frontiers | Research Topics

Advances in marine and freshwater monitoring to support aquatic ecosystem conservation and restoration

Edited by
Elisabetta Manea, Caterina Bergami
and Robert Ptacnik

Published in
Frontiers in Environmental Science
Frontiers in Marine Science

ISSN 1664-8714
ISBN 978-2-8325-3884-5
DOI 10.3389/978-2-8325-3884-5

About Frontiers

Frontiers is more than just an open access publisher of scholarly articles: it is a pioneering approach to the world of academia, radically improving the way scholarly research is managed. The grand vision of Frontiers is a world where all people have an equal opportunity to seek, share and generate knowledge. Frontiers provides immediate and permanent online open access to all its publications, but this alone is not enough to realize our grand goals.

Frontiers journal series

The Frontiers journal series is a multi-tier and interdisciplinary set of open-access, online journals, promising a paradigm shift from the current review, selection and dissemination processes in academic publishing. All Frontiers journals are driven by researchers for researchers; therefore, they constitute a service to the scholarly community. At the same time, the *Frontiers journal series* operates on a revolutionary invention, the tiered publishing system, initially addressing specific communities of scholars, and gradually climbing up to broader public understanding, thus serving the interests of the lay society, too.

Dedication to quality

Each Frontiers article is a landmark of the highest quality, thanks to genuinely collaborative interactions between authors and review editors, who include some of the world's best academicians. Research must be certified by peers before entering a stream of knowledge that may eventually reach the public - and shape society; therefore, Frontiers only applies the most rigorous and unbiased reviews. Frontiers revolutionizes research publishing by freely delivering the most outstanding research, evaluated with no bias from both the academic and social point of view. By applying the most advanced information technologies, Frontiers is catapulting scholarly publishing into a new generation.

What are Frontiers Research Topics?

Frontiers Research Topics are very popular trademarks of the *Frontiers journals series*: they are collections of at least ten articles, all centered on a particular subject. With their unique mix of varied contributions from Original Research to Review Articles, Frontiers Research Topics unify the most influential researchers, the latest key findings and historical advances in a hot research area.

Find out more on how to host your own Frontiers Research Topic or contribute to one as an author by contacting the Frontiers editorial office: frontiersin.org/about/contact

Advances in marine and freshwater monitoring to support aquatic ecosystem conservation and restoration

Topic editors

Elisabetta Manea — UMR8222 Laboratoire d’Ecogéochimie des Environnements Benthiques (LECOB), France

Caterina Bergami — Institute of Marine Science, National Research Council (CNR), Italy

Robert Ptacnik — Wasser Cluster Lunz, Austria

Citation

Manea, E., Bergami, C., Ptacnik, R., eds. (2023). *Advances in marine and freshwater monitoring to support aquatic ecosystem conservation and restoration*. Lausanne: Frontiers Media SA. doi: 10.3389/978-2-8325-3884-5

Table of contents

frontiers | Frontiers in Environmental Science

TYPE Editorial
PUBLISHED 23 October 2023
DOI 10.3389/fenvs.2023.1304545

EDITED AND REVIEWED BY
Angela Helen Arthington,
Griffith University, Australia

*CORRESPONDENCE
Caterina Bergami,
✉ caterina.bergami@ismar.cnr.it

RECEIVED 29 September 2023
ACCEPTED 12 October 2023
PUBLISHED 23 October 2023

CITATION
Manea E, Bergami C and Ptacnik R (2023), Editorial: Advances in marine and freshwater monitoring to support aquatic ecosystem conservation and restoration.
Front. Environ. Sci. 11:1304545.
doi: 10.3389/fenvs.2023.1304545

Editorial: Advances in marine and freshwater monitoring to support aquatic ecosystem conservation and restoration

Elisabetta Manea[1,2], Caterina Bergami[3]* and Robert Ptacnik[4]

[1]Laboratoire d'Ecogeochimie des Environnements Benthiques (LECOB), Sorbonne Université, Centre National de la Recherche Scientifique (CNRS), Banyuls-Sur-Mer, France, [2]National Research Council, Institute of Marine Sciences, CNR-ISMAR, Venice, Italy, [3]National Research Council, Institute of Marine Sciences, CNR-ISMAR, Milan, Italy, [4]WasserCluster Lunz—Biologische Station, Lunz am See, Austria

KEYWORDS

monitoring networks, monitoring data, freshwater, marine, transitional, aquatic ecosystems, restoration, conservation

Editorial on the Research Topic
Advances in marine and freshwater monitoring to support aquatic ecosystem conservation and restoration

Monitoring, conserving, and restoring aquatic ecosystems are priorities addressed by European and global initiatives, put in place to achieve declared national and global conservation and sustainability goals. These initiatives are dictated by both legally binding EU frameworks (e.g., Water and Marine Strategy Framework directives, WFD and MSFD, respectively; EC, 2000; EC, 2008), and global initiatives—i.e., Essential Ocean and Biodiversity Variables frameworks (EOVs and EBVs) under the Global Ocean Observing System (GOOS), and the Group on Earth Observations Biodiversity Observation Network (GEO BON), respectively (Pereira et al., 2013; Miloslavich et al., 2018). Nonetheless, the extent to which all these initiatives can provide lasting positive effects on conservation and restoration targets is often limited by the lack of robust baseline data and systematic monitoring and protocols, which in turn are constrained by the limited number of long-term monitoring programs and limited dedicated funding. Harmonization of methods, data structure, and handling is a further limitation when it comes to providing a comprehensive assessment of aquatic habitats in times of global change.

This Research Topic provides an overview of important advancements in the research field of monitoring as a supporting tool for the conservation/restoration of aquatic ecosystems (freshwater, marine, and transitional), and of innovative and under-development monitoring practices and approaches at both local and large scales (i.e., local, national, transnational).

This Research Topic contains sixteen articles that address encompassing all major aquatic domains: freshwater (7), marine (5), and transitional (4) ecosystems, and are focused on different habitats and groups of organisms (e.g., benthic and pelagic habitats, fishes, benthic organisms, algae, and seagrasses) and environmental parameters (e.g., oxygen, chlorophyll). Despite their heterogeneity, they possess the common scope of exploring, developing, and testing different monitoring approaches with the aim of favoring conservation and restoration strategies.

Podda et al. use long-term data from river systems in Sardinia to assess the effect of dams on the population dynamics of the European Eel. Using boosted regression trees, they show that especially time of dam construction, as well as dam height, impair mobility and dispersal of Eel into the catchments, and make a strong case for de-regulation of rivers.

Some studies are more methodological. For instance, Di Muri et al. present a case study focused on the biogeography of two invasive crustaceans and describe the procedures, resources, and analytical web services implemented to investigate the trophic habits of these taxa by using carbon and nitrogen stable isotope data. They offer a number of analytical tools to determine the variability of the trophic position of invasive crustaceans in a spatially explicit context and to model it as a function of relevant environmental predictors. Moe et al. provide information on the Water Information System for Europe (WISE) biology data, their accessibility, and re-usability, and illustrate current or planned applications and indicator development for European-scale assessments.

Three methodological papers assess the adoption of (semi-) automated methods for sampling Chlorophyll-a (Chl-a) in coastal waters and lakes (Rogora et al. Alikas et al., and Farinha et al.). In the study of Alikas et al. *in vitro*, fluorescence, and spectral approaches to measure Chl-a are compared in two distinct lakes in Estonia, characterized by diverse trophic conditions. They explore the potential to combine the different methods for improving Chl-a measurement accuracy. Rogora et al. focus on Chl-a data, with the aim to test whether *in situ* fluorescence measurements may provide an estimate of lake phytoplankton biovolume and its seasonal dynamic. Their results confirm the use of *in situ* sensors as a reliable approach to measure algal pigments, especially to assess their variability in the short-term, but also to describe the seasonal pattern of phytoplankton biovolume. Farinha et al. present and validate the use of MEDUSA, an Unmanned Aerial-Aquatic Vehicle capable of performing underwater sampling and inspection. This system is successful in acquiring samples from shore and at high precision in depth and filtered water volume, enabling the acquisition of accurate Chl-a measurements that are on par with manual sampling methods.

Leoni et al. investigate another important environmental parameter, focusing on the role of sediments in Dissolved Oxygen (DO) consumption in the Venice Lagoon (Italy), and measuring the Sediment Oxygen Demand (SOD) rate in four test areas with benthic chambers. They assess how the presence of the MOSE infrastructure, which protects the lagoon from high tide-derived flooding, will affect DO concentration and the functioning of the waterbody during its closures.

Mackin-Mclaughlin et al. and Tesfaye et al. proposed approaches to improve the assessment and monitoring of aquatic habitats and associated species. Mackin-Mclaughlin et al. test the performance of predictive modeling approaches to enable marine coastal habitats monitoring. The authors employ habitat mapping techniques to spatially characterize the distribution of benthic organisms along the western coast of Placentia Bay, an Ecologically and Biologically Significant Area (EBSA) in Newfoundland, Canada. They find the use of fine-scale environmental information from benthic videos to consistently improve model accuracy, highlighting the need for in-field data Research Topic. They provide valuable knowledge on marine epifaunal association, distributions, and richness in the case study area, thus strongly supporting the current and future monitoring of Placentia Bay habitats. Tesfaye et al. focus on the Římov Reservoir (Czech Republic) lake's pelagic habitat and compare the consolidated CEN (European Committee for Standardization) protocol to assess fish abundance and biomass, with alternative approaches, which turned out to be effective. These incorporate information on pelagic habitats volume avoiding under-representation of any habitat in the assessment. They additionally evaluate the composition and trend changes of fish populations over time.

Transitional waters and coastal wetlands are the areas of interest in the papers from Petrocelli et al. and Duan et al., respectively. Duan et al. use shorebird survey and land-use data to characterize the effects of long-term habitat change (1995–2020) on shorebird populations in the Yellow River Delta (China). They hypothesize that habitat changes pose a more serious threat to threatened, large-bodied, and coastal specialist species than to non-threatened, small-bodied, and generalist/inland specialist species. Their findings provide useful insights to conserve and manage key shorebird habitats in the area. Petrocelli et al. analyze the 11-year monitoring data on non-indigenous species (NIS) of seaweeds in the Mar Piccolo of Taranto (Italy). To investigate spatial and temporal differences in seaweed assemblages, multivariate analyses are performed considering the NIS and the most important native species in terms of temporal occurrence. The Mar Piccolo seems not particularly suitable for NIS settlement and development, especially if coming from cold-temperate zones.

Two papers are specifically dedicated to the identification of gaps in the current conservation networks and related monitoring efforts (Gianni et al. and Castellan et al.). Gianni et al. develop and apply a conceptual model to some selected Adriatic Natura 2000 (N2K) sites to review and assess the management and monitoring effectiveness of the sites, and to suggest possible improvements. They aim to inform the management of N2K sites by providing a knowledge baseline to support the implementation of the Adriatic Sea ecological observing system. Castellan et al. assess the effectiveness of the current legislative framework in providing instruments to protect mesophotic ecosystems in the Mediterranean Sea, through literature revision, highlighting a heterogeneous coverage of information related to mesophotic habitats and associated taxa and a lack of conservation efforts towards mesophotic zones. They provide suggestions to improve the management regime of these ecosystems starting from the setting up of routine and *ad hoc* monitoring of mesophotic and deep-sea habitats to advance the knowledge needed to inform their conservation.

Radwan et al. and Vieira et al. test the use of indicators to favor consistency in monitoring efforts worldwide. In particular, the first study explores the host-parasite-metals interactions and the potential to use the parasites' presence as a bio-indicator of the health status of Nile tilapia (*Oreochromis niloticus*), an important source of protein for local people. After characterizing the accumulation dynamics of heavy metals in the fish tissue, the authors observe significant relationships between parasite presence and heavy metal concentration. Meanwhile, the potential to adopt an interspecific boundary line (IBL) as an indicator of the health status of seagrass meadows is explored by

Veira and colleagues. The IBL is adopted to define the maximum possible efficiency in space occupation of 18 species of seagrasses in Costa Rica, and its efficiency as an indicator is tested against 5,052 observations from 78 studies. The authors prove the effectiveness of IBL for monitoring the health of seagrass populations.

Finally, Orlando-Bonaca et al. highlight the importance of monitoring environmental conditions for identifying suitable restoration locations and ensuring efficiency in restoration actions. They set up a restoration system for the macroalga *Gongolaria barbata*, a *Cystoseira* s.l. species, in the marine protected area of Miramare (Trieste, Italy) and in Piran (Slovenia) to deepen knowledge of the reproductive potential and success of donor populations and evaluate the out-planting success in relation to the different donor and receiving sites. Additionally, they test the effectiveness of *ex-situ* and hybrid methods combined with mesocosm cultivation and suspended culture in the field.

We thank all contributing authors and hope that you will enjoy reading their papers. We hope that these papers will support progressive advancement in monitoring practices as the base of effective conservation and restoration of aquatic ecosystems.

Author contributions

EM: Conceptualization, Writing–review and editing. CB: Conceptualization, Writing–original draft, Writing–review and editing. RP: Writing–review and editing.

Funding

The author(s) declare that no financial support was received for the research, authorship, and/or publication of this article.

Acknowledgments

We wish to express our gratitude to all colleagues who submitted manuscripts to this Research Topic and to all the reviewers for their time, attentive criticisms, and constructive comments and suggestions.

Conflict of interest

The authors declare that the research was conducted in the absence of any commercial or financial relationships that could be construed as a potential conflict of interest.

Publisher's note

References

European Commission (2000). Directive 2000/60/EC of the European parliament and of the council of 23 October 2000 establishing a framework for community action in the field of water policy (Water framework directive). *Off. J. Eur. Union* 73.

European Commission (2008). Directive 2008/56/EC of the European parliament of the council of 17 June 2008 establishing a framework for community action in the field of marine environmental policy (Marine strategy framework directive). *Off. J. Eur. Union* 27.

Miloslavich, P., Bax, N. J., Simmons, S. E., Klein, E., Appeltans, W., Aburto-Oropeza, O., et al. (2018). Essential ocean variables for global sustained observations of biodiversity and ecosystem changes. *Glob. Change Biol.* 24 (6), 2416–2433. doi:10.1111/gcb.14108

Pereira, H. M., Ferrier, S., Walters, M., Geller, G. N., Jongman, R. H. G., Scholes, R. J., et al. (2013). Essential biodiversity variables. *Science* 339 (6117), 277–278. doi:10.1126/science.1229931

frontiers | Frontiers in Environmental Science

ORIGINAL RESEARCH
published: 23 June 2022
doi: 10.3389/fenvs.2022.890039

Fish Parasites and Heavy Metals Relationship in Wild and Cultivated Fish as Potential Health Risk Assessment in Egypt

Mahmoud Radwan[1]*, Mahmoud Mahrous M. Abbas[1], Moharam Adel Mohamed Afifi[1], Amaal Mohammadein[2] and Jamila S. Al Malki[2]

[1]Marine Biology Branch, Zoology Department, Faculty of Science, Al-Azhar University, Cairo, Egypt, [2]Department of Biology, College of Science, Taif University, Taif, Saudi Arabia

Edited by:
Elisabetta Manea,
National Research Council (CNR), Italy

Reviewed by:
Edison Barbieri,
Agência de Agronegócio e Tecnologia de São Paulo (APTA), Brazil
Wynand Malherbe,
North-West University, South Africa

***Correspondence:**
Mahmoud Radwan
MahmoudKhriy.201@azhar.edu.eg

Specialty section:
This article was submitted to Freshwater Science, a section of the journal Frontiers in Environmental Science

Received: 05 March 2022
Accepted: 10 May 2022
Published: 23 June 2022

Citation:
Radwan M, Abbas MMM, Afifi MAM, Mohammadein A and Al Malki JS (2022) Fish Parasites and Heavy Metals Relationship in Wild and Cultivated Fish as Potential Health Risk Assessment in Egypt. Front. Environ. Sci. 10:890039. doi: 10.3389/fenvs.2022.890039

Despite wide studies of biomonitoring aquatic environment through dynamics of host–parasite interaction, bio-indicators to track the influence and accumulation of heavy metals on fish are still few. The present study sheds light on the relation between fish parasites and heavy metals as it threatens fish's health and, as a consequence, that of humans after fish consumption. Samples of Nile tilapia (*Oreochromis niloticus*) were collected in Burullus Lake, a wild fish source, and from a private fish farm in Kafr El-Sheikh Governorate, in Egypt. They were exposed to various pollutants associated with anthropogenic activities to determine the levels of accumulation of Fe, Zn, and Cu, along with the top three most toxic metals (As, Cd, and Pb) in water and fish tissues of gills, intestine, liver, and muscles in both wild and farmed *O. niloticus*. The results showed the order of abundance: Fe < Zn < Pb < Cu < As < Cd. In waters of both farmed and wild fish, there was a significant negative relation between parasite prevalence and heavy metals, including Zn, Pb, and As. Also, there was a significant positive relation between parasite prevalence with Cu while no significant relation was found with Fe and Cd. Heavy metal content was significantly higher ($p > 0.05$) in non-infected than infected farmed and wild *O. niloticus*. In addition, a significantly decreased concentration ($p > 0.05$) of essential heavy metal was recorded in wild fish compared to farmed specimens, while non-essential heavy metal was significantly higher ($p > 0.05$) in wild compared to farmed fish. Bioaccumulation factors (BAF) of different organs of *O. niloticus* were ranked in ascending order: Liver > Gills > Intestine > Muscles. In general, the risk assessment showed safe human consumption of farmed and wild fish under the reported environmental conditions in this study. Moreover, the parasite's presence can be adopted as a surrogate indicator to estimate the potential impact of heavy metal pollution and accumulation.

Keywords: Nile tilapia, aquatic pollution, infection, bioaccumulation factor, hazard index

INTRODUCTION

Aquaculture has grown to become a major source of low-cost protein in many countries globally, and production has doubled in the last 10 years, especially in Egypt, where aquaculture accounts for more than 80% of Egypt's total fish production (GAFRD, 2019; David et al., 2021). In poor countries, fish provides up to approximately 30% of the total animal protein consumed per capita (Wang et al., 2015). Nile tilapia, *Oreochromis niloticus,* is considered the most important and well-known farmed fish in Egypt and Africa (Authman et al., 2012; Abdel-hakim et al., 2016). It has grown more than twenty-fold in the last 20 years (Henriksson et al., 2017).

Due to their environmental persistence and incapacity to dissolve, metals are considered a particular cause of concern across the world (Abah et al., 2016; Jiang et al., 2018). Contaminants are accumulated in aquatic species, such as fish, either directly from contaminated water or indirectly through the food chain (Abah et al., 2016; Ahmed et al., 2020). Some heavy metals are important for fish metabolism within accepted ranges, but when their quantities exceed these ranges, they become extremely hazardous (Keke et al., 2015; Padrilah et al., 2018). Fish uptake the heavy metals directly from the water *via* their skin and gills, as well as through the consumption of contaminated food (Hassan et al., 2018). As such, the concentration of metal in a fish tissue depends on its amount in the water and its prey (Mousa et al., 2015). With the capability of metals to bioaccumulate within the fish organs, these may constitute a health risk for consumers (Tytła, 2019). It is vital to estimate the risks of metals on human health as a result of targeted fish intake (Salam et al., 2019).

Concentrations of heavy metals do not have to reach high levels in the organism's body to be dangerous, since even if accumulated in low quantities in the body tissues, they can exceed the allowed limits (Sardar et al., 2013). As a result, the consequences of heavy metals' negative effects on fish can be exploited in biomonitoring freshwater environments. In parallel, the quality of fish living in environments subject to agricultural drainage and the fresh water of the Nile should be examined to assess their acceptability and safety for human consumption.

Metals, such as Cu, Mn, Zn, and Fe, are classified as essential for enzyme functioning and play vital roles in a variety of biological mechanisms. Nonetheless, when an organism assimilates them in high quantities over long periods, they can become poisonous. In parallel, Cr, Pb, and Cd are categorized as non-essential metals as they have no biological significance for living creatures. Furthermore, even in small amounts, they are hazardous (Ju et al., 2017; Mehana et al., 2020).

Fish consumption is a small part of the overall human diet, whereas the risk range provided by the US Environmental Protection Agency (EPA) is for the total dietary intake of metals. However, the metal accumulation risk through fish consumption should not be ignored. Furthermore, given harmful metals' non-biodegradability and probable accumulation in fish tissues, metal supplementation in fish feed should be reduced, and fish should be monitored regularly to help reduce the risk of non-essential metal poisoning for consumers (Resma et al., 2020).

Analyses of fish-parasite-metals interactions have been proposed as an efficient monitoring method for assessing the health of the environmental fish ecosystem, with parasites indicating the presence of various contaminants in aquatic habitats, including toxic metals and sewage pollutants (Mehana et al., 2020).

Indeed, fish parasites help their hosts survive in heavy metal-polluted environments by collecting larger quantities of heavy metals and therefore acting as metal sinks (Eissa et al., 2012).

This study intended to explore the following:

1. The metal content in water, gills, intestines, livers, and edible tissues of both farmed and wild *Oreochromis niloticus;*
2. The potential human health risks associated with the consumption of both farmed and wild fish with the use of combined indices;
3. The role and relationships between heavy metal accumulation and fish parasite infestation in monitoring ecosystem pollutions.

Moreover, by examining the possible relationship between parasites and heavy metals as bio-monitors of pollution, the current study fills a significant gap in the ecotoxicology field.

MATERIAL AND METHODS

Collection of Fish and Water Samples

Water samples were taken from two different locations. The first location was Burullus Lake (lake origin), while the second was a private fish farm in the governorate of Kafr El-Sheikh in Egypt (Farmed origin) (**Figure 1**). A total of 538 Nile Tilapia specimens, *O. niloticus*, were taken, 324 males and 214 females, with a standard length of 17.48 ± 6.87 cm and an average weight of 236.26 ± 14.35 g. Fish were taken simultaneously with the water samples from the same location and transported to the Marine Biology Department of the Faculty of Science at Al-Azhar University in Egypt.

Physico-Chemical Parameters

Physico-chemical parameters (pH, turbidity, TDS, ammonia, NO_2, NO_3, total alkalinity, total hardness, total phosphate, H_2S, and dissolved oxygen) were measured in the water of Burullus Lake and the private fish farm according to procedures outlined by the American Public Health Association (APHA, 2005). The pH levels were determined using a digital pH meter. Total dissolved solids were calculated using a digital TDS meter (TDS). Ammonia (NH_3), nitrite (NO_2), nitrate (NO_3), and total phosphate levels were measured using colorimetric methods. Water alkalinity was precisely evaluated following sample collection using phenolphthalein and methyl orange as indicators. The Winkler method was used to analyze dissolved oxygen and titration methods were utilized to estimate H_2S.

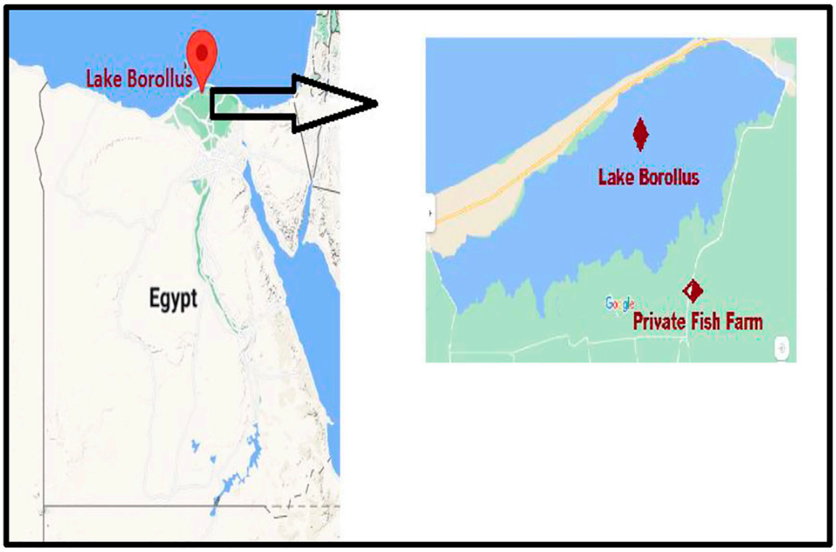

FIGURE 1 | Map showing the Burullus Lake and the Private Fish Farm location.

Length-Weight Relationship

After collection, the standard length of each fish was measured to the nearest millimeter. The body weight was also determined to the nearest 0.1 g. The Length-weight relationship was determined by using power equation or its logarithmic modification according to the following method:

$$\text{Log W} = \text{Log a} \pm \text{b Log L}$$

(Lagler, 1956).where W is the weight of the fish in grams; L is the standard length in centimeter; and a and b are constants, whose values are estimated by the least square method.

By grouping the fish in 10 mm length groups, the empirical and calculated weights were determined.

Parasitological Assessments

Specimens were examined in the laboratory. The gills, intestines, muscles, and liver were isolated. After incisions on the ventral side, the excised organs were initially checked externally for parasites with a magnifying glass. The alimentary tracts were then isolated under a stereomicroscope in 0.09% sterile saline for parasite extraction (Marcogliese and Pietrock, 2011). According to Sohn's (2009) procedures, 1 g of each tissue was placed between two glass slides and investigated for the detection of encysted metacercariae using a binocular dissecting microscope. Distinct parasites were carefully removed, and morphological features were utilized to differentiate them at the species level. Their proportions were documented, as well as whether they appeared alone or in clusters. They were not tarnished when they were photographed (Elsheikha and Elshazly, 2008; El-Shahawy et al., 2017). However, the approaches described in Yamaguti (1963), Cheng (1973), and Radwan (2022) were used to identify helminths. Cestodes, nematodes, and trematodes were relaxed in warm water for 6 h before being fixed in 5% formalin and transferred to 70% ethanol (Oros et al., 2010).

According to Radwan et al. (2021) and El-Shahawy et al. (2017), the specimens were stained with acetic acid alum carmine in 70% acid ethanol, dehydrated in ascending concentrations of ethanol, cleaned with clove oil, and permanently mounted in Canada balsam for microscopic examination. Parasites prevalence (PP) and intensity (IN) in fish were estimated according to the following formula:

$$\text{FPP}\,(\%) = (\text{No. HI}/\text{No. HE}) \times 100$$

where FPP (%) denotes fish PP; No. HI represents the number of individuals of a host species infected with a particular parasite species; and No. HE indicates the number of hosts investigated.

$$\text{IN} = \text{TNPS}/\text{NIHS}$$

where IN is the intensity; TNPS is the total number of parasite individuals in a sample of host species; and NIHS is the number of infected hosts in the sample.

Heavy Metals Analysis

Sample Digestion

The studied organs (intestine, gills, liver, and muscles) of infected and non-infected fish were selected for heavy metals analysis after parasitological inspection. The organs (0.5 g each) were treated with 5 ml of concentrated nitric acid, warmed on the hot plate at 100°C for 10 h, cooled at room temperature, and thoroughly digested. The digested sample was transferred to a volumetric flask, and the volume was diluted to a final volume of 50 ml with deionized water. Heavy metals in water samples were determined using an acid digestion technique for total metals. The digested solution was poured into a volumetric flask and then diluted to a final volume of 100 ml with deionized water. After that, the diluted solution of organs and water samples were tested (AOAC, 2012).

ICP Analysis

Heavy metal (zinc Zn, cadmium Cd, copper Cu, iron Fe, lead Pb, and arsenic As) levels were measured in diluted solutions of tissues and water samples. The heavy metals levels in the serial dilutions (water and fish samples, $n = 5$) were determined using an inductively coupled plasma optical emission spectrophotometer (ICP-OES, Model 4300 DV, Perkin Elmer, Shelton, CT, United States). To estimate the ppm of each analysis in the digested solution, samples were treated with a multi-element standard solution containing 1 μg/L of each metal used for calibration curve calculation. The Quality Control sample was analyzed every ten samples to ensure that the calibration accuracy and instrument drift were both within acceptable limits (within 20% of the known QC values acceptable). In each analytical batch, blank samples were run in duplicate in random order and utilized to calculate the technique detection limit. The heavy metals levels in the water samples were measured in mg/L and the fish samples in mg/kg on a wet weight basis (Abbas et al., 2021).

Bioaccumulation Factor Calculation

The BAF is the ratio between heavy metals deposited in fish tissues and in the water. It was calculated using the following equation:

$$\mathrm{BAF} = \mathrm{C - fish/C - water}$$

(Adolfsson-Erici et al., 2012).where BAF is the bioaccumulation factor, C-fish is the heavy metal levels in fish organs (ppm), and C-water is the heavy metal levels in water (ppm).

Human Risk Assessment Calculation

To assess the human risk of heavy metals absorption through the ingestion of the analyzed fish, the approach provided by the US Environmental Protection Agency was adopted (USEPA 2018). The average daily dosage (EDI; an average daily intake of a given chemical over a lifetime) determined the degree of exposure produced by oral human ingestion of certain heavy metals found in fish tissues. The average daily dose (ADD) was calculated using the following equation, which is given as $\mathrm{mg}^{-1}\,\mathrm{kg}^{-1}\,\mathrm{day}^{-1}$.

$$\mathrm{EDI} = (\mathrm{CF} \times \mathrm{IR} \times \mathrm{ER} \times \mathrm{EP} / \mathrm{BW} \times \mathrm{AT}) \times 10^{-3}$$

(Mwakalapa et al., 2019).where CF is the average heavy metals concentration in fish muscle—mg/kg wet wt.; IR refers to the daily intake (DI) of fish consumed (kg/day), which in this study was considered to be 7.9 g/day for children (age 6–11 years old) and 20.1 g/day for adults; ER is the exposure rate (365 days/year); EP is the exposure period over a lifetime (suspected to be 70 years old); BW is the body weight, which for adults was considered to be 70 kg (Mannzhi et al., 2021) and for children 6–11 years old 52.5 kg body weight which refers to the 95th percentile (USEPA, 2008); AT is the average lifetime (70 years × 365 days/year).

The target hazard quotient (THQ), a non-cancer indicator of unfavorable health consequences due to the ingestion of particular heavy metals contaminants in fish samples, was used to quantify human risk. THQ was computed using the equation below, which was derived from the proportion of ADD to ORD (oral reference dose of heavy metals).

$$\mathrm{THQ} = \mathrm{EDI/ORD}$$

(USEPA, 2018). where ORD refers to the oral reference doses of heavy metals (mg/kg/days) for an adult person weighing 70 kg, it's recommended as an upper limit of heavy metals oral consumption. ORDs for Cu, Pb, Zn, Cd, As, and Fe are 0.04, 0.00357, 0.3, 0.001, 0.0003, and 0.7 mg/kg/day, respectively (USEPA, 2018). When the target hazard quotient (THQ) falls below 1.0, it indicates that unfavorable health effects on people are improbable. If the calculated THQ is greater than 1.0, people should expect unfavorable health consequences.

The hazard index (HI) is a scientific formula that measures the effect of non-carcinogenic hazards by the sum of THQ values of the metals under investigation as follows:

$$\mathrm{HI} = \mathrm{THQ(Cd)} + \mathrm{THQ(Pb)} + \mathrm{THQ(Fe)} + \mathrm{THQ(Cu)} + \mathrm{THQ(As)} + \mathrm{THQ(Zn)}$$

(USEPA, 2011). When the HI value is higher than 10, the exposed persons have a higher non-carcinogenic risk.

Data Analysis

The normal distribution and homogeneity of variance were demonstrated using Levene's test. The statistical analysis was performed using IBM, SPSS Statistical Program, Version 22; SPSS Inc., IL, United States. The one-way ANOVA was applied and when significant differences were found, multivariate, post hoc Tukey evaluations were utilized to quantify the statistical difference between the heavy metals' levels in various fish organs for each metal. The correlations between physico-chemical parameters and heavy metal levels in farmed and wild fish were investigated using Pearson's correlation coefficient. The T-test was used to compare infected and non-infected fish, and the statistical significance was established at $p < 0.05$.

RESULTS

Water Quality

Data indicated that fish farm waters had significantly higher levels of ammonia (mg/L), pH, turbidity (%), nitrogen dioxide (mg/L), TDS (mg/L), nitrate (mg/L), total alkalinity (mg/L), total hardness (mg/L), phosphate (mg/L), and hydrogen sulfide (mg/L) compared to the water of Burullus Lake. The only exception to this pattern was the dissolved oxygen (mg/L). On the contrary, Fe, Zn, Pb, Cu, and As levels in Burullus Lake waters were much lower than in fish farm waters. Concentrations of heavy metals in Burullus Lake and fish farm water were reported in this order: Fe, Zn, Pb, Cu, As, and Cd (**Table 1**, **2**).

TABLE 1 | Water quality parameters and heavy metal concentrations of the water collected from fish farm and Burullus Lake. At $p < 0.05$, results from the same row with different alphabetic letters are statistically different.

	Fish farm	Lake burullus	Drinking water		Aquatic life	WHO (2011)
			EWQS	WHO	CCME	
Water quality parameters						
PH	8.37 ± 0.39^{a}	7.17 ± 0.95^{b}	6.5–8.5	6.5–8.5	6.5–9	
Turbidity (%)	84.33 ± 5.25^{a}	68.67 ± 0.58^{b}		1000		
TDS (mg/L)	836.00 ± 19.80^{a}	772.00 ± 34.39^{b}				
Ammonia (mg/L)	1.28 ± 0.09^{a}	0.80 ± 0.13^{b}				
NO_2 (mg/L)	0.41 ± 0.03^{a}	0.31 ± 0.02^{b}		1		
NO_3 (mg/L)	0.81 ± 0.01^{a}	0.57 ± 0.06^{b}		50		
Total alkalinity (mg/L)	207.33 ± 2.87^{a}	186.33 ± 4.93^{b}				
Total hardness (mg/L)	235.33 ± 1.70^{a}	203.67 ± 5.51^{b}	500	500		
Phosphate (mg/L)	0.35 ± 0.05^{a}	0.21 ± 0.02^{b}				
H_2S (mg/L)	0.93 ± 0.04^{a}	0.75 ± 0.05^{b}				
Dissolved Oxygen (mg/L)	7.67 ± 0.38^{b}	8.44 ± 0.81^{a}			5.5–9.5	
Heavy metal concentrations						
Fe (PPm)	0.865 ± 0.061^{a}	0.561 ± 0.072^{b}				1
Zn (PPm)	0.6907 ± 0.060^{a}	0.481 ± 0.036^{b}				1
Pb (PPm)	0.088 ± 0.008^{a}	0.067 ± 0.008^{b}				0.05
Cu (PPm)	0.072 ± 0.015^{a}	0.056 ± 0.010^{b}				1
AS (PPm)	0.050 ± 0.004^{a}	0.046 ± 0.007^{b}				0.05
Cd (PPm)	0.004 ± 0.001	0.004 ± 0.001				0.01

$^{a,\,b}$Results at $p < 0.05$, results from the same row with different alphabets small letters are statistically different.

TABLE 2 | Comparison between HMs levels of (μg/L = ppb) in Burullus Lake water of the present study with the previous studies.

References	HM levels values (μg/L) in water					
	Cu	Zn	Fe	AS	Cd	Pb
Shakweer and Radwan (2004)	8.48	11.07	1031	55	6.5	5
Radwan (2005)	12.43	15.68	1920	--	5.3	7.3
Saeed and Shaker (2008)	35	50	425	--	--	65
Masoud et al. (2011)	3.3	30.75	1737	14	4.6	4.13
Basiony (2014)	23.42	64.15	1550			12.07
El-Alfy (2015)	7.28	2.92	14.64	37	12.3	8.88
El-Batrawy et al. (2018)	2.05	10.5	29.38	--	--	5.98
Present study						
Burullus Lake	56	481	561	46	4	67
Fish Farm	72	691	865	50	4	88

Length-Weight Relationship of Uninfected and Infected Fish

Figure 2A–D shows the length-weight relationship of *O. niloticus* fish and its relationship with parasite infection. The wild and farmed infected and non-infected *O. niloticus* specimens exhibited b values ranging from 2.56 to 2.92. The value of "b" was less than 3 in the infected and non-infected fish of both wild and farmed fish, indicating a negative allometric growth pattern for fish regardless of their infection status. Nearly, all species' length and weight had a strong and very significant correlation (r > 0.96).

Parasitological Outcomes

The parasitic infection rate was 71.34% in farmed fish, while in wild fish it was 61.16%. Furthermore, farmed fish infection was lower in the liver (11.78%), increased gradually in the gills (14.65%), and intestine (16.88%), and reached a higher rate (28.03%) in muscle tissue. The parasitic infection in different organs in lake fish fluctuated between (9.82%) in the liver and (21.43%) in muscles. Farmed fish organs were more susceptible to infection than lake fish. Moreover, organs were ordered as muscles, gills, liver, and intestine according to the ratio of infection (**Table 3**).

Table 4 showed that the prevalence of protozoa was higher in farmed *O. niloticus* fish (14.01%) in comparison to lake fish (7.59%). Trematodes have fluctuated between 31.53% in farmed fish and 31.70% in lake fish. The prevalence of cestodes was 4.14% in farmed fish and 4.91% in lake fish, respectively. Furthermore, the highest prevalence of Acanthocephala was found in lake fish, while the lowest rate was found in farmed fish, at 21.66% and 16.96%, respectively.

A total of 13 parasites, were isolated from the examined fish. Platyhelminthes, two trematodes (*Cichlidogyrus tilapiae*, *Enterogyrus cichlidarum*), one cestode (Procercoid and plerocercoid stage of *Polyonchobothrium clarias*), two nematodes (*Procamallanus sp* and *Paracamallanus* sp), one acanthocephala (*Acanthosentis tilapiae*), were found, as well as seven species of encysted metacercariae *Centrocestusn formosanus*, *Heterphyes* sp., *Pygidiopsis genata*, *Diplostomum tilapiae*, *Cyanodiplostomum* sp., *Opisthorchis* sp., *Prohemistomum* sp., (**Table 5** and **Figure 3A–O**).

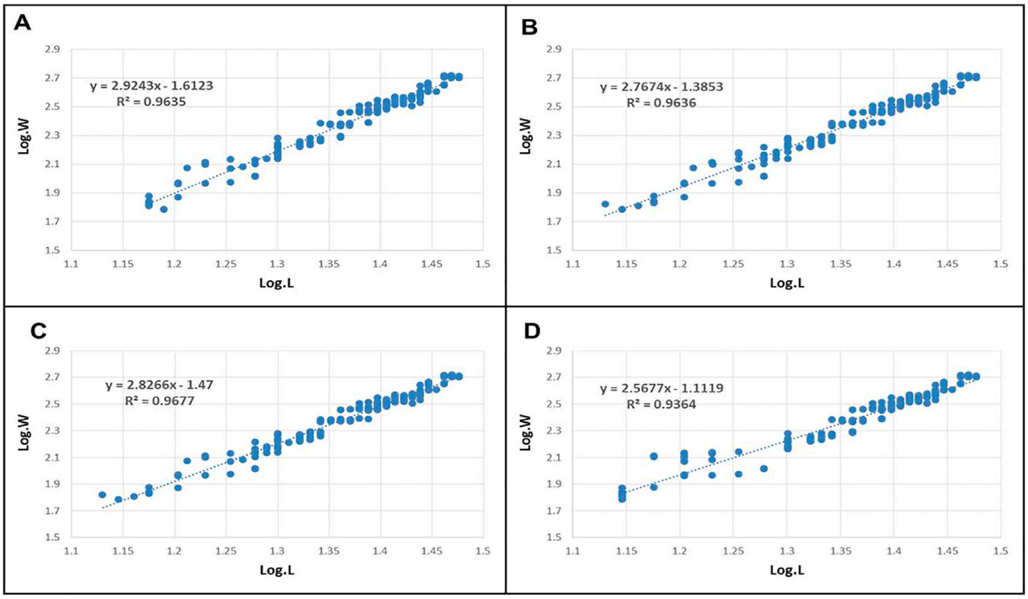

FIGURE 2 | Length-weight relationship of lake and farmed Nile Tilapia, *O. niloticus*. **(A)**: Non-infected farmed fish **(B)**: Infected farmed fish; **(C)**: Non-infected lake fish **(D)**: Infected lake fish.

TABLE 3 | Number of infected specimens of *O. niloticus* considering the different analyzed organs and their percentage on the total number of fish examined.

Organs	Farmed fish examined (314)		Lake fish examined (224)	
	No. of infected	PP (%)	No. of infected	PP (%)
Gill	46	14.65	28	12.5
Muscles	88	28.03	48	21.43
Intestine	53	16.88	39	17.41
Liver	37	11.78	22	9.82
Total infected	224	71.34	137	61.16

TABLE 4 | Prevalence of different parasites species (PP) among the examined fish *O. niloticus,* collected from Fish Farm and Burullus Lake.

Organs	Farmed fish		Lake fish	
	No. of infected	PP (%)	No. of infected	PP (%)
Nematoda	44	14.01	17	7.59
Trematodes	99	31.53	71	31.70
Cestoda	13	4.14	11	4.91
Acanthocephala	68	21.66	38	16.96
Total infected	224	71.34	137	61.16

PP, parasites Prevalence.

Pearson Correlation Coefficients

Table 6 showed the Pearson correlation between parasite prevalence, physico-chemical parameters, and water heavy metals. There was a positive correlation between parasite prevalence and turbidity, nitrogen dioxide, nitrate, total alkalinity, and phosphate (r = 0.75, 0.69, 0.65, and 0.67; $p < 0.05$). The parasite prevalence of farmed and lake fish was correlated negatively with pH and dissolved oxygen (r = –0.51 and –49 previously and –0.66 and –0.58 later; $p < 0.05$). In both fish farm and Burullus Lake waters, there was a significant negative correlation between parasite prevalence (PP) and water heavy metals, including PP-Zn, PP-Pb, and PP-As. However, there was a significant positive correlation between PP and Cu. There is no significant link between PP-Fe and PP-Cd.

Level of Heavy Metals in Fish Organs

Non-essential heavy metal concentrations, As, Cd, and Pb, were significantly higher in both non-infected lake and farmed fish compared to the infected specimens ($p < 0.05$), while the concentrations of the essential metals Fe, Zn, and Cu were significantly lower in non-infected fish than in infected specimens. However, for both infected and non-infected fish, there was a substantial ($p < 0.05$) increase in non-essential heavy metals in lake fish compared to farmed fish. Similarly, for both infected and non-infected groups, organs of lake and farmed Nile tilapia had the same sequence of essential and non-essential metals: Fe > Zn > Pb > Cu > As > Cd (**Table 7**).

Table 8 revealed that the Pearson correlation had a strong positive correlation ($p < 0.05$) for Fe-Zn, Fe-Pb, Fe-Cu, Zn-Pb, Zn-Cu, and Pb-Cu. However, As and Cd showed no significant correlation with the remaining examined elements in infected and non-infected groups of farmed fish. In contrast, in lake fish, there was a substantial positive correlation ($p < 0.05$) between Fe-Zn, Fe-Pb, and Zn-Pb, as well as a non-significant correlation between the other analyzed metals.

Bioaccumulation Factors of Heavy Metals in Fish Organs

BAF of heavy metals in organs of lake and farmed Nile Tilapia are shown in **Figures 4**, **5**. BAF was evaluated from water to fish and in

TABLE 5 | Parasites species isolated from farmed and wild fish, *O. niloticus.*

Phylum	Family	Species	Farmed fish	Wild fish
Trematoda	*Dactylogyridae*	*Cichlidogyrus tilapiae*	a	b
	Ancyrocephalidae	*Enterogyrus cichlidarum*	c	c
	Heterophyidae	*Centrocestus formosanus*	a	b
		Heterphyes sp	a	c
		Pygidiopsis genata	c	b
	Diplostomatidae	*Diplostomum tilapiae*	a	b
	Cyanodiplostomatide	*Cyanodiplostomum sp*	a	b
	Opisthorchiidae	*Opisthorchis* sp	a	c
	Cyathocotylidae	*Prohemistomum sp*	a	b
Cestoda	*Ptychobothriidae*	Procercoid and pleurocercoid stage of *Polyonchobothrium clarias*	c	b
Nematoda	*Camallanidae*	*Procamallanus sp*	c	b
		Paracamallanus sp	c	
Acanthocephalan	*Quadrogyridae*	*Acanthosentis tilapiae*	a	b

[a] *Max. mean for intensity of infection.*
[b] *Min,*
[c] *medium*

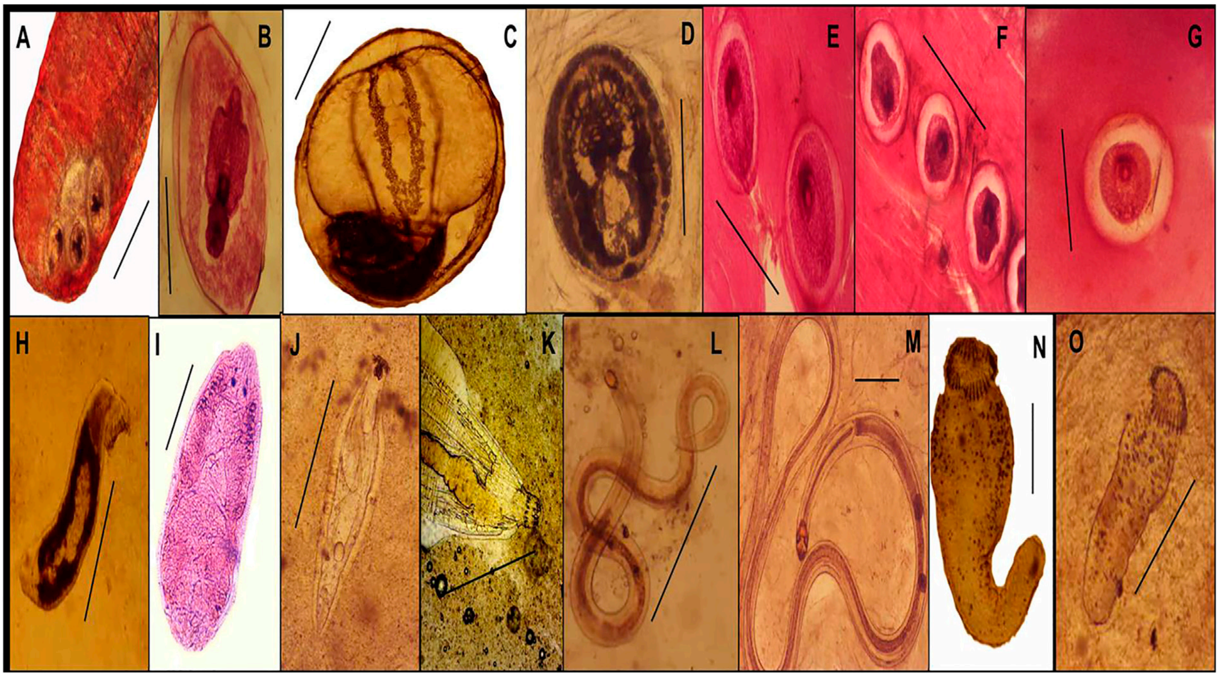

FIGURE 3 | Encysted metacercariae (EMC) of identified infected fishes (Scale bar = 50 μm). **(A)**: *Centrocestus formosanus*. **(B)**: *Diplostomum tilapiae* stained with acetic acid alum carmine. **(C)**: *Opisthorchis sp*. **(D)**: *Cyanodiplostomum sp*. **(E)**: *Prohemistomum* sp. stained with acetic acid alum carmine **(F)**: *Pygidiopsis genata* stained with acetic acid alum carmine **(G)**: *Heterphyes* sp. stained with acetic acid alum carmine **(H–O)**. Helminth parasites identified in infected fish (Scale bar = 0.5 mm). **(H)**: *Cichlidogyrus tilapiae*. **(I)**: *Enterogyrus cichlidarum,* stained with acetic acid alum carmine **(J)**: *Acanthosentis tilapiae.* **(K)**: anterior part of *A. tilapiae.* **(L)**: *Procamallanus* sp. **(M)**: *Paracamallanus* sp. **(N,O)**: Procercoid and pleurocercoid stage of *Polyonchobothrium clarias.*

various organs of lake and farmed fish with increasing order of metal ions according to BAF Liver > BAF Gills > BAF Intestine > BAF Muscles. However, BAF in infected organs of lake and farmed fish was lower when compared to non-infected fish. In the infected and non-infected organs of lake fish, the highest accumulation factor was detected for Cd, while the lowest factor was observed for Cu. On the other hand, the intestine, liver, and gills of farmed fish organs accumulated the majority of Cd from the water, whereas Zn had the lowest accumulation factor. Fe was accumulated in the muscles to the maximum extent in farmed fish.

Human Health Assessment

Table 9 reports the estimated daily intake (EDI, mg/kg/day) and target hazard quotients (THQ) for trace metals in the muscles of

TABLE 6 | Pearson correlation coefficients between water quality and water-heavy metals with parasites prevalence of *O. niloticus*, collected from Fish Farm and Burullus Lake.

Parasites prevalence	Fish farm	Burullus lake
Water quality		
pH	–0.59[a]	–0.49
Turbidity (%)	0.75	0.77
TDS (mg/L)	–0.33	–0.42
Ammonia (mg/L)	–0.48	–0.43
NO2 (mg/L)	0.58	0.89
NO3 (mg/L)	0.69	0.94
Total alkalinity (mg/L)	0.65	0.55
Total hardness (mg/L)	–0.65	–0.56
Phosphate (mg/L)	0.67	0.65
H2S (mg/L)	–0.34	–0.22
Dissolved Oxygen (mg/L)	–0.66	–0.58
Water heavy metals		
Fe (ppm)	0.20	0.14
Zn (ppm)	–0.96	–0.97
Pb (ppm)	–0.69	–0.58
Cu (ppm)	0.89	0.84
AS (ppm)	–0.56	–0.59
Cd (ppm)	–0.19	–0.28

[a] *Correlation is significant at the 0.05 level (2-tailed).*
[b] *Correlation is significant at the 0.01 level (2-tailed).*

lake and farmed fish. Children's EDI in farmed *O. niloticus* muscles varied from 5 × 10^{-6} to 2 × 10^{-3} mg/kg/day, while adults' EDI ranged from 9 × 10^{-6} to 3 × 10^{-3} mg/kg/day. In lake fish, however, EDI varied from 8 × 10^{-5} to 1 × 10^{-2} mg/kg/day for children, and from 4 × 10^{-5} to 3 × 10^{-2} mg/kg/day for adults. Furthermore, the THQ in this investigation was all lower than 1, indicating that eating lake and farmed fish had no negative health consequences for both age groups. **Figure 6** shows the hazard index (HI) for heavy metals in the muscles of lake and farmed fish. The HI values determined for this study were all lower than 1, indicating that lake and farmed fish intake is safe. In both groups examined, lake fish had higher HI values than farmed fish. For both children and adults, it was greater in lake fish than in farmed fish. Furthermore, for both children and adults, it was greater in non-infected muscles than in infected muscles.

DISCUSSION

Water Quality and Fish Parasites Relationship

Water quality is an essential factor in the growth of healthy fish. Therefore, the risk of infections is linked to the water's sanitary conditions as well as to the overall fish health (Ojwala et al., 2018). The values of pH in this study were neutral, even though the optimal pH range for freshwater fish was between 6.5 and 7.0. Also, a pH range of 6.1–8.0 was deemed adequate for fish reproduction and survival (Makori et al., 2017). According to the results from Soltan et al. (2016), reduced water transparency can be linked to a higher abundance of phytoplankton, but in lakes, it is possible that it can be due to untreated wastewater (Negm et al., 2017). Total ammonia was also found to be higher in fish farms than in lakes, which might be due to large fish stocks, fish excretion, and the breakdown of extra un-consumed diet, all of which are ammonia sources in ponds. These findings corroborate previous research (Konsowa, 2007; Radwan et al., 2021; Radwan, 2022).

The elevated level of dissolved oxygen concentration (DO) detected in the farm water might be related to the abundance and distribution of phytoplankton, which promotes photosynthesis, resulting in the creation of a huge quantity of DO (El-Nemaki et al., 2008). This is consistent with other observations by Soltan et al. (2016). On the other hand, a depletion in DO concentrations might be owing to a higher usage rate caused by biological processes and high temperature (Radwan, 2005; Goheret al., 2015; El Sayed et al., 2020). Dissolved oxygen and pH, on the other hand, displayed a strong negative relation with the Parasites Prevalence (PP) in lake and farmed Nile Tilapia. This observation agrees with Zargar et al. (2012) and Radwan et al. (2021) who observed strong negative relationships between parasite presence frequency and pH and DO concentrations. Meanwhile, these findings contradict the findings of Sosanya (2002) who found a positive relationship between water contaminants and parasite prevalence rates. Furthermore, H_2S is very hazardous to fish. Boyd (1985) indicated a safe H_2S concentration for freshwater fish of 0.002 mg/L. The correlation coefficient of physico-chemical elements with parasite prevalence in this study implies that the measured factors have an influence on the PP (Wali et al., 2016; Qayoom and Shah, 2017; Radwan et al., 2021). Turbidity, total alkalinity, NO_2, NO_3, and phosphate were shown to be substantially related to PP (Abba et al., 2018; Ojwala et al., 2018).

Length-Weight Relationship

The present study showed that the values of "b" of infected fishes were significantly lower than "3" which indicates a negative allometric growth, i.e., the fish grows but it is slender (Bagenal and Tesch, 1978). Negative allometric growth is an indication of slow growth, which might be due to the non-availability of food or weakened immune status (Veeramani et al., 2010; Ndeda et al., 2013). On the other hand, the variation of growth patterns may be due to ecological parameters through periods of study, which include several biotic and abiotic interactions contingent on seasonality (Ngodhe and Owuor-JB, 2019). In contrast, parasites are also known to act as stressors on their hosts and then cause altered growth in their hosts (Froese, 2006; Kahraman et al., 2014).

Parasitological Outcomes

Parasite prevalence (PP) was found to be higher in farmed fish than in lake Nile Tilapia in the current investigation. This may be attributed to stoking density of fish at farms and feeding habits, which depend mainly on artificial feed and other natural aquatic pollutants (Enyidi and Eneje, 2015). Parasites prevalence may also be related to increased fish numbers in culture systems and variations in physico-chemical variables related to a larger density of fish in the cultivated site than in the lake (Violante-González

TABLE 7 | Heavy metal concentrations in different organs of lake and farmed *O. niloticus*. Different superscript letters in the same column and metal are significantly different (T-test, $p < 0.05$). While results from the same row and origin with different alphabetic letters are statistically different (ANOVA, $p < 0.05$).

Hm	Fish status	Fish origin							
		Farmed fish				Lake fish			
		Liver	Gills	Intestine	Muscles	Liver	Gills	Intestine	Muscles
		Essential heavy metals							
Cu	Non-infected fish	0.98 ± 0.01^{aA}	0.81 ± 0.17^{bA}	0.68 ± 0.06^{cA}	0.38 ± 0.15^{dA}	0.41 ± 0.05^{aA}	0.40 ± 0.01^{bA}	0.23 ± 0.07^{cA}	0.17 ± 0.01^{dA}
	Infected fish	0.92 ± 0.11^{aB}	0.77 ± 0.12^{bB}	0.63 ± 0.09^{cB}	0.29 ± 0.22^{dB}	0.35 ± 0.03^{aB}	0.34 ± 0.04^{bB}	0.19 ± 0.03^{cB}	0.12 ± 0.01^{dB}
Zn	Non-infected fish	5.52 ± 0.24^{aA}	4.50 ± 0.62^{bA}	3.62 ± 0.06^{cA}	3.41 ± 0.91^{dA}	4.75 ± 0.85^{aA}	3.73 ± 0.47^{bA}	2.89 ± 0.15^{cA}	2.67 ± 0.28^{dA}
	Infected fish	5.30 ± 0.30^{aB}	4.34 ± 0.99^{bB}	3.49 ± 0.41^{cB}	3.29 ± 0.77^{dB}	4.66 ± 0.83^{aB}	3.57 ± 0.20^{bB}	2.75 ± 0.40^{cB}	2.55 ± 0.31^{dB}
Fe	Non-infected fish	29.10 ± 2.18^{aA}	22.73 ± 1.33^{bA}	17.41 ± 2.07^{cA}	11.28 ± 1.08^{dA}	27.49 ± 2.32^{aA}	21.52 ± 2.50^{bA}	15.19 ± 1.96^{cA}	9.03 ± 0.96^{dA}
	Infected fish	28.21 ± 1.15^{aB}	21.77 ± 1.57^{bB}	17.10 ± 0.57^{cB}	9.89 ± 0.49^{dB}	26.60 ± 1.00^{aB}	20.79 ± 0.75^{bB}	15.06 ± 0.69^{cB}	7.64 ± 0.58^{dB}
		Non-essential heavy metals							
Pb	Non-infected fish	3.58 ± 0.35^{aA}	2.76 ± 0.32^{bA}	1.55 ± 0.15^{cA}	0.24 ± 0.17^{dA}	4.37 ± 0.35^{aA}	3.48 ± 0.32^{bA}	2.36 ± 0.15^{cA}	0.62 ± 0.05^{dA}
	Infected fish	3.36 ± 0.32^{aB}	2.58 ± 0.05^{bB}	1.33 ± 0.19^{cB}	0.20 ± 0.20^{dB}	3.48 ± 0.35^{aB}	2.72 ± 0.05^{bB}	2.07 ± 0.04^{cB}	0.55 ± 0.06^{dB}
As	Non-infected fish	0.58 ± 0.06^{aA}	0.45 ± 0.05^{bA}	0.43 ± 0.10^{cA}	0.23 ± 0.10^{dA}	1.02 ± 0.05^{aA}	0.86 ± 0.20^{bA}	0.84 ± 0.05^{cA}	0.73 ± 0.06^{dA}
	Infected fish	0.52 ± 0.04^{aB}	0.44 ± 0.05^{bB}	0.39 ± 0.04^{cB}	0.15 ± 0.07^{dB}	1.01 ± 0.10^{aB}	0.81 ± 0.14^{bB}	0.79 ± 0.06^{cB}	0.61 ± 0.07^{dB}
Cd	Non-infected fish	0.41 ± 0.05^{aA}	0.36 ± 0.06^{bA}	0.21 ± 0.03^{cA}	0.04 ± 0.01^{dA}	0.81 ± 0.06^{aA}	0.65 ± 0.05^{bA}	0.49 ± 0.10^{cA}	0.20 ± 0.05^{dA}
	Infected fish	0.39 ± 0.06^{aB}	0.30 ± 0.06^{bB}	0.18 ± 0.03^{cB}	0.03 ± 0.01^{dB}	0.77 ± 0.04^{aB}	0.64 ± 0.12^{bB}	0.44 ± 0.06^{cB}	0.17 ± 0.05^{dB}

$^{a,\ b}$Results at $p < 0.05$, results from the same row with different alphabets small letters are statistically different.

Different superscript capital letters in the same column and metal are significantly different Q29 (T-test, $p < 0.05$). While results from the same row and origin with different alphabetic small letters are statistically different (ANOVA, $p < 0.05$).

et al., 2009; Ibrahim and Soliman, 2010). This research also revealed that trematodes have been the most common source of parasite infection in fish populations. This finding might be due to fish skin that may be more sensitive to infective parasite stages penetration and the detritus and benthic invertebrates consumed by this fish at different periods. Nile Tilapia is considered an intermediate host which is suitable for many parasite phases when favorable physico-chemical properties are present (El-Shahawy et al., 2017; Shehata et al., 2018; Radwan, 2022).

Assay of Heavy Meals in Water and Fish Tissues

Heavy metals concentrations are essential indicators of fish health and the aquatic environment (Padrilah et al., 2018). Heavy metals estimated levels (Fe, Zn, Pb, Cu, and As) in the water of Burullus Lake and fish farm were within the standard allowed values except for Pb, which exceeded the maximum permitted levels (WHO, 2011), as a result of contamination by industrial effluents and municipal sewage concentrations that might be blamed (Chen et al., 2010; Nafea and Zyada, 2015). Moreover, HM levels in the current study's findings (Burullus Lake and Farmed fish waters) are still within the range of prior examinations, except for Zn, Cu, and Pb, which were greater in both analyzed locations than in past studies (Younes and Nafea, 2012; Ghabour et al., 2013; El-Batrawy et al., 2018; Melegy et al., 2019). The following is the order of the metals: $Fe < Zn < Pb < Cu < As < Cd$ as reported in other studies (Darwish, 2016; El Morshedy, 2017; El-Batrawy et al., 2018).

Metal levels (Fe, Zn, Cu, As, Cd, and Pb) in the non-infected lake and farmed Nile Tilapia were significantly higher than in the infected fish. This may be due to parasites accumulating high levels of metal in their tissues, thereby acting as metal sinks for their fish host and helping in their survival in the presence of

TABLE 8 | Pearson correlations between heavy metal concentrations of lake and farmed in *O. niloticus.*

	Farmed fish						Lake fish					
	Fe	**Zn**	**Pb**	**Cu**	**As**	**Cd**	**Fe**	**Zn**	**Pb**	**Cu**	**As**	**Cd**
Non- Infected fish												
Fe	1						1					
Zn	0.82^{a}	1					0.80^{a}	1				
Pb	0.86^{a}	0.78^{a}	1				0.83^{a}	0.77^{a}	1			
Cu	0.87^{a}	0.82^{a}	0.86^{a}	1			0.53	0.38	0.52	1		
As	0.53	0.22	0.54	0.51	1		0.37	0.18	0.44	0.13	1	
Cd	0.36	0.21	0.42	0.43	0.47	1	0.63^{b}	0.65^{b}	0.67^{b}	0.62^{b}	0.77^{b}	1
Infected fish												
Fe	1						1					
Zn	0.74^{a}	1					0.85^{a}	1				
Pb	0.97^{a}	0.75^{a}	1				0.97^{a}	0.82^{a}	1			
Cu	0.85^{a}	0.73^{a}	0.88^{a}	1			0.50	0.47	0.38	1		
As	0.38	0.23	0.46	0.37	1		0.34	0.28	0.36	0.29	1	
Cd	0.35	0.08	0.32	0.43	0.32	1	0.84^{a}	0.78^{a}	0.86^{a}	0.62^{b}	0.62^{b}	1
Prevalence	-0.97^{b}	-0.93^{b}	-0.97^{b}	−0.61	−0.63	−0.52	-0.92^{b}	-0.94^{b}	-0.95^{b}	−0.59	−0.56	−0.57

aCorrelation is significant at the 0.01 level (2-tailed)

bCorrelation is significant at the 0.05 level (2-tailed)

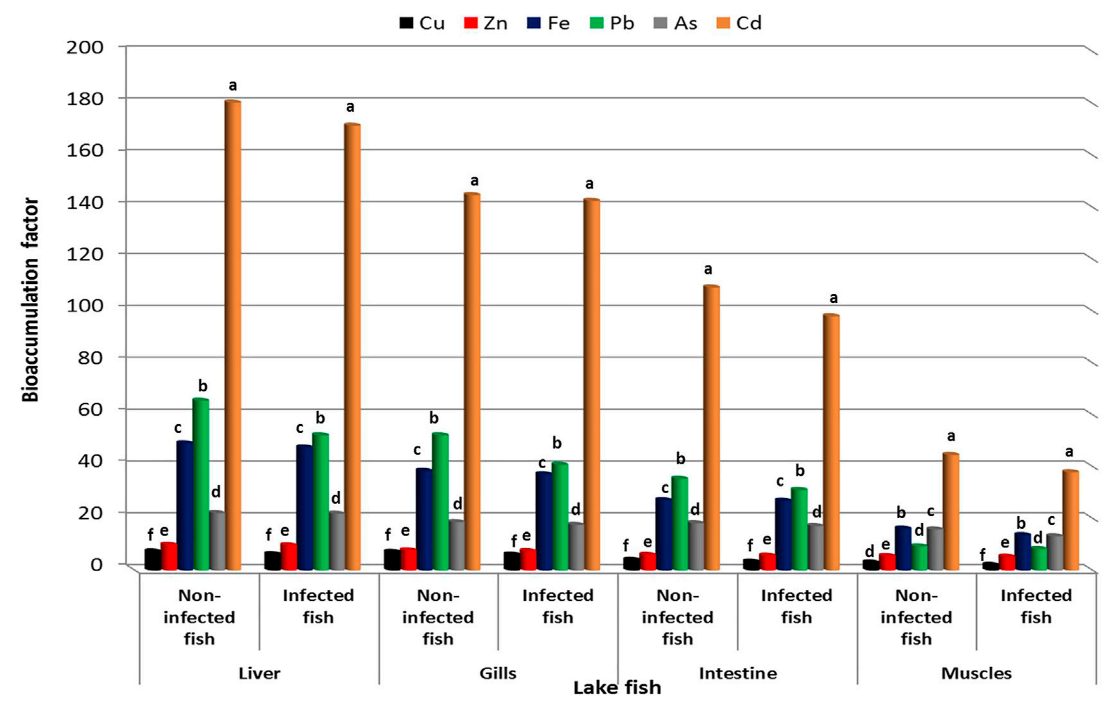

FIGURE 4 | Bioaccumulation factor of heavy metals in different organs of lake Nile Tilapia, *O. niloticus*.

toxins. These observations agree with Sures (2007), Azmat et al. (2008), and Eissa et al. (2012). Furthermore, infected fish had decreased concentration of some heavy metals, which included Cu, Fe, Pb, and Zn, according to some studies (Oyoo-Okoth et al., 2010; Dural et al., 2011). This result is supported by Shahat et al. (2011) who observed that parasitic-infected organs had lower amounts of Cu, Cd, and Pb than non-infected fish. Similarly, gastrointestinal parasitic worms appeared capable to decrease levels of heavy metals in fish muscle by accumulating them (Al-Hasawi, 2019; Mehana et al., 2020).

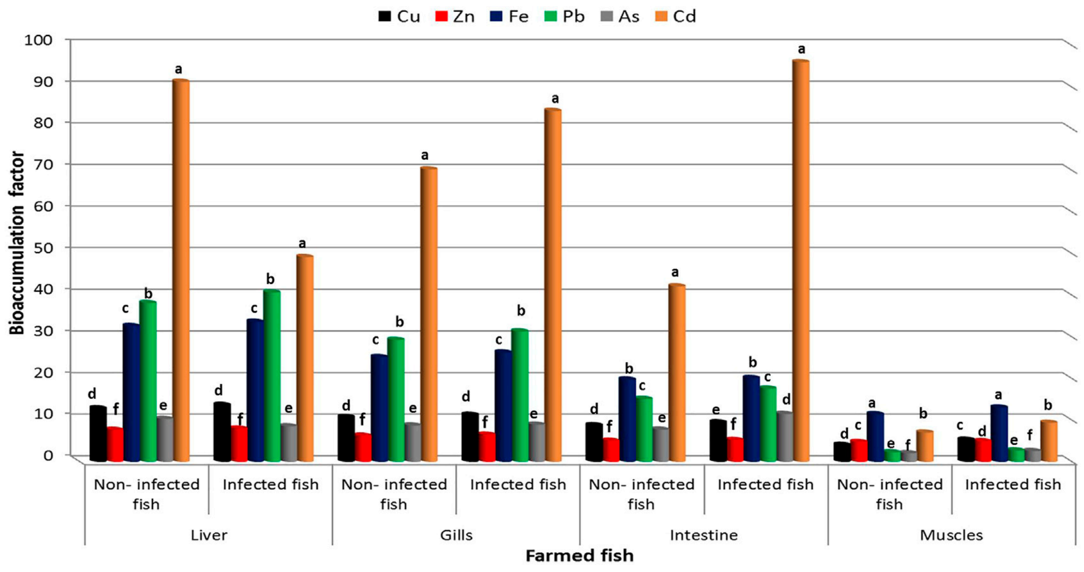

FIGURE 5 | Bioaccumulation factor of heavy metals in different organs of farmed Nile Tilapia, *O. niloticus*.

TABLE 9 | Estimated daily intake (EDI, mg/kg/day) and target hazard quotients (THQ) for HMs in muscles of farmed and lake *O. niloticus*.

HRA-heavy metals	**Fish origin**								
	Farmed fish				**Lake fish**				
	EDI		**THQ**		**EDI (mg/kg/day)**		**THQ**		
	Children	**Adults**	**Children**	**Adults**	**Children**	**Adults**	**Children**	**Adults**	**HM PTDI**
Non-infected fish									
Cu	6×10^{-5}	1×10^{-4}	3×10^{-5}	5×10^{-5}	1.4×10^{-2}	2.7×10^{-2}	6.4×10^{-3}	1.2×10^{-2}	35
Zn	5×10^{-4}	1×10^{-3}	4×10^{-4}	8×10^{-4}	2×10^{-3}	3×10^{-3}	1.3×10^{-3}	2.6×10^{-3}	70
Fe	2×10^{-3}	3×10^{-3}	1.4×10^{-3}	3×10^{-3}	2×10^{-3}	5×10^{-3}	1.9×10^{-3}	3.7×10^{-3}	50
As	4×10^{-5}	7×10^{-5}	9×10^{-5}	2×10^{-4}	1×10^{-2}	2×10^{-2}	2.67×10^{-2}	5.09×10^{-2}	0.14
Cd	3×10^{-5}	7×10^{-5}	1×10^{-4}	2×10^{-4}	1×10^{-4}	2×10^{-4}	4×10^{-4}	7×10^{-4}	0.07
Pb	6×10^{-6}	1×10^{-5}	3×10^{-5}	6×10^{-5}	6×10^{-3}	1.1×10^{-2}	3.02×10^{-2}	5.74×10^{-2}	0.25
Infected fish									HM ORDs
Cu	4×10^{-5}	8×10^{-5}	2×10^{-5}	3×10^{-5}	1.1×10^{-2}	2.1×10^{-2}	4.5×10^{-3}	8.6×10^{-3}	0.04
Zn	5×10^{-4}	9×10^{-4}	4×10^{-4}	7×10^{-4}	2×10^{-3}	3×10^{-3}	1.3×10^{-3}	2.4×10^{-3}	0.30
Fe	1×10^{-3}	3×10^{-3}	1×10^{-3}	2×10^{-3}	2×10^{-3}	4×10^{-3}	1.6×10^{-3}	3.1×10^{-3}	0.70
As	3×10^{-5}	6×10^{-5}	8×10^{-5}	2×10^{-4}	9×10^{-3}	1.6×10^{-2}	2.36×10^{-2}	4.51×10^{-2}	0.003
Cd	2×10^{-5}	4×10^{-5}	9×10^{-5}	2×10^{-4}	8×10^{-5}	1×10^{-4}	3×10^{-4}	6×10^{-4}	0.001
Pb	5×10^{-6}	9×10^{-6}	3×10^{-5}	5×10^{-5}	5×10^{-3}	9×10^{-3}	2.56×10^{-2}	4.88×10^{-2}	0.0036

Cu, Zn, and Pb concentrations were found to be higher in Burullus Lake compared to previous studies, while Cd and Fe were decreased (Shakweer and Radwan, 2004; Radwan 2005; Saeed and Shaker, 2008; Masoud et al., 2011; Basiony, 2014; El-Alfy, 2015; El-Batrawy et al., 2018). However, in the fish farm, Cu, Zn, As and Pb concentrations were higher compared to the previous studies (Radwan 2005; Masoud et al., 2011; Basiony, 2014; El-Alfy, 2015; El-Batrawy et al., 2018), while Cd and Fe concentrations were lower compared to previous studies (Shakweer and Radwan, 2004; Saeed and Shaker, 2008).

The level of heavy metals concentration in fish tissues is influenced by various factors such as water quality, fish species, and maturity stage (Łuczy´nska and Paszczyk, 2019). The non-essential heavy metals such as As, Cd, and Pb were much higher than the levels recommended by USEPA (2010) and FAO (2016), which may be caused by the increase in human activities in the lake or fish farms. On the other hand, Yildiz, (2008), Fallah et al. (2011), Kim et al. (2018), and Simukoko et al. (2022) reported that a diet that contains animal protein ingredients has a much higher level of heavy metals, especially of the essential heavy metals such as Zn, Fe, and Cu.

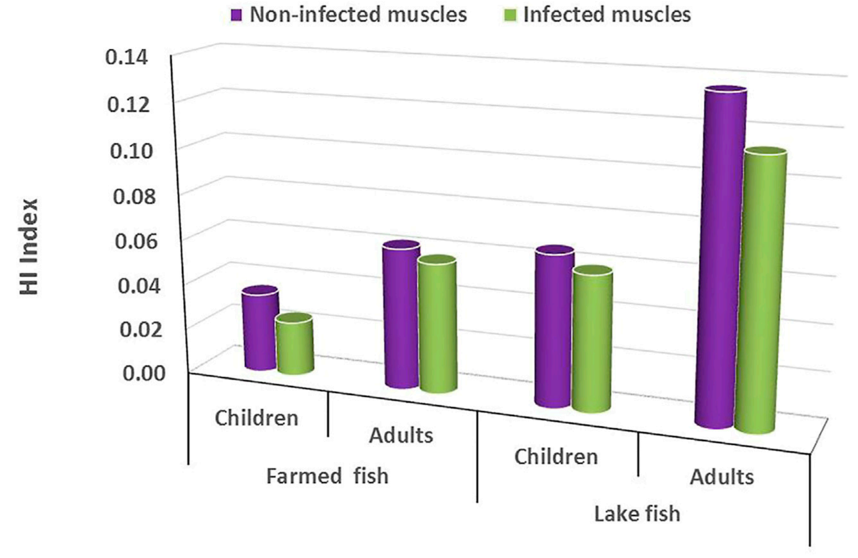

FIGURE 6 | Hazard index (HI) for heavy metals in the muscles of lake and farmed Nile Tilapia, *O. niloticus*.

Non-essential heavy metal levels (As, Cd, and Pb) in cultivated Nile Tilapia were much lower than in lake fish, maybe due to the fact that lake fish live for several years while cultivated fish are caught within 6 months (Oumar et al., 2018). When compared to cultivated Nile Tilapia and lake fish, Nile Tilapia can absorb contaminants with long biological half-lives, such as, Cd, and Pb, throughout a long lifespan. These findings agree with Chatta et al. (2016), who reported that the farmed *Cirrhinus mrigala* and *Labeo rohita* accumulated less Cd and Pb than the lake ones. Lake fish also had higher levels of non-essential heavy metals due to a longer lifetime and exposure, but they also had reduced levels of essential metals because they were not fed a commercial diet (Simukoko et al., 2022).

Bioaccumulation Factor of HM Levels in Fish Tissues

The bioaccumulation (BAF) of heavy metal levels in fish tissues is the percentage of heavy metal levels in tissues to their levels in the aquatic environment (Hatem et al., 2015). In the current study, gill, muscles, liver, and intestine tissues presented a strong probability of heavy metal bioaccumulation in fish. All gill and liver samples had a high BAF value, whereas the muscle and intestine presented lower values. This revealed that the heavy metals were accumulating in fish tissues after being absorbed from the water. The BAF in the current study revealed that the heavy metal levels in the analyzed tissues were in the following order: liver > gills > intestines > muscles, as already reported in a previous study (Maurya et al., 2019). Active metabolic tissues, such as the kidneys, gills, and liver, accumulate more heavy metals than less metabolically active tissues, such as the muscles and skin (Ali et al., 2019). Generally, muscles store the lowest amount of heavy metals (Ronagh et al., 2009). These results are nearly similar to those reported by Badr et al. (2014), who concluded that the level of heavy metals in Nile Tilapia tissues were higher in the liver than in gills and muscle.

In general, the current study found that the tissues of lake and cultivated Nile Tilapia contained more iron (Fe) than every heavy metal tested, with cadmium (Cd) being the lowest, and concentrations of heavy metals were in the sequence Fe > Zn > Pb > Cu > As > Cd. The increase in Fe accumulation in fish tissue in all tested organs was greater than the increase of other metals. This might be related to an increase in the total dissolved Fe in water of fish farms and lakes, with a consequent increase in free metal Fe levels and hence metal absorption by various organs. These results are supported by Tayel et al. (2008) and Al-Halani et al. (2021), who determined that the heavy metal concentration in lake fish tissues, *Dicentrarchus labrax*, occurred in the following order: Fe > Zn > Mn > Cu > Pb > Ni > Cr > Cd.

Human Health Risk Assessment

Humans consume large amounts of fish, and fish muscles are a good source of protein. As a result, determining the human daily consumption of heavy metals from fish is important (Rajeshkumar and Li, 2018). The daily intake of metal through the consumption of commercially relevant fish species by people who eat a normal quantity of fish on a regular basis corresponds to a hazard index (HI) of 1.0, as suggested by USEPA (2018).

To explain the safe levels of heavy metals, the average daily intake was utilized (Keshavarzi et al., 2018). The oral reference dose (ORD) is an oral reference dosage established on the basis of worldwide and Egyptian fish consumption and daily exposure levels. This research focused on the estimated daily intake (EDI) (mg/kg/day). Target hazard quotient (THQ) and HI were used to determine the levels of heavy metals in the muscles of farmed and lake Nile Tilapia. EDI levels in cultivated Nile Tilapia muscles ranged from 1×10^{-5} to 0.193 mg/kg/day. On the other hand, the lake fish had a range of 2×10^{-4} to 0.024 mg/kg/day. The EDI distribution against the examined heavy metals was arranged in the following order: Cd > As > Cu > Pb > Zn > Fe. The measured EDI of both groups was compared to the

FAO/WHO (2004). Similarly, for permissible tolerable daily intake (PTDI), which is the acceptable tolerable daily intake for 70 kg weight, it was determined that the metals' mean EDI levels have to be lower than the PTDI values (FAO, 2016).

The THQ values estimate— for this study were all lower than one, indicating that eating cultivated and lake Nile Tilapia will not harm people. According to Lei et al. (2015), if the HI value is lower than one (HI1), the impacts on humans would be unfavorable, HI > 1 would most likely have a negative impact, and HI > 10 would have strong or chronic acute consequences.

Human health risk assessment due to exposure to heavy metals through farmed and lake Nile Tilapia consumption revealed no significant non-carcinogenic adverse health risk to humans, as all calculated values for THQ and HI were lower than 1, indicating that the analyzed fish would not cause any health problems in both children and adults.

CONCLUSION

Generally, all studied metals in the water were found to be lower than the permissible limits, except for Pb. HM levels were significantly lower in infected than in non-infected Nile tilapia. HM levels in lake and farmed Nile tilapia tissues in the area of study were mostly recognized by the legislation of national and international limits for not determining human risk upon their consumption. THQ and HI values calculated for HMs levels of lake and farmed Nile tilapia predicted for adults and children were below the threshold level of 1. Parasites are capable to decrease concentrations of heavy metals in the tissues of fish by accumulating them. Also, they are a possible application as early warning indicators of heavy metal pollution in fish. Fish farmers lacked knowledge of diseases that affect fish and the importance of water quality in disease transmission. Heavy metal levels in fish tissue and water must be continuously monitored not just for human health but also to inform aquaculture management. In addition, employing the EDI, THQ, and HI indices to estimate human health risk is a highly recommended method.

DATA AVAILABILITY STATEMENT

The raw data supporting the conclusion of this article will be made available by the authors, without undue reservation.

ETHICS STATEMENT

All applicable international, national, and/or institutional guidelines for the care and use of fish were followed by the authors.

AUTHOR CONTRIBUTIONS

MR. Conceptualization, formal analysis, investigation, methodology, validation, writing—original draft writing—review, and editing. MA. Conceptualization, formal analysis, investigation, methodology, validation, writing. MM. The investigation, methodology, validation, writing—original draft. Finally, all authors have read and approved the manuscript. AM: Formal analysis, Methodology, Conceptualization, Editing. JA: Formal analysis, Methodology, Visualization, Editing.

FUNDING

This research was funded by The Taif University researchers, supporting project number (TURSP-2020/299), Taif University, Taif, Saudi Arabia.

ACKNOWLEDGMENTS

The authors would like to thank the Deanship of Scientific Research, Taif University for the financial support. The authors would also like to thank the research staff of the departments of Zoology, Al-Azhar University for the scientific guidance.

REFERENCES

Abah, J., Mashebe, P., and Onjefu, S. (2016). Preliminary Assessment of Some Heavy Metals Pollution Status of Lisikili River Water in Zambezi Region, Namibia. *Int. J. Environ. Pollut. Res.* 4, 13–30.

Abba, A. M., Abdulkarim, B., Omenesa, R. L., Abdulhamid, Y., and Mudassir, I. (2018). Study on Physico-Chemical Parameters and Prevalence of Fish Parasites in Jibia Reservoir Katsina State Nigeria. *UMYU J. Microbiol. Res.* 3 (2), 1–6.

Abbas, M. M. M., Shehata, S. M., Talab, A. S., and Mohamed, M. H. (2021). Effect of Traditional Processing Methods on the Cultivated Fish Species, Egypt. Part I. Mineral and Heavy Metal Concentrations. *Biol. Trace Elem. Res.* 200, 2391–2405. doi:10.1007/s12011-021-02840-w

Abdel-hakim, N. F., Helal, A., Salem, M., Zaghloul, M., and Hanbal, M. (2016). Effect of Some Heavy Metals on Physiological and Chemical Parameters in Nile tilapia (*Oreochromis niloticus* L.). *J. Egypt. Acad. Soc. Environ. Dev. D, Environ. Stud.* 17, 81–95. doi:10.21608/jades.2016.63382

Adolfsson-Erici, M., Åkerman, G., and Mclachlan, M. S. (2012). Measuring Bioconcentration Factors in Fish Using Exposure to Multiple Chemicals and Internal Benchmarking to Correct for Growth Dilution. *Environ. Toxicol. Chem.* 31, 1853–1860. doi:10.1002/etc.1897

Ahmed, N. F., Sadek, K. M., Soliman, M. K., Khalil, R. H., Khafaga, A. F., Ajarem, J. S., et al. (2020). Moringa Oleifera Leaf Extract Repairs the Oxidative Misbalance Following Sub-chronic Exposure to Sodium Fluoride in Nile tilapia *oreochromis Niloticus*. *Animals* 10, 626. doi:10.3390/ani10040626

Al-Halani et al., A. A., Soliman, A., and Shady, S. H. H. (2021). The Seasonal Assessment of Heavy Metals Bioaccumulation in European Seabass (*Dicentrarchus labrax*). *Egypt. J. Aqua. Biolo. Fish.* 25 (5), 607–626. doi:10.21608/ejabf.2021.205025

Al-Hasawi, Z. M. (2019). Environmental Parasitology: Intestinal Helminth Parasites of the Siganid Fish *Siganus Rivulatus* as Bioindicators for Trace Metal Pollution in the Red Sea. *Parasite* 26, 12. doi:10.1051/parasite/2019014

Ali, H., Khan, E., and Ilahi, I. (2019). Environmental Chemistry and Ecotoxicology of Hazardous Heavy Metals: Environmental Persistence, Toxicity, and Bioaccumulation. *J. Chem.* 2019, 1–14. doi:10.1155/2019/6730305

AOAC [Association of Official Analytical Chemists] (2012). *Official Methods of Analysis*. 15th ed. Washington, DC USA: Association of official analytical chemists Inc, 478.

APHA (2005). *Standard Methods for Examination of Water and Wastewater*. 21st. Edn. Washington DC, USA: American Public Health Association APHA, the American Water Works Association AWWA, and the Water Environment Federation WEF.

Authman, M. M. N., Abbas, W. T., and Gaafar, A. Y. (2012). Metals Concentrations in Nile tilapia *Oreochromis niloticus* (Linnaeus, 1758) from Illegal Fish Farm in Al-Minufiya Province, Egypt, and Their Effects on Some Tissues Structures. *Ecotoxicol. Environ. Saf.* 84, 163–172. doi:10.1016/j.ecoenv.2012.07.005

Azmat, R., Fayyaz, S., Kazi, N., Mahmood, S. J., and Uddin, F. (2008). Natural Bioremediation of Heavy Metals through Nematode Parasite of Fish. *Biotechnology* 7 (1), 139–143. doi:10.3923/biotech.2008.139.143

Badr, A. M., Mahana, N. A., and Eissa, A. (2014). Assessment of Heavy Metal Levels in Water and Their Toxicity in Some Tissues of Nile Tilapia (*Oreochromis niloticus*) in River Nile Basin at Greater Cairo, Egypt. *Glob. Veterinaria* 13 (4), 432–443. doi:10.5829/idosi.gv.2014.13.04.8561

Bagenal, T. B., and Tesch, F. W. (1978). "Age and Growth," in *Methods of Assessment of Fish Production in Fresh Waters*. Editor T. Bagenal (Oxford: Oxford Blackwell Scientific Publication), 101–136.

Basiony, A. I. (2014). *Environmental Studies on Heavy Metals Pollution and Management of Lake Burullus, Egypt*. M.Sc. Thesis. Port Said, Egypt: Faculty of science, Port Said University.

Boyd, C. E. (1985). Chemical Budgets for Channel Catfish Ponds. *Trans. Am. Fish. Soc.* 114, 291–298. doi:10.1577/1548-8659(1985)114<291:cbfccp>2.0.co;2

Chatta, A. M., Khan, M. N., Mirza, Z. S., Ali, A., and Ali, A. (2016). Heavy Metal (Cadmium, Lead, and Chromium) Contamination in Farmed Fish: a Potential Risk for Consumers' Health. *Turk. J. Zool.* 40, 248–256. doi:10.3906/zoo-1506-1

Chen, Z., Salem, A., Xu, Z., and Zhang, W. (2010). Ecological Implications of Heavy Metal Concentrations in the Sediments of Burullus Lagoon of Nile Delta, Egypt. Estuarine. *Estuar. Coast. Shelf Sci.* 86 (3), 491–498. doi:10.1016/j.ecss.2009.09.018

Cheng, T. (1973). *General Parasitology*. New York USA: Academic Press, 965.

Darwish, S. I. (2016). *Water Quality and Heavy Metals Pollution in Soil, Water and Fish in Lake Burullus*. Ph.D. Thesis. Alexandria: Faculty Of Agriculture Saba Basha- Alexandria University. Dep. of fish production.

David, L. H., Pinho, S. M., Agostinho, F., Kimpara, J. M., Keesman, K. J., and Garcia, F. (2021). Emergy Synthesis for Aquaculture: A Review on its Constraints and Potentials. *Rev. Aqua.* 13, 1119–1138. doi:10.1111/raq.12519

Dural, M., Genc, E., Sangun, M. K., and Güner, O. (2011). Accumulation of Some Heavy Metals in Hysterothylacium Aduncum (Nematoda) and its Host Sea Bream, Sparusaurata (Sparidae) from North-Eastern Mediterranean Sea (Iskenderun Bay). *Environ. Monit. Assess.* 174 (1–4), 147–155. doi:10.1007/s10661-010-1445-0

Eissa, I. A. M., Gehan, I. S., Wafeek, M., and Nashwa, A. S. (2012). Bioremediation for Heavy Metals in Some Red Sea Fishes in Suez, Egypt. *SCVMJ, XVII* 18 (2), 341–356.

El Morshedy, E. M. (2017). *Effect of Pollution on Water Quality, Soil and Fish Performance in Lakes and Fish Farm Ponds*. Ph.D. Thesis. Alexandria: Faculty Of Agriculture Saba Basha- Alexandria University. Dep. of fish production.

El Sayed, S. M., Hegab, M. H., Mola, H. R. A., Ahmed, N. M., and Goher, M. E. (2020). An Integrated Water Quality Assessment of Damietta and Rosetta Branches (Nile River, Egypt) Using Chemical and Biological Indices. *Environ. Monit. Assess.* 192, 228. doi:10.1007/s10661-020-8195-4

El-Alfy, M. A. (2015). *Comparative Ecological Studies on the Northern Deltaic Lakes Using Geographic Information system-Egypt*. Ph.D. Thesis. Mansoura: Faculty of science, Mansoura University.

El-Batrawy, O. A., El-Gammal, M. I., Mohamadein, L. I., Darwish, D. H., and El-Moselhy, K. M. (2018). Impact Assessment of Some Heavy Metals on tilapia Fish, *Oreochromis niloticus*, in Burullus Lake, Egypt. *J. Basic Appl. Zool.* 79, 13. doi:10.1186/s41936-018-0028-4

El-Nemaki, F. A., Ali, N. A., Zeinhom, M. M., and Radwan, O. A. (2008). "Impacts of Different Water Resources on the Ecological Parameters and Quality of tilapia Production at ElAbbassa Fish Farms in EGYPT," in Proceedings of the 8th International Symposium on Tilapia in Aquaculture.

El-Shahawy, I. S., El-Seify, M. O., Metwally, A. M., and Fwazi, M. M. (2017). Survey on Endoparasitic Fauna of Some Commercially Important Fishes of the River Nile, Southern of Egypt (Egypt). *Rev. Méd Vét* 168 (4-6), 126–134.

ElSheikha, H. M., and Elshazly, A. M. (2008). Host-dependent Variations in the Seasonal Prevalence and Intensity of Heterophyid Encysted Metacercariae (Digenea: Heterophyidea) in Brackish Water Fish in Egypt. *Vet. Parasitol.* 153, 65–72. doi:10.1016/j.vetpar.2008.01.026

Enyidi, U. D., and Eneje, U. I. (2015). Parasites of African Catfish *Clarias gariepinus* Cultured in Homestead Ponds. *Res. J. Agric.* 2 (12), 1–10.

Fallah, A. A., Saei-Dehkordi, S. S., Nematollahi, A., and Jafari, T. (2011). Comparative Study of Heavy Metal and Trace Element Accumulation in Edible Tissues of Farmed and Wild Rainbow Trout (*Oncorhynchus mykiss*) Using ICP-OES Technique. *Microchem. J.* 98, 275–279. doi:10.1016/j.microc.2011.02.007

FAO (2016). *Fishery Information Data and Statistics Unit. FISHSTAT, Databases and Statistics*. Rome, Italy: Food and Agriculture Orga,nization of the United Nation.

FAO/WHO (2004). "FAO/WHO Summary of Evaluations Performed by the Joint FAO/WHO Expert Committee on Food Additives (JECFA 1956e2003)," in *Evaluation of Certain Contaminants in Food: Sixty-Fourth Report of the Joint (2004)*.

Froese, R. (2006). Cube Law, Condition Factor and Weight-Length Relationships: History, Meta-Analysis and Recommendations. *J. Appl. Ichthyol.* 22 (4), 241–253. doi:10.1111/j.1439-0426.2006.00805.x

GAFRD (2019). "General Authority for Fish Resources Development," in *Fish Statistics Yearbook* (Cairo, Arab Republic of Egypt: Agriculture Ministry Press).

Ghabour, T. K., Rahim, I. S., and Morgan, R. S. (2013). Heavy Metals Status of Some Wetlands of Egypt. *J. Appl. Sci. Res.* 9 (7), 4345–4350.

Goher, M. E., Abdo, M. H., Mangood, A. H., and Hussein, M. M. (2015). Water Quality and Potential Health Risk Assessment for Consumption of *Oreochromis niloticus* from El-Bahr El-Pharaony Drain, Egypt. *Fresenius Environ. Bull.* 24 (11), 3590–3602.

Hassan, A., Moharram, S., and El Helaly, H. (2018). Role of Parasitic Helminths in Bioremediating Some Heavy Metal Accumulation in the Tissues of *Lethrinus Mahsena*. *Turk. J. Fish. Aquat. Sci.* 18, 435–443. doi:10.4194/1303-2712-v18_3_09

Hatem, A. J., Azim, B., Nguyen, B., Sylvain, G., and Zoppoli, C. S. (2015). Genomic Aberrations in Young and Elderly Breast Cancer Patients. *BMC Med.* 13, 266. doi:10.1186/s12916-015-0504-3

Henriksson, P. J. G., Dickson, M., Allah, A. N., Al-Kenawy, D., and Phillips, M. (2017). Benchmarking the Environmental Performance of Best Management Practice and Genetic Improvements in Egyptian Aquaculture Using Life Cycle Assessment. *Aquaculture* 468, 53–59. doi:10.1016/j.aquaculture.2016.09.051

Ibrahim, M. M., and Soliman, M. F. M. (2010). Prevalence and Site Preferences of Heterophyid Metacercariae in *Tilapia Zilli* from Ismalia Freshwater Canal, Egypt. *Parasite* 17 (3), 233–239. doi:10.1051/parasite/2010173233

Jiang, Z., Xu, N., Liu, B., Zhou, L., Wang, J., Wang, C., et al. (2018). Metal Concentrations and Risk Assessment in Water, Sediment and Economic Fish Species with Various Habitat Preferences and Trophic Guilds from Lake Caizi, Southeast China. *Ecotoxicol. Environ. Saf.* 157, 1–8. doi:10.1016/j.ecoenv.2018.03.078

Ju, Y.-R., Chen, C.-W., Chen, C.-F., Chuang, X.-Y., and Dong, C.-D. (2017). Assessment of Heavy Metals in Aquaculture Fishes Collected from Southwest Coast of Taiwan and Human Consumption Risk. *Int. Biodeterior. Biodegrad.* 124, 314–325. doi:10.1016/j.ibiod.2017.04.003

Kahraman, A., Göktürk, D., and Aydin, E. (2014). Length-Weight Relationships of Five Fish Species from the Sakarya River, Turkey. *Annu. Rev. Res. Biol.* 4 (15), 2476–2483. doi:10.9734/arrb/2014/7513

Keke, U. N., Arimoro, F. O., Ayanwale, A. V., and Aliyu, S. M. (2015). Physicochemical Parameters and Heavy Metals Content of Surface Water in Downstream Kaduna River, Zungeru, Niger State, Nigeria. *Appl. Sci. Res. J.* 3, 46–57.

Keshavarzi, B., Hassanaghaei, M., Moore, F., Rastegari Mehr, M., Soltanian, S., Lahijanzadeh, A. R., et al. (2018). Heavy Metal Contamination and Health Risk Assessment in Three Commercial Fish Species in the Persian Gulf. *Mar. Pollut. Bull.* 129, 245–252. doi:10.1016/j.marpolbul.2018.02.032

Kim, H.-T., Loftus, J. P., Mann, S., and Wakshlag, J. J. (2018). Evaluation of Arsenic, Cadmium, Lead and Mercury Contamination in Over-the-counter Available Dry Dog Foods with Different Animal Ingredients (Red Meat, Poultry, and Fish). *Front. Vet. Sci.* 5, 264. doi:10.3389/fvets.2018.00264

Konsowa, A. H. (2007). Ecological Studies on Fish Farms of El-Fayoum Depression. *E. J. Aquat. Res.* 33 (1), 290–299.

Lagler, K. F. (1956). *Fresh Water Fishery Biology*. 2nd Ed. Dubuque, Iowa: W.M.C. Brown Comp, 421.

Lei, M., Tie, B.-q., Song, Z.-g., Liao, B.-H., Lepo, J. E., and Huang, Y.-z. (2015). Heavy Metal Pollution and Potential Health Risk Assessment of White Rice Around Mine Areas in Hunan Province, China. *Food Sec.* 7 (1), 45–54. doi:10.1007/s12571-014-0414-9

Łuczy´nska, J., and Paszczyk, B. (2019). Health Risk Assessment of Heavy Metals and Lipid Quality Indexes in Freshwater Fish from Lakes of Warmia and Mazury Region, Poland. *Int. J. Environ. Res. Public Health* 16, 3780. doi:10.3390/ijerph16193780

Makori, A. J., Abuom, P. O., Kapiyo, R., Anyona, D. N., and Dida, G. O. (2017). Effects of Water Physico-Chemical Parameters on tilapia (*Oreochromis niloticus*) Growth in Earthen Ponds in Teso North Sub-County, Busia County. *Fish. Aquat. Sci.* 20, 30. doi:10.1186/s41240-017-0075-7

Mannzhi, M. P., Edokpayi, J. N., Durowoju, O. S., Gumbo, J., and Odiyo, J. O. (2021). Assessment of Selected Trace Metals in Fish Feeds, Pond Water and Edible Muscles of *Oreochromis mossambicus* and the Evaluation of Human Health Risk Associated with its Consumption in Vhembe District of Limpopo Province, South Africa. *Toxicol. Rep.* 8, 705–717. doi:10.1016/j.toxrep.2021.03.018

Marcogliese, D. J., and Pietrock, M. (2011). Combined Effects of Parasites and Contaminants on Animal Health: Parasites Do Matter. *Trends Parasitol.* 27 (27), 123–130. doi:10.1016/j.pt.2010.11.002

Masoud, M. S., Fahmy, M. A., Ali, A. E., and Mohamed, E. A. (2011). Heavy Metal Speciation and Their Accumulation in Sediments of Lake Burullus, Egypt. *Afr. J. Environ. Sci. Technol.* 5, 280–298.

Maurya, P. K., Malik, D. S., Yadav, K. K., Kumar, A., Kumar, S., and Kamyab, H. (2019). Bioaccumulation and Potential Sources of Heavy Metal Contamination in Fish Species in River Ganga Basin: Possible Human Health Risks Evaluation. *Toxicol. Rep.* 6 (6), 472–481. doi:10.1016/j.toxrep.2019.05.012

Mehana, E.-S. E., Khafaga, A. F., Elblehi, S. S., Abd El-Hack, M. E., Naiel, M. A. E., Bin-Jumah, M., et al. (2020). Biomonitoring of Heavy Metal Pollution Using Acanthocephalans Parasite in Ecosystem: an Updated Overview. *Animals* 10, 811. doi:10.3390/ani10050811

Melegy, A. A., El-Bady, M. S., and Metwally, H. I. (2019). Monitoring of the Changes in Potential Environmental Risk of Some Heavy Metals in Water and Sediments of Burullus Lake, Egypt. *Bull. Natl. Res. Cent.* 43, 143. doi:10.1186/s42269-019-0182-y

Mousa, M. A., Ibrahim, A. A. E., Hashem, A. M., and Khalil, N. A. (2015). The Effect of Water Quality on the Immunoreactivity of Stress-Response Cells and Gonadotropin-Secreting Cells in the Pituitary Gland of Nile tilapia, *Oreochromis niloticus. J. Exp. Zool.* 323, 146–159. doi:10.1002/jez.1901

Mwakalapa, E. B., Simukoko, C. K., Mmochi, A. J., Mdegela, R. H., Berg, V., Bjorge Müller, M. H., et al. (2019). HMs Levels in Cultivated and Wild Milkfish (*Chanos Chanos*) and Wild Mullet (*Mugil cephalus*) along the Coasts of Tanzania and Associated Health Risk for Humans and Fish. *Chemosphere* 224, 176–186. doi:10.1016/j.chemosphere.2019.02.063

Nafea, E. M. A., and Zyada, M. A. (2015). Biomonitoring of Heavy Metals Pollution in Lake Burrullas, Northern Delta, Egypt. *Afr. J. Environ. Sci. Technol.* 9 (1), 1–7. doi:10.5897/AJEST2014.1764

Ndeda, V. M., Aketch, B. O, and Onyango, D. M. (2013). Effect of Diplostomum Species on Length–Weight Relationship of Farmed Nile tilapia in Kibos Area, Kisumu City, Kenya. *Fish. Aquac. J*, 1–9.

Negm, A., Abdel-Aziz, T. M., Salem, M. N., and Yousef, W. (2017). "Morphology of the Nile River Due to a Flow Rate over the Maximum Current: Case Study Damietta Branch," in *The Nile River,*. Editor A. M. Negm (Springer International Publishing AG), 239–257. Hdb Env Chem. doi:10.1007/698_2017_3

Ngodhe, S. O., and Owuor-Jb, O. (2019). Assessment of Length-Weight Relationship and Condition Factor of Nile Tilapia (*Oreochromis Niloticus*) in Cage and Open Waters in Winam Gulf of L. Victoria, Kenya. *Ijesnr* 22 (3), 556088. doi:10.19080/ijesnr.2019.22.556088

Ojwala, R. A., Otachi, E. O., and Kitaka, N. K. (2018). Effect of Water Quality on the Parasite Assemblages Infecting Nile tilapia in Selected Fish Farms in Nakuru County, Kenya. *Parasitol. Res.* 117 (11), 3459–3471. doi:10.1007/s00436-018-6042-0

Oros, M., Scholz, T., Hanzelová, V., and Mackiewicz, J. S. (2010). Scolex Morphology of Monozoic Cestodes (Caryophyllidea) from the Palaearctic Region: A Useful Tool for Species Identification. *Folia Parasit.* 57, 37–46. doi:10.14411/fp.2010.006

Oumar, D., Flibert, G., Tidjani, A., Rirabe, N., Patcha, M., Bakary, T., et al. (2018). Risks Assessments of Heavy Metals Bioaccumulation in Water and tilapia Nilotica Fish from Maguite Island of Fitri Lake. *Curr. J. Appl. Sci. Technol.* 26, 1–9. doi:10.9734/cjast/2018/39384

Oyoo-Okoth, E., Admiraal, W., Osano, O., Hoitinga, L., and Kraak, M. H. S. (2010). Metal Specific Partitioning in a Parasite-Host Assemblage of the Cestode Ligula Intestinalis and the Cyprinid Fish Rastrineobola Argentea. *Sci. Total Environ.* 408 (7), 1557–1562. doi:10.1016/j.scitotenv.2009.11.054

Padrilah, S. N., Shukor, M. Y. A., Yasid, N. A., Ahmad, S. A., Sabullah, M. K., and Shamaan, N. A. (2018). Toxicity Effects of Fish Histopathology on Copper Accumulation. *Pertanika J. Trop. Agric. Sci.* 2018, 519–540.

Qayoom, I., and Shah, F. A. (2017). Parasitic Bioload in Schizothoracine Fishes of Kashmir Valley with Respect to the Tropic Status of Anchar Lake. *Res. J. Agric. Sci.* 8 (2), 364–369.

Radwan, A. M. (2005). Some Factors Affecting the Primary Production of Phytoplankton in Burullus Lake. *Egypt. J. Aquatic Res.* 31 (2), 72–88.

Radwan, M., Shehata, S., Abdelhadi, Y., Mohammed, R., Mohamed, M., and Magdy, M. (2021). Histopathological, Haematological and Biochemical Indices of *Clarias gariepinus* (Burchell, 1822) Parasitized by Endoparasitic Fauna in Fish Farm of the Northeastern Egypt. *Turkish J. Fish. Aquatic Sci.* 21, 465–478. doi:10.4194/1303-2712-v21_9_05

Radwan, M. (2022). Vital Economic Threat of Predatory Birds and Parasites to Cultivated Fishes in Egypt. *Aquaculture* 548, 737666. doi:10.1016/j.aquaculture.2021.737666

Rajeshkumar, S., and Li, X. (2018). Bioaccumulation of Heavy Metals in Fish Species from the Meiliang Bay, Taihu Lake, China. *Toxicol. Rep.* 5, 288–295. doi:10.1016/j.toxrep.2018.01.007

Resma, N. S., Meaze, A. K. M. M. H., Hossain, S., Khandaker, M. U., Kamal, M., and Deb, N. (2020). The Presence of Toxic Metals in Popular Farmed Fish Species and Estimation of Health Risks through Their Consumption. *Phys. Open* 5, 100052. doi:10.1016/j.physo.2020.100052

Ronagh, M. T., Savari, A., Papahn, F., and Hesni, M. A. (2009). Bioaccumulation of Heavy Metals in Euryglossa Orientalis from the Hendijan Seaport (Coastal of Persian Gulf). *J. Biol. Sci.* 9, 272–275. doi:10.3923/jbs.2009.272.275

Saeed, S. M., and Shaker, I. M. (2008). "Assessment of Heavy Metals Pollution in Water and Sediments and Their Effect on *Oreochromis niloticus* in the Northern Delta Lakes, Egypt," in Proceedings of the 8th International Symposium on Tilapia in Aquaculture, Cairo, 12-14 October 2008, 475–490.

Salam, M. A., Paul, S. C., Noor, S. N. B. M., Siddiqua, S. A., Aka, T. D., Wahab, R., et al. (2019). Contamination Profile of Heavy Metals in Marine Fish and Shellfish. *Glob. J. Environ. Sci. Manag.* 5, 225–236. doi:10.22034/gjesm.2019.02.08

Sardar, K., Shafaqat, A., Hameed, S., Afzal, S., Fatima, S., Shakoor, M. B., et al. (2013). Heavy Metals Contamination and what Are the Impacts on Living Organisms. *Greener J. Environ. Manag. Public Saf.* 2, 172–179. doi:10.15580/GJEMPS.2013.4.060413652

Shahat, M. A ., Amer, O. S. O., AbdAllah, A. T ., Abdelsater, N., and Moustafa, M. A. (2011). The Distribution of Certain Heavy Metals between Intestinal Parasites and Their Fish Hosts in the River Nile at Assuit Province, Egypt. *Egypt. J. Hosp. Med.* 43, 241–257. doi:10.21608/ejhm.2011.16783

Shakweer, L. M., and Radwan, A. M. (2004). Environmental and Fishery Investigations on Lake Burullus. 2, B. Rates of Trace Elements Accumulation in the Macrophytes and Fish at Lake Borollus. *Egypt. J. Aquat. Res.* 30, 99–120.

Shehata, S. M., Mohammed, R. A., Ghanem, M. H., Abdelhadi, Y. M., and Radwan, M. K. (2018). Impact of the Stresses Environmental Condition on the Prevalence of Parasite in Freshwater Aquaculture. *J. Fish. Sci.* 12 (2), 1–8. doi:10.21767/1307-234x.1000147

Simukoko, C. K., Mwakalapa, E. B., Bwalya, P., Muzandu, K., Berg, V., Mutoloki, S., et al. (2022). Assessment of HMs Levels in Wild and Cultivated tilapia (*Oreochromis niloticus*) on Lake Kariba, Zambia: Implications for Human and Fish Health. *Food Addit. Contam. Part A* 39 (1), 74–91. doi:10.1080/19440049.2021.1975830

Sohn, W.-M. (2009). Fish-borne Zoonotic Trematode Metacercariae in the Republic of Korea. *Korean J. Parasitol.* 47, S103–S113. doi:10.3347/kjp.2009.47.S.S103

Soltan, M., Hassaan, M., and Khattaby, A. (2016). Agricultural Drainage Water as a Source of Water for Fish Farming in Egypt. *Ecol. Evol. Biol.* 1 (3), 68–75. doi:10.11648/j.eeb.20160103.15

Sosanya, M. O. (2002). *Fish Parasite as Indicators of Environmental Quality*. M. Sc Thesis. Ibadan: University of Ibadan, 142.

Sures, B. (2007). Host-parasite Interactions from an Ecotoxicological Perspective. *Parassitologia* 49 (3), 173–176.

Tayel, S. I., Yacoub, A. M., and Mahmoud, S. A. (2008). Histopathological and Haematological Responses to Freshwater Pollution in the Nile Catfish *Clarias gariepinus*. *J. Egypt. Acad. Soc. Environ. Dev.* 9 (4), 43–60.

Tytła, M. (2019). Assessment of Heavy Metal Pollution and Potential Ecological Risk in Sewage Sludge from Municipal Wastewater Treatment Plant Located in the Most Industrialized Region in Poland - Case Study. *Int. J. Environ. Res. Public Health* 16, 2430–2516. doi:10.3390/ijerph16132430

USEPA (2010). *Lists of Contaminants and Their Maximum Contaminant Levels (MCLs)*. Washington, DC: USEPA.

USEPA (2011). *Risk Assessment Guidance for Superfund. Volume I: (Part A: Human Health Evaluation Manual; Part E, Supplemental Guidance for Dermal Risk Assessment; Part F, Supplemental Guidance for Inhalation Risk Assessment)*. Washington, DC: US Environmental Protection Agency.

USEPA (2018). *US EPA Regional Screening Levels (RSLs) (November 2018)*. Dataset- California open data. Available at: https://data.ca.gov/dataset/us-epa-regional-screening-levels-rsls-november-2018/resource/b66c9172-a61a-4131-997f- 01f45a473a08 (Accessed Jul 28, 2021).

USEPA, United States Environmental Protection Agency (2008). *Child-Specific Exposure Factors Handbook*. EPA/600/R-06/096F. Washington. District of Columbia: National Center for Environmental Assessment Office of Research and Development, 1–687. Available at: http://www.epa.gov/ncea.

Veeramani, T., Ravi, V., and Kesavan, K. (2010). Length-weight Relationship of Parrot Fish, Scarus Ghobban, (Forsskal 1775) from Nagapattinam, Southeast Coast of India. *Adv. Biol. Res.* 4 (3), 182–184. doi:10.1186/1752-0509-4-95

Violante-González, J., García-Varela, M., Rojas-Herrera, A., and Guerrero, S. G. (2009). Diplostomiasis in Cultured and Wild tilapia *Oreochromis niloticus* in Guerrero State, Mexico. *Parasitol. Res.* 105 (3), 803–807. doi:10.1007/s00436-009-1458-1

Wali, A., Balkhi, M.-u. H., Maqbool, R., Darzi, M. M., Shah, F. A., Bhat, F. A., et al. (2016). Distribution of Helminth Parasites in Intestines and Their Seasonal Rate of Infestation in Three Freshwater Fishes of Kashmir. *J. Parasitol. Res.* 2016, 1–16. doi:10.1155/2016/8901518

Wang, Q., Cheng, L., Liu, J., Li, Z., Xie, S., and De Silva, S. S. (2015). Freshwater Aquaculture in PR China: Trends and Prospects. *Rev. Aquacult.* 7, 283–302. doi:10.1111/raq.12086

WHO (2011). *Guidelines for Drinking-Water Quality*. 4th edn. Geneva, Switzerland: World Health Organization.

Yamaguti, S. (1963). *Systema Helminthum*, 5. New York and London: Acanthocephala Wiley Interscience.

Yildiz, M. (2008). Mineral Composition in Fillets of Sea Bass (*Dicentrarchus labrax*) and Sea Bream (*Sparus aurata*): A Comparison of Cultured and Wild Fish. *J. Appl. Ichthyol.* 24, 589–594. doi:10.1111/j.1439-0426.2008.01097.x

Younes, A. M., and Nafea, E. M. (2012). Impact of Environmental Conditions on the Biodiversity of Mediterranean Sea Lagoon, Burullus Protected Area, Egypt. *World Appl. Sci. J.* 19 (10), 1423–1430. doi:10.5829/idosi.wasj.2012.19.10.66110

Zargar, U. R., Yousuf, A. R., Chishti, M. Z., Ahmed, F., Bashir, H., and Ahmed, F. (2012). Effects of Water Quality and Trophic Status on Helminth Infections in the Cyprinid Fish, Schizothorax niger Heckel, 1838 from Three Lakes in the Kashmir Himalayas. *J. Helminthol.* 86 (01), 70–76. doi:10.1017/S0022149X11000071

Conflict of Interest: The authors declare that the research was conducted in the absence of any commercial or financial relationships that could be construed as a potential conflict of interest.

frontiers | Frontiers in Environmental Science

ORIGINAL RESEARCH
published: 18 July 2022
doi: 10.3389/fenvs.2022.876369

When the Eel Meets Dams: Larger Dams' Long-Term Impacts on *Anguilla anguilla* (L., 1758)

Cinzia Podda, Francesco Palmas, Antonio Pusceddu and Andrea Sabatini*

Department of Life and Environmental Sciences, University of Cagliari, Cagliari, Italy

Diadromous fish, like the European eel *Anguilla anguilla* (L., 1758), are highly threatened by dams that disrupt river connectivity, consequently impeding fish movements to reach feeding and spawning habitats. In this study, variation in eel occurrence between a historical period (1940–1970) and recent data (2016–2020) was assessed throughout the Sardinian rivers' network (more than 450 sites). Using Boosted Regression Trees (BRT) we investigated relationships between eel's occurrence and a set of spatial and temporal environmental variables including a set of dams' construction features for each period. An overall decrease by 65% of eel's occurrence was noticed during the ca. 80-years period under scrutiny. Considering a subset (105 and 88 sites for the historical and the recent period, respectively) characterized by the presence of larger dams (height >15 m), eel's occurrence dropped by 85%. Conversely, eel's occurrence dropped only by ca. 44% in dam-free sites. During the historical period, eel's occurrence was mostly affected by time since the initial habitat fragmentation, flow, distance to dams, connectivity, and dams' height. In the most recent period, eel's occurrence is mostly affected by dams' building year, dam-to-sea distance, and, again, dams' height. Results pinpoint that dams' construction features and the time from their construction have significant negative effects on eel's occurrence. Addition of future effective eel restoration practices, apart any other adverse environmental stressor, must consider dams' removal, wherever socially sustainable or alternatively, the modification of construction features of dams (like excessive height) and the addition of fish ladders.

Keywords: Diadromous species, European eel, freshwater ecosystems, damming, river fragmentation

Edited by:
Robert Ptacnik,
Wasser Cluster Lunz, Austria

Reviewed by:
Jeyaraj Antony Johnson,
Wildlife Institute of India, India
Maria Filomena Magalhães,
Faculty of Sciences, University of Lisbon, Portugal

****Correspondence:***
Cinzia Podda
cpodda@unica.it

Specialty section:
This article was submitted to Freshwater Science,
a section of the journal
Frontiers in Environmental Science

Received: *15 February 2022*
Accepted: *23 June 2022*
Published: *18 July 2022*

Citation:
Podda C, Palmas F, Pusceddu A and Sabatini A (2022) When the Eel Meets Dams: Larger Dams' Long-Term Impacts on Anguilla anguilla (L., 1758). Front. Environ. Sci. 10:876369. doi: 10.3389/fenvs.2022.876369

INTRODUCTION

Freshwaters are biodiversity hotspots with 13,000 fish species inhabiting rivers and lakes (Lévêque et al., 2008). Free-flowing rivers provide migration routes for aquatic and riparian species, allow the transportation of sediments and nutrients, enable groundwater recharge, and mitigate flooding (Poff et al., 1997; Tickner et al., 2020). At the same time, rivers are essential elements for biodiversity and humans' wellbeing (Addams et al., 2009; Russi et al., 2013). Rivers are among the most threatened ecosystems by anthropogenic disturbances (Vörösmarty et al., 2010) including a large variety of obstacles (e.g., dams and weirs, road crossings, hydroelectric power plants, water abstraction for irrigation, flood control systems for municipal water security) (Welcomme, 1995; Jungwirth et al., 2000; Nilsson et al., 2005). Dams' construction has seen an acceleration worldwide during 1950/1960s (Dynesius and Nilsson, 1994; Postel and Richter, 2003; MacGregor et al., 2009), and more than two thirds of larger rivers have been fragmented (Grill et al., 2015). At present, ca. 2.8 million dams are operating and roughly 3,700 major dams are being constructed or planned (Zarfl et al., 2015; Grill et al., 2019).

Environmental alterations caused by anthropogenic obstacles affect the natural hydrology and connectivity of stream networks, and their ability to transport sediments (Bednarek 2001; Fullerton et al., 2010; Grill et al., 2015; Rincón et al., 2017). Modifying the river flow (Grill et al., 2015), dams pose increasing threats to freshwater ecosystems and mobile biota, particularly fish (Arthington et al., 2016). These barriers play a role in the degradation of water quality (Chowdhury and Kipgen, 2013; Galipeau et al., 2013; Opperman et al., 2019; Barbarossa et al., 2020), cause variations in temperature and water flows (Poff et al., 1997; Richter et al., 2010; Opperman et al., 2017), impair biodiversity, and in particular impede migration, threat the spawning habitats and alter the natural gene flows (Silva et al., 2018; Wilkes et al., 2018; Birnie-Gauvin and Aarestrup, 2019), ultimately increasing the risk of extinction of fish (Lucas and Baras, 2001; Ding et al., 2018). In addition, to adequate habitat for spawning and development, fish require connectivity to migrate freely between different areas of the river and to lakes and to the sea. High connectivity between freshwater and marine habitats facilitates the exchange of matter, energy, and nutrients, with species contributing to the longitudinal transfer and supporting important ecosystem services (Holmlund and Hammer, 1999). For instance, anthropogenic intervention in river discharge result in reduced flushing up to unnaturally extended periods of estuary mouth closure and reduce the connectivity between freshwater habitats and the sea (Potter et al., 2010; Lloyd et al., 2012; Podda et al., 2020). In many estuarine systems, especially those with Mediterranean climate, sand bars are deposited during low flow periods at the river mouth, resulting in truncation of the connection between freshwater and marine habitats (Potter et al., 2010; Suari et al., 2019; Podda et al., 2020). These interruptions and the river flow alteration can have severe implications especially for diadromous species (Gillanders et al., 2003), like the European eel *Anguilla anguilla* (L., 1758). This diadromous species demonstrates high plasticity in habitat use (Daverat et al., 2006), and is currently exposed to numerous threats along the migratory routes in both marine and freshwater realms (Culurgioni et al., 2014, 2015; Bevacqua et al., 2015; Aalto et al., 2016; Baltazar-Soares et al., 2014; Dekker and Beaulaton, 2016; Drouineau et al., 2018; Podda et al., 2021). Because of these hazards, *A. anguilla* is progressively declining since the 1970s (ICES, 2021), and is currently classified as Critically Endangered (CR) (IUCN, 2014; Pike et al., 2020) and protected according to the European Council regulation 1100/2007 (EC, 2007).

One of the major threats to the European eel is the presence of large instream barriers restricting access to juveniles leaving the sea after recruitment (Dekker, 2003; Piper et al., 2013; Tamario et al., 2019). The more so as the natural recruitment is the only source of supply of the species (Pedersen and Rasmussen, 2016). Despite their extraordinary climb ability, only a minor proportion of eels can successfully overcome large dams (White and Knights, 1997). Furthermore, direct mortality and sublethal injuries can occur during obstacle passages because of impingements on hard structures, even in the absence of turbines (Bruijs and Durif, 2009). Moreover, increased costs of metabolic energy caused by obstacle passage may have a delayed impact on eel's migration success and fecundity (Van Ginneken and van den Thillart, 2000). Delays induced by dams can impair escapement, especially when the migration suitability window is limited (Verbiest et al., 2012; Drouineau et al., 2017).

In this study, the impacts of large dams on the occurrence of the European eel *A. anguilla* in the Sardinian hydrographic district (Central-Western Mediterranean) have been investigated considering how the pre and post dams' building can affect the long-term presence of eels. We studied relationships among current and historical occurrence of the European eel hypothesizing potential negative effects of a set of temporal, spatial, and dams' related descriptors using a multivariate approach.

MATERIALS AND METHODS

Study Area

Sardinia (Italy) is the second largest island in the Mediterranean (area = 24,106 km^2). Its hydrographic district coincides with the entire regional territory (**Figure 1**). The Sardinian hydrographic network is characterized by a reduced number of perennial rivers and the prevalence of intermittent streams (Palmas et al., 2022). Mediterranean climate is typically bi-seasonal with severe drought summer and rainy autumn/winter that determine irregular flow and strong seasonal hydrological fluctuations (Sabatini et al., 2011, 2018; Palmas et al., 2020; Podda et al., 2020). Average annual precipitations range from 500 to 900 mm (De Waele et al., 2010; Moccia et al., 2020). Artificial interruptions of longitudinal river continuity, like dams, strongly influence the annual hydrological cycle of these streams (Naselli-Flores and Luglié, 2014). An increasing construction of artificial barriers has been observed since the end of the 19th century to provide water for human use (Marchetto et al., 2009; Montaldo and Sarigu, 2017).

Eels' Data

Two datasets were collected in the frame of the monitoring program for the official Fish Inventory of the Sardinian region (VV.AA., 2022).

The point-to-point historical occurrence data available from 1940 (1940–1970, hereafter historical period), derive from scientific and informative publications of regional origin for a total of 238 sites (**Supplementary Table S1**), and were georeferenced in a Geographical Information System (GIS) through the Open-Source Software Quantum Gis 2.18.3 (QGIS) (http://www.qgis.org/).

Recent occurrence data (2016–2020; hereafter current period) were collected for 214 sites. Surveys were conducted mainly during the dry season using electrofishing (0-4 Ampere, 0-600 Volt) in habitats ranging from sea level to 1,262 m a.s.l. For comparisons, current data were then integrated into the GIS layer including historical data. Sites have been selected in proportion to the amplitude of the hydrographic basin and in order to have a historical continuity with the data deriving from the previous historical period allowing an appropriate spatial

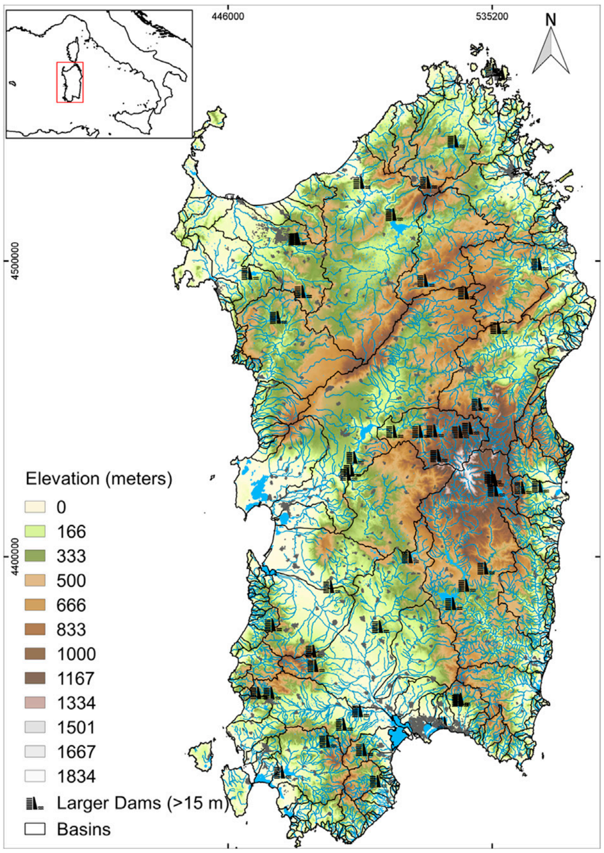

FIGURE 1 | Study area, location of rivers and larger dams (height >15 m) in the Sardinian hydrographic district.

coverage in relation to the extension of the whole hydrographic network of Sardinia (VV.AA., 2022).

Datasets were analyzed separately, and sites influenced by at least one downstream dam were identified. In each dataset, sites located on free-flow rivers or under dams have been analyzed separately from those located above dams.

Data Analysis

Twelve variables, ten continuous and two dummies, have been investigated as potential factors explaining the eel's occurrence related to dams' effects. The variables were subdivided into four categories: temporal, spatial, dams' features, and site-specific, respectively (**Table 1**). Geospatial information on dams were acquired from the Regional Land Information System of Sardinia (RAS, 2021).

Differences between the percentage of eel's occurrence during the historical and recent period were evaluated using the X^2 test (p-value < 0.05). Pairwise collinearity in explanatory variables was examined by scatter plots to exclude redundancy between paired variables disregarding combinations with Spearman's rho >0.7. Variables were discarded from the pairwise combination based on the Variance Inflation Factor (VIF) discarding observation with VIF > 3 (Zuur et al., 2010).

The set of dams' descriptors for the two datasets was fitted using Boosted Regression Tree models (BRT) (Friedman 2001; Elith et al., 2008). BRT is a machine-learning method for data exploration and analysis recently introduced into the fields of ecology and conservation biology (Déath, 2007; Elith et al., 2008). BRTs are suited to select the most relevant predictors from a large set of candidate variables, do not depend on the normality and homoscedasticity of the data, integrate nonlinear responses, and reduce the problem of 'overfitting' (Elith et al., 2008). BRTs allow to calculate multiple regression models (regression trees) and include an adaptive method to combine many simple models to give improbe predictive performance (boosting). Within the BRT model, terms that are used to optimize predictive performance are represented by the learning rate, tree complexity, and bagging factor (Friedman, 2001; Elith et al., 2008). BRTs were adjusted with a learning rate to return an optimal number of regression trees (1,000–1,500), which has been associated with data overfitting. Trees' complexity of two refers to the number of nodes in a tree that has been selected (Elith et al., 2008). We use tree complexity to control the number of nodes, to set the maximum number of interactions between predictor variables that are possible, and we used a bagging factor of 0.5 (Friedman, 2001). Variable selection is not necessary for constructing BRTs because they generally ignore non-informative predictors (Elith et al., 2008). The BRT analysis was conducted using the Bernoulli family of occurrence. For visualizing the results, we calculated the partial dependencies that depict the relationships between the response and each predictor variable while controlling for the average effects of the remaining predictors (Friedman, 2001; Friedman and Meulman, 2003).

Our approach did not allow to assess confidence intervals for BRTs, used when a large number of BRT sub-models are fitted. The partial dependence plots for parameters with a contribution >10% were used to visualize the effect of each variable on eel's occurrence. As this method does not deliver p-values, but uses internal validation processes, BTRs performance were evaluated using the amount of total deviance explained (%) and cross-validated correlation between model prediction and observed data (CV correlation) (Derville et al., 2016; Nieto and Mélin, 2017; Ju et al., 2021; Saha et al., 2021). Statistical analyses were conducted using the open-source R software (R Core Team, 2021). Specifically, *gbm* (Greenwell et al., 2020), and *dismo* (Hijmans et al., 2011) packages for BRT analyses, and partial dependence plots with smoothing for each variable.

RESULTS

Dams in the Sardinian Hydrographic District

Although the first dam in Sardinia date back to the end of the 19th century, a rapid increase in dams' construction has been observed from the late 1960s to the late 1990s (**Figure 2A**). More than 50% of the 54 larger dams (>15 m height, mean height ± Standard Deviation—SD, 42.5 ± 22.3 m) were built between 1940 and 1960 (**Figure 2B**), with two of the most recent dams not completely built yet. Furthermore, Sardinia is currently

TABLE 1 | Description of the investigated variables.

Variable Name (ABBREVIATION)	Description	Type	Unit
Year of fragmentation (FRAGMENTATION)	Number of years since dam construction compared to sampling year or the year of construction of the oldest dam in cases with multiple dams	Temporal	
Year of dam building (YEAR)	Year of construction of the nearest dam downstream the site	Temporal	
Height (HEIGHT)	Dam height	Dam feature	m
Volume (VOL)	Dam volume	Dam feature	m^3
Flow (FLOW)	Dam flow	Dam feature	m^{3s-1}
Elevation (ELEV)	Elevation above sea level	Dam feature	m
Distance of the dam from the site (D_STA)	The distance of the dam from the site	Spatial	km
Distance of the dam from the sea (D_SEA)	The distance of the dam from the sea	Spatial	km
Dendritic Connectivity Index (DCI) (Cote et al., 2009)	Proxy of the fragmentation of the longitudinal river connectivity caused by dams in relation to the presence of eels. DCI = 100 l L^{-1} where l is the current length of the river from the sea to the first barrier without fish passage, and L is the maximum historical eel migration distance for each site	Spatial	%
Number of dams (DAM)	Number of downstream dams in each site	Site-specific	1 or 2 in the historical dataset From 1 to 6 in the current dataset
River mouth condition (MOUTH)		Site-specific	0 = closed, for rivers which don't flow into a lagoon 1 = open, rivers which flow into a lagoon
Fishing pressure (FISH)	Presence of fishing pressure along the river to its river mouth, (http://www.sardegnaagricoltura.it)	Site-specific	0 = absence of fishing activities 1 = presence of fishing activities

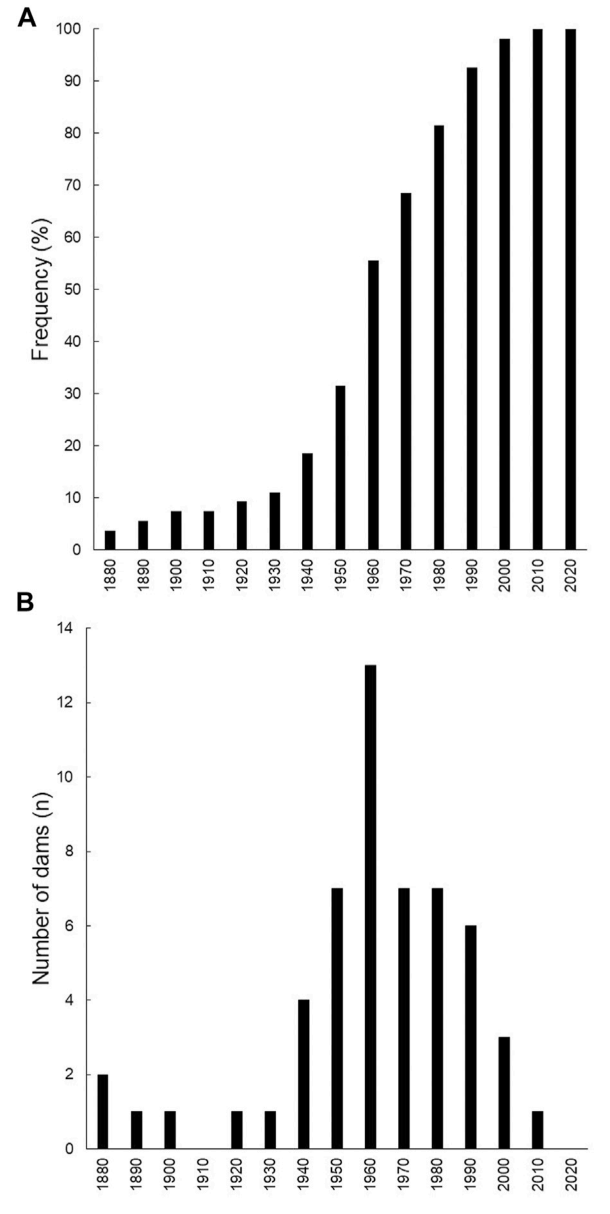

FIGURE 2 | (A) Cumulative frequency in dam building in Sardinia (%). **(B)** Number of dams in Sardinia.

lacking river flow regulations, and fishways or fish ladders are mainly absent or not working with one single exception (i.e., Casteldoria dam, height = 26.6 m, 40°53.3843 N–08°53.7534 E, recently built, 2015).

Eel's Occurrence in Sardinian Rivers

Comparing sites correspondence (one observation per site for each dataset) between the historical and the current datasets, a total of 54 sites matched (23% and 25% of number of sites, respectively). The analysis of the historical period (1940–1970) revealed that eel's occurrence amounted of ca. 95% (**Figure 3A**). In the current period (2016–2020) we observed a strong contraction (ca. 65%, X^2, $p < 0.001$) of eel's occurrence, which decreased to only 30% (**Figure 3B**).

Considering only sites with downstream dams (88 and 105 sites for the historical and current period, respectively), eel's occurrence dropped from 92% to 7% respectively, with a total (statistically significant) decrease of ca. 85% (X^2, $p < 0.001$). In this subset, the proportion of sites influenced by downstream dams was ca. 37% and 49% for the two periods, respectively.

During the historical period, 96% of free flow sites (i.e., sites without dams or sites without downstream dams) had eels, whereas in the current period this value dropped to 52%, with a decreasing rate between the two periods of ca. 44% (X^2, $p < 0.001$).

Effect of Larger Dams on Eel's Occurrence

After analyzing dams' descriptors through Spearman correlation (**Supplementary Figures S1, S2**) and using VIF score >3 as a threshold (**Supplementary Tables S2, S3**), only eight descriptors were included for the modeling of the data from the historical period, and seven for the current one. Five descriptors were common between the datasets: dendritic connectivity index (DCI), height (HEIGHT) and flow (FLOW) of dams, river mouth condition (MOUTH), and fishing pressure (FISH). The predictors in the modeling of the historical period also included the temporal fragmentation (FRAGMENTATION), the distance of dams from each site (D_STA) and the dams' elevation (ELEV), while the year of dams' building (YEAR) and the distance of dams from the sea (D_SEA) were included in the modeling of the current period.

The historical BRT model shows that five descriptors cumulatively explain 88.4% of the model: FRAGMENTATION (relative contribution = 22.3%), FLOW (22.2%), D_STA (14.7%), DCI (14.6%), HEIGHT (14.6%). Explained deviance (51%) and CV correlation (0.40) suggest that the relationships between dams' characteristics and the eel's occurrence are quite robust. The partial dependence plots obtained after BRT models (**Figure 4**) show that the contribution of FRAGMENTATION to eel's occurrence is greatest 20 years after dams' building. The difference across that threshold is very narrow, with a value of 91% and 94% occurrence, below and above downstream dams, respectively. The contribution of FLOW to eel's occurrence is maximum over a threshold of ca. 1,300 m^3s^{-1}, with a value of 87% below and 100% above the threshold. The highest effect of D_STA is observed more than 5 km far from dams, where mean eel's occurrence is 75%, whereas at closer sites this value is 96%. The HEIGHT effect was highest above ca. 60 m, where eel's occurrence (100%) was higher than that (90%) in sites with downstream dams <60 m height. The index of river connectivity (DCI) has the highest effect on eel's occurrence within the interval of 60%–80% DCI with mean eel's occurrence of 86% below 60% of DCI, and 100% above this threshold.

The BRT model for the most recent period reveals that three descriptors, YEAR (54.6% of relative contribution), D_SEA (21.3%), and HEIGHT (13.4%), explain cumulatively 91% of the model. There is well goodness of fit of the BRT with an explained deviance of 62% and a CV correlation of 0.67. The partial dependence plots obtained after BRT models (**Figure 5**) show that the effect of dams' age is highest (25%) after 1980 (i.e., dams with less than ca. 40 years) and drops to 2% in more

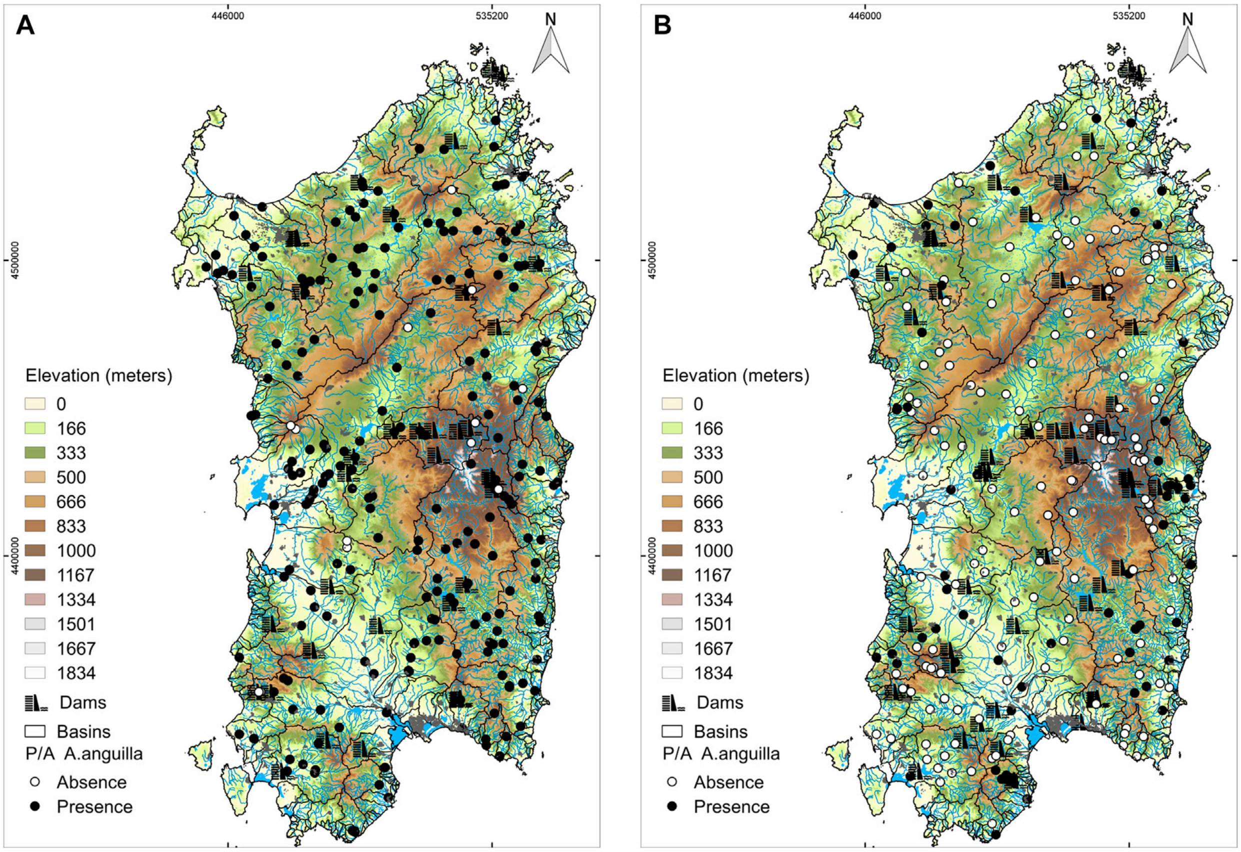

FIGURE 3 | (A) Historical European eel's occurrence (1940–1970). **(B)** Current European eel's occurrence (2016–2020)

recent years. The contribution of D_SEA to eel's occurrence is highest below 20 km, with the highest mean occurrence (13%) in sites close to the sea and the lowest (2%) in the farthest ones. The highest contribution of HEIGHT is observed for dams between 30 and 80 m, which have a mean eel's occurrence of 5%. In sites with dams <30 m occurrence is 10%, whereas in sites with dams >80 m (some of which are still not completed) the mean eel's occurrence is 7%.

DISCUSSION

Impacts of Large Dams on Eel's Occurrence

A. anguilla is worldwide ranked as critically endangered species due to an ample array of often synergistic, anthropogenic threats (Jacoby et al., 2015; Miller et al., 2016; Drouineau et al., 2018). Moreover, the presence of dams, causing a physical interruption of river connectivity, river flow reduction or modification, and loss and deterioration of habitats, may also critically affect eel's survival during their freshwater life stage (Feunteun, 2002; Tamario et al., 2019; Watz et al., 2019).

The dramatic decline of the European eel's recruitment reported worldwide (Dekker, 2003, 2004; ICES, 2021) also affects the Sardinian rivers' network, where we observed a huge decrease in eel's occurrence. Indeed, considering only free-flow sites (i.e., sites in dam-free rivers or sites without downstream dams), the European eel occupied most of the main Sardinian rivers until the 1970s (ca. 95%). The overall 44% reduction in species' occurrence between the two periods in these sites suggests that a relevant proportion of such a decline is independent by dams. Nevertheless, the decline of eel's occurrence in Sardinian rivers is also severely affected by damming with eel's occurrence in sites above dams dropping by 85% between the two periods. Our results, ultimately, confirm that dams have a severe impact on eels due to the fragmentation of migration habitats and the alteration of river flow (Poff and Schmidt, 2016; Dias et al., 2017).

We hypothesized that dams' height (Larinier, 2001; Merg et al., 2020), dams' age (Atkinson et al., 2020) and the decreased river flow due to the oldest dams (Legault et al., 2003) could negatively affect eel's migration.

In both periods under scrutiny, as expected, the height of dams could have had a negative effect on eel's occurrence and such an impact was lower during the old period but severely exacerbated in recent years. In the most recent period, the eel's occurrence above dams >80 m high is, counterintuitively, higher than that in lower dams. This apparent discrepancy can be ascribed to the fact that especially some of the very tall dams (>80 m) were built only very recently, thus the presence of eels above the dam stems from times before the dam was finalized or filled. For catadromous fish,

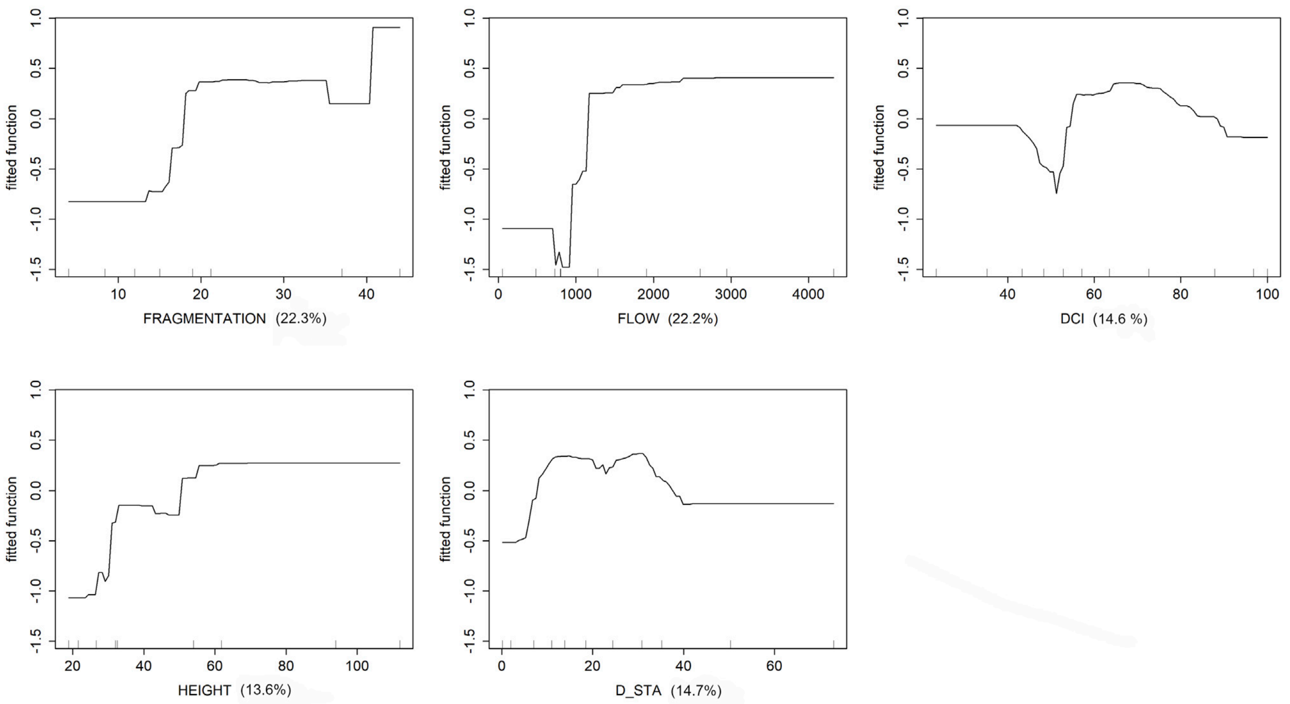

FIGURE 4 | Partial dependence plots of the five variables (FRAGMENTATION, FLOW, D_STA, DCI, and HEIGHT) affecting eels 'occurrence in Sardinian rivers during the historical period (1940–70). The relative contribution of each variable is reported within parenthesis. Black lines refer to the raw model output.

including eels, climbing out of the water to surpass a barrier is challenging and linked to high metabolic costs (Edeline et al., 2004; Briand et al., 2005; Bult and Dekker 2007).

The age of the dams (estimated using either year of construction–in the most recent period—or temporal fragmentation—in the old one) negatively influence eel's occurrence. We contend that the oldest dams installed in Sardinia, possibly due to technical and financial limitations, have been built in rivers of lower order or in the upper part of the rivers, thus having a minor negative effect on the overall river connectivity (Segurado et al., 2013). In the most recent period, the strongest impact of fragmentation by dams could be attributable to the technological progress and modernization that allowed building dams with more effective water retention and, thus, the stronger capacity of interrupting the river flow in more downstream river sections (Haidvogl, 2018; Merg et al., 2020). Nevertheless, the effect of river flow is a major factor influencing eel's occurrence only in the old period. The minimum or nihil effect of river flow and the DCI index on eel's occurrence in the most recent period could be attributable to the very low river flow in the last 30 years, caused by prolonged drought, which, most probably impaired eels' ability to migrate upstream. The negative effect of dams appears more evident during the old period, when either river flow or the DCI index explains significant proportions of eel's occurrence variations. The major role of river flow and the DCI index, in the old period only, and their ininfluence in the most recent one, is corroborated by the intensity of water flow involved in the route choice (Legault et al., 2003), causing the silencing of environmental stimuli when it is too low (Trancart et al., 2018, 2020) and, in the most extreme cases, interrupting downstream (Durif, 2003) and upstream migration (Podda et al., 2020).

In both periods, the distance from the sea explains significant proportions of eel's occurrence. The more distant from the sea the more probable is the presence of natural (and artificial) obstacles to be crossed by fish (Merg et al., 2020), which, indeed, becomes a severe impediment to migration, especially when river connectivity is limited due to low river flow.

Giving Future to the European Eel

Our study reveals that different dams' attributes can explain the current decline of *A. anguilla*. Along with damming, other factors, associated with excessive human pressure but also with climate change, are severely impairing eel's occurrence. To foster the conservation of the European eel, many authors have pushed to mitigate its commercial exploitation (Nielsen and Prouzet, 2008; Henderson et al., 2011; Aalto et al., 2016; ICES, 2021). In addition, we contend that a strong effort should be paid to eliminate highly impacting artificial barriers or, at least, to mitigate their impacts with more sustainable actions, tools, and devices. While creating unobstructed migration routes between the spawning area in the sea and freshwater growth habitats could be preferable (Feunteun, 2002; Drouineau et al., 2018; Rodeles et al., 2021), the removal of artificial barriers could be, locally, socially, and economically impracticable. Some attempts have been made and succeeded with other catadromous endangered species (Graf, 2003; Stanley and Doyle, 2003; Harris et al., 2016), including the American eel

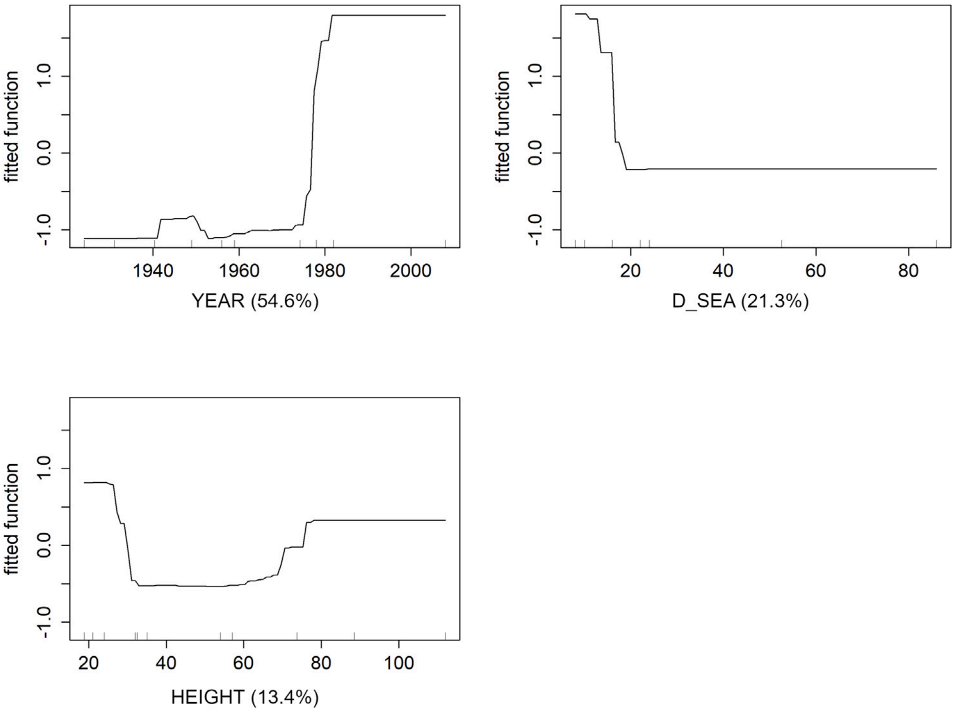

FIGURE 5 | Partial dependence plots of the three variables (YEAR, D_SEA, and HEIGHT) affecting eels 'occurrence in Sardinian rivers during the recent period (2016–20). The relative contribution of each variable is reported within parenthesis. Black lines refer to the raw model output.

Anguilla rostrata (Lesueur, 1817) (Hitt et al., 2012; Turner et al., 2018). The removal of artificial barriers could be not exempt from collateral negative effects, including, for instance, the facilitation of biological invasions (Rahel, 2013; Milt et al., 2018), the spill of toxic sediments, and sudden changes in hydromorphology (Stanley and Doyle, 2003; Gangloff, 2013).

Except these general suggestions, in our context it could be crucial to control and reducing the uptake of water for human use above dams and, at the same time, ensuring a Minimum Vital Flow (MVF; Moccia et al., 2020) that guarantees the morphological, hydrological, physical-chemical, and biological integrity downstream will enable the protection of eel's habitats in the short and long term (Dudgeon et al., 2006). A potentially compensative solution for partial restoration of dammed river connectivity, without eliminating dams, could also profit of the construction of artificial fishways to allow eels' passage beyond dams (Seliger and Zeiringer, 2018), management measures both still lacking in Sardinia. Moreover, it would be advisable that any management, operation, and maintenance of large dams in Sardinia would be implemented within a regional control system aimed at harmonizing and standardizing information to support a correct use and management of these structures. Although this study was conducted on a purely regional scale, our results highlighted the major impact of dams on the European eel's occurrence in Sardinian rivers and its apparent worsening in the last 10 years. We conclude that, based on the general current crisis of this species, urgent actions are needed worldwide to restore their habitats by reducing humans' pressure, ensuring a minimum vital flow, abating, wherever possible, artificial barriers to river connectivity, or, at least, implementing natural migration routes with artificial fishways.

DATA AVAILABILITY STATEMENT

The raw data supporting the conclusions of this article will be made available by the authors, without undue reservation.

AUTHOR CONTRIBUTIONS

CP led conceptualization, field sampling, data curation, software realization, statistical analysis, formal writing, and original draft. FP conducted field sampling, software realization, writing, review, and editing. AP contributed for the supervision, writing, review, and editing. AS led the project administration, supervision, writing, review, and editing.

FUNDING

This study has been carried out in the context of the agreements: "Rep. RAS n. 27002–1 A.D.A. of 18.12.2015 and Rep. RAS n. 7304–12 A.D.A. of 29.03.2018," Sardinian Regional Government. CP gratefully acknowledges Sardinian Regional Government for the financial support of her PhD scholarship (P.O.R. Sardegna F.S.E.—Operational Program of the Autonomous Region of Sardinia, European Social Fund 2014–2020—Axis III Education and training, Thematic goal 10, Investment Priority 10ii), Specific goal 10.5.

REFERENCES

Aalto, E., Capoccioni, F., Terradez Mas, J., Schiavina, M., Leone, C., De Leo, G., et al. (2016). Quantifying 60 Years of Declining European Eel (*Anguilla anguilla* L., 1758) Fishery Yields in Mediterranean Coastal Lagoons. *ICES J. Mar. Sci.* 73, 101–110. doi:10.1093/icesjms/fsv084

Addams, L., Boccaletti, G., Kerlin, M., and Stuchtey, M. (2009). *Charting OurWater Future. Economic Frameworks to Inform Decision-Making.* https://www.mckinsey.com/~/media/mckinsey/dotcom/client_service/sustainability/pdfs/charting%20our%20water%20future/charting_our_water_future_full_report_.ashx.

Arthington, A. H., Dulvy, N. K., Gladstone, W., and Winfield, I. J. (2016). Fish Conservation in Freshwater and Marine Realms: Status, Threats and Management. *Aquat. Conserv. Mar. Freshw. Ecosyst.* 26, 838–857. doi:10.1002/aqc.2712

Atkinson, S., Bruen, M., O' Sullivan, J. J., Turner, J. N., Ball, B., Carlsson, J., et al. (2020). An Inspection-Based Assessment of Obstacles to Salmon, Trout, Eel and Lamprey Migration and River Channel Connectivity in Ireland. *Sci. Total Environ.* 719, 137215. doi:10.1016/j.scitotenv.2020.137215

Baltazar-Soares, M., Biastoch, A., Harrod, C., Hanel, R., Marohn, L., Prigge, E., et al. (2014). Recruitment Collapse and Population Structure of the European Eel Shaped by Local Ocean Current Dynamics. *Curr. Biol.* 24 (1), 104–108. doi:10.1016/j.cub.2013.11.031

Barbarossa, V., Schmitt, R. J. P., Huijbregts, M. A. J., Zarfl, C., King, H., and Schipper, A. M. (2020). Impacts of Current and Future Large Dams on the Geographic Range Connectivity of Freshwater Fish Worldwide. *Proc. Natl. Acad. Sci. U.S.A.* 117, 3648–3655. doi:10.1073/pnas.1912776117

Bednarek, A. T. (2001). Undamming Rivers: a Review of the Ecological Impacts of Dam Removal. *Environ. Manag.* 27, 803–814. doi:10.1007/s002670010189

Bevacqua, D., Melià, P., Gatto, M., and De Leo, G. A. (2015). A Global Viability Assessment of the European Eel. *Glob. Change Biol.* 21, 3323–3335. doi:10.1111/gcb.12972

Birnie-Gauvin, K., and Aarestrup, K. (2019). A Call for a Paradigm Shift: Assumed-to-be Premature Migrants Actually Yield Good Returns. *Ecol. Freshw. Fish.* 28, 62–68. doi:10.1111/eff.12431

Briand, C., Fatin, D., Feunteun, E., and Fontenelle, G. (2005). Estimating the Stock of Glass Eels in an Estuary by Mark-Recapture Experiments Using Vital Dyes. *Bull. Fr. Pêche Piscic.* 378, 23–46. doi:10.1051/kmae:2005002

Bruijs, M. C. M., and Durif, C. M. F. (2009). "Silver Eel Migration and Behaviour," in *Spawning Migration of the European Eel*. Editors G. Thillart, S. Dufour, and J. C. Rankin (Dordrecht: Fish & Fisheries SeriesSpringer), 30, 65–95. doi:10.1007/978-1-4020-9095-0_4

Bult, T. P., and Dekker, W. (2007). Experimental Field Study on the Migratory Behaviour of Glass Eels (*Anguilla anguilla*) at the Interface of Fresh and Salt Water. *ICES J. Mar. Sci.* 64 (7), 1396–1401. doi:10.1093/icesjms/fsm105

Chowdhury, A. R., and Kipgen, N. (2013). Deluge amidst Conflict: Hydropower Development and Displacement in the North-east Region of India. *Prog. Dev. Stud.* 13, 195–208. doi:10.1177/1464993413486545

Cote, D., Kehler, D. G., Bourne, C., and Wiersma, Y. F. (2009). A New Measure of Longitudinal Connectivity for Stream Networks. *Landsc. Ecol.* 24 (1), 101–113. doi:10.1007/s10980-008-9283-y

Cottiglia, M. (1968). La Distribuzione Dell'ittiofauna Dulciacquicola in Sardegna. *Riv. Idrob.* 7 (1), 64–115.

Culurgioni, J., Figus, V., Cabiddu, S., De Murtas, R., Cau, A., and Sabatini, A. (2015). Larval Helminth Parasites of Fishes and Shellfishes from Santa Gilla Lagoon (Sardinia, Western Mediterranean), and Their Use as Bioecological Indicators. *Estuaries Coasts* 38, 1505–1519. doi:10.1007/s12237-014-9894-2

Culurgioni, J., Sabatini, A., De Murtas, R., Mattiucci, S., and Figus, V. (2014). Helminth Parasites of Fish and Shellfish from the Santa Gilla Lagoon in Southern Sardinia, Italy. *J. Helminthol.* 88, 489–498. doi:10.1017/S0022149X13000461

Déath, G. (2007)., 88. 0.CO, 2432–251. doi:10.1890/0012-9658(2007)88[243Boosted Trees for Ecological Modeling and Prediction*EcologyBTFEMA]2*

Daverat, F., Limburg, K., Thibault, I., Shiao, J., Dodson, J., Caron, F., et al. (2006). Phenotypic Plasticity of Habitat Use by Three Temperate Eel Species, *Anguilla anguilla, A. Japonica* and *A. rostrata*. *Mar. Ecol. Prog. Ser.* 308, 231–241. doi:10.3354/meps308231

De Waele, J., Martina, M. L. V., Sanna, L., Cabras, S., and Cossu, Q. A. (2010). Flash Flood Hydrology in Karstic Terrain: Flumineddu Canyon, Central-East Sardinia. *Geomorphology* 120, 162–173. doi:10.1016/j.geomorph.2010.03.021

Dekker, W., and Beaulaton, L. (2016). Climbing Back up what Slippery Slope? Dynamics of the European Eel Stock and its Management in Historical Perspective. *ICES J. Mar. Sci.* 73, 5–13. doi:10.1093/icesjms/fsv132

Dekker, W. (2003). Did Lack of Spawners Cause the Collapse of the European Eel, *Anguilla anguilla* ? *Fish. Manag. Ecol.* 10, 365–376. doi:10.1111/j.1365-2400.2003.00352.x

Dekker, W. (2004). *Slipping through Our Hands – Population Dynamics of the European Eel. PhD Thesis*. Amsterdam, Netherlands: University of Amsterdam. Available at: http://www.diadfish.org/doc/these_2004/dekker_thesis_eel.pdf.

Derville, S., Constantine, R., Baker, C., Oremus, M., and Torres, L. (2016). Environmental Correlates of Nearshore Habitat Distribution by the Critically Endangered Maũi Dolphin. *Mar. Ecol. Prog. Ser.* 551, 261–275. doi:10.3354/meps11736

Dias, M. S., Tedesco, P. A., Hugueny, B., Jézéquel, C., Beauchard, O., Brosse, S., et al. (2017). Anthropogenic Stressors and Riverine Fish Extinctions. *Ecol. Indic.* 79, 37–46. doi:10.1016/j.ecolind.2017.03.053

Ding, L., Chen, L., Ding, C., and Tao, J. (2018). Global Trends in Dam Removal and Related Research: A Systematic Review Based on Associated Datasets and Bibliometric Analysis. *Chin. Geogr. Sci.* 29, 1–12. doi:10.1007/s11769-018-1009-8

Drouineau, H., Bau, F., Alric, A., Deligne, N., Gomes, P., and Sagnes, P. (2017). Silver Eel Downstream Migration in Fragmented Rivers: Use of a Bayesian Model to Track Movements Triggering and Duration★. *Aquat. Living Resour.* 30, 5–9. doi:10.1051/alr/2017003

Drouineau, H., Carter, C., Rambonilaza, M., Beaufaron, G., Bouleau, G., Gassiat, A., et al. (2018). River Continuity Restoration and Diadromous Fishes: Much More Than an Ecological Issue. *Environ. Manag.* 61, 671–686. doi:10.1007/s00267-017-0992-3

Dudgeon, D., Arthington, A. H., Gessner, M. O., Kawabata, Z.-I., Knowler, D. J., Lévêque, C., et al. (2006). Freshwater Biodiversity: Importance, Threats, Status and Conservation Challenges. *Biol. Rev.* 81, 163–182. doi:10.1017/S1464793105006950

Durif, C. M. F. (2003). *La migration d'avalaison de l'anguille européenne* Anguilla anguilla*: Caractérisation des fractions dévalantes, phénoméne de migration et franchissement d'obstacles*. PhD Thesis. Toulouse: University of Paul Sabatier.

Dynesius, M., and Nilsson, C. (1994). Fragmentation and Flow Regulation of River Systems in the Northern Third of the World. *Science* 266 (5186), 753–762. doi:10.1126/science.266.5186.753

E.C. (2007). Council Regulation (EC) No. 1100/2007 of 18 September 2007, Establishing Measures for the Recovery of the Stock of European Eel. *Official J. Eur. Union L* 248, 17–23.

Edeline, E., Dufour, S., Briand, C., Fatin, D., and Elie, P. (2004). Thyroid Status Is Related to Migratory Behavior in *Anguilla anguilla* Glass Eels. *Mar. Ecol. Prog. Ser.* 282, 261–270. doi:10.3354/meps282261

Elith, J., Leathwick, J. R., and Hastie, T. (2008). A Working Guide to Boosted Regression Trees. *J. Anim. Ecol.* 77, 802–813. doi:10.1111/j.1365-2656.2008.01390.x

Feunteun, E. (2002). Management and Restoration of European Eel Population (*Anguilla anguilla*): An Impossible Bargain. *Ecol. Eng.* 18, 575–591. doi:10.1016/S0925-8574(02)00021-6

SUPPLEMENTARY MATERIAL

The Supplementary Material for this article can be found online at: https://www.frontiersin.org/articles/10.3389/fenvs.2022.876369/full#supplementary-material

Friedman, J. H. (2001). Greedy Function Approximation: A Gradient Boosting Machine. *Ann. Stat.* 29 (5), 1189–1232. doi:10.1214/aos/1013203451

Friedman, J. H., and Meulman, J. J. (2003). Multiple Additive Regression Trees with Application in Epidemiology. *Stat. Med.* 22, 1365–1381. doi:10.1002/sim.1501

Fullerton, A. H., Burnett, K. M., Steel, E. A., Flitcroft, R. L., Pess, G. R., Feist, B. E., et al. (2010). Hydrological Connectivity for Riverine Fish: Measurement Challenges and Research Opportunities. *Freshw. Biol.* 55, 2215–2237. doi:10.1111/j.1365-2427.2010.02448.x

Galipeau, B. A., Ingman, M., and Tilt, B. (2013). Dam-Induced Displacement and Agricultural Livelihoods in China's Mekong Basin. *Hum. Ecol.* 41, 437–446. doi:10.1007/s10745-013-9575-y

Gangloff, M. M. (2013). Taxonomic and Ecological Tradeoffs Associated with Small Dam Removals. *Aquat. Conserv. Mar. Freshw. Ecosyst.* 23, 475–480. doi:10.1002/aqc.2383

Graf, W. L. (2003). "Dam Removal Research – Status and Prospects," in *Proceedings of the Heinz Center's Dam Removal Research Workshop* (Pennsylvania Avenue, Washington D.C: The H. John Heinz III Center for Science, Economics and the Environment), 23–24.

Greenwell, B., Boehmke, B., and Cunningham, J. (2020). *Gbm: Generalized Boosted Regression Models*. R Package Version 2.1.5. Available online: https://CRAN.R-project.org/package=gbm.

Grill, G., Lehner, B., Lehner, B., Lumsdon, A. E., Zarfl, C., MacDonald, G. K., et al. (2015). An Index-Based Framework for Assessing Patterns and Trends in River Fragmentation and Flow Regulation by Global Dams at Multiple Scales. *Environ. Res. Lett.* 10 (1), 015001. doi:10.1088/1748-9326/10/1/015001

Grill, G., Lehner, B., Thieme, M., Geenen, B., Tickner, D., Antonelli, F., et al. (2019). Mapping the World's Free-Flowing Rivers. *Nature* 569, 215–221. doi:10.1038/s41586-019-1111-9

Haidvogl, G. (2018). "Historic Milestones of Human River Uses and Ecological Impacts," in *Riverine Ecosystem Management*. Editors S. Schmutz and J. Sendzimir (Cham: Springer), 8, 19–39. Aquatic Ecology Series. doi:10.1007/978-3-319-73250-3_2

Harris, J. H., Kingsford, R. T., Peirson, W., and Baumgartner, L. J. (2017). Mitigating the Effects of Barriers to Freshwater Fish Migrations: The Australian Experience. *Mar. Freshw. Res.* 68, 614–696. doi:10.1071/MF15284

Henderson, P. A., Plenty, S. J., Newton, L. C., and Bird, D. J. (2011). Evidence for a Population Collapse of European Eel (*Anguilla anguilla*) in the Bristol Channel. *J. Mar. Biol. Ass.* 92 (4), 843–851. doi:10.1017/s002531541100124x

Hijmans, R. J., Phillips, S., Leathwick, J., and Elith, J. (2011). *Dismo: Species Distribution Modeling. R Package Version 1.1-4*. Available online: https://CRAN.R-project.org/package=dismo.

Hitt, N. P., Eyler, S., and Wofford, J. E. B. (2012). Dam Removal Increases American Eel Abundance in Distant Headwater Streams. *Trans. Am. Fish. Soc.* 141, 1171–1179. doi:10.1080/00028487.2012.675918

Holmlund, C. M., and Hammer, M. (1999). Ecosystem Services Generated by Fish Populations. *Ecol. Econ.* 29 (2), 253–268. doi:10.1016/S0921-8009(99)00015-4

ICES (2021). Joint EIFAAC/ICES/GFCM Working Group on Eels (WGEEL). *ICES Sci. Rep.* 3 (85). doi:10.17895/ices.pub.8143

IUCN (2014). The IUCN Red List of Threatened Species. *Anguilla anguilla*. Available at: http://www.iucnredlist.org.

Jacoby, D. M. P., Casselman, J. M., Crook, V., DeLucia, M.-B., Ahn, H., Kaifu, K., et al. (2015). Synergistic Patterns of Threat and the Challenges Facing Global Anguillid Eel Conservation. *Glob. Ecol. Conservation* 4, 321–333. doi:10.1016/j.gecco.2015.07.009

Ju, M.-C., Zhang, T.-L., Li, X.-K., Li, B.-Y., Li, Y.-P., Liu, Q.-Y., et al. (2021). Large Scale Environmental Drivers of Biocrust Distribution and Development across a Sandy Desert in China. *Catena* 200, 105137. doi:10.1016/j.catena.2020.105137

Jungwirth, M., Muhar, S., and Schmutz, S. (2000). Fundamentals of Fish Ecological Integrity and Their Relation to the Extended Serial Discontinuity Concept. *Hydrobiologia* 422, 85–97. doi:10.1023/A:101704552723310.1007/978-94-011-4164-2_7

Lévêque, C., Oberdorff, T., Paugy, D., Stiassny, M. L. J., and Tedesco, P. A. (2008). Global Diversity of Fish (Pisces) in Freshwater. *Hydrobiologia* 595, 545–567. doi:10.1007/s10750-007-9034-0

Larinier, M. (2001). *Dams, Fish and Fisheries: Opportunities, Challenges and Conflict Resolution*. FAO fisheries technical paper.Environmental Issues, Dams and Fish Migration

Legault, A., Acou, A., Guillouët, J., and Feunteun, E. (2003). Suivi De La Migration D'avalaison Des Anguilles Par Une Conduite De Debit Reserve. *Bull. Fr. Pêche Piscic.* 368, 43–54. doi:10.1051/kmae:2003035

Lloyd, L. N., Anderson, B. G., Cooling, M., Gippel, C. J., Pope, A. J., and Sherwood, J. E. (2012). *Estuary Environmental Flows Assessment Methodology for Victoria*. Melbourne, Victoria, Australia: Victorian Government Department of Sustainability and Environment.

Lucas, M. C., and Baras, E. (2001). *Migration of Freshwater Fishes*. Oxford GBR: Blackwell Science Ltd.

Mac Gregor, R., Casselman, J., Allen, W., Haxton, T., Dettmers, J., Mathers, A., et al. (2009). Natural Heritage, Anthropogenic Impacts, and Biopolitical Issues Related to the Status and Sustainable Management of American Eel: a Retrospective Analysis and Management Perspective at the Population Level. *Am. Fish. Soc. Symp.* 69, 713–740. doi:10.1158/0008-5472.sabcs-09-2053

Manca, G. (1965). "Contributo Alla Conoscenza Della *Salmo trutta Macrostigma* Dum," in *Sardegna* (University of Cagliari), 92.

Marchetto, A., Padedda, B. M., Mariani, M. A., Lugliè, A., and Sechi, N. (2009). A Numerical Index for Evaluating Phytoplankton Response to Changes in Nutrient Levels in Deep Mediterranean Reservoirs. *J. Limnol.* 68 (1), 106–121. doi:10.4081/jlimnol.2009.106

Merg, M.-L., Dézerald, O., Kreutzenberger, K., Demski, S., Reyjol, Y., Usseglio-Polatera, P., et al. (2020). Modeling Diadromous Fish Loss from Historical Data: Identification of Anthropogenic Drivers and Testing of Mitigation Scenarios. *Plos One* 15 (7), e0236575. doi:10.1371/journal.pone.0236575

Miller, M. J., Feunteun, E., and Tsukamoto, K. (2016). Did a "Perfect Storm" of Oceanic Changes and Continental Anthropogenic Impacts Cause Northern Hemisphere Anguillid Recruitment Reductions? *ICES J. Mar. Sci.* 73, 43–56. doi:10.1093/icesjms/fsv063

Milt, A. W., Diebel, M. W., Doran, P. J., Ferris, M. C., Herbert, M., Khoury, M. L., et al. (2018). Minimizing Opportunity Costs to Aquatic Connectivity Restoration while Controlling an Invasive Species. *Conserv. Biol.* 32, 894–904. doi:10.1111/cobi.13105

Moccia, D., Salvadori, L., Ferrari, S., Carucci, A., and Pusceddu, A. (2020). Implementation of the EU Ecological Flow Policy in Italy with a Focus on Sardinia. *Adv. Ocean. Limnol.* 11 (1). doi:10.4081/aiol.2020.8781

Montaldo, N., and Sarigu, A. (2017). Potential Links between the North Atlantic Oscillation and Decreasing Precipitation and Runoff on a Mediterranean Area. *J. Hydrology* 553, 419–437. doi:10.1016/j.jhydrol.2017.08.018

Naselli-Flores, L., and Lugliè, A. (2014). Laghi artificiali dell'Italia meridionale e delle isole maggiori. *Biol. Ambient.* 28, 1–8.

Nielsen, T., and Prouzet, P. (2008). "Capture-based Aquaculture of the Wild European Eel (*Anguilla anguilla*)," in *Capture-based Aquaculture. Global Overview*. Editors A. Lovatelli and P. F. Holthus (Rome: FAO Fisheries Technical Paper).

Nieto, K., and Mélin, F. (2017). Variability of Chlorophyll-A Concentration in the Gulf of Guinea and its Relation to Physical Oceanographic Variables. *Prog. Oceanogr.* 151, 97–115. doi:10.1016/j.pocean.2016.11.009

Nilsson, C., Reidy, C. A., Dynesius, M., and Revenga, C. (2005). Fragmentation and Flow Regulation of the World's Large River Systems. *Science* 308 (5720), 405–408. doi:10.1126/science.1107887

Opperman, J., Baruch-Mordo, S., Carvallo, J., Kammen, D., Kiesecker, J., and Weber, C. (2019). Sustaining the Last Rivers. *Amer. Sci.* 107, 302. doi:10.1511/2019.107.5.302

Opperman, J. J., Moyle, P. B., Larsen, E. W., Florsheim, J. L., and Manfree, A. D. (2017). *Floodplains: Processes and Management for Ecosystem Services*. Berkeley, CA, USA: University of California Press.

Palmas, F., Cau, A., Podda, C., Musu, A., Serra, M., Pusceddu, A., et al. (2022). Rivers of Waste: Anthropogenic Litter in Intermittent Sardinian Rivers, Italy (Central Mediterranean). *Environ. Pollut.* 302, 119073. doi:10.1016/j.envpol.2022.119073

Palmas, F., Righi, T., Musu, A., Frongia, C., Podda, C., Serra, M., et al. (2020). Pug-Headedness Anomaly in a Wild and Isolated Population of Native Mediterranean Trout *Salmo trutta* L., 1758 Complex (Osteichthyes: Salmonidae). *Diversity* 12 (9), 353. doi:10.3390/d12090353

Pedersen, M. I., and Rasmussen, G. H. (2016). Yield Per Recruit from Stocking Two Different Sizes of Eel (*Anguilla anguilla*) in the Brackish Roskilde Fjord. *ICES J. Mar. Sci.* 73, 158–164. doi:10.1093/icesjms/fsv167

Pike, C., Crook, V., and Gollock, M. (2020). "*Anguilla anguilla*," in *The IUCN Red List of Threatened Species*. e.T60344A152845178.

Piper, A. T., Wright, R. M., Walker, A. M., and Kemp, P. S. (2013). Escapement, Route Choice, Barrier Passage and Entrainment of Seaward Migrating European Eel, *Anguilla anguilla*, within a Highly Regulated Lowland River. *Ecol. Eng.* 57, 88–96. doi:10.1016/j.ecoleng.2013.04.030

Podda, C., Palmas, F., Frau, G., Chessa, G., Culurgioni, J., Diciotti, R., et al. (2020). Environmental Influences on the Recruitment Dynamics of Juvenile European Eels, *Anguilla anguilla* , in a Small Estuary of the Tyrrhenian Sea, Sardinia, Italy. *Aquat. Conserv. Mar. Freshw. Ecosyst.* 30 (8), 1638–1648. doi:10.1002/aqc.3362

Podda, C., Sabatini, A., Palmas, F., and Pusceddu, A. (2021). Hard Times for Catadromous Fish: the Case of the European Eel (*Anguilla anguilla*, L. 1758). *Adv. Ocean. Limnol.* 12 (2), 9997. doi:10.4081/aiol.2021.9997

Poff, N. L., Allan, J. D., Bain, M. B., Karr, J. R., Prestegaard, K. L., Richter, B. D., et al. (1997). The Natural Flow Regime. *BioScience* 47, 769–784. doi:10.2307/1313099

Poff, N. L., and Schmidt, J. C. (2016). How Dams Can Go with the Flow. *Science* 353, 1099–1100. doi:10.1126/science.aah557110.1126/science.aah4926

Pomini, F. P. (1940). Ricerche su Salmo macrostigma Dum. *Boll. Pesca Pisc. Idrob.* 16 (3), 3–63.

Postel, S., and Richter, B. D. (2004). *Rivers for Life: Managing Water for People and Nature*, 41. Washington DC: Island Press, 41–4059. doi:10.5860/choice.41-4059Rivers for Life: Managing Water for People and Nature*Choice Rev. Online*

Potter, I. C., Chuwen, B. M., Hoeksema, S. D., and Elliott, M. (2010). The Concept of an Estuary: a Definition that Incorporates Systems Which Can Become Closed to the Ocean and Hypersaline. *Estuar. Coast. Shelf Sci.* 87, 497–500. doi:10.1016/j.ecss.2010.01.021

R Core Team (2021). *R: A Language and Environment for Statistical Computing.* [WWW Document]. R Found. Stat. Comput. Vienna. URL: https://www.r-project.org.

Rahel, F. J. (2013). Intentional Fragmentation as a Management Strategy in Aquatic Systems. *Bioscience* 63, 362–372. doi:10.1525/bio.2013.63.5.9

Regione Autonoma della Sardegna (2021). *Sardegna Geo-Portale*. Available at: http://www.sardegnageoportale.it/index.html.

Richter, B. D., Postel, S., Revenga, C., Scudder, T., Lehner, B., Churchill, A., et al. (2010). Lost in Development's Shadow: The Downstream Human Consequences of Dams. *Water Altern.* 3 (2), 14–42.

Rincón, G., Solana-Gutiérrez, J., Alonso, C., Saura, S., and García de Jalón, D. (2017). Longitudinal Connectivity Loss in a Riverine Network: Accounting for the Likelihood of Upstream and Downstream Movement across Dams. *Aquat. Sci.* 79, 573–585. doi:10.1007/s00027-017-0518-3

Rodeles, A. A., Galicia, D., and Miranda, R. (2021). A Simple Method to Assess the Fragmentation of Freshwater Fish Meta-Populations: Implications for River Management and Conservation. *Ecol. Indic.* 125, 107557. doi:10.1016/j.ecolind.2021.107557

Russi, D., Ten Brink, P., Farmer, A., Badura, T., Coates, D., Förster, J., et al. (2013). *The Economics of Ecosystems and Biodiversity for Water and Wetlands.* Available at: https://www.cbd.int/financial/values/g-ecowaterwetlands-teeb.pdf.

Sabatini, A., Cannas, R., Follesa, M. C., Palmas, F., Manunza, A., Matta, G., et al. (2011). Genetic Characterization and Artificial Reproduction Attempt of Endemic Sardinian troutSalmo truttaL., 1758 (Osteichthyes, Salmonidae): Experiences in Captivity. *Italian J. Zoology* 78, 20–26. doi:10.1080/11250003.2010.497171

Sabatini, A., Podda, C., Frau, G., Cani, M. V., Musu, A., Serra, M., et al. (2018). Restoration of Native Mediterranean Brown Trout *Salmo Cettii* Rafinesque, 1810 (Actinopterygii: Salmonidae) Populations Using an Electric Barrier as a Mitigation Tool. *Eur. Zoological J.* 85, 137–149. doi:10.1080/24750263.2018.1453554

Saha, S., Arabameri, A., Saha, A., Blaschke, T., Ngo, P. T. T., Nhu, V. H., et al. (2021). Prediction of Landslide Susceptibility in Rudraprayag, India Using Novel Ensemble of Conditional Probability and Boosted Regression Tree-Based on Cross-Validation Method. *Sci. Total Environ.* 764, 142928. doi:10.1016/j.scitotenv.2020.142928

Segurado, P., Branco, P., and Ferreira, M. T. (2013). Prioritizing Restoration of Structural Connectivity in Rivers: a Graph Based Approach. *Landsc. Ecol.* 28 (7), 1231–1238. doi:10.1007/s10980-013-9883-z

Seliger, C., and Zeiringer, B. (2018). "Riverine Ecosystem Management," in *Riverine Ecosystem Management. Science for Governing towards a Sustainable Future*. Editors S. Schmutz and J. Sendzimir (Amsterdam: Springer). doi:10.1007/978-3-319-73250-3

Silva, A. T., Lucas, M. C., Castro-Santos, T., Katopodis, C., Baumgartner, L. J., Thiem, J. D., et al. (2018). The Future of Fish Passage Science, Engineering, and Practice. *Fish. Fish.* 19, 340–362. doi:10.1111/faf.12258

Stanley, E. H., and Doyle, M. W. (2003). Trading off: the Ecological Effects of Dam Removal. *Front. Ecol. Environ.* 1, 15–22. doi:10.1890/1540-9295(2003)001[0015:toteeo]2.0.co;2

Suari, Y., Amit, T., Gilboa, M., Sade, T., Krom, M. D., Gafny, S., et al. (2019). Sandbar Breaches Control of the Biogeochemistry of a Micro-estuary. *Front. Mar. Sci.* 6, 1–15. doi:10.3389/fmars.2019.00224

Tamario, C., Calles, O., Watz, J., Nilsson, P. A., and Degerman, E. (2019). Coastal River Connectivity and the Distribution of Ascending Juvenile European Eel (*Anguilla anguilla* L.): Implications for Conservation Strategies Regarding Fish-passage Solutions. *Aquat. Conserv. Mar. Freshw. Ecosyst.* 29, 612–622. doi:10.1002/aqc.3064

Tickner, D., Opperman, J. J., Abell, R., Acreman, M., Arthington, A. H., Bunn, S. E., et al. (2020). Bending the Curve of Global Freshwater Biodiversity Loss: an Emergency Recovery Plan. *BioScience* 70, 330–342. doi:10.1093/biosci/biaa002

Trancart, T., Carpentier, A., Acou, A., Charrier, F., Mazel, V., Danet, V., et al. (2020). When "Safe" Dams Kill: Analyzing Combination of Impacts of Overflow Dams on the Migration of Silver Eels. *Ecol. Eng.* 145, 105741. doi:10.1016/j.ecoleng.2020.105741

Trancart, T., Tétard, S., Acou, A., Feunteun, E., Schaeffer, F., and de Oliveira, E. (2018). Silver Eel Downstream Migration in the River Rhine, Route Choice, and its Impacts on Escapement: A 6-year Telemetry Study in a Highly Anthropized System. *Ecol. Eng.* 123, 202–211. doi:10.1016/j.ecoleng.2018.09.002

Turner, S. M., Chase, B. C., and Bednarski, M. S. (2018). Evaluating the Effect of Dam Removals on Yellow-Phase American Eel Abundance in a Northeastern U.S. Watershed. *North Am. J. Fish. Manage* 38, 424–431. doi:10.1002/nafm.10040

VV, A. A. (2022). *Carta Ittica Della Sardegna – D.G.R. N. 2/28*, 428. del 20/01/2022. Regione Autonoma della Sardegna (ADA/STNPF)/Università degli Studi di Cagliari (DISVA)Available online: https://delibere.regione.sardegna.it/protected/58916/0/def/ref/DBR58914/ (accessed on march 21, 2022).

Vörösmarty, C. J., McIntyre, P. B., Gessner, M. O., Dudgeon, D., Prusevich, A., Green, P., et al. (2010). Global Threats to Human Water Security and River Biodiversity. *Nature* 467, 7315555–561. doi:10.1038/nature09440

Van Ginneken, V. J. T., and van den Thillart, G. E. E. J. M. (2000). Eel Fat Stores Are Enough to Reach the Sargasso. *Nature* 403, 156–157. doi:10.1038/35003110

Verbiest, H., Breukelaar, A., Ovidio, M., Philippart, J.-C., and Belpaire, C. (2012). Escapement Success and Patterns of Downstream Migration of Female Silver Eel *Anguilla anguilla* in the River Meuse. *Ecol. Freshw. Fish.* 21, 395–403. doi:10.1111/j.1600-0633.2012.00559.x

Watz, J., Nilsson, P. A., Degerman, E., Tamario, C., and Calles, O. (2019). Climbing the Ladder: an Evaluation of Three Different Anguillid Eel Climbing Substrata and Placement of Upstream Passage Solutions at Migration Barriers. *Anim. Conserv.* 22 (5), 452–462. doi:10.1111/acv.12485

Welcomme, R. L. (1995). Relationships between Fisheries and the Integrity of River Systems. *Regul. Rivers Res. Mgmt.* 11, 121–136. doi:10.1002/rrr.3450110110

White, E. M., and Knights, B. (1997). Environmental Factors Affecting Migration of the European Eel in the Rivers Severn and Avon, England. *J. Fish Biol.* 50, 1104–1116. doi:10.1111/j.1095-8649.1997.tb01634.x

Wilkes, M. A., Mckenzie, M., and Webb, J. A. (2018). Fish Passage Design for Sustainable Hydropower in the Temperate Southern Hemisphere: An Evidence Review. *Rev. Fish. Biol. Fish.* 28 (1), 117–135. doi:10.1007/s11160-017-9496-8

Zarfl, C., Lumsdon, A. E., Berlekamp, J., Tydecks, L., and Tockner, K. (2015). A Global Boom in Hydropower Dam Construction. *Aquat. Sci.* 77, 161–170. doi:10.1007/s00027-014-0377-0

Zuur, A. F., Ieno, E. N., and Elphick, C. S. (2010). A Protocol for Data Exploration to Avoid Common Statistical Problems. *Methods Ecol. Evol.* 1, 3–14. doi:10.1111/j.2041-210X.2009.00001.x

Conflict of Interest: The authors declare that the research was conducted in the absence of any commercial or financial relationships that could be construed as a potential conflict of interest.

frontiers | Frontiers in Environmental Science

TYPE Original Research
PUBLISHED 10 October 2022
DOI 10.3389/fenvs.2022.1000665

Sediment oxygen demand rate in a flow regulated lagoon (Venice, Italy)

Simone Leoni, Janusz Dominik, Daniele Cassin, Giorgia Manfè, Davide Tagliapietra, Francesco Acri and Roberto Zonta*

Consiglio Nazionale delle Ricerche - Istituto di Scienze Marine (CNR-ISMAR), Venezia, Italy

OPEN ACCESS

EDITED BY
Caterina Bergami,
Institute of Marine Science, National Research Council (CNR), Italy

REVIEWED BY
Daniele Brigolin,
Università Iuav di Venezia, Italy
Michele Mistri,
University of Ferrara, Italy

*CORRESPONDENCE
Roberto Zonta,
r.zonta@ismar.cnr.it

SPECIALTY SECTION
This article was submitted to Freshwater Science, a section of the journal Frontiers in Environmental Science

RECEIVED 22 July 2022
ACCEPTED 27 September 2022
PUBLISHED 10 October 2022

CITATION
Leoni S, Dominik J, Cassin D, Manfè G, Tagliapietra D, Acri F and Zonta R (2022), Sediment oxygen demand rate in a flow regulated lagoon (Venice, Italy). *Front. Environ. Sci.* 10:1000665.
doi: 10.3389/fenvs.2022.1000665

From October 2020, the MOSE system went into operation in the three inlets to protect Venice and its lagoon from flooding caused by high tide events in the Adriatic Sea. While the MOSE increases the prospect of physical defense, how will the new status of a regulated lagoon affect the functioning of the waterbody? In particular, the dissolved oxygen balance in the water column can be affected by the expected increase in water residence times. Sediments play an important role in oxygen consumption in the water column and for this reason sediment oxygen demand (SOD) was studied *in situ* for the first time, in 16 sites at four lagoon areas. SOD rate, measured throughout 2021 with specially made benthic chambers, varied in the different areas and with seasons (from 0.63 to 24.00 g m^{-2} d^{-1}), with higher values at the more confined sites and significantly lower values in those belonging to the open lagoon. Based on SOD rate, consumption times of dissolved oxygen in the water column were estimated at the MOSE closures, from saturation values to hypoxia and in the temperature range of 11.7–33.3°C. Especially in the confined sites, sediments can exert an important depleting action on dissolved oxygen already at water temperatures above 20°C, which are not particularly high for the lagoon.

KEYWORDS

benthic chamber, climate changes, lagoons, MOSE system, sediment oxygen demand, Venice

Introduction

Dissolved oxygen (DO) in the water column is essential for aquatic life and its concentration is a direct indicator of ecosystem health (Vellidis et al., 2006; MacPherson et al., 2007). Low DO concentrations are harmful to aquatic life, to the point that hypoxia (< 2.8 mg L^{-1}) or anoxia (absence of oxygen) events entail damage to the population structure and ecosystem functioning (Diaz and Rosenberg, 1995; Altieri and Diaz, 2019). Oxygen solubility in water is inversely proportional to temperature and decreases in warmer waters (Garcia and Gordon, 1992). As the threat from global warming increases, one of the main consequences is the decrease in oxygen in aquatic environments (Breitburg et al., 2018; Pitcher et al., 2021). Other processes that decrease DO concentration include water column stratification that reduces the downward supply of O_2-rich surface waters (Manabe et al., 1991; Collins et al., 2013; Breitburg et al., 2018), land use and agricultural activities that implicate nutrient enrichment in water (Kemp et al., 2005), and nocturnal oxygen consumption *via* respiration (Caraco and Caraco, 2002).

Major sources of DO are photosynthetic production and re-aeration from the atmosphere, whereas natural sinks are sediment oxygen demand (SOD) and biochemical oxygen demand (BOD) of the water column (Rounds and Doyle 1997; Rong et al., 2016). SOD is the rate at which DO is removed from the water by biochemical processes in the sediment (Hatcher, 1986). It includes depletion due to both biological respiration of benthic organisms (biological SOD, BSOD) and chemical oxidation of reduced compounds (chemical SOD, CSOD) arising from anaerobic metabolism (Walker and Snodgrass, 1986; Chau, 2002; Doyle and Lynch, 2005). BSOD is governed by aerobic heterotrophs that utilize organic material as an energy source (Middelburg et al., 2005); CSOD involves anaerobic bacteria which degrade organic matter, determining the sulphate reduction (e.g., Zaggia et al., 2007) and releasing reduced compounds (mainly of nitrogen, manganese, and iron) that react with molecular oxygen (Rounds and Doyle, 1997; Todd et al., 2010).

Oxygen concentration is strongly dependent on the air-sea exchange in surface waters, whereas in shallow systems - such as lagoons - exchange across the sediment-water interface is often important (Pitcher et al., 2021). Due to the high sediment surface area to water volume ratios, lagoon sediments influence the dynamics of oxygen and play an important regulatory function for the whole ecosystem (Giordani et al., 2008; Brigolin et al., 2021). Lagoons are also places with high organic matter inputs (Viaroli et al., 2008). Settled organic material is actively decomposed by microbial processes and the DO level consequently decreases (Castel et al., 1996). Systems with long water residence times and stratified water columns are more prone to be subjected to hypoxia events (NRC, 2000).

Serious anoxic events occurred in the Venice Lagoon (Figure 1) during the warm months of the 1980s (Sfriso et al., 1987; Sfriso et al., 1995; Zirino et al., 2016), due to the rot of *Ulva rigida* after major blooms. Since 1990, water conditions in the lagoon have changed, thanks to a concomitance of climatic situations, increased water turbidity, and biomass harvesting (Sfriso and Marcomini, 1996). While events of that severity did not recur after the 1980s, hypoxia/anoxia conditions have been observed in some sectors of the lagoon since the early 2010s (Bernardi Aubry et al., 2020), although generally lasting less than 24 h (ISPRA and ARPAV, 2016; ISPRA and ARPAV, 2018; ISPRA and ARPAV, 2021).

The MOSE system was operated for the first time in October 2020 (Mel et al., 2021) to protect Venice and the lagoon against

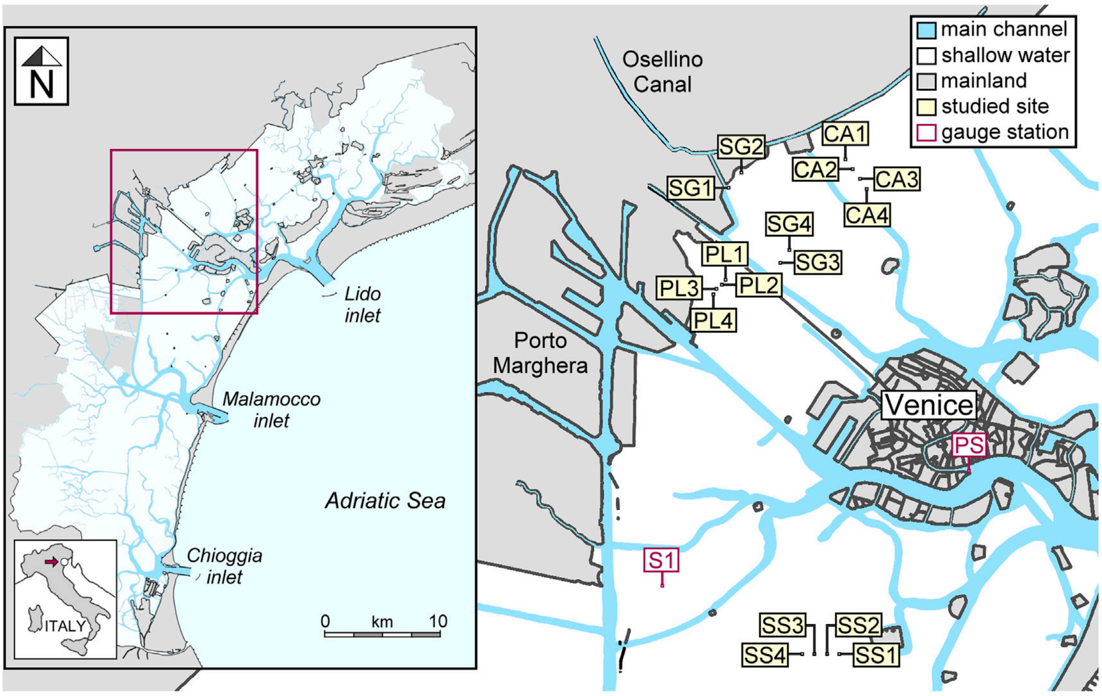

FIGURE 1
Location of the 16 measurement sites in the four selected areas of the Venice Lagoon (in the insert). S1 (45°24.7934′N 12°16.4518′E) and PS (45°25.8656′N 12°20.1826′E) identify the DO gauge station of the SAMANET network and the tide gauge of *Punta Salute* (managed by the Venice Municipality), respectively.

flooding during high sea-level events. The MOSE (Scotti, 2005; Trincardi et al., 2016) consists of mobile gates clustered into barriers installed on the bottom of the three inlets of the lagoon, which rise up and temporarily seal off the waterbody from the sea during high tide events. Although the MOSE system can potentially be operated in the future to improve the water exchange with the sea through appropriate maneuvers of the barriers, it is expected to increase the water renewal time in the lagoon as a whole (Ferrarin et al., 2013). Due to the anticipated sea-level rise and the higher incidence of severe storms, the number of times the MOSE is placed in operation is also foreseen to increase (Lionello, 2012; Cavaleri et al., 2020). Moreover, an increase in the frequency of summer heatwaves due to climate change (Molina et al., 2020) is occurring in the Mediterranean region, which may lead to a greater duration and severity of hypoxic events in the Venice Lagoon (Brigolin et al., 2021).

In this context, the aim of this study was to investigate the importance of sediments in the DO consumption in the Venice Lagoon, measuring the SOD rate in four test areas with benthic chambers. A further objective of the study was the evaluation of how much the sediment can affect the concentration of DO in the water column during MOSE closures.

Materials and methods

Study site

Venice Lagoon is widely described in the literature in terms of functioning and ecosystem characteristics (e.g., Zonta et al., 2018 - and references therein). With a surface area of 550 km^2 and a mean water depth of about 1 m, it includes islands, tidal marshes, mudflats, and a complex network of tidal channels up to 10 m deep (Figure 1). Shallow water areas account for 75% of the total surface area (ca. 415 km^2). The lagoon is linked to the Adriatic Sea by three inlets (Lido, Malamocco and Chioggia), which enable the exchange of water during tidal cycles. The mean tidal excursion is 30 and 80 cm respectively in neap and spring tide conditions (Zaggia et al., 2007).

Four shallow water areas were selected for the study: *Campalto* (CA), *San Giuliano* (SG), *Pili* (PL), and *Sacca Sessola* (SS). In each area, four sites were identified for the SOD measurements and numbered from 1 to 4, for a total of 16 sites (Figure 1). The sites of the CA area were arranged along a perpendicular to the lagoon-mainland interface, at a distance of about 200 m from each other, while the sites of the PL area were located along a line of about 210 m, parallel to the easternmost sector of the industrial area of Porto Marghera. In the SG area, two sites were closer to the mainland (SG1 and SG2) and the other two sites (SG3 and SG4) were located further south, towards the open lagoon north of the City of Venice; of the former two, one (SG1) was located in the shallow waters of the mouth of the Osellino canal, a 47-km-long watercourse draining a crop area of 50 km^2 (Zonta et al., 2005). The distance of SG1 - SG2 from SG3 - SG4 was about 1,400 m. Sites in the SS area were located along a line in the central zone of the lagoon, at a distance of about 200 m from each other.

TABLE 1 Number of cases (and percentage) of hourly DO data below 30 and 50% of saturation value, recorded from June to September in the period 2018–2021. Data from SAMANET measuring network.

Year	DO < 30%		DO < 50%	
	# Cases	% Cases	# Cases	% Cases
2018	321	11.0	916	31.3
2019	111	3.8	457	15.6
2020	176	6.0	622	21.2
2021	28	1.0	269	9.2

The Venice Water Authority (*Provveditorato Interregionale per le Opere Pubbliche del Veneto - Trentino Alto Adige - Friuli Venezia Giulia*) manages an O_2 saturation (DO%) measurement network in the lagoon (named SAMANET), including station S1 (Figure 1) which is located not far from this study's measurement areas. The station is subjected to a greater water exchange than most of the measurement sites, thanks to its proximity to the main tidal channels. Consequently, the concentration of DO in the water column is assumed to be generally higher at station S1 than in our measurement sites. In the warm months from June to September of the years in the period 2018–2021, the hourly DO values recorded by the station were below 50% in 9.2%–31.3% of cases and below 30% in 1%–11% of cases (Table 1).

SOD measurements were carried out approximately on a monthly basis at the 16 sites in the period March - November 2021. Geographic coordinates of site and bathymetric heights are shown in Table 2, referring to the tidal zero level in the lagoon.

Sediment analyses

Small sediment cores (length 10 cm, diameter 6.4 cm) were collected in the 16 sites in May 2021 by utilizing a piston corer, taking care of not disturbing the upper sediment layers. Two sediment samples were obtained from each core, corresponding to the surface (0–1) and sub-surface (1–2 cm) layers. Samples were sieved through a 1 mm Teflon mesh to remove debris and organic fragments, and then carefully homogenized. An aliquot of about 2 g of wet sediment was weighed and dispersed in distilled water before grain-size measurement with a laser diffraction particle size analyzer (Mastersizer 2000; Malvern Instruments, Malvern, United Kingdom). The instrument provided the volumetric percentage of particles belonging to 100 diameter classes in the range of 0.1–2,000 μm.

Total nitrogen (TN) and total carbon (TC) were determined on duplicate samples using a ThermoFisher Flash 2000 IRMS

TABLE 2 Coordinates in the WGS84 reference system and bathymetric height of the 16 sites; the latter refers to the zero-tide level recorded by the *Punta Salute* tide gauge (PS, Figure 1).

SITE	CA1	CA2	CA3	CA4	SG1	SG2	SG3	SG4
lat. N	45° 28.6095′	45° 28.5156′	45° 28.4461′	45° 28.3525′	45° 28.3775′	45° 28.5035′	45° 27.7413′	45° 27.8186′
lon. E	12° 18.4965′	12° 18.5723′	12° 18.6865′	12° 18.7773′	12° 17.0104′	12° 17.1360′	12° 17.5941′	12° 17.6936′
depth (m)	0.22	0.26	0.41	0.52	0.28	0.24	0.57	0.56

SITE	PL1	PL2	PL3	PL4	SS1	SS2	SS3	SS4
lat. N	45° 27.5210′	45° 27.4875′	45° 27.4630′	45° 27.4403′	45° 24.2138′	45° 24.2252′	45° 24.2246′	45° 24.2294′
lon. E	12° 16.9414′	12° 16.9200′	12° 16.8984′	12° 16.8728′	12° 18.6400′	12° 18.4768′	12° 18.3308′	12° 18.1776′
depth (m)	0.47	0.49	0.53	0.53	0.86	0.92	1.05	1.08

Elemental Analyzer (EA, ThermoFisher Scientific Inc, Aurora, OH, United States). Samples for total organic carbon (TOC) measurements were first decarbonated with HCl 1.5 N. As determined by replicate analyses of the same sample, each measurement had an average standard deviation (STD) of ± 0.01% for TN and ± 0.07% for TOC. Total inorganic carbon (TIC) was calculated as the difference between TC and TOC and converted to carbonates, assuming that it was entirely bound as $CaCO_3$.

Water content (W_C) was determined from an aliquot of sample dried in an oven at 105°C until it reached a constant weight (Percival and Lindsay, 1997). Based on variation coefficients of five replicate measurements in three sediment samples, the analytical error of W_C determination was less than 0.88%. W_C was not corrected for salt, as this correction is negligible.

Sediment porosity (Φ) was calculated following Hobbs (1983), as described in Zonta et al. (2021). Organic matter (OM) content was calculated as 1.7 TOC in %, and its density of 1.25 g cm^{-3} was assumed (Avnimelech et al., 2001). The density of the mineral fraction was calculated assuming densities of $CaCO_3$ and the remaining Al-Si fraction of 2.8 g cm^{-3} and 2.65 g cm^{-3}, respectively.

Characteristics of the benthic chambers

Benthic chambers are used to incubate *in situ* a known volume of water above a given sediment surface, measuring over time the consumption of the DO concentration in the isolated water. The PVC cylindrical benthic chambers were made in-house (Figure 2), introducing some changes to the commonly used design for SOD measurements (Murphy and Hicks, 1986; Coenen et al., 2019). A method for measuring the SOD flow rate *in situ* has not been standardized (Coenen et al., 2019), and it may be worth experimenting with any technical improvements.

Chambers had an internal diameter of 30 cm and a height of 27 cm, 6 cm of which are intended to be driven into the sediment; the opacity of the material inhibited photosynthesis during incubation. The lower edge of the cylinder was tapered to facilitate the insertion of the chamber into the sediment. Two centimeter-steel rods embedded with the chamber, allowed the chamber to be driven into the sediment at the correct level of penetration from a boat. As the 2 bars protruded from the base of the chamber by 15 cm, they also strengthened the stability of the apparatus once driven into the sediment. In the case of sites with sediments that have a greater sandy component, a housing is present on the head of the benthic chamber to allow it to be pushed into the sediment, utilizing a wooden pole.

A multiparameter water quality probe (Aquaprobe AP 2000; Aquaread Ltd, England) was inserted in the centre of the chamber to measure dissolved oxygen (optically, mg L^{-1}), temperature (°C), pH, turbidity (NTU), and water depth (cm). The probe was mounted vertically in the center of the chamber, thanks to a sleeve consisting of three layers of material (Plastazote® compressed between two layers of PVC), which maintains the hermetic seal of the chamber. The probe was connected to a data-logger (Aquameter, Aquaread Ltd, England), programmed to acquire data every 5 min, but allowing instantaneous readings. The chambers exposed a 0.071 m^2 area of sediment to 14.6 L of enclosed water; the correction was made for the volume occupied by both multiprobe and hydraulic circuits inside the chamber. Several tests were carried out to verify that the benthic chamber was completely sealed once it was embedded in the sediment.

A pump powered by a 12-V lead-acid rechargeable battery was used to continuously recirculate the water inside the chamber. The blade shape of the pump propeller was modified to reduce its flow rate to 100 L h^{-1}; this means that the volume of incubated water was completely recirculated in about 9 min. The water circuit inside the chamber had a "recirculating fountain" configuration. The water intake (Figure 2B), located under the probe, suctioned the water from about 2 cm above the water-sediment interface; it

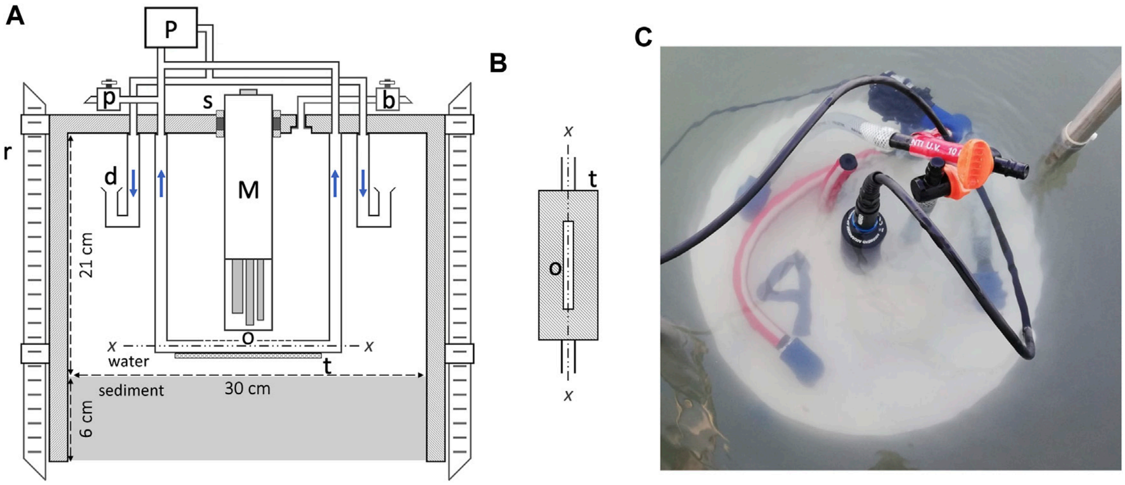

FIGURE 2
(A): schematic drawing of the SOD chamber (not in scale): pump (P); funnel-shaped flow diffusers (d); pump-priming cock (p); air bleed cock (b); multiprobe (M); centimeter steel rods, integral with the chamber (r); composite sleeve in PVC and Plastazote® (s); rectangular suction opening (o); PVC shielding plate (t). **(B)**: detail of the suction opening (o). **(C)**: photo of a chamber being immersed in the water column before deployment in the sediment.

consisted of a rectangular opening shielded towards the sediment by a thin sheet of PVC, to prevent the aspirated flow from causing the sediment to be resuspended. The outlet took place through two diffusers that directed the flow towards the upper part of the chamber.

The purpose of the water circulation is to achieve an approximately uniform DO concentration within the chamber, avoiding the occurrence of vertical concentration gradients and making the distance of the probe from the sediment surface substantially irrelevant. In natural systems, a diffusive boundary layer (DBL) (Jørgensen and Revsbech, 1985; Glud et al., 1994; Glud, 2008) at the sediment-water interface reduces the oxygen uptake and may lead to an underestimation of the SOD rate (Doyle and Rounds, 2003). DBL effectiveness is inversely related to the water flow velocity above the interface with the sediment. Inside the chamber, the water intake, which is designed to bring water near the sediment interface, has the purpose of counteracting the formation of DBL during the measurement or - at least - reducing the "effective DBL thickness" (Jørgensen and Des Marais, 1990). In any case, the diffusive oxygen uptake rate in coastal marine sediments makes up roughly only a half of the total uptake rate, the rest being due to irrigation and faunal respiration (Glud, 2008). In all the measurements carried out in this study, the same water recirculation speed was set to ensure repeatability and comparability of the measurement.

On the other hand, sediment resuspension within the chamber increases the surface area of the bottom material in contact with water, leading to an overestimation of the SOD rate (Doyle and Rounds, 2003). Therefore, every effort was made in the set-up of the benthic chamber to avoid resuspension. The shape and position of the inflow diffusers, the conformation of the pump intake inside the chamber, and the flow rate adjustment, obtained by modifying the propeller blades of the pump, were fundamental to this purpose. Laboratory tests were carried out to verify that the chamber did not generate resuspension of sediments during the measurement due to an excessive current speed at the water-sediment interface. To this purpose, silt-clayey sediments similar to those from the 16 measurement sites were used in the test, and the absence of resuspension in the incubated water was monitored with a small camera and a turbidity sensor. In the field, the turbidity sensor of the multi-probe used inside the benthic chamber constituted the ultimate check of the absence of resuspension phenomena throughout the measurement.

Preparation and use of the chamber *in situ*

Probes were calibrated before each field campaign using specific Aquaread standards for each sensor. The chamber was completely immersed in the water column by holding it by the 2-cm-steel rods (Figure 2C). Then the pump was turned on and primed, and it was ensured that all the air was expelled from the chamber through the bleed valve, which was finally closed. Hence the chamber was lowered and pushed into the bottom sediment; this step was done with care to minimize disturbance to the bottom. The benthic chamber had to remain completely submerged during the entire measurement period. It could be correctly deployed when the height of the water column was equal to at least 40 cm and could be used for measuring up to a

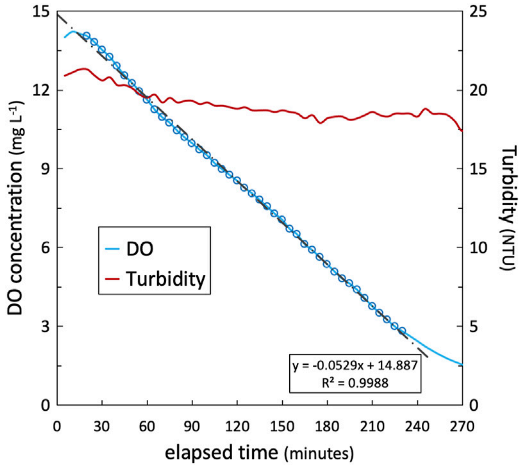

FIGURE 3
Example of oxygen depletion curve for a chamber placed at site CA2 (July 2021). The turbidity trend is superimposed. Slope m is calculated for the approximately straight section of the oxygen-depletion curve, which is highlighted with light blue dots.

minimum height of 25 cm. The final driving depth of the chamber could be precisely recorded, thanks to a centimeter-scale placed on the steel rods.

The chambers were deployed for periods ranging from 100 to 200 min and, less frequently, for longer periods. The pump, battery, and data logger were placed in a resealable polyethylene box, hung to a post driven into the sediment in the proximity of the benthic chamber.

SOD rate calculation

A typical plot of DO concentration depletion vs. time elapsed is shown in Figure 3.

With a linear regression applied to the approximately straight section of the curve, the slope m ($mg\ L^{-1}\ min^{-1}$) was determined and the SOD was obtained as in Murphy and Hicks (1986):

$$SOD_T = 1.44 * V * A^{-1} * m \tag{1}$$

where SOD_T is the sediment oxygen demand rate ($g\ m^{-2}\ d^{-1}$) at water temperature T (°C), V is the volume of incubated water (L), A is the area of sediment enclosed by the chamber (m^2), and 1.44 is a unit-conversion factor (from $mg\ min^{-1}$ to $g\ d^{-1}$).

Equation 1 can be rewritten as:

$$SOD_T = K * m \tag{2}$$

where K includes the geometric parameters of the chamber and the conversion for units of measurement. Chambers used in this study were characterized by K = 298; when the chamber insertion depth was slightly different from the expected 7 cm, a volume correction was made resulting in a K value in the range 270–327, comparable with that of other studies (Steeby et al., 2004 (K = 260); Ziadat and Berdanier, 2004 (K = 363); Doyle and Lynch, 2005 (K = 333); Utley et al., 2008 (K = 347); De Vittor et al., 2016 (K = 305)).

To compare SOD rates measured at different temperatures, the values are corrected to 20°C through a van't Hoff equation (Thomann and Mueller, 1987), as temperature affects the solubility of oxygen in water:

$$SOD_{20} = SOD_T * 1.065^{(20-T)}, \quad T \geq 10\,°C \tag{3}$$

which is no longer valid for T < 10°C (Rounds and Doyle, 1997).

The initial small increase of DO concentration observed in Figure 3 is due to the water mixing inside the chamber generated by the circulation induced by the pump. The inflection of the curve that sometimes occurs just below the DO concentration of 3 $mg\ L^{-1}$ reflects a situation where the respiration of microorganisms at the sediment surface begins to be oxygen limited. Beyond this point, this process may negatively influence the SOD rate value (Doyle and Lynch, 2005), and therefore SOD rate was calculated in the DO ≥ 3 $mg\ L^{-1}$ range.

In the first period of the study, measurements were done to determine the rate of DO depletion due to the oxygen demand rate of the water incubated inside the chamber (WOD), in order to be subtracted (*blank correction*) from the measured DO depletion rate values (Rounds and Doyle, 1997; Doyle and Lynch, 2005). This was done by filling with site water a thick 10 L opaque polyethylene container, which was left at the bottom for the entire duration of the measurement. The water-column oxygen demand was then determined by comparing the DO concentration at the beginning and end of the water incubation period.

WOD measurement can be affected by significant errors (Caldwell and Doyle, 1995; Heckathorn and Gibs, 2010) as waters incubated in the measuring chamber and the *blank* one may be dissimilar. As observed in other studies (Caldwell and Doyle, 1995; Rounds and Doyle, 1997; Wood, 2001; Heckathorn and Gibs, 2010) the WOD was found to be very small (1%–4%) compared to the measured SOD rate and its measurement was no longer deemed necessary, although it cannot be excluded that it was not negligible in particular environmental conditions encountered during the study.

A total of 141 measurements were performed at the 16 sites and the SOD rate was determined with linear regressions with coefficient of determination $R^2 > 0.94$.

Results and discussion

Sediment characteristics

Sediment analyses (TN, TOC, grain size, TIC, porosity) performed on samples from the 16 sites showed comparable

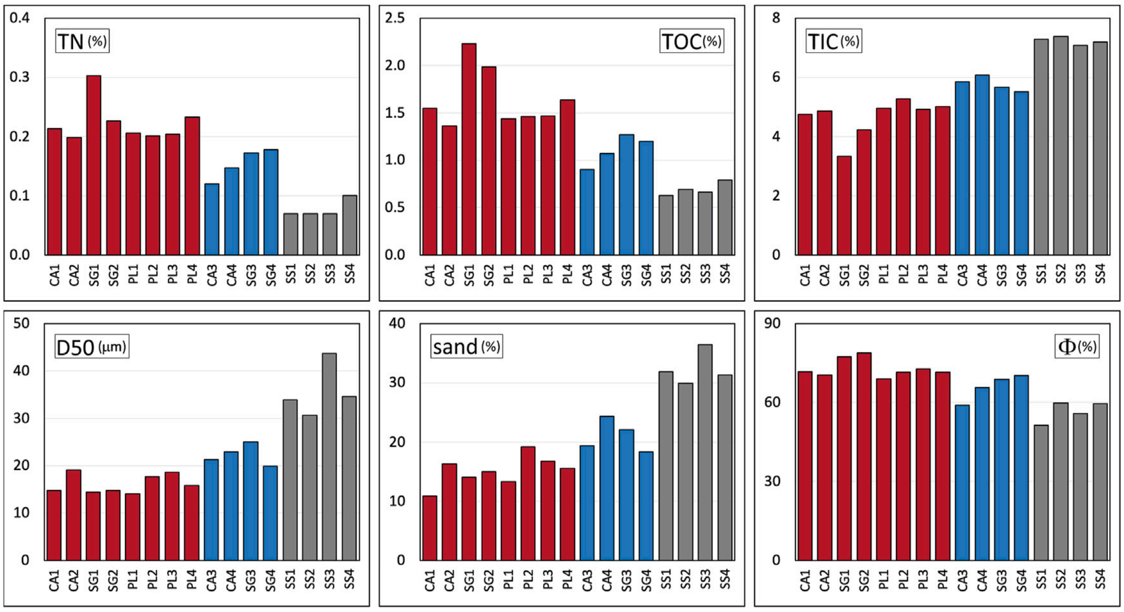

FIGURE 4
TN, TOC and TIC concentration values, D50 diameter, sand content (63–500 μm) and porosity in the 0–2 cm sediment layer of the 16 sites. Bar coloring highlights the three groups of sites.

values in the two sampling layers (0–1 and 1–2 cm) except for some variables at a few sites; therefore, the mean values between the two layers were considered. Value distributions among sites are shown in Figure 4. Grain-size characteristics are expressed as both the D50 value (median particle size, which is the particle size when the cumulative percentage reaches 50%) and sand content (in the dimensional range 63–500 μm).

The sediment of the Venice Lagoon has been extensively investigated since the 1980s, in terms of composition, texture, and contamination, over the entire waterbody as well as in sectors of interest for specific environmental problems (e.g., Zonta et al., 2018 and references therein). The obtained data reflected the known characteristics of the lagoon sediments. A clear difference was observed between sites of the SS area compared to the others, with the former characterized by a coarser particle size, lower porosity, a greater presence of TIC and a lower content of TOC and TN.

CA, SG, and PL areas are located close to the lagoon-mainland interface, which has higher water renewal times (Cucco and Umgiesser, 2006; Ferrarin et al., 2013), lower salinity (Guerzoni and Tagliapietra, 2006) and finer-sized sediments (Zonta et al., 2018) than the SS area, which belongs to the central lagoon. The lagoon sector that includes CA, SG, and PL areas is classified as a “marginal” water body, based on the classification of the Water Framework Directive (WFD), as a result of the resolution of the transition gradient in discrete water bodies in the lagoon (Tagliapietra et al., 2011; ISPRA and ARPAV, 2018). This sector is interested by the presence of the mouths of freshwater tributaries delivering nutrients and chemical compounds from the drainage basin (Collavini et al., 2005), and it is particularly vulnerable to low oxygen conditions in the summer months (ISPRA and ARPAV, 2016; ISPRA and ARPAV, 2018; ISPRA and ARPAV, 2021). The lagoon sector that includes the SS area is instead classified as “open lagoon”, characterized by greater salinity, water exchange, and bathymetry, due to the water circulation driven by the inlets that allow water exchange with the Adriatic Sea.

Among the 12 sites located in the “marginal” sector, two groups can be distinguished on the basis of sediment variables. The first group includes the four sites within the CA and SG areas furthest away from the lagoon-mainland interface (CA3, CA4, SG3, SG4); the second one includes the other four sites (CA1, CA2, SG1, SG2) and the four sites of the PL area.

In the CA area there is a gradient of fine particle content decreasing from the mainland towards the lagoon (from CA1 to CA4), and the sediment of the two more confined sites (CA1 and CA2) has a higher concentration of TN and TOC than the other two (CA3 and CA4). Similarly, these differences are observed between the SG sites close to the mainland (SG1 and SG2) and the more distant ones (SG3 and SG4). SG1 has the finest median grain size and the greatest content of TN and TOC among the 16 sites, due to the proximity of the mouth of the Osellino canal, which is a source of fresh water and fine particles from the drainage basin into the lagoon. Incidentally, small but significant

FIGURE 5
SOD_T and SOD_{20} 2021 monthly trend rates at the 16 sites. Water temperature measured inside the benthic chamber is also shown. Two measurements were done in the CA area in June, and two in SG both in August and September.

differences are observed due to the greater proximity of SG3, compared to SG4, to a main channel that determines the tidal impulse propagation and therefore the water renewal in the area.

Grain size, porosity, and TIC in these sites are not expected to change substantially in the short term, as evidenced by the scarce variations of the measured values between the upper layer (0–1) and the subsurface layer (1–2 cm), in agreement with previous studies (Sfriso et al., 2005; Zonta et al., 2018). TOC and TN may instead be subject to greater annual variability.

SOD values distribution

Two field tests were conducted to verify the repeatability of the SOD rate measurement. For this purpose, four benthic chambers were placed within a small area at the CA3 and CA4 sites. Low coefficients of variation (CV%) were obtained for the SOD rate (6.2 and 14.8%, respectively), which we attribute more to the heterogeneous nature of the bottom sediments than to possible artifacts in the measurement.

Distributions of the measured SOD_T and SOD_{20} values over the year are shown in Figure 5, together with the water temperature (T) measured inside the benthic chamber. SOD_T values ranged from 0.63 to 24.00 g m^{-2} d^{-1} and T values from 11.7 to 33.3°C. Higher values were registered in the warm months in all sites, due to the increase of the rate of oxygen-depleting processes. A significant values increase was recorded as early as June in the more confined sites of CA (CA1 and CA2) and SG (SG1 and SG2) areas, whereas it occurred in July in the PL area.

Towards the end of the year, a more or less marked increase in the SOD_T rate was observed in several sites, despite the decrease in water temperature. Particularly, in the SS3 and SS4 sites, the highest values of the study were recorded in October and rates remained relatively high in November. We ascribed these values to the presence of macroalgae fragments (*Ulva* spp. and *Gracilaria* spp.) near the water-sediment interface, some of which may have become trapped in the benthic chamber, producing an extra contribution to oxygen consumption.

Correcting the SOD_T value by the water temperature resulted in a more flattened SOD_{20} rate distribution. The latter, however, retained considerable variability between sites and months of measurement (from 0.87 to 14.48 g m^{-2} d^{-1}).

Relation between SOD rate and sediment characteristics

The SOD_{20} records were in agreement with the subdivision of the 16 sites in the three groups observed on the basis of sediment

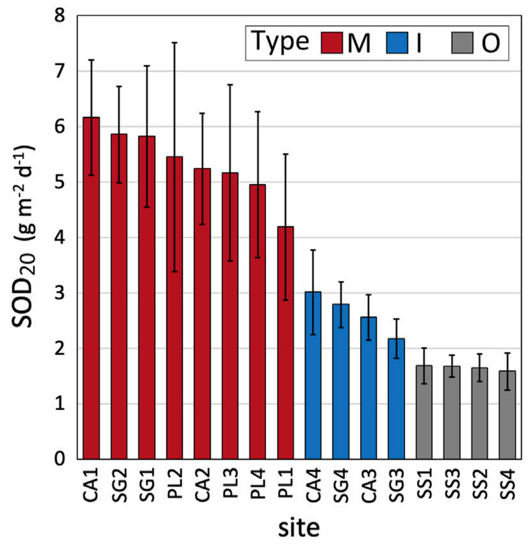

FIGURE 6
Mean SOD_{20} rate for the whole period in the 16 sites, in increasing order; the line indicates the standard deviation value. Bar coloring highlights the three types of sites.

TABLE 3 Pearson correlation matrix calculated among variables measured in the sediment collected in May 2021 at 16 sites, mean SOD_{20} rate in the 2021 and site depth. Two SOD_{20} rates measured in SS3 and SS4 in October were excluded. All correlation coefficients are significant at $\alpha < 0.05$. Distribution normality for each variable was verified using the Kolmogorov-Smirnov test ($p > 0.01$).

	SOD_{20}	TN	TOC	TIC	D50	Sand	Φ
TN	0.88						
TOC	0.88	0.97					
TIC	−0.89	−0.97	−0.96				
D50	−0.84	−0.88	−0.84	0.88			
sand	−0.85	−0.89	−0.84	0.91	0.97		
Φ	0.86	0.93	0.94	−0.92	−0.85	−0.85	
depth	−0.83	−0.81	−0.80	0.89	0.90	0.92	−0.78

characteristic (Figure 4). Figure 6 shows mean SOD_{20} values (from 1.58 to 6.16 g m^{-2} d^{-1}) recorded over the entire measurement period. The more confined eight sites (CA1, CA2, SG1, SG2, and the four sites in the PL area) had the highest SOD_{20} values (Type M sites–*marginal*), whereas the lowest ones were recorded in the SS area (Type O sites–*open lagoon*). The remaining four sites (CA3, CA4, SG3, SG4) had intermediate values (Type I sites–*intermediate*).

The subdivision of the 16 sites in three types is highlighted in the dendrogram of Figure 7, obtained from a cluster analysis performed on SOD_{20}, TN and D50 values. It is important to underline how small distances in the position of a pair of sites (1 and 2) with respect to the other (3 and 4) in the SG area and especially in the CA area determined different characteristics of the sediment and consequently different SOD rates.

The correspondence between the sediment characteristics and the mean SOD_{20} rates is summarized by the correlation matrix shown in Table 3. Data normality for each variable was verified using the Kolmogorov-Smirnov test ($p > 0.01$) after a Iglewicz and Hoaglin outlier test (Iglewicz and Hoaglin, 1993). The latter indicated the two aforementioned values recorded in the SS3 and SS4 sites in October as outliers, which were therefore excluded from the statistics.

Two elements (regression of SOD_{20} concerning TN and D50, respectively) of the correlation matrix in Table 3 are shown in Figure 8 to highlight the differentiation of the 16 sites into three types. Various authors have considered sediment grain size and organic matter concentration (frequently measured with the *Loss on Ignition* technique) with respect to the variation of SOD rate in statistical analyses (e.g., Butts and Evans, 1979; Wood, 2001; Doyle and Lynch, 2005; Foster et al., 2016). Generally, clear-cut relationships were not obtained but instead a more or less defined linear dependence. The degree of correlation obtained in the present study was relatively high among all the variables involved. The reason presumably lay in both having compared mean values of SOD_{20} measured for a long period and the selection of a set of sites with quite diversified characteristics - even if typical of the Venice Lagoon.

Among the few studies of sediment and DO in the Venice Lagoon, Melaku Canu et al. (2003) developed an ecological model that simulated the evolution of nine ecological state variables, including DO concentration. In the mass balance components, they assumed a value of SOD_{20} = 1.08 g m^{-2} d^{-1}. Based on the experimental results of our study, the value assumed in the model seems excessively low, being respectively about 66 and 20% of the mean SOD_{20} rate value measured in sites representative of the open lagoon (Type O, 1.65) and the more confined sites (Type M, 5.35 g m^{-2} d^{-1}). SOD rate distribution values obtained from the study may be useful for mathematical models aimed at the simulation of the distribution of DO concentration in the lagoon system.

The correction of SOD_T measurement (Eq. 3) - which produces the SOD_{20} value - removes the effect of temperature on the solubility of the oxygen in the water column, but other factors still introduce a dependence of SOD_{20} on T. Observing the temporal trend of SOD_{20} (Figure 5), the permanence of an indirect relationship with the temperature after the rate correction is in fact evident, in particular in the Type M sites that in the summer period showed significantly higher values than in the other months.

In addition to temperature and sediment characteristics, SOD is influenced by variables that depend on the conditions of the water column (available oxygen, velocity of the current on the sediments, aeration), as well as the chemistry of the interstitial water. Even more important factors are the quality and quantity

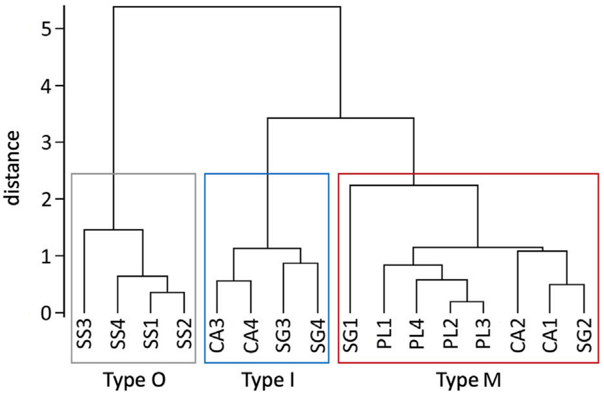

FIGURE 7
Dendrogram obtained from a cluster analysis performed on mean SOD_{20} rate, TN concentration, and D50 data (complete-linkage hierarchical clustering).

of the organic matter and the composition of the biological community (Bowie et al., 1985), which change with the availability of DO and nutrients.

The consumption of organic matter is due to the growth dynamics of the microbial populations, which in turn are linked to temperature and organic matter supply and type, as well as the composition of the biological community and biotic interactions. Temperature affects the metabolism of oxygen-consuming microorganisms in the sediment, their density, and community structure (Arnosti et al., 1998; Thamdrup et al., 1998; Zakem et al., 2021). The characteristics of the organic matter are also of considerable importance in this process since the rate of degradation depends on its lability (Boudreau, 1992; Kirchman et al., 2005; Fagervold et al., 2014; Zakem et al., 2021). The dependence of the SOD rate on the presence of microbial communities and other organisms in the sediment is beyond the scope of this study.

Estimating water column DO depletion due to the sediment during MOSE closures

According to the present management scenario, the MOSE gates would temporarily isolate the Venice Lagoon from the Adriatic Sea during tides greater than 110 cm (*safeguard threshold*, Ruol et al., 2020) above the *Punta Salute* reference level (PS, Figure 1). The latter is 26 cm below the current mean sea level. The 110-cm level is a compromise among the physical protection of the city, ensuring the naval commercial traffic through the inlets, and maintaining the water exchanges between the lagoon and the sea (Trincardi et al., 2016). When a high tide event is forecasted, the gates are closed before the 110-cm level is reached, depending on the meteorological situation (wind speed, rainfall intensity); when a normal storm occurs, the MOSE is closed with a water level equal to 90 cm (Umgiesser, 2020).

In the absence of exchange between lagoon and sea, the water will be stagnant and the oxygen "starvation" of the sediment could have a greater negative effect on the oxygen balance. To evaluate the effect of sediment on oxygen depletion, we considered a simplified scenario: 1) the water column is stationary (no tide or wind-induced current) and sediment resuspension does not occur; 2) the water level at all sites is that corresponding to a level of 90 cm at station PS; 3) the initial oxygen concentration in the water column is equal to 9.17 mg L^{-1}, i.e., the saturation concentration value at 20°C; 4) there is neither production nor consumption of oxygen due to aeration and processes in the water column; 5) the water column is mixed and there is no the formation of a DBL at the sediment interface.

The time (t_{HYP}) to reach the hypoxia value (2.8 mg L^{-1}) in the whole water column due to the SOD rate alone, during the closing of the MOSE, was estimated in the 16 sites and at different water temperatures. The rate value of SOD_T was used as it reflects - unlike SOD_{20} - the actual DO consumption of the sediment at a given T.

In Eq. 2, m is expressed as the ratio between the difference in oxygen concentration at saturation and at the limit of hypoxia and the time to reach that limit, obtaining:

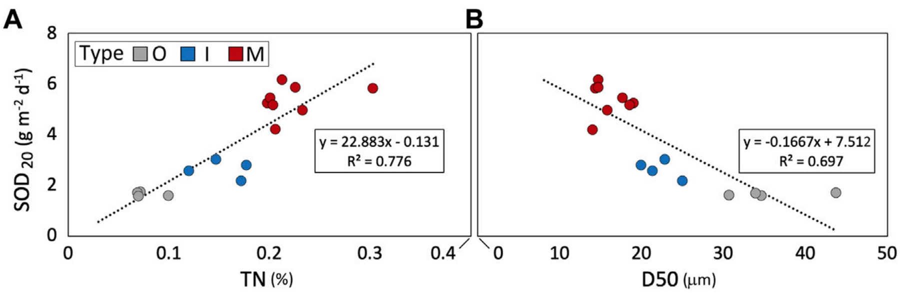

FIGURE 8
Regression plot between mean SOD_{20} and **(A)** TN concentration and **(B)** D50. The three types of sediments are highlighted with different colors.

TABLE 4 Estimated time elapsing (t_{HYP}) from the DO saturation to the limit of hypoxia values in the whole water column, due to the SOD_T rate at the conditions simulating the MOSE closure.

Date of deployment	**T**	**t HYP**	**T**	**t HYP**	**T**	**t HYP**	**T**	**t HYP**
	˚C	**hour**	**˚C**	**hour**	**˚C**	**hour**	**˚C**	**hour**
	CA1		**CA2**		**CA3**		**CA4**	
16/03/2021	11.74	62	11.62	90	11.84	148	11.83	184
29/03/2021					16.24	215	16.90	84
17/05/2021	22.66	28	22.62	25	22.45	61	22.38	86
11/06/2021	26.55	11	26.72	15			26.27	22
17/06/2021	33.27	9					32.00	38
20/07/2021	30.65	11	30.69	11	29.96	29	29.75	31
25/08/2021	25.93	19	26.24	20	25.54	44		
22/09/2021	19.63	38	20.50	48	23.32	93	19.62	153
26/10/2021	13.12	80	14.24	83	13.78	138	13.31	138
12/11/2021	12.35	46	13.60	59	13.02	93	12.46	109
	SG1		**SG2**		**SG3**		**SG4**	
17/03/2021	12.42	89	12.98	69	12.03	207		
16/04/2021	16.43	50	15.98	47			14.81	85
17/05/2021	20.96	39	21.22	24	20.91	99	20.58	49
11/06/2021	26.96	12	28.27	12			26.54	42
20/07/2021	28.29	29	28.53	12	28.30	57	28.72	49
03/08/2021	27.36	10	29.23	12	27.02	38	27.02	44
25/08/2021	26.99	21	27.02	16			26.98	67
07/09/2021			24.82	27			25.15	67
22/09/2021	21.91	25	23.02	25	22.20	101	22.87	89
26/10/2021	13.91	45	14.64	76	13.45	207	13.36	206
12/11/2021	13.38	60	14.81	50	14.30	175	13.76	130
	PL1		**PL2**		**PL3**		**PL4**	
24/03/2021	12.26	200	12.17	233	12.42	115	12.36	118
15/04/2021	14.02	237	13.33	332	15.75	251	15.95	115
14/05/2021	20.58	92	21.70	71	21.84	53	21.45	59
10/06/2021			25.87	35	26.41	41	26.30	37
19/07/2021	28.39	25	28.02	9	28.52	11	28.59	13
23/08/2021	27.78	21	27.88	18	27.15	17	28.00	16
20/09/2021	25.96	16	25.00	25	25.14	29	25.27	52
25/10/2021	15.83	96	17.03	56	16.74	66	18.20	54
17/11/2021	15.56	44	14.58	38	15.23	46	14.72	46
	SS1		**SS2**		**SS3**		**SS4**	
24/03/2021	13.22	368	13.69	259	13.58	298	13.60	348
15/04/2021	13.42	171	13.17	223	13.21	346	13.55	328
14/05/2021	20.15	237	20.49	205	20.26	278	20.45	226
10/06/2021	25.70	213	25.14	146	25.68	112		
19/07/2021	29.08	91	28.94	60	28.73	83	28.71	192
23/08/2021	27.20	70			26.88	97	26.66	123
20/09/2021	23.97	160	22.60	192	22.76	158	23.50	146
25/10/2021	15.04	138	15.07	309	14.45	93	15.15	70
17/11/2021	13.28	239	13.23	208	13.30	207	13.50	151

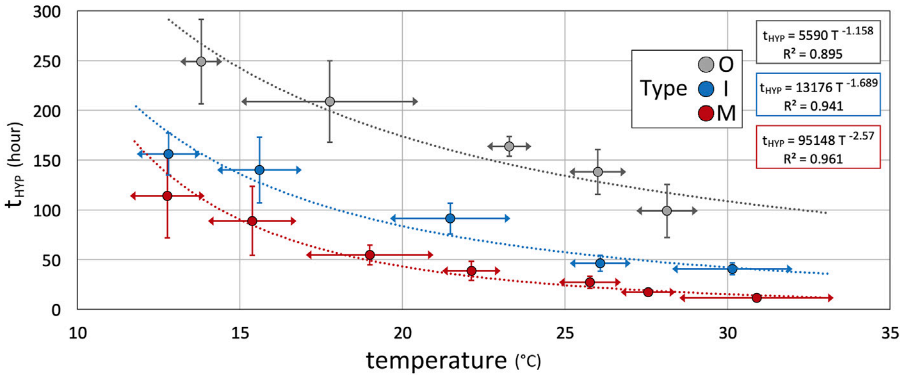

FIGURE 9
Plot of the relationship between temperature and t_{HYP} for the three types of sites. Dots represent mean values of t_{HYP} in the selected T range, highlighted by horizontal arrows; vertical segments indicate the respective t_{HYP} standard deviation.

$$t_{HYP}{}^{BC} = (K*6.37)*SOD_T{}^{-1} \tag{4}$$

where $t_{HYP}{}^{BC}$ is the time in minutes elapsed to enter the hypoxia condition within the benthic chamber and K is defined in Eq. 2; the concentration of 6.37 (mg L^{-1}) is the difference between DO content in water at saturation and the hypoxia limit.

Considering the entire water column, the time to hypoxia t_{HYP}, in hours, results from a proportion:

$$t_{HYP} = t_{HYP}{}^{BC}*H*(60*h)^{-1} = 0.57*K*H*\left(10^2*SOD_T\right)^{-1} \tag{5}$$

where the height of the water column (H) is given by 90 cm plus the bathymetric height at the site (Table 2), and h is the height of incubated water inside the benthic chamber; 60 is the conversion factor between minutes and hours. Obtained values of t_{HYP} are shown in Table 4; they range from a maximum of 368 h (SS1, in March, with T = 13.22°C) to a minimum of 9 h (CA1 with T = 33.27 and PL2 with T = 28.02°C, both in July).

Figure 9 shows the power regression obtained for the mean t_{HYP} values over selected intervals of T, for the three types of sites; data normality for each type was verified using the Kolmogorov-Smirnov test ($p > 0.01$). Type M sites were prone to reach hypoxic conditions within 48 h of MOSE closure at a water temperature of about 22°C. For temperatures around 30°C, these conditions can be reached in about half a day. Despite being located near Type M sites, oxygen consumption in Type I sites was significantly slower and remained on the order of 2 days even at higher water temperatures. Instead, Type O sites showed a greater "resistance" to the depletion of oxygen caused by the closure of the MOSE, with a t_{HYP} always greater than 4 days.

Following the first closure of the MOSE system, on 3 October 2020, the gates were raised on 34 occasions until 11 December 2021 (MOSE, 2022), mainly in autumn, since floods conditions frequently occur in that period, due to several forcing weather-marine factors (Camuffo, 1993). The mean daily temperatures recorded at the PS station on these 34 days ranged from a minimum of 6.8 to a maximum of 16.5°C (mean 10.1 ± 2.8°C standard deviation). The longest closure period lasted about 42 h (from 4 to 6 December 2020), with an average water temperature of 8.90°C. The climatic conditions in which the MOSE is currently activated are not such as to trigger a relevant consumption of DO by the lagoon sediments. If in the future the MOSE closures will take place with higher temperatures and/or for longer periods, the sediment could play an important negative role in the oxygen balance in the water column, starting from the marginal areas.

Brigolin et al. (2021) investigated the relationship between sediment early diagenesis and hypoxia conditions in the water column in five sites of the central lagoon, analyzing sediment cores in the laboratory by using microelectrodes. The investigation was based on the Diffusive Oxygen Uptake rates (DOU), measured through the O_2 concentration gradient calculated over 400 μm in the sediment micro-profile. They estimated that the DO hypoxic level at T = 25°C is reached in the water column in 5–18 days, depending on site. As in our scenario, they neglected oxygen renewal associated with primary production, exchange with the atmosphere, and advection. For sites where sediment is less likely to consume the DO of the water column (Type O) our estimated t_{HYP} at 25°C is around 5 days, which corresponds to the worst situation measured by Brigolin et al. (2021). The difference between the two results can be ascribed to the different measurement methodology and to the fact that DOU constitutes only a fraction of the Total Oxygen Uptake (TOU) (Jørgensen et al., 2022). Whatever the method (sediment cores in the laboratory or benthic chambers in the field), the measurement systems are only an imperfect model of natural conditions and their relative advantages or disadvantages are questionable (Coenen et al., 2019 and references therein). If the sediment at the measurement site is heterogeneous, especially in respect to macrobenthos activity, drastic differences may result

(Coenen et al., 2019) due to the disparity between areas of the sediment surfaces examined.

Conclusion

A new era of "regulated flows" has begun for the Venice Lagoon as a result of the start of operations of the MOSE system in October 2020, which temporarily seals the water body during high tide events in the Adriatic Sea. The regulation of the tidal flow is expected to lead to a general increase in the water renewal time in the lagoon and this motivated the investigation of the oxygen-consuming action of the sediment.

SOD rate was measured in a range of water temperature from 11.7 to 33.3°C. The measured SOD rate values (SOD_T) ranged from 0.63 to 24.00 $g\ m^{-2}\ d^{-1}$; once standardization was carried out at a temperature of 20°C (SOD_{20}), the resulting range of variation was equal to 0.87–14.48 $g\ m^{-2}\ d^{-1}$.

Sediment characteristics and SOD value distribution reflected different lagoon conditions, in terms of bathymetry, hydrodynamics, and water renewal. A subdivision of the sites into three typologies was observed based on the distribution of SOD_{20} values and sediment characteristics. Four sites belonging to the open lagoon (named Type O- *open lagoon*), characterized by coarser particle size, a greater presence of TIC, and less TOC and TN, showed lower SOD values. The eight more confined sites (Type M - *marginal*) showed instead the higher values of SOD, particularly in the warm months. The remaining four sites (Type I - *intermediate*) had intermediate both sediment features and SOD values.

The dependence of the SOD rate on both availability and type of organic matter presence and composition and growth of microbial communities, which is beyond the scope of this study, should be investigated at different water temperatures in an adequate number of lagoon sites.

In a simplified scenario, which involved the absence of both primary production and water renewal/aeration, the incidence of sediment on the DO concentration in the water column has been estimated at the closure of the MOSE, for different range of water temperatures and the three types of sites. In a still and completely mixed water column, it was found that the time (t_{HYP}) elapsing from the saturation of DO (9.17 $mg\ L^{-1}$) to the hypoxia values (2.8 $mg\ L^{-1}$) has a different power relationship with the temperature in the three types of sites. In the confined sites, DO concentration in the water column can be depleted in about a day, at temperatures of ca. 25°C.

The MOSE system is currently activated for short periods in the cold months, when low water temperatures do not trigger a relevant consumption of DO by the lagoon sediments. However, the ongoing climate change could lead to longer lasting MOSE closure with higher temperatures in the future. At that point the sediment will be able to exert a strong action of oxygen consumption in the water column, especially in the marginal areas of the lagoon.

Data availability statement

The raw data supporting the conclusions of this article will be made available by the authors, without undue reservation.

Author contributions

Conceptualization, SL, DT, and RZ; Methodology, DC, SL, GM, and RZ; Validation, JD, SL, DT, and RZ; Formal Analysis, FA, DC, SL, and RZ; Investigation, SL, DC, GM, FA, and RZ; Resources, DC and GM; Data Curation, SL and RZ; Writing—Original Draft Preparation, SL and RZ; Writing—Review and Editing, JD, SL, DT, and RZ; Visualization, SL and RZ; Supervision, RZ; Project Administration, RZ; Funding Acquisition, RZ.

Funding

Scientific activity performed in the Research Programme Venezia 2021 (Scientific research program for a "regulated" lagoon), coordinated by CORILA (Consortium for coordination of research activities concerning the Venice Lagoon system), with the contribution of the Ministero delle Infrastrutture e della Mobilità Sostenibili - Provveditorato Interregionale per le Opere Pubbliche del Veneto - Trentino Alto Adige - Friuli Venezia Giulia.

Acknowledgments

We thank Loris Dametto and Gianfranco Magris (CNR ISMAR, Venice, Italy), Daniele Curiel and Emiliano Checchin (SELC, Venice, Italy) for the support provided in the field activities. Roberto Pini (CNR IRET, Pisa, Italy) carried out the analysis to determine sediment grain size. Leonardo Langone and Fabio Savelli (Laboratory for the measurement of N and C contents and stable isotopes - CNR ISMAR, Bologna, Italy) performed the elementary analyzes. Paola Focaccia (CNR ISMAR, Bologna, Italy) took care of the administrative aspects of the project. The DO% data of station S1 (SAMANET network) was provided by the Ministero delle Infrastrutture e della Mobilità Sostenibili - Provveditorato Interregionale per le Opere Pubbliche del Veneto - Trentino Alto Adige - Friuli Venezia Giulia. Franca Pastore (Centro Previsioni e Segnalazioni Maree, Venice Municipality) provided recordings of tide and temperature data acquired from the *Punta Salute* (PS) tide gauge. Caterina Dabalà (CORILA) assisted in retrieving data from institutional measurement stations. The authors gratefully thank Alberto Zirino (Scripps Institution of Oceanography, US) for the constructive comments and recommendations, and Carlo Corsaro for revising the English language.

Conflict of interest

The authors declare that the research was conducted in the absence of any commercial or financial relationships that could be construed as a potential conflict of interest.

The handling editor CB declared a shared affiliation with the authors at the time of review.

Publisher's note

References

Altieri, A. H., and Diaz, R. J. (2019). "Dead zones: Oxygen depletion in coastal ecosystems," in *World seas: An environmental evaluation. Ecological issues and environmental impacts*. Editor C. Sheppard. 2nd Edition (Academic Press), Vol. III, 453–473. doi:10.1016/B978-0-12-805052-1.00021-8

Arnosti, C., Jorgensen, B. B., Sagemann, J., and Thamdrup, B. (1998). Temperature dependence of microbial degradation of organic matter in marine sediments: Polysaccharide hydrolysis, oxygen consumption, and sulfate reduction. *Mar. Ecol. Prog. Ser.* 165, 59–70. doi:10.3354/meps165059

Avnimelech, Y., Ritvo, G., Meijer, L. E., and Kochba, M. (2001). Water content, organic carbon and dry bulk density in flooded sediments. *Aquac. Eng.* 25, 25–33. doi:10.1016/S0144-8609(01)00068-1

Bernardi Aubry, F., Acri, F., Scarpa, G. M., and Braga, F. (2020). Phytoplankton–macrophyte interaction in the lagoon of Venice (northern Adriatic Sea, Italy). *Water* 12, 2810. doi:10.3390/w12102810

Boudreau, B. P. (1992). A kinetic model for microbic organic-matter decomposition in marine sediments. *FEMS Microbiol. Lett.* 11 (1), 1–14. doi:10.1111/j.1574-6968.1992.tb05789.x

Bowie, G. L., Mills, W. B., Porcella, D. B., Campbell, C. L., Pagenkopf, J. R., Rupp, G. L., et al. (1985). *Rates, constants, and kinetics formulations in surface water quality modeling*. second edition. Athens, GA: United States Environmental Protection Agency. EPA/600/3-85/040.

Breitburg, D., Levin, L. A., Oschlies, A., Grégoire, M., Chavez, F. P., Conley, D. J., et al. (2018). Declining oxygen in the global ocean and coastal waters. *Science* 359, eaam7240. doi:10.1126/science.aam7240

Brigolin, D., Rabouille, C., Demasy, C., Bombled, B., Monvoisin, G., and Pastres, R. (2021). Early diagenesis in sediments of the Venice lagoon (Italy) and its relationship to hypoxia. *Front. Mar. Sci.* 7, 575547. doi:10.3389/fmars.2020.575547

Butts, T. A., and Evans, R. L. (1979). *Sediment oxygen demand in a shallow oxbow lake*. Urbana, IL: Illinois State Water Survey, Circular, 136.

Caldwell, J. M., and Doyle, M. C. (1995). Sediment oxygen demand in the lower willamette river, Oregon, 1994. *U.S. Geol. Surv. Water-Resources Investig. Rep.* 95, 4196. doi:10.3133/wri954196

Camuffo, D. (1993). Analysis of the sea surges at Venice from A.D. 782 to 1990. *Theor. Appl. Climatol.* 47, 1–14. doi:10.1007/BF00868891

Caraco, N. F., and Caraco, J. J. (2002). Contrasting impacts of a native and alien macrophyte on dissolved oxygen in a large river. *Ecol. Appl.* 12, 1496–1509. doi:10.1890/1051-0761(2002)012[1496:cioana]2.0.co;2

Castel, J., Caumette, P., and Herbert, R. (1996). Eutrophication gradients in coastal lagoons as exemplified by the Bassin d'Arcachon and the Etang du Prevost. *Hydrobiologia* 329, ix–xxviii. doi:10.1007/BF00034542

Cavaleri, L., Bajo, M., Barbariol, F., Bastianini, M., Benetazzo, A., Bertotti, L., et al. (2020). The 2019 flooding of Venice and its implications for future predictions. *Oceanogr. Wash. D. C).* 33, 42–49. doi:10.5670/oceanog.2020.105

Chau, K. W. (2002). Field measurements of SOD and sediment nutrient fluxes in a landlocked embayment in Hong Kong. *Adv. Environ. Res.* 6 (2), 135–142. doi:10.1016/S1093-0191(00)00075-7

Coenen, E. N., Christensen, V. G., Bartsch, L. A., Kreiling, R. M., and Richardson, W. N. (2019). Sediment oxygen demand: A review of *in situ* methods. *J. Environ. Qual.* 48, 403–411. doi:10.2134/jeq2018.06.0251

Collavini, F., Bettiol, C., Zaggia, L., and Zonta, R. (2005). Pollutant loads from the drainage basin to the Venice Lagoon (Italy). *Environ. Int.* 31 (7), 939–947. doi:10.1016/j.envint.2005.05.003

Collins, M., Knutti, R., Arblaster, J., Dufresne, J. L., Fichefet, T., Friedlingstein, P., et al. (2013). "Long-term climate change: Projections, commitments and irreversibility," in *Climate change 2013: The physical science basis. Contribution of working group I to the fifth assessment report of the intergovernmental panel on climate change*. Editors T. F. Stocker, D. Qin., G.-K. Plattner, M. Tignor, S. K. Allen, J. Boschung, et al. (Cambridge, United Kingdom and New York, NY, USA: Cambridge University Press), 1029–1136.

Cucco, A., and Umgiesser, G. (2006). Modeling the Venice lagoon residence time. *Ecol. Modell.* 193, 34–51. doi:10.1016/j.ecolmodel.2005.07.043

De Vittor, C., Relitti, F., Kralj, M., Covelli, S., and Emili, A. (2016). Oxygen, carbon, and nutrient exchanges at the sediment-water interface in the Mar Piccolo of Taranto (Ionian Sea, southern Italy). *Environ. Sci. Pollut. Res.* 23, 12566–12581. doi:10.1007/s11356-015-4999-0

Diaz, R. J., and Rosenberg, R. (1995). Marine benthic hypoxia: A review of its ecological effects and the behavioral responses of benthic macrofauna. *Oceanog. Mar. Biol. Annu. Rev.* 33, 245–303. doi:10.1126/science.1156411

Doyle, M. C., and Lynch, D. D. (2005). *Sediment oxygen demand in lake ewauna and the klamath river, Oregon, June 2003*. U.S. Geological Survey Scientific Investigations. Report 2005-5228.

Doyle, M. C., and Rounds, S. (2003). *The effect of chamber mixing velocity on bias in measurement of sediment oxygen demand rates in the tualatin river basin, Oregon*. Portland, OR: U.S. Geological Survey: Water-Resources Investigations. Report 03-4097.

Fagervold, S. K., Bourgeois, S., Pruski, A. M., Charles, F., Kerhervé, P., Vétion, G., et al. (2014). River organic matter shapes microbial communities in the sediment of the Rhône prodelta. *ISME J.* 8, 2327–2338. doi:10.1038/ismej.2014.86

Ferrarin, C., Ghezzo, M., Umgiesser, G., Tagliapietra, D., Camatti, E., Zaggia, L., et al. (2013). Assessing hydrological effects of human interventions on coastal systems: Numerical applications to the Venice lagoon. *Hydrol. Earth Syst. Sci.* 17, 1733–1748. doi:10.5194/hess-17-1733-2013

Foster, G. M., King, L. R., and Graham, J. L. (2016). *Sediment oxygen demand in eastern Kansas streams, 2014 and 2015*. Reston, VA: U.S. Geological Survey Investigations. Report 2016-5113.

Garcia, H. E., and Gordon, L. I. (1992). Oxygen solubility in seawater: Better fitting equations. *Limnol. Oceanogr.* 37 (6), 1307–1312. doi:10.4319/lo.1992.37.6.1307

Giordani, G., Austoni, M., Zaldivar, J. M., Swaney, D. P., and Viaroli, P. (2008). Modelling ecosystem functions and properties at different time and spatial scales in shallow coastal lagoons: An application of the LOICZ biogeochemical model. *Estuar. Coast. Shelf Sci.* 77, 264–277. doi:10.1016/j.ecss.2007.09.017

Glud, R. N., Gundersen, J. K., Jorgensen, B. B., Revsbech, N. P., and Schulz, H. D. (1994). Diffusive and total oxygen-uptake of deep-sea sediments in the eastern south-atlantic-ocean: *In situ* and laboratory measurements. *Deep Sea Res. Part I Oceanogr. Res. Pap.* 41 (11-12), 1767–1788. doi:10.1016/0967-0637(94)90072-8

Glud, R. N. (2008). Oxygen dynamics of marine sediments. *Mar. Biol. Res.* 4, 243–289. doi:10.1080/17451000801888726

Guerzoni, S., and Tagliapietra, D. (2006). *Atlante della laguna - Venezia tra terra e mare*. Venezia (Italy): Ed. Marsilio, 42–43. ISBN88-317-8764-0 (*in Italian*). English version available at the website: atlante.silvenezia.it/en/start_atlante_ns.phtml.

Hatcher, K. J. (1986). "Introduction to part 1: Sediment oxygen demand processes," in *Sediment oxygen demand: Processes, modeling and measurement*. Editor K. J. Hatcher (Athens, GA, USA: Institute of Natural Resources, University of Georgia), 3–8.

Heckathorn, H. A., and Gibs, J. (2010). *Sediment oxygen demand in the saddle river and salem river watersheds*. New Jersey: U.S. Geological Survey Scientific Investigations. Report 2010–5093.

Hobbs, C. H. (1983). A method for determining the dry bulk density of subaqueous sediments. *J. Sediment. Res.* 53, 663–665. doi:10.2110/jsr.53.663

Iglewicz, B., and Hoaglin, D. C. (1993). How to detect and handle outliers. *Am. Soc. Qual. Control (ASQC), Basic reference Qual. control* 16, 87. ISBN 0-87389-247-X.

ISPRA and ARPAV (2016). "Monitoraggio della Laguna di Venezia ai sensi della Direttiva 2000/60/CE finalizzato alla definizione dello stato ecologico," in

Valutazione dei dati acquisiti nel monitoraggio ecologico 2013-2015 ai fini della classificazione ecologica dei corpi idrici lagunari, 114. (in Italian).

ISPRA and ARPAV (2018). "Monitoraggio della Laguna di Venezia ai sensi della Direttiva 2000/60/CE finalizzato alla definizione dello stato ecologico," in *Valutazione dei dati acquisiti nel monitoraggio ecologico 2014-2016 ai fini della classificazione ecologica dei corpi idrici lagunari*, 117. (in Italian).

ISPRA and ARPAV (2021). "Monitoraggio della Laguna di Venezia ai sensi della Direttiva 2000/60/CE finalizzato alla definizione dello stato ecologico," in *Valutazione dei dati acquisiti nel monitoraggio ecologico 2017-2019 ai fini della classificazione ecologica dei corpi idrici lagunari*, 112. (in Italian).

Jørgensen, B. B., and Des Marais, D. J. (1990). The diffusive boundary layer of sediments: Oxygen micro gradients over a microbial mat. *Limnol. Oceanogr.* 35 (6), 1343–1355. doi:10.4319/lo.1990.35.6.1343

Jørgensen, B. B., and Revsbech, N. P. (1985). Diffusive boundary layers and the oxygen uptake of sediments and detritus1. *Limnol. Oceanogr.* 30 (1), 111–122. doi:10.4319/lo.1985.30.1.0111

Jørgensen, B. B., Wenzhöfer, F., Egger, M., and Glud, R. N. (2022). Sediment oxygen consumption: Role in the global marine carbon cycle. *Earth-Science Rev.* 228, 103987. doi:10.1016/j.earscirev.2022.103987

Kemp, W. M., Boynton, W. R., Adolf, J. E., Boesch, D. F., Boicourt, W. C., Brush, G., et al. (2005). Eutrophication of chesapeake bay: Historical trends and ecological interactions. *Mar. Ecol. Prog. Ser.* 303, 1–29. doi:10.3354/meps303001

Kirchman, D. L., Malmstrom, R. R., and Cottrell, M. T. (2005). Control of bacterial growth by temperature and organic matter in the Western Arctic. *Deep Sea Res. Part II Top. Stud. Oceanogr.* 52 (24-26), 3386–3395. doi:10.1016/j.dsr2.2005.09.005

Lionello, P. (2012). The climate of the Venetian and North Adriatic region: Variability, trends, and future change. *Phys. Chem. Earth Parts A/B/C* 40-41, 1–8. doi:10.1016/j.pce.2012.02.002

MacPherson, T. A., Cahoon, L. B., and Mallin, M. A. (2007). Water column oxygen demand and sediment oxygen flux: Patterns of oxygen depletion in tidal creeks. *Hydrobiologia* 586 (1), 235–248. doi:10.1007/s10750-007-0643-4

Manabe, S., Stouffer, R. J., Spelman, M. J., and Bryan, K. (1991). Transient responses of a coupled ocean-atmosphere model to gradual changes of atmospheric CO_2. Part I. Annual mean response. *J. Clim.* 4 (8), 785–818. doi:10.1175/1520-0442(1991)004<0785:TROACO>2.0.CO;2

Mel, R. A., Viero, D. P., Carniello, L., Defina, A., and D'Alpaos, L. (2021). The first operations of MO.S.E. system to prevent the flooding of Venice: Insights on the hydrodynamics of a regulated lagoon. *Estuar. Coast. Shelf Sci.* 261 (1-2), 107547. doi:10.1016/j.ecss.2021.107547

Melaku Canu, D., Solidoro, C., and Umgiesser, G. (2003). Modelling the responses of the Lagoon of Venice ecosystem to variations in physical forcings. *Ecol. Modell.* 170, 265–289. doi:10.1016/j.ecolmodel.2003.07.004

Middelburg, J. J., Duarte, C. M., and Gattuso, J. P. (2005). "Respiration in coastal benthic communities," in *Respiration in aquatic ecosystems*. Editors P. A. Del Giorgio and P. J. LeB. Williams (New York: Oxford University Press), 206–224.

Molina, M. O., Sánchez, E., and Gutiérrez, C. (2020). Future heat waves over the Mediterranean from an Euro-CORDEX regional climate model ensemble. *Sci. Rep.* 10, 8801. doi:10.1038/s41598-020-65663-0

MOSE (2022).*MOSE*. Available at: https://www.mosevenezia.eu/il-mose-in-funzione (Accessed June 6, 2022).

Murphy, P. J., and Hicks, D. B. (1986). "*In situ* method for measuring sediment oxygen demand," in *Sediment oxygen demand: Processes, modeling, and measurement*. Editor K. J. Hatcher (Athens: Institute of Natural Resources, University of Georgia), 307–330.

NRC, National Research Council (2000). *Clean coastal waters: Understanding and reducing the effects of nutrient pollution*. Washington, D.C: National Academy Press.

Percival, J. B., and Lindsay, P. J. (1997). "Measurement of physical properties of sediments," in *Manual of physico-chemical analysis of aquatic sediments*. Editors A. Mudrock, J. M. Azcue, and P. Mudrock (Boca Raton, FL: CRC Press), 7–45.

Pitcher, G. C., Aguirre-Velarde, A., Breitburg, D., Cardich, J., Carstensen, J., Conley, D. J., et al. (2021). System controls of coastal and open ocean oxygen depletion. *Prog. Oceanogr.* 197, 102613. doi:10.1016/j.pocean.2021.102613

Rong, N., Shan, B., and Wang, C. (2016). Determination of sediment oxygen demand in the Ziya River watershed, China: Based on laboratory core incubation and microelectrode measurements. *Int. J. Environ. Res. Public Health* 13 (2), 232. doi:10.3390/ijerph13020232

Rounds, S. A., and Doyle, M. C. (1997). "Sediment oxygen demand in the tualatin river basin, Oregon, 1992-96," in *U.S. Geological survey on water-resources investigations report 97-4103*, 19.

Ruol, P., Favaretto, C., Volpato, M., and Martinelli, L. (2020). Flooding of piazza san marco (Venice): Physical model tests to evaluate the overtopping discharge. *Water* 12, 427. doi:10.3390/w12020427

Scotti, A. (2005). "Engineering interventions in Venice and the Venice lagoon," in *Flooding and environmental challenges for Venice and its lagoon: State of knowledge*. Editors C. A. Fletcher and T. Spencer (UK: Cambridge University Press), 245–256. ISBN-13 978-0-521-84046-0.

Sfriso, A., Favaretto, M., Ceoldo, S., Facca, C., and Marcomini, A. (2005). Organic carbon changes in the surface sediments of the Venice lagoon. *Environ. Int.* 31, 1002–1010. doi:10.1016/j.envint.2005.05.010

Sfriso, A., and Marcomini, A. (1996). Decline of Ulva growth in the lagoon of Venice. *Bioresour. Technol.* 58, 299–307. doi:10.1016/s0960-8524(96)00120-4

Sfriso, A., Marcomini, A., and Pavoni, B. (1987). Relationships between macroalgal biomass and nutrient concentrations in a hypertrophic area of the Venice lagoon. *Mar. Environ. Res.* 22, 297–312. doi:10.1016/0141-1136(87)90005-5

Sfriso, A., Marcomini, A., and Zanette, M. (1995). Heavy metals in sediments, SPM, and phytozoobenthos of the Lagoon of Venice. *Mar. Pollut. Bull.* 30 (2), 116–124. doi:10.1016/0025-326X(94)00109-M

Steeby, J. A., Hargreaves, J. A., Tucker, C. S., and Cathcart, T. P. (2004). Modeling industry-wide sediment oxygen demand and estimation of the contribution of sediment to total respiration in commercial channel catfish ponds. *Aquac. Eng.* 31, 247–262. doi:10.1016/j.aquaeng.2004.05.006

Tagliapietra, D., Zanon, V., Frangipane, G., Umgiesser, G., and Sigovini, M. (2011). "Physiographic zoning of the Venetian lagoon," in *Scientific research and safeguarding of Venice - volume VII - 2007-2010 results*. Editor P. Campostrini (Venice, Italy: CORILA Publ.), 161–164. ISBN: 9788889405215 888940521X.

Thamdrup, B., Hansen, J. W., and Jørgensen, B. B. (1998). Temperature dependence of aerobic respiration in a coastal sediment. *FEMS Microbiol. Ecol.* 25 (2), 189–200. doi:10.1111/j.1574-6941.1998.tb00472.x

Thomann, R. V., and Mueller, J. A. (1987). *Principles of surface water quality modeling and control*. New York: Harper and Rowe, 291–293.

Todd, M. J., Lowrance, R. R., Goovaerts, P., Vellidis, G., and Pringle, C. M. (2010). Geostatistical modeling of the spatial distribution of sediment oxygen demand within a Coastal Plain blackwater watershed. *Geoderma* 159 (1-2), 53–62. doi:10.1016/j.geoderma.2010.06.015

Trincardi, F., Barbanti, A., Bastianini, M., Cavaleri, L., Chiggiato, J., Papa, A., et al. (2016). The 1966 flooding of Venice: What time taught us for the future. *Oceanogr. Wash. D. C).* 29 (4), 178–186. doi:10.5670/oceanog.2016.87

Umgiesser, G. (2020). The impact of operating the mobile barriers in Venice (MOSE) under climate change. *J. Nat. Conserv.* 54, 125783. doi:10.1016/j.jnc.2019.125783

Utley, B. C., Vellidis, G., Lowrance, R., and Smith, M. C. (2008). Factors affecting sediment oxygen demand dynamics in blackwater streams of Georgia's coastal plain. *J. Am. Water Resour. Assoc.* 44, 742–753. doi:10.1111/j.1752-1688.2008.00202.x

Vellidis, G., Barnes, P., Bosch, D. D., and Cathey, A. M. (2006). Mathematical simulation tools for developing dissolved oxygen TMDLS. *Trans. ASABE* 49 (4), 1003–1022. ISSN 0001–2351. doi:10.13031/2013.21743

Viaroli, P., Bartoli, M., Giordani, G., Naldi, M., Orfanidis, S., and Zaldivar, J. M. (2008). Community shifts, alternative stable states, biogeochemical controls and feedbacks in eutrophic coastal lagoons: A brief overview. *Aquat. Conserv.* 18, 105–117. doi:10.1002/aqc.956

Walker, R. R., and Snodgrass, W. J. (1986). Model for sediment oxygen demand in lakes. *J. Environ. Eng. New. York.* 112, 25–43. doi:10.1061/(ASCE)0733-9372(1986)112:1(25)

Wood, T. M. (2001). *Sediment oxygen demand in upper klamath and agency lakes, Oregon, 1999*. Portland, OR: U.S. Geological Survey Water-Resources Investigations. Report 01-4080.

Zaggia, L., Rosso, J., and Zonta, R. (2007). Sulphate reduction in the sediment of the Venice canals (Italy). *Mar. Pollut. Bull.* 10-12, 415–424. doi:10.1016/j.marpolbul.2007.09.004

Zakem, E. J., Cael, B. B., and Levine, N. M. (2021). A unified theory for organic matter accumulation. *Proc. Natl. Acad. Sci. U. S. A.* 118 (6), e2016896118. doi:10.1073/pnas.2016896118

Ziadat, A. H., and Berdanier, B. W. (2004). Stream depth significance during *in-situ* sediment oxygen demand measurements in shallow streams. *J. Am. Water Resour. Assoc.* 40 (3), 631–638. doi:10.1111/j.1752-1688.2004.tb04448.x

Zirino, A., Elwany, H., Facca, C., Maicù, F., Neira, C., and Mendoza, G. (2016). Nitrogen to phosphorus ratio in the Venice (Italy) Lagoon (2001–2010) and its relation to macroalgae. *Mar. Chem.* 180, 33–41. doi:10.1016/j.marchem.2016.01.002

Zonta, R., Costa, F., Collavini, F., and Zaggia, L. (2005). Objectives and structure of the DRAIN project: An extensive study of the delivery from the drainage basin of the Venice lagoon (Italy). *Environ. Int.* 31 (7), 923–928. doi:10.1016/j.envint.2005.05.002

Zonta, R., Botter, M., Cassin, D., Bellucci, L. G., Pini, R., and Dominik, J. (2018). Sediment texture and metal contamination in the Venice lagoon (Italy): A snapshot before the installation of the MOSE system. *Estuar. Coast. Shelf Sci.* 205, 131–151. doi:10.1016/j.ecss.2018.03.007

Zonta, R., Fontolan, G., Cassin, D., and Dominik, J. (2021). X-Ray computed tomography as a tool for screening sediment cores: An application to the lagoons of the Po river delta (Italy). *J. Mar. Sci. Eng.* 9, 323. doi:10.3390/jmse9030323

frontiers | Frontiers in Environmental Science

TYPE Original Research
PUBLISHED 20 October 2022
DOI 10.3389/fenvs.2022.999483

Spatial distribution of benthic flora and fauna of coastal placentia bay, an ecologically and biologically significant area of the island of newfoundland, atlantic Canada

Julia Mackin-McLaughlin[1,2]*, Shreya Nemani[1,2], Benjamin Misiuk[3], Adam Templeton[1], Patrick Gagnon[4], Evan Edinger[2] and Katleen Robert[1]

[1]School of Ocean Technology, Fisheries and Marine Institute of Memorial University of Newfoundland, St. John's, NL, Canada, [2]Department of Geography, Memorial University of Newfoundland, St. John's, NL, Canada, [3]Department of Oceanography, Dalhousie University, Halifax, NS, Canada, [4]Department of Ocean Sciences, Ocean Sciences Centre, Memorial University of Newfoundland, St. John's, NL, Canada

Coastal habitats have the potential to be biodiversity hotspots that provide important ecosystem services, but also hotspots for human development and exploitation. Continued use of coastal ecosystem services requires establishing baselines that capture the present state of the benthos. This study employs habitat mapping to establish a baseline describing the spatial distribution of benthic organisms along the western coast of Placentia Bay, an Ecologically and Biologically Significant Area (EBSA) in Newfoundland, Canada. The influence of seafloor characteristics on the distribution of four dominant epifaunal assemblages and two macrophyte species were modelled using two machine learning techniques: the well-established Random Forest and the newer Light Gradient Boosting Machine. When investigating model performance, the inclusion of fine-scale (<1 m) substrate information from the benthic videos was found to consistently improve model accuracy. Predictive maps developed here suggest that the majority of the surveyed areas consisted of a species-rich epifaunal assemblage dominated by ophiuroids, porifera, and hydrozoans, as well as prominent coverage by *Agarum clathratum* and non-geniculate crustose coralline algae. These maps establish a baseline that enables future monitoring of Placentia Bay's coastal ecosystem, helping to conserve the biodiversity and ecosystem services this area provides.

KEYWORDS

marine habitat mapping, machine learning, multiscale, benthic epifauna, benthic algae

EDITED BY
Elisabetta Manea,
Institute of Marine Science, National Research Council (CNR), Italy

REVIEWED BY
Giorgio Castellan,
Institute of Marine Science, National Research Council (CNR), Italy
Thadickal V Joydas,
King Fahd University of Petroleum and Minerals, Saudi Arabia

*CORRESPONDENCE
Julia Mackin-McLaughlin,
jamackinmclaughlin@vims.edu

SPECIALTY SECTION
This article was submitted to Freshwater Science,
a section of the journal
Frontiers in Environmental Science

RECEIVED 21 July 2022
ACCEPTED 03 October 2022
PUBLISHED 20 October 2022

CITATION
Mackin-McLaughlin J, Nemani S, Misiuk B, Templeton A, Gagnon P, Edinger E and Robert K (2022), Spatial distribution of benthic flora and fauna of coastal placentia bay, an ecologically and biologically significant area of the island of newfoundland, atlantic Canada.
Front. Environ. Sci. 10:999483.
doi: 10.3389/fenvs.2022.999483

Introduction

Human reliance on coastal ecosystem services places stress on benthic habitats, which may impact future availability of those services (Costanza et al., 1997; Barbier et al., 2011) and also biodiversity (Lotze et al., 2006), warranting management actions that balance coastal ecosystem function and human use. Considering the modern trend of increased utilization of ocean resources (Bennett et al., 2019), it is imperative to understand the current distribution of biota and non-living resources (i.e. oil, mined goods), against which change can be monitored over time (Shumchenia and King, 2010; Siwabessy et al., 2018). Conserving ecosystem function and services requires effective ecosystem-based management, which aims to preserve biodiversity and functionality by recognizing complex ecological linkages at varying scales, instead of relying on policies managing individual species (O'Higgins et al., 2020). The resultant holistic management therefore works to balance stakeholder involvement with sustainable practice (Long et al., 2015).

The benthos plays an important role in providing physical structure to the marine environment, supporting the ecological niches of other biota and serving as an indicator of ecosystem health which may be monitored to inform conservation priorities (Brey, 2012; Oug et al., 2012, Alexandridis et al., 2017). Benthic epifaunal invertebrates form the trophic basis for marine food webs (Iken et al., 2010), influencing both benthic and pelagic zones *via* cycling of energy, nutrients, and organic matter (Sandnes et al., 2000; Hajializadeh et al., 2020; Lam-Gordillo et al., 2021), and acting as ecosystem engineers (Reise, 1985; Meadows et al., 2012). The majority of benthic species are relatively immobile, if not completely sessile (Bilyard, 1987), and are long-lived, resulting in prolonged exposure to stressors and disturbances (Wei et al., 2019; Meng et al., 2021). Therefore, long-term monitoring of ecosystem function and health may benefit from the inclusion of epibenthic invertebrates as bioindicators.

Brown kelp, primarily of the order *Laminariales*, are one particular taxon known to enhance local biodiversity (Steneck et al., 2002; Krumhansl et al., 2016). They act as both primary and secondary producers, sequester carbon, provide shelter from predators, act as nursery grounds (Gagnon et al., 2003), and provide the physical framework to increase habitat complexity (Steneck et al., 2002). Kelp beds in temperate and sub-polar coastal regions of the northwest Atlantic are subject to periodic decimation by the herbivorous green sea urchin (*Strongylocentrotus droebachiensis*), resulting in coastal barrens that are less productive, which may extend 1000s of km (Filbee-Dexter and Scheibling, 2014). In the Northeast Atlantic, some of the few remaining floral species not consumed by urchins may include the kelp *Agarum clathratum* and non-geniculate crustose coralline algae (CCA). *A. clathratum* presumably deters urchins *via* phenolic compounds that render them unpalatable (Vadas, 1968; Vadas, 1977). For urchins, CCA are a poor nutritional substitute compared to kelps (Agatsuma, 2000; Kelly et al., 2008). Both *A. clathratum* and CCA are associated with a unique suite of invertebrates [Ojeda and Dearborn, 1989; Freiwald, 1993; Bégin et al., 2004; Swanson et al., 2006; Chenelot et al., 2011; Blain and Gagnon, 2014; Tebben et al., 2015; Jørgensbye and Halfar, 2017], potentially boosting subtidal biodiversity.

Benthic fauna and flora associate strongly with the physical structure of the seafloor (Auster and Langton, 1998; Kostylev et al., 2001), and geospatial models based on remotely sensed data may be used to support our understanding of spatial ecological patterns and the physical factors that drive them. The defined species-environmental relationships can be used to develop a baseline grounded in the function of an ecosystem that qualifies the composition and distribution of the benthos in a target area. These resultant habitat maps have been utilized for fisheries management (Brown et al., 2012), to inform effective Marine Protected Areas (MPAs) (Lacharite and Brown, 2019), for observing the impacts following ecological disturbance (e.g. oil spills (Botello et al., 2015)), and the first step in the establishment of long-term monitoring programs of coastal biodiversity (Obst et al., 2018). The effectiveness of a baseline relies on accurate and robust modelling techniques employed during its development, and these techniques are being improved continuously as there is an urgent need for such spatial data products.

This study aims to establish a baseline describing the benthic epifaunal assemblages and two marine algae species (*A. clathratum* and CCA) found in the subtidal zone of an Ecologically and Biologically Significant Area (EBSA) in Newfoundland, Canada (Templeman, 2007; DFO, 2016). An EBSA is an area notable for its distinct ecosystem characteristics, role in species' life stages (i.e. feeding/spawning grounds), resilience, and socio-economic utilization (DFO, 2004). The Placentia Bay EBSA has exhibited growth in vessel traffic and coastline activities that will likely shift the state of the benthos (DFO, 2007; LGL, 2018). The baseline established here will enable documenting changes to the dominant epifauna and marine algae using spatially explicit predictions of their current distribution based on the relationships with the physical structure of the seafloor. While modeling the relationship between seafloor features and biota, the performance of a new machine-learning algorithm, Light Gradient Boosting Machine (LightGBM), is tested against a well-established algorithm, Random Forest (RF). The predictive models and habitat maps developed in this study may be applied for future monitoring of changes in ecosystem structure and health within the Placentia Bay EBSA.

Methods

Study area

Placentia Bay is a deep-water embayment located on the southern side of the Island of Newfoundland, in the province of

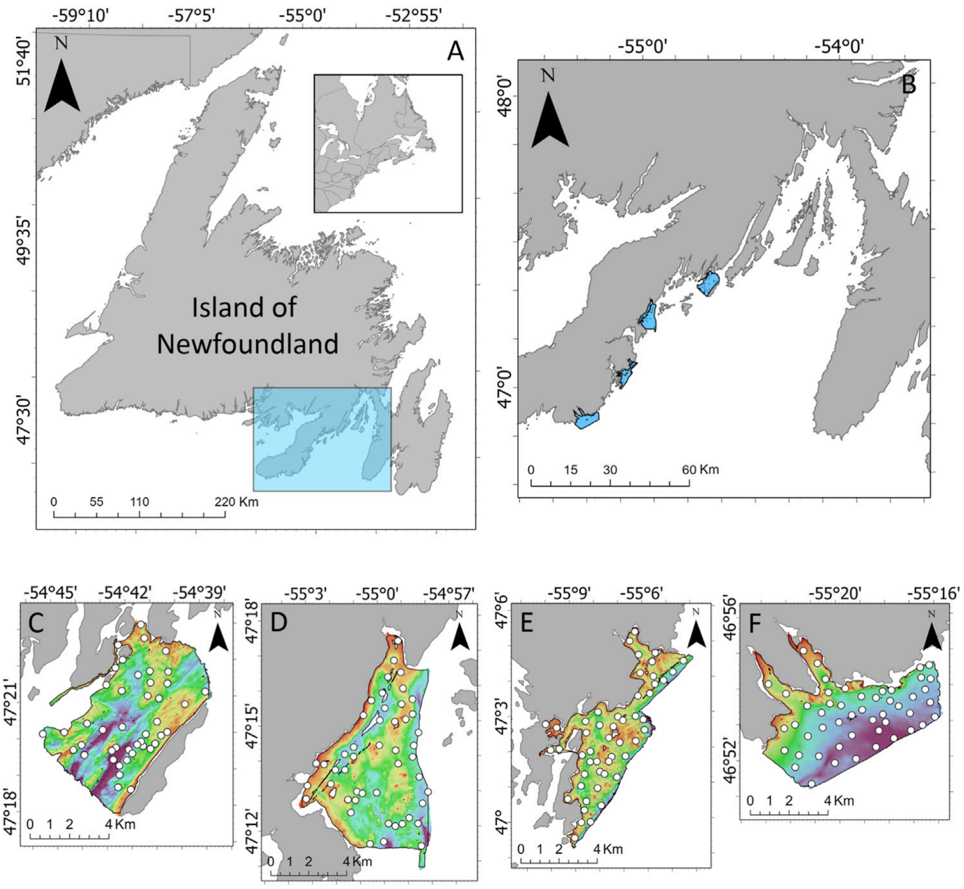

FIGURE 1
(A) Location of Placentia Bay (highlighted in the blue box) on the southern coast of the Island of Newfoundland, located on the eastern coast of Canada. **(B)** Locations of the four survey areas along the west coast of Placentia Bay. Bathymetry and ground-truth locations for **(C)** Rushoon, **(D)** D'Argent Bay, **(E)** Burin, and **(F)** St. Lawrence.

Newfoundland and Labrador (Atlantic Canada). Following an overview of its ecosystem status, present fish distribution and spawning locations, and a species inventory, Placentia Bay was designated by the Government of Canada Department of Fisheries and Oceans as an EBSA (Templeman, 2007; DFO, 2016). Any severe disturbance (i.e. oil spill) would be of greater ecological consequence within the EBSA boundary than if the same perturbation occurred beyond its extent (DFO, 2004). Placentia Bay hosts important capelin spawning beaches, seagrass meadows, seabird colonies, and herring aggregations (Sjare et al., 2003). It is also a location where charismatic megafauna such as whales (DFO, 2018) and leatherback turtles (DFO, 2012b) may be observed. Paired with its ecological relevance, Placentia Bay has local socio-economic importance, including traditional and commercial fisheries of groundfish and shellfish (Robichaud and Rose, 2006; DFO, 2012a; DFO, 2019), a growing finfish aquaculture industry (LGL, 2018), and frequent marine traffic, including oil tankers. Placentia Bay is considered to be amongst marine areas at greatest risk of oil spill across Canada (DFO, 2007).

Four survey areas along the west coast of Placentia Bay were selected for this study: Rushoon, D'Argent Bay, Burin and St-Lawrence (Figure 1). These sites are notable for their local ecological importance. Rushoon was the northernmost site surveyed, and is likely one of the more pristine of the four due to its remoteness. This may be subject to change, as development of salmon aquaculture progresses in the area, which may impact the local environment (LGL, 2018). Further southwest, D'Argent Bay was selected for its capelin spawning sites, herring aggregations, and high occurrence of whales (Sjare et al., 2003). Burin is near a relatively large cluster of towns, including the towns of Burin and Marystown. Finally, closest to the mouth of Placentia Bay, St. Lawrence was selected for its capelin spawning sites, as well as its role as an important seabird habitat (White, 2018).

TABLE 1 Acquisition information for multibeam echosounder (MBES) and ground-truth (GT) surveys.

Site	Survey period—MBES	MBES survey area (km^2)	Survey period—gt	Number of sites	Camera system
Rushoon	June—July 2019	39	August 2019	44	FDR-X300
D’Argent Bay	December, February 2018 and April 2019	43	July—August 2019	48	
Burin	May 2019	24	July 2020	50	Deep Trekker DTPod
St. Lawrence	July—August 2020	37	August 2020	50	

Environmental survey

Multibeam echosounder (MBES) surveying was carried out between winter 2018 and summer 2020 (Table 1) on board the 27’ Fisheries and Marine Institute research vessel *D. Cartwright*. MBES uses sound waves that travel from the sensor to the seafloor and back again, forming a swath of depth soundings across the path of the vessel. As sound waves echo back from the seafloor, the strength of their return is also measured, and this acoustic backscatter can be indicative of substrate types. Harder substrates like bedrock or boulders return a higher backscatter signal, while softer sediments like mud or sand will produce a weaker signal (Lamarche et al., 2011; Lurton and Lamarche, 2015; Calvert et al., 2015). Bathymetry and backscatter were collected using a Kongsberg EM 2040P, operating at 400 kHz. Positioning data were obtained using a Fugro 3,610 differential GPS with a Seastar subscription that provided spatial accuracy of up to 8 cm. Sound Velocity Profiles (SVP) between the transducer and seafloor were obtained using an AML BaseX sound velocity profiler, while sound velocity measurements at the MBES transducer head were obtained by an AML Micro SV sound speed sensor.

Raw sonar files for each survey area were imported into the Quality Positioning Services (QPS) Qimera v2.0.3 software. Bathymetric data were adjusted for Rushoon and D’Argent Bay using observations from the Argentia tide station (Station #835, https://www.tides.gc.ca/en/stations/835) and for Burin and St. Lawrence using the St. Lawrence tide station (Station #755, https://www.tides.gc.ca/en/stations/00755).). SVPs were imported into each respective Qimera project: 25 for D’Argent Bay, 19 for Rushoon, 19 for Burin, and 17 for St. Lawrence. Spline filters were employed to automatically remove outliers, and once processing was completed, a bathymetric surface was exported as a Floating Point GeoTIFF Grid at 5 × 5 m spatial resolution for each area. Processed files were additionally exported to. GSF format, and were imported into QPS Fledermaus Geocoder Toolbox (FMGT) v.7.8.4. For backscatter processing. Backscatter mosaics were exported at 5 × 5 m spatial resolution. All environmental rasters were projected to UTM Zone 21.

Bathymetric surfaces were used to derive terrain features that have been found to influence benthic biota distribution. These features can act as surrogates for variables that are difficult to measure directly (e.g. slope can act as a proxy for finer-scale currents). Six terrain features identified by Lecours et al., 2016a that capture a large amount of topographic information were calculated in ESRI ArcGIS using the Terrain Attribute Selection for Spatial Ecology toolbox (TASSE) (Lecours, 2015). These included slope (change in elevation), eastness and northness (orientation, calculated as the sine and cosine of slope), relative difference to the mean value (RDMV; relative position), and standard deviation (SD) of bathymetry (a measure of rugosity). Additionally, bathymetric position index (BPI) and vector ruggedness measure (VRM) were also selected to potentially provide information on seafloor structure. BPI is an adaptation of the topographic position index (Weiss, 2001) that measures the relative position of an area to the surrounding seabed (Lecours et al., 2016b). Positive and negative values represent peaks and troughs, respectively. VRM incorporates both slope and aspect in a single measure of surface roughness that is independent of slope (Hobson, 1972; Sappingtom et al., 2007; Martín-García et al., 2013), unlike SD. BPI, and VRM were derived from the bathymetric surfaces using the Benthic Terrain Modeller (BTM) Version 3.0 (Wright et al., 2012). Additionally, a layer measuring the distance from the coast was calculated within each survey area using the ‘Euclidean Distance’ tool in ESRI ArcGIS, which has previously been used to inform on benthic assemblage distributions (Degraer et al., 2008; Richmond and Stevens, 2014; Vassallo et al., 2018).

Features were derived from backscatter mosaics based on the spatial distribution of the varying shades of grey denoting backscatter intensity (Haralick et al., 1973). Three features were calculated using a grey-level co-occurrence matrix *via* the R package ‘GLCM’ (Zvoleff, 2020): contrast (local variation), homogeneity (closeness of distribution), and entropy (randomness) (Haralick et al., 1973). These features were selected for their common application in previous studies of similar systems (Blondel and Sichi, 2009; Samsudin and Hasan, 2017; Shang et al., 2021).

Terrain features were calculated across a range of spatial scales (i.e. using moving-windows of varying sizes), as no single scale can account for all ecological processes of a benthic ecosystem (Dolan, 2012; Lecours et al., 2015). All features (except for BPI) were derived using a 3x3-cell window, with

TABLE 2 Multiscale environmental features calculated at each site.

Feature	Scale (m)	Unit	Software	Software source
Bathymetry (m)	-	meters	-	-
Slope	15, 45, 175	degrees	TASSE	Lecours, (2015)
Eastness	15, 45, 175	unitless	TASSE	Lecours, (2015)
Northness	15, 45, 175	unitless	TASSE	Lecours, (2015)
RDMV	15, 45, 175	unitless	TASSE	Lecours, (2015)
SD	15, 45, 175	meters	TASSE	Lecours, (2015)
Fine BPI	15, 45, 175	meters	BTM	Wright et al. (2012)
Broad BPI	15, 45, 175	meters	BTM	Wright et al. (2012)
VRM	15, 45, 175	unitless	BTM	Wright et al. (2012)
Backscatter	-	Value (dB)	-	
Contrast	15, 45, 175	unitless	GLCM	Zvoleff (2020)
Entropy	15, 45, 175	unitless	GLCM	Zvoleff (2020)
Homogeneity	15, 45, 175	unitless	GLCM	Zvoleff (2020)
Distance to Coast (km)	5	meters	'Euclidean Distance'	
Bedrock (%)		%	ImageJ	
Boulder (%)		%	ImageJ	
Gravel (%)		%	ImageJ	
Fine sediment (%)		%	ImageJ	
Red Algae (%)		%	ImageJ	
Agarum clathratum (%)		%	ImageJ	
Saccharina latissima (%)		%	ImageJ	

additional scales obtained using the "calculate-average" approach (Dolan and Lucieer, 2014; Misiuk et al., 2021), by focal averaging using increasing window sizes (13 × 13-and 35 × 35-cell windows; Table 2). BPI layers were calculated by setting the outer and inner radii (in cells) of an annulus (ring-shape) and calculating the mean elevation value of all cells within the analysis neighborhood (Walbridge et al., 2018). BPI was calculated using the Benthic Terrain Modeler Toolbox, with outer and inner radii of 60 and 3, 150 and 45, 260 and 13, 630 and 195, 700 and 35, and 1750 and 525 cells.

Benthic biota

Ground-truthing sites (n = 192) across all four survey areas were selected using a Generalized Random Tessellation Stratified (GRTS) survey design (Supplementary Table S1) (Stevens and Olsen, 2004), stratified by bathymetry and backscatter. For the St. Lawrence sites, MBES data were unavailable prior to ground-truthing, and bathymetry was interpolated from depth soundings on a nautical chart (e.g. Great St. Lawrence Harbour, Marine Chart CA4642_2). Ground-truthing consisted of underwater video with two systems: a Sony FDR-X3,000 Action Cam (1920 × 1,080 pixels, 60 frames/sec), contained in a Deep Blue Abysso waterproof housing, paired with two 3,500 lumen neutral white light Cree LED bulbs and two green lasers spaced 10 cm apart; and a Deep Trekker DTPod (1920 × 1,080 pixels, 30 frames/sec) with an integrated light and two red lasers spaced 2.5 cm apart. For both systems, a live video feed was used to adjust the height of camera above the seabed. Boat positioning at the start and end of each transect was obtained using the onboard Garmin GPS 16x; the midpoint of each transect was used to extract point-wise data from terrain features.

Two-minutes of continuous video were annotated using the Monterey Bay Aquarium Research Institute's (MBARI) Video Annotation and Reference System (VARS) (Schlining and Stout, 2006). The presence or absence of *Agarum clathratum* and non-geniculate coralline algae (CCA) were recorded. Because of varying coverage across different ground-truthing sites, CCA were divided into three classes: full coverage, partial coverage, and absent. The full-coverage class was assigned when most of the seafloor was covered by CCA. Partial coverage was given when at least half of the substrate was covered. If little to no CCA was present, the site was marked as absent. Because abundance of

S. droebachiensis may influence macroalgae distributions, counts at each site were included as a possible predictor variable.

All epifauna larger than 2 cm were counted and identified to the lowest possible taxonomic level, using expert knowledge and published species guides (Gosner, 1979; Harvey-Clark, 1997; Martinez and Martinez, 2003; Fox et al., 2014; Salvo et al., 2018). When species identification was not feasible, a morphotype approach was employed (Howell et al., 2019). The total number of individual species/morphotypes per transect was calculated and converted to densities by estimating the total area recorded for each transect. Using the Blender v.2.8.2, 12 frames at 10 s intervals were extracted and the distance between lasers was measured and used to calculate transect width with ImageJ. This was averaged and multiplied by the total length of the transect. Species/morphotypes that had an abundance of <5 individuals across all ground-truthing sites were removed to reduce the influence of low-abundance species. The dominant assemblages for ground-truthing sites with <5 faunal counts could not be characterized (De la Torriente et al., 2018); these sites were removed prior to analysis.

The species matrix was Hellinger transformed to reduce the importance of larger epifaunal abundances (Legendre and Gallagher, 2001; Borcard et al., 2011). Faunal assemblages were clustered using the average hierarchical clustering method 'Unweighted Pair-Group Method using arithmetic Averages' (UPGMA) (Sokal and Michener, 1958), with hierarchical relationships plotted as a dendrogram. The UPGMA approach is fast, simple, and may even outperform other clustering algorithms (Kreft and Jetz, 2010). Dissimilarity values between two branches of the derived dendrogram (i.e., "fusion levels") were plotted to determine the optimal number of faunal assemblages. Silhouette widths were additionally calculated and plotted for each fusion level, providing a metric for distinguishing assemblages. Silhouette widths range from -1 to 1, with one representing assemblages that are clearly distinguished (Borcard et al., 2011). Once faunal assemblages were identified, the characteristic species or morphotypes of each assemblage were identified using an IndVal procedure (Legendre, 2013). A species accumulation curve was developed for each assemblage to identify if species richness was effectively captured (Ugland et al., 2003; Bevilacqua et al., 2018).

Model development

For both the assemblages and for each marine algae taxa model, a Boruta Feature Selection (Kurse and Rudnicki, 2010) algorithm was run separately to include terrain features grouped by scale (window of analysis: 3 × 3, 13 × 13, 35 × 35 cells) in order to reduce the number of candidate terrain features and promote model parsimony and support performance (Nemani et al., 2021). Important variables are identified by the Boruta wrapper as it compares the importance of a variable with a randomly shuffled version containing the same distribution of values (i.e., "shadow features"). A variable is deemed important if it consistently contributes more to the model than its shadow variable. Degenhardt et al., 2019 found that the Boruta algorithm generally outperformed other selection methods, and previous successful applications can be found in Li et al., 2016, Diesing and Thorsnes, (2017) and Nemani et al., 2021. Variables identified as "important" or "tentative" were selected for model training here. Variables were further dropped that had absolute correlation values exceeding 0.7, as determined using the R function 'corrplot' (Wei, 2013). In these cases, the variable with the lower impact on model accuracy was dropped.

Separate multiclass classification Random Forest (RF) and Light Gradient Boosting Machine (LightGBM) models were developed for the epifaunal dataset, the *A. clathratum* dataset, and the CCA dataset. Each model was trained with 2/3 of the samples, which included a proportional representation of classes (i.e. presence and absence of *A. clathratum* or epifaunal assemblage). The remaining 1/3 was reserved to test model performance. Model accuracy was assessed using the test data by computing a confusion matrix of predicted and observed classes (Congalton, 1991), from which overall accuracy and Cohen's kappa were derived. Overall accuracy is the number of accurately predicted classifications divided by the total number of observations. The kappa statistic incorporates the chance of random agreement between observed and predicted classes based on their prevalence (Cohen, 1960; Allouche et al., 2006). Both the RF and LightGBM models were run with and without fine-scale (<1 m) substrate % coverage to understand the importance of fine-scale features in explaining spatial patterns. Using both the RF and LightGBM models and the environmental data layers, full-coverage predictive maps were developed for the distribution of epifaunal assemblages, presence/absence of *A. clathratum*, and for the absence/partial/full coverage of CCA. Since substrate % coverage features were not spatially continuous, full-coverage predictions were based on the terrain feature-only models.

RF is a well-established ensemble machine-learning algorithm that builds a 'forest' of classification trees from which predictions are obtained through majority voting. It employs 'bagging', where the data are repeatedly bootstrapped to train different classification trees (Quinlan, 1986), which are uncorrelated. Additionally, each tree split uses a random subset of variables, instead of the entire set. RF models were trained using the R package 'randomForest' (Liaw and Weiner, 2002), with the default number of variables included in each split ('mtry') retained for each model. Random Forest has been used successfully for predictive models with limited sample sizes similar to the number of observations in this study (Stephens and Diesing, 2014; Robert et al., 2015; McLaren

TABLE 3 Parameters selected for LightGBM model tuning.

Parameter	Description	Range tested
'objective'	Sets the model as regression or classification	'multi_class' *
'metric'	How the model performance is evaluated	'multi_error' *
'num_class'	Number of classes predicted	number of faunal assemblages*
'is_unbalance'	Algorithm automatically balances weights of classes	TRUE, FALSE
'force_col_wise'	Manages model instability when there is a large number of columns (features)	TRUE, FALSE
'max_depth'	Controls the maximum distance between a tree's root node and each leaf node	10, 20, 40, 80
'num_leaves'	Maximum number of leaves for each learner; manages complexity; adjust with 'max_depth'	(2ˆmax_depth)
'learning_rate'	Boosting learning rate	0.05, 0.1, 0.25, 0.5
'num_iterations'	Number of trees to build; with larger values, adjust with smaller 'learning_rate'	100, 200, 300, 400
'feature_fraction'	Sets % of features selected as a subset for each iteration (tree)	0.8, 0.9, 0.95
'lambda_l1'	L1 regularization	0.2, 0.4
'lambda_l2'	L2 regularization	0.2, 0.4
'min_gain_to_split'	Sets the minimum improvement value when evaluating gains at a split	0.2, 0.4
'early_stopping_rounds'	Stops training when validation metric does not improve; adjust with 'num_iterations'	10% of 'num_iterations'

* Core features that do not change during any model iteration.

TABLE 4 Indicator species by IndVal analysis of faunal assemblages.

Name	*n* sites	Indicator morphotype/species	Species present	Unique to this cluster	Images*
OPH	*64*	Ophiuroidea spp. Porifera sp.5 Hydrozoa sp.1	51	8	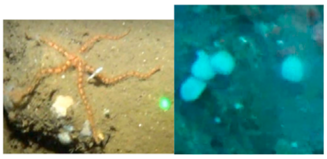
SDR	*21*	*Strongylocentrotus droebachiensis* Stauromedusae sp.2	20	none	
MIX	*26*	Hormathia sp.1 Cerianthidae sp.3 Cnidaria sp.1 Sagittidae sp.1	42	1	
EPA	*8*	*Echinarachnius parma* *Pseudopleuronectes americanus*	15	1	

n indicates the number of ground-truthing sites identified as containing each assemblage.

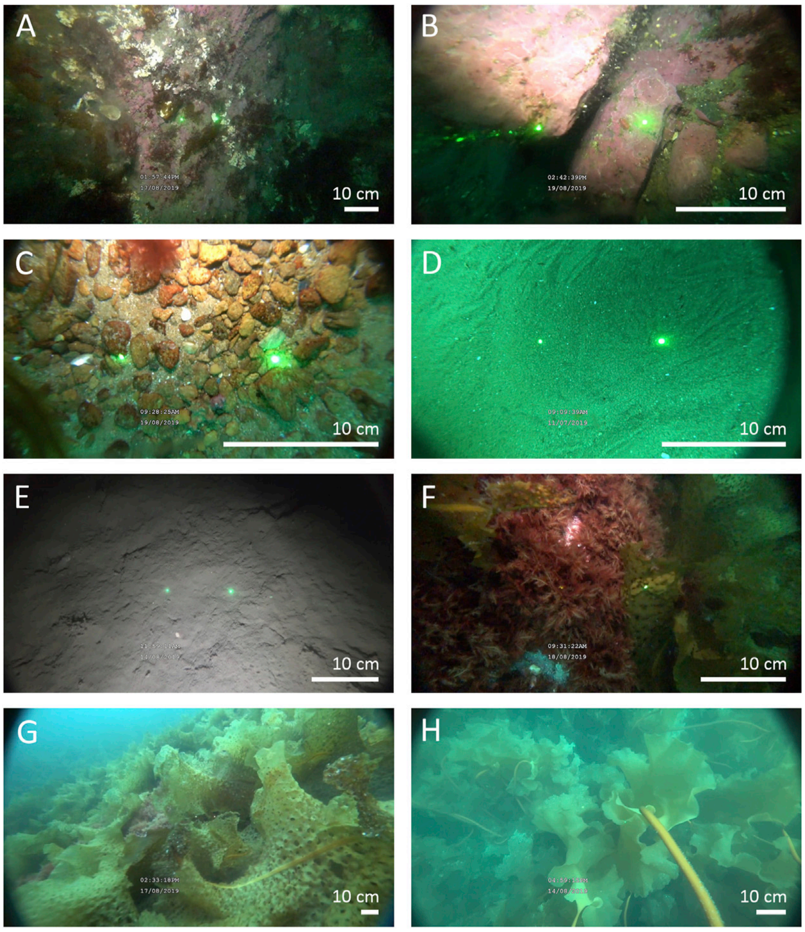

FIGURE 2
Images of the substrate classes identified during video annotation: **(A)** bedrock, **(B)** boulder, **(C)** gravel mix, **(D)** fine-sediment (sand), **(E)** fine-sediment (mud), **(F)** filamentous red algae (excluding coralline algae), **(G)** *Agarum clathratum*, and **(H)** sugar kelp (*Saccharina latissima*). Distance between lasers was 10 cm for the Sony FDR-X300 camera and 2.5 cm for the Deep Trekker DTPod.

et al., 2019; Misiuk et al., 2019; Ilich et al., 2021; Janowski et al., 2021).

LightGBM is a relatively recent Gradient Boosting Decision Tree algorithm (Ke et al., 2017). Unlike RF, LightGBM uses 'boosting' rather than 'bagging' to enhance performance. Boosting is another ensemble method in which classification trees are grown on the residuals from previous trees (Vaghela et al., 2009; Schapire and Freund, 2013). Tree growth and learning rate are controlled by a suite of tunable parameters (Table 3). The parameters recommended in the LightGBM release 3.2.1.99 guide (Zhang et al., 2012) were chosen to tune the model.

A variable importance plot was derived for each model, ranking variables based on their predictive importance. The RF model used Gini Importance, which measures the total decrease in node impurity by calculating the sum over the number of splits including a variables, across all trees (Friedman et al., 2001). LightGBM implements a gain-based method that is similar to the Gini Importance used by RF (Lundberg et al., 2020), but excludes unimportant features. Univariate partial dependence plots were derived from the best-performing model to visualize the relationship between an individual variable and a faunal assemblage or marine algae (Marini et al., 2015; Vassallo et al., 2018).

By comparing model accuracy and ranked variable importance, preliminary modelling using the derived terrain features suggested that important variables may be missing. Substrate heterogeneity information extracted from videos of the seafloor was tested to improve model performance. Substrate observations were obtained from the underwater video collected for biological analysis (described below). An image was extracted every 10 s from each video using Blender v.2.8.2 and images were imported to ImageJ (Image processing and analysis in Java). A 50-square grid was superimposed on each image and each square

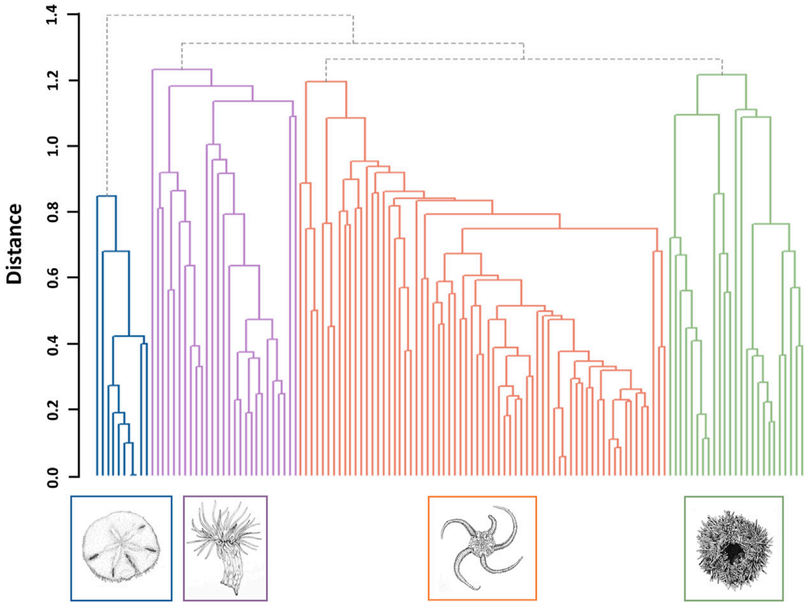

FIGURE 3
Dendrogram of the four dominant epifaunal assemblages identified at sites across the west coast of Placentia Bay. Illustrations by J. Mackin-McLaughlin.

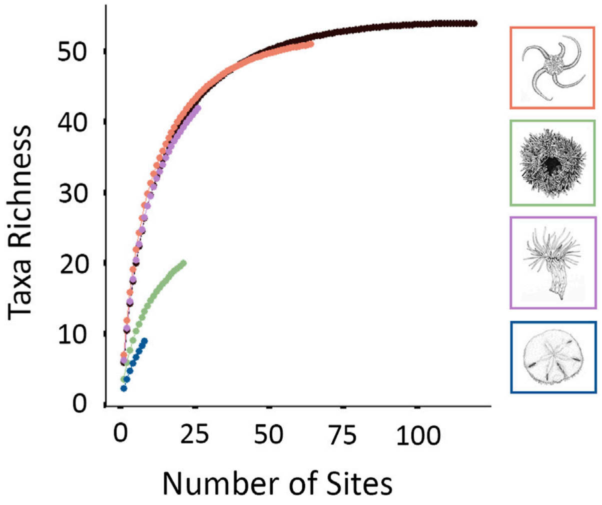

FIGURE 4
A species accumulation curve was developed for each faunal assemblage and for the summation of species observed across all sites included in analysis (in black).

was labelled as one of seven classes: bedrock, boulder, gravel-mix, fine sediment (including both mud and sand), red algae (excluding coralligenous algae), *Agarum clathratum*, and *Saccharina latissima* (Figure 2). Following Connell et al., 2014, red algae can be qualitatively categorized as turfs (i.e. loosely to densely aggregated filamentous algae <15 cm tall and covering an area greater than 1 m^2). Biogenic substrates were included because observing the sediment underneath was often not possible and algae presence is likely to influence the presence of other epifauna. The number of occurrences of each class was divided by the total number of grids for a ground-truth site, yielding fine-scale (<1 m) percent cover for each substrate class.

Results

Epifaunal assemblages

Of the 192 ground-truthing sites collected, 117 fulfilled the criteria for assemblage identification. One site (Rushoon-53) exhibited two distinct epifaunal assemblages and substrate types, and was split into two, producing 118 total samples. From these, a total of 12,096 individuals were counted and 55 taxa were identified (Supplementary Table S2), 14 of which (25.5%) were identified to species level. The brittle star morphotype ‘Ophiuroidea spp.’ had the highest overall abundance (6,693 individuals; 55.5% of all counts), followed by ‘*Hormathia* sp.1’ (1,631 individuals; 13.5%), *Strongylocentrotus droebachiensis* (766 individuals; 6.3%), and *Echinarachnius parma* (627 individuals; 5.2%). Porifera had the highest taxa diversity with 14 morphotypes. Echinodermata was

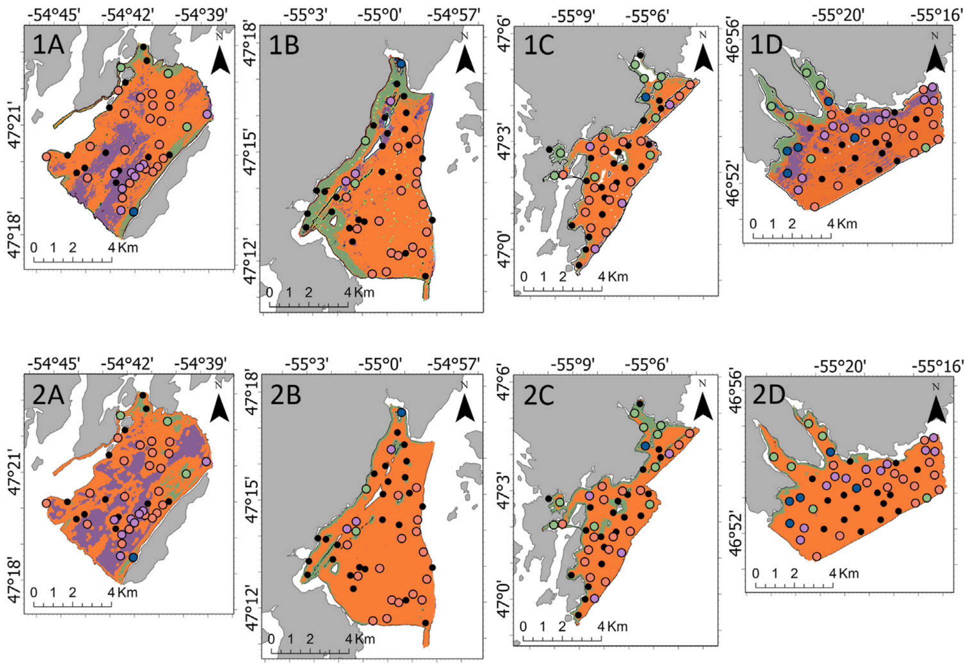

FIGURE 5
Predicted spatial coverage of the identified four assemblages by the 1) Random Forest and 2) Light Gradient Boosting Machine models across the four target survey areas: **(A)** Rushoon, **(B)** D'Argent Bay, **(C)** Burin, and **(D)** St. Lawrence.

second in taxa diversity (7 morphotypes; six species), followed by Cnidaria (8 morphotypes; two species).

Four epifaunal assemblages were identified (Figure 3; Table 4). Sixty-four of 119 sites (53.8%) were identified as OPH, typified by 'Ophiuroidea spp.', 'Porifera sp.5', and 'Hydrozoa sp.1'. OPH contained the highest taxa richness (51 taxa: 39 morphotypes, 12 species), as well as the most taxa unique to a single assemblage (8 taxa). SDR represented 21 sites (17.6%) and contained 13 morphotypes and seven species, with *S. droebachiensis* and 'Stauromedusae sp.2' as the typifying taxa. MIX was found at 26 sites (21.8%) and had the second highest taxa richness, with 30 morphotypes and 12 species. It was typified by '*Hormathia* sp.1', 'Cerianthidae sp.3', 'Cnidaria sp.1', and 'Sagittidae sp.1'. EPA was the rarest assemblage, with only eight representative sites (6.7%). EPA had the lowest taxa richness, with only eight morphotypes and seven species, and was typified by *E. parma* and *Pseudopleuronectes americanus*, with the former unique to this assemblage. While OPH exhibited the highest taxa richness, species accumulation curves indicate that the species/morphotypes richness of SDR, MIX, and EPA are underrepresented (Figure 4). Greater surveying effort could reveal additional species/morphotypes for each assemblage. However, this lack of plateau may also be the result of removing species with <5 occurrences across all ground-truthing sites.

Model performance and predicted distribution

Following the Boruta algorithm and assessment of collinearity, 18 variables were included in the epifaunal models, 18 in the *A. clathratum* models, and 24 in the CCA models. Without fine-scale substrate % features, the RF model accuracy was 61.0% (kappa = 0.31) and the LightGBM model accuracy was 68.3% (kappa = 0.47). With the addition of fine-scale substrate features, the epifaunal RF test accuracy increased to 78.1% (kappa = 0.62), and the LightGBM model accuracy increased to of 78.1% (kappa = 0.62). Both the RF and LightGBM models overestimated the occurrence of OPH, and as a result, a large number of SDR and MIX observations were incorrectly classified as OPH. This is evidenced in the RF and LightGBM predictive maps, where OPH was predicted to cover the majority of each survey area, excluding Rushoon (Figure 5). RF, however, included a greater coverage of SDR along the coastal side of D'Argent Bay and of MIX along the interior of St. Lawrence. LightGBM underestimated the coverage of both SDR and MIX in D'Argent Bay and St. Lawrence, respectively, even though ground-truthing sites assigned as those assemblages were observed. RF correctly identified all EPA observations while LightGBM was unable to correctly predict any of the EPA sites.

Only ground-truthing sites within the observed depth range for each marine algae were included. For *A. clathratum* model

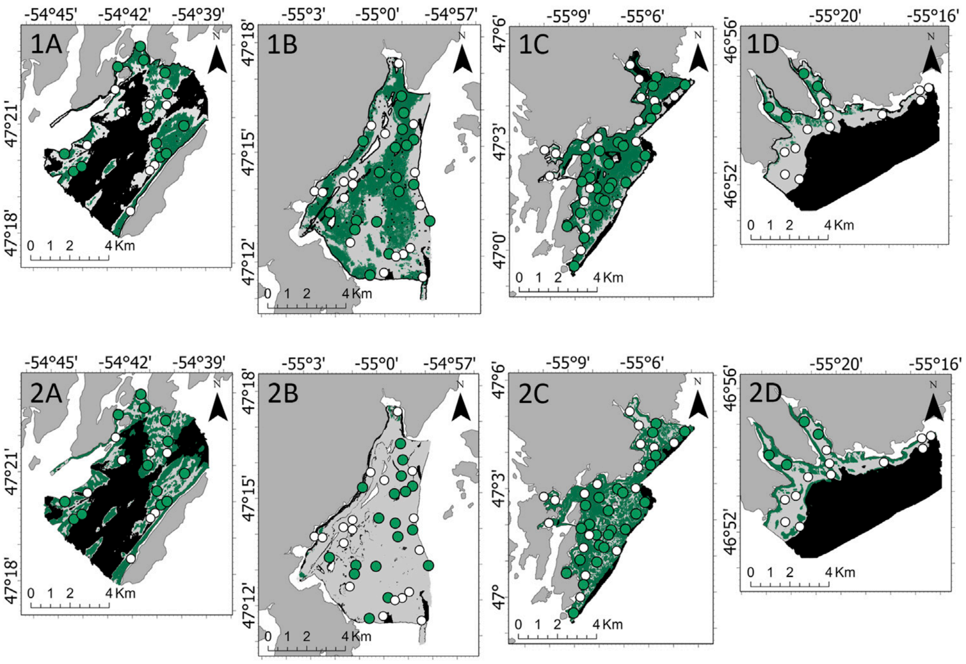

FIGURE 6
Predicted absence (white) and presence (green) of *Agarum clathratum* by the 1) Random Forest and 2) Light Gradient Boosting Machine models across the four target survey areas: **(A)** Rushoon, **(B)** D'Argent Bay, **(C)** Burin, and **(D)** St. Lawrence. No predictions were developed where black is seen, as depth exceeded the range established in *A. clathratum* model development.

development, 115 sites at a depth range of 15–66 m were included. *A. clathratum* was present at 60 of 115 ground-truth sites, the majority of which occurred in Burin (25 of 60 sites; 41.7%). *A. clathratum* was present at over 50% of sites in all survey areas except for St. Lawrence. Model performance without fine-scale substrate % features was 82.1% (kappa = 0.64) for the RF model and 87.2% (kappa = 0.74) for the LightGBM model. Maps derived from these models predicted a majority coverage of *A. clathratum* across Burin, though a patchwork of absences is predicted by LightGBM in the interior of Burin's extent. Differences in predicted *A. clathratum* extent is apparent in Rushoon and St. Lawrence. The greatest discrepancies were observed in D'Argent Bay though, with very little coverage predicted by LightGBM compared to RF (Figure 6).

132 sites were included in the CCA model at a depth range of 15–78 m. For CCA, 42 sites had full coverage (31.8%) and 31 sites had partial coverage (23.5%). Rushoon had the highest number of ground-truthing sites with full coverage off CCA (15 of 27). Aside from one instance of full coverage, the northeastern coast of St. Lawrence was characterized by partial coverage of CCA. Few absences of CCA were observed in D'Argent Bay (7 out of 36 sites) and Burin (11 out of 45 sites). When models were developed without fine-scale substrate % coverage, the CCA RF model had an accuracy of 68.9% (kappa = 0.49) and the LightGBM model had an accuracy of 68.9% (kappa = 0.51). Predictive maps derived from these differed in the concentration of absences, with LightGBM predicting an underestimation across all four survey areas of both partial and full coverage (Figure 7).

The accuracy of all marine algae models was increased with the introduction of fine-scale substrate % coverage features. The *A. clathratum* RF and LightGBM model accuracies increased to 89.7% (kappa = 0.80) and 92.3% (kappa = 0.85), respectively and both the CCA RF and LightGBM accuracies increased to 82.2% (kappa = 0.72).

Species-Environment relationships

Depth was the most important variable for explaining the distribution of epifaunal assemblages, according to the RF model (Figure 8). OPH and MIX were associated with deeper portions of the surveyed areas, while SDR and EPA were generally observed at depths shallower than 50 m. Relationships between EPA and the five most important variables appeared opposite to those observed for the other assemblages (according to the best-preforming RF model) (Figure 9). EPA was the only assemblage that was more prevalent with increased coverage of fine sediment and flat terrain. Assemblages SDR, MIX, and OPH appeared more

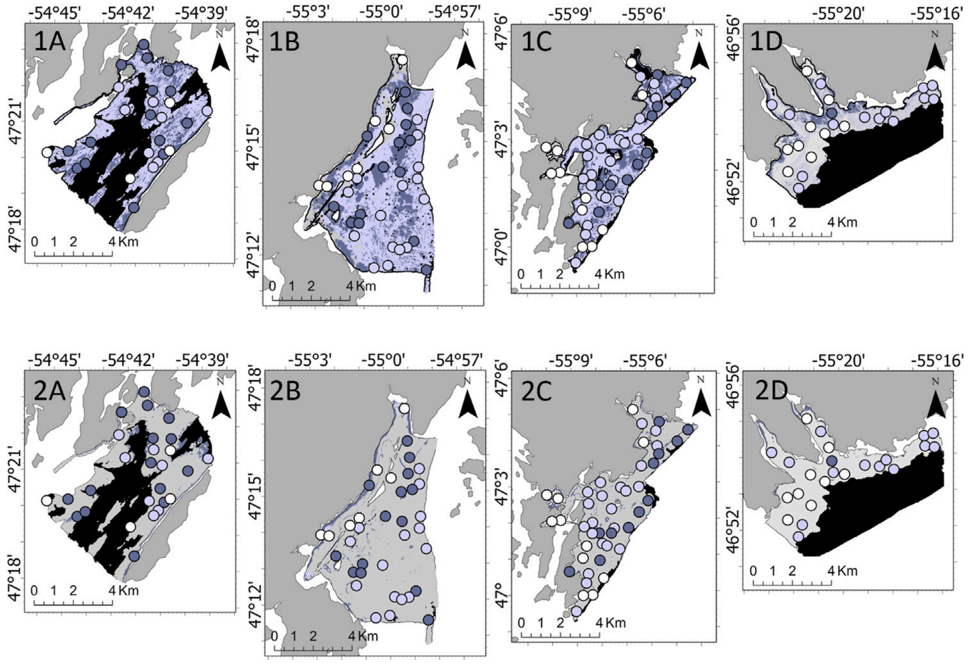

FIGURE 7
Predicted absence (white), partial coverage (light purple), and full coverage (dark purple) of non-geniculate crustose coralline algae (CCA) by the 1) Random Forest and 2) Light Gradient Boosting Machine models across the four target survey areas: **(A)** Rushoon, **(B)** D'Argent Bay, **(C)** Burin, and **(D)** St. Lawrence. No predictions were developed where black is seen, as depth exceeded the range established in CCA model development.

prevalent at areas of rugged and boulder terrain, according to models. EPA was most prevalent within 2 km of the coast, with decreasing occurrence with greater distance. Unlike SDR and MIX, OPH was most prominent at sites closer to shore, but also occurred at the furthest offshore sites that were sampled.

Fine-scale substrate % coverage was identified as being even more important than depth to explain the spatial patterns of both *A. clathratum* and CCA models (Figure 8). Specifically, the presence of even low % coverage of fine sediment influences the presence of both *A. clathratum* and CCA. The predicted presence of either marine algae was higher with increasing coverage of harder substrates, including both boulder (%) and gravel (%) coverage (Figure 10).

According to both RF and LightGBM models, bathymetry was the second most important variable influencing the distribution of *A. clathratum*, with the majority of occurrences constrained to depths of 15–48 m. Bathymetry appeared less important for predicting CCA distribution in the RF model, and was not included at all in the CCA LightGBM model. The model suggested that softer sediments were more influential than harder substrate in determining the presence of *A. clathratum* (Figure 10). For CCA models, partial and full coverage were associated with higher backscatter values, while sites with absences were characterized by lower backscatter (Figure 11).

Discussion

The west coast of Placentia Bay hosts a diverse and heterogeneous collection of benthic invertebrates, with prominent populations of *A. clathratum* and substantial CCA coverage. Fine-scale (<1 m) substrate features appear highly important for explaining observed spatial patterns. Performance improved in all cases when substrate features were included in the models, yet ultimately, these variables could not be used for continuous spatial prediction due to their discontinuous coverage. This highlights the importance of fine-scale substrate as a benthic habitat driver. Nonetheless, the models developed in this study provide valuable insight into the species-environment relationships driving the distribution of the heterogeneous benthic biota found in Placentia Bay–a necessary step in establishing a baseline for monitoring changes over time.

Depth has often been identified as an important variable in explaining benthic biota distribution (Bekkby et al., 2009; Gorman et al., 2013; Neves et al., 2014; Schückel et al., 2015; Bekkby et al., 2019). However, depth is likely acting as a proxy for other co-varying and harder to characterize variables, such as light availability, temperature, salinity, wave action, or ice scouring (Elith and Leathwick, 2009; Sandman et al., 2013). For example, in the case of the spatial distribution

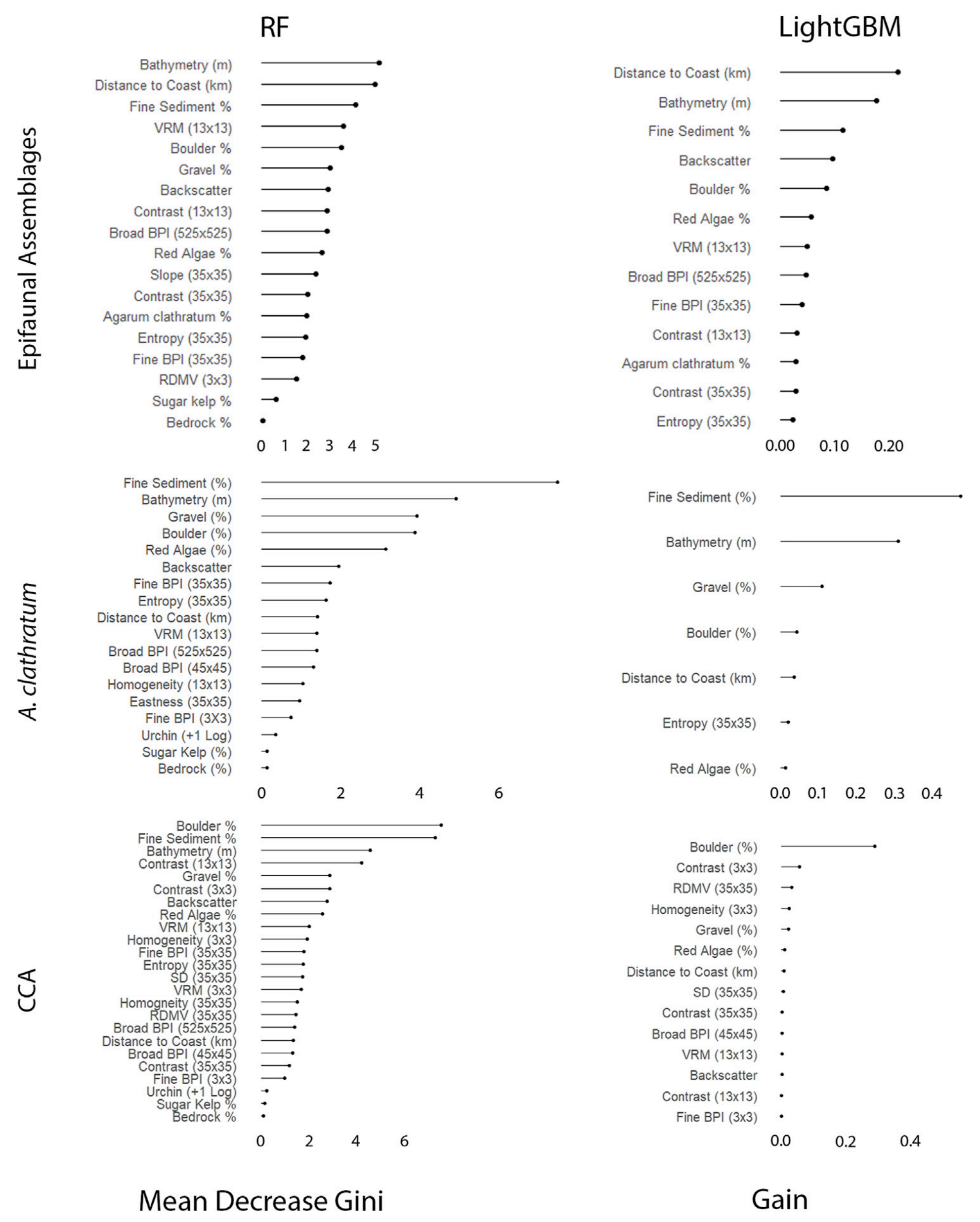

FIGURE 8
Order of variable importance as determined by the Random Forest (RF) and Light Gradient Boosting Machine (LightGBM) for the epifaunal, *Agarum clathratum*, and non-geniculate crustose coralline algae (CCA).

of *A. clathratum* and CCA within Placentia Bay, depth likely acts as a proxy for light attenuation. *A. clathratum* extends to greater depths than most kelp species due to its shade-tolerance (Krause-Jensen et al., 2019), with an observed depth limit in this study of up to 66 m, consistent with findings along coastal Greenland (Krause-Jensen et al., 2019). CCA are even more tolerant of low-light conditions due to their low photosynthetic capacity (Littler et al., 1985; Roberts et al., 2002; Nelson, 2009). CCA are found within most coastal habitats (Littler et al., 1985), including Antarctica (Zaneveld and Sanford, 1965; Schwarz et al., 2005; Castellan et al., 2021), and are observed at depths greater than any other local marine algae species (McConnaughey and Whelan, 1997). This may explain the exclusion of bathymetry from the CCA LightGBM model. Dean et al., 2015 observed a similar pattern with coralline algae along the Great Barrier Reef, where depth had little effect on their distribution compared to physical features.

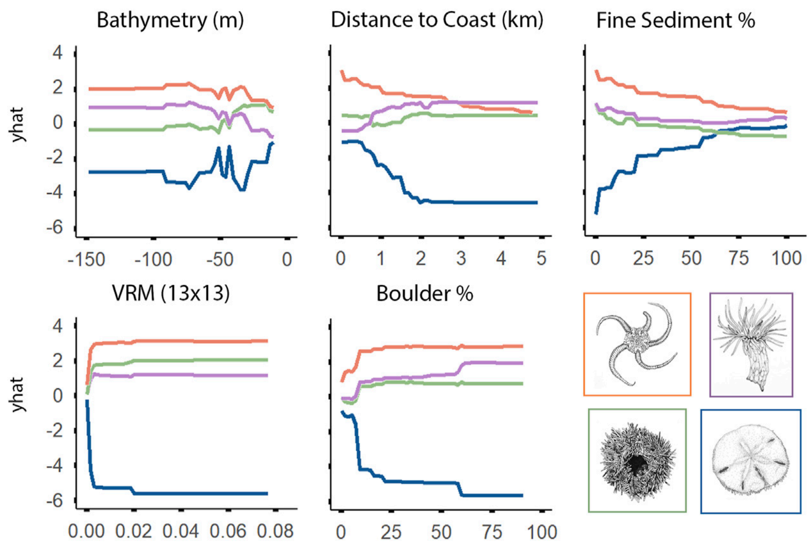

FIGURE 9
Univariate partial dependence plots derived from the Random Forest classification model for the top five most important explanatory environmental features explaining the distribution of individual epifaunal assemblages. The 'yhat' axis refers to the value of partial dependence function. The partial response of the epifaunal assemblages to all features is provided in Supplementary Figure S1.

In the case of EPA, shallower depths may be associated with a greater abundance of food for the typifying species *E. parma*, such as benthic diatoms, which are known to migrate to shallowed depths as they grow older and larger (Cabanac and Himmelman, 1996; Cabanac and Himmelman, 1998). In contrast, OPH and MIX were found across most of the depth range surveyed. The dominant epifauna of these assemblages included porifera and cnidarians, with dense ophiuroid beds in OPH and abundant *Hormathia* sp.1 aggregations in MIX. As these epifauna rely on filter- and suspension-feeding techniques, their survival may depend on food transport from the euphotic zone (Maldonado et al., 2017). Food transport may be constrained by both hydrography and depth in coastal environments (Grebmeier and Barry, 1991; Graf, 1992; Piepenburg, 2005; Sswat et al., 2015).

Mean current circulation in Placentia Bay is counterclockwise, with currents entering on the eastern coast and exiting on the west (Ma et al., 2012). The west coast is therefore subject to upwelling currents that may be beneficial to filter- and suspension feeders (Ma et al., 2012), such as the porifera and cnidarians (i.e. *Hormathia* sp.1) observed within the OPH and MIX assemblages. Sponge aggregations (Hogg et al., 2010) and *Hormathia digitata* (Dunlop et al., 2020) are known to associate with strong, nutrient-enriched currents delivering a constant food supply–though the current strength in these small embayments is strongly influenced by the complex bathymetry and shoreline (Largier, 2020). *A. clathratum* and CCA were found on westward-facing substrate in line with Placentia Bay's south westerly currents [Supplementary Figures S2,3]. Kelp beds are well-adapted to environments of moderate wave exposure (Gorman et al., 2013; Bekkby et al., 2019), as wave action boosts nutrient supply and uptake, ensures continuous light exposure (Hurd et al., 1996; Hepburn et al., 2007; Bekkby et al., 2019), and reduce survivability of epiphytes (Strand and Weisner, 1996). However, at exposed areas such as St. Lawrence, which may experience excessive wave action, growth may be inhibited due to abrasions or transport (Marrack, 1999; Sañé et al., 2016).

With the exception of EPA, hard substrates were associated with suitable habitat for all epifaunal assemblages, *A. clathratum,* and CCA. Fine sediments and sedimentation may reduce habitat suitability for these sessile organisms by inhibiting feeding strategies. Large kelps such as *A. clathratum* additionally require a stable foundation for holdfast attachment to endure currents and storm surge (Morrison et al., 2009; Watanabe et al., 2014; Masteller et al., 2015). In contrast, *E. parma* would preferentially inhabit coarse sand areas (Stanley and James, 1971; Sisson et al., 2002), enabling filtering where coarse sand traps particulate matter for consumption without excess fouling (Bland et al., 2019), and burying to avoid predation (Manderson et al., 1999; Pappal et al., 2012) and damaging storm surge (O'Neill, 1978). Distance from the coast may act as a surrogate for sedimentation rate (Stephens and Diesing, 2015; Misiuk et al., 2018). In the case of CCA, growth occurs only on hard substrate (Connell, 2005; Gagnon et al., 2012, Jørgensbye and Halfar, 2017), with fine sediment additionally reducing light availability for photosynthesis (Konar and Iken, 2005; Jørgensbye and Halfar, 2017).

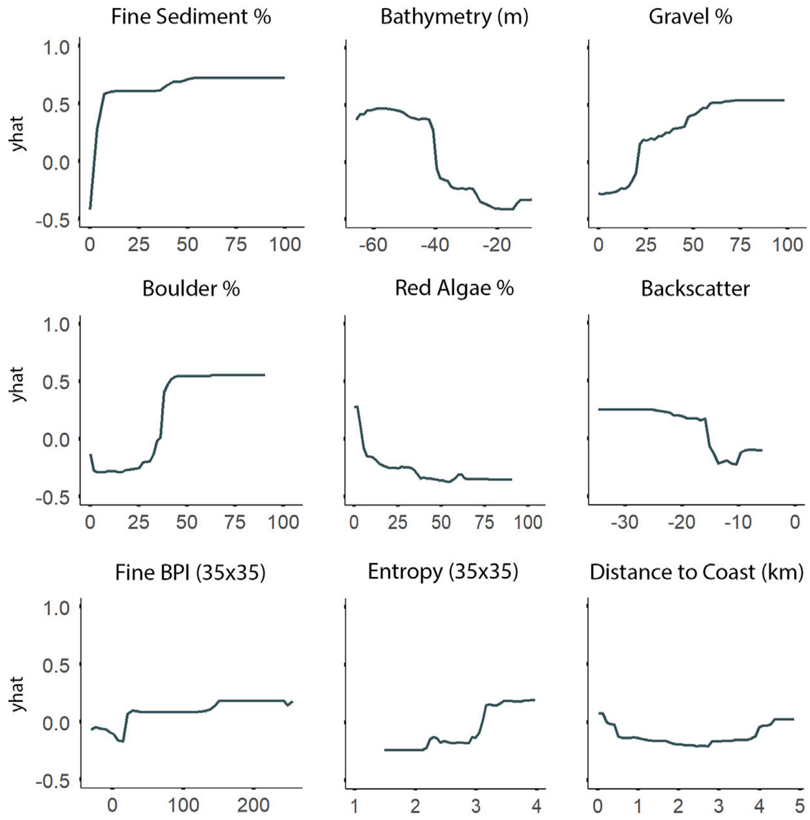

FIGURE 10
Partial dependence plots derived from the Random Forest classification model for the most important explanatory environmental features describing the distribution of *Agarum clathratum*. The 'yhat' axis refers to the value of partial dependence function. The partial response of *A. clathratum* to all features is provided in Supplementary Figure S2.

Smaller grain sizes, like gravel, are more likely to be reworked in a dynamic environment, limiting consistent light exposure and increasing physical damage and making it more difficult for CCA to establish growth due to abrasion (Foster, 2001; Hetzinger et al., 2006).

Removal of fine-scale substrate features from the RF models produced a substantial drop in predictive accuracy (~25%). Owing to the highly heterogeneous nature of the seafloor in Placentia Bay, the ability to capture increased structural complexity can allow for the identification of potential 'keystone structures', (i.e. structures that directly bolster species richness) (Tews et al., 2004). For example, '*Hormathia* sp.1' was often seen attached to the sporadic boulders scattered across the silt-covered seafloor in the deep channels within Rushoon. Drop stones resulting from glacial retreat (Shaw et al., 2011) have been shown to increase diversity of more homogeneous sediment dominated areas (Meyer et al., 2016). This fine-scale feature cannot currently be captured by acoustic surveying techniques such as MBES, but new methods such as synthetic apertures sonar may provide this capability (Gini et al., 2021).

Increased physical habitat complexity has previously been linked to increases in abundance and diversity (Barry and Dayton, 1991; Bracewell et al., 2018). In coastal environments, rocky shores play a critical role in structuring coastal benthic communities (Menge, 1982; Underwood and Denley, 1984). Within Placentia Bay, boulder and gravel fields occur along the offshore extent of D'Argent Bay and Burin and along the shoreline of Rushoon and St. Lawrence. These fields may provide a level of stability and topographical diversity that could increase structural availability for sessile invertebrates (MacArthur and Wilson, 1967; Liversage and Chapman, 2018; Franz et al., 2021), such as the sponges and anemones observed in Rushoon and St. Lawrence. These areas were found to be associated with a higher presence of arcto-boreal species, such as the different morphotypes of porifera and anthozoan as well as species of echinoderms and crustaceans. 1,064 individuals from 25 morphotypes of the Phylum Porifera were recorded in these areas, further increasing habitat complexity by acting as biogenic substrate for associated fauna (Buhl-Mortensen et al., 2017; Hogg et al., 2010, Maldonado et al., 2017). Those areas may represent rocky reefs–an ecologically important habitat

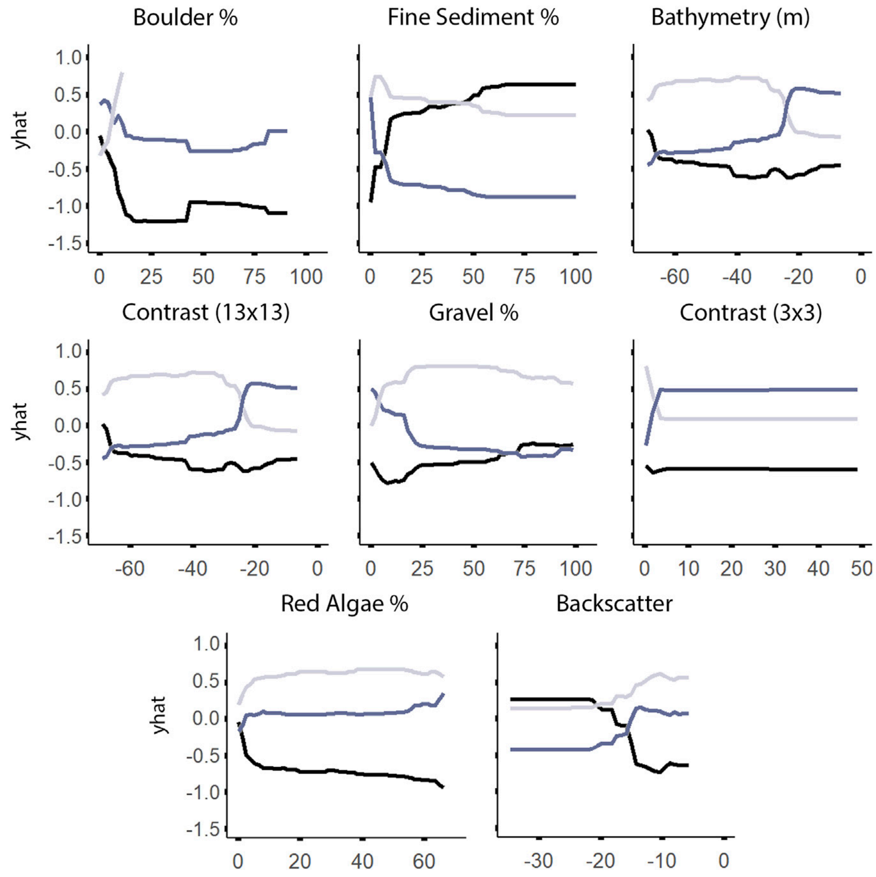

FIGURE 11
Univariate partial dependence plots derived from the Random Forest classification model for the most important explanatory environmental features describing the distribution of non-geniculate crustose coralline algae (CCA). The 'yhat' axis refers to the value of partial dependence function. The partial response of absence, partial coverage, and full coverage of CCA to all features is provided in Supplementary Figure S3.

characterized as a subtidal natural hard substrate, which has been linked to increased biodiversity (Taylor, 1998; Kostylev et al., 2005; Wahl, 2009).

Rocky reefs from temperate to Arctic environments are often covered with canopy-forming kelp species. Likely, the dense coverage of *A. clathratum* observed in the subtidal would also contribute to increased epifaunal richness (Blain and Gagnon, 2014; Teagle et al., 2017). Fewer species were observed than expected in the SDR assemblage, but this may have resulted from limited visibility of the seafloor due to obstruction by *A. clathratum* blades.

Few other brown kelp species were observed during ground-truthingan exception being two sites in Rushoon fully covered by the sugar kelp *S. latissima*. *A. clathratum* was often found to co-exist with red algae though. The potential for increased coverage by red algae is an example of an observable change made possible by comparing to the baseline established in this study. As compared to kelp beds, low-lying red algae turfs are a fast-growing and stress-tolerant opportunistic group (Airoldi, 1998; Filbee-Dexter and Wernberg, 2018), and high turnover rates allow them to succeed kelp forests that have been weakened by thermal stress (Scheibling and Gagnon, 2006; Filbee-Dexter et al., 2016; Wernberg et al., 2019). Kelp is more susceptible to stress due to ocean warming and increased storm activity, concurrent with cyclical herbivorous pressure by *S. droebachiensis* (Filbee-Dexter and Wernberg, 2018). Once it supersedes kelp, red algae turfs cover the substrate, preventing kelp from resettling and inducing phase shifts to environments with reduced oxygen and increased sediment accumulation (Gorgula and Connell, 2004), further negatively impacting settlement of kelp spores (Norton and Fetter, 1981; Gorman and Connell, 2009; Connell and Russell, 2010). Kelp is susceptible to stress due to ocean warming and increased storm activity, concurrent with cyclical herbivorous pressure by *S. droebachiensis*. No observations of turf-dominated areas show shifting back to kelp (Filbee-Dexter and Wernberg, 2018).

The performances of the RF algorithm, which is well-established in the field of benthic habitat mapping, and the newer LightGBM were comparable considering only model accuracy and variable importance estimates. However, disagreements occurred over the predictions of the rarer assemblages, especially when both model types were used to develop predictive maps. LightGBM is a powerful modelling technique, but it was developed to manage large datasets (e.g., 1,00,000 s of observations) (Ke et al., 2017). Sample sizes of this magnitude are uncommon in marine ecology [Benkendorf and Hawkins, 2020; Luan et al., 2020]. The small sample size in this study likely resulted in overfitting of the LightGBM models, apparent, for example, in the prediction of CCA absences. Ground-truthing samples indicated extensive full and partial coverage of CCA in D'Argent Bay and Burin; however, LightGBM predicted very sparse CCA coverage for most of the areas.

LightGBM advertises faster training speed, low memory usage (Ke et al., 2017; McCarty et al., 2020), and in-depth control over boosting and model learning *via* tunable parameters. The latter point, though, requires the user to be confident in their understanding of each parameter. In contrast, RF has only two parameters that generally require manipulation, and even appears quite robust to these in practice, making it a more user-friendly algorithm (Brieman, 2001; Liaw and Weiner, 2002). RF has demonstrated repeated success in benthic habitat mapping studies comparing techniques (Lucieer et al., 2013; Robert et al., 2015; Rooper et al., 2017; Misiuk et al., 2019; Pillay et al., 2020; Shang et al., 2021). However, RF may be biased towards computational efficiency in favor of accuracy (Fernandez-Delgado et al., 2011; Wainberg et al., 2016). The comparison carried out here supports the continued use of RF as a modelling technique that can perform well with the limited amount of data that is common in marine studies. It will be of great interest to determine whether the newer LightGBM algorithm shows better performance with larger datasets.

The subtidal zone of western Placentia Bay is host to a diverse and heterogeneous benthic environment that supports multiple ecosystem services. The baseline information provided by this study provides information necessary to monitor potential changes in biodiversity and ecosystem function within the Placentia Bay EBSA. The communities of OPH and MIX are notable for their epifaunal diversity, comprising structure-forming sessile invertebrates. Biogenic structural heterogeneity is often linked to increased biodiversity (Buhl-Mortensen et al., 2010; Thomsen et al., 2010; Lefcheck et al., 2017; Kazanidis et al., 2021), which may support ecosystem health. Coastal townships of Placentia Bay also rely on the health of this benthic ecosystem, which support local livelihoods, but which may be threatened under increased anthropogenic activity (e.g. aquaculture, oil shipping) and shifts in ocean temperature and pH (Doney et al., 2009). Proactive management action may mitigate potential detrimental changes brought on by these stressors.

Conclusion

The predictive maps developed in this study indicate a heterogenous benthic ecosystem in the western part of the Placentia Bay EBSA, composed of habitat-forming biotasuch as marine algae and sessile invertebrates including porifera and anemones. This contributes substantiallyto baseline understanding of marine epifaunal distributions and richness in a subtidal area of recognized ecological and socio-economic importance. Concurrent with predictive geospatial modelling, investigation of fine-scale (<1 m) substrate characteristics highlight their importance as benthic habitat drivers. All models tested here performed better with the addition of discrete fine-scale substrate observations compared to the use of spatially continuous acoustic backscatter proxies. The LightGBM models had higher accuracies, but often demonstrated signs of overfitting as compared with the predictive maps derived from the RF models. The fundamental knowledge derived from these models provide information that is critically needed for monitoring the health of the Placentia Bay EBSA over time.

Data availability statement

The datasets presented in this study can be found in online repositories. The names of the repository/repositories and accession number(s) can be found below: https://slgo.ca/en/coastal-environment-baseline-program/.

Author contributions

JM-M collected ground-truthing data for Burin and St. Lawrence, with Rushoon and D'Argent Bay collected by SN. Acoustic surveying of all study areas was conducted on the R/V Cartwright by AT and Kirk Regular (latter not included). Data processing, analysis, and model development and interpretation was conducted by JM-M with assistance from SN and BM. JM-M and SN collaborated in creating a species guide for the identification of all observed benthic flora and fauna (>2 cm) to the lowest taxonomic level possible. BM assisted with processing multibeam echosounder data from the survey areas. Project initiation with the Fisheries and Oceans Canada and the organization of fieldwork was led by KR. All writing was initially done by JM-M with editorial input from SN, AT, BM, KR, EE, and PG.

Conflict of interest

The authors declare that the research was conducted in the absence of any commercial or financial relationships that could be construed as a potential conflict of interest.

Publisher's note

Supplementary material

The Supplementary Material for this article can be found online at: https://www.frontiersin.org/articles/10.3389/fenvs.2022.999483/full#supplementary-material

References

Agatsuma, Y. (2000). Food consumption and growth of the juvenile sea urchin *Strongylocentrotus intermedius*. *Fish. Sci.* 66, 467–472. doi:10.1046/j.1444-2906.2000.00075.x

Airoldi, L. (1998). Roles of disturbance, sediment stress, and substratum retention on spatial dominance in algal turf. *Ecology* 79, 2759–2770. doi:10.1890/0012-9658(1998)079[2759:rodssa]2.0.co;2

Alexandridis, N., Bacher, C., Desroy, N., and Jean, F. (2017). Building functional groups of marine benthic macroinvertebrates on the basis of general community assembly mechanisms. *J. Sea Res.* 121, 59–70. doi:10.1016/j.seares.2017.01.007

Allouche, O., Tsoar, A., and Kadmon, R. (2006). Assessing the accuracy of species distribution models: Prevalence, kappa and the true skill statistic (TSS). *J. Appl. Ecol.* 43, 1223–1232. doi:10.1111/j.1365-2664.2006.01214.x

Auster, P. J., and Langton, R. W. (1998). The effects of fishing on fish habitat. *Am. Fish. Soc. Symposium* 22, 150–187.

Barbier, E. B., Hacker, S. D., Kennedy, C., Koch, E. W., Stier, A. C., and Silliman, B. R. (2011). The value of estuarine and coastal ecosystem services. *Ecol. Monogr.* 81, 169–193. doi:10.1890/10-1510.1

Barry, J. P., and Dayton, P. H. (1991). "Physical heterogeneity and the organisation of marine Communities," in *Ecological heterogeneity*. Editors J. Kolasa, and S. T. A. Pickett (New York, NY: Springer-Verlag), 270–320.

Bégin, C., Johnson, L. E., and Himmelman, J. H. (2004). Macroalgal canopies: Distribution and diversity of associated invertebrates and effects on the recruitment and growth of mussels. *Mar. Ecol. Prog. Ser.* 271, 121–132. doi:10.3354/meps271121

Bekkby, T., Rinde, E., Erikstad, L., and Bakkestuen, V. (2009). Spatial predictive distribution modelling of the kelp species *Laminaria hyperborea*. *ICES J. Mar. Sci.* 66, 2106–2115. doi:10.1093/icesjms/fsp195

Bekkby, T., Smit, C., Gundersen, H., Rinde, E., Steen, H., Tveiten, L., et al. (2019). The abundance of kelp is modified by the combined impact of depth, waves and currents. *Front. Mar. Sci.* 6, 1–10. doi:10.3389/fmars.2019.00475

Benkendorf, D. J., and Hawkins, C. P. (2020). Effects of sample size and network depth on a deep learning approach to species distribution modeling. *Ecol. Inf.* 60, 101137. doi:10.1016/j.ecoinf.2020.101137

Bennett, N. J., Cisneros-Montemayor, A. M., Blythe, J., Silver, J. J., Signh, G., Andrews, N., et al. (2019). Towards a sustainable and equitable blue economy. *Nat. Sustain.* 2, 991–993. doi:10.1038/s41893-019-0404-1

Bevilacqua, S., Ugland, K. I., Plicanti, A., Scuderi, D., and Terlizzi, A. (2018). An approach based on the total-species accumulation curve and higher taxon richness to estimate realistic upper limits in regional species richness. *Ecol. Evol.* 8, 405–415. doi:10.1002/ece3.3570

Bilyard, G. R. (1987). The value of benthic infauna in marine pollution monitoring studies. *Mar. Pollut. Bull.* 18, 581–585. doi:10.1016/0025-326X(87)90277-3

Blain, C., and Gagnon, P. (2014). Canopy-forming seaweeds in urchin-dominated systems in eastern Canada: Structuring forces or simple prey for keystone grazers. *PLoS ONE* 9, e98204. doi:10.1371/journal.pone.0098204

Bland, A., Konar, B., and Edwards, M. (2019). Spatial trends and environmental drivers of epibenthic shelf community structure across the Aleutian Islands. *Cont. Shelf Res.* 175, 12–29. doi:10.1016/j.csr.2019.01.006

Blondel, P., and Sichi, O. G. (2009). Textural analyses of multibeam sonar imagery from Stanton Banks. Northern Ireland continental shelf. *Appl. Acoust.* 70, 1288–1297. doi:10.1016/j.apacoust.2008.07.015

Borcard, D., Gillet, F., and Legendre, P. (2011). *Numerical ecology with R*. New York: Springer.

Botello, A. V., Soto, L. A., Ponce-Velez, G., and Villanueva, S. (2015). Baseline for PAHs and metals in NW Gulf of Mexico related to the Deepwater Horizon oil spill. *Estuar. Coast. Shelf Sci.* 156, 124–133. doi:10.1016/j.ecss.2014.11.010

Bracewell, S. A., Clark, G. F., and Johnston, E. L. (2018). Habitat complexity effects on diversity and abundance differ with latitude: An experimental study over 20 degrees. *Ecology* 99, 1964–1974. doi:10.1002/ecy.2408

Brey, T. (2012). A multi-parameter artificial neural network model to estimate macrobenthic invertebrate productivity and production. *Limnol. Oceanogr. Methods* 10, 581–589. doi:10.4319/lom.2012.10.581

Brieman, L. (2001). Random forests. *Mach. Learn.* 45, 5–32. doi:10.1023/A:1010933404324

Brown, C. J., Sameoto, J. A., and Smith, S. J. (2012). Multiple methods, maps, and management applications: Purpose made seafloor maps in support of ocean management. *J. Sea Res.* 72, 1–13. doi:10.1016/j.seares.2012.04.009

Buhl-Mortensen, L., Vanreusel, A., Gooday, A. J., Levin, L. A., Priede, I. G., Buhl-Mortensen, P., et al. (2010). Biological structures as a source of habitat heterogeneity and biodiversity on the deep ocean margins. *Mar. Ecol. Berl.* 31, 21–50. doi:10.1111/j.1439-0485.2010.00359.x

Buhl-Mortensen, P., Buhl-Mortensen, L., and Purser, A. (2017). "Trophic ecology and habitat provision in cold-water coral ecosystems," in *Marine animal forests*. Editors S. L. RossiBramanti, A. Gori, and C. Orejas (Cham: Springer).

Cabanac, A., and Himmelman, J. H. (1998). Directional movement of the sand dollar *Echinarachnius parma*. *Ophelia* 48, 93–102. doi:10.1080/00785236.1998.10428679

Cabanac, A., and Himmelman, J. H. (1996). Population structure of the sand dollar *Echinarachnius parma* in the subtidal zone of the northern Gulf of St. Lawrence, eastern Cananda. *Can. J. Zool.* 74, 698–709. doi:10.1139/z96-079

Calvert, J., Strong, J. A., Service, M., McGonigle, C., and Quinn, R. (2015). An evaluation of supervised and unsupervised classification techniques for marine benthic habitat mapping using multibeam echosounder data. *ICES J. Mar. Sci.* 72, 1498–1513. doi:10.1093/icesjms/fsu223

Castellan, G., Angeletti, L., Canese, S., Mazzoli, C., Montagna, P., Schiaparelli, S., et al. (2021). Visual imaging of benthic carbonate-mixed factories in the ross sea region marine protected area, Antarctica. *Minerals* 11, 833. doi:10.3390/min11080833

Chenelot, H., Jewett, S. C., and Hoberg, M. K. (2011). Macrobenthos of the nearshore aluetian archipelago, with emphasis on invertebrates associated with *clathromorphum* nereostratum (rhodophyta, corallinaceae). *Mar. Biodivers.* 41, 413–424. doi:10.1007/s12526-010-0071-y

Cohen, J. (1960). A coefficient of agreement for nominal scales. *Educ. Psychol. Meas.* 20, 37–46. doi:10.1177/001316446002000104

Congalton, R. G. (1991). A review of assessing the accuracy of classifications of remotely sensed data. *Remote Sens. Environ.* 37, 35–46. doi:10.1016/0034-4257(91)90048-B

Connell, S., and Russell, B. D. (2010). The direct effects of increasing CO_2 and temperature on non-calcifying organisms: Increasing the potential for phase shifts in kelp forests. *Proc. R. Soc. B* 277, 1409–1415. doi:10.1098/rspb.2009.2069

Connell, S. D. (2005). Assembly and maintenance of subtidal habitat heterogeneity: Synergistic effects of light penetration and sedimentation. *Mar. Ecol. Prog. Ser.* 289, 53–61. doi:10.3354/meps289053

Connell, S. D., Foster, M. S., and Airoldia, L. (2014). What are algal turfs? Towards a better description of turfs. *Mar. Ecol. Prog. Ser.* 495, 299–307. doi:10.3354/meps10513

Costanza, R., d'Arge, R., deGroot, R., Farber, S., Grasso, M., Hannon, B., et al. (1997). The value of the world's ecosystem services and natural capital. *Nature* 387, 253–260. doi:10.1038/387253a0

De la Torriente, A., Serrano, A., Fernanzdez-Salas, L. M., Garcia, M., and Aguilar, R. (2018). Identifying epibenthic habitats on the Seco de los Olivos Seamount: Species assemblages and environmental characteristics. *Deep Sea Res. Part I Oceanogr. Res. Pap.* 135, 9–22. doi:10.1016/j.dsr.2018.03.015

Dean, A. J., Steneck, R. S., Tager, D., and Pandolfi, J. M. (2015). Distribution, abundance and diversity of crustose coralline algae on the Great Barrier Reef. *Coral Reefs* 34, 581–594. doi:10.1007/s00338-015-1263-5

Degenhardt, F., Seifert, S., and Szymczak, S. (2019). Evaluation of variable selection methods for random forests and omics data sets. *Brief. Bioinform.* 20, 492–503. doi:10.1093/bib/bbx124

Degraer, S., Verfaillie, E., Willems, W., Adiaens, E., Vincx, M., and Van Lancker, V. (2008). Habitat suitability modelling as a mapping tool for macrobenthic communities: An example from the Belgian part of the North Sea. *Cont. Shelf Res.* 28, 369–379. doi:10.1016/j.csr.2007.09.001

DFO (2004). *Identification of ecologically and biologically significant areas*. Ottawa, ON. DFO Canadian Science Advisory Secretariat. Ecosystem Status Report 2004/006.

DFO (2018). *Identification of habitat important to the Blue whale in the western north atlantic*. Ottawa, ON. DFO Canadian Science Advisory Secretariat Science Advisory Report #2018/003.

DFO (2007). *Placentia Bay integrated management plan*. Ottawa, ON. DFO Canadian Science Advisory Secretariat 2007/1292.

DFO (2019). *Re-Evaluation of the Placentia Bay-Grand Banks area to identify ecologically and biologically significant areas*. St. John's, NL. DFO Canadian Science Advisory Secretariat Science Advisory Report. 2019/040.

DFO (2016). *Refinement of information relating to ecologically and biologically significant areas (EBSAs) identified in the Newfoundland and Labrador (NL) bioregion*. St. John's, NL. DFO Canadian Science Advisory Secretariat #2016/032.

DFO (2012a). *State of the ocean for the Placentia Bay – grand banks large ocean management area*, 2983. Ottawa, ON: DFO Canadian Manuscript Report of Fisheries and Aquatic Sciences. viii + 34 p.

DFO (2012b). *Using satellite tracking data to define important habitat for leatherback turtles in Atlantic Canada*. Ottawa, ON. DFO Canadian Science Advisory Secretariat Science Advisory Report #2012/036.

Diesing, M., and Thorsnes, T. (2017). Mapping of cold-water coral carbonate mounds based on geomorphometric features: An object-based approach. *Geosciences* 8, 34. doi:10.3390/geosciences8020034

Dolan, M. F. J. (2012). *Calculation of slope angle from bathymetry data using GIS – effects of computation algorithms, data resolution and analysis scale*. Trondheim, Norway: Geological Survey of Norway. NGU Report, 2012.041.

Dolan, M. F. J., and Lucieer, V. L. (2014). Variation and uncertainty in bathymetric slope calculations using geographic information systems. *Mar. Geod.* 37, 187–219. doi:10.1080/01490419.2014.902888

Doney, S. C., Fabry, V. J., Feely, R. A., and Kleypas, J. A. (2009). Ocean acidification: The other CO_2 problem. *Ann. Rev. Mar. Sci.* 1, 169–192. doi:10.1146/annurev.marine.010908.163834

Dunlop, K., Harendza, A., Plassen, L., and Keeley, N. (2020). Epifaunal habitat associations on mixed and hard bottom substrates in coastal waters of northern Norway. *Front. Mar. Sci.* 7, 568802. doi:10.3389/fmars.2020.568802

Elith, J., and Leathwick, J. R. (2009). Species distribution models: Ecological explanation and prediction across space and time. *Annu. Rev. Ecol. Evol. Syst.* 40, 677–697. doi:10.1146/annurev.ecolsys.110308.120159

Fernandez-Delgado, M., Riberio, J., Cernadas, E., and Ameneiro, S. B. (2011). Direct parallel perceptions (DPP): Fast analytical calculation of the parallel perceptions weights with margin control for classification tasks. *Neural Netw. IEEE Trans.*22, 1837–1848. doi:10.1109/TNN.2011.2169086

Filbee-Dexter, K., Feehan, C. J., and Scheibling, R. E. (2016). Large-scale degradation of a kelp ecosystem in an ocean warming hotspot. *Mar. Ecol. Prog. Ser.* 543, 141–152. doi:10.3354/meps11554

Filbee-Dexter, K., and Scheibling, R. E. (2014). Sea urchin barrens as alternative stable states of collapsed kelp ecosystems. *Mar. Ecol. Prog. Ser.* 495, 1–25. doi:10.3354/meps10573

Filbee-Dexter, K., and Wernberg, T. (2018). Rise of turfs: A new battlefront for globally declining kelp forests. *Bioscience* 68, 64–76. doi:10.1093/biosci/bix147

Foster, M. S. (2001). Rhodoliths: Between rocks and soft places. *J. Phycol.* 37, 659–667. doi:10.1046/j.1529-8817.2001.00195.x

Fox, J., Lambert, G., and Salomonsen, H. (2014). *Basic identification guide of common bycatch species – fishing intensity trial*. Bangor, United kingdom: Bangor University.

Franz, M., von Ronn, G. A., Barboza, F. R., Karez, R., Reimers, H. C., Schwarzer, K., et al. (2021). How do geological structure and biological diversity relate? Benthic communities in boulder fields of the southwestern baltic sea. *Estuaries Coasts* 44, 1994–2009. doi:10.1007/s12237-020-00877-z

Freiwald, A. (1993). Coralline algal maerl frameworks-Islands within the phaeophytic kelp belt. *Facies* 29, 133–148. doi:10.1007/BF02536925

Friedman, J., Hastie, T., and Tibshirani, R. (2001). *The elements of statistical learning*, 1. Berlin: Springer.

Gagnon, P., Himmelman, J. H., and Johnson, L. E. (2003). Algal colonization in urchin barrens: Defense by association during recruitment of the Brown alga *Agarum cribrosum*. *J. Exp. Mar. Biol. Ecol.* 290, 179–196. doi:10.1016/S0022-0981(03)00077-7

Gagnon, P., Matheson, K., and Stapleton, M. (2012). Variation in rhodolith morphology and biogenic potential of newly discovered rhodolith beds in Newfoundland and Labrador (Canada). *Bot. Mar.* 55, 85–99. doi:10.1515/bot-2011-0064

Gini, C., Robert, K., Jamieson, J., and Dillon, J. (2021). *Interferometric synthetic aperture sonar as a tool for seafloor geological mapping on the grand banks offshore atlantic Canada: Preliminary results*. [Conference presentation] European Geophysical Union General Assembly, virtual. St. John's, NL: Memorial University of Newfoundland.

Gorgula, S. K., and Connell, S. D. (2004). Expansive covers of turf-forming algae on human-dominated coast: The relative effects of increasing nutrient and sediment loads. *Mar. Biol.* 145, 613–619. doi:10.1007/s00227-004-1335-5

Gorman, D., Bajjouk, T., Populus, J., Vasquez, M., and Erhold, A. (2013). Modeling kelp forest distribution and biomass along temperate rocky coastlines. *Mar. Biol.* 160, 309–325. doi:10.1007/s00227-012-2089-0

Gorman, D., and Connell, S. D. (2009). Recovering subtidal forests in human-dominated landscapes. *J. Appl. Ecol.* 46, 1258–1265. doi:10.1111/j.1365-2664.2009.01711.x

Gosner, K. L. (1979). *A field guide to the atlantic seashore: Invertebrates and seaweeds of the atlantic coast from the Bay of fundy to cape hatteras; text and illustrations*. Boston: Houghton Mifflin.

Graf, G. (1992). Benthic-pelagic coupling: A benthic view. *Oceanogr. Mar. Biol.* 30, 149–190.

Grebmeier, J. M., and Barry, J. P. (1991). The influence of oceanographic processes on pelagic-benthic coupling in polar regions: A benthic perspective. *J. Mar. Syst.* 2, 495–518. doi:10.1016/0924-7963(91)90049-z

Hajializadeh, P., Safaie, M., Naderloo, R., Shojaei, M. G., Gammal, J., Villnas, A., et al. (2020). Species composition and functional traits of macrofauna in different mangrove habitats in the Persian gulf. *Front. Mar. Sci.* 7, 575480. doi:10.3389/fmars.2020.575480

Haralick, R. M., Shanmugam, K., and Dinstein, I. (1973). Textural features for image classification. *IEEE Trans. Syst. Man. Cybern.* SMC-3, 610–621. doi:10.1109/TSMC.1973.4309314

Harvey-Clark, C. (1997). *Eastern tidepool & reef: North-central atlantic marine life*. Surrey: Hancock House Publishers.

Hepburn, C. D., Holborow, J. D., Wing, S. R., Frew, R. D., and Hurd, C. L. (2007). Exposure to waves enhances the growth rate and nitrogen status of the giant kelp *Macrocystis pyrifera*. *Mar. Ecol. Prog. Ser.* 339, 99–108. doi:10.3354/meps339099

Hetzinger, S., Halfar, J., Riegl, B., and Godinez-Orta, L. (2006). Sedimentology and acoustic mapping of modern rhodolith facies on a non-tropical carbonate shelf (Gulf of California, Mexico). *J. Sediment. Res.* 76, 670–682. doi:10.2110/jsr.2006.053

Hobson, R. D. (1972). "Surface roughness in topography: A quantitative approach," in *Spatial analysis in geomorphology*. Editor R. J. Chorley (London: Methuen & Co.), 221–245.

Hogg, M. M., Tendal, O. S., Conway, K. W., Pomponi, S. A., van Soest, R. W. M., Gutt, J., et al. (2010). *Deep-sea sponge-grounds: Reservoirs of biodiversity*. Cambridge, UK: UNEP-WCMC. UNEP-WCMC Biodiversity Series No.32.

Howell, K. L., Davies, J. S., Allcock, A. L., Braga-Henriques, A., Buhl-Mortensen, P., Carreiro-Silva, M., et al. (2019). A framework for the development of a global standardised marine taxon reference image database (SMarTaR-ID) to support image-based analyses. *PLoS ONE* 14, e0218904. doi:10.1371/journal.pone.0218904

Hurd, C. L., Harrison, P. J., and Druehl, K. D. (1996). Effect of seawater velocity on inorganic nitrogen uptake by morphologically distinct forms of *Macrocystis intergrifolia* from wave-sheltered and exposed sites. *Mar. Biol.* 126, 205–214. doi:10.1007/BF00347445

Iken, K., Bluhm, B., and Dunton, K. (2010). Benthic food-web structure under differing water mass properties in the southern Chukchi Sea. *Deep Sea Res. Part II Top. Stud. Oceanogr.* 57, 71–85. doi:10.1016/j.dsr2.2009.08.007

Ilich, A. R., Brizzolara, J. L., Grasty, S. E., Gray, J. W., Hommeyer, M., Lembke, C., et al. (2021). Integrating towed underwater video and multibeam acoustics for marine benthic habitat mapping and fish population estimation. *Geosciences* 11, 176. doi:10.3390/geosciences11040176

Janowski, L., Wroblewski, R., Dworniczak, J., Kolakowski, M., Rogowska, K., Wojcik, M., et al. (2021). Offshore benthic habitat mapping based on object-based image analysis and geomorphometric approach. A case study from the Slupsk Bank, Southern Baltic Sea. *Sci. Total Environ.* 801, 149712. doi:10.1016/j.scitotenv.2021.149712

Jørgensbye, H. I. O., and Halfar, J. (2017). Overview of coralline red algal crusts and rhodolith beds (Corallinales, Rhodophyta) and their possible ecological importance in Greenland. *Polar Biol.* 40, 517–531. doi:10.1007/s00300-016-1975-1

Kazanidis, G., Henry, L. A., and Roberts, J. M. (2021). Hidden structural heterogeneity enhances marine hotspots' biodiversity. *Coral Reefs* 40, 1615–1630. doi:10.1007/s00338-021-02114-w

Ke, G., Meng, Q., Finley, T., Wang, T., Chen, W., Ma, W., et al. (2017). LightGBM: A highly efficient gradient boosting decision tree. *Adv. Neural Inf. Process. Syst.* 2017, 3147–3155.

Kelly, J. R., Scheibling, R. E., Iverson, S. J., and Gagnon, P. (2008). Fatty acid profiles in the gonads of the sea urchin *Strongylocentrotus droebachiensis* on natural algal diets. *Mar. Ecol. Prog. Ser.* 373, 1–9. doi:10.3354/meps07746

Konar, B., and Iken, K. (2005). Competitive dominance among sessile marine organisms in a high Arctic boulder community. *Polar Biol.* 29, 61–64. doi:10.1007/s00300-005-0055-8

Kostylev, V. E., Erlandsson, J., Ming, M. Y., and Williams, G. A. (2005). The relative importance of habitat complexity and surface area in assessing biodiversity: Fractal application on rocky shores. *Ecol. Complex.* 2, 272–286. doi:10.1016/j.ecocom.2005.04.002

Kostylev, V. E., Todd, B. J., Fader, G. B. J., Courtney, R. C., Cameron, G. D. M., and Pickrill, R. A. (2001). Benthic habitat mapping on the Scotian Shelf based on multibeam bathymetry, surficial geology and sea floor photographs. *Mar. Ecol. Prog. Ser.* 219, 121–137. doi:10.3354/meps219121

Krause-Jensen, D., Sejr, M. K., Bruhn, A., Rasmussen, M. B., Christensen, P. B., Hansen, J. L. S., et al. (2019). Deep penetration of kelps offshore along the west coast of Greenland. *Front. Mar. Sci*. 6, 375. doi:10.3389/fmars.2019.00375

Kreft, H., and Jetz, W. (2010). A framework for delineating biogeographical regions based on species distributions. *J. Biogeogr.* 37, 2029–2053. doi:10.1111/j.1365-2699.2010.02375.x

Krumhansl, K. A., Okamoto, D. K., Rassweiler, A., Novak, M., Bolton, J. J., Cavanaugh, K. C., et al. (2016). Global patterns of kelp forest change over the past half-century. *Proc. Natl. Acad. Sci. U. S. A.* 113, 13785–13790. doi:10.1073/pnas.1606102113

Kurse, M. B., and Rudnicki, W. R. (2010). Feature selection with the Boruta package. *J. Stat. Softw.* 26, 1–13. doi:10.18637/jss.v036.i11

Lacharite, M., and Brown, C. J. (2019). Utilizing benthic habitat maps to inform biodiversity monitoring in marine protected areas. *Aquat. Conserv.* 29, 938–951. doi:10.1002/aqc.3074

Lam-Gordillo, O., Baring, R., and Dittmann, S. (2021). Taxonomic and functional patterns of benthic communities in southern temperate tidal flats. *Front. Mar. Sci.* 8, 113202. doi:10.3389/fmars.2021.723749

Lamarche, G., Lurton, X., Verdier, A. L., and Augustin, J. M. (2011). Quantitative characterisation of seafloor substrate and bedforms using advanced processing of multibeam backscatter—application to cook strait, New Zealand. *Cont. Shelf Res.* 31, S93–S109. doi:10.1016/j.csr.2010.06.001

Largier, J. L. (2020). Upwelling bays: How coastal upwelling controls circulation, habitat, and productivity in bays. *Ann. Rev. Mar. Sci.* 12, 415–447. doi:10.1146/annurev-marine-010419-011020

Lecours, V., Brown, C. J., Devillers, R., Lucieer, V. L., and Edinger, E. N. (2016a). Comparing selections of environmental variables for ecological studies: A focus on terrain attributes. *PLoS ONE* 11, e0167128. doi:10.1371/journal.pone.0167128

Lecours, V., Devillers, R., Schneider, D. C., Lucieer, V. L., Brown, C. J., and Edinger, E. N. (2015). Spatial scale and geographic context in benthic habitat mapping: Review and future directions. *Mar. Ecol. Prog. Ser.* 525, 259–284. doi:10.3354/meps11378

Lecours, V., Dolan, M. F. J., Micallef, A., and Lucieer, V. L. (2016b). A review of marine geomorphometry, the quantitative study of the seafloor. *Hydrol. Earth Syst. Sci.* 20, 3207–3244. doi:10.5194/hess-20-3207-2016

Lecours, V. (2015). *Terrain Attribute selection for spatial ecology (TASSE)*. V.1.0.. Quebec City, Quebec: University of Quebec. doi:10.13140/RG.2.2.15014.52800

Lefcheck, J. S., Marion, S. R., and Orth, R. J. (2017). Restored eelgrass (zostera marina L.) as a refuge for epifaunal biodiversity in mid-western atlantic coastal bays. *Estuaries Coasts* 40, 200–212. doi:10.1007/s12237-016-0141-x

Legendre, P., and Gallagher, E. D. (2001). Ecologically meaningful transformations for ordination of species data. *Oecologia* 129, 271–280. doi:10.1007/s004420100716

Legendre, P. (2013). "Indicator species: Computation," in *Encyclopedia of biodiversity*. Second Edition, 4, 264–268. doi:10.1016/B978-0-12-384719-5.00430-5

LGL (2018). *Fish and fish habitat. Component study for the environmental impact statement of the Placentia Bay atlantic salmon aquaculture project*. Marystown, NL: Rep. by LGL Limited, St. John's, NL for Grieg NL, 71. LGL Rep. FA0144-2+ appendices.

Li, J., Tran, M., and Siwabessy, J. (2016). Selecting optimal random forest predictive models: A case study on predicting the spatial distribution of seabed hardness. *PLoS ONE* 11, e0149089. doi:10.1371/journal.pone.0149089

Liaw, A., and Weiner, M. (2002). Classification and regression by randomForest. *R. News* 2, 18–22.

Littler, M. M., Littler, D. S., Blair, S. M., and Norris, J. N. (1985). Deepest known plant life discovered on an uncharted seamount. *Science* 227, 57–59. doi:10.1126/science.227.4682.57

Liversage, K., and Chapman, M. G. (2018). Coastal ecological engineering and habitat restoration: Incorporating biologically diverse boulder habitat. *Mar. Ecol. Prog. Ser.* 593, 173–185. doi:10.3354/meps12541

Long, R. D., Charles, A., and Stephenson, R. L. (2015). Key principles of marine ecosystem-based management. *Mar. Policy* 57, 53–60. doi:10.1016/j.marpol.2015.01.013

Lotze, H. K., Lenihan, H. S., Bourque, B. J., Bradbury, R. H., Cooke, R. G., Kay, M. C., et al. (2006). Depletion, degradation, and recovery potential of estuaries and coastal seas. *Science* 312, 1806–1809. doi:10.1126/science.1128035

Luan, J., Zhang, C. L., Xu, B. D., Xue, Y., and Ren, Y. P. (2020). The predictive performances of random forest models with limited sample size and different species traits. *Fish. Res.* 227, 105534. doi:10.1016/j.fishres.2020.105534

Lucieer, V., Hill, N. A., Barret, N. S., and Nichol, S. (2013). Do marine substrates 'look' and 'sound' the same? Supervised classification of multibeam acoustic data using autonomous underwater vehicle images. *Estuar. Coast. Shelf Sci.* 117, 94–106. doi:10.1016/j.ecss.2012.11.001

Lundberg, S. M., Erion, G., Chen, H., DeGrave, A., Prutkin, J. M., Nair, B., et al. (2020). Explainable AI for trees: From local explanations to global understanding. *Nat. Mach. Intell.* 2, 56–67. doi:10.1038/s42256-019-0138-9

Lurton, X., and Lamarche, G. (Eds). (2015). *Backscatter measurements by seafloor-mapping sonars. Guidelines and Recommendations*. Auckland, New Zealand: GeoHab, 200. Available at: http://geohab.org/wp-content/uploads/2014/05/BSWG-REPORT-MAY2015.pdf.

Ma, Z., Han, G., and DeYoung, B. (2012). Modelling temperature, currents and stratification in Placentia Bay. *Atmosphere-Ocean* 50, 244–260. doi:10.1080/07055900.2012.677413

MacArthur, R. H., and Wilson, E. O. (1967). *The theory of island biogeography*. Princeton: Princeton University Press.

Maldonado, M., Aguilar, R., Bannister, R. J., Bell, J. J., Conway, K. W., DaytonDíaz, P. C., et al. (2017). "Sponge grounds as key marine habitats: A synthetic review of types, structure, functional roles, and conservation concerns," in *Marine animal forests: The ecology of benthic biodiversity hotspots*. Editors L. Bramanti, A. Gori, C. Orejas, and S. Rossi (Cham: Springer), 145–183.

Manderson, J. P., Pheln, B. A., Bejda, A. J., Stehlik, L. L., and Stoner, A. W. (1999). Predation by striped searobin (*Prionotus evolans*, triglidae) on young-of-the-year winter flounder (*Pseudopleuronectus americanus*, walbum): Examining prey size selection and prey choice using field observations and laboratory experiments. *J. Exp. Biol. Ecol.* 242, 211–231. doi:10.1016/S0022-0981(99)00105-7

Marini, C., Fossa, F., Paoli, C., Bellingeri, M., Gnone, G., and Vassallo, P. (2015). Predicting bottlenose dolphin distribution along Liguria coast (northwestern Mediterranean Sea) through different modeling techniques and indirect predictors. *J. Environ. Manag.* 150, 9–20. doi:10.1016/j.jenvman.2014.11.008

Marrack, E. C. (1999). The relationship between water motion and living rhodolith beds in the southwestern gulf of California, Mexico. *Palaios* 14, 159–171. doi:10.2307/3515371

Martín-García, L., González-Lorenzo, G., Brtio-Izquierdo, I. T., and Barquín-Diez, J. (2013). Use of topographic predictors for macrobenthic community mapping in the marine reserve of La palma (canary islands, Spain). *Ecol. Model.* 263, 19–31. doi:10.1016/j.ecolmodel.2013.04.005

Martinez, A. J., and Martinez, C. S. (2003). *Marine life of the north atlantic: Canada to new england*. New York: Aqua Quest Publications.

Masteller, C. C., Finnegan, N. J., Warrick, J. A., and Miller, I. M. (2015). Kelp, cobbles, and currents: Biologic reduction of coarse grain entrainment stress. *Geology* 43, 543–546. doi:10.1130/G36616.1

McCarty, D. A., Kim, H. W., and Lee, H. K. (2020). Evaluation of light gradient boosted machine learning technique in large scale land use and land cover classification. *Environments* 7, 84. doi:10.3390/environments7100084

McConnaughey, T. A., and Whelan, J. F. (1997). Calcification generates protons for nutrient and bicarbonate uptake. *Earth-Science Rev.* 42, 95–117. doi:10.1016/S0012-8252(96)00036-0

McLaren, K., McIntyre, K., and Prospere, K. (2019). Using the random forest algorithm to integrate hydroacoustic data with satellite images to improve the mapping of shallow nearshore benthic features in a marine protected area in Jamaica. *GIsci. Remote Sens.* 56, 1065–1092. doi:10.1080/15481603.2019.1613803

Meadows, P. S., Meadows, A., and Murray, J. M. H. (2012). Biological modifiers of marine benthic seascapes: Their role as ecosystem engineers. *Geomorphology* 157, 31–48. doi:10.1016/j.geomorph.2011.07.007

Meng, Z., Han, Q. X., and Wang, X. B. (2021). Distribution pattern of macrobenthic composition, diversity and secondary production in Hangzhou Bay, northern East China Sea. *Regional Stud. Mar. Sci.* 47, 101956. doi:10.1016/j.rsma.2021.101956

Menge, B. A. (1982). “Effects of feeding on the environment: Asteroidea,” in *Echinoderm nutrient*. Editors M. Jangoux, and J. Lawrence. 1st edition (Rotterdam: A.A. Balkema), 521–551.

Meyer, K. S., Young, C. M., Sweetman, A. K., Taylor, J., Soltwedel, T., and Bergmann, M. (2016). Rocky islands in a Sea of mud: Biotic and abiotic factors structuring deep-sea dropstone communities. *Mar. Ecol. Prog. Ser.* 556, 45–57. doi:10.3354/meps11822

Misiuk, B., Diesing, M., Aitken, A., Brown, C. J., Edinger, E. N., and Bell, T. (2019). A spatially explicit comparison of quantitative and categorical modelling approaches for mapping seabed sediments using random forest. *Geosciences* 9, 254. doi:10.3390/geosciences9060254

Misiuk, B., Lecours, V., and Bell, T. (2018). A multiscale approach to mapping seabed sediments. *PLoS ONE* 13, e0193647. doi:10.1371/journal.pone.0193647

Misiuk, B., Lecours, V., Dolan, M. F. J., and Robert, K. (2021). Evaluating the suitability of multi-scale terrain Attribute calculation approaches for seabed mapping applications. *Mar. Geod.* 44, 327–385. doi:10.1080/01490419.2021.1925789

Morrison, L., Feely, M., Stengel, D. B., Blamey, N., Dockery, P., Sherlock, A., et al. (2009). Seaweed attachment to bedrock: Biophysical evidence for a new geophycology paradigm. *Geobiology* 7, 477–487. doi:10.1111/j.1472-4669.2009.00206.x

Nelson, W. A. (2009). Calcified macroalgae – critical to coastal ecosystems and vulnerable to change: A review. *Mar. Freshw. Res.* 60, 787–801. doi:10.1071/MF08335

Nemani, S., Cote, D., Shaw, J., Templeton, A., Misiuk, B., Mackin-McLaughlin, J., et al. (2021). A multi-scale feature selection approach for predicting benthic assemblages. *Estuar. Coast. Shelf Sci.* 277, 108053. doi:10.1016/j.ecss.2022.108053

Neves, B. M., Du Preez, C., and Edinger, E. (2014). Mapping coral and sponge habitats on a shelf-depth environment using multibeam sonar and ROV video observations: Learmonth Bank, northern British Columbia, Canada. *Deep Sea Res. Part II Top. Stud. Oceanogr.* 99, 169–183. doi:10.1016/j.dsr2.2013.05.026

Norton, T. A., and Fetter, R. (1981). The settlement of *Sargassum muticum* propagules in stationary and flowing water. *J. Mar. Biol. Assoc. U. K.* 61, 929–940. doi:10.1017/S0025315400023067

Obst, M., Vicario, S., Lundin, K., Berggren, M., Karlsson, A., Haines, R., et al. (2018). Marine long-term biodiversity assessment suggests loss of rare species in the Skagerrak and Kattegat region. *Mar. Biodivers.* 48, 2165–2176. doi:10.1007/s12526-017-0749-5

O’Higgins, T. G., Lago, M., and DeWitt, T. H. (2020). *Ecosystem-based management, ecosystem services and aquatic biodiversity: Theory, tools and applications*. Cham, Switzerland: Springer Nature Switzerland AG.

Ojeda, F. P., and Dearborn, J. H. (1989). Community structure of macroinvertebrates inhabiting the rocky subtidal zone in the gulf of Maine: Seasonal and bathymetric distribution. *Mar. Ecol. Prog. Ser.* 57, 147–161. doi:10.3354/meps057147

O’Neill, P. L. (1978). Hydrodynamic analysis of feeding in sand dollars. *Oecologia* 34, 157–174. doi:10.1007/BF00345164

Oug, E., Fleddum, A., Rygg, B., and Olsgard, F. (2012). Biological traits analyses in the study of pollution gradients and ecological functioning of marine soft bottom species assemblages in a fjord ecosystem. *J. Exp. Mar. Biol. Ecol.* 432, 94–105. doi:10.1016/j.jembe.2012.07.019

Pappal, A. L., Rountree, R. A., and MacDonald, D. G. (2012). Relationship between body size and habitat complexity preference in age-0 and -1 year winter flounder *Pseudopleuronectus americanus*. *J. Fish. Biol.* 81, 220–229. doi:10.1111/j.1095-8649.2012.03328.x

Piepenburg, D. (2005). Recent research on arctic benthos: Common notions need to be revised. *Polar Biol.* 28, 733–755. doi:10.1007/s00300-005-0013-5

Pillay, T., Cawthra, H. C., and Lombard, A. T. (2020). Characterisation of seafloor substrate using advanced processing of multibeam bathymetry, backscatter, and sidescan sonar in Table Bay, South Africa. *Mar. Geol.* 429, 106332. doi:10.1016/j.margeo.2020.106332

Quinlan, J. R. (1986). Induction of decision trees. *Mach. Learn.* 1, 81–106. doi:10.1007/BF00116251

Reise, K. (1985). *Tidal flat ecology: An experimental approach to species interactions*. Berlin: Springer-Verlag.

Richmond, S., and Stevens, T. (2014). Classifying benthic biotopes on sub-tropical continental shelf-reefs: How useful are abiotic surrogates. *Estuar. Coast. Shelf Sci.* 138, 79–89. doi:10.1016/j.ecss.2013.12.012

Robert, K., Jones, D. O. B., Tyler, P. A., Van Rooij, D., and Huvenne, V. A. I. (2015). Finding the hotspots within a biodiversity hotspot: Fine-scale biological predictions within a submarine canyon using high-resolution acoustic mapping techniques. *Mar. Ecol. Berl.* 36, 1256–1276. doi:10.1111/maec.12228

Roberts, R. D., Kühl, M., Glud, R. N., and Rysgaard, S. (2002). Primary production of crustose coralline red algae in a high arctic Fjord[1]. *J. Phycol.* 38, 273–283. doi:10.1046/j.1529-8817.2002.01104.x

Robichaud, D., and Rose, G. A. (2006). Density-dependent distribution of demersal juvenile atlantic cod (*Gadus morhua*) in Placentia Bay, Newfoundland. *ICES J. Mar. Sci.* 63, 766–774. doi:10.1016/j.icesjms.2005.12.002

Rooper, C. N., Zimmerman, M., and Prescott, M. M. (2017). Comparison of modeling methods to predict the spatial distribution of deep-sea coral and sponge in the Gulf of Alaska. *Deep Sea Res. Part I Oceanogr. Res. Pap.* 126, 148–161. doi:10.1016/j.dsr.2017.07.002

Salvo, F., Oldford, V., Bungay, T., Boone, C., and Hamoutene, D. (2018). *Guide for video monitoring of hardbottom benthic communities of the south coast of Newfoundland for aquaculture impact assessments*. St. John’s, Newfoundland: Fisheries and Oceans Canada. Canadian Technical Report of Fisheries and Aquactic Sciences.

Samsudin, S. A., and Hasan, R. C. (2017). Assessment of multibeam backscatter texture analysis for seafloor sediment classification. *Int. Arch. Photogramm. Remote Sens. Spat. Inf. Sci.* 42-4, 177–183. doi:10.5194/isprs-archives-XLII-4-W5-177-2017

Sandman, A. N., Wikström, S. A., Blomqvist, M., Kautsky, H., and Isaeus, M. (2013). Scale-dependent influence of environmental variables on species distribution: A case-study on five coastal benthic species in the baltic sea. *Ecography* 36, 354–363. doi:10.1111/j.1600-0587.2012.07053.x

Sandnes, J., Forbes, T., Hansen, R., Sandnes, B., and Rygg, B. (2000). Bioturbation and irrigation in natural sediments, described by animal-community parameters. *Mar. Ecol. Prog. Ser.* 197, 169–179. doi:10.3354/meps197169

Sañé, E., Chiocci, F. L., Basso, D., and Martorelli, E. (2016). Environmental factors controlling the distribution of rhodoliths: An integrated study based on seafloor sampling, ROV and side scan sonar data, offshore the W-Pontine Archipelago. *Cont. Shelf Res.* 129, 10–22. doi:10.1016/j.csr.2016.09.003

Sappingtom, J. M., Longshore, K. M., and Thompson, D. B. (2007). Quantifying landscape ruggedness for animal habitat analysis: A case study using bighorn sheep in the mojave desert. *J. Wildl. Manag.* 71, 1419–1426. doi:10.2193/2005-723

Schapire, R. E., and Freund, Y. (2013). *Boosting: Foundations and algorithms*. Cambridge, MA: MIT Press.

Scheibling, R. E., and Gagnon, P. (2006). Competitive interactions between the invasive green alga *Codium fragile* spp. *tomentosoides* and native canopy-forming seaweeds in Nova Scotia (Canada). *Mar. Ecol. Prog. Ser.* 325, 1–14. doi:10.3354/meps325001

Schlining, B. M., and Stout, N. J. (2006). “MBARI’s video annotation and reference system,” in Proceedings of the Marine Technology Society/Institute of

Electrical and Electronics Engineers Ocean Conference (Boston, MA: OCEANS), 1–5. doi:10.1109/OCEANS.2006.306879

Schückel, U., Beck, M., and Kroncke, I. (2015). Macrofauna communities of tidal channels in jade Bay (German wadden sea): Spatial patterns, relationships with environmental characteristics, and comparative aspects. *Mar. Biodivers.* 45, 841–855. doi:10.1007/s12526-014-0308-2

Schwarz, A. M., Hawes, I., Andrew, N., Mercer, S., Cummings, V., and Thrush, S. (2005). Primary production potential of non-geniculate coralline algae at Cape Evans, Ross Sea, Antarctica. *Mar. Ecol. Prog. Ser.* 294, 131–140. doi:10.3354/meps294131

Shang, X. D., Robert, K., Misiuk, B., Mackin-McLaughlin, J., and Zhao, J. H. (2021). Self-adaptive analysis scale determination for terrain features in seafloor substrate classification. *Estuar. Coast. Shelf Sci.* 254, 107359. doi:10.1016/j.ecss.2021.107359

Shaw, J., Potter, D. P., and Kostylev, V. E. (2011). *Seascapes, Placentia Bay, Newfoundland and Labrador*. Ottawa, ON: Geological Survey of Canada. Open File 6683, scale 1:250,000. doi:10.4095/288644

Shumchenia, E. J., and King, J. W. (2010). Comparison of methods for integrating biological and physical data for marine habitat mapping and classification. *Cont. Shelf Res.* 30, 1717–1729. doi:10.1016/j.csr.2010.07.007

Sisson, J. D., Shimeta, J., Zimmer, C. A., and Traykovski, P. (2002). Mapping epibenthic assemblages and their relations to sedimentary features in shallow-water, high-energy environments. *Cont. Shelf Res.* 22, 565–583. doi:10.1016/S0278-4343(01)00074-7

Siwabessy, P. J. W., Tran, M., Picard, K., Brooke, B. P., Huang, Z., Smit, N., et al. (2018). Modelling the distribution of hard seabed using calibrated multibeam acoustic backscatter data in a tropical, macrotidal embayment: Darwin Harbour, Australia. *Mar. Geophys. Res.* 39, 249–269. doi:10.1007/s11001-017-9314-7

Sjare, B., Nakashima, B. S., and Mercer, D. (2003). *Integrating scientific and local ecological knowledge to identify potential critical habitats: A case study in Placentia Bay, Newfoundland. Fisheries and Oceans Canada, science*. Ottawa, ON: DFO Canadian Science Advisory Secretariat #2003/114.

Sokal, R. R., and Michener, C. D. (1958). A statistical method for evaluating systematic relationships. *J. Biomed. Sci. Eng.* 2, 1409–1438.

Sswat, M., Gulliksen, B., Menn, I., Sweetman, A. K., and Piepenburg, D. (2015). Distribution and composition of the epibenthic megafauna north of Svalbard (Arctic). *Polar Biol.* 38, 861–877. doi:10.1007/s00300-015-1645-8

Stanley, D. J., and James, N. P. (1971). "Distribution of *Echinarachnius parma* (lamarck) and associated fauna on sable Island Bank, Southeast Canada," in *Smithsonian contributions to the Earth Sciences* (Washington, DC: Smithsonian), 1–24. doi:10.5479/si.00810274.6.1

Steneck, R. S., Graham, M. H., Bourque, B. J., Corbett, D., Erlandson, J. M., Estes, J. A., et al. (2002). Kelp forest ecosystems: Biodiversity, stability, resilience and future. *Environ. Conserv.* 29, 436–459. doi:10.1017/S0376892902000322

Stephens, D., and Diesing, M. (2014). A comparison of supervised classification methods for the prediction of substrate type using multibeam acoustic and legacy grain-size data. *PLoS ONE* 9 (4), e93950. doi:10.1371/journal.pone.0093950

Stephens, D., and Diesing, M. (2015). Towards quantitative spatial models of seabed sediment composition. *PLoS ONE* 10 (11), e0142502. doi:10.1371/journal.pone.0142502

Stevens, D. L., and Olsen, A. R. (2004). Spatially balanced sampling of natural resources. *J. Am. Stat. Assoc.* 99, 262–278. doi:10.1198/016214504000000250

Strand, J. A., and Weisner, S. E. B. (1996). Wave exposure related growth of epiphyton: Implications for the distribution of submerged macrophytes in eutrophic lakes. *Hydrobiologia* 325, 113–119. doi:10.1007/BF00028271

Swanson, R. L., de Nys, R., Huggett, M. J., Green, J. K., and Steinberg, P. D. (2006). *In situ* quantification of a natural settlement cue and recruitment of the Australian sea urchin *Holopneustes purpurascens*. *Mar. Ecol. Prog. Ser.* 314, 1–14. doi:10.3354/meps314001

Taylor, R. B. (1998). Density, biomass and productivity of animals in four subtidal rocky reef habitats: The importance of small mobile invertebrates. *Mar. Ecol. Prog. Ser.* 172, 37–51. doi:10.3354/meps172037

Teagle, H., Hawkins, S. J., Moore, P. J., and Smale, D. A. (2017). The role of kelp species as biogenic habitat formers in coastal marine ecosystems. *J. Exp. Mar. Biol. Ecol.* 492, 81–98. doi:10.1016/j.jembe.2017.01.017

Tebben, J., Motti, C. A., Siboni, N., Tapiolas, D. M., Negri, A. P., Schupp, P. J., et al. (2015). Chemical mediation of coral larval settlement by crustose coralline algae. *Sci. Rep.* 5, 10803. doi:10.1038/srep10803

Templeman, N. D. (2007). *Placentia bay-grand banks large ocean management area ecologically and biologically significant areas*. St. John's, NL. DFO Canadian Science Advisory Secretariat #2007/52.

Tews, J., Brose, U., Grimm, V., Tielbörger, K., Wichmann, M. C., Schwager, M., et al. (2004). Animal species diversity driven by habitat heterogeneity/diversity: The importance of keystone structures. *J. Biogeogr.* 31, 79–92. doi:10.1046/j.0305-0270.2003.00994.x

Thomsen, M. E., Wernberg, T., Altieri, A. H., Tuya, F., Gulbransen, D., McGlathery, K. J., et al. (2010). Habitat cascades: The conceptual context and global relevance of facilitation cascades via habitat formation and modification. *Integr. Comp. Biol.* 50, 158–175. doi:10.1093/icb/icq042

Ugland, K. I., Gray, J. S., and Ellingsen, K. E. (2003). The species accumulation curve and estimation of species richness. *J. Anim. Ecol.* 72, 888–897. doi:10.1046/j.1365-2656.2003.00748.x

Underwood, A. J., and Denley, E. J. (1984). "Paradigms, explanations, and generalisations in models for structure of intertidal communities on rocky shores," in *Ecological communities: Conceptual issues and the evidence*. Editors D. R. Strong, D. Simberloff, L. G. Abele, and A. B. Thistle (Princeton, NJ: Princeton University Press), 151–180.

Vadas, R. L. (1977). Preferential feeding: An optimization strategy in sea urchins. *Ecol. Monogr.* 47, 337–371. doi:10.2307/1942173

Vadas, R. L. (1968). *The ecology of Agarum and the kelp bend community*. Seattle (WA): University of Washington. [dissertation].

Vaghela, V. B., Ganatra, A., and Thakkar, A. (2009). "Boost a weak learner to a strong learner using an ensemble system Approach," in IEEE International Advance Computing Conference, (Patiala, India: IEEE), 1432–1436.

Vassallo, P., Bianchi, C. N., Paoli, C., Holon, F., Navone, A., Bavestrello, G., et al. (2018). A predictive approach to benthic marine habitat mapping: Efficacy and management implications. *Mar. Pollut. Bull.* 131, 218–232. doi:10.1016/j.marpolbul.2018.04.016

Wahl, M. (2009). "Habitat characteristics and typical functional groups," In *Marine hard bottom communities*. Editor M. Wahl (Berlin: Springer), 7–17.

Wainberg, M., Alipanahi, B., and Frey, B. J. (2016). Are random forests truly the best classifiers. *BMC Genomics* 17, 787. doi:10.1186/s12864-016-3121-4

Walbridge, S., Slocum, N., Pobuda, M., and Wright, D. J. (2018). Unified geomorphological analysis workflows with benthic terrain modeler. *Geosciences* 8, 94. doi:10.3390/geosciences8030094

Watanabe, H., Ito, M., Matsumoto, A., and Arakwawa, H. (2014). Effects of sediment influx on the settlement and survival of canopy-forming macrophytes. *Sci. Rep.* 6, 18677. doi:10.1038/srep18677

Wei, C. L., Cusson, M., Archambault, P., Belley, R., Brown, T., Burd, B. J., et al. (2019). Seafloor biodiversity of Canada's three oceans: Patterns, hotspots, and potential drivers. *Divers. Distrib.* 26, 226–241. doi:10.1111/ddi.13013

Wei, T. (2013). *Corrplot: Visualization of a correlation matrix*. R package v.0.73. CRAN.

Weiss, A. D. (2001). "Topographic positions and landform analysis," in *ESRI international user conference* (San Diego California: ESRI).

Wernberg, T., Krumhansl, K., Filbee-Dexter, K., and Pendersen, M. F. (2019). "Chapter 3 – status and trends for the world's kelp forests," in *World seas: An environmental evaluation*. Editor C. Sheppard (Cambridge MA: Academic Press), 57–78.

White, N. (2018). *Special marine areas in Newfoundland and labrador*. 2nd Edition. Prepared for CPAWS-NL. 162 pg.

Wright, D. J., Slocum, N., Pobuda, M., and Wright, D. J. (2012). Unified geomorphological analysis workflows with Benthic terrain modeler. *Geosci.* 8, 94. doi:10.3390/geosciences8030094

Zaneveld, J. S., and Sanford, R. B. (1965). Crustose corallinaceous algae (rhodophyta) of the New Zealand and united-states scientific expedition to the ross, balleny islands, and macquarie ridge. *Blumea* 26, 205–231.

Zhang, H., Zhang, J., and Zheng, Y. (2012). "Discriminative learning for anatomical structure detection and segmentation," in *Ensemble machine learning*. Editors C. Zhang, and Y. Ma (New York, NY: Springer), 160.

Zvoleff, A. (2020). *Image texture measures from grey-level co-occurrence matrices (GLCM)*. R package, v.1.0. CRAN.

frontiers | Frontiers in Environmental Science

TYPE Original Research
PUBLISHED 04 November 2022
DOI 10.3389/fenvs.2022.1009033

What are we protecting? An analysis of the current conservation framework addressing Mediterranean mesophotic habitats

G. Castellan[1]*, M. Abbiati[1,2,3], L. Angeletti[1†], F. Foglini[1], V. Grande[1], P. Montagna[4,5] and M. Taviani[1,6]

[1]Institute of Marine Sciences, National Research Council (CNR-ISMAR), Bologna, Italy, [2]Dipartimento Dei Beni Culturali, Università di Bologna, Ravenna, Italy, [3]Consorzio Nazionale Interuniversitario per le Scienze Del Mare (CoNISMa), Roma, Italy, [4]Institute of Polar Sciences, National Research Council (CNR-ISP), Bologna, Italy, [5]Lamont Doherty Earth Observatory of Columbia University, Palisades, NY, United States, [6]Stazione Zoologica Anton Dohrn, Naples, Italy

Mesophotic ecosystems in the Mediterranean Sea are biodiversity hotspots distributed from ca 30 m down to 180 m, depending upon the depth of the light compensation point. Overall, the taxonomic composition of Mediterranean mesophotic ecosystems is dominated by corals and sponges, with subordinate bryozoans, mollusks, ascidians, and shade-adapted algae. As for most marine ecosystems, the mesophotic habitats are increasingly exposed to natural and anthropogenic threats, including seawater-temperature rise, more intense and frequent heat waves, progressive ocean acidification, fishing activities, and littering. The establishment of effective governance guidelines is, therefore, the necessary rationale to guarantee the good environmental status of such widespread, highly diverse, service-provider natural resources. However, an in-depth quantification of the extent to which Mediterranean mesophotic habitats and taxa are included in conservation measures is lacking. In this article, we review the available literature information on mesophotic habitats in the Mediterranean Sea to evaluate the efficiency of the current legislative framework in providing instruments to protect this natural heritage. Our analysis allows identifying gaps in the current conservation network, ultimately suggesting functional integrative actions for effective conservation measures and the long-term survival of the Mediterranean mesophotic ecosystems.

KEYWORDS

marine conservation, biodiversity, policy, mesophotic ecosystems, monitoring, Mediterranean Sea

OPEN ACCESS

EDITED BY
Elisabetta Manea,
National Research Council (CNR), Italy

REVIEWED BY
Soha Shabaka,
National Institute of Oceanography and Fisheries (NIOF), Egypt
Lorenzo Bramanti,
UMR8222 Laboratoire d'Ecogéochimie des Environnements Benthiques (LECOB), France

*CORRESPONDENCE
G. Castellan,
giorgio.castellan@bo.ismar.cnr.it

†PRESENT ADDRESS
L. Angeletti,
National Research Council, Institute of Marine Biological Resources and Biotechnologies (CNR-IRBIM)

SPECIALTY SECTION
This article was submitted to Conservation and Restoration Ecology, a section of the journal Frontiers in Environmental Science

RECEIVED 01 August 2022
ACCEPTED 18 October 2022
PUBLISHED 04 November 2022

CITATION
Castellan G, Abbiati M, Angeletti L, Foglini F, Grande V, Montagna P and Taviani M (2022), What are we protecting? An analysis of the current conservation framework addressing Mediterranean mesophotic habitats. *Front. Environ. Sci.* 10:1009033.
doi: 10.3389/fenvs.2022.1009033

1 Introduction

Global biodiversity loss is the largest ecological crisis our society is facing together with climate change. Invaluable genetic resources are being lost and ecosystem processes destroyed due to anthropogenic activities (Lande, 1998; Brooks et al., 2006; Danovaro et al., 2021). Current rates of extinction are 1,000 times higher than those of pre-human levels, and future rates might be 100 times higher than those of today (Pimm et al., 1995). The Intergovernmental Science-Policy Platform on Biodiversity and Ecosystem Services assessment highlighted that almost two-thirds of marine environments have been "severely altered" by human activity causing massive marine biodiversity loss in the last 40 years (Díaz et al., 2019) with a substantial erosion of the environmental services and goods on which we depend (Worm et al., 2006).

The international community delineated the path to strengthen marine protection by 2020 and strike the Aichi Target 11 of the Convention on Biological Diversity, which called for 10% of coastal and marine areas to be "conserved through effectively and equitably managed, ecologically representative, and well-connected systems of protected areas and other effective area-based conservation measures." Several European member states claimed the achievement of the target, but nearly 90% of the European Marine Protected Areas (MPAs) are not managed effectively (WWF, 2019) and the network of MPAs is not ecologically coherent yet (i.e., representing all natural communities within an area, maintaining ecological and evolutionary processes, and ensuring resilience to large-scale disturbances and to long-term changes), according to the European Environment Agency assessment (EEA, 2015).

Protecting the marine species and resources in their totality is arguably utopistic (Brooks et al., 2006), and we need to identify priorities for conservation (habitats and species) and guide government agencies and environmental organizations toward the best compromise. Many "shortcuts" have been adopted for monitoring management plans, defining "keystone," "indicator," "flagship," "umbrella," and "charismatic" species (Vane-Wright et al., 1991; Roberge and Angelstam, 2004; Mace et al., 2006).

The information on the species identified as priorities is, however, dramatically scarce. Despite various studies estimating that between 1.4 and 1.6 million species live in the oceans (Bouchet, 2006), currently, less than 15% of the about 240,000 known marine species are considered by the IUCN Red List, the most comprehensive indicator of the health of the world's biodiversity (https://www.iucnredlist.org/about/barometer-of-life). Summing up, if the status of marine species and habitats is still practically unknown, how can we effectively define what is of priority?

Providing an answer is tremendously and worryingly hard. Geographical gaps exist in implementing conservation measures, with an unbalance in the coverage of protected areas across regions (with Mediterranean and Macaronesian areas as the tail light, EEA, 2015), and between coastal and deep habitats, which are operationally more difficult to reach and remain strongly underrepresented in the conservation and monitoring plans (MedPAN and SPA/RAC, 2017).

Currently, protected areas between 50 m and 200 m depth cover 13.18% of the European designations (MedPAN and SPA/RAC, 2017). This depth range largely overlaps with the mesophotic domain (from 30 m depth down to the photosynthetic compensation point) that might cover a consistent portion of the entire Mediterranean Sea (Castellan et al., 2022). Ecologically relevant habitats occur within this depth layer, whose composition largely varies depending on the geographic area (Pyle and Copus, 2019). Coralligenous formations (Ballesteros, 2006), rhodoliths *s.l.* (Foster et al., 2013; Basso et al., 2017), sponge grounds (Idan et al., 2018; Goren et al., 2021), structures built by stony corals and mollusks (Taviani et al., 2012; Corriero et al., 2019; Angeletti and Taviani, 2020; Angeletti et al., 2020; Cardone et al., 2020), and cnidarian forests (Bo et al., 2011; Cau et al., 2015; Boavida et al., 2016; Chimienti et al., 2020 among many others) dominate the mesophotic zone of the Mediterranean Sea. It is well established that mesophotic habitats provide various ecosystem services, for example, acting as hotspots of biodiversity, potential sources of commercial species, and carbon sinks (Rossi et al., 2017). Despite their recognized importance, mesophotic habitats do not directly receive protection from marine conservation networks (Rocha et al., 2018; Soares et al., 2020). The lack of a clear definition of the mesophotic zone (Castellan et al., 2022) together with the complex patterns of genetic connectivity of mesophotic assemblages, characterized by critical areas of discontinuities (Costantini et al., 2018), surely did not facilitate the delineation of conservation measures specifically targeting mesophotic habitats. Given their heterogeneous nature in terms of the main structuring taxa, mesophotic habitats are characterized as the perfect ground to test if the current conservation network in the Mediterranean Sea is good enough to favor their long-term preservation or whether we need *ad hoc* measures.

Here, we analyze the available information on mesophotic-benthic habitats and their taxonomic composition in the Mediterranean Sea to evaluate the efficiency of the current legislative framework in providing instruments to protect this natural heritage. Our contribution not only aims at identifying persisting biases and gaps but also provides a first assessment of the extent to which the conservation network addresses mesophotic habitats across the basin, suggesting potential integrative actions for their long-term survival.

2 Materials and methods

2.1 Literature review

A systematic analysis of the literature was conducted up to 31 May 2022. To identify documents regarding mesophotic habitats in the Mediterranean Sea, the query "Mediterranean" was used in the mesophotic.org database (http://www.

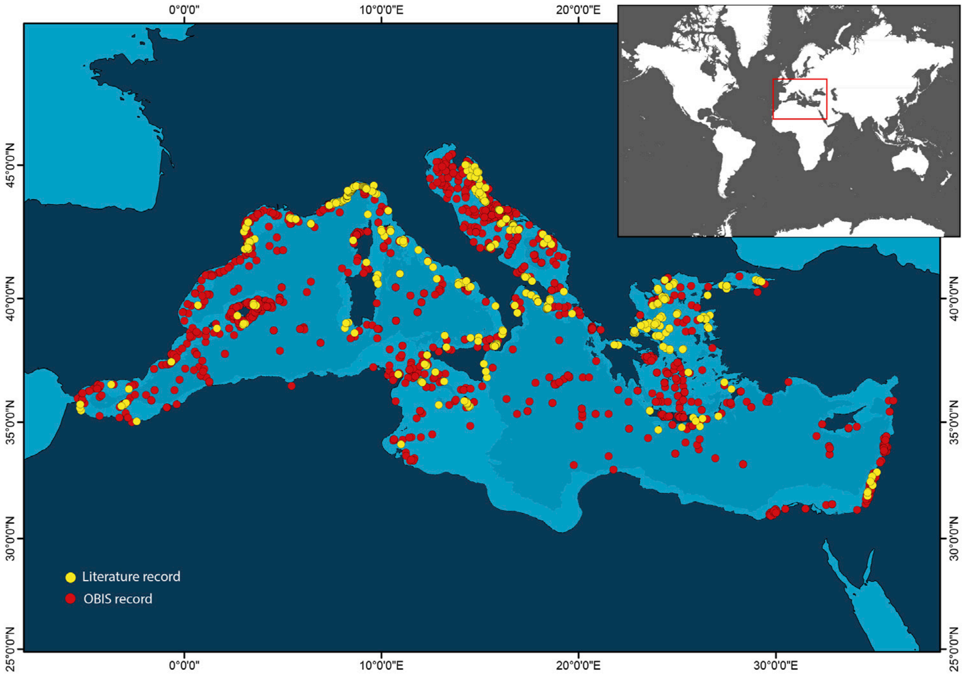

FIGURE 1
Map showing the distribution of available information on mesophotic habitats and taxa in the Mediterranean Sea. Yellow and red dots refer to the literature records (scientific articles and reports) and species occurrences from OBIS repository (obis.org), respectively.

mesophotic.org/), while "twilight AND Mediterranean" and "mesophotic AND Mediterranean" were used in Elsevier's Scopus database (scopus.com). A cross-check between the results from these two databases was performed to exclude duplicates. The records were then screened to remove non-benthic studies (e.g., fish fauna). The typology of habitat, according to the definitions provided in the literature records, and taxonomic lists, whenever present, were extracted (Supplementary Tables S1, S2).

2.2 Data repositories

Literature records were integrated with information from the open-access Ocean Biogeographic Information System (OBIS), held by the UNESCO/IOC project office for IODE in Oostende (Belgium), which provides taxonomically and geographically resolved data for over 47 million observations of marine species. Taxonomic occurrences for the Mediterranean Basin were sorted using the depth range of 30–190 m as a constraint (according to the estimation in Castellan et al., 2022). Duplicated taxa were removed to obtain a list of single taxa observed in the mesophotic depth range. Finally, records were filtered to isolate only benthic taxa (Supplementary Table S2).

2.3 Conservation status

International binding and not-binding instruments in the field of conservation of marine environments were extensively analyzed to extract lists of habitats and taxa currently identified as protected or used to define areas that might deserve management and/or conservation measures. Mesophotic benthic habitat typologies and taxa from the literature and data stored in repositories were compared to those listed in conservation instruments, reporting information on the conservation rank, whenever specified. The number of habitats and taxa currently listed in policy instruments was calculated as percentages.

3 Results

3.1 Conservation status of Mediterranean mesophotic habitats

The screening of literature records on mesophotic benthic habitats in the Mediterranean Sea resulted in 93 scientific documents, including peer-reviewed articles and technical reports (Figure 1; Supplementary Table S1). Most of the literature is represented by single-taxon studies, whilst community composition assessments and area-based censuses

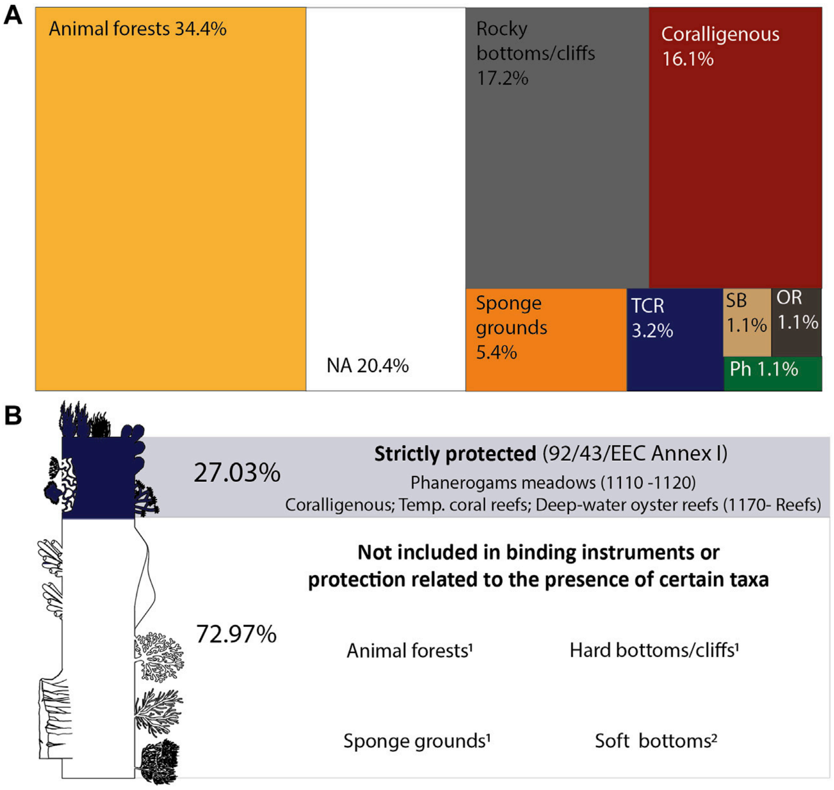

FIGURE 2
Proportion of mesophotic habitats studied in the Mediterranean Sea **(A)** and the proportion of records targeting habitats included in the current International Policy Framework **(B)**. [1]Habitats defined as VME in FAO, 2009. [2]Only soft-bottom habitats (1110-Sandbanks) shallower than 20 m depth are listed under the Habitats Directive (Romão, 1996). TCR: temperate coral reefs; SB: soft bottom; OR: deep-water oyster reef; Ph: Phanerogam meadows; NA: not available.

TABLE 1 Description of the target mesophotic habitats from the literature analysis. Definitions reported here summarize those provided in the bibliographic records. See Supplementary Table S1 for further information.

Habitat	Description
Animal forests	Single- or multi-species assemblages dominated by sessile suspension feeders (octocorals, hydrozoans, and bryozoans) large in number on hard and soft substrates
Hard bottom/cliffs	Associations of different taxa (octocorals, hydrozoans, bryozoans, and brachiopods) patchily populating on hard and rocky bottoms
Coralligenous formations	Structures built by red algae (*Rhodophyta*) populated by highly diverse associations of bryozoans, corals, and sponges
Sponge grounds	Extensive aggregations of *Porifera* populating on hard or soft bottoms
Temperate coral reefs	Single- and multi-species assemblages of scleractinian corals, mainly represented by specimens of the *Caryophylliidae* family, creating three-dimensional frameworks
Deep-water oyster reefs	Three-dimensional formations built by *Neopycnodonte cochlear* populated by sponges, bryozoans, ascidians, and polychaetes
Phanerogam meadows	Extensive communities of marine phanerogams forming sea meadows
Soft bottoms	Bottoms of unconsolidated, unvegetated substrates populated by patches of vagile (mainly echinoderms) and/or erected sessile fauna (polychaetes and soft corals)

are scarce. About 80% of the records defined or reported a description of the target habitats, while the remaining 20% lacked this information since they were represented by large-scale studies encompassing various and unspecified situations or because they were simply not provided (Figure 2). We identified eight categories of habitats, as listed in Table 1.

Most of the studies providing information on habitats focused on animal forests (34.4%), with those formed by octocorals and antipatharians as the preferred targets (Figure 2). Although not forming animal forests, cnidarians also represented a frequent focus in the mesophotic literature on hard bottoms/cliffs, accounting for 17.2% of the whole record. Coralligenous formations were the third most frequently studied habitat (16%), followed by sponge grounds (5.4%), temperate coral reefs (3.2%) and deep-water oyster reefs, phanerogam meadows, and soft bottoms (about 1.1% each).

By analyzing the policy framework currently in force, the Habitats Directive resulted as the main instrument for the establishment of binding measures on marine habitats in the Mediterranean area, with four out of the eight habitats identified in the literature listed in its annexes. Phanerogam meadows are listed as "*Posidonia* beds" (code 1120) and "Mediterranean *Cymodocea* and *Zostera* beds" under "sandbanks which are slightly covered by seawater all the time" (code 1110). Coral and oyster reefs and coralligenous are listed as biogenic or geogenic concretions under "reefs" (code 1170).

Although habitats related to soft bottoms may fall under Habitat 1110, the interpretation manual (Romão, 1996) that specifies this category mainly refers to situations shallower than 20 m depth, thus not encompassing mesophotic situations. Animal forests, sponge grounds, and hard and soft bottoms are, instead, not directly included in the Habitats Directive and conservation or management actions are strictly related to the presence of taxa that are listed under Annex IV or other binding instruments (Figure 2).

3.2 Conservation status of Mediterranean mesophotic taxa

The taxonomic lists included in the literature documented the occurrence of 507 benthic taxa within the mesophotic depth range and 3,146 taxa were further obtained from the OBIS repository, resulting in 3,653 different mesophotic-benthic taxa for the Mediterranean Sea (Supplementary Table S1). The final dataset was highly diverse, encompassing 21 Phyla, 53 Orders, and more than 800 Families. Arthropods, mollusks, and annelids accounted for ca. 68% of the entire dataset (~ 26%, ~ 21%, and ~ 20%, respectively), followed by sponges (~10%), cnidarians (~8%), and bryozoans (~5%).

About 69.5% of the identified taxa are currently not included in the legal framework, whilst ca. 30.5% resulted as listed under policy instruments, comprising both those are binding and not-binding (Figure 3). Most of these were represented by sponges, annelids, and bryozoans, followed, by arthropods and cnidarians. The proportions of the listed taxa varied significantly when considering only binding instruments, with the annelids completely disappearing and cnidarians covering about 53% of all the species included in the policy framework, followed by sponges, arthropods, and mollusks (Figure 3).

4 Discussion

Conservation efforts in Europe, similarly to other regions around the globe, against biodiversity loss and the impact on ecosystem functions and services has been focused on setting the instruments and priorities for the management of habitat degradation and species protection, their sustainable exploitation, and their monitoring (Figure 4). Considerable advances in the conservation of biodiversity have been documented in the last decades, with 18.5% of the European land area and almost 10% of the total EU marine area currently covered by conservation and/or management measures (EEA, 2020). This substantial effort, however, proves insufficient to reduce biodiversity loss (European Commission, 2020), with only 15% of the habitats and 27% of the species listed in the Habitats Directive have been saved from the risk of extinction to date (European Commission, 2020). Although this insufficient advance is surely related to the multiple impact the biodiversity is facing, lessons from the past provide evidence that conservation goals need to be coupled with adequate planning and prompt integration of scientific information into governance in order to be effective (Guidetti et al., 2008; Yates et al., 2019).

4.1 Policy framework on the conservation and management of marine natural resources in the Mediterranean Sea

4.1.1 International Union for Conservation of Nature, Red List

The IUCN Red List (iucnredlist.org) was established in 1964 and is the world's most comprehensive inventory on the extinction risk for flora and fauna that aims at catalyzing action for biodiversity conservation and promoting the protection of species. It collects information on geographic distribution range, population size trends, habitat and ecology, and the extinction risk of more than 142,500 species by classifying them into nine threatening levels based on reports performed by experts. Despite being largely used as a reference to integrate conservation directives by government agencies, wildlife departments, and conservation-related organizations, the list does not have legislative implications and cannot establish binding restrictions or measures. The list mainly includes land species, whilst marine species represent a small amount of the species assessed (less than 15% https://www.iucnredlist.org/about/barometer-of-life).

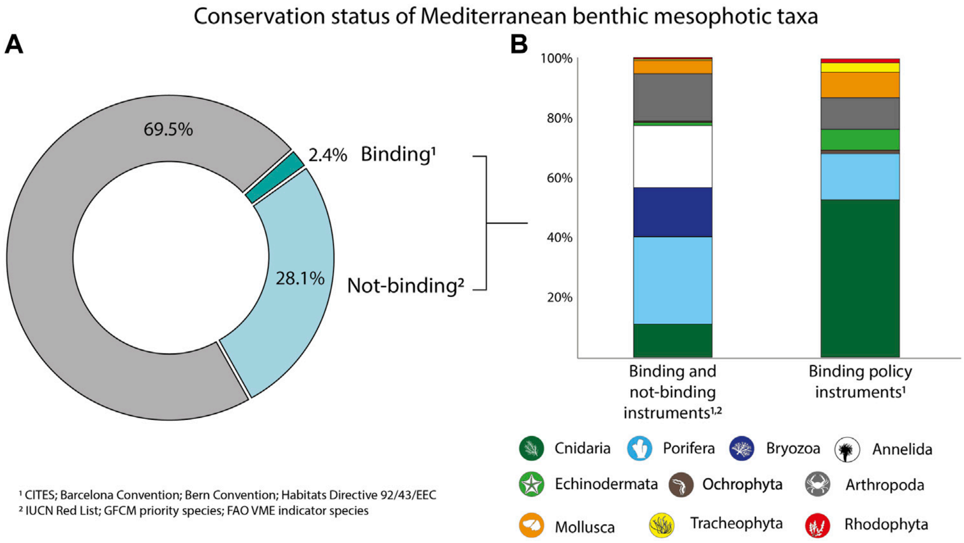

FIGURE 3
Portion of benthic mesophotic taxa included in the International Legal Framework, considering both binding and not-binding instruments **(A)**, and percentage contribution of the identified Phyla to taxa listed under legal instruments **(B)**.

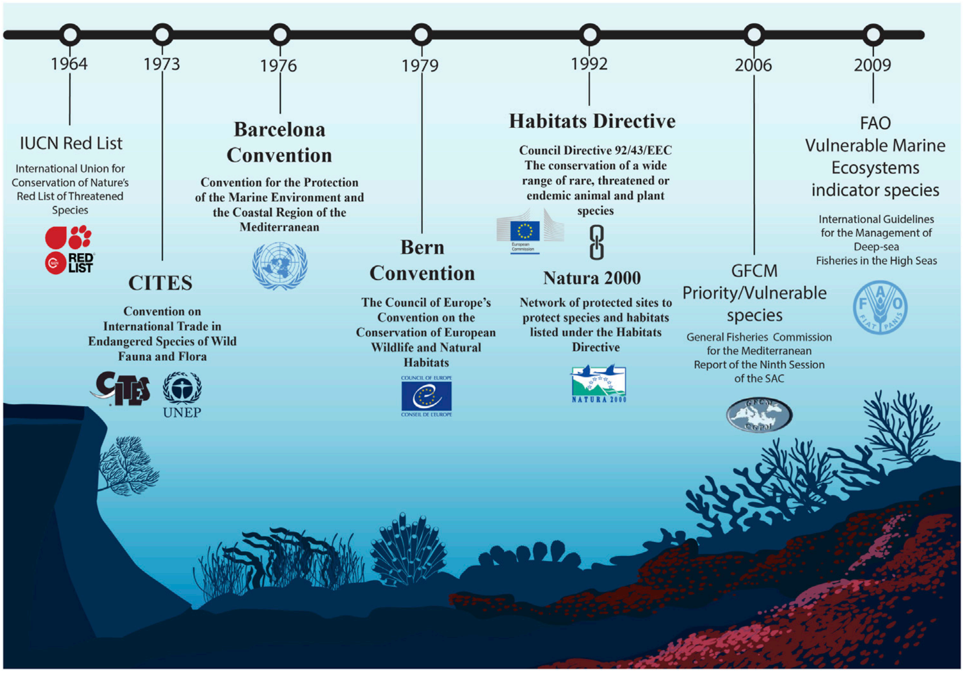

FIGURE 4
International Legislative Framework, comprising binding (bold font) and not-binding instruments, which also includes Mediterranean mesophotic habitats and taxa. The establishment years and depositary organisms are reported.

4.1.2 Convention on International Trade in Endangered Species of wild fauna and flora

CITES (cites.org) was signed in 1973 and entered into force in 1975 to control international trade in wild species of flora and fauna and their by-products for conservation purposes and avoid them becoming threatened through international commerce. CITES does not directly address issues of habitat destruction and biodiversity loss, but it was intended to supplement the management and/or protection of wildlife. It represents a functional mechanism to control the commercial exploitation and alleviate pressure on wild populations (Vincent et al., 2014). The relevance of the convention is that it is legally binding for the states that joined CITES and remains one of the most world's powerful tools for wildlife conservation. The species covered by CITES are listed in three appendices, according to the degree of restriction in trade. Appendix I includes species for which trade is forbidden. Appendix II refers to species for which trade is restricted and has to be authorized through an international licensing system supported by national managing and scientific authorities. Appendix III refers to species that are protected at least in one country, which can impose controls on trade. Appendices I and II are amended and updated every two/3 years at the Conference of the Parties, participated by 184 states. Currently, the lists contain roughly 1,000 marine species (https://cites.org/eng/app/appendices.php).

4.1.3 The Convention for the Protection of the Mediterranean Sea against Pollution—Barcelona Convention

The Barcelona Convention was adopted in 1976 in Barcelona and entered into force in 1978 in the European Union, while its amendments came into force in 2004 (unep.org/unepmap/who-we-are/contracting-parties/barcelona-convention-and-amendments). The convention comprises a protocol promoting the creation of protected areas and the conservation and regulation of threatened or endangered species of flora and fauna. Annex I of the convention delineates the criteria for the selection of the marine areas to be protected. Annexes II and III provide lists of threatened or endangered species and those whose exploitation requires regulation, including about 130 marine species (https://rac-spa.org/annexes).

4.1.4 The Council of Europe's Convention on the Conservation of European Wildlife and Natural Habitats—Bern Convention

The Bern Convention (82/72/EEC) came into force in 1982, and it was among the first international agreements aimed at conserving habitats and wild species. The convention establishes general guidelines to develop conservation measures and includes a list of specific species to be protected. Despite its adoption occurred when the information on marine environments was in its infancy, its lists are constantly updated with biannual reports (coe.int/en/web/bern-convention/biennial-reports). The Bern Convention's lists of species to be protected include ca. 200 marine species, encompassing mammals, invertebrates, fishes, and algae (https://eunis.eea.europa.eu/references/2443).

4.1.5 Council Directive 92/43/EEC—Habitats Directive

Building on the Bern Convention, the European Habitats Directive was first adopted in 1992 by the European Union (92/43/EEC). Contrary to the Bern Convention, this directive is a European law and is mandatorily transposed to the national laws of EU countries. The Habitats Directive is, together with the Birds Directive, the main legislation regarding Europe's nature conservation policy as its annexes list the protected habitats and species in the EU. It went through a number of updates and corrections, mainly to the annexes, the last in 2007. Annexes II and IV form the basis for the protected species lists in many European countries, delineating the types of habitats and the animal and plant species whose conservation requires the designation of special areas of conservation and animal and plant species of community interest in need of strict protection (ec.europa.eu/environment/nature/legislation/habitatsdirective/index_en.htm). Together with the Birds Directive (2009/147/EC), species and habitats listed under the Habitats Directive represent the backbone of Natura 2000, the largest network of Sites of Community Importance (SCIs) and conservation areas in the world aiming at ensuring the long-term survival of species and habitats of community interest (ec.europa.eu/environment/nature/natura2000/index_en.htm). Unlike the Bern Convention, the Directive's annexes are, however, not periodically updated and have remained practically unchanged from its establishment, including only five marine habitats and 18 marine species (rac-spa.org/annexes).

4.1.6 General Fisheries Commission for the Mediterranean—Priority and vulnerable species

The General Fisheries Commission for the Mediterranean (FAO-GFCM) is a regional fishery management organization under the Food and Agriculture Organization of the United Nations whose main objective is to ensure the conservation of living marine resources, including aquaculture systems and their sustainable use in the Mediterranean and Black seas (fao.org/gfcm/en/). FAO-GFCM was established in 1949 and counts 22 contracting partners (19 Mediterranean states, 3 Black Sea states, and the European Union). It has authority to deliberate binding recommendations for fishery monitoring and management. During the Ninth Session that took place in 2006, the Scientific Advisory Committee (SAC) on Fisheries identified a list of priority species for the Mediterranean and the Black seas (https://www.fao.org/3/a0889b/a0889b00.htm). Mainly having authority on fishing and aquaculture activities, the overwhelming majority of the roughly 100 marine species included in the lists are represented by cetaceans, sharks, and rays, whilst benthic species are only five (four decapod species and the cnidarian *Corallium rubrum*, https://www.fao.org/gfcm/activities/fisheries/stock-assessment/priority-species/en/).

4.1.7 FAO International Guidelines for the Management of Deep-sea Fisheries in the High Seas

The concept of vulnerable marine ecosystems (VMEs) was formally defined after the United Nations General Assembly (UNGA) in 2004 (A/RES/61/105, 2007). VMEs are groups of species, communities, or habitats that may be vulnerable to the impact from fishing activities. The FAO International Guidelines for the Management of Deep-sea Fisheries in the High Seas (FAO, 2009) were built on the UNGA Resolution 61/105 and provide details on the VME, criteria to identify them, and examples of species groups, communities, and potentially vulnerable habitats. Despite the presence of VMEs leading to the establishment of management measures, that, however, only act on restricting fishing activities (Fishery Restricted Areas, FRA, fao.org/gfcm/data/maps/fras/en/), the guidelines have no binding force (fao.org/in-action/vulnerable-marine-ecosystems/background/international-framework/en/). The list of taxa that may form VMEs has been also integrated into Annex 1.c of *Monitoring the incidental catch of vulnerable species in the Mediterranean and Black Sea fisheries: methodology for data collection* to promote the collection of data on VME-forming species (FAO. 2019).

To date, the European Union's most important instrument for the constitution of conservation areas in the marine environment is represented by the Natura 2000 sites network whose designation is based upon the Habitats Directive (92/43/EEC). As established in Article 19 of the Directive, the list of habitats should be subjected to updates and amendments each time new countries join the European Union (Cardoso, 2012). However, the growth rate of technical and scientific progresses is arguably different from that of new member state inclusion, and no considerable modifications have been registered solely as a consequence of new knowledge so far (Fois et al., 2021). Consequently, the lists of habitats and species currently included in the Habitats Directive annexes rely upon outdated information, whilst some habitats of community interest are still not considered (Evans, 2006).

4.2 Conservation network addressing Mediterranean mesophotic habitats and species

Information on mesophotic habitats of the Mediterranean Sea has been largely collected in the early 2000s (e.g., Cerrano et al., 2019), providing evidence on the paramount ecological importance of habitats populating this depth range that serve as areas for spawning, breeding, feeding, and growth to maturity (e.g., Lesser et al., 2009; Bramanti et al., 2017; Capdevila et al., 2018; Santín et al., 2019). The analysis of the literature identified eight categories of mesophotic habitats in the Mediterranean Sea from reefs to soft bottoms patchily populated by erect megafauna. Four of these are included in binding instruments (i.e., Habitats Directive), corresponding to biogenic structures and phanerogam meadows. These habitats, however, covered a small portion of the literature, whilst about 73% of records focused on habitats currently listed in not-binding instruments or whose protection is related to the presence of certain taxa. As a case in point, animal forests resulted as the most studied habitat, accounting for ca. 34% of the literature records. These are known to represent hotspots of biodiversity and ecological services (Gori et al., 2017), but their protection is strictly related to the taxonomic composition: forests formed by *Callogorgia verticillata*, for instance, are considered of priority for protection and for the establishment of conservation measures since the species are listed in Barcelona Convention Annex II. On the contrary, *Paramuricea clavata*, gorgonid largely studied in the Mediterranean Sea (e.g., Linares et al., 2008 amongst many others), is currently not listed in any binding directives. So, identifying and collecting scientific information on situations hosting *P. clavata* forests may not be enough to lead to conservation actions.

Likewise, sponge grounds represented ca. 5% of the literature records, but this habitat is not included in the Habitats Directive and the chance to be subjected to conservation measures relies upon the presence of species listed under binding legal instruments. Despite 359 taxa of *Porifera* that were identified through the literature analysis, only 13 species, however, resulted as included in binding instruments to date. Similar arguments can be made for hard- and soft-bottom habitats, whose protection emerged as completely dependent on the occurrence of taxa listed in binding instruments.

If establishing conservation measures relying upon certain taxa which might surely represent a successful strategy to contrast biodiversity loss, it endows lists of species included in legally binding instruments a critical role. Of the more than 3,600 benthic mesophotic taxa identified from our analysis, 2.4% are currently listed under binding instruments, encompassing eight Phyla out of the 22 documented in the literature and open-access databases. Not only do the taxa need to be listed in binding instruments to be considered for protection, but also the different annexes or appendices within the same instrument have different reasoning. Annex II of the Habitats Directive, for instance, lists species for which members have to be designated protected areas, whilst Annex IV comprises strictly protected species but for which no legal obligation to protect the habitat exists. Listing species in Annex II is, therefore, more legally binding, but no marine benthic species are included yet. In natural systems, discerning species protection from habitat conservation might be tricky since the first concur in forming habitats, while habitats support the presence of species.

There is no doubt that finding solutions to contrast the jeopardization of benthic habitats is incredibly hard. A successful path toward the effective conservation of mesophotic-benthic habitats might be the improvement of legal conservation instruments to be more adaptive and promptly incorporate the available scientific knowledge (Manea et al., 2020).

However, the spatial distribution of information on mesophotic habitats and taxa in the Mediterranean Sea is heterogeneous. Most of the information comes from the northwestern sector of the basin, whilst in the easternmost Levantine Sea and the African coasts and margins, the number of available records is limited (Figure 1). The sole analysis of the literature records would lead to a notable underestimation of the diversity of mesophotic habitats and related taxa in the southeastern Mediterranean Sea. If the scientific knowledge that should fuel improvements in conservation measures to include mesophotic habitats and species occurring in the easternmost Mediterranean Sea is missing, evidence of the collapse of native mesophotic biodiversity by non-indigenous species is largely documented in the literature (Albano et al., 2021).

A starting point might be to update lists of species included in binding instruments by integrating information included in not legally binding conservation tools. These already provide data on population trends (IUCN Red List) and/or scientific evidence that some benthic taxa occurring within the mesophotic depths may form ecologically relevant habitats crucial for human supplies (GFCM priority species and VME indicator species). For instance, considering the taxa listed in binding and not-binding (at any "concerning" level) instruments, the portion of mesophotic benthic taxa in the Mediterranean Sea considered by the conservation network would increase from 2.4% to about 30% of those identified from our analysis. Including these taxa and habitats into legally binding instruments does not necessarily lead to their strict protection but might fuel the monitoring of their conservation status through programs already in force. Despite presenting strong legal (Fraschetti et al., 2018) and conceptual limitations (Fanelli et al., 2021), the Marine Strategy Framework Directive (MSFD 2008/56/EC) set the path for monitoring the Good Environmental Status (GES) of marine biodiversity in the EU, channeling scientific information into conservation instruments (Danovaro et al., 2020).

Ensuring routine monitoring of mesophotic and deep-sea habitats is, however, much more demanding in terms of funds, time, and on-field effort with respect to coastal situations (Danovaro et al., 2020). Stable funding for the onset of innovative cabled ocean observatories, infrastructure that provides real-time data on benthic-mesophotic habitats (Levin et al., 2019), represents a new frontier that might not only lead to novel scientific insights but also provide long-term data to improve the efficiency of the current marine conservation framework.

Data availability statement

The original contributions presented in the study are included in the article/Supplementary Material; further inquiries can be directed to the corresponding author.

Author contributions

Conceived the study: GC; methods: GC and LA; writing original draft: GC; discussion writing, review, and editing: GC, MA, LA, VG, PM, and MT; data interpretation: GC, LA, FF, and VG.

Funding

This work was supported by the H2020 Project Reliance (grant agreement no.: 101017501), the DG Environment programme IDEM (grant agreement no.: 11.0661/2017/750680/SUB/EN V.C2), and MIUR-PRIN 2017 GLIDE 2017FREXZY. This contribution is an overgrowth of a chapter of GC dissertation, co-financed by the Ph.D. program in Cultural and Natural Heritage of the University of Bologna.

Acknowledgments

The authors thank the guest editors Elisabetta Manea and Caterina Bergami for accepting the kind invitation to contribute to the special issue. The authors also thank the Department of Cultural and Natural Heritage of the University of Bologna for supporting the activities performed during the Ph.D. program. This is an ISMAR-CNR Bologna scientific contribution n. 2069.

Conflict of interest

The authors declare that the research was conducted in the absence of any commercial or financial relationships that could be construed as a potential conflict of interest.

Publisher's note

Supplementary material

The Supplementary Material for this article can be found online at: https://www.frontiersin.org/articles/10.3389/fenvs.2022.1009033/full#supplementary-material

References

Albano, P. G., Steger, J., Bošnjak, M., Dunne, B., Guifarro, Z., Turapova, E., et al. (2021). Native biodiversity collapse in the eastern Mediterranean. *Proc. R. Soc. B* 288, 20202469. doi:10.1098/rspb.2020.2469

Angeletti, L., Canese, S., Cardone, F., Castellan, G., Foglini, F., and Taviani, M. (2020). A brachiopod biotope associated with rocky bottoms at the shelf break in the central Mediterranean Sea: Geobiological traits and conservation aspects. *Aquat. Conserv.* 30, 402–411. doi:10.1002/aqc.3255

Angeletti, L., and Taviani, M. (2020). Offshore *Neopycnodonte* oyster reefs in the Mediterranean Sea. *Diversity* 12, 92. doi:10.3390/d12030092

Ballesteros, E. (2006). Mediterranean coralligenous assemblages: A synthesis of present knowledge. *Oceanogr. Mar. Biology:An Annu. Rev.* 44, 123–195. doi:10.1201/9781420006391-7

Basso, D., Babbini, L., Ramos-Esplá, A. A., and Salomidi, M. (2017). “Mediterranean rhodolith beds,” in *Rhodolith/maërl beds: A global perspective coastal research library*. Editors R. Riosmena-Rodríguez, W. Nelson, and J. Aguirre (Cham: Springer International Publishing), 281–298. Available at:Accessed March 27, 2019]. doi:10.1007/978-3-319-29315-8_11

Bo, M., Bertolino, M., Borghini, M., Castellano, M., Harriague, A. C., Camillo, C. G. D., et al. (2011). Characteristics of the mesophotic megabenthic assemblages of the vercelli seamount (north tyrrhenian sea). *PLOS ONE* 6, e16357. doi:10.1371/journal.pone.0016357

Boavida, J., Assis, J., Silva, I., and Serrão, E. A. (2016). Overlooked habitat of a vulnerable gorgonian revealed in the Mediterranean and Eastern Atlantic by ecological niche modelling. *Sci. Rep.* 6, 36460. doi:10.1038/srep36460

Bouchet, P. (2006). “The magnitude of marine biodiversity,” in *The exploration of marine biodiversity: Scientific and technological challenges*. Editor C. M. Duarte (Madrid: Fundación BBVA), 31–62.

Bramanti, L., Benedetti, M. C., Cupido, R., Cocito, S., Priori, C., Erra, F., et al. (2017). “Demography of animal forests: The example of mediterranean gorgonians,” in *Marine animal forests: The ecology of benthic biodiversity hotspots*. Editors S. Rossi, L. Bramanti, A. Gori, and C. Orejas (Cham: Springer International Publishing), 529. Available at:. doi:10.1007/978-3-319-21012-4_13

Brooks, T. M., Mittermeier, R. A., da Fonseca, G. A. B., Gerlach, J., Hoffmann, M., Lamoreux, J. F., et al. (2006). Global biodiversity conservation priorities. *Science* 313, 58–61. doi:10.1126/science.1127609

Capdevila, P., Linares, C., Aspillaga, E., Riera, J. L., and Hereu, B. (2018). Effective dispersal and density-dependence in mesophotic macroalgal forests: Insights from the Mediterranean species *Cystoseira zosteroides*. *PLOS ONE* 13, e0191346. doi:10.1371/journal.pone.0191346

Cardone, F., Corriero, G., Longo, C., Mercurio, M., Onen Tarantini, S., Gravina, M. F., et al. (2020). Massive bioconstructions built by *Neopycnodonte cochlear* (Mollusca, Bivalvia) in a mesophotic environment in the central Mediterranean Sea. *Sci. Rep.* 10, 6337. doi:10.1038/s41598-020-63241-y

Cardoso, P. (2012). Habitats directive species lists: Urgent need of revision. *Insect Conserv. divers.* 5, 169–174. doi:10.1111/j.1752-4598.2011.00140.x

Castellan, G., Angeletti, L., Montagna, P., and Taviani, M. (2022). Drawing the borders of the mesophotic zone of the Mediterranean Sea using satellite data. *Sci. Rep.* 12, 5585. doi:10.1038/s41598-022-09413-4

Cau, A., Follesa, M. C., Moccia, D., Alvito, A., Bo, M., Angiolillo, M., et al. (2015). Deepwater corals biodiversity along roche du large ecosystems with different habitat complexity along the south Sardinia continental margin (CW Mediterranean Sea). *Mar. Biol.* 162, 1865–1878. doi:10.1007/s00227-015-2718-5

Cerrano, C., Bastari, A., Calcinai, B., Camillo, C. D., Pica, D., Puce, S., et al. (2019). Temperate mesophotic ecosystems: Gaps and perspectives of an emerging conservation challenge for the Mediterranean Sea. *Eur. Zoological J.* 86, 370–388. doi:10.1080/24750263.2019.1677790

Chimienti, G., De Padova, D., Mossa, M., and Mastrototaro, F. (2020). A mesophotic black coral forest in the Adriatic Sea. *Sci. Rep.* 10, 8504. doi:10.1038/s41598-020-65266-9

Corriero, G., Pierri, C., Mercurio, M., Marzano, C. N., Tarantini, S. O., Gravina, M. F., et al. (2019). A Mediterranean mesophotic coral reef built by non-symbiotic scleractinians. *Sci. Rep.* 9, 3601. doi:10.1038/s41598-019-40284-4

Costantini, F., Ferrario, F., and Abbiati, M. (2018). Chasing genetic structure in coralligenous reef invertebrates: Patterns, criticalities and conservation issues. *Sci. Rep.* 8, 5844. doi:10.1038/s41598-018-24247-9

Danovaro, R., Aronson, J., Cimino, R., Gambi, C., Snelgrove, P. V. R., and Van Dover, C. (2021). Marine ecosystem restoration in a changing ocean. *Restor. Ecol.* 29, e13432. doi:10.1111/rec.13432

Danovaro, R., Fanelli, E., Canals, M., Ciuffardi, T., Fabri, M.-C., Taviani, M., et al. (2020). Towards a marine strategy for the deep Mediterranean Sea: Analysis of current ecological status. *Mar. Policy* 112, 103781. doi:10.1016/j.marpol.2019.103781

Díaz, S., Settele, J., Brondízio, E. S., Ngo, H. T., Agard, J., Arneth, A., et al. (2019). Pervasive human-driven decline of life on Earth points to the need for transformative change. *Science* 366 (6471), Eaax3100. doi:10.1126/science.aax3100

EEA (2020). *Management effectiveness in the EU's Natura 2000 network of protected areas*. Prepared for the EEA by The Institute for European Environment Policy (IEEP), UNEP-WCMC and Trinomics. Copenhagen, Denmark, 87.

EEA (2015). Marine protected areas in Europe's seas -An overview and perspectives for the future. EEA Report, no 3/2015.

European Commission (2020). *The state of nature in the European Union. Report on the status and trends in 2013 - 2018 of species and habitat types protected by the Birds and Habitats Directives*. Brussels: European Commission. 15.10.2020 COM 635 final.

Evans, D. (2006). The habitats of the European Union habitats directive. *Biol. Environ.* 106B, 167–173. doi:10.1353/bae.2006.0032

Fanelli, E., Bianchelli, S., Foglini, F., Canals, M., Castellan, G., Güell-Bujons, Q., et al. (2021). Identifying priorities for the protection of deep Mediterranean Sea ecosystems through an integrated approach. *Front. Mar. Sci.* 8, 698890. doi:10.3389/fmars.2021.698890

Food and Agriculture Organization (FAO) (2009). *International guidelines for the management of deep-sea fisheries in the High seas*. Rome, Italy: FAO, 73.

Food and Agriculture Organization (FAO) (2019). *Monitoring the incidental catch of vulnerable species in Mediterranean and Black Sea fisheries: Methodology for data collection*. Rome: FAO. FAO Fisheries and Aquaculture Technical Paper No. 640.

Foster, M. S., Amado-Filho, G. M., Kamenos, N. A., Riosmena-Rodriguez, R., and Steller, D. L. (2013). in *Rhodoliths and rhodolith beds" in research and discoveries: The revolution of science through SCUBA*. Editors M. A. Lang, R. L. Marinelli, S. J. Roberts, and P. R. Taylor (Washington, DC: Smithsonian Contributions to the Marine Sciences), 143–155.

Fraschetti, S., Pipitone, C., Mazaris, A. D., Rilov, G., Badalamenti, F., Bevilacqua, S., et al. (2018). Light and shade in marine conservation across European and contiguous seas. *Front. Mar. Sci.* 5. doi:10.3389/fmars.2018.00420

Goren, L., Idan, T., Shefer, S., Ilan, M., Hernandez, D., Yates, K. K., et al. (2021). Acidification in the U.S. Southeast: Causes, potential consequences and the role of the Southeast Ocean and coastal acidification network. *Front. Mar. Sci.* 7, 1–548. doi:10.3389/fmars.2020.00548

Gori, A., Bavestrello, G., Grinyó, J., Dominguez-Carrió, C., Ambroso, S., and Bo, M. (2017). “Animal forests in deep coastal bottoms and continental shelf of the Mediterranean Sea,” in *Marine animal forests: The ecology of benthic biodiversity hotspots*. Editors S. Rossi, L. Bramanti, A. Gori, and C. Orejas (Cham: Springer International Publishing), 1–28. doi:10.1007/978-3-319-17001-5_5-2

Grassle, J. F., and Maciolek, N. J. (1992). Deep-sea species richness: Regional and local diversity estimates from quantitative bottom samples. *Am. Nat.* 139, 313–341. doi:10.1086/285329

Guidetti, P., Milazzo, M., Bussotti, S., Molinari, A., Murenu, M., Pais, A., et al. (2008). Italian marine reserve effectiveness: Does enforcement matter? *Biol. Conserv.* 141, 699–709. doi:10.1016/j.biocon.2007.12.013

Idan, T., Shefer, S., Feldstein, T., Yahel, R., Huchon, D., and Ilan, M. (2018). Shedding light on an East-Mediterranean mesophotic sponge ground community and the regional sponge fauna. *Mediterr. Mar. Sci.* 19, 84–106. doi:10.12681/mms.13853

Lande, R. (1998). Anthropogenic, ecological and genetic factors in extinction and conservation. *Popul. Ecol.* 40, 259–269. doi:10.1007/BF02763457

Lesser, M. P., Slattery, M., and Leichter, J. J. (2009). Ecology of mesophotic coral reefs. *J. Exp. Mar. Biol. Ecol.* 375, 1–8. doi:10.1016/j.jembe.2009.05.009

Levin, L. A., Bett, B. J., Gates, A. R., Heimbach, P., Howe, B. M., Janssen, F., et al. (2019). Global observing needs in the deep ocean. *Front. Mar. Sci.* 6. doi:10.3389/fmars.2019.00241

Linares, C., Coma, R., Garrabou, J., Díaz, D., and Zabala, M. (2008). Size distribution, density and disturbance in two Mediterranean gorgonians: *Paramuricea clavata* and *Eunicella singularis*. *J. Appl. Ecol.* 45, 688–699. doi:10.1111/j.1365-2664.2007.01419.x

Manea, E., Bianchelli, S., Fanelli, E., Danovaro, R., and Gissi, E. (2020). Towards an ecosystem-based marine spatial planning in the deep Mediterranean Sea. *Sci. Total Environ.* 715, 136884. doi:10.1016/j.scitotenv.2020.136884

MedPAN and SPA/RAC (2017). *The 2016 status of marine protected areas in the mediterranean*. Editors B. Meola and C. Webster. Tunis: SPA/RAC & MedPAN.

Pimm, S. L., Russell, G. J., Gittleman, J. L., and Brooks, T. M. (1995). The future of biodiversity. *Science* 269, 347–350. doi:10.1126/science.269.5222.347

Pyle, R. L., and Copus, J. M. (2019). "Mesophotic coral ecosystems: Introduction and overview, " in *Mesophotic coral ecosystems*. Editors Y. Loya, K. A. Puglise, and T. C. L. Bridge (Cham: Springer International Publishing), 3–27. doi:10.1007/978-3-319-92735-0_1

Roberge, J. -M., and Angelstam, P. (2004). Usefulness of the umbrella species concept as a conservation tool. *Conserv. Biol.* 18, 76–85. doi:10.1111/j.1523-1739.2004.00450.x

Rocha, L. A., Pinheiro, H. T., Shepherd, B., Papastamatiou, Y. P., Luiz, O. J., Pyle, R. L., et al. (2018). Mesophotic coral ecosystems are threatened and ecologically distinct from shallow water reefs. *Science* 361, 281–284. doi:10.1126/science.aaq1614

Romão, C. (1996). *Interpretation manual of European union habitats. Version EUR 15. Directorate general XI 'environment, nuclear safety and civil protection' of the European commission*. Bruxelles: European Commission.

Rossi, S., Bramanti, L., Gori, A., and Orejas, C. (2017). "Animal forests of the world: An overview,"In. *Marine animal forests: The ecology of benthic biodiversity hotspots*. Editors S. Rossi, L. Bramanti, A. Gori, and C. Orejas (Cham: Springer International Publishing), 1–28. Available at:. doi:10.1007/978-3-319-21012-4_1

Santín, A., Grinyó, J., Ambroso, S., Uriz, M. J., Dominguez-Carrió, C., and Gili, J. M. (2019). Distribution patterns and demographic trends of demosponges at the Menorca Channel (northwestern Mediterranean Sea). *Prog. Oceanogr.* 173, 9–25. doi:10.1016/j.pocean.2019.02.002

Soares, M. D. O., Araújo, J. T. D., Ferreira, S. M. C., Santos, B. A., Ruela Heimbürger Boavida, J., Costantini, F., et al. (2020). Why do mesophotic coral ecosystems have to be protected? *Sci. Total Environ.* 726, 138456. doi:10.1016/j.scitotenv.2020.138456

Taviani, M., Angeletti, L., Campiani, E., Ceregato, A., Foglini, F., Maselli, V., et al. (2012). Drowned karst landscape offshore the Apulian margin (southern Adriatic Sea, Italy). *J. Caves. Karst Stud.* 74/2, 197–212. doi:10.4311/2011JCKS0204

Vane-Wright, R. I., Humphries, C. J., and Williams, P. H. (1991). What to protect?—Systematics and the agony of choice. *Biol. Conserv.* 55, 235–254. doi:10.1016/0006-3207(91)90030-D

Vincent, A. C. J., Sadovy de Mitcheson, Y. J., Fowler, S. L., and Lieberman, S. (2014). The role of CITES in the conservation of marine fishes subject to international trade. *Fish. Fish. (Oxf).* 15, 563–592. doi:10.1111/faf.12035

Worm, B., Barbier, E. B., Beaumont, N., Duffy, J. E., Folke, C., Halpern, B. S., et al. (2006). Impacts of biodiversity loss on ocean ecosystem services. *Science* 314, 787–790. doi:10.1126/science.1132294

Yates, K. L., Clarke, B., and Thurstan, R. H. (2019). Purpose vs performance: What does marine protected area success look like? *Environ. Sci. Policy* 92, 76–86. doi:10.1016/j.envsci.2018.11.012

frontiers | Frontiers in Environmental Science

TYPE Original Research
PUBLISHED 16 November 2022
DOI 10.3389/fenvs.2022.1023269

OPEN ACCESS

EDITED BY
Caterina Bergami,
National Research Council (CNR), Italy

REVIEWED BY
Jingmin Zhu,
Zhejiang Ocean University, China
Manuel Cánovas,
Catholic University of the North, Chile

*CORRESPONDENCE
André Tristany Farinha,
a.farinha17@imperial.ac.uk
Mirko Kovac,
mirko.kovac@empa.ch

†These authors share first authorship

SPECIALTY SECTION
This article was submitted to Freshwater Science,
a section of the journal
Frontiers in Environmental Science

RECEIVED 19 August 2022
ACCEPTED 02 November 2022
PUBLISHED 16 November 2022

CITATION
Farinha AT, di Tria J, Reyes M, Rosas C, Pang O, Zufferey R, Pomati F and Kovac M (2022), Off-shore and underwater sampling of aquatic environments with the aerial-aquatic drone MEDUSA.
Front. Environ. Sci. 10:1023269.
doi: 10.3389/fenvs.2022.1023269

Off-shore and underwater sampling of aquatic environments with the aerial-aquatic drone MEDUSA

André Tristany Farinha[1*†], Julien di Tria[1†], Marta Reyes[2], Constanca Rosas[1], Oscar Pang[1], Raphael Zufferey[1,3], Francesco Pomati[2] and Mirko Kovac[1,4*]

[1]Aerial Robotics Laboratory, Department of Aeronautics, Imperial College London, London, United Kingdom, [2]Department of Aquatic Ecology, Eawag: Swiss Federal Institute of Aquatic Science and Technology, Dübendorf, Switzerland, [3]Biorobotics Laboratory, École Polytechnique Fédérale de Lausanne, Lausanne, Switzerland, [4]Materials and Technology Center of Robotics, Department of Functional Materials, Empa - Swiss Federal Laboratories for Materials Science and Technology, Dübendorf, Switzerland

Monitoring of aquatic habitats for water quality and biodiversity requires regular sampling, often in off-shore locations and underwater. Such sampling is commonly performed manually from research vessels, or if autonomous, is constrained to permanent installations. Consequentially, high frequency ecological monitoring, such as for harmful algal blooms, are limited to few sites and/or temporally infrequent. Here, we demonstrate the use of MEDUSA, an Unmanned Aerial-Aquatic Vehicle which is capable of performing underwater sampling and inspection at up to 10 m depth, and is composed of a multirotor platform, a tether management unit and a tethered micro Underwater Vehicle. The system is validated in the task of vertical profiling of Chlorophyll-a levels in freshwater systems by means of a custom solid sample filtering mechanism. This mechanism can collect up to two independent samples per mission by pumping water through a pair of glass-fibre GF/F filters. Chlorophyll levels measured from the solid deposits on the filters are consistent and on par with traditional sampling methods, highlighting the potential of using UAAVs to sample aquatic locations at high frequency and high spatial resolution.

KEYWORDS

environmental sensing, aerial-aquatic robotics, aquatic habitats, water sampling, UAV (unmanned aerial vehicle)

1 Introduction

Aquatic ecosystems—both freshwater and marine—are fundamental to both Earth system dynamics and to human society Wang-Erlandsson et al. (2022). Water bodies provide the foundation for our life, health, and wealth, through "ecosytem services" such as nutrients' cycling and primary production, climate regulation, clean water and fisheries, as well as tourism by means of aesthetics and recreational values of natural aquatic resources D'Alelio et al. (2021). Aquatic ecosystems are however very fragile and extensively perturbed by anthropogenic activities at local and global scales Wang-Erlandsson et al. (2022). Given the importance of aquatic resources for biodiversity, conservation and ecosystem services, there is a scientific interest and a societal need to monitor ecosystem state and water quality, ideally at low cost, high frequency and large spatial scales. Such needs imply the selection of relevant ecosystem variables to monitor, and of monitoring tools that minimize the imposed trade-offs between spatial and temporal resolution, and costs.

The estimation of abundance and diversity of phytoplankton in pelagic aquatic ecosystems is the most common, and often mandatory, biological parameter to monitor, to evaluate the quality of water bodies. Phytoplankton is a key component of all aquatic food-webs, encompassing a variety of photosynthetic organisms from eukaryotic microalgae to cyanobacteria. Having a short lifespans and being regulated by essential inorganic resources (including human pollutants), phytoplankton communities are sensitive to environmental conditions and represent effective indicators of environmental change, ecosystem health and water quality (Directives originating from the EU, 2000; Xu et al., 2001). One alarming response of phytoplankton to anthropogenic pollution, and a worldwide threat to aquatic ecosystem services, is the formation of blooms, i.e., mass accumulation of microalgae Isles and Pomati (2021). Phytoplankton blooms are increasing worldwide due to eutrophication and climate warming Huisman et al. (2018); Ho et al. (2019), with annual societal costs in the billions of Euros. In freshwaters, dense and often toxic blooms are associated with cyanobacteria Huisman et al. (2018). Forecasting or real time detection of algal blooms is a central concern in ecosystem management. The ability to promptly identify blooms would allow stakeholders to respond to human health or ecosystem service concerns. However, current early warning approaches suffer from severe drawbacks due to lack of spatial and temporal resolution in sampling and detection of these events.

Although automated instruments are available and used Lombard et al. (2019); Merz et al. (2021), phytoplankton monitoring is most commonly performed by dedicated personnel, making it difficult, time consuming and expensive Pomati et al. (2011). Dedicated laboratories perform sample collection, transport and storage for subsequent analysis by technicians and trained taxonomists, in case identification of microalgae is necessary. In many monitoring programs, particularly those concerning public health issues like harmful algal blooms, sampling should be rapid and target multiple locations and ideally multiple depths underwater, which is inconvenient and often difficult to achieve. Some locations, or deep chlorophyll-a (Chl-a) maxima which often characterise algal blooms, might not be easily accessible, limiting our ability to detect potential environmental threats. Aquatic ecosystem monitoring would hence tremendously benefit from autonomous sampling devices for phytoplankton monitoring, which allow multiple sample collection in offshore and/or inaccessible sites.

As summarised in Figure 1, the use of UAVs for water sampling shows potential for automating sampling and expanding the breadth of water research. In fact, the use of UAVs for this task is not a novel concept, having been employed by Ore et al. (2015) and Schwarzbach et al. (2014), and subsequently used in various different applications Lally et al. (2019). Amongst these, several are of particular interest. The sampling of a remote crater lake showcases UAV based water sampling as an adequate method for sampling in remote and hazardous regions Terada et al. (2018). The surface mapping of water quality using water samples and on-board sensors demonstrates the usage of UAVs for mapping of spatial gradients in bodies of water, Koparan et al. (2020). Finally, simultaneous sampling and sensor deployment showcases the potential of integrating these methods in real-time networks Ribeiro et al. (2016). Here, we would like to highlight two distinguishable methods used for water sample collection. The first relies on a pump to fill a container present on-board the UAV, while the second is much more widely used and relies on a cable suspended payload with a container that can be passively triggered by buoyancy Benson et al. (2019), by a microcontroller Koparan et al. (2020); Terada et al. (2018), or by a messenger probe Koparan et al. (2018). The latter is remarkably similar to standard depth water samplers and if employed for depth sampling, could constitute a simple alternative to the method here presented.

Remote water sampling at depth with autonomous vehicles has been previously performed using non-flying Autonomous Underwater Vehicles (AUVs) Zhang et al. (2019), but these systems are normally bulky and heavy, hindering access to many research sites. Being inherently lightweight and facilitating access to remote locations through flight, UAV based methods can be of particular interest in many applications. Thus far, two UAV systems have used sensor probes lowered from UAVs Chung et al. (2015); Ore and Detweiler (2018) to measure thermophysical properties of water at depth. Concerning water sampling at depth, an author has done it successfully at up to 3 m depth using multiple cable suspended samplers actuated by a microcontroller Koparan et al. (2019). Also using a cable suspended sampler, another author has commercialised a method that has been successfully demonstrated up to an impressive depth of 92 m Castendyk et al. (2019).

In light of this recent work, we find there is a lack of fully integrated UAV solutions which perform targeted sampling at accurate depths, i.e., not relying on sampler depths set *a priori* to flight (Koparan et al. (2019)) or not requiring multiple flights and interfaces for a signle sample (Castendyk et al. (2019)). A new

FIGURE 1
Sampling methods used in this publication. A multiparametric probe collects data autonomously along a vertical profile of the lake in a fixed location. A Niskin bottle is used off-board a motor-boat to collect water at depth for later filtration and analysis. The MEDUSA system developed for remote acquisition of water samples at depth.

class of vehicles capable of seamless motion in water and air is, in our view, a necessity in this effort.

Unmanned Aerial-Aquatic Vehicles (UAAVs)[1] are hybrid unmanned vehicles capable of traveling through air and water, normally fully integrated into a single package. These robots are capable of performing a new class of hybrid aerial-aquatic missions in challenging environments, creating opportunities for novel data-gathering strategies. This is achieved by providing in essence, means for researchers to access water-bodies from more convenient launch points, collect aerial data of said water-bodies, and perform direct measurements at the water surface or/and at depth at multiple locations. Literature in the UAAV field is extensive, Zeng et al. (2022), and varied mission profiles have been proposed thus far, Farinha et al. (2021). Amongst other achievements, UAAVs have been shown overcoming obstacles and escaping cluttered aquatic environments (Zufferey et al. (2019a); Siddall et al. (2017); Tétreault et al. (2020)), autonomously traveling underwater (Lyu et al. (2022)), and performing long duration sailing missions (Zufferey et al. (2019b)). These technologies are expected to extend hybrid sensing mission capabilities in aquatic environments by performing both remote observation and direct sampling. The direct sampling component can be valuable as a ground-truth mechanism in remote observation missions, but even more so in disciplines that require knowledge of water properties at depth, where sampling is more labour intensive.

Aerial-aquatic locomotion within a single vehicle often comes at the cost of compromising performance and limiting operational envelope. We previously investigated separating the aquatic and aerial components into two agents, taking advantage of the robustness of standard multicopter configurations and the simplicity of modular systems, Debruyn et al. (2020). This solution (the MEDUSA system - Multi-Environment Dual-robot for Underwater Sample Acquisition) proved to be simple and reliable, as well as easily expandable for different sensing and locomotion requirements. In this paper we demonstrate the application of the MEDUSA concept on the task of freshwater monitoring. The primary developments and contributions are the following: 1) Development of an autonomous filtration depth sampling system for use with an UAV; 2) Extension of the previous prototype's operational envelope by redesigning the micro Underwater Vehicle (μUV) and its buoyancy control subsystem for operations at depth; 3) Redesign of the communication between the different agents into a more streamlined and robust package; 4) Field demonstration of vertical profiling of aquatic environments and Chlorophyll-a monitoring with MEDUSA.

2 Materials and methods

2.1 System operational envelope

By having the capacity to operate in air and in water at depth, MEDUSA type systems are especially indicated for sample collection and underwater inspection. The system here described is capable of collecting up to two independent water

---

[1] Also designated as Hybrid Aerial Underwater Vehicles (HAUVs) and Aquatic Unmanned Aerial Vehicles (AquaUAVs).

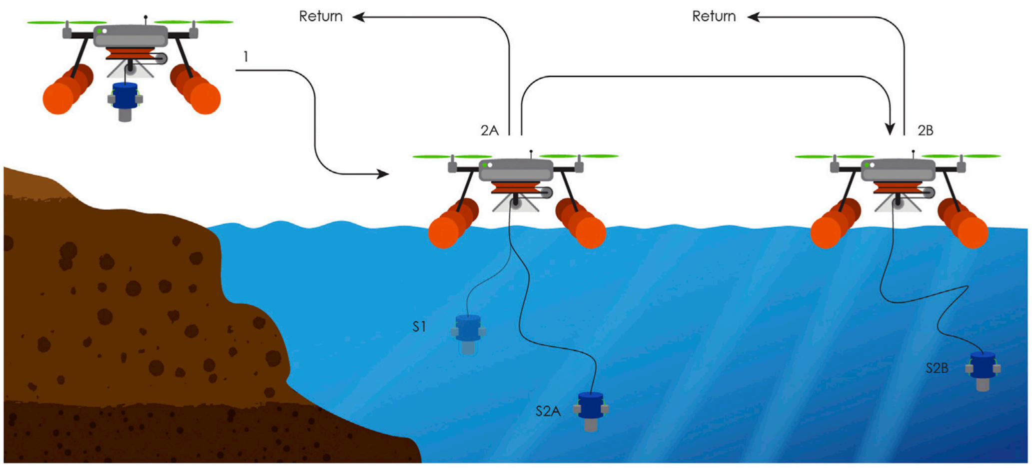

FIGURE 2
Mission profile for the MEDUSA system. Take-off from shore - 1 fly to aquatic location of interest - 2A land on the water surface - S1 collect first water sample at desired depth - S2A collect second water sample at different depth (OR) 2B fly to second location of interest and collect second sample S2B- return to shore.

TABLE 1 Masses of principal components in the MEDUSA system.

Frame (kg)	Propulsion	Batteries	Avionics & wiring	Coiling system	Underwater vehicle (μUV)	μUV ballast	Landing gear	Total
2	1.800 kg	1.446 kg	0.207 kg	0.997 kg	0.676 kg	0.312 kg	1.52 kg	8 kg

samples, speeding up the characterisation of gradients, and enabling a variety of hybrid aerial-aquatic missions as shown in Figure 2. This system can vertically take-off and land on solid ground or the water surface, and collect up to two water samples. These samples can be collected from a single location at different depths (S1, S2A), or from two different locations (S1, S2B). This provides flexibility in the characterisation of water bodies in their depth and span.

The underwater operational envelope is restricted by the length of the tether to a half sphere of 10 m radius. Consequentially, the sampling depth is also restricted to a maximum depth of 10 m, which is generally sufficient to cover the entirety of the epilimnion layer of stratified lakes, where most of the phytoplankton production occurs.

2.2 System design

The MEDUSA system is composed of a standard multicopter platform, a water-landing system, a tether management unit and a micro underwater vehicle, with masses discretised in Table 1.

Details on this implementation of MEDUSA are shown in Figure 3. The flying component is based on the *Tarot X6* hexacopter frame with the *DJI E1200 Standard* propulsion system and 6.6 Ah of installed battery capacity. We use a *Pixhawk four* flight controller and the *H-RTK F9P* RTK GNSS system for position control. Communication is done *via* 900 MHz for long range radio-control and Mavlink stream for the ground-station, while analog video-feed is provided over 2.4 GHz.

The water landing gear is composed of eight spherical floats, which are chosen for its low weight (each weighs 120 g), buoyancy (each supports 1.2 kg) and high-visibility (in red and white). The floats are mounted in such a way that it creates a wide and stable floating platform on the water for the UAV. The heavier system components e.g., coiling system and *μUV* are located in the centre of the floating platform to maintain stability while the UAV is floating on water.

The coiling unit holds 11 m of Ethernet cable. Among the eight color wires in the cable, power and ground take two lines each, serial communication two more, analog video takes another and one is left free. The tension for power transmission is boosted

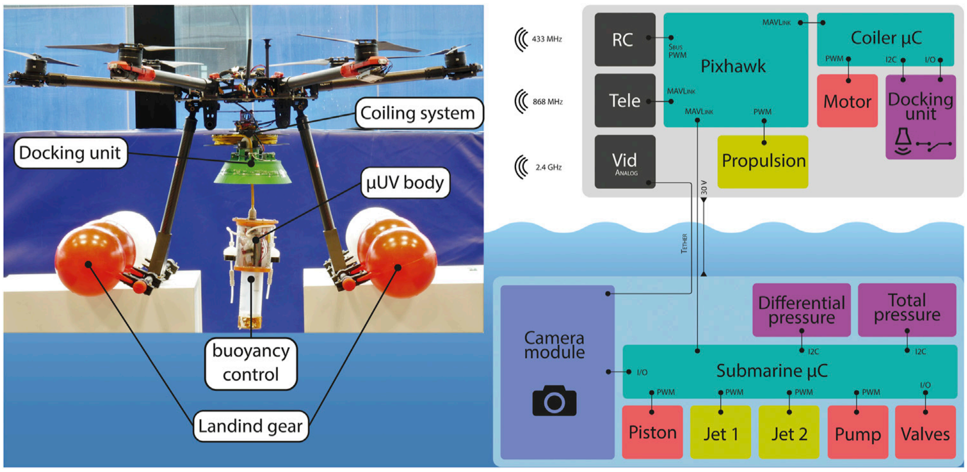

FIGURE 3
Principal mechanical subsystems that compose the MEDUSA system (left). On the left, electronics framework including: controllers, sensors, actuators and communication protocols for both the aerial (top) and underwater system (bottom).

to 30V, which keeps the voltage drop in the line bellow 4.4%, reducing power loss. Waterproofing at the μUV interface is ensured by using a waterproof cable gland connector, which also facilitates disassembly. The tether feeding is done by a high-torque continuous-rotation servo motor and managed by an *Arduino-nano* using PWM signal. Given we're using a "dumb-servo", the docking unit is fitted with contact switches to detect the terminus of recoil, while depth measured by the μUV provides information on the length of deployed cable. The docking unit is further fitted with a sonar range-finder to detect the approach of the μUV and slow down before docking contact.

The μUV is shaped as a cylindrical container, composed of a transparent polycarbonate tube capped on both ends by machined Aluminium 6,068 lids. One end can be opened and holds the tether connector while the other end holds a custom PCB. The PCB includes power modules, actuator drivers, sensors and an *Arduino-nano* micro-controller. Buoyancy control is achieved using a linear actuator connected to a piston, and a total pressure sensor provides feedback for the control loop. An FPV-flight analog camera placed in the μUV provides visual feedback *via* the video transmitter on-board the multicopter. It is worth noting that a major design challenge of a micro Underwater Vehicle (μUV) with appropriate mass for flight, is its compactness. This is made obvious by the mass of ballast used (30% of the μUV mass), to raise the system's mass to a neutral buoyancy point. For this reason, the μUV needs to be designed for minimum volume, not mass.

2.2.1 Sampling system design

The design of a water sampling system to be integrated on an UAV comes with considerable technical challenges and design constraints. First, the UAV payload is limited and mission range is directly affected by an additional load. Secondly, the sample volume is dependant on the water properties of interest, varying the return payload depending on the application. Lastly, the UAV needs to be stable pre and post sample acquisition. A sampling solution that allows for flexibility in sampling volumes and negligible added payload in the form of water is filtration. Even though this method does not allow for some types of *a posterirori* analysis that require a liquid sample, thermophysical properties of water can still be measured *in situ* (albeit with lower precision), using on-board sensors. Nevertheless, filtration alone can provide relevant information such as concentration of suspended particles (e.g., algae, bacteria, zooplankton), their elemental composition (e.g., stoichiometry), and the biodiversity of the ecosystem based on environmental DNA Deiner et al. (2017). The sampling system demonstrated here is shown in Figure 4 and is capable of acquiring two independent samples per flight. This is achieved by using a pair of micro solenoid valves for flow diversion (or 2/3 solenoid valves), which open three parallel and independent lines. Two of these lines are used for sampling and have an inline filter holder for glass fibre filters (GF/F-filters). Further efforts are taken towards ensuring that no cross-contamination occurs, by dedicating the third line for purging before each sample; and by including a non-return valve at the end of each sampling line, thus avoiding the occurrence of reflux. Another feature of this design is scalability. Considering the 2/3 valve - filter holder - non-return valve as a single block, one can place as many of these as necessary in parallel to perform as many samples as required, adding only 40 g per additional line.

Filtration sampling methods rely on accurate knowledge of the volume of filtered water. The use of a peristaltic pump is thus

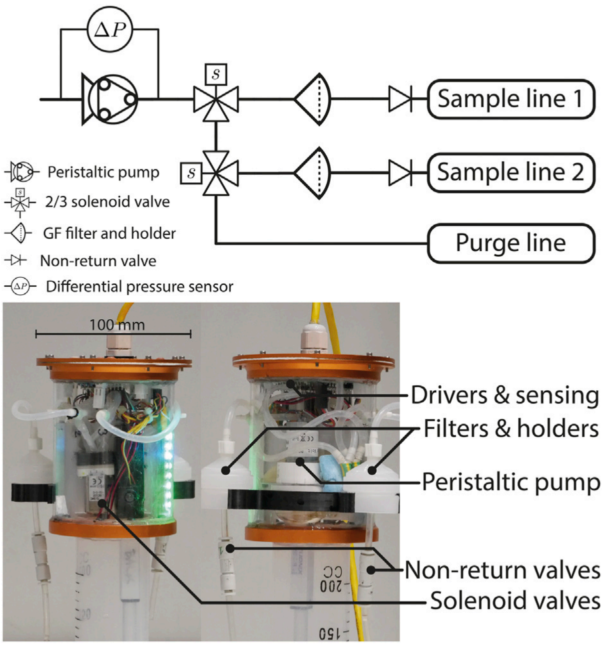

FIGURE 4
Filter based sampling system integrated in the μUV: hydraulic diagram (top), and physical components (bottom).

clearly advantageous, due to its mostly linear characteristic (i.e., the pump's rotation speed and flow rate remain constant with pressure loading). There is however a source of inaccuracy that should be accounted for, which is stall. In fact, peristaltic pumps have drastically reduced flow rates above certain pressure loading values, a condition that is reached as particles deposit on the filters and block the flow. The inclusion of a differential pressure sensor to measure the pressure loading on the pump allows a sample to be cut-off as soon as the pump starts operating outside its linear regime, thus leading to accurate and consistent sampling volume estimations.

2.2.2 Dual system communication setup

The integration of the system's aerial and underwater components is done using customised open-source frameworks, i.e., *PX4* (Meier et al. (2015)) for the flight control, *Arduino* for underwater control and sampling, and *MAVLink* (Koubâa et al. (2019)) for communication between the Ground Control Station (GCS), UAV and μUV. Control of the vehicle is done *via* the Radio Control (RC) and GCS which also receives feedback information; a complete list of control inputs and available feedback information is provided in Table 2.

Figure 5A shows a visualisation of the two modes for the μUV's depth control. A first mode uses the tether system to pull the μUV upwards, and the μUV's weight with the piston fully retracted for downwards movement. A second mode uses a piston actuated by a linear actuator, which controls the μUV's depth using a PID control loop and a total pressure sensor for feedback. Even though the second mode increases the system's complexity and weight, it achieves tasks that would not be possible otherwise, such as underwater current compensation and depth control when moving in 3D space. For both cases, depth control is achieved using depth setpoints set *via* the MDSA_DEPTH_TGT parameter editable through the GCS, or *via* the RC using the pitch stick mapped to the actuator_control_0 topic.

As shown in Figure 5B, the timing, switching logic and actuation happens internally in the μUV, which uses the actuator_control_0 topic to trigger sample collection and manual stopping. The value of MDSA_SMPL_NB (Table 2) is incremented every time a sample is triggered and a switching logic chooses valve and pump actuation status that diverts the flow appropriately to either one of the samples or, when necessary, the purging line. In addition to the manual RC override, samples will automatically be stopped after a target volume set in the GCS is reached or the maximum Δp measured in-line is reached. The sample volume is calculated using a calibration curve that uses only the μC clock for the elapsed time.

2.3 Sampling procedures

In order to test and prove the functionality of the pump system on a real case scenario, a test was performed in Greifensee, Switzerland, with the aim of collecting a gradient of chlorophyll values water samples at different depths. Samples were collected from a boat by the monitoring station 47.36668 °N, 8.6651 °E (WGS 84). For this purpose glass microfiber filters, Grade GF/F (Whatman), 25 mm diameter and a pore size of 0.7 µm were used. To test the performance of the UAAV sampling system, manual samples were collected in parallel and manually filtered with syringes and filter holders as done in the UAVV system. Surface sample was taken directly from the boat by manually filling a syringe with surface water and measuring the volume of filtered water. Water samples at the different depths were collected with a niskin bottle, parallel to the UAAV system and the same filtering procedure was repeated. All filters were stored at 4°C and in the dark, and frozen (−20°C) once in the lab until sample processing.

2.3.1 On-site benchmarking

For the comparison of drone-sampled Chl-a with depth profiles, we used data from an Idronaut multiparametric probe and automated profiler (relevant information can be found in previous publications) Pomati et al. (2011); Merz et al. (2021). Water parameters monitored included pressure (i.e., depth), temperature, conductivity, oxygen, PAR (photosynthetic Active Radiation), turbidity, phycocyanin and

TABLE 2 List of parameters and topics used to handle the underwater locomotion mission section, sampling control, depth control and tether extension/retraction.

Group	Parameter/topic	Radio-control	Ground control station
Sampling	MDSA_SMPL_STTUS	set - start/stop/auto sample	—
	MDSA_SMPL_VOL	—	view - current sample volume
	MDSA_SMPL_TGVL	—	set - next sample target volume
	MDSA_SMPL_DP	—	view - current sample Δp
	MDSA_SMPL_NB	—	view - sample number
Underwater Control	MDSA_DEPTH_TGT	—	set - depth target
	MDSA_DEPTH_CUR	—	view - current depth
	MDSA_C_MODE	set - depth control mode	view/set - depth control mode
	actuator_control_0 [1]	set - forward motion	—
	actuator_control_0 [2]	set - yaw rate	—
	actuator_control_0 [3]	set - depth/buoyancy	—
Mission Control	actuator_control_0 [5]	set - flight/underwater mode	—
	actuator_control_0 [6]	set - hold/retract/deploy tether	—

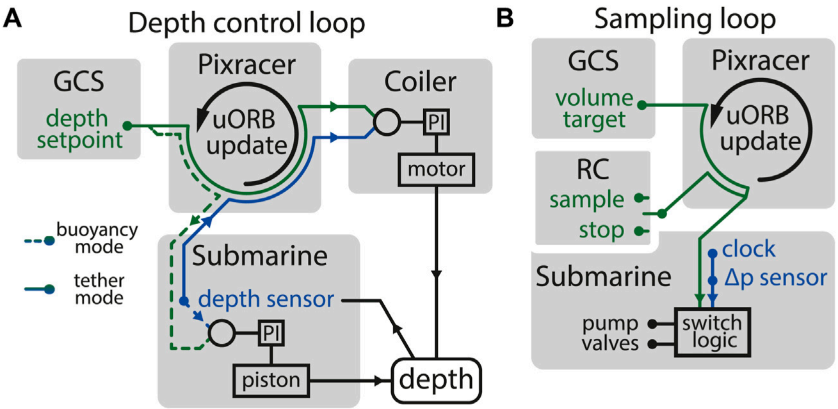

FIGURE 5
Distribution of actuators, sensors, control logic and user interfaces used across the MEDUSA system for: **(A)** *μUV* depth control and **(B)** sample collection logic.

chlorophyll-a, these last three using a Trilux fluorometer (https://chelsea.co.uk/).

2.3.2 Chlorophyll-a extraction

Chl-a extraction was done in the laboratory according to the standard procedure in Carranzo (2012). Using 90 percent ethanol, samples were vortexed, afterwards sonicated in an ice-waterbath for 15 min and stored at 4°C overnight. Extracted samples were filtered with 0.2 μm cellulose acetate syringe filters to remove particles and measured at 665 and 750 nm using a photospectrometer.

3 Results

Videos of the MEDUSA system in action during field trials and sampling tests can be found in Supplementary Video S1. Full system tests (flight - sample - sample - return) were performed in various locations in the United Kingdom, Switzerland and Croatia, in fresh and seawater. During these tests, samples were acquired at a maximum distance of 65 m from shore, and the maximum distance covered in flight was 600 m. The system achieved flight times of up to 13 min, however, we estimate the current setup can operate for 27 min if the maximum available battery payload is used. Flights were performed with winds up to 25 knots in a sheltered location where waves do not develop. While the wind was not a challenge for flight, it lead to rather fast drifting while MEDUSA floats on the water surface. This does not necessarily lead to failure, however, the μUV tends to get dragged behind it, which makes the depth control highly inaccurate. In terms of water surface state, all flights and landing attempts were performed on Douglas scale 0 to 1. One attempt was made for take-off in scale two conditions, however, a safe take-off was not possible. With increasing degrees of swell, it is not only take-off and landing that becomes challenging, but also deployment and recovery of the μUV can become impossible due to aggravated motion of the tether relatively to the coiling system. We've observed during sampling that the depth holding accuracy of the μUV is of ±3 cm, which outperforms other depth samplers we found in the literature. This estimate is however based on the on-board total pressure sensor, so it does not account for sensor bias that can occur due to local atmosphere or water density.

System tests where the acquired samples were analysed, were performed in three different locations in Switzerland: Zurich lake (47.319756, 8.553111) where there are no flight restrictions in place, Greifensee (47.366402, 8.665131) which a nature reserve with limited boat and flight activities allowed, and the EAWAG ponds facility (47.405155, 8.608538), where flight plans need to be approved by the flight authorities due to the proximity of the Dubendorf airbase. Taking into account these restrictions, full system tests were performed in Zurich lake, while in Greifensee the UAV was kept onboard a motorboat and the μUV lowered into the water using the depth control systems in place, and in the ponds facility the UAV was left to freely float in the ponds and the aquatic phase of the mission was carried out as in a full system trials.

3.1 Freshwater chlorophyll sampling

Samples were obtained in Greifensee from surface level to 9 m depth. The obtained Chlorophyll-a values are shown in Figure 6A alongside corresponding data from manual samples and from the Chl-a sensor values (from the multiparametric probe) logged at the time of sampling. It is shown that the UAAV and manual samples mostly match, with exception of the samples at 2 m depth. However, this mismatch is most likely a result of an error either with the manual sampling depth or with the sample tagging, as emphasised by the fact that the UAAV-based samples better follow the trend shown by the multi-parametric sensor values. It is also apparent that manual and UAAV samples show slightly lower Chl-a values than the sensor data. We expect, however, the latter ones to be less precise in absolute terms, as they are based on pigment fluorescence after light excitation, which can be influenced by a number of confounding factors, Falkowski and Kiefer (1985).

In order to assess the contamination between sampler one and two in consecutive samples, pairs of consecutive S1 and S2 samples were ordered and a contamination hypothesis given by $Chl_{M2} = (1 - \epsilon)\,(Chl_{S2} + \alpha Chl_{S1})$ is tested for the ordered pairs as well as 1,000 random permutations of the same pairs. Where Mi and Si indexes correspond respectively to manual and UAV-sampler-i based samples of the same location and ϵ is the absolute error incurred by the measurement performed with sampler 1 before a measurement of a different location with sampler 2. As shown in Supplementary Figure S1, the confidence interval for the contamination ratio α is comparable to values encountered in other random permutations, which indicates contamination is likely not happening.

In order to validate the sampling system, samples taken using MEDUSA were taken in tandem with manual ones. The relation between the manual and UAAV based samples can be found in Figure 6B, where 27 valid sample pairs are discretized. Despite some variation in the 3–5 $\mu g/L$ range, the data follows a close fit of a line of slope one intersecting at the origin, showcasing a one to one relation between the manual and UAAV-based methods. These results, however, show only that Chl-a values obtained using MEDUSA are comparable to manual methods. A full description of the method's precision would require several more samples across the full range of Chl-a concentrations.

All UAAV-based samples were acquired with varying volumes, which were the result of the samples being cut-off when the Δp loading on the pump exceeded a threshold of 1,000 kPa. Figure 6C showcases 4 such samples where the system's water outlet was collected onto a set of scales and the measured value compared to the prediction used by MEDUSA. Sample 1 corresponds to the filtering of clear water and thus the Δp remains constant and equivalent to the pressure loading of the valves, filter and tubing. In this situation, MEDUSA will cut-off the sample after reaching a predefined maximum volume, which is here set to 200 ml. Subsequent samples correspond to increasingly more turbid water. Thus, the sampled volume does not reach the set maximum volume, but the maximum Δp, after which the flow rate is no longer constant and the predicted sampled volume accumulates error.

4 Discussion

There are three main features that distinguish the method here described from the previous literature on UAV based depth water sampling (Ore and Detweiler (2018); Koparan et al. (2019); Castendyk et al. (2019)).

Firstly, as opposed to Ore and Detweiler (2018); Castendyk et al. (2019), the MEDUSA system lands on water to collect samples instead of hovering above it. This is done with the intention of saving energy while the samples are being collected, and thus increasing the system's effective range. However, it also comes at an increased payload which has the opposite effect. Our

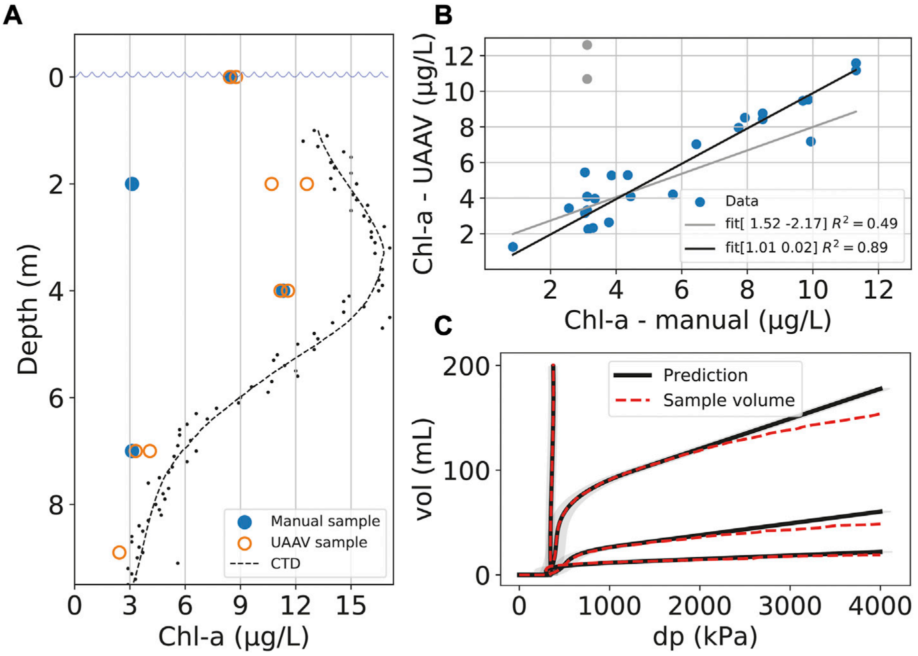

FIGURE 6
(A) Vertical section of the Chlorophyl-a values found at the Greifensee research station (47.366402, 8.665131) on the 30th of September 2021: manual sampling values obtained with a Niskin bottle, UAAV values obtained with MEDUSA and CTD values obtained using the automated multiparametric probe. **(B)** Correlation of UAAV - manual samples obtained in the same location/depth at several locations. In grey, the removed datapoints where a manual sampling error is likely to have occurred. **(C)** Evolution of filtered volume with differential pressure measued in the sampler, comparing volumes predicted using the linear model used in the sampler and the real measured volume. At 1,000 kPa, the limit for sample cut-off put in place to avoid non-linear effects.

experiments show that by flying without the water landing gear, MEDUSA can extend its flight time by ~ 2 minutes, an 18% increase. Depending on the sample volume being collected, the sample time can go well beyond this (it will take 150 s to collect 200 ml for example), so there is a clear advantage in increasing the mission times like this. Moreover, given the μUV can perform other more lengthy tasks, such as underwater inspection, the range benefits become even greater. Adversely, landing on water means the UAV is more exposed to the water surface and operating conditions are limited to very calm sea states. However, designing the UAV component to be fully waterproof and capable of providing buoyancy with it is main body (as some commercial platforms do) would improve stability in waves and make the system more robust.

Secondly, the usage of a filtration system to collect samples. This system has the advantage of not changing the UAV's dynamics after sample collection, however, the mass of the samples we collected thus far ($20 \sim 200 mg$) is rather insignificant when compared with the mass of the entire system (8 kg). Nevertheless, these volumes are comparable to the ones found in the literature Koparan et al. (2019). Instead, we have found that the main advantage of the system is on a practical level: by providing a solid sample on a filter and eliminating the need to do filtration manually after collection. There is also the fact that storing the water inside the μUV would be rather challenging, but this is more a consequence of our design choices and not necessarily the case for other UAAVs. Furthermore, even though the fact that samples will generally have different volumes can initially seem convoluted, however, given the that the condition for sample termination is the clogging of the filter; samples will, in principle, always contain enough solids to perform the necessary analysis.

Finally, the integration of underwater locomotion and flight in a single robot. Besides the obvious additional tasks that can be performed by the underwater robot, it allows us to accurately control the depth of the μUV. We have estimated the accuracy in depth control to be ±3 cm from the information of the depth sensor. However, no baseline measurement was used to confirm this value, and we do not claim to have a more accurate depth control than in Ore and Detweiler (2018). Another useful feature is the fact that we have access to real-time data about the samples, μUV depth and visual feedback, which allows for missions to be adjust in real-time. On the other hand, this level of integration creates the need for coiling heavy and stiff electrical cable which hinders operations. The impact of this is clearly seen as Castendyk et al. (2019) can achieve much greater depths than what would be feasible with such a cable. There is, however, room to improve the cable used by using higher performance tethers for underwater rovers, or even by providing the μUV with it is own power supply to reduce the number of lines necessary in the line. This, of course, comes with it is own challenges.

4.1 System design and field trials: Lessons learnt

Most UAAV systems we are aware of have operated at shallower depths than here described, which constituted a challenge in itself and lead to unexpected design choices. We summarise here some lessons learnt on the system design and trials, which we hope will prove useful in designing a similar system.

The design of the μUV is much more driven by volume limitations than weight. So, keeping all sealed components outside the chamber helped keep the volume low and consequentially reduce the payload in flight. Furthermore, the μUV is also much less subject to drag, as travel speeds are considerably low. It is thus not disadvantageous to design configurations with large cross-sections, if this results in simpler deployment and recovery by the UAV.

Opening and closing a sealed compartment in the field is troublesome, especially with live electronics in wet environments. We found that keeping the filter holders outside the μUV makes the process of recovering and replacing filters considerably safer and simpler.

A more effective coiling system than the one here described would use a stepper motor with encoder driving the winch with larger gear ratio through a timing belt. This results in a higher rotating torque setup with precise measurement of cable length, though, at the expense of weight and complexity.

The beyond visual-line-of-sight (BVLOS) requirement in remote water sampling mission imposes challenges in on-site operation, especially in terms of landing and take-off maneuvers, which are dependent on local water surface conditions, weather, obstacles, and animal activities. To give the pilot a better situational awareness during flight, the onboard camera on the UAV and μUV proved to be a simple and effective setup. The camera on the UAV, being mounted properly facing downward, allows the pilot to examine the sampling site prior to landing, and see the deployment of the coiling system. The camera onboard the μUV, on the other hand, allows the pilot to have a clear view of the underwater operation and water condition, and assists in the retrieval process of the μUV. The LED indicators on the μUV can also be seen through the cameras which allows immediate diagnosis of any system failures onboard.

Another operational challenge encountered is related to the difference in density between salt and fresh water. This was overcome by using two different ballast masses in both environments, however, the μUV system would ideally provide sufficient volume variation to account for this difference, which is considerably difficult to achieve with piston systems.

4.2 Conclusion

The primary objective of this work was to showcase a novel method of sampling aquatic environments at depth and demonstrate it in the particular case of Chlorophyll-a measurements. The MEDUSA system was shown to be successful in acquiring samples from shore and at high precision in depth and filtered sample volume. This enables us to acquire accurate Chlorophyll-a measurements that are on-par with manual sampling methods. The underwater component of MEDUSA is equipped with a novel depth sampler which is fully integrated with a modified open-source flight controller, and is demonstrated to operate at up to 9 m depth. This same implementation of the MEDUSA concept can be directly used for other *a posterirori* analysis such as measurements of isotope concentrations, biomass or eDNA.

Some challenges remain when it comes to implementing this research in daily freshwater monitoring applications. For instance, increasing the number of samples per flight would improve usability considerably, especially if the system can perform one full vertical profile per flight. This is easily achieved thanks to the modularity of the sampling system, however, it will come at a payload cost. This is not due to the increased component mass, but rather to the increased internal volume which needs to be compensated by ballast.

Finally, we have shown that aerial-aquatic drones can be successful in improving access and facilitating water sampling at depth, opening new paths in fresh-water research, amongst other fields. We anticipate that this technology will improve data gathering processes and help answer various ecological and environmental questions.

Data availability statement

The raw data supporting the conclusions of this article will be made available by the authors, without undue reservation.

Author contributions

AF, JT, CR, RZ, MR, FP, and MC worked on the conceptual design of the MEDUSA platform. The μUV, UAV and other subsystems were jointly developed by AF, JT, CR, and OP. AF and JT jointly worked on the software development of the MEDUSA software. Flight tests and system trials were performed by AF, JT, CR, OP, RZ, FP, and MK. Sample analysis and manual samples were performed and supervised by MR and FP. Data processing was performed by AF and MR. AF wrote the first draft of the manuscript and all authors contributed with additional content, read and approved the final version.

Funding

This work was supported by NERC and NPIF grant NE/R012229/1, and carried out within the framework of the EUROfusion Consortium. As well as the Engineering and Physical Sciences Research Council (EP/R009953/1, EP/N018494/1, EP/R026173/1, EP/S031464/1); the EU H2020 AeroTwin project (grant ID 810321). The work of MK is supported by the Royal Society Wolfson fellowship (RSWF/R1/18003). The Greifensee monitoring station is funded by the Swiss National Science Foundation (project 182124 Aquascope - www.aquascope.ch).

Acknowledgments

The authors thank the members of the Aerial Robotics Lab, Imperial College London, and Materials and Technology Centre of Robotics, EMPA, for their support and numerous stimulating discussions.

Conflict of interest

The authors declare that the research was conducted in the absence of any commercial or financial relationships that could be construed as a potential conflict of interest.

Publisher's note

Supplementary material

The Supplementary Material for this article can be found online at: https://www.frontiersin.org/articles/10.3389/fenvs.2022.1023269/full#supplementary-material

References

Benson, J., Hanlon, R., Seifried, T. M., Baloh, P., Powers, C. W., Grothe, H., et al. (2019). Microorganisms collected from the surface of freshwater lakes using a drone water sampling system (dowse). *Water* 11, 157. doi:10.3390/w11010157

Carranzo, I. V. (2012). "Standard methods for examination of water and wastewater," in *Anales de hidrología médica* (Spain: Universidad Complutense de Madrid), 5, 185.

Castendyk, D., Straight, B., Voorhis, J., Somogyi, M., Jepson, W., and Kucera, B. (2019). "Using aerial drones to select sample depths in pit lakes," in *Mine closure 2019: Proceedings of the 13th international conference on mine closure*. Editors A. Fourie, and M. Tibbett (Australia: Australian Centre for Geomechanics), 1113–1126. doi:10.36487/ACG_rep/1915_89_Castendyk

Chung, M., Detweiler, C., Hamilton, M., Higgins, J., Ore, J.-P., and Thompson, S. (2015). Obtaining the thermal structure of lakes from the air. *Water* 7, 6467–6482. doi:10.3390/w7116467

D'Alelio, D., Russo, L., Hay Mele, B., and Pomati, F. (2021). Intersecting ecosystem services across the aquatic continuum: From global change impacts to local, and biologically driven, synergies and trade-offs. *Front. Ecol. Evol.* 9, 628658. doi:10.3389/fevo.2021.628658

Debruyn, D., Zufferey, R., Armanini, S. F., Winston, C., Farinha, A., Jin, Y., et al. (2020). Medusa: A multi-environment dual-robot for underwater sample acquisition. *IEEE Robot. Autom. Lett.* 5, 4564–4571. doi:10.1109/LRA.2020.3001534

Deiner, K., Bik, H. M., Mächler, E., Seymour, M., Lacoursière-Roussel, A., Altermatt, F., et al. (2017). Environmental dna metabarcoding: Transforming how we survey animal and plant communities. *Mol. Ecol.* 26, 5872–5895. doi:10.1111/mec.14350

Directives originating from the EU (2000). Directive 2000/60/ec of the European parliament and of the council of 23 october 2000 establishing a framework for community action in the field of water policy. *OJ L* 327, 1–73.

Falkowski, P., and Kiefer, D. A. (1985). Chlorophyll a fluorescence in phytoplankton: Relationship to photosynthesis and biomass. *J. Plankton Res.* 7, 715–731. doi:10.1093/plankt/7.5.715

Farinha, A., Di Tria, J., Zufferey, R., Armanini, S. F., and Kovac, M. (2021). "Challenges in control and autonomy of unmanned aerial-aquatic vehicles," in 2021 29th Mediterranean Conference on Control and Automation (MED), Puglia, Italy., 22-25 June 2021, 937–942. doi:10.1109/MED51440.2021.9480342

Ho, J. C., Michalak, A. M., and Pahlevan, N. (2019). Widespread global increase in intense lake phytoplankton blooms since the 1980s. *Nature* 574, 667–670. doi:10.1038/s41586-019-1648-7

Huisman, J., Codd, G. A., Paerl, H. W., Ibelings, B. W., Verspagen, J. M., and Visser, P. M. (2018). Cyanobacterial blooms. *Nat. Rev. Microbiol.* 16, 471–483. doi:10.1038/s41579-018-0040-1

Isles, P. D., and Pomati, F. (2021). An operational framework for defining and forecasting phytoplankton blooms. *Front. Ecol. Environ.* 19, 443–450. doi:10.1002/fee.2376

Koparan, C., Koc, A. B., Privette, C. V., and Sawyer, C. B. (2020). Adaptive water sampling device for aerial robots. *Drones* 4, 5. doi:10.3390/drones4010005

Koparan, C., Koc, A. B., Privette, C. V., and Sawyer, C. B. (2019). Autonomous *in situ* measurements of noncontaminant water quality indicators and sample collection with a uav. *Water* 11, 604. doi:10.3390/w11030604

Koparan, C., Koc, A. B., Privette, C. V., Sawyer, C. B., and Sharp, J. L. (2018). Evaluation of a uav-assisted autonomous water sampling. *Water* 10, 655. doi:10.3390/w10050655

Koubâa, A., Allouch, A., Alajlan, M., Javed, Y., Belghith, A., and Khalgui, M. (2019). Micro air vehicle link (mavlink) in a nutshell: A survey. *IEEE Access* 7, 87658–87680. doi:10.1109/ACCESS.2019.2924410

Lally, H., O'Connor, I., Jensen, O., and Graham, C. (2019). Can drones be used to conduct water sampling in aquatic environments? A review. *Sci. total Environ.* 670, 569–575. doi:10.1016/j.scitotenv.2019.03.252

Lombard, F., Boss, E., Waite, A. M., Vogt, M., Uitz, J., Stemmann, L., et al. (2019). Globally consistent quantitative observations of planktonic ecosystems. *Front. Mar. Sci.* 6, 196. doi:10.3389/fmars.2019.00196

Lyu, C., Lu, D., Xiong, C., Hu, R., Jin, Y., Wang, J., et al. (2022). Toward a gliding hybrid aerial underwater vehicle: Design, fabrication, and experiments. *J. Field Robot.* 39, 543–556. doi:10.1002/rob.22063

Meier, L., Honegger, D., and Pollefeys, M. (2015). "Px4: A node-based multithreaded open source robotics framework for deeply embedded platforms," in 2015 IEEE international conference on robotics and automation (ICRA), Seattle, Washington, USA., 26-30 May 2015, 6235.

Merz, E., Kozakiewicz, T., Reyes, M., Ebi, C., Isles, P., Baity-Jesi, M., et al. (2021). Underwater dual-magnification imaging for automated lake plankton monitoring. *Water Res.* 203, 117524. doi:10.1016/j.watres.2021.117524

Ore, J.-P., and Detweiler, C. (2018). Sensing water properties at precise depths from the air. *J. Field Robot.* 35, 1205–1221. doi:10.1002/rob.21807

Ore, J.-P., Elbaum, S., Burgin, A., and Detweiler, C. (2015). Autonomous aerial water sampling. *J. Field Robot.* 32, 1095–1113. doi:10.1002/rob.21591

Pomati, F., Jokela, J., Simona, M., Veronesi, M., and Ibelings, B. W. (2011). An automated platform for phytoplankton ecology and aquatic ecosystem monitoring. *Environ. Sci. Technol.* 45, 9658–9665. doi:10.1021/es201934n

Ribeiro, M., Ferreira, A. S., Gonçalves, P., Galante, J., and de Sousa, J. B. (2016). "Quadcopter platforms for water sampling and sensor deployment," in *OCEANS 2016 MTS/IEEE monterey* (Manhattan, New York, U.S.: IEEE). doi:10.1109/OCEANS.2016.7761400

Schwarzbach, M., Laiacker, M., Mulero-Pázmány, M., and Kondak, K. (2014). "Remote water sampling using flying robots," in 2014 International Conference on Unmanned Aircraft Systems (ICUAS), Orlando, Florida, USA, 27-30 May 2014, 72–76. doi:10.1109/ICUAS.2014.6842240

Siddall, R., Ancel, A., and Kovač, M. (2017). Wind and water tunnel testing of a morphing aquatic micro air vehicle. *Interface Focus* 7, 20160085. doi:10.1098/rsfs.2016.0085

Terada, A., Morita, Y., Hashimoto, T., Mori, T., Ohba, T., Yaguchi, M., et al. (2018). Water sampling using a drone at yugama crater lake, kusatsu-shirane volcano, Japan. *Earth Planets Space* 70, 64–69. doi:10.1186/s40623-018-0835-3

Tétreault, E., Rancourt, D., and Desbiens, A. L. (2020). Active vertical takeoff of an aquatic UAV. *IEEE Robot. Autom. Lett.* 5, 1–4851. doi:10.1109/LRA.2020.3003296

Wang-Erlandsson, L., Tobian, A., van der Ent, R. J., Fetzer, I., te Wierik, S., Porkka, M., et al. (2022). A planetary boundary for green water. *Nat. Rev. Earth Environ.* 3, 380–392. doi:10.1038/s43017-022-00287-8

Xu, F.-L., Tao, S., Dawson, R. W., Li, P.-g., and Cao, J. (2001). Lake ecosystem health assessment: Indicators and methods. *Water Res.* 35, 3157–3167. doi:10.1016/s0043-1354(01)00040-9

Zeng, Z., Lyu, C., Bi, Y., Jin, Y., Lu, D., and Lian, L. (2022). Review of hybrid aerial underwater vehicle: Cross-domain mobility and transitions control. *Ocean. Eng.* 248, 110840. doi:10.1016/j.oceaneng.2022.110840

Zhang, Y., Ryan, J. P., Kieft, B., Hobson, B. W., McEwen, R. S., Godin, M. A., et al. (2019). Targeted sampling by autonomous underwater vehicles. *Front. Mar. Sci.* 415. doi:10.3389/fmars.2019.00415

Zufferey, R., Ortega, A., Farinha, A., Siddall, R., Armanini, S. F., Nasr, M., et al. (2019a). Consecutive aquatic jump-gliding with water-reactive fuel. *Sci. Robot.* 4, eaax7330. doi:10.1126/scirobotics.aax7330

Zufferey, R., Ortega, A., Raposo, C., Armanini, S. F., Farinha, A., Siddall, R., et al. (2019b). Sailmav: Design and implementation of a novel multi-modal flying sailing robot. *IEEE Robot. Autom. Lett.* 4, 2894–2901. doi:10.1109/LRA.2019.2921507

frontiers | Frontiers in Marine Science

TYPE Original Research
PUBLISHED 23 November 2022
DOI 10.3389/fmars.2022.960249

EDITED BY
Elisabetta Manea,
National Research Council (CNR), Italy

REVIEWED BY
Loubna Boutahar,
Sevilla University (Spain) and
Mohammed V University
(Morocco), Spain
Joanne Irene Ellis,
University of Waikato, New Zealand

*CORRESPONDENCE
Vasco M. N. C. S. Vieira
vasco.vieira@tecnico.ulisboa.pt

SPECIALTY SECTION
This article was submitted to
Marine Conservation and
Sustainability,
a section of the journal
Frontiers in Marine Science

RECEIVED 02 June 2022
ACCEPTED 18 October 2022
PUBLISHED 23 November 2022

CITATION
Vieira VMNCS, Lobo-Arteaga J,
Santos R, Leitão-Silva D, Veronez A,
Neves JM, Nogueira M, Creed JC,
Bertelli CM, Samper-Villarreal J and
Pettersen MRS (2022) Seagrasses
benefit from mild anthropogenic
nutrient additions.
Front. Mar. Sci. 9:960249.
doi: 10.3389/fmars.2022.960249

Seagrasses benefit from mild anthropogenic nutrient additions

Vasco M. N. C. S. Vieira[1]*, Jorge Lobo-Arteaga[2,3], Rafael Santos[2,4], David Leitão-Silva[2,4], Arthur Veronez[5,6], Joana M. Neves[2,3], Marta Nogueira[2], Joel C. Creed[7], Chiara M. Bertelli[8], Jimena Samper-Villarreal[9] and Mats R. S. Pettersen[1]

[1]Marine Environment and Technology Center, Instituto Superior Técnico, Universidade Técnica de Lisboa, Lisbon, Portugal, [2]Portuguese Institute for Sea and Atmosphere, Algés, Portugal, [3]Marine and Environmental Sciences Centre, Universidade Nova de Lisboa, Caparica, Portugal, [4]Barreiro School of Technology, Polytechnic Institute of Setubal, Lavradio, Portugal, [5]Centre for Functional Ecology, Universidade de Coimbra, Coimbra, Portugal, [6]Centro de Ciências do Mar (CCMAR) - Universidade do Algarve, Faro, Portugal, [7]Departamento de Ecologia, Universidade do Estado do Rio de Janeiro, Rio de Janeiro, Brazil, [8]Department of Biosciences, Swansea University, Swansea, United Kingdom, [9]Centro de Investigación en Ciencias del Mar y Limnología (CIMAR), Universidad de Costa Rica, San José, Costa Rica

Seagrasses are declining globally, in large part due to increased anthropogenic coastal nutrient loads that enhance smothering by macroalgae, attenuate light, and are toxic when in excessive concentrations of inorganic nitrogen and phosphorus. However, as sanitation is improved many seagrass meadows have been observed to recover, with a few studies suggesting that they may even benefit from mild anthropogenic nutrient additions. Monitoring seagrass demography and health has faced difficulties in establishing the adequate variables and metrics. Such uncertainty in the methods has caused uncertainty of the significance of results presented and compromised extrapolations to other seasons, areas, or species. One solution has come from within the plant self-thinning theories. During the 1980s, an interspecific boundary line (IBL) was determined as the upper limit of the combination of plant density and above-ground biomass for any stand on Earth, setting their maximum possible efficiency in space occupation. Recently, two meta-analyses to determine specific IBLs for algae and for seagrasses have been performed. The recently updated seagrass dataset comprises 5,052 observations from 78 studies on 18 species. These IBLs opened new perspectives for monitoring: the observed distance of a stand to the respective IBL (i.e., each stand's relative efficiency of space occupation) was demonstrated to be a valuable indicator of a population's health. Thus, this metric can be used to determine the impact of nutrients and pollutants on algae and seagrass populations. Furthermore, because the IBLs are common to all species, they may be used to compare all species from any location worldwide. This novel approach showed that *Halodule wrightii*, *Halodule beaudettei*, *Halophila baillonii*, *Zostera marina*, and *Zostera noltei* meadows benefit from anthropogenic additions of nitrogen and phosphorus, as long as these additions are moderate. In fact, the healthier *Z. noltei* meadows in Portugal (and among the healthiest meadows worldwide) were the ones exposed to effluents from wastewater treatment plants (WWTP) and a food factory. We conclude that those effluents are providing water with enough quality and that their optimal management should coordinate the technological solutions of the WWTP with the natural potential of seagrass meadows as water purifiers and biomass producers.

KEYWORDS

seagrass, water quality, indicator, coastal, eutrophication, monitoring, mitigation, valuation

Introduction

Seagrass meadows are one of the most common marine coastal biotopes, representing hotspots for biodiversity and productivity (Morrison et al., 2014; Hyman et al., 2019; McHenry et al., 2021; Surugiu et al., 2021). Seagrasses are keystone species in these biotopes, providing many services to both ecosystems and human populations. The most common are nursery and shelter for fish, bivalves, arthropods, and marine invertebrates—some of them commercially exploited—food, and water purification (Morrison et al., 2014; Nordlund et al., 2016). Recently, seagrass meadows have been revealed as an important carbon sink (Bedulli et al., 2020; Ricart et al., 2020) as well as a sustainable source of renewable raw material and energy for construction and industry (Ntalos and Sideras, 2014; Plis et al., 2016; Hamdaoui et al., 2018; Jedidi and Abrough, 2020; Rammou et al., 2021), and soilless agriculture (Parente et al., 2014).

Seagrasses have declined globally during the 20th century due to increased anthropogenic impacts, especially those affecting water quality. The most common negative impact is increased nutrient load to coastal systems originating from agricultural runoff and urban effluents. In many cases, this has led to eutrophication, resulting in smothering by drift or epiphytic macroalgae, light attenuation due to increased phytoplankton and turbidity, and the toxic effects of excessive concentrations of inorganic nitrogen (N) and phosphorus (P) (Burkholder et al., 2007; Lee et al., 2007). Other negative impacts include clam harvesting (Cabaço et al., 2005; Garmendia et al., 2017), herbicides (McMahon et al., 2005; Waycott et al., 2005; Negri et al., 2015; Espel et al., 2019), pesticides (Bester, 2000; Waycott et al., 2005; Espel et al., 2019), and industrial contamination (Waycott et al., 2005; Fraser and Kendrick, 2017; Espel et al., 2019; Lafratta et al., 2019). However, evidence is accumulating on the recovery of some seagrass beds worldwide (Greening et al., 2014; Bertelli et al., 2018; Burdick et al., 2020; Orth et al., 2020). This trend is particularly true for European seagrasses, for which a reversal was determined from the 2000s onward (de los Santos et al., 2019). This improvement was likely associated with the significant European-wide efforts that took place through the latter decades to improve sanitation and protect coastal habitats. A few studies have suggested that seagrass stands may even benefit from mild anthropogenic nutrient additions (Cabaço et al., 2013; Vieira et al., 2018).

Inference about the demography and health of seagrass stands is complex as we face difficulties in finding adequate variables, metrics, and models. Often, studies have been performed exclusively on a single species, comprising only a narrow band of its geographical distribution, and sometimes over only part of the seasonal cycle (Cabaço et al., 2007, 2008; Romero et al., 2007; García-Marín et al., 2013; Jones and Unsworth, 2016; Jones et al., 2018). This has brought great uncertainty on the significance of the results presented and compromised extrapolations to other seasons, geographical areas, or species. Broader studies still face problems with numerical methods. Examples of this are the debate between Cabaço et al. (2013) and Vieira et al. (2015), or inadequate analyses such as flawed PCA applications lacking criteria to screen the meaningful principal components and the variables significantly contributing to each of these components. Concomitantly, the efficiency of space occupation and its related phalanx and guerrilla clonal growth forms were used as indicators of the health of seagrass meadows (Sintes et al., 2005) as well as of meadows of other clonal plants in wetlands and their response to environmental stressors (Chen et al., 2011, 2014, 2017; Geremew et al., 2018). Healthier meadows adopt the phalanx strategy by simultaneously growing new shoots and increasing their biomass. Weak or unhealthy stands adopt the guerilla strategy by simultaneously losing shoots and decreasing their biomass. One aspect that has been at the core of monitoring of seagrass systems has been the widespread use of seagrass population parameters as indicators of health. Following on from that has been the attempt to establish a biomass–density relationship for seagrasses and place it on the core of the metrics and models inferring the health of seagrass stands (Cabaço et al., 2007, 2008, 2013; Romero et al., 2007;

García-Marín et al., 2013; Jones and Unsworth, 2016, 2019; Jones et al., 2018; Vieira et al., 2018).

Biomass–density relationships started to be investigated in the plant kingdom from the 1960s onward (Yoda et al., 1963; White and Harper, 1970). Some patterns emerged about how biomass and density interact through intraspecific competition and plant growth which led to some generalizations. The most outstanding aspects were the "Law of Constant Final Yield" and the theory related to self-thinning, the concurrent increase in biomass with reduction in density due to mortality through intraspecific competition. The dynamic self-thinning trajectory of plant stands, also known as the "-3/2 power law" (Hutchings, 1979; Weller, 1989), was at the time considered the only theory in ecology worthy of being named a "law" (Harper quotea in Hutchings, 1983). Alongside this, an interspecific boundary line (IBL) was determined as the upper limit for any plant stand on Earth, thus setting the maximum for efficient packing of biomass in space in plant stands (Weller, 1989; Scrosati, 2000). Recently, revised IBLs have been determined for algae (Creed et al., 2019) and for seagrasses (Vieira et al., 2018, 2019). Both the self-thinning theory and IBL determination rely on the stand biomass (B) *vs.* density (D) plotted on log scales, i.e., $\log_{10}B=a+b\times\log_{10}D$. In the case of seagrasses, "density" refers to $\text{shoots}\cdot\text{m}^{-2}$ and its original IBL had constants a = 4.569 and b = -0.438 (Vieira et al., 2018). The determination of IBL specific of algae and of seagrasses allowed updated analytical tools offering new perspectives in the research and monitoring of these taxa as well as their communities and ecosystems. Given that the IBL sets the maximum space occupation efficiency, each stand's distance to the IBL has been used as a robust indicator of how good/healthy (small distance) or how bad/impacted (large distance) the stand is. Following this rationale, the distance to the IBL has been shown as a valuable tool to access the effects of nutrients, pollutants, seasonality, light, temperature, and depth in algae (Creed et al., 2019) and seagrass (Vieira et al., 2018; Creed et al., 2019). Furthermore, because the seagrass IBL is common to all seagrass species, using the distance to the IBL (d_{grass}) allows different seagrass species to be analyzed together.

Here, we use the d_{grass} metric as an indicator in order to examine the health of seagrass stands subject to varying concentrations of nitrogen and phosphorus as a consequence of anthropogenic additions to natural background levels. We reanalyze data from previous publications of *Zostera noltei* Hornemann, 1832, *Zostera marina* Linnaeus, 1753, *Halodule wrightii* Asch., *Halodule beaudettei* Hartog, *Halophila baillonii* Ascherson, 1874, and *Cymodocea nodosa* (Ucria) Asch and analyze our own new data from *Z. noltei* meadows in the Tagus and Sado estuaries, Portugal.

Methods

This study includes results of monitoring of *Z. noltei* in Portugal, *Z. noltei* and *C. nodosa* in Italy, *Z. marina* in the British Isles, *H. wrightii* in Brazil, and *H. beaudettei* and *H. baillonii* in Costa Rica. The monitoring of *Z. noltei* in the Tagus and Sado estuaries, Portugal, was an unpublished experiment performed during the summer of 2021. Therefore, below we present the methods in detail. The remaining studies with *Z. noltei*, *Z. marina*, *H. wrightii*, *H. beaudettei*, and *H. baillonii* have already been published. Therefore, we present only the fundamental aspects of those studies. Further details about their field sampling and laboratory procedures are provided in their respective publications.

Z. noltei was monitored in the Tagus and Sado estuaries, Portugal (Figure 1A), during the summer of 2021. Sampling took place during July because that is when meadows peak their biomass, density, efficiency of space occupation, and health (Vieira et al., 2018). The rivers Tagus and Sado have meso-tidal estuaries, with a mean tidal amplitude of 2.4 m. Detailed characterizations are available of the geography and hydrodynamics of the Tagus (Dias et al., 2013) and Sado (Biguino et al., 2021) estuaries. Roughly 3 million people live in the region, mainly around the Tagus estuary, where the Portuguese capital, Lisbon, is located. Natural sources of nutrients to these systems are riverine discharge and tidal transport of nutrients upwelled in the coastal ocean during the summer upwelling season. The main anthropogenic sources of nutrients are urban effluents and agriculture, the latter being most intense in livestock and rice fields. The Tagus monitoring included nine stations (Figure 1B). Stations "T.Al1" and "T.Al2" were inside the Tagus Estuary Natural Reserve and thus expected to be the most pristine sites. Station "T.Al3" was along the Alcochete city margin. Stations "T.Sam1," "T.Sam2," and "T.Sam3" were next to the Samouco locality. Station "T.Sex" was located at the Seixalinho wastewater treatment plant (WWTP) runoff. Station "T.Rib1" was located at the Ribeiralves fish factory runoff, and "T.Rib2" was approximately 300 m away. All stations were located at mid intertidal heights. The Sado monitoring included six stations (Figure 1C). Station "S.ST" was along the main channel, closest to the estuary inlet and next to the "Sol Troia" resort. It was the only station located at the lower intertidal limit, only emersed during spring tides. In the Sado estuary, stations "S.Com1," "S.Com2," and "S.Com3" were located along the Comporta channel whereas stations "S.Cr1" and "S.Cr2" were located in the main channel next to the Carrasqueira village. All these stations were located at mid intertidal heights. The area next to the Comporta and Carrasqueira villages, and landward for tens of km along the main channel is intensively occupied by rice fields. In each location, three cores (11 cm diameter, 20 cm length) were taken from the center of the seagrass patch. Hence, the three distinct d_{grass} observations corresponded to the three cores taken at each location. While immersed, each location was sampled for water properties (temperature, N, P, and Si) three times: soon after immersion, during peak high tide, and soon before emersion. The data from these three time instances were averaged, hence the nutrient concentrations common to all three data points from each location. In the laboratory, the seagrasses were cleaned from sediment and measured for counts of shoots and nodes. Above-ground and below-ground biomasses were separated, dried in the

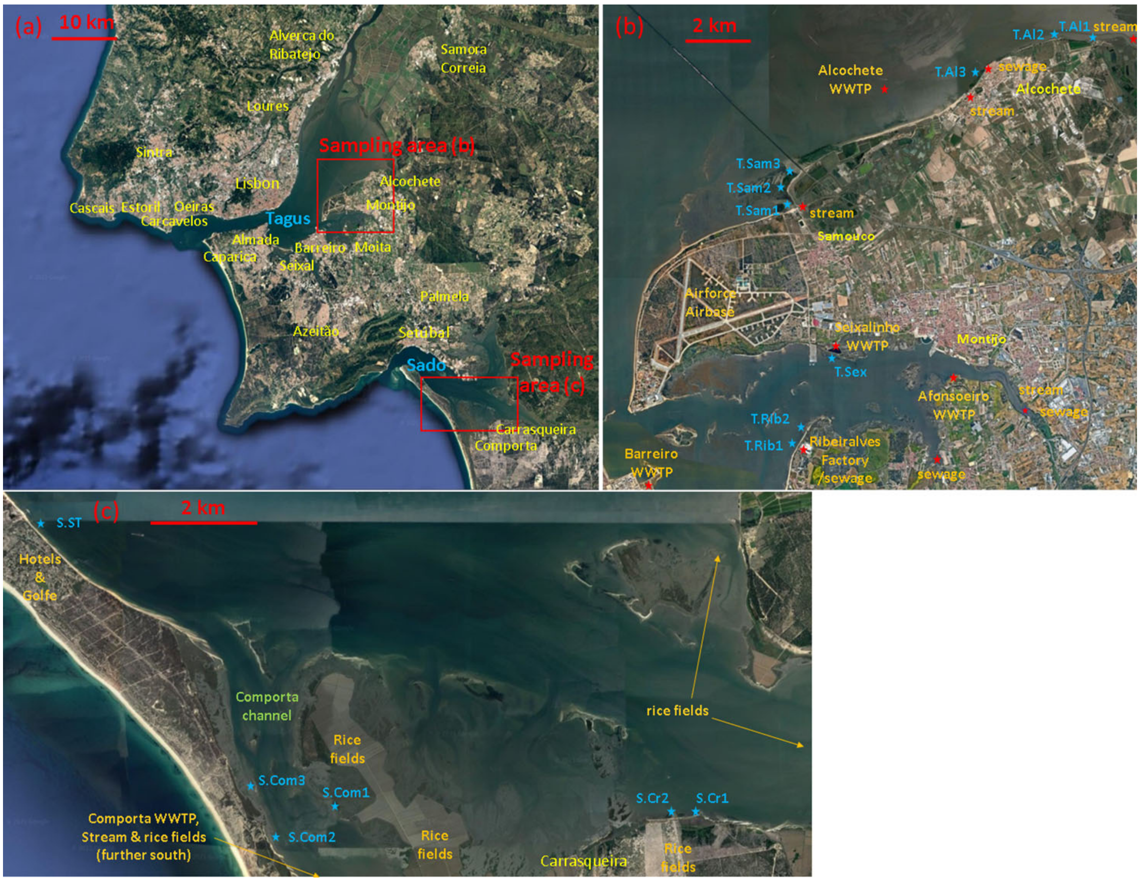

FIGURE 1
Region of study with the Tagus and Sado estuaries, urban areas, locations of sampling sites, and anthropogenic sources of nutrient enrichment. Aerial photos obtained from Google Maps. **(A)** Lisbon and Setubal metropolitan areas with Tagus and Sado estuaries, **(B)** sampling locations in the Tagus estuary, and **(C)** sampling locations in the Sado estuary.

oven for 48 h at 60°C, and weighed. Samples for nutrients in the water column were filtered through a 0.45-µm membrane (Whatman cellulose acetate) to 25-ml plastic bottles and frozen until analysis in the laboratory. Ammonium and phosphates were analyzed by colorimetry in a Skalar autoanalyzer SAN+ (Hansen and Koroleff, 1999).

Z. noltei was monitored in Ria Formosa, south Portugal, during 2001 and 2002, along a distance gradient from Montenegro's WWTP (Cabaço et al., 2008). One census per season was performed in the stations S1, S2, S3, and S4, located 270, 520, 610, and 1,500 m away from WWTP, respectively. Monitoring included the above- and below-ground biomass, shoot density, and morphometrics of *Z. noltei*, as well as concentrations of ammonium and phosphates.

Z. marina was monitored at 11 locations along the British Isles (Jones and Unsworth, 2016; Jones et al., 2018). The monitoring during the summer season (May to August 2013) certified that the meadows were sampled during the seasonal peak of biomass, density, efficiency of space occupation, and health (Vieira et al., 2018). Monitoring included the above- and below-ground biomass and shoot density of *Z. marina*, as well as above-ground $\delta^{15}N$ isotopic ratios. The seagrass biomass and density, presented by (Jones and Unsworth, 2016; Jones et al., 2018), were relative to quadrat area (0.25 m^2). In this work, as well as in previous ones, we present the data standardized to unit area (1 m^2).

C. nodosa and *Z. noltei* were monitored in an intermixed meadow at 5-m depth in a protected embayment adjacent to the Aragonese Castle on the island of Ischia in the Gulf of Naples, Italy (Kraemer and Mazella, 1999). Monitorization took place from October 1994 to October 1995. Three quadrats were sampled each month. Ammonium concentrations were measured in the water and in the sediment.

H. wrightii was monitored along southeast Brazil (Bertelli et al., 2020). The ecological and environmental characteristics were quantified in April 2017 in 10 seagrass meadows along the coast of Rio de Janeiro and São Paulo states, Brazil. At each site, single transect lines (50 -10 m depending on the size of the meadow) running parallel to the shore were placed through the middle of the seagrass meadow and along the outer (deep) edge of the meadow. Monitoring included above- and below-ground biomass and shoot density of *H. wrightii*, as well as above-ground concentrations of N and of the $\delta^{15}N$ isotopic ratios.

H. beaudettei and *H. baillonii* were monitored along the Pacific coast of Costa Rica at Potrero during February 2016 (Samper-Villarreal et al., 2018), at Playa Refugio Animal, Playa Colibrí, Golfito, and Puerto Jiménez during May 2016 (Samper-Villarreal and Cortés, 2020); at Potrero, Jobo, and Matapalito during August 2017, December 2017, and May 2018 (Samper-Villarreal et al., 2020); and at Sámara Bay during August 2018 and March 2019 (Samper-Villarreal et al., 2022). Measured seagrass variables included, among others, above- and below-ground biomass, shoot density, and above- and below-ground concentrations of N as well as $\delta^{15}N$ isotopic ratios.

Seagrasses couple their growth in biomass and density (Figure 2, Supplementary Material Figure S1, Cabaço et al., 2013, 2019; Vieira et al., 2018), thus allowing the use of the distance to the seagrass IBL (d_{grass}) as a proxy for their health (Vieira et al., 2018). Adopting the phalanx strategy, healthier meadows approach the IBL (and d_{grass} approaches zero) by simultaneously growing new shoots and increasing their biomass. Adopting the guerilla strategy, weak or unhealthy stands depart the IBL (and d_{grass} departs from zero) by simultaneously losing shoots and decreasing their biomass. The $d_{grass} = (\log_{10}\dot{B} - \log_{10}B)\cdot\cos\theta$. Here, $\dot{B}$ is the theoretical maximum biomass given an observed density. It is estimated from the IBL as $\log_{10}\dot{B} = a + b\cdot\log_{10}D$. Coefficients are $a = 4.708$, $b = -0.489$, $\theta = \mathrm{arctg}(|b|)=0.455$, and thus, $\cos\theta = 0.898$. The seagrass data compiled to estimate this IBL were here updated with 26 more studies providing 1,221 more observations. The current full data set, with 5,052 observations from 78 studies on 18 seagrass species, confirmed the seagrass clonal growth form (Figures 2, S1) but led to a re-estimation of the seagrass IBL with slightly different coefficients.

The d_{grass} indicator was compared with the concentrations of ammonium, phosphate, and the $\delta^{15}N$ isotope. In the studies by (Jones and Unsworth, 2016; Jones et al., 2018), Bertelli et al. (2020); Samper-Villarreal and Cortés (2020), and Samper-Villarreal et al.

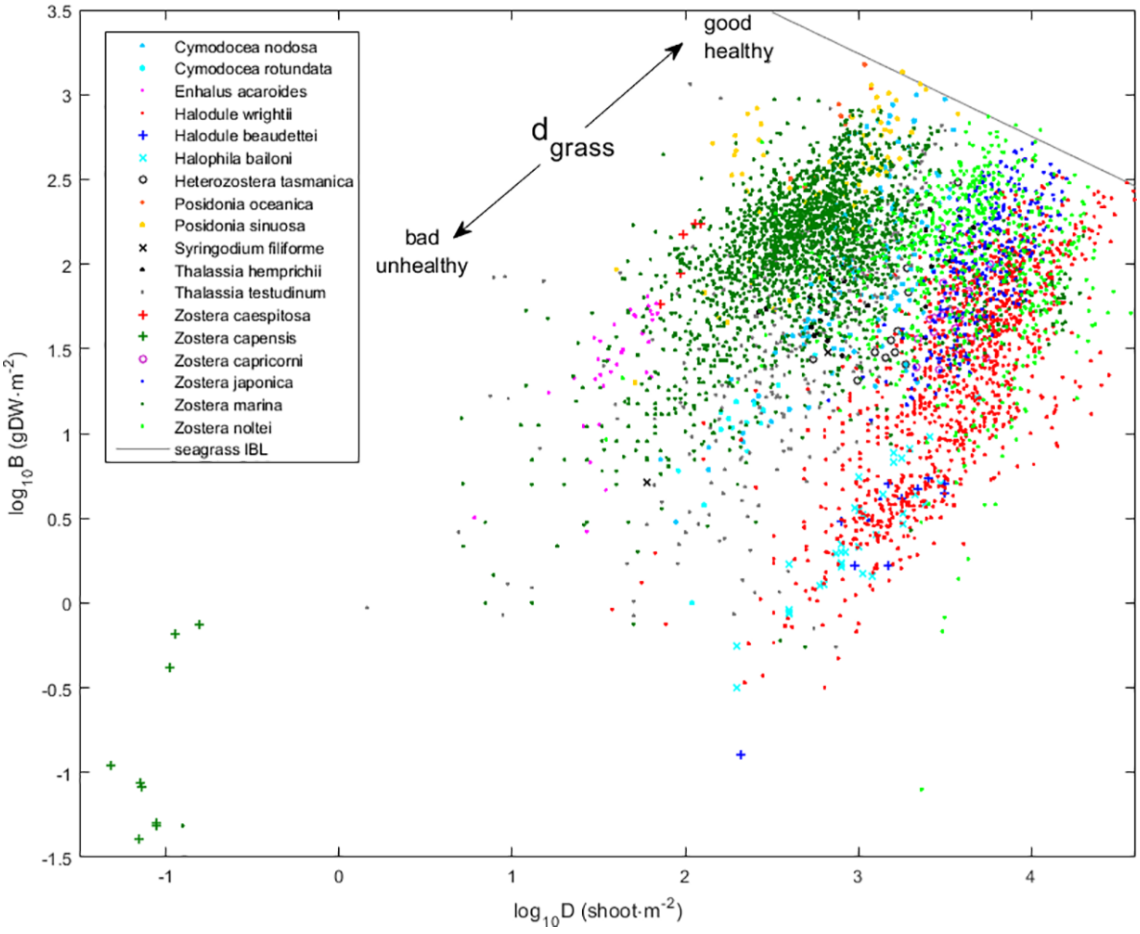

FIGURE 2
The meta-analysis on the biomass–density relations of 18 seagrass species and the derived seagrass IBL. B, biomass in grams of dry weight (g DW) per square meter; D, density of shoots per square meter.

(2018, 2020, 2022), the proportion of the $\delta^{15}N$ isotope to the total N in the leaf content was considered to be an indicator of the N provenience: lower proportions (below 4 ppt) usually correspond to N coming from natural sources, whereas higher proportions (above 4 ppt) usually correspond to N coming from anthropogenic sources, namely, urban sewage and livestock effluents (following Macko and Ostrom, 1994; McClelland et al., 1997; McClelland and Valiela, 1998; Kjønaas and Wright, 2007; Bruland and MacKenzie, 2010; Román et al, 2019).

Third-order polynomials were fit to the non-linear relations between d_{grass} (response) and nutrients (predictor). Distinct fitting methods were applied, namely, ordinary least squares (OLS), weighted least squares (WLS), iterative reweighted least squares (IRLS), linear-in-the-parameters oblique least squares (LOLS), and maximum likelihood estimation (MLE). A detailed presentation of these methods and their comparison is presented by Vieira et al. (2016). Their application was done using the Matlab software developed by Vieira et al. (2016). The best fits should be those presenting the highest R^2 and the lowest root mean square deviation (RMSD, also known as root mean square error: RMSE). However, the data distribution was strongly biased (assymetrical), with many more observations on the side of lower nutrient concentrations. Consequently, the highest R^2 and the lowest RMSD optimized the fit on the side of lower nutrient concentrations but at the cost of poor fits on the side of higher nutrient concentrations. This problem was overcome by attributing relative weights to the data on each side and applying an MLE using the Newton–Raphson method (Vieira et al., 2016).

Results

The *Z. noltei* meadows monitored in south and central Portugal, namely, in Ria Formosa and in the Tagus and Sado estuaries, had smaller d_{grass} (indicative of healthier meadows) under moderate nutrient concentrations in the water (Figures 3A, B). The healthier Ria Formosa meadow was S2 located 510 m away from the WWTP (Figure 3C). The only

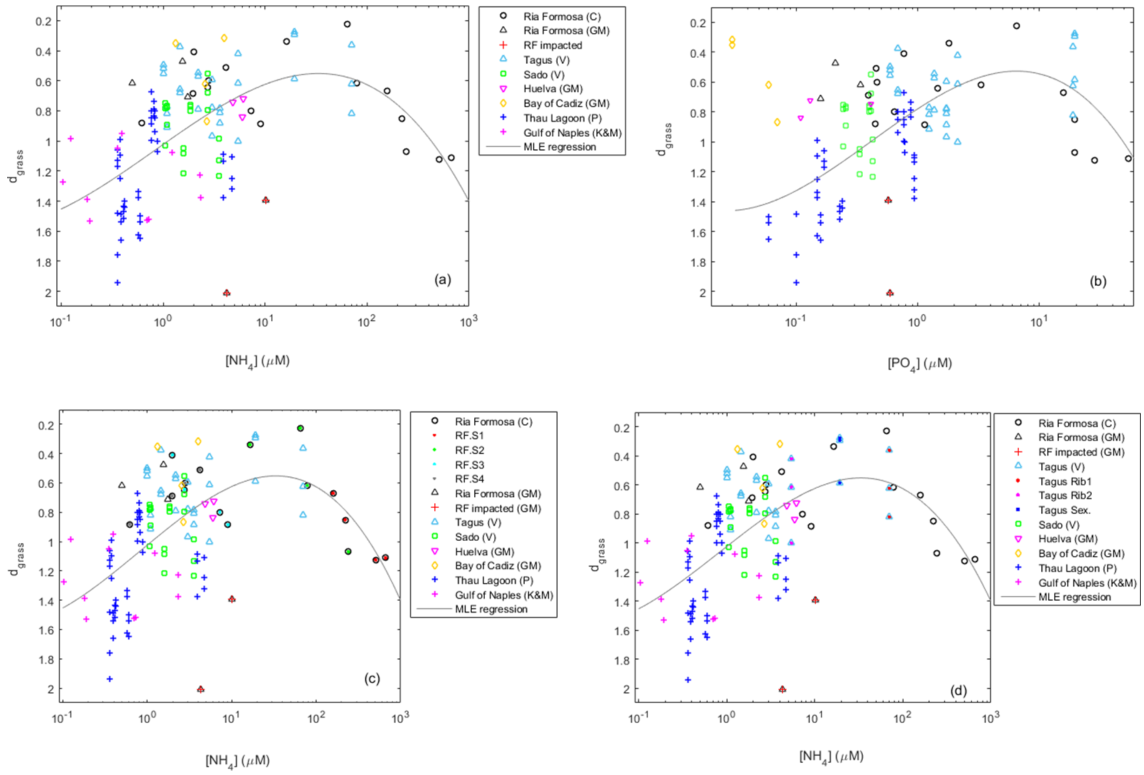

FIGURE 3
Health of *Zostera noltei* meadows in Portugal, namely, in the Ria Formosa lagoon system and the Tagus and Sado estuaries, and its dependency on ammonium **(A, C, D)** and phosphate **(B)** concentrations in the water. *Z. noltei* meadows in Portugal are compared with other *Z. noltei* meadows from elsewhere. Original data comes from this study (V), Kraemer and Mazella (1999) (K&M), Plus et al. (2001) (P), Cabaço et al. (2008) (C), and García-Marín et al. (2013) (GM). The *Z. noltei* health is indicated by its efficiency of space occupation, in its turn indicated by its distance (d_{grass}) to the seagrass IBL. Panel **(C)** highlights the Ria Formosa (RF) case, with stations S1, S2, S3, and S4 sorted in increased distance from Montenegro's WWTP. Panel **(D)** highlights the Tagus case. The Seixalinho station (Sex) is immediately outside Seixalinho WWTP, whereas Ribeiralves stations are immediately outside (Rib1) and 300 m away (Rib2) from Ribeiralves fish factory effluent. Trends fit by maximum likelihood estimation (MLE).

time S2 was in a poor condition was during winter under a peak of excess ammonium. In the Tagus estuary, the healthier meadows were located exactly next to the Seixalinho WWTP and the Ribeiralves factory effluent (Figure 3D), where the ammonium concentrations were similar to those observed for the Ria Formosa meadows S2 and S3 located at intermediate distances from the Montenegro WWTP (Figures 3C, D). Under lower nutrient loads, the d_{grass} of *Z. noltei* meadows increased (i.e., departed the IBL), suggesting that they were under nutrient deprivation. These lower loads occurred in the Ria Formosa and Tagus meadows furthest away from the WWTPs, and in the Sado meadows, which were all far from WWTP (Figures 3C, D). Furthermore, the Sado meadows were even less healthy than the Tagus and Ria Formosa meadows under equivalently low ammonium loads (Figure 3A), suggesting that the lack of phosphate worsened its condition (Figure 3B). Under the highest nutrient loads, *Z. noltei* meadows also increased d_{grass} (i.e., departed the IBL), suggesting that they were suffering from toxicity (Figures 3A, B). This happened in the Ria Formosa S1 meadow located closer to the Montenegro WWTP. Comparison with *Z. noltei* meadows from other locations and reported in other studies shows that the meadows from Ria Formosa and the Tagus estuary under moderate anthropogenic nutrient additions were among the healthier ever reported (Figure 3).

The *C. nodosa* and *Z. noltei* meadows monitored in the Bay of Naples, Italy, had smaller d_{grass} (indicative of healthier meadows) under intermediate nutrient concentrations in the water and in the sediment (Figure 4). It is noteworthy that both species exhibited very similar responses.

In order to have a global perspective, we plotted all data showing how the health of seagrass meadows may depend on the concentrations of ammonium or phosphate, in the water or in the sediment (Figure 5). Overall, seagrasses improved their efficiency of space occupation (and thus, their health) as nutrient concentrations increased, with the healthier meadows occurring under moderate nutrient concentrations. Only under the most extreme nutrient concentrations observed in this dataset were the seagrass meadows less healthy. From all these cases, the healthier meadows, occupying almost all the space available (i.e., d_{grass} close to zero), were located in coastal systems subject to anthropogenic pressure, as were the cases of *Z. noltei* in Ria Formosa (from Cabaço et al., 2008), in the Tagus estuary (from this study), and in the Bay of Cadiz (from García-Marín et al., 2013), and of *Z. japonica* in Dadae Bay (from Lee et al., 2006), in Koje Bay (from Kim et al., 2018), and in Willapa Bay (from Ruesink et al., 2009). It was also the case of *T. testudinum* in Laguna Madre and in Corpus Christy Bay, for both the control and the ammonium-enriched meadows (from Lee and Dunton, 2000).

The *Z. marina* meadows in the British Isles showing smaller d_{grass} (thus in better health) were in Priory Bay, Isle of Wight, Mannin Bay, Ireland, and Kircubbin Bay, Northern Ireland (Figure 6). With $\delta^{15}N$ within 5 to 11 ppt, these meadows were clearly under anthropogenic nutrient input. They were particularly better than the meadow sampled in the pristine Isles of Sicily (with $\delta^{15}N \leq 5$ ppt), or the heavily impacted meadows sampled in Studland Bay (with $\delta^{15}N$ within 11 to 13 ppt) or in Southend-On-Sea (with $\delta^{15}N > 15$ ppt). Nevertheless, there were also meadows showing $\delta^{15}N$ signals suggesting moderate-to-large anthropogenic sources of N (5 ppt< $\delta^{15}N$

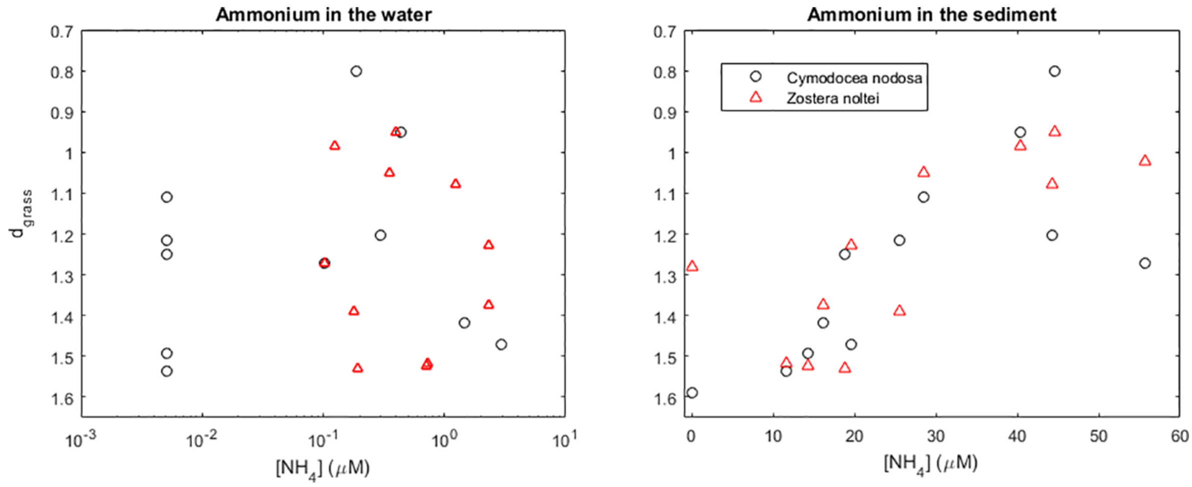

FIGURE 4
Health of *Cymodocea nodosa* and *Zostera noltei* meadows in the Bay of Naples, Italy, and their relation with the ammonium concentration in the water and sediment. Seagrass health is indicated by their distance (d_{grass}) to the seagrass IBL (i.e., their efficiency of space occupation). In some locations, samples were taken from both the middle (Middle) and the edge (Edge) of the meadow. Trends fit by maximum likelihood estimation (MLE).

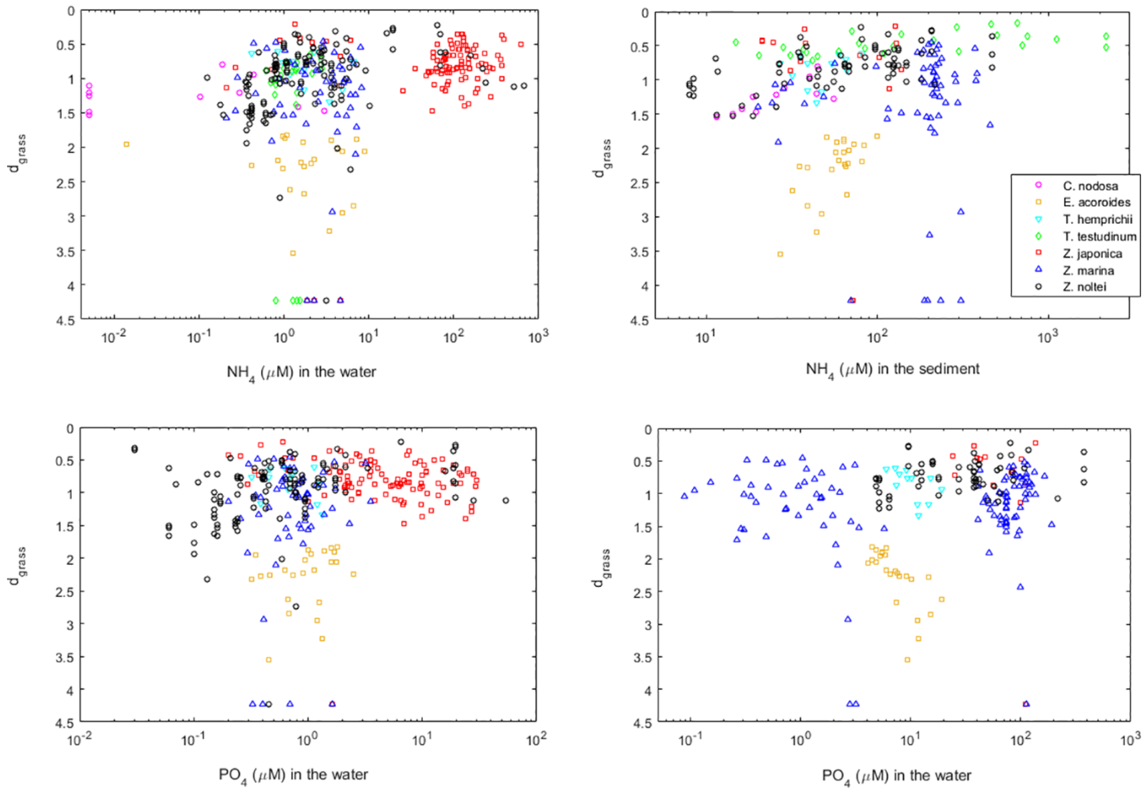

FIGURE 5
Health of seagrasses worldwide and their relation with the concentrations of ammonium and phosphate in the water and in the sediments. Seagrass health is indicated by their distance (d_{grass}) to the seagrass IBL (i.e., their efficiency of space occupation).

<10 ppt) for which the d_{grass} was large, thus indicating unhealthy stands. Therefore, there was something else in addition to the source of N that severely affected the health of *Z. marina* meadows in the British Isles.

The *H. wrightii* in Brazil, as well as the *H. beaudettei* and *H. baillonii* in Costa Rica, benefited from moderate nutrient enrichment (Figure 6). The meadows showing smaller d_{grass} were those with a $\delta^{15}N$ proportion within 4 to 6 ppt, indicating moderate anthropogenic N enrichment. For the *H. wrightii* in Brazil, these meadows were in Ossos, Manguinhos, dos Anjos, and Pedro. The meadows showing $\delta^{15}N$ proportions either above (Catita and Praia Grande) or below (Siriuba, Ilha do Japonês, Ilha G1 - Abraão and Saco do Céu) these bounds also showed larger d_{grass}. Furthermore, the samples taken from the middle of the meadow systematically indicated better health than the samples taken from the edge. For *H. beaudettei* and *H. baillonii* in Costa Rica, within each location sampled at different time instances, the respective meadow was generally healthier (smaller d_{grass}) as the proportion of $\delta^{15}N$ in above-ground biomass increased. In order to have a global perspective, we plotted all data showing how the health of seagrass meadows may depend on anthropogenic nutrient additions as inferred from the proportion of the $\delta^{15}N$ isotope (Figure 7). Overall, seagrasses were healthier under moderate nutrient addition. For the tropical seagrasses, the optimal $\delta^{15}N$ was roughly around 5 to 6 ppt, whereas for temperate seagrasses, the optimal $\delta^{15}N$ was slightly higher, around 8 ppt.

Discussion

The monitoring of *Z. noltei* in Portugal showed that the nutrient concentrations immediately next to a WWTP and a food factory in the heavily populated Tagus estuary (outside the Natural Reserve) during the summer of 2021 were only as moderate as the nutrient concentrations 500 and 600 m away from a WWTP inside the Ria Formosa Natural Reserve during 2001 and 2002. Under these moderate nutrient concentrations were found the healthier *Z. noltei* meadows ever reported (considering their efficiency of space occupation). The main determinant of their health seems to have been the concentration of ammonium in the water. Concentrations too high were toxic for *Z. noltei* whereas concentrations too low were limiting for their growth. Nevertheless, under similarly

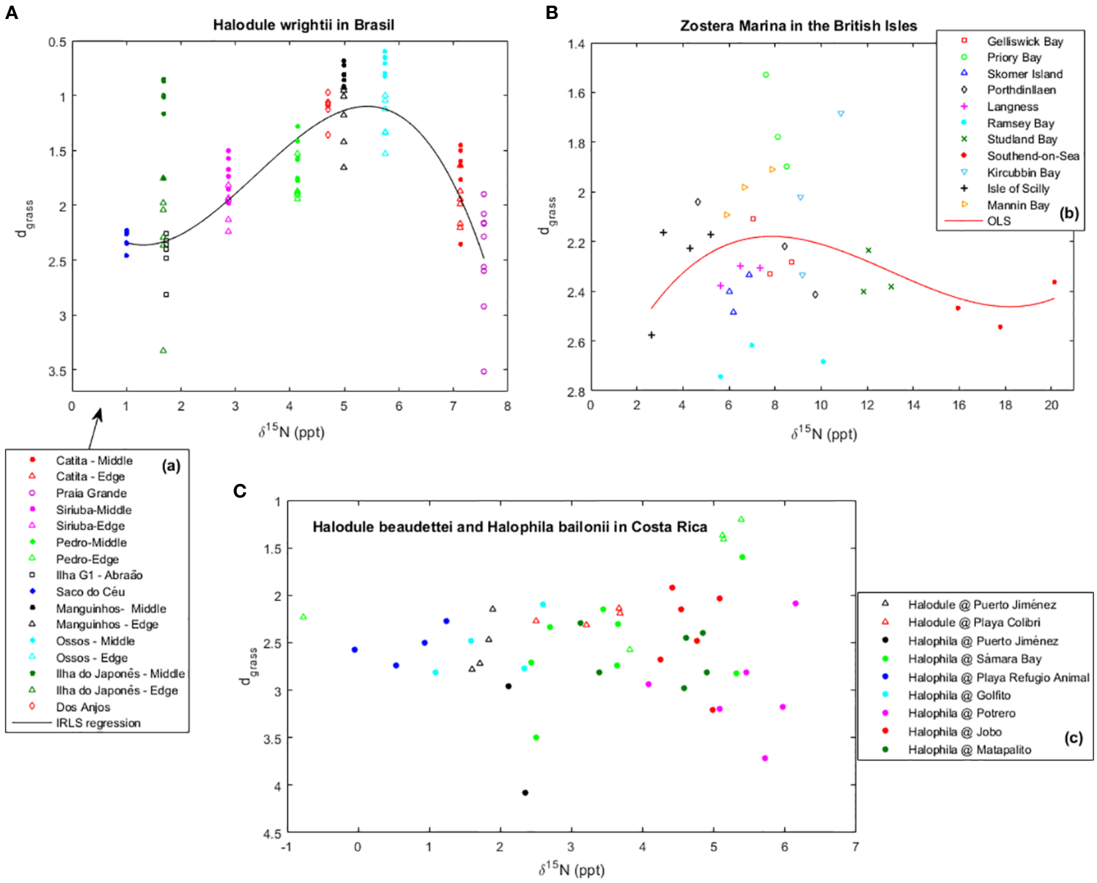

FIGURE 6
Health of **(A)** Halodule wrightii meadows in Brazil, **(B)** Zostera marina meadows in the British Isles, and **(C)** Halodule beaudettei and Halophila baillonii meadows in Costa Rica and their relation with the proportion of the δ^{15}N isotope to total N in seagrass leaf content. Seagrass health is indicated by their distance (d_{grass}) to the seagrass IBL (i.e., their efficiency of space occupation). In some locations, samples were taken from both the middle (Middle) and the edge (Edge) of the meadow. Trends fit by maximum likelihood estimation (MLE).

low ammonium concentrations, the Sado meadows were seemingly less healthy than the Tagus and Ria Formosa meadows. The reason for this may have been the significantly lower phosphate concentrations in the Sado estuary. The increased vulnerability to ammonium and the light environment under phosphate deficiency had already been reported for *Z. noltei* in the Bay of Cadiz, Spain (Brun et al., 2008). The present contrast between Sado and the other sites, particularly regarding the phosphate concentrations, may result from the distinct types of anthropogenic inputs. Rice crops are abundant both in the Sado River and in the Tagus river and its Sorraia tributary. Rice is not cultivated anywhere within the Ria Formosa basin. However, in the Sado estuary rice crops are the main source of anthropogenic inputs, with crops abounding in the estuary and right next to the sampling sites. In the Tagus estuary, urban effluents and livestock gain preponderance, with many being located right next to the sampling sites, whereas rice crops are located many kms further upstream. Rice (*Oryza* sp.) growth and production have a high demand and uptake of P, with crops generally being limited by P availability and consumption (Beyrouty et al., 1994; Akinrinde and Gaizer, 2006; Julia et al., 2016; Rajaona et al., 2017; Jiang et al., 2021). It is therefore feasible that the P concentrations observed in the Sado estuary lower than the observed in the Tagus estuary and Ria Formosa are driven by P uptake by rice crops and that this relative P deficiency drives the relatively less healthy status of the *Z. noltei* meadows in the Sado estuary. The monitoring of *Z. marina* in the British Isles, of *H. wrightii* in Brazil, and of *H. beaudettei* and *H. baillonii* in Costa Rica showed that the meadows in better conditions were found in locations subject to mild or moderate nutrient additions to the natural background. In the cases of the tropical *H. wrightii*, *H. beaudettei*, and *H. baillonii*, the optimal proportion of the δ^{15}N isotope to the total N in leaf content was roughly within

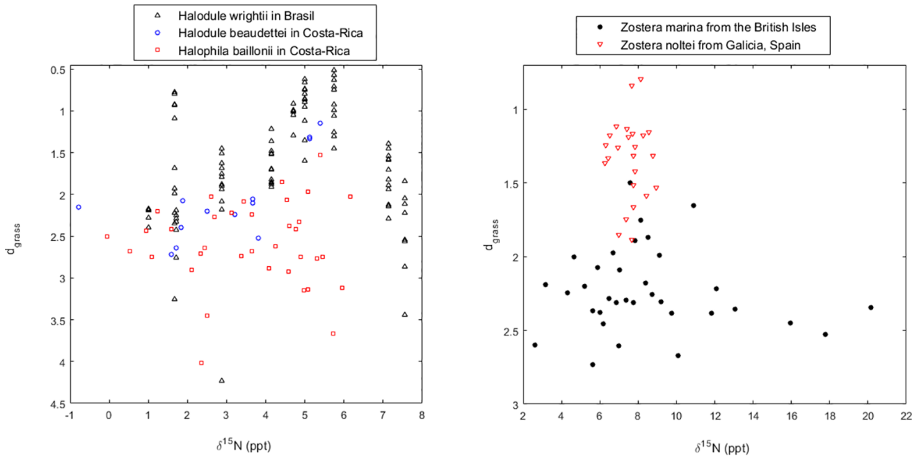

FIGURE 7
Health of seagrasses worldwide and their relation with the proportion of the δ^{15}N isotope to total N in seagrass leaf content. Seagrass health is indicated by their distance (d_{grass}) to the seagrass IBL (i.e., their efficiency of space occupation).

4 to 5 ppt. In the case of the temperate *Z. marina* and *Z. noltei*, the optimal range placed slightly higher around 8 ppt. The meadows under lower nitrogen enrichment were less healthy, presumably due to nitrogen deficiency, whereas meadows under higher nitrogen enrichment were also less healthy, presumably due to nitrogen toxicity. Overall, our results suggest that *H. wrightii* meadows in Brazil, *H. beaudettei* and *H. baillonii* in Costa Rica, *Z. noltei* meadows in Portugal, and *Z. marina* meadows in the British Isles may benefit from anthropogenic nitrogen additions, as long as these additions are moderate, and that such meadows can in fact do better than the meadows in pristine environments.

Our findings match previous studies on the physiological and demographic responses of seagrass beds to nutrient concentrations. The review by Touchette and Burkholder (2000) also determined that many seagrass species respond favorably to mild or moderate nutrient enrichment and that only when enrichment is too high do the seagrasses respond unfavorably with decreasing survival and/or growth. In this case, the negative response can be a direct physiological response to N or P toxicity or an indirect effect of eutrophication due to stimulation of algal overgrowth or smothering and associated light reduction. In the review by Waycott et al. (2005) of four seagrass species in the Great Barrier Reef, nutrients were only reported as limiting growth due to their weak supply. N or P toxicity was never found. Reported pollutants with negative impacts were only herbicides, pesticides, and other chemical contaminants. Our findings, together with the concordant previous findings reported above, contradict the former generalized negative perception that anthropogenic nutrient additions, however small these additions may be, are always harmful to seagrass beds.

A large contribution to this biased perception may have come from the lack of an adequate indicator for the health of seagrass meadows. This handicap has been solved by the distance to the seagrass IBL (d_{grass}), reflecting the efficiency of space occupation by the respective stand. The application of this new indicator to several species scattered worldwide showed that all monitored species benefit from moderate anthropogenic nutrient additions, which explains the recent recovery of seagrass meadows in populated coastlines where the improved management of wastewaters reduced but not eradicated the anthropogenic input of nutrients (Greening et al., 2014; Bertelli et al., 2018; de los Santos et al., 2019; Burdick et al., 2020; Orth et al., 2020). Furthermore, our results suggest that, in situations where WWTP are the main source of anthropogenic nutrient enrichment (i.e., agricultural runoff is reduced), modern wastewater treatment cleans the wastewater well enough to improve the health of nearby seagrass meadows, and their level of reduced nutrient inputs may even promote seagrass growth.

Seagrasses provide many ecosystem services, including CO_2 trapping, as well as shelter and food for commercially exploited species (Nordlund et al., 2016; de los Santos et al., 2020). Furthermore, the restoration of formerly deteriorated seagrass habitat leads to rapid recovery of coastal ecosystem services (Orth et al., 2020). Here, we determined that moderate anthropogenic nutrient additions have the potential to enhance these ecosystem services in seagrass meadows. Instead of trying to minimize the nutrient load in effluents from human origin as much as possible, society might better divert its focus to identifying maximal (beneficial) nutrient loads at specific sites for different species as well as improving strategies to maximize nutrient dilution when discharged to the sea, so that the threshold concentrations for inorganic nitrogen and phosphorus to become toxic are not exceeded.

In addition to the detrimental concentrations of inorganic N and P, seagrass meadows are subject to a multitude of other stressors, acting alone or in consonance. Large nutrient inputs result in eutrophication, which, in estuarine and lagoon systems, take the form of extensive algal blooms often smothering seagrass meadows (Brun et al., 2003; Burkholder et al., 2007; Pergent et al., 2008; Cognat et al., 2018), or epiphytes and phytoplankton reducing light availability (Brun et al., 2003; Plus et al., 2003). Such was the case for *Z. noltei* in the Tagus estuary, with particular incidence in Samouco, where an extensive mat of mainly *Ulva* sp. but also some *Enteromorpha* sp. and *Sargassum* sp. covered almost all of the seafloor. During the summer of 2021 monitoring, patches with *Z. noltei* were sparce, and the healthy but sparse Samouco patches still showed some algae coverage (Supplementary Figure S2). During a subsequent monitoring in the summer of 2022, patches with *Z. noltei* in Samouco were even harder to find among the many tons of green algae, but the few patches left showed some of the best efficiencies of space occupation (d_{grass}) reported in the data set of seagrasses worldwide. This sparse coverage of extremely healthy *Z. noltei* patches mingled among an extensive green algae bloom suggests that moderate anthropogenic nutrient additions may lead seagrass meadows to their best health provided that the collateral effects of eutrophication are avoided. Otherwise, the formation of extensive algal mats covering the seagrasses, epiphytes, and/or phytoplankton becomes largely detrimental to seagrass meadows (Brun et al., 2003; Plus et al., 2003; Burkholder et al., 2007; Pergent et al., 2008; Cognat et al., 2018; and present study). Also, temperature affects and interacts with other factors that determine seagrass performance. Temperature affects the photosynthetic efficiency (P–I) curve of seagrasses (Plus et al., 2005; Lee et al., 2007; Vieira et al., 2018), their nutrient uptake and metabolic rates (Plus et al., 2001, 2003; Lee et al., 2007), and the toxicity of inorganic N and P, herbicides, and trace metals (Gamain et al., 2018). In the Tagus and Sado estuaries, during the summer, water temperature was always above 24°C and in their landward sections often above 30°C, which is considered too warm for temperate seagrasses (Lee et al., 2007). However, the largest stressor to *Z. noltei* in the Tagus and Sado estuaries was by far clam harvesting. During the July 2021 monitoring, the *Z. noltei* meadows in the Ribeiralves stations were composed of a few healthy patches interspersed within the bare sediment, with the daily pressure of tens of clandestine clam harvesters plucking their shoots and breaking their roots. By August 2021, these meadows had entirely disappeared, never to reappear thus far. The same happened in many other stations and locations in the Tagus and Sado estuaries. As examples, the *Z. noltei* meadow in the original Comporta 2 station had also disappeared by July 2022. The beach front along Alcochete is abundant in clandestine recreational clam harvesters daily destroying *Z. noltei* patches spersed within the bare sediment (Supplementary Figure S3).

Data availability statement

The original contributions presented in the study are provided online at http://dx.doi.org/10.13140/RG.2.2.32343.14240.

Author contributions

VV contributed to the conceptualization, design, field sampling, model and software development, data analysis, and writing of the manuscript. RS, DL-S, JC, CB, and JS-V contributed to the field sampling. JL-A, RS, DL-S, AV, JN, MN, JC, CB, and MP contributed to the laboratorial work. JL-A, MN, JC, CB, and JS-V contributed to reviewing the manuscript. All authors contributed to the work and approved the submitted version.

Funding

This work was funded by Portuguese National Funding through FCT - Fundação para a Ciência e Tecnologia, I. P., through project LA/P/0083/2020 (LA LARSyS - MARETEC) and project LA/P/0069/2020 granted to the Associate Laboratory ARNET. The present work was supported by the Marine and Environmental Sciences Centre (MARE) which is financed by national funds from FCT/MCTES (UIDB/04292/2020) Joana M. Neves was supported by a PhD fellowship (UI/BD/150954/2021) from FCT. This work was supported by Fundação Carlos Chagas Filho de Amparo à Pesquisa do Estado do Rio de Janeiro (JCC, FAPERJ- E26/201.286/2014) and Conselho Nacional de Desenvolvimento Científico e Tecnológico (JCC, CNPq- 307117/2014–6) and Santander Bank staff mobility funding through Swansea University, UK. Studies in Costa Rica were funded by the Vicerrectoría de Investigación at the Universidad de Costa Rica. The funders took no part in the design of the study, in the collection, analysis, and interpretation of data, and in writing the manuscript.

Acknowledgments

Our acknowledgments are given to Instituto para a Conservação da Natureza e das Florestas (ICNF), Reserva Natural do Estuario do Tejo (RNET), and Reserva Natural do Estuário do Sado (RNES) for authorizing sampling *Zostera noltei* in their natural parks, and to OceanAlive.org for the support in planning the Sado field campaign. To Benjamin Jones for providing additional information.

Conflict of interest

The authors declare that the research was conducted in the absence of any commercial or financial relationships that could be construed as a potential conflict of interest.

Publisher's note

Supplementary material

The Supplementary Material for this article can be found online at: https://www.frontiersin.org/articles/10.3389/fmars.2022.960249/full#supplementary-material

References

Akinrinde, E., and Gaizer, T. (2006). Differences in the performance and phosphorus-use efficiency of some tropical rice (Oryza sativa l.) varieties. *Pak. J. Nutr.* 5 (3), 206–211. doi: 10.3923/pjn.2006.206.211

Bedulli, C., Lavery, P. S., Harvey, M., Duarte, C. M., and Serrano, O. (2020). Contribution of seagrass blue carbon toward carbon neutral policies in a touristic and environmentally-friendly island. *Front. Mar. Sci.* 7. doi: 10.3389/fmars.2020.00001

Bertelli, C. M., Creed, J. C., Nuuttila, H. K., and Unsworth, R. K. F. (2020). The response of the seagrass halodule wrightii ascherson to environmental stressors. *Est. Coast. Shelf Sci.* 238, 106693. doi: 10.1016/j.ecss.2020.106693

Bertelli, C. M., Robinson, M. T., Mendzil, A. F., Pratt, L. R., and Unsworth, R. K. F. (2018). Finding some seagrass optimism in Wales, the case of zostera noltii. *Mar. pollut. Bull.* 134, 216–222. doi: 10.1016/j.marpolbul.2017.08.018

Bester, K. (2000). Effects of pesticides on seagrass beds. *Helgol Mar. Res.* 54, 95–98. doi: 10.1007/s101520050007

Beyrouty, C. A., Grigg, B. C., Norman, R. J., and Wells, B. R. (1994). Nutrient uptake by rice in response to water management. *J. Plant Nutr.* 17 (1), 39–55. doi: 10.1080/01904169409364708

Biguino, B., Sousa, F., and Brito, A. C. (2021). Variability of currents and water column structure in a temperate estuarine system (Sado estuary, Portugal). *Water* 13 (2), 187. doi: 10.3390/w13020187

Bruland, G. L., and MacKenzie, R. A. (2010). Nitrogen source tracking with δ n content of coastal wetland plants in Hawaii. *J. Environ. Qual.* 39, 409–419. doi: 10.2134/jeq2009.0005

Brun, F., Olivé, I., Malta, E., Vergara, J., Hernández, I., and Pérez-Lloréns, J. (2008). Increased vulnerability of zostera noltii to stress caused by low light and elevated ammonium levels under phosphate deficiency. *Mar. Ecol.Prog. Ser.* 365, 67–75. doi: 10.3354/meps07512

Brun, F. G., Vergara, J. J., Navarro, G., Hernández, I., and Pérez-Lloréns, J. L. (2003). Effect of shading by ulva rigida canopies on growth and carbon balance of the seagrass zostera noltii. *Mar. Ecol. Prog. Ser.* 265, 85–96. doi: 10.3354/meps265085

Burdick, D. M., Edwardson, K. J., Gregory, T., Matso, K., Mattera, T., Paly, M., et al. (2020). A case for restoration and recovery of zostera marina l. in the great bay estuary. *PREP Rep. Publ.* 441, 1–19.

Burkholder, J. M., Tomasko, D. A., and Touchette, B. W. (2007). Seagrasses and eutrophication. *J. Exp. Mar. Biol. Ecol.* 350, 46–72. doi: 10.1016/j.jembe.2007.06.024

Cabaço, S., Alexandre, A., and Santos, R. (2005). Population-level effects of clam harvesting on the seagrass zostera noltii. *Mar. Ecol. Prog. Ser.* 298, 123–129. doi: 10.3354/meps298123

Cabaço, S., Apostolaki, E. T., Garcıa-Marín, P., Gruber, R., Hernandez, I., Martınez-Crego, B., et al. (2013). Effects of nutrient enrichment on seagrass population dynamics: evidence and synthesis from the biomass–density relationships. *J. Ecol.* 101, 1552–1562. doi: 10.1111/1365-2745.12134

Cabaço, S., Machás, R., and Santos, R. (2007). Biomass–density relationships of the seagrass zostera noltii: A tool for monitoring anthropogenic nutrient disturbance. *Estuar. Coast. Shelf. Sci.* 74, 557–564. doi: 10.1016/j.ecss.2007.05.029

Cabaço, S., Machás, R., Vieira, V., and Santos, R. (2008). Impacts of urban wastewater discharge on seagrass meadows (Zostera noltii). *Estuar. Coast. Shelf. Sci.* 78, 1–13. doi: 10.1016/j.ecss.2007.11.005

Chen, X.-S., Deng, Z.-M., Xie, Y.-H., Li, F., Hou, Z.-Y., and Li, X. (2014). Demography of carex brevicuspis (Cyperaceae) rhizome populations: A wetland sedge that produces both elongated and shortened rhizomes. *Nord. J. Bot.* 32, 251–256. doi: 10.1111/j.1756-1051.2013.00094.x

Chen, X., Liao, Y., Xie, Y., Li, F., Deng, Z., Hou, Z., et al. (2017). Concurrent effects of sediment accretion and nutrient availability on the clonal growth strategy of carex brevicuspis – a wetland sedge that produces both spreading and clumping ramets. *Front. Plant Sci.* 8. doi: 10.3389/fpls.2017.01685

Chen, X.-S., Xie, Y.-H., Deng, Z.-M., and Hou, Z.-Y. (2011). A change from phalanx to guerrilla growth form is an effective strategy to acclimate to sedimentation in a wetland sedge species carex brevicuspis (Cyperaceae). *Flora* 206 (4), 347–350. doi: 10.1016/j.flora.2010.07.006

Cognat, M., Ganthy, F., Auby, I., Barraquand, F., Rigouin, L., and Sottolichio, A. (2018). Environmental factors controlling biomass development of seagrassmeadows of zostera noltei after a drastic decline (Arcachon bay, France). *J. Sea Res.* 140, 87–104. doi: 10.1016/j.seares.2018.07.005

Creed, J., Vieira, V.M.N.C.S., Norton, T. A., and Caetano, D. (2019). A meta-analysis shows that seaweeds surpass plants, setting life-on-Earth's limit for biomass packing. *BMC Ecol.* 19 (6), 1–11. doi: 10.1186/s12898-019-0218-z

Dias, J. M., Valentim, J. M., and Sousa, M. C. (2013). A numerical study of local variations in tidal regime of tagus estuary, Portugal. *PloS One* 8 (12), e80450. doi: 10.1371/journal.pone.0080450

Espel, D., Diepens, N. J., Boutron., O., Buffan-Dubaua, E., Chéraind, Y., Coulet, E., et al. (2019). Dynamics of the seagrass zostera noltei in a shallow Mediterranean lagoon exposed to chemical contamination and other stressors. *Est. Coast. Shelf Sci.* 222, 1–12. doi: 10.1016/j.ecss.2019.03.019

Fraser, M. W., and Kendrick, G. A. (2017). Belowground stressors and long-term seagrass declines in a historically degraded seagrass ecosystem after improved water quality. *Sci. Rep.* 7 (1), 2045–2322. doi: 10.1038/s41598-017-14044-1

Gamain, P., Feurtet-Mazel, A., Maury-Brachet, R., Auby, I., Pierron, F., Belles, A., et al. (2018). Can pesticides, copper and seasonal water temperature explain the seagrass zostera noltei decline in the arcachon bay? *Mar. Poll. Bull.* 134, 66–74. doi: 10.1016/j.marpolbul.2017.10.024

García-Marín, P., Cabaço, S., Hernández, I., Vergara, J. J., Silva, J., and Santos, R. (2013) Multimetric index based on the seagrass zostera noltii (ZoNI) for ecological quality assessment of coastal and estuarine in SW Iberian peninsula. *Mar. pollut. Bull.* 68, 46–54. doi: 10.1016/j.marpolbul.2012.12.025

Garmendia, J. M., Valle, M., Borja, Á., Chust, G., Lee, D.-J., Rodríguez, J. G., et al. (2017). Effect of trampling and digging from shellfishing on zostera noltei (Zosteraceae) intertidal seagrass beds. *Sci. Mar.* 81 (1), 121–128. doi: 10.3989/scimar.04482.17A

Geremew, A., Stiers, I., Sierens, T., Kefalew, A., and Triest, L. (2018). Clonal growth strategy, diversity and structure: A spatiotemporal response to sedimentation in tropical cyperus papyrus swamps. *PloS One* 13 (1), e0190810. doi: 10.1371/journal.pone.0190810

Greening, H., Janicki, A., Sherwood, E. T., Pribble, R., and Johansson, J. O. R. (2014). Ecosystem responses to long-term nutrient management in an urban estuary: Tampa bay, Florida, USA. *Estuar. Coast. Shelf. Sci.* 151, A1–A16. doi: 10.1016/j.ecss.2014.10.003

Hamdaoui, O., Ibos, L., Mazioud, A., Safi, M., and Limam, O. (2018). Thermophysical characterization of posidonia oceanica marine fibers intended to be used as an insulation material in Mediterranean buildings. *Constr. Build. Mater.* 180, 68–76. doi: 10.1016/j.conbuildmat.2018.05.195

Hansen, H., and Koroleff, F. (1999). "Determination of nutrients," in *Methods of seawater analysis*. Eds. K. Grasshoff, K. Kremling and M. Ehrhardt (Weinheim: Wiley-VCH Verlag), 159–226.

Hutchings, M. J. (1979). Weight–density relationships in ramet populations of clonal perennial herbs, with special reference to the 3/2 power law. *J. Ecol.* 67, 21–33. doi: 10.2307/2259334

Hutchings, M. J. (1983). Ecology's law in search of a theory. *New Scientist* 98, 765–767.

Hyman, A. C., Frazer, T. K., Jacoby, C. A., Frost, J. R., and Kowalewski, M. (2019). Long-term persistence of structured habitats: seagrass meadows as enduring hotspots of biodiversity and faunal stability. *Proc. R. Soc B.* 286, 1912 doi: 10.1098/rspb.2019.1861

Jedidi, M., and Abroug, A. (2020). Valorization of posidonia oceanica balls for the manufacture of an insulating and ecological material. *Jordan J. Civ. Eng.* 14 (3), 417–430.

Jiang, B., Shen, J., Sun, M., Hu, Y., Jiang, W., Wang, J., et al. (2021). Soil phosphorus availability and rice phosphorus uptake in paddy fields under various agronomic practices. *Pedosphere* 31 (1), 103–115. doi: 10.1016/S1002-0160(20)60053-4

Jones, B. L., Cullen-Unsworth, L. C., and Unsworth, R. F. K. (2018). Tracking nitrogen source using δ15N reveals human and agricultural drivers of seagrass degradation across the British isles. *Front. Plant Sci.* 9. doi: 10.3389/fpls.2018.00133

Jones, B. L., and Unsworth, R. K. F. (2016). *The perilous state of seagrass in the British isles* Vol. 3 (London: Royal Society Open Science), 150596. doi: 10.1098/rsos.150596

Julia, C., Wissuwa, M., Kretzschmar, T., Jeong, K., and Rose, T. (2016). Phosphorus uptake, partitioning and redistribution during grain filling in rice. *Ann. Bot.* 118 (6), 1151–1162. doi: 10.1093/aob/mcw164

Kim, S.H., Kim, J.W., Kim, Y.K., and Lee, K.-S. (2018) Growth responses of the intertidal seagrass Zosterajaponica to manipulated sea level rise conditions. *Bull Mar Sci.* 94 (4), 1379–1393. doi: 10.5343/bms.2017.1139

Kjønaas, O. J., and Wright, R. F. (2007). Use of 15N-labelled nitrogen deposition to quantify the source of nitrogen in runoff at a coniferous-forested catchment at gårdsjön, Sweden. *Environ. pollut.* 147, 791–799. doi: 10.1016/j.envpol.2006.06.019

Kraemer, G. P., and Mazella, L. (1999). Nitrogen acquisition, storage, and use by the co-occurring Mediterranean seagrasses cymodocea nodosa and zostera noltii. *Mar. Ecol. Prog. Ser.* 183, 95–103. doi: 10.3354/meps183095

Lafratta, A., Serrano, O., Masqué, P., Mateo, M. A., Fernandes, M., Gaylard, S., et al. (2019). Seagrass soil archives reveal centennial-scale metal smelter contamination while acting as natural filters. *Sci. Tot. Environ.* 649, 1381–1392. doi: 10.1016/j.scitotenv.2018.08.400

Lee, K.-S., and Dunton, K. H. (2000). Effects of nitrogen enrichement on biomass allocation, growth, and leaf morphology of the seagrass thalassia testudinum. *Mar. Ecol. Prog. Ser.* 196, 39–48. doi: 10.3354/meps196039

Lee, S. Y., Kim, J. B., and Lee, S. M. (2006). Temporal dynamics of subtidal zostera marina and intertidal zostera japonica on the southern coast of Korea. *Mar. Ecol.* 27, 133–144. doi: 10.1111/j.1439-0485.2006.00089.x

Lee, K.-S., Park, S. R., and Kim, Y. K. (2007). Effects of irradiance, temperature, and nutrients on growth dynamics of seagrasses: a review. *J. Exp. Mar. Biol. Ecol.* 350, 144–175. doi: 10.1016/j.jembe.2007.06.016

Macko, S. A., and Ostrom, N. E. (1994). "Pollution studies using stable isotopes," in *Stable isotopes in ecology and environmental science*. Eds. K. Lajtha and R. H. Michener (Oxford: Blackwell Scientific Publications), 45–62.

McClelland, J. W., and Valiela, I. (1998). Linking nitrogen in estuarine producers to land-derived sources. *Limnol. Oceanogr.* 43, 577–585. doi: 10.4319/lo.1998.43.4.0577

McClelland, J. W., Valiela, I., and Michener, R. H. (1997). Nitrogen-stable isotope signatures in estuarine food webs: A record of increasing urbanization in coastal watersheds. *Limnol. Oceanogr.* 42, 930–937. doi: 10.4319/lo.1997.42.5.0930

McHenry, J., Rassweiller, A., Hernan, G., Uejio, C. K., Pau, S., Dubel, A. K., et al. (2021). Modelling the biodiversity enhancement value of seagrass beds. *Divers. Distrib.* 27 (11), 2036–2049. doi: 10.11117/ddi.13379

McMahon, K., Nash, S. B., Eaglesham, G., Müller, J. F., Duke, N. C., and Winderlich, S. (2005). Herbicide contamination and the potential impact to seagrass meadows in hervey bay, Queensland, Australia. *Mar. pollut. Bull.* 51 (1-4), 325–334. doi: 10.1016/j.marpolbul.2004.10.045

Morrison, M. A., Lowe, M. L., Grant, C., Smith, P. J., Carbines, G., Reed, J., et al. (2014). "Seagrass meadows as biodiversity and productivity hotspots," in *New Zealand aquatic environment and biodiversity report no 137*. (Wwllington, New Zealand: Ministry for Primary Industries)

Negri, A. P., Flores, F., Mercurio, P., Mueller, J. F., and Collier, C. J. (2015). Lethal and sub-lethal chronic effects of the herbicide diuron on seagrass. *Aquat. Toxicol.* 165, 73–83. doi: 10.1016/j.aquatox.2015.05.007

Nordlund, L. M., Koch, E. W., Barbier, E. B., and Creed, J. C. (2016). Seagrass ecosystem services and their variability across genera and geographical regions. *PloS One* 11 (10), e0163091. doi: 10.1371/journal.pone.0163091

Ntalos, G., and Sideras, A. (2014). The usage of posidonia oceanica as raw material for wood composite and thermal energy production. *Mater. Methods Technol.* 8, 605–611.

Orth, R. J., Lefcheck, J. S., McGlathery, K. S., Aoki, L., Luckenbach, M. W., Moore, K. A., et al. (2020). Restoration of seagrass habitat leads to rapid recovery of coastal ecosystem services. *Sci. Adv.* 6, 41. doi: 10.1126/sciadv.abc6434

Parente, A., Serio, F., Montesano, F. F., Mininni, C., and Santamaria, P. (2014). The compost of posidonia oceanica residues: A short review on a new component for soiless growing media. *Acta Hortic.* 1034, 291–298. doi: 10.17660/ActaHortic.2014.1034.36

Pergent, G., Boudouresque, C.-F., Dumay, O., Pergent-Martini, C., and Wyllie-Echeverria, S. (2008). Competition between the invasive macrophyte caulerpa taxifolia and the seagrass posidonia oceanica: Contrasting strategies. *BMC Ecol.* 8 (20), 1–13. doi: 10.1186/1472-6785-8-20

Plis, A., Lasek, J. A., Zuwała, J., Yu, C.-C., and Iluk, A. (2016). Combustion performance evaluation of posidonia oceanica using TGA and bubbling fluidized-bed combustor (batch reactor). *J. Sustain. Min.* 15 (4), 181–190. doi: 10.1016/j.jsm.2017.03.006

Plus, M., Auby, I., Verlaque, M., and Levavaseur, G. (2005). Seasonal variations in photosynthetic irradiance response curves of macrophytes from a Mediterranean lagoon. *Aquat. Bot.* 81, 157–173. doi: 10.1016/j.aquabot.2004.10.004

Plus, M., Chapelle, A., Ménesguen, A., Deslous-Paoli, J.-M., and Auby, I. (2003). Modelling seasonal dynamics of biomasses and nitrogen contents in a seagrass meadow (Zostera noltii hornem.): Application to the thau lagoon (French Mediterranean coast). *Ecol. Model.* 161, 213–238. doi: 10.1016/S0304-3800(02)00350-2

Plus, M., Deslous-Paoli, J.-M., and Dagault, F. (2001). Factors influencing primary production of seagrass beds (Zostera noltii hornem.) in the thau lagoon (French Mediterranean coast). *J. Exp. Mar. Biol. Ecol.* 259, 63–84. doi: 10.1016/S0022-0981(01)00223-4

Rajaona, A., Rakotoson, T., Wright, H., Ramarolahy, J., Senthilkumar, K., Saito, K., et al. (2017). "Responses of grain yield and p uptake to water management and phosphorus in lowland irrigated rice (Oryza sativa l.)," in *Future agriculture: Social-ecological transitions and bio-cultural shifts* (Germany: Tropentag), 20–22.

Rammou, E., Mitani, A., Ntalos, G., Koutsianitis, D., Taghiyari, H. R., and Papadopoulos, A. N. (2021). The potential use of seaweed (Posidonia oceanica) as an lternative lignocellulosic raw material for wood composites manufacture. *Coatings* 11 (1), 2079–6412. doi: 10.3390/coatings11010069

Ricart, A. M., York, P. H., Bryant, C. V., Rasheed, M. A., Ierodiaconou, D., and Macreadie, P. I. (2020). High variability of blue carbon storage in seagrass meadows at the estuary scale. *Sci. Rep.* 10 (1), 5865. doi: 10.1038/s41598-020-62639-y

Román, M., Emilio, F., Zamborain-Mason, J., and Martínez, G. (2019). Anthropogenic impact on zostera noltei seagrass meadows (NW Iberian peninsula) assessed by carbon and nitrogen stable isotopic signatures. *Estuaries Coast.* 42, 987–1000. doi: 10.1007/s12237-019-00549-7

Romero, J., Martínez-Crego, B., Alcoverro, T., and Pérez, M. (2007). A multivariate index based on the seagrass posidonia oceanica (POMI) to assess ecological status of coastal waters under the water framework directive (WFD). *Mar. pollut. Bull.* 55, 196–204. doi: 10.1016/j.marpolbul.2006.08.032

Ruesink, J. L., Hong, J.-S., Wisehart, L., Hacker, S. D., Dumbauld, B. R., Hessing-Lewis, M., et al. (2009). Congener comparison of native (Zostera marina) and introduced (Z. japonica) eelgrass at multiple scales within a pacific Northwest estuary. *Biol. Invasions.* 12, 1773–1789. doi: 10.1007/s10530-009-9588-z

Samper-Villarreal, J., Bolañosa, R. C., Heidemeyer, M., Vargas, M. M., and Vargas, R. M. (2020). Characterization of seagrasses at two new locations in the Eastern tropical pacific (El jobo and matapalito, Costa Rica). *Aquat. Bot.* 165, 103237. doi: 10.1016/j.aquabot.2020.103237

Samper-Villarreal, J., and Cortés, J. (2020). Seagrass characterization on the southern pacific coast of Costa Rica: history, vegetation, and environment. *Bot. Mar.* 63 (5), 429–438. doi: 10.1515/bot-2020-0022

Samper-Villarreal, J., Moya-Ramírez, J., and Cortés, J. (2022). First characterization of seagrasses at Samara bay, pacific coast of Costa Rica. *Aquat. Bot.* 178, 103486. doi: 10.1016/j.aquabot.2021.103486

Samper-Villarreal, J., Rojas-Ortega, G., Vega-Alpízar, J. L., and Cortés, J. (2018). New sighting of seagrasses in the Eastern tropical pacific (Bahía potrero, Costa Rica). *Aquat. Bot.* 151, 25–29. doi: 10.1016/j.aquabot.2018.07.010

de los Santos, C. B., Krause-Jensen, D., Alcoverro, T., Marbà, N., Duarte, C. M., van Katwijk, M. M., et al. (2019). Recent trend reversal for declining European seagrass meadows. *Nat. Commun.* 10 (1), 3356. doi: 10.1038/s41467-019-11340-4 de los Santos, C. B., Scott, A., Arias-Ortiz, A., Jones, B., Kennedy, H., Mazarrasa, I., et al. (2020). "Out of the blue - the value of seagrasses to the environment and to people," in *Seagrass ecosystem services: assessment and scale of benefits*. Eds. M. Potouroglou, G. Grimsditch, L. Weatherdon and S. Lutz, (Nairobi: UNEP) 94.

Scrosati, R. A. (2000). The interspecific biomass–density relationship for terrestrial plants: where do clonal red seaweeds stand and why? *Ecol. Lett.* 3, 191–197. doi: 10.1046/j.1461-0248.2000.00133.x

Sintes, T., Duarte, C. M., and Kendrick, G. A. (2005). Non-linear processes in seagrass colonisation explained by simple clonal growth rules. *Oikos* 108 (1), 165–175. doi: 10.1111/j.0030-1299.2005.13331.x

Surugiu, V., Adrian, T., Ilie, S., and Quijón, P. A. (2021). A hotspot in the Romanian black Sea: Eelgrass beds drive local biodiversity in surrounding bare sediments. *Front. Mar. Sci*. 8 doi: 10.3389/fmars.2021.745137

Touchette, B. W., and Burkholder, J. M. (2000). Review of nitrogen and phosphorus metabolism in seagrasses. *J. Exp. Mar. Biol. Ecol.* 250 (1-2), 133–167. doi: 10.1016/s0022-0981(00)00195-7

Vieira, V.M.N.C.S., Engelen, A. H., Huanel, O. R., and Guillemin, M.-L. (2016). Linear-in-the-parameters oblique least squares: a case study with the estimation of density-dependent survival in algae with isomorphic biphasic life-cycles. *PloS One* 11 (12), e0167418. doi: 10.1371/journal.pone.0167418

Vieira, V. M., Leitão, F., and Mateus, M. (2015). Biomass–density data analysis: a comment on cabaço et al., (2013). *J. Ecol.* 103, 537–540. doi: 10.1111/1365-2745.12294

Vieira, V.M.N.C.S., Lopes, I. E., and Creed, J. C. (2018). The biomass–density relationship in seagrasses and its use as an ecological indicator. *BMC Ecol.* 18, 44. doi: 10.1186/s12898-018-0200-1

Vieira, V.M.N.C.S., Lopes, I. E., and Creed, J. C. (2019). A model for the biomass-density dynamics of seagrasses developed and calibrated on global data. *BMC Ecol.* 19 (1), 4. doi: 10.1186/s12898-019-0221-4

Waycott, M., Longstaff, B. J., and Mellors, J. (2005). Seagrass population dynamics and water quality in the great barrier reef region: a review and future research directions. *Mar. pollut. Bull.* 51 (1-4), 343–350. doi: 10.1016/j.marpolbul.2005.01.017

Weller, D. E. (1989). The interspecific size-density relationship among crowded plant stands and its implications for the -3/2 power rule of self-thinning. *Am. Nat.* 133, 20–41. doi: 10.1086/284899

White, J., and Harper, J. L. (1970). Correlated change in plant size and number in plant populations. *J. Ecol.* 58, 467–485. doi: 10.2307/2258284

Yoda, K., Kira, T., Ogawa, H., and Hozumi, K. (1963). Self-thinning in overcrowded pure stands under cultivated and natural conditions (Intraspecific competition among higher plants. *J. Biol. Osaka. City. Univ.* 14, 107–129.

frontiers | Frontiers in Marine Science

TYPE Original Research
PUBLISHED 28 November 2022
DOI 10.3389/fmars.2022.988584

EDITED BY
Elisabetta Manea,
National Research Council (CNR), Italy

REVIEWED BY
Eva Cacabelos,
University of the Azores, Portugal
Antonella Petrocelli,
National Research Council (CNR), Italy

*CORRESPONDENCE
Martina Orlando-Bonaca
Martina.Orlando@nib.si

SPECIALTY SECTION
This article was submitted to
Marine Conservation and
Sustainability,
a section of the journal
Frontiers in Marine Science

RECEIVED 07 July 2022
ACCEPTED 10 November 2022
PUBLISHED 28 November 2022

CITATION
Orlando-Bonaca M, Savonitto G, Asnaghi V, Trkov D, Pitacco V, Šiško M, Makovec T, Slavinec P, Lokovšek A, Ciriaco S, Chiantore M, Kaleb S, Descourvières EP, Srijemsi M and Falace A (2022) Where and how - new insight for brown algal forest restoration in the Adriatic. *Front. Mar. Sci.* 9:988584. doi: 10.3389/fmars.2022.988584

Where and how - new insight for brown algal forest restoration in the Adriatic

Martina Orlando-Bonaca[1*], Gilda Savonitto[2], Valentina Asnaghi[3,4], Domen Trkov[1], Valentina Pitacco[1], Milijan Šiško[1], Tihomir Makovec[1], Petra Slavinec[1], Ana Lokovšek[1], Saul Ciriaco[5], Mariachiara Chiantore[3,4], Sara Kaleb[2], Emmanuelle Patricia Descourvières[2], Marina Srijemsi[2] and Annalisa Falace[2]

[1]Marine Biology Station Piran, National Institute of Biology, Piran, Slovenia, [2]Department of Life Sciences, University of Trieste, Trieste, Italy, [3]Department of Earth, Environment and Life Sciences, University of Genoa, Genoa, Italy, [4]NBFC, National Biodiversity Future Center, Palermo, Italy, [5]World Wide Fund for Nature (WWF) Marine Protected Area of Miramare, Trieste, Italy

Several anthropogenic factors are responsible for the decline of *Cystoseira sensu lato* (hereafter *Cystoseira*) forests along Mediterranean coasts. Some *Cystoseira* species are already regionally extinct, and their decline has been widely recorded. Sustainable and efficient techniques for the restoration of *Cystoseira* are needed. In this context, the objectives of this study were i) to analyse the reproductive traits of three populations of *Gongolaria barbata* from three nearby donor sites in the northern Adriatic Sea, assessing the differences in their reproductive potential and reproductive success; and ii) to evaluate the outplanting success in terms of the effectiveness of *G. barbata* restoration, in relation to the different donor and receiving sites (Miramare MPA and in front of the Marine Biology Station Piran - MBSP) and implemented methods (*ex situ* and hybrid method combining a mesocosm cultivation and a suspended culture in the field). After 2 weeks of cultivation in mesocosms, half of the tiles with germlings were transported to the receiving sites and placed on suspended lantern nets (hybrid method), which were later (after 3 months) transferred to the seabed on concrete plates with protective cages. The remaining tiles were placed on the seabed on concrete plates with protective cages after a 4-week culture (*ex situ* method). At both sites, lantern nets and plates were randomly placed at 3 m depth. Thallus length was measured monthly in each treatment. Seedlings in suspended culture showed lower performance at the Miramare MPA, most likely due to the unfavourable environmental conditions. The satisfactory results obtained at MBSP demonstrate the efficiency of the hybrid method and confirm its potential to reduce the cost and time required for cultivation. Since unpredictable climatic events pose the greatest threat to restoration performance, these challenges must be considered when establishing new restoration practices. Moreover, herbivore regulation is extremely urgent and should be planned and implemented on a larger regional scale.

KEYWORDS

Gongolaria barbata, canopy-forming algae, restoration, *ex situ*, cultivation, Mediterranean

Introduction

Canopy-forming fucoids are dominant foundation species found on almost all Mediterranean coasts (Bulleri et al., 2012; Gianni et al., 2013; Assis et al., 2020; Bringloe et al., 2020). In particular, *Cystoseira sensu lato* (Fucales, Phaeophyta) species (hereafter referred to as *Cystoseira*), recently subdivided into the three genera *Cystoseira*, *Ericaria* and *Gongolaria* (Molinari-Novoa and Guiry, 2020), can thrive from intertidal to circalittoral rocky bottoms, forming dense forests that are among the most productive assemblages in the Mediterranean coastal zone, with different species replacing each other along a bathymetric gradient (Boudouresque and Lück, 1972; Giaccone, 1973; Ballesteros, 1989; Rull and Gómez Garreta, 1989; Otero-Schmitt and Pérez-Cirera, 1996; Ballesteros et al., 1998; Pizzuto, 1999; Ballesteros et al., 2009).

Important ecosystem services (De La Fuente et al., 2019a) provided by these brown algal forests include high primary production (Ballesteros et al., 2009; Mačić and Svirčev, 2014), rich understory communities of algae and invertebrates (Pitacco et al., 2014; Bianchelli et al., 2016; Mancuso et al., 2021), outstanding fish densities and diversity (Orlando-Bonaca and Lipej, 2005; Cheminée et al., 2013), and a long term carbon sink (Peleg et al., 2020). Other benefits of *Cystoseira* to humans include the production of several bioactive metabolites (Bruno de Sousa et al., 2017a), with antioxidant, anti-inflammatory, antifungal, antiviral and antibacterial effects (Mhadhebi et al., 2011; Vizetto-Duarte et al., 2016; Bruno de Sousa et al., 2017b; De La Fuente et al., 2020).

As a result of multiple anthropogenic impacts (e.g., coastal urbanisation, eutrophication, sediment loading and overgrazing), *Cystoseira* stands have gradually disappeared in many Mediterranean coastal areas, often being replaced by filamentous or ephemeral taxa (e.g., Mangialajo et al., 2008; Falace et al., 2010; Vergés et al., 2014; Thibaut et al., 2015; Rindi et al., 2017; Rindi et al., 2018; Catra et al., 2019; Mariani et al., 2019; Bernal-Ibáñez et al., 2021; Orlando-Bonaca et al., 2021a; Orfanidis et al., 2021). In addition, human changes in the marine environment also affect connectivity, leading to habitat fragmentation and loss, and genetic disjunction even at small spatial scales (Alberto et al., 2010).

Furthermore, an important feature of *Cystoseira* settlements is that their zygotes sink rapidly (Clayton, 1990), so that they fall and stick to the substrate near the parent algae. Due to their low dispersal, the colonisation of new or damaged areas is therefore difficult, so habitat fragmentation has a major impact on these species.

The first strategy to address the decline of *Cystoseira* and their habitat was their protection through international agreements (e.g., Bern Convention, Barcelona Convention, Directive 92/43/EEC, European Red List of Habitats). Nevertheless, there is little evidence of natural recovery of degraded *Cystoseira* forests (but see Munda, 2000; Perkol-Finkel and Airoldi, 2010; Iveša et al., 2016; Medrano et al., 2020a).

Restoration of affected areas, but only those where disturbance is no longer present or has been mitigated, is so important as it can greatly accelerate habitat recovery.

Restoration is increasingly recognized as an appropriate strategy to actively trigger the recovery of degraded coastal habitats (Abelson et al., 2020), as proposed in the recently proclaimed UN Decade of Ecosystem Restoration (2021–2030; Waltham et al., 2020). However, implementing successful restoration efforts requires detailed knowledge of the current and past distribution of lost habitats and species, the pressures that led to their decline, and accurate characterization of donor populations (Gann et al., 2019). In recent years, several restoration attempts have been made in the Mediterranean region through different projects to address the loss of *Cystoseira* (Falace et al., 2018; Verdura et al., 2018; De La Fuente et al., 2019b; Medrano et al., 2020b; Orlando-Bonaca et al., 2021b; Savonitto et al., 2021).

Restoration of brown algal forests can be achieved through: transplantation of adult thalli (Falace et al., 2006; Susini et al., 2007), deployment of bags with fertile receptacles *in situ*, attached to a hoe and fixed to the seafloor at selected restoration sites (Verdura et al., 2018; Medrano et al., 2020b), and the outplanting of juveniles grown *ex situ* under laboratory conditions (Falace et al., 2006; Sales et al., 2011; Falace et al., 2018; Verdura et al., 2018; De La Fuente et al., 2019b; Savonitto et al., 2021; Orlando-Bonaca et al., 2021b; Lardi et al., 2022).

The latter two techniques are recommended for the recovery of endangered species to avoid depleting donor populations (De La Fuente et al., 2019b).

A sharp decline of Fucales has also been reported in the northern Adriatic basin (Falace et al., 2010; Orlando-Bonaca and Rotter, 2018; Orlando-Bonaca et al., 2021a), leading to displacement by turf-forming taxa in shallow waters. The occurrence of these low-lying algae is likely related to human-induced hydromorphological changes to the shoreline and high sediment resuspension rates (Falace et al., 2010; Orlando-Bonaca and Rotter, 2018) rather than nutrient enrichment, as the northern Adriatic is considered oligotrophic (Mozetič et al., 2012).

Moreover, negative impacts from native herbivorous fish have also been documented: for *Sargassum vulgare* C. Agardh (Orlando-Bonaca and Mavrič, 2014) and recently for the transplanted *Gongolaria barbata* (Stackhouse) Kuntze (Orlando-Bonaca et al., 2021b; Savonitto et al., 2021). Currently, *G. barbata* and *Cystoseira compressa* (Esper) Gerloff and Nizamuddin are quite common in the Gulf of Trieste only on the Slovenian coast, while they have almost disappeared on the Italian coast. Other species from this group are already rare in Slovenian waters and extinct in Italian waters of the Gulf of Trieste.

Based on previous results of *G. barbata* restoration in the northern Adriatic (Orlando-Bonaca et al., 2021b; Savonitto et al., 2021), the present study aimed to evaluate the performance of different donor populations in close proximity to each other in the restoration of two receiving sites. To successfully reduce cultivation time (to avoid lengthy maintenance and minimise costs), we compared the performance of the *ex situ* method (already consolidated at the same sites in the ROC-POP LIFE and J1-1702 projects) with a hybrid method combining cultivation in mesocosm and suspended culture in the field.

In this context, the objectives of this study were (1) to analyse the reproductive traits of three populations of *G. barbata* from three nearby donor sites (i.e., Izola, Strunjan, Piran) in order to assess the differences in their reproductive potential and reproductive success, and (2) to evaluate the restoration success in relation to the different donor and receiving sites (Miramare MPA vs. Marine Biology Station Piran) and the methods used. The added value of our work is that by combining two methods, for the first time different donor and receiving sites were compared in terms of restoration success of *G. barbata*.

Materials and methods

Study area

The study area is located in the Gulf of Trieste (Figure 1), a shallow, semi-enclosed bay in the northernmost part of the Adriatic and Mediterranean Seas. The gulf stretches from Cape Savudrija (Croatia) to Grado (Italy) and includes the entire Slovenian coast, with an average depth of about 21 m. The area is known for the lowest winter temperatures (mostly below 10°C) in the Mediterranean and the prevailing winds, which blow mainly from the northeast in an offshore direction (Boicourt et al., 2021). Maximum summer seawater temperatures reach 28°C (data from VIDA oceanographic buoy, https://www.nib.si/mbp/en/). The average salinity is about 37 and is mainly influenced by the freshwater inflow from the Soča (Isonzo) River, while the water circulation is mainly counterclockwise in the lower layer and clockwise in the surface layer (Stravisi, 1983).

The rationale of the experiment, aimed at testing the effect of three donor and two receiving sites, and cultivation methods (hybrid vs. *ex situ*) on the restoration efficiency of *G. barbata*, is shown in Figure 2.

Fertile apices of *G. barbata* were collected in Slovenia from three donor populations located in:

- Izola (45.543567, 13.676371), which is characterised by a healthy and dense populations of *G. barbata* and *C. compressa*;
- Strunjan Natural Park (45.53379, 13.638281), where *G. barbata* forms healthy stands in association with *C. compressa* and *Ericaria crinita* (Duby) Molinari and Guiry;
- Piran (45.5284, 13.5754), where belts of *G. barbata* are present in association with *C. compressa* and *E. crinita*.

The distances along the coastline between the donor sites (at an isobath depth of 2 m) are: Izola-Strunjan = 4.621 km, and Strunjan-Piran = 6.873 km. All donor sites have a shallow, rocky seabed and are moderately exposed to wave action. Due to overgrazing by native herbivorous species such as *Sarpa salpa* (L., 1758) at the Piran sampling site in March 2021, the number of apices collected in this area was lower than at the other two donor sites (authors' *pers. obs.*).

The germlings were cultivated in the two nursery facilities at the University of Trieste (UNITS) and at the Marine Biology Station Piran (MBSP).

The cultured germlings were outplanted in:

- the 'no-take' zone of the Miramare MPA in Italy (45.701802, 13.714223), where *G. barbata* once occurred (Bussani and Vuković, 1992) and was recently reintroduced as part of the ROC-POP LIFE project (Savonitto et al., 2021). The MPA is located in a highly urbanized coastal system and is affected by herbivorous fish grazing (Savonitto et al., 2021; Bevilacqua et al., 2022);
- the coastal area off the Marine Biology Station Piran (hereafter MBSP) in Slovenia (45.5177, 13.5680), where

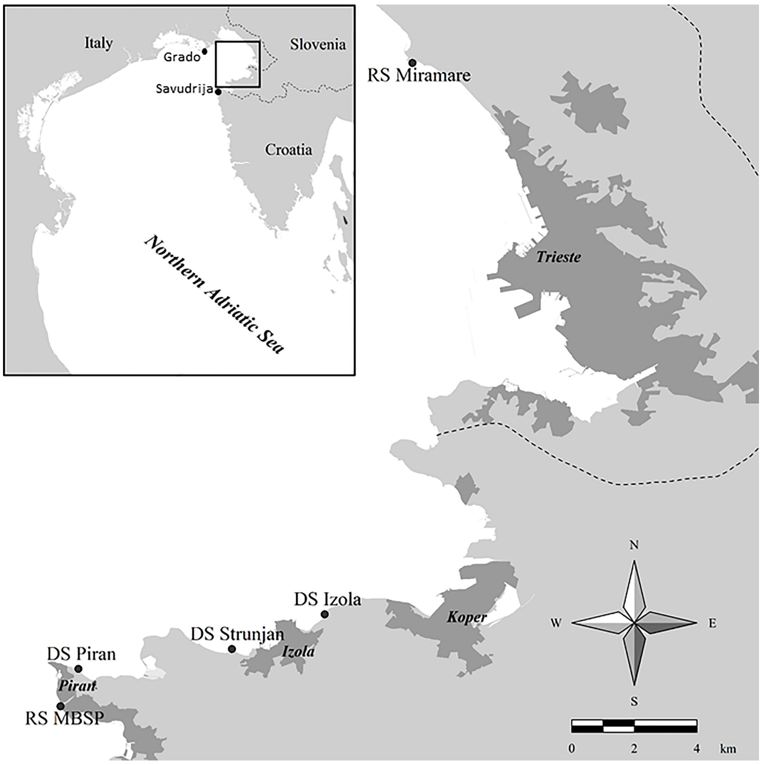

FIGURE 1
Map of the study area showing donor (= DS) and receiving sites (=RS) for *Gongolaria barbata*.

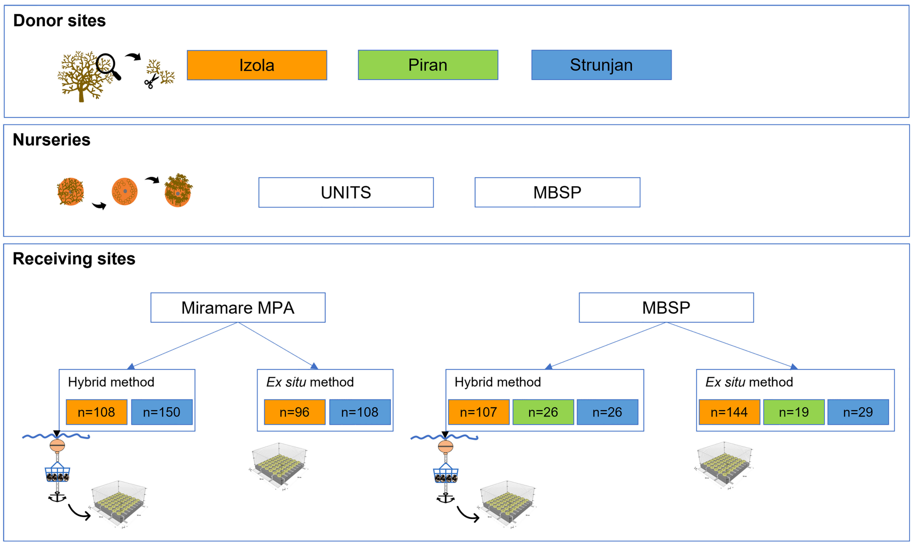

FIGURE 2
Experiment on *G. barbata* restoration in the northern Adriatic Sea. UNITS, University of Trieste (Italy), MBSP, Marine Biology Station Piran (Slovenia). It shows: i) the three donor sites where fertile receptacles were collected; ii) the two nursery facilities where germlings were cultivated on clay tiles starting from the fertile receptacles; iii) the two receiving sites where the tiles coming from different donor populations were outplanted using either the hybrid or *ex situ* method.

less than a decade ago there was a dense brown algal forest consisting mainly of *G. barbata* and *C. compressa.* This habitat was completely destroyed in 2016 due to invasive encroachment for beach construction, when no precautions were taken to limit environmental damage. This site is also affected by fish grazing pressure (Orlando-Bonaca et al., 2021b).

Culture in mesocosms

Cultures of *G. barbata* were carried out following the protocol of Falace et al. (2018) further improved in De La Fuente et al. (2019b).

In early April 2021, apices with mature receptacles were collected simultaneously at 1-2 m depth at the three donor sites. They were then transported to the nursery facilities within a few hours under cool (4°C) and dark conditions. At the laboratory, the receptacles were cleaned with filtered seawater to remove epibionts, and stored at 4°C for 24 h to promote gamete release.

In parallel, approximately 100 randomly selected apices from each donor site were stored at -4°C for further analyses (i.e., morphometric measurements).

In environmentally controlled rooms, approximately 50 mg FW fertile apices were placed on each rough clay tile (4.5 cm diameter with a central hole of 0.6 cm diameter), in aquaria filled with filtered seawater (0.22 µm filter membrane) enriched with Von Stosch solution and germanium dioxide (for details, see Falace et al., 2018; De La Fuente et al., 2019b), and oxygenated with air pumps and bubblers.

At UNITS, 10 aquaria with 50-55 tiles each were used. A total of 204 tiles were seeded with Izola apices and 303 with Strunjan apices. At MBSP, 6 aquaria were used, each containing 50-55 tiles. In total, 251 tiles were seeded with apices from Izola and 55 with apices from Piran. The tiles were labelled according to the donor populations. The differences in culturing efforts and, thus, the unbalanced experimental design depend on the availability of fertile material, which is related to the size of the populations themselves (i.e., Strunjan is larger in terms of population size, while the Piran population was severely damaged by fish grazing during the fertile season).

Temperature was set at 15°C, light intensity at 125 µmol m^{-2} s^{-1}, and photoperiod at 15:9 h light:dark to simulate conditions during the reproductive period of *G. barbata* at donor sites. Air temperature was automatically set by the room controller and water temperature was measured daily with a thermometer in each aquarium to ensure it was constant.

Apices placed on the tiles for seeding were removed after twenty-four hours (T0). To avoid nutrient limitation, the culture medium was renewed every 3-5 days. Both the aquaria and the tiles within each aquarium were randomly repositioned at each periodic change of culture medium to provide random culture conditions to all the tiles.

Cultures lasted two weeks for tiles destined for the hybrid method and 4 weeks for tiles destined for the *ex situ* method.

Hybrid method

To test whether it is possible to shorten the cultivation time in mesocosm, an *in situ* suspended culture was established after a shorter cultivation time (i.e., 2 weeks).

Therefore, after 2 weeks of culture in the mesocosms (on April 23rd, T2), about half of the tiles were randomly selected and transported to the receiving sites, where they were fixed to plastic lantern nets (55 cm diameter) suspended at 2 m depth, as described in Savonitto et al. (2021); 108 tiles with germlings from Izola and 150 from Strunjan were placed in the Miramare MPA, while 107 from Izola, 26 from Strunjan and 26 from Piran were placed in front of MBSP.

After 3 months in the lantern nets (July), the tiles were placed on the rocky bottom using outplanting modules. The modules consisted of 50x50 cm concrete plates (each capable of holding up to 48-54 tiles) covered with iron anti-grazing cages (mesh size 1x1 cm^2) and secured with metal wedges, as described in Orlando-Bonaca et al. (2021b). Tiles were randomly positioned on the modules, interspersing tiles hosting juveniles from the different donor populations.

In the Miramare MPA, the tiles without juveniles were excluded, so that finally 69 tiles from Strunjan and 7 tiles from Izola were placed on two plates. In front of the MBSP, all tiles were laid on three plates on the seabed near the lantern nets.

Ex situ method

After 4 weeks of cultivation in the mesocosms (on May 7th, T4), the tiles destined for the *ex situ* method were transported to the receiving sites and attached with screws to preassembled outplanting modules (see above). As with the hybrid method, tiles from the different donor sites were marked and randomly placed on the plates (4 plates at Miramare MPA and 4 in front of MBSP). The plates for the two methods were placed very close to each other on the seafloor.

Specifically, 96 tiles with juveniles from Izola and 108 from Strunjan were located in the Miramare MPA, while 144 from Izola, 19 from Strunjan and 29 from Piran were placed in front of the MBSP.

Tiles were monitored in the Miramare MPA and MBSP by SCUBA-divers, and iron cages were cleaned regularly with a wire brush to remove epibionts and sediment, at least twice a month at Miramare, an MPA with dedicated staff, whereas in front of the MBSP they were cleaned only once a month during routine monitoring. The difference in frequency of cleaning was due to the different degree of protection and monitoring to which the two receiving sites are subject.

Collected data

During mesocosm culture, the following data were collected and processed(Table 1):

- Morphometric measurements of receptacles (i.e., length and width in mm): 100 receptacles from each donor site (Izola, Strunjan, Piran) were randomly collected and photographed under a stereomicroscope (Leica MZ 6, Leica Microsystems, Wetzlar, Germany) with a Nikon Coolpix 4500 camera (Nikon Corporation, Tokyo, Japan) (at T0);
- Reproductive traits: 20 tiles per donor site (Izola and Strunjan) were randomly selected at UNITS (at T0) to determine the:
  (i) reproductive potential as *RP = N. of conceptacles per receptacle* of all the receptacles on each tile. The number of conceptacles was determined by counting the total number of ostioles protruding from the outer surface of the receptacle using a stereomicroscope (Supplement 1);
  (ii) reproductive success (*RS = N. of zygotes per tile x N. of conceptacles per tile*$^{-1}$) by photographic sampling with a Nikon D300 camera (Nikon Corporation, Tokyo, Japan).
- Germling density (i.e., number of germlings per tile): at weeks 1 (T1), 2 (T2), 3 (T3, only at MBSP), and 4 (T4) after fertilisation, germling density was estimated on pictures (photographic sampling with a Nikon D300 camera) randomly selecting 42 tiles from Izola (henceforth as juvIZ) and 76 from Strunjan (juvST) at UNITS, while 30 from Izola (juvIZ) and 10 from Piran (juvPI) at MBSP. No data are available at T4 for juvPI cultured at MBSP.
- Germling length and width: at T4, 40 germlings per donor site (only the donor populations from Izola and Strunjan were considered: juvIZ and juvST at UNITS, juvIZ at MBSP) were randomly selected and photographed directly on the tiles under a stereomicroscope to measure their length and width. They were randomly selected each time, thus not repeated measures. No data are available at T4 for juvPI cultured at MBSP.
- Light intensity (Lux) and seawater temperature (°C) were measured from the time of outplanting on the seabed (T4) using a HOBO Pendant Data Logger (UA-OOx) at the MBSP receiving site.

In the laboratory, receptacles' length and width, number of zygotes per tile at T0, number of germlings per tile at T1, T2, T3 and T4, and length and width of germlings at T4 were determined by analysing the photos with ImageJ software (Schneider et al., 2012).

In the field, thalli lengths were measured by SCUBA divers at Miramare MPA and MBSP on 20 randomly selected tiles per method and donor site monthly from May to November (7 times). In November, the percentage survival rate (i.e., the % of tiles that had juveniles on them) was determined by SCUBA divers. It is noteworthy that length data are not available for the hybrid method juveniles outplanted in the Miramare MPA from August onwards, as the mortality rate was 100%.

For the assessment of reproductive traits, germling density and germling morphometry in the laboratory and thallus length in the field, the tiles have been considered as replicates, even acknowledging an issue of spatial pseudoreplication since some of the tiles belong to the same aquarium/outplanting module. Logistical constraints did not allow us to have all completely independent replicates but care in interspersion and randomisation allowed us to reduce the risk of an aquarium/module effect. This aspect has been considered in results interpretation, keeping in mind the risk of inflated Type I errors in case of simple pseudoreplication (Millar and Anderson, 2004).

Statistical analysis

One-way ANOVA design was applied to test for possible differences between donor sites (Izola, Piran and Strunjan) in

TABLE 1 Summary of data collected during the mesocosm culture at UNITS and MBSP.

Sampling time	Sample size	Variable	Calculation/Unit
T0	100 receptacles per donor site	Receptacle length and width	Length and width (mm)
	20 random tiles per site	Receptacle reproductive potential*	N. of conceptacles per receptacle of all the receptacles on the tile
		Reproductive success*	N. zygotes released per tile x N. receptacles per tile
T1 = 1 week	At UNITS: 42 tiles from Izola and 76 from Strunjan; At MBSP: 30 from Izola and 10 from Piran	Germling density	N. germlings per tile
T2 = 2 weeks			
T3 = 3 weeks			
T4 = 4 weeks^{+}	40 germlings per donor site	Germling length and width	Length and width (mm)

*Only at UNITS, on tiles seeded with apices from Izola and Strunjan. $^{+}$At MBSP, missing data for Piran.

receptacle morphometry (length and width, n=100), reproductive potential (RP, n=20), reproductive success (RS, n=20) and germling morphometry (length and width, n=40) after 4 weeks of culture. Verification of the assumptions (normality with the Kolmogorov-Smirnov test and homoscedasticity with the Bartlett's test) was performed prior to conducting the analyses. If the assumptions were not fulfilled, square root transformation of the response variable was applied and assumptions re-tested. If still not compliant with ANOVA assumptions, the non-parametric equivalent of ANOVA, the Kruskal-Wallis test, was performed.

Differences in germling density on the tiles according to donor populations (juvIZ, juvPI and juvST) were assessed applying a linear mixed model, after checking for normality of the response variables, using the variable "Donor population" as fixed, while "Time" as random.

As for the field data, two separate analyses were performed on the response variable thallus length measured at the last monitoring time (November 2021, n=20). Potential differences linked to the donor population and the outplanting method has been investigated through a two-way ANOVA design, testing the effect of the fixed orthogonal factors "Donor population" (3 levels: juvIZ, juvPI, juvST), "Outplanting method" (2 levels: *ex situ*, hybrid) and their interaction. This test has been performed only on MBSP data, because this was the receiving site hosting all donor populations and where it was possible to carry out both methods till the end of the experimentation. A second two way ANOVA design has been applied only considering the *ex situ* method data for testing the effect of the fixed orthogonal factors "Donor population" (2 levels: juvIZ, juvST), "Receiving site" (2 levels: Miramare MPA, MBSP) and their interaction. Normality and homoscedasticity assumptions were tested by Kolmogorov-Smirnov test and Bartlett's test respectively, and a square root transformation was required.

For all analyses, *post-hoc* comparisons on significant terms were performed by Tukey test and significant differences are shown on the corresponding plots and table (for field data). All statistical analyses and plots were performed with "stats" and "car" packages of the free software RStudio (RStudio Team, 2021).

Results

- Culture in mesocosm

Morphometry of the receptacles

Significant differences were found in the length and width of the receptacles between the three donor sites, with the receptacles in Izola being longer and larger (length: 6.02 ± 0.26 SE mm; width: 0.96 ± 0.02 SE mm) than those from Piran (length: 4.66 ± 0.16 SE mm; width: 0.78 ± 0.02 SE mm; p-value < 0.001) and Strunjan (length: 4.70 ± 0.18 SE mm; width: 0.83 ± 0.02 SE mm; p-value < 0.001). No significant differences were found between Piran and Strunjan (Figure 3, Table 2).

The fertile apical fronds from Piran and Strunjan generally had short, simple and cylindrical receptacles that were sparsely mucronate and had few or no aerocysts (Figure 3C). In contrast, fronds from Izola had long fusiform or mucronate receptacles, predominantly prominent conceptacles, and there were numerous single or concatenated aerocysts (Figure 3C; Table 3).

Reproductive traits

The Izola population receptacles had significantly higher reproductive potential (30.5 ± 0.4 SE conceptacles receptacle^{-1}) compared to Strunjan (25.0 ± 0.3 SE conceptacles receptacle^{-1}; p-value < 0.001; Figure 4A, Table 2). Conversely, the reproductive success of Izola receptacles (0.4 ± 0.1 SE zygotes conceptacle^{-1}; p-value < 0.01) was significantly lower than those from Strunjan (0.8 ± 0.1 SE zygotes conceptacle^{-1}; Figure 4B, Table 2).

Germling density

Germling density gradually decreased from the first to the fourth week in culture (Figure 5). After 4 weeks, it ranged from 132 ± 15 SE germlings per tile (juvIZ) to 73 ± 8 SE germlings per tile (juvST) (Figure 5). JuvST had significantly different germling density (p-value < 0.001, Table 2), and showed higher values at earlier sampling times (T1-T2), than juvIZ and juvPI, which were again significantly different (p-value = 0.02, Table 2).

Morphometry of germlings after 4 weeks

After 4 weeks in culture, significant differences in length and width were observed between juvIZ (length: 1.15 ± 0.07 SE mm; width: 0.29 ± 0.01 SE mm) and juvST (length: 0.65 ± 0.03 SE mm; width: 0.17 ± 0.01 SE mm), with juvIZ having higher values in both morphometric parameters (p-value < 0.001, Figures 6A, B; Table 2).

For these last parameters (i.e., reproductive traits, germling density and morphometry), also considering the pseudoreplication issue, the low p-values of statistical tests (always lower than 0.01) allowed us to consider our results reliable.

- Field data

The two-way ANOVA on MBSP data showed a significant effect of the interactions "Donor population" x "Outplanting Method" (p-value =0.0001, Table 4).

The three populations showed no differences in performance when the hybrid method was applied, while juvIZ performed differently from juvPI and juvST in the *ex situ* method (p-value <0.001). JuvIZ performed better if outplanted through the *ex situ* method compared to hybrid (p-value <0.001), while no differences were observed for juvPI and juvST (Table 4, Figure 7A).

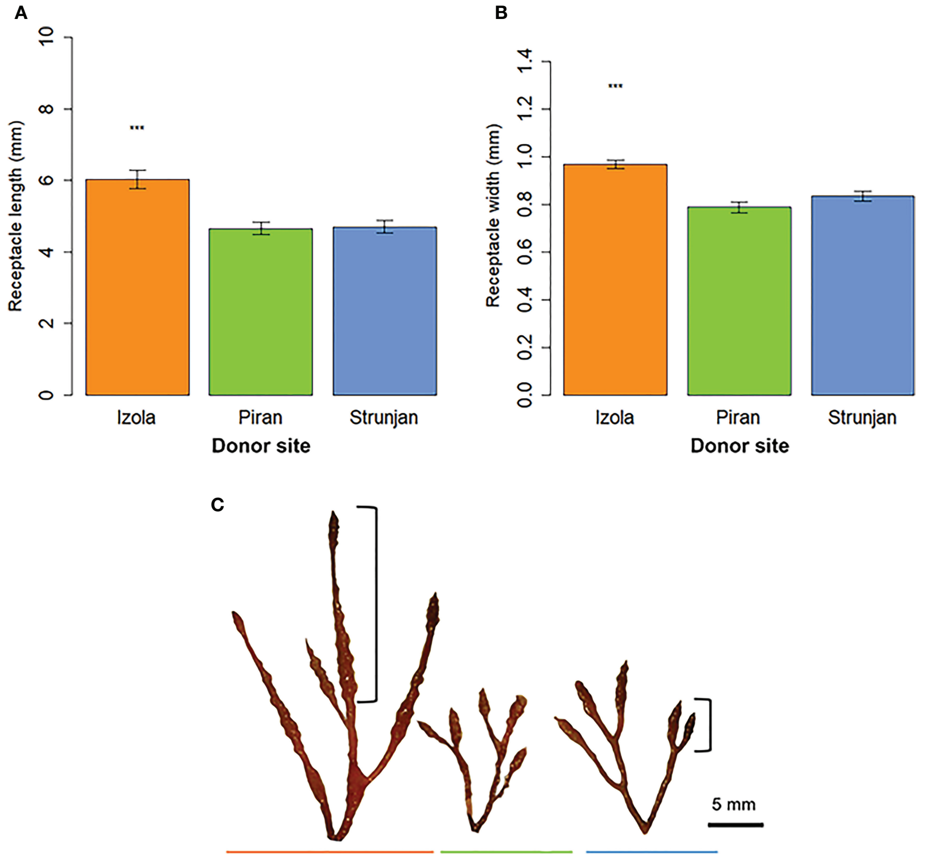

FIGURE 3
G barbata receptacles' **(A)** length and **(B)** width in the three donor sites (mean ± SE); **(C)** fertile apices of *G barbata* populations from Izola (orange), Piran (green) and Strunjan (blue) sampling sites. Significance levels: '***' p-value < 0.001.

Significant differences were observed in the *ex situ* method between the two receiving sites: thalli of both donor populations outplanted in Miramare MPA showed significantly higher performances compared to the ones in MBSP (p-value <0.0001, Figure 7B, Table 4). In both receiving sites, juvIZ performed significantly better than juvST (p-value=0.007, Figure 7B, Table 4). At 7 months (November 2021), the average length of thalli outplanted by the *ex situ* method at Miramare MPA ranged from 8.4 ± 0.7 SE (juvST) to 9.1 ± 0.6 SE cm (juvIZ), while at MBSP it ranged from 2.3 ± 0.4 SE (juvST) to 4.9 ± 0.3 SE cm (juvIZ).

It was not possible to compare the two methods in the Miramare MPA receiving site at 7 months because after only 3 months in the field (July 2021), a lower length (0.3 ± 0.1 SE – juvIZ; 0.5 ± 0.1 SE cm – juvST) was observed and in August (i.e., after 1 month on the sea bottom) juvenile mortality was 100%. For this reason, monitoring of the hybrid method was interrupted at this site.

The extremely low p-values of the statistical tests (always lower than 0.001) allowed us to consider our results reliable even acknowledging that some of the replicates should be considered pseudoreplicated in space.

In front of the MBSP, the percentage of tiles with germlings (% survival) ranged from 58% (juvST), 70% (juvIZ) and 90% (juvPI) for the *ex situ* method, while for the hybrid method it was 41% for juvST, 83% for juvIZ and 100% for juvPI (Figure 8A). At Miramare MPA, the percentage of tiles with germlings in November 2021 ranged from 44% (juvST) to 78% (juvIZ) for the *ex situ*, while it was 0% for the hybrid method for both juvIZ and juvST (Figure 8B).

Discussion

For restoration, it is important to gain a deeper knowledge of the phenology of the species to be restored. In the last forty years, many studies have investigated the phenology of *Cystoseira* spp., highlighting that they usually undergo both morphological and reproductive changes during the year (e.g., Gómez-Garreta et al., 1982; Hoffmann et al., 1992;

TABLE 2 Results of statistical analyses on laboratory data.

Response variable	Statistics	Tested factor			
Receptacle length	Anova		SS	F	p-value
		Donor site	3.465	11.3	<0.0001
		Residuals	47.531		
				chi-sq	p-value
Receptacle width	KW test	Donor site		36.904	<0.0001
				chi-sq	p-value
Reproductive potential	KW test	Donor site		101.09	<0.0001
			SS	F	p-value
Reproductive success	Anova	Donor site	0.455	7.7237	0.008
		Residuals	2.237		
			Std.Error	t-value	p-value
Germling density	Linear mixed model	Intercept	0.507	8.194	<0.0001
		Donor pop: juvPI	0.166	-2.224	0.027
		Donor pop: juvST	0.084	7.079	<0.0001
		Random effect: Time	1.008		
				chi-sq	p-value
Germling length	KS test	Donor population		13.433	0.0002
				chi-sq	p-value
Germling width	KS test	Donor population		31.015	<0.0001

Alongi et al., 1999; Marzocchi et al., 2003; Falace et al., 2005; Falace and Bressan, 2006; Medrano et al., 2020a). Nevertheless, few studies focused on phenotypic variation among populations of fucoid species and also reported significant differences in reproductive traits (De Paula and De Oliveira, 1982; Silva et al., 2004; Sadogurska et al., 2021).

Within its geographical range, *G. barbata* shows considerable ecological plasticity and outstanding morphological variability due to environmental factors (Ercegović, 1952; Falace and Bressan, 2006). In the present study, we found relevant differences in the shape and size of apical fronds and the number of aerocysts between populations of *G. barbata* from Izola and those from Strunjan and Piran (Tables 2 and 3): long spindle-shaped receptacles, bearing aerocysts and always ending with a mucron for the population from Izola (Falace et al., 2005; Falace and Bressan, 2006), while the populations from Strunjan and Piran had short cylindrical receptacles bearing almost no aerocysts and not always mucronated (Orlando-Bonaca et al., 2021b).

In the Black Sea, Sadogurska et al. (2021) reported that this variability might depend on the hydrodynamic regime and season and observed two main morphologies. At sheltered sites, *G. barbata* had long, sickle-shaped receptacles, sometimes with protruding conceptacles, and numerous concatenated aerocysts. In contrast, on exposed shores, *G. barbata* had small, oval or spindle-shaped receptacles with

TABLE 3 Comparison of *Gongolaria barbata* populations sampled at Izola, Strunjan and Piran donor sites, in terms of receptacles' features (numeric values are expressed as mean ± SE).

Donor sites	Izola	Piran	Strunjan
Cryptostomata	numerous	numerous	numerous
Aerocysts	abundant, oval to spindle shaped, isolated or in chains (up to 5 aerocysts)	absent or few isolated	absent or few isolated
Receptacle shape	simple, fusiform mucronate or pedicellate	simple or bifid, cylindrical, mucronate	simple or bifid, cylindrical, mucronate
Receptacle length	6.02 ± 0.26 mm, range 1.28 – 15.12 mm	4.66 ± 0.16, range 1.61 – 10.89 mm	4.70 ± 0.18 mm, range 1.71 – 10.22 mm
Receptacle width	0.96 ± 0.02 mm, range 0.53 – 1.62 mm	0.78 ± 0.02 mm, range 0.29 – 1.31 mm	0.83 ± 0.02 mm, range 0.35 – 1.45 mm
Conceptacle	prominent	smooth or slightly prominent	smooth or slightly prominent
Conceptacles receptacle^{-1}	30.45 ± 0.45 conceptacles receptacle^{-1} (up to 93 conceptacles receptacle^{-1})		24.96 ± 0.25 conceptacles receptacle^{-1} (up to 65 conceptacles receptacle^{-1})

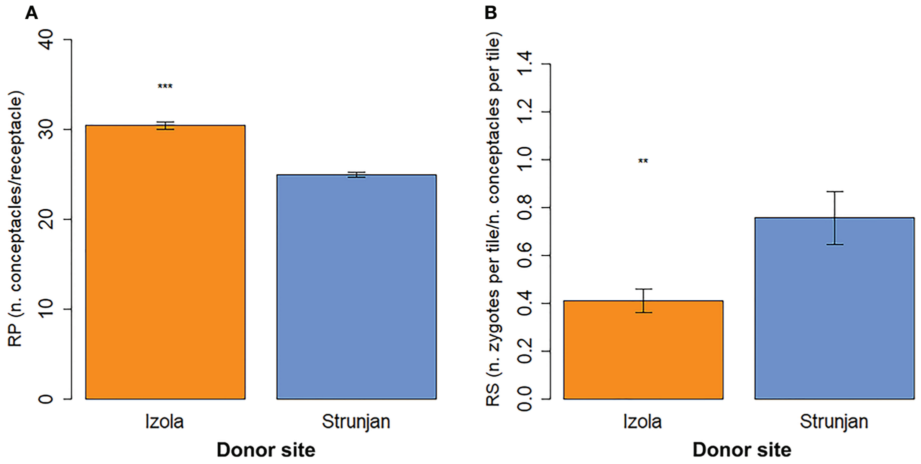

FIGURE 4
Reproductive potential **(A)** and reproductive success **(B)** of the receptacles from Izola and Strunjan donor sites (mean ± SE). Significance levels: '***' p-value < 0.001, '**' p-value < 0.01.

smooth surfaces and few aerocysts. Nevertheless, molecular analyses revealed minor differences between the Black Sea samples of *G. barbata*, representing smaller infraspecific variations. Sadogurska et al. (2021) therefore concluded that the morphological variability of *G. barbata* in the Black Sea is not due to infraspecific taxa, but to considerable ecological plasticity and seasonal variation. Consequently, the populations sampled for the present study could represent two different ecotypes.

Although the donor sites on the Slovenian coast are close to each other (see Materials and methods), they have different environmental characteristics. The Izola donor site is located at the edge of Koper Bay, which is characterised by high sedimentation and suspension rates reflected in increased water turbidity (Ogorelec et al., 1991). The area is exposed to large freshwater inputs from the Rižana and Badaševica rivers (Cozzi et al., 2012) and is located close to the port of Koper. In addition, some unidentified sources of pollution (probably municipal sewage) affect the ecological status of macroalgae in this area (Orlando-Bonaca and Rotter, 2018; Orlando-Bonaca et al., 2021c). In contrast, Strunjan and Piran are exposed to lower anthropogenic pressures (Orlando-Bonaca et al., 2015), as they are located on a coastline that is still in a pristine state. Moreover, these two sites are located outside the bays of Koper and Piran, which are known to have the highest sedimentation and suspension rates in Slovenian marine waters (Ogorelec et al., 1991). Consequently, the three donor populations might be adapted to different sedimentation rates, salinity, and turbidity,

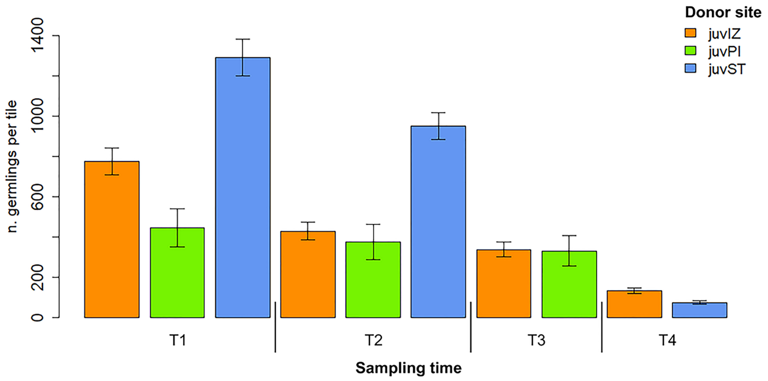

FIGURE 5
Germlings density (mean ± SE) on tiles from apices collected in Izola (juvIZ), Piran (juvPI) and Strunjan juvST (data for juvIZ are pooled for UNITS and MBSP). No data are available for juvST cultivated at UNITS at T3, and for juvPI cultivated at MBSP at T4.

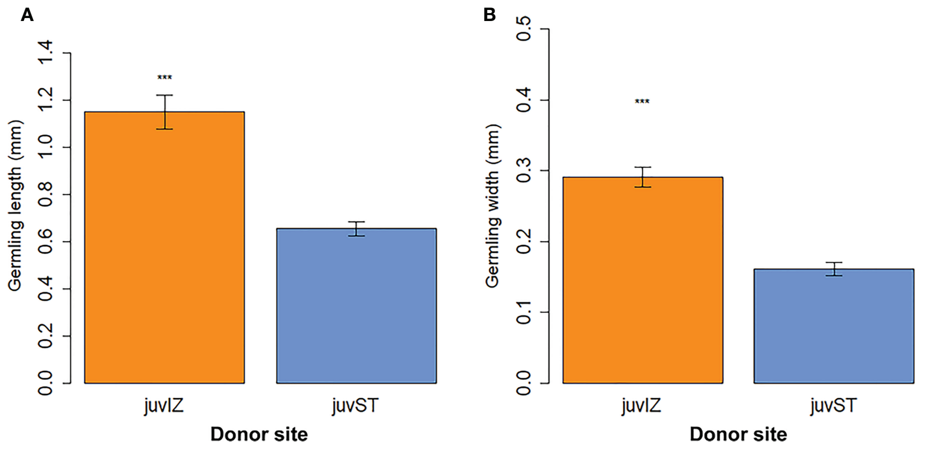

FIGURE 6
Germling size (mean ± SE) after 4 weeks of culture (data for juvIZ are pooled for UNITS and MBSP): **(A)** length (mm) and **(B)** width (mm). No data available for juvPI cultivated at MBSP. Significance levels: '***' p-value < 0.001.

affecting the length of receptacles and the presence of aerocysts. In environments with high water turbidity, the development of aerocysts stimulates the algae to stretch upwards and in this way improve their access to light (Lüning, 1991). The elongated shape of the receptacles could be another adaptation to increase surface area and better capture light to improve photosynthesis. Therefore, the Izola population could be a morphotype adapted to higher sedimentation.

The fertile apices of the Izola population not only had longer and larger receptacles (Figure 3), but also a higher number of conceptacles per receptacle (RP, Figure 4A; Table 2). However, the number of zygotes per tile relative to the number of conceptacles per tile (RS) was higher in the *G. barbata* population from Strunjan (Figure 4B; Table 2). Furthermore, the density of juvIZ and juvPI was lower than that of juvST after one (T1) and two weeks of culture (T2) (Figure 5). Nevertheless, the progressive decrease in seedling density over time (T4), which can be explained at least in part by the process of "self-thinning" of a growing plant population (Ang and De Wreede, 1992; Steen and Scrosati, 2004), was more pronounced in juvST. Not only the density but also the dimensions of juvST were smaller than those of juvIZ at T4 (Figure 6). This result indicates that the population from Strunjan, although more successful in the first two weeks of culture, was less successful than the others after three to four weeks.

The success of outplanting juveniles in the field was highly variable and depended on both the location of the donor/receiving sites and the outplanting method. As with the *ex situ* method, the greatest differences in Slovenia (MBSP) were due to the different donor sites. This is because although all experimental tiles were exposed to the same environmental conditions (Supplement 2), juvIZ thalli grew significantly better than juvST and juvPI (Figure 7A). This was probably due to pre-adaptation to the high sediment resuspension rate

TABLE 4 Results of the statistical analyses on field data. In the footnotes, results of *post-hoc* comparisons are reported.

	Statistics	Tested factor	SS	F	p-value
Juveniles' length in MBSP	Anova	Donor pop	0.86	14.20	<0.0001
		Method	0.11	3.74	0.055
		Donor pop X Method	0.58	9.55	0.0001
		Residuals	4.31		
Post-hoc: Donor pop*Method: *ex situ*: juvIZ ≠ juvST=juvPI; hybrid: juvIZ=juvST=juvPI; juvIZ: *ex situ* ≠ hybrid					
			SS	F	p-value
Juveniles length using the *ex situ* method	Anova	Donor pop	44.17	7.47	0.007
		Receiving site	458.55	77.53	<0.0001
		Donor pop X Rec site	15.71	2.66	0.107
		Residuals	538.24		

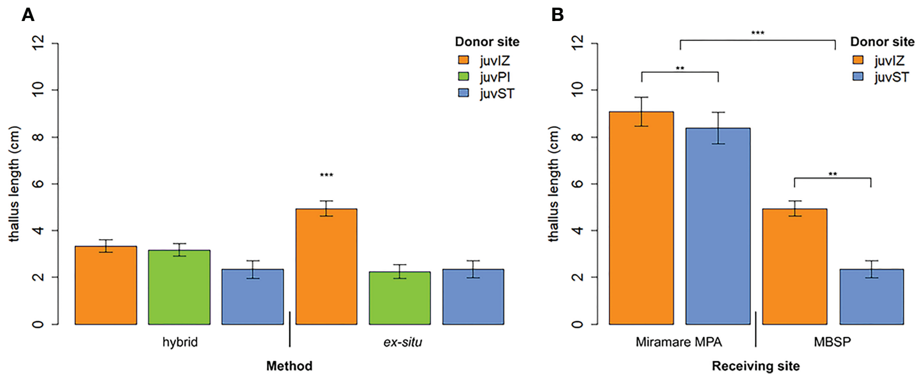

FIGURE 7
Thallus length (mean ± SE) after 7 months in the field (November 2021) **(A)** comparing juvIZ, juvST and juvPI and the two outplanting methods at the receiving site in front of the MBSP; **(B)** comparing juvIZ and juvST in the two receiving sites (Miramare and MBSP) for the *ex situ* method. Significance levels: '***' p-value < 0.001, '**' p-value < 0.01.

characteristic of this receiving site. The MBSP receiving site is located at the edge of Piran Bay, which has a similar water turbidity, suspension and sedimentation rate as the Izola donor site at the edge of Koper Bay (Ogorelec et al., 1991). In addition, the tiles were placed near an underwater pipe, to prevent the protective cages from being damaged by fishermen's trawls, as the site is not a protected area. However, during monitoring, it was found that the proximity of the pipe reduces hydrodynamics and exposes juvenile thalli to higher sediment resuspension during growth. This may have favoured the growth of juvIZ, which are adapted to similar environmental conditions, and disadvantaged juvST and juvPI. Indeed, sedimentation may be one of the most important factors affecting the survival and development of early life stages of macroalgae (Vadas et al., 1992; Schiel and Foster, 2006; Irving et al., 2009). In addition, the lower frequency of cage cleaning in the MBSP site and the resulting lower light experienced by the juveniles under the cages may have contributed to their slower growth.

For the hybrid method, the main differences were due to the receiving site: the method performed much better at MBSP than at Miramare (Figure 8). As this method performed better at Miramare in 2019 (Savonitto et al., 2021), these poorer results could be related to a series of unfavourable environmental conditions that occurred in the Italian part of the Gulf of Trieste in spring and early summer 2021. An impressive bloom of the jellyfish *Rhizostoma pulmo*, followed by a massive bloom of *Noctiluca scintillans*, which was much more pronounced in the Italian waters than in the Slovenian ones (ARPA FVG, 2021), characterised the area during the laying of the tiles on the lantern nets and in the following crucial weeks (Supplement 3). In addition, the tiles on the lantern nets were colonised by mussel and oyster recruits from June onwards, and

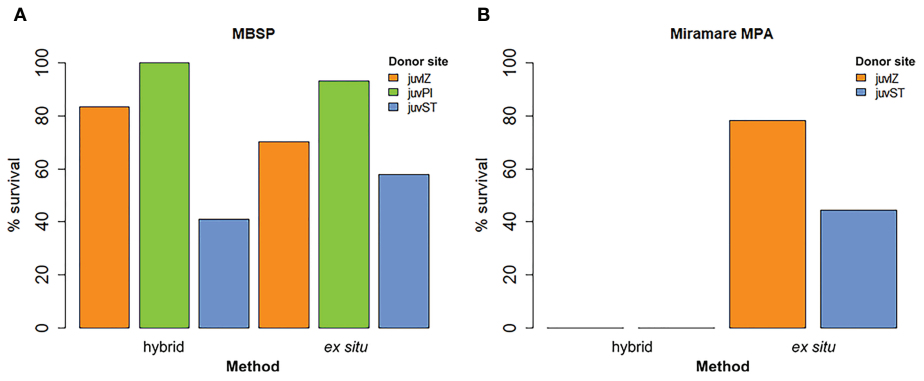

FIGURE 8
Percentage survival data in the hybrid and *ex situ* method in November 2021 in the receiving sites **(A)** in front of the MBSP and **(B)** in Miramare MPA.

this trend intensified in July (i.e., at the time of outplanting on the sea bottom), favoured by a mussel farm near the MPA that probably served as a larval source. Thus, the molluscs probably displaced the *G. barbata* seedlings as already observed in *Cystoseira* populations (Gros, 1978; Benedetti-Cecchi et al., 1996; Thibaut et al., 2005; Mačić et al., 2010; Perkol-Finkel and Airoldi, 2010). Nevertheless, the satisfactory results of the hybrid method at MBSP support the pilot application reported by Savonitto et al. (2021). At MBSP, the lantern net allowed us to successfully reduce the culture time required for seedlings to reach a "refuge size," and it also seemed to limit the presence of mesograzers, which typically occur on vegetated rocky bottoms. In addition, this intermediate step of keeping seedlings in suspended culture in the sea prior to final outplanting on the seafloor reduced the risk of bacterial or microalgal outbreaks, which are common with prolonged culture in mesocosms (Orlando-Bonaca et al., 2021b; Lardi et al., 2022). Nevertheless, it should be further tested in Slovenian coastal waters to improve the outcomes in terms of thalli growth.

Shortened times in mesocosms correspond to reduced maintenance and overall costs, which is necessary for scaling up efforts beyond a purely experimental scale, as is now required by international policies and standards (Gann et al., 2019).

Controlling grazers with protective cages improved overall outplanting performance, as it has already been shown that the loss of a protective cage for only one week resulted in significant overgrazing of juveniles by herbivorous fish (Orlando-Bonaca et al., 2021b). *S. salpa*, which is very abundant in the Miramare MPA and also along the Slovenian coast, is most likely the main predator of *G. barbata* recruits in the Gulf of Trieste, as schools were regularly observed near the experimental plots during monitoring by divers and with the camera also in 2021 (authors' *pers. obs.*). Conversely, the influence of grazing by sea urchins and mesograzers (e.g., molluscs, crustaceans) was likely negligible, as our underwater observations showed. In any case, thalli cannot be kept in a cage indefinitely. In spring 2022, the cage that had protected thalli outplanted in spring 2020 (Orlando-Bonaca et al., 2021b) was removed, and after several months without protection, thalli were bitten at the tips but were at least 30 cm long overall (unpublished data). In contrast, the sharp decline of macroalgae in the Miramare MPA has not only affected *Cystoseira*, as the system has "tipped" into an alternative state dominated by turf algae and other grazing-resistant species (e.g., *Dictyota* spp., crustose calcareous Rhodophytes; Falace et al., 2010; Bevilacqua et al., 2022). Reversing this state would require enormous effort and the constant maintenance of grazing protection, with great uncertainty about the long-term viability of transplanted stands.

Our results suggest that the characteristics of the donor site may confer higher fitness to the cultured seedlings when they are in the field, as shown by the higher growth of juvIZ under sediment resuspension in front of the MBSP.

Despite its late start compared to restoration on land, marine restoration holds enormous potential as an important tool for developing strategies to ensure that the oceans continue to provide the goods and services on which the well-being of life on Earth depends (Danovaro et al., 2021). The results of this study suggest that outplanting of infralittoral canopy-forming species such as *G. barbata* in the northern Adriatic should be further tested and improved, at least on the Slovenian coasts of the Gulf of Trieste. Although the cultivation of *Cystoseira* is already consolidated, albeit with room for improvement (Falace et al., 2018; Verdura et al., 2018; De La Fuente et al., 2019b; Savonitto et al., 2019; Savonitto et al., 2021; Orlando-Bonaca et al., 2021b; Lardi et al., 2022), positive results from the laboratory phase do not guarantee success in outplanting at sea. Successful reestablishment of brown algal forests, even in MPAs, is influenced by factors other than nutrient enrichment and other pollutants, some of which cannot be controlled [i.e., climate change-related trends and events (Grbec et al., 2018), complex and unpredictable environmental dynamics such as jellyfish or *N. scintillans* blooms (ARPA FVG, 2021)] and others that are more measurable/controllable, such as overgrazing by herbivorous fishes (Gianni et al., 2017). Since environmental conditions influenced by both natural and anthropogenic forces appear to play a critical role in restoration effectiveness, monitoring these variables in donor and receiving sites prior to implementing restoration activities can help determine the best location for restoration and/or predict restoration success. As protection is easier and cheaper than restoration, herbivore regulation (to reduce herbivore density) is extremely urgent and should be planned and implemented on a larger regional scale to save not only brown algal forests, but also other endangered infralittoral vegetation and the habitat/biota they sustain.

Data availability statement

The raw data supporting the conclusions of this article will be made available by the authors, without undue reservation.

Author contributions

MO-B: Conceptualization, Investigation, Data curation, Methodology, Writing - original draft, Writing - review & editing. GS: Conceptualization, Investigation, Data curation, Methodology, Formal analysis, Writing - original draft, Writing - review & editing. VA: Data curation, Methodology, Formal analysis, Writing - original draft, Writing - review & editing. DT: Conceptualization, Investigation, Writing - review & editing. VP: Conceptualization, Investigation, Writing - review & editing. MŠ: Investigation, Writing - review & editing. TM: Investigation, Writing - review & editing. PS: Investigation, Writing - review & editing. AL:

Investigation, Writing - review & editing. SC: Conceptualization, Investigation, Writing - review & editing. MC: Writing - review & editing. SK: Investigation, Writing - review & editing. ED: Investigation, Writing - review & editing. MS: Investigation, Writing - review & editing. AF: Conceptualization, Investigation, Data curation, Methodology, Writing - original draft, Writing - review & editing. All authors contributed to the article and approved the submitted version.

Funding

The Slovenian authors acknowledge the project (Factors affecting Adriatic brown algal forests and solutions for habitat restoration, J1-1702) was financially supported by the Slovenian Research Agency. The activities performed by the Italian authors were financed by the LIFE financial instrument of the European Community, project ROC-POP-LIFE (LIFE16 NAT/IT/000816).

Acknowledgments

The Slovenian authors would like to thank Lovrenc Lipej, Leon Lojze Zamuda, Borut Mavrič, Ana Fortič and Tristan Bartole for their help during the fieldwork. All authors thank the reviewers and the editor for their careful review of the manuscript and their constructive comments and suggestions.

Conflict of interest

The authors declare that the research was conducted in the absence of any commercial or financial relationships that could be construed as a potential conflict of interest.

Publisher's note

Supplementary material

The Supplementary Material for this article can be found online at: https://www.frontiersin.org/articles/10.3389/fmars.2022.988584/full#supplementary-material

SUPPLEMENT 1
(A) Receptacles of *Gongolaria barbata* with several conceptacles, **(B)** ostioles, **(C)** the circles indicate the ostioles. The reproductive potential was assessed by counting the number of ostioles per receptacle, as each ostiole is considered as a proxy of a conceptacle; **(D)** the ostiole allows eggs and/or zygotes to emerge from the conceptacle.

SUPPLEMENT 2
Sea temperature and light intensity measured on experimental plates in front of the MBSP from May to December 2021. Trends in sea temperature and light intensity did not deviate significantly, apart from one event. On 18 and 19 July, isolated thunderstorms with showers and north-easterly winds were recorded, leading to a decrease in water temperature.

SUPPLEMENT 3
Unfavourable environmental dynamics that characterized the Italian part of the Gulf of Trieste (northern Adriatic) in spring 2021. **(A)** *Rhizostoma pulmo* on a lantern net in the Miramare MPA (credits: Marco Segarich); **(B)** Jellyfish bloom in Trieste, Italy (credits: Repubblica; https://www.repubblica.it/green-and-blue/2022/04/26/news/bloom_meduse_trieste_riscaldamento_mare_pesca_intensiva-346958254/); *Noctiluca scintillans* bloom **(C)** next to Miramare MPA (credits: Area Marina Protetta Miramare) and d) inside the MPA, on the experimental plots (credits: Legambiente FVG; https://www.legambientefvg.it/component/content/article/2-uncategorised/2411-i-complessi-equilibri-degli-ecosistemi-marini-che-succede-nel-nostro-golfo?Itemid=337).

References

Abelson, A., Reed, D. C., Edgar, G. J., Smith, C. S., Kendrick, G. A., Orth, R. J., et al. (2020). Challenges for restoration of coastal marine ecosystems in the anthropocene. *Front. Mar. Sci.* 7, 544105. doi: 10.3389/fmars.2020.544105

Alberto, F., Raimondi, P., and Reed, D. (2010). Habitat continuity and geographic distance predict population genetic differentiationin giant kelp. *Ecology* 91, 49–56. doi: 10.1890/09-0050.1

Alongi, G., Catra, M., and Cormaci, M. (1999). Fenologia morfologica e riproduttiva di *Cystoseira elegans* sauvageau (Cystoseiraceae, phaeophyta). *Bollett. Accad. Gioenia Sci. Nat. Catania* 31, 189–200.

Ang, P. O.Jr., and De Wreede, R. E. (1992). Density-dependence in a population of *Fucus distichus*. *Mar. Ecol. Prog. Ser.* 90 (2), 169–181. doi: 10.3354/meps090169

ARPA FVG (2021) *Fioritura di "Noctiluca scintillans" e le acque del golfo si colorano di rosso*. Available at: https://www.arpa.fvg.it/temi/temi/acqua/news/fioritura-di-noctiluca-scintillans-e-le-acque-del-golfo-si-colorano-di-rosso/ (Accessed 13 June 2022).

Assis, J., Fragkopoulou, E., Neiva, J., Abecasis, D., Faugeron, S., and Serrão, E. A. (2020). A fine-tuned global distribution dataset of marine forests. *Sci. Data* 7, 1–9. doi: 10.1038/s41597-020-0459-x

Ballesteros, E. (1989). Production of seaweeds in northwestern Mediterranean marine communities: its relation with environmental factors. *Sci. Mar.* 53 (2–3), 357–364. Available at: https://digital.csic.es/handle/10261/28562.

Ballesteros, E., Garrabou, J., Hereu, B., Zabala, M., Cebrian, E., and Sala, E. (2009). Deep-water stands of *Cystoseira zosteroides* c. agardh (Fucales, ochrophyta) in the northwestern Mediterranean: insights into assemblage structure and population dynamics. *Estuar. Coast. Shelf Sci.* 82, 477–484. doi: 10.1016/j.ecss.2009.02.013

Ballesteros, E., Sala, E., Garrabou, J., and Zabala, M. (1998). Community structure and frond size distribution of a deep water stand of *Cystoseira spinosa* (Phaeophyta) in the northwestern Mediterranean. *Eur. J. Phycol.* 33 (2), 121–128. doi: 10.1080/09670269810001736613

Benedetti-Cecchi, L., Nuti, S., and Cinelli, F. (1996). Analysis of spatial and temporal variability in interactions among algae, limpets and mussels in low-shore habitats on the west coast of Italy. *Mar. Ecol. Prog. Ser.* 144, 87–96. doi: 10.3354/meps144087

Bernal-Ibáñez, A., Gestoso, I., Wirtz, P., Kaufmann, M., Serrão, E. A., Canning-Clode, J., et al. (2021). The collapse of marine forests: drastic reduction in populations of the family sargassaceae in Madeira island (NE Atlantic). *Reg. Environ. Change* 21, 71. doi: 10.1007/s10113-021-01801-2

Bevilacqua, S., Vellani, V., Fabbrizio, P., Falace, A., Ciriaco, S., Segarich, M., et al. (2022). Multidecadal monitoring highlighted long-term stability of protected assemblages within a Mediterranean marine reserve. *Estuar. Coast. Shelf Sci.* 274, 107946. doi: 10.1016/j.ecss.2022.107946

Bianchelli, S., Buschi, E., Danovaro, R., and Pusceddu, A. (2016). Biodiversity loss and turnover in alternative states in the Mediterranean Sea: a case study on meiofauna. *Sci. Rep.* 6, 34544. doi: 10.1038/srep34544

Boicourt, W. C., Ličer, M., Li, M., Vodopivec, M., and Malačič, V. (2021). "Sea State: recent progress in the context of climate change," in *Coastal ecosystems in transition: a comparative analysis of the northern Adriatic and Chesapeake bay. geophysical monograph series.* Eds. T. Malone, A. Malej and J. Faganeli (Hoboken, NJ: American Geophysical Union: Wiley), 21–48. doi: 10.1002/9781119543626.ch3

Boudouresque, C. F., and Lück, H. B. (1972). Recherches de bionomie structurale au niveau d'un peuplement benthique sciaphile. *J. Exp. Mar. Biol. Ecol.* 8 (2), 133–144. doi: 10.1016/0022-0981(72)90016-0

Bringloe, T. T., Starko, S., Wade, R. M., Vieira, C., Kawai, H., De Clerck, O., et al. (2020). Phylogeny and evolution of the brown algae. *Crit. Rev. Plant Sci.* 39 (4), 281–321. doi: 10.1080/07352689.2020.1787679

Bruno de Sousa, C., Gangadhar, K. N., Macridachis, J., Pavão, M., Morais, T. R., Campino, L., et al. (2017a). *Cystoseira* algae (Fucaceae): update on their chemical entities and biological activities. *Tetrahedron: Asymmetry* 28, 1486–1505. doi: 10.1016/j.tetasy.2017.10.014

Bruno de Sousa, C., Gangadhar, K. N., Morais, T. R., Conserva, G. A., Vizetto-Duarte, C., Pereira, H., et al. (2017b). Antileishmanial activity of meroditerpenoids from the macroalgae *Cystoseira baccata*. *Exp. Parasitol.* 174, 1–9. doi: 10.1016/j.exppara.2017.01.002

Bulleri, F., Benedetti-Cecchi, L., Cusson, M., Maggi, E., Arenas, F., Aspden, R., et al. (2012). Temporal stability of European rocky shore assemblages: variation across a latitudinal gradient and the role of habitat-formers. *Oikos* 121, 1801–1809. doi: 10.1111/j.1600-0706.2011.19967.x

Bussani, M., and Vuković, A. (1992). Le alghe di miramare. *Hydrores Inf.* 10, 4–48.

Catra, M., Alongi, G., Leonardi, R., Negri, M., Sanfilippo, R., Sciuto, F., et al. (2019). Degradation of a photophilic algal community and its associated fauna from eastern Sicily (Mediterranean Sea). *Mediterr. Mar. Sci.* 20 (1), 74–89. doi: 10.12681/mms.17765

Cheminée, A., Sala, E., Pastor, J., Bodilis, P., Thiriet, P., Mangialajo, L., et al. (2013). Nursery value of *Cystoseira* forests for Mediterranean rocky reef fishes. *J. Exp. Mar. Biol. Ecol.* 442, 70–79. doi: 10.1016/j.jembe.2013.02.003

Clayton, M. N. (1990). The adaptive significance of life history characters in selected orders of marine brown macroalgae. *Aust. J. Ecol.* 15, 439–452. doi: 10.1111/j.1442-9993.1990.tb01469.x

Cozzi, S., Falconi, C., Comici, C., Čermelj, B., Kovač, N., Turk, V., et al. (2012). Recent evolution of river discharges in the gulf of Trieste and their potential response to climate changes and anthropogenic pressure. *Estuar. Coast. Shelf Sci.* 115, 14–24. doi: 10.1016/j.ecss.2012.03.005

Danovaro, R., Aronson, J., Cimino, R., Gambi, C., Snelgrove, P. V. R., and Van Dover, C. (2021). Marine ecosystem restoration in a changing ocean. *Restor. Ecol.* 29 (S2), e13432. doi: 10.1111/rec.13432

De La Fuente, G., Asnaghi, V., Chiantore, M., Thrush, S., Povero, P., Vassallo, P., et al. (2019a). The effect of *Cystoseira* canopy on the value of midlittoral habitats in NW Mediterranean, an emergy assessment. *Ecol. Modell.* 404, 1–11. doi: 10.1016/j.ecolmodel.2019.04.005

De La Fuente, G., Chiantore, M., Asnaghi, V., Kaleb, S., and Falace, A. (2019b). First *ex situ* outplanting of the habitat-forming seaweed *Cystoseira amentacea* var. *stricta* from a restoration perspective. *PeerJ* 7, e7290. doi: 10.7717/peerj.7290

De La Fuente, G., Fontana, M., Asnaghi, V., Chiantore, M., Mirata, S., Salis, A., et al. (2020). The remarkable antioxidant and anti-inflammatory potential of the extracts of the brown alga *Cystoseira amentacea* var. *stricta*. *Mar. Drugs* 19 (1), 2. doi: 10.3390/md19010002

De Paula, E. J., and De Oliveira, E. C. (1982). Wave exposure and ecotypical differentiation in *Sargassum cymosum* (Phaeophyta – fucales). *Phycologia* 21 (2), 145–153. doi: 10.2216/i0031-8884-21-2-145.1

Ercegović, A. (1952). "Jadranske cistozire," in *Sur les cystoseira adriatiques* (Split: Institut za Oceanografiju i Ribarstvo), 212.

Falace, A., Alongi, G., Cormaci, M., Furnari, G., Curiel, D., Cecere, E., et al. (2010). Changes in the benthic algae along the Adriatic Sea in the last three decades. *Chem. Ecol.* 26 (S1), 77–90. doi: 10.1080/02757541003689837

Falace, A., and Bressan, G. (2006). Seasonal variations of *Cystoseira barbata* (Stackhouse) c. agardh frond architecture. *Hydrobiologia* 555 (1), 193–206. doi: 10.1007/s10750-005-1116-2

Falace, A., Kaleb, S., de la Fuente, G., Asnaghi, V., and Chiantore, M. (2018). *Ex situ* cultivation protocol for *Cystoseira amentacea* var. *stricta* (Fucales, phaeophyceae) from a restoration perspective. *PloS One* 13 (2), e0193011. doi: 10.1371/journal.pone.0193011

Falace, A., Zanelli, E., and Bressan, G. (2005). Morphological and reproductive phenology of *Cystoseira compressa* (Esper) gerloff & nizamuddin (Fucales, fucophyceae) in the gulf of Trieste (North Adriatic Sea). *Annales Ser. Hist. Nat.* 15 (1), 71–78. Available at: http://www.dlib.si/details/URN:NBN:SI:doc-QTHLRV24.

Falace, A., Zanelli, E., and Bressan, G. (2006). Algal transplantation as a potential tool for artificial reef management and environmental mitigation. *Bull. Mar. Sci.* 8, 161–166. Available at: https://www.webofscience.com/wos/WOSCC/full-record/000235074300014"WOS:000235074300014.

Gann, G. D., McDonald, T., Walder, B., Aronson, J., Nelson, C. R., Jonson, J., et al. (2019). International principles and standards for the practice of ecological restoration. *Restor. Ecol.* 27, S1–S46. doi: 10.1111/rec.13035

Giaccone, G. (1973). Écologie et chorologie des *Cystoseira* de méditerranée. *Rapp. Commun. Int. Mer Médit.* 22, 49–50.

Gianni, F., Bartolini, F., Airoldi, L., Ballesteros, E., Francour, P., Guidetti, P., et al. (2013). Conservation and restoration of marine forests in the Mediterranean Sea and the potential role of marine protected areas. *Adv. Oceanogr. Limnol.* 4 (2), 83–101. doi: 10.1080/19475721.2013.845604

Gianni, F., Bartolini, F., Pey, A., Laurent, N., Martins, G. M., Airoldi, L., et al. (2017). Threats to large brown algal forests in temperate seas: The overlooked role of native herbivorous fish. *Sci. Rep.* 7, 6012. doi: 10.1038/s41598-017-06394-7

Gómez-Garreta, M., Ribera Siguán, M. A., and Seoane Camba, J. A. (1982). Estudio fenológico de varias especies del género *Cystoseira* en mallorca. *Collect. Bot.* 13 (2), 841–855.

Grbec, B., Matić, F., Beg Paklar, G., Morović, M., Popović, R., and Vilibić, I. (2018). Long-term trends, variability and extremes of *in situ* sea surface temperature measured along the Eastern Adriatic coast and its relationship to hemispheric processes. *Pure Appl. Geophys.* 175, 4031–4046. doi: 10.1007/s00024-018-1793-1

Gros, C. (1978). "Le genre cystoseira sur la côte des albères," in *Répartition - Écologie - morphogenèse* (Université Pierre et Marie Curie, Paris: PhD Thesis).

Hoffmann, L., Renard, R., and Demoulin, V. (1992). Phenology, growth and biomass of *Cystoseira balearica* in calvi (Corsica). *Mar. Ecol. Progr. Ser.* 80 (2), 249–254. doi: 10.3354/meps080249

Irving, A. D., Balata, D., Colosio, F., Ferrando, G. A., and Airoldi, L. (2009). Light, sediment, temperature, and the early life-history of the habitat-forming alga *Cystoseira barbata*. *Mar. Biol.* 156 (6), 1223–1231. doi: 10.1007/s00227-009-1164-7

Iveša, L., Djakovac, T., and Devescovi, M. (2016). Long-term fluctuations in *Cystoseira* populations along the west istrian coast (Croatia) related to eutrophication patterns in the northern Adriatic Sea. *Mar. pollut. Bull.* 106 (1–2), 162–173. doi: 10.1016/j.marpolbul.2016.03.010

Lardi, P. I., Varkitzi, I., Tsiamis, K., Orfanidis, S., Koutsoubas, D., Falace, A., et al. (2022). Early development of *Gongolaria montagnei* (Fucales, phaeophyta) germlings under laboratory conditions, with a view to enhancing restoration potential in the Eastern Mediterranean. *Bot. Mar.* 65 (4), 279–287. doi: 10.1515/bot-2021-0105

Lüning, K. (1991). *Seaweeds: Their environment, biogeography, and ecophysiology* (Hoboken, NJ: Wiley Interscience publication. John Wiley & Son, Inc.) 527.

Mačić, V., Antolic, B., Thibaut, T., and Svirčev, Z. (2010). Distribution of the most common *Cystoseira* c. agardh species (Heterokontophyta, fucales) on the coast of Montenegro (south-east Adriatic sea). *Fresenius Environ. Bull.* 19 (6), 1191–1198. Available at: https://hal.archives-ouvertes.fr/hal-00927240.

Mačić, V., and Svirčev, Z. (2014). Macroepiphytes on *Cystoseira* species (Phaeophyceae) on the coast of Montenegro. *Fresenius Environ. Bull.* 23 (1), 29–34. Available at: https://www.scopus.com/record/display.uri?eid=2-s2.0-84896913751&origin=inward&txGid=75e02f797b95afbd8db2004f018f608d.

Mancuso, F. P., Milazzo, M., and Chemello, R. (2021). Decreasing in patch-size of *Cystoseira* forests reduces the diversity of their associated molluscan assemblage in Mediterranean rocky reefs. *Estuar. Coast. Shelf Sci.* 250, 107163. doi: 10.1016/j.ecss.2020.107163

Mangialajo, L., Chiantore, M., and Cattaneo-Vietti, R. (2008). Loss of fucoid algae along a gradient of urbanisation, and structure of benthic assemblages. *Mar. Ecol. Progr. Ser.* 358, 63–74. doi: 10.3354/meps07400

Mariani, S., Cefalì, M. E., Chappuis, E., Terradas, M., Pinedo, S., Torras, X., et al. (2019). Past and present of fucales from shallow and sheltered shores in Catalonia. *Reg. Stud. Mar. Sci.* 32, 100824. doi: 10.1016/j.rsma.2019.100824

Marzocchi, M., Curiel, D., Dri, C., and Scattolin, M. (2003). Fenologia morfologica e riproduttiva di *Cystoseira barbata* (Stackhouse) c. agardh var. *barbata* (Fucales, fucophyceae) nella laguna di venezia (Nord adriatico). *Lav. Soc Ven. Sc. Nat.* 28, 21–23.

Medrano, A., Hereu, B., Cleminson, M., Pagès-Escolà, M., la Rovira, G., Solà, J., et al. (2020a). From marine deserts to algal beds: *Treptacantha elegans* revegetation to reverse stable degraded ecosystems inside and outside a no-take marine reserve. *Rest. Ecol.* 28 (3), 632–644. doi: 10.1111/rec.13123

Medrano, A., Hereu, B., Mariani, S., Neiva, J., Paulino, C., Rovira, G., et al. (2020b). Ecological traits, genetic diversity and regional distribution of the macroalga *Treptacantha elegans* along the Catalan coast (NW Mediterranean Sea). *Sci. Rep.* 10 (1), 1–10. doi: 10.1038/s41598-020-76066-6

Mhadhebi, L., Laroche-Clary, A., Robert, J., and Bouraoui, A. (2011). Anti-inflammatory, antiproliferative and antioxidant activities of organic extracts from the Mediterranean seaweed, *Cystoseira crinita*. *Afr. J. Biotechnol.* 10, 16682–16690. doi: 10.5897/AJB11.218

Millar, R. B., and Anderson, M. J. (2004). Remedies for pseudoreplication. *Fish. Res.* 70 (2-3), 397–407. doi: 10.1016/j.fishres.2004.08.016

Molinari-Novoa, E., and Guiry, M. (2020). Reinstatement of the genera *Gongolaria* boehmer and *Ericaria* stackhouse (Sargassaceae. phaeophyceae). *Not. Algarum* 172, 1–10.

Mozetič, P., Francé, J., Kogovšek, T., Talaber, I., and Malej, A. (2012). Plankton trends and community changes in a coastal sea (northern adriatic): bottom-up vs. top-down control in relation to environmental drivers. *Estuar. Coast. Shelf Sci.* 115, 138–148. doi: 10.1016/j.ecss.2012.02.009

Munda, I. M. (2000). Long-term marine floristic changes around rovinj (Istrian coast, north Adriatic) estimated on the basis of historical data from Paul kuckuck's field diaries from the end of the 19th century. *Nova Hedwigia* 71 (1–2), 1–36. doi: 10.1127/nova/71/2000/1

Ogorelec, B., Mišič, M., and Faganeli, J. (1991). Marine geology of the gulf of Trieste (northern adriatic): Sedimentological aspects. *Mar. Geol.* 99, 79–92. doi: 10.1016/0025-3227(91)90084-H

Orfanidis, S., Rindi, F., Cebrian, E., Fraschetti, S., Nasto, I., Taskin, E., et al. (2021). Effects of natural and anthropogenic stressors on fucalean brown seaweeds across different spatial scales in the Mediterranean Sea. *Front. Mar. Sci.* 8. doi: 10.3389/fmars.2021.658417

Orlando-Bonaca, M., Francé, J., Mavrič, B., Grego, M., Lipej, L., Flander-Putrle, V., et al. (2015). A new index (MediSkew) for the assessment of the *Cymodocea nodosa* (Ucria) ascherson meadow's status. *Mar. Environ. Res.* 110, 132–141. doi: 10.1016/j.marenvres.2015.08.009

Orlando-Bonaca, M., and Lipej, L. (2005). Factors affecting habitat occupancy of fish assemblage in the gulf of Trieste (Northern Adriatic Sea). *Mar. Ecol.* 26 (1), 42–53. doi: 10.1111/j.1439-0485.2005.00037.x

Orlando-Bonaca, M., and Mavrič, B. (2014). Recurrence of *Sargassum vulgare* c. agardh in Slovenian coastal waters (Adriatic sea). annales. *Ser. Hist. Nat.* 24 (2), 109–114. Available at: https://www.dlib.si/details/URN:NBN:SI:doc-WAXUZLDP.

Orlando-Bonaca, M., Pitacco, V., Bajt, O., Falnoga, I., Jagodic Hudobivnik, M., Mazej, D., et al. (2021c). Spatial and temporal distribution of trace elements in *Padina pavonica* from the northern Adriatic Sea. *Mar. pollut. Bull.* 172, 112874. doi: 10.1016/j.marpolbul.2021.112874

Orlando-Bonaca, M., Pitacco, V., and Lipej, L. (2021a). Loss of canopy-forming algal richness and coverage in the northern Adriatic Sea. *Ecol. Indic.* 125, 107501. doi: 10.1016/j.ecolind.2021.107501

Orlando-Bonaca, M., Pitacco, V., Slavinec, P., Šiško, M., Makovec, T., and Falace, A. (2021b). First restoration experiment for *Gongolaria barbata* in Slovenian coastal waters. what can go wrong? *Plants* 10 (2), 239. doi: 10.3390/plants10020239

Orlando-Bonaca, M., and Rotter, A. (2018). Any signs of replacement of canopy-forming algae by turf-forming algae in the northern Adriatic Sea? *Ecol. Indic.* 87, 272–284. doi: 10.1016/j.ecolind.2017.12.059

Otero-Schmitt, J., and Pérez-Cirera, J. L. (1996). Epiphytism on *Cystoseira* (Fucales, phaeophyta) from the Atlantic coast of northwest Spain. *Bot. Mar.* 39(1–6), 445–465. doi: 10.1515/botm.1996.39.1-6.445

Peleg, O., Guy-Haim, T., Yeruham, E., Silverman, J., and Rilov, G. (2020). Tropicalisation may invert trophic state and carbon budget of shallow temperate rocky reefs. *J. Ecol.* 108 (3), 884–854. doi: 10.1111/1365-2745.13329

Perkol-Finkel, S., and Airoldi, L. (2010). Loss and recovery potential of marine habitats: an experimental study of factors maintaining resilience in subtidal algal forests at the Adriatic sea. *PloS One* 5 (5), e10791. doi: 10.1371/journal.pone.0010791

Pitacco, V., Orlando-Bonaca, M., Mavrič, B., Popovič, A., and Lipej, L. (2014). Mollusc fauna associated with the *Cystoseira* algal associations in the gulf of Trieste (northern Adriatic Sea). *Medit. Mar. Sci.* 15 (2), 225–238. doi: 10.12681/mms.466

Pizzuto, F. (1999). On the structure, typology and periodism of a *Cystoseira brachycarpa* j. agardh emend. giaccone community and of a *Cystoseira crinita* duby community from the eastern coast of Sicily (Mediterranean Sea). *Plant Biosyst.* 133 (1), 15–35. doi: 10.1080/11263509909381529

Rindi, L., Dal Bello, M., and Benedetti-Cecchi, L. (2018). Experimental evidence of spatial signatures of approaching regime shifts in macroalgal canopies. *Ecology* 99, 1709–1715. doi: 10.1002/ecy.2391

Rindi, L., Dal Bello, M., Dai, L., Gore, J., and Benedetti-Cecchi, L. (2017). Direct observation of increasing recovery length before collapse of a marine benthic ecosystem. *Nat. Ecol. Evol.* 1 (6), 1–7. doi: 10.1038/s41559-017-0153

RStudio Team (2021). *RStudio: Integrated development environment for r* (Boston, MA: RStudio, PBC). Available at: https://www.rstudio.com/.

Rull, J. L., and Gómez Garreta, A. (1989). Distribución de las algas epífitas sobre los ejemplares de *Cystoseira mediterranea* sauv. *An. Jardín Bot. Madrid* 46(1), 99–106. Available at: https://dialnet.unirioja.es/servlet/articulo?codigo=2955200.

Sadogurska, S. S., Neiva, J., Falace, A., Serrão, E. A., and Israel, A. (2021). The genus *Cystoseira s.l.* (Ochrophyta, fucales, sargassaceae) in the black Sea: morphological variability and molecular taxonomy of *Gongolaria barbata* and endemic *Ericaria crinita* f. *bosphorica* comb. nov. *Phytotaxa* 480 (1), 1–21. doi: 10.11646/phytotaxa.480.1.1

Sales, M., Cebrian, E., Tomas, F., and Ballesteros, E. (2011). Pollution impacts and recovery potential in three species of the genus *Cystoseira* (Fucales, heterokontophyta). *Estuar. Coast. Shelf Sci.* 92 (3), 347–357. doi: 10.1016/j.ecss.2011.01.008

Savonitto, G., Alongi, G., and Falace, A. (2019). Reproductive phenology, zygote embryology and germling development of the threatened *Carpodesmia barbatula* (= *Cystoseira barbatula*) (Fucales, phaeophyta) towards its possible restoration. *Webbia* 74 (2), 317–323. doi: 10.1080/00837792.2019.1692594

Savonitto, G., de la Fuente, G., Tordoni, E., Ciriaco, S., Srijemsi, M., Bacaro, G., et al. (2021). Addressing reproductive stochasticity and grazing impacts in the restoration of a canopy-forming brown alga by implementing mitigation solutions. *Aquat. Conserv.: Mar. Freshw. Ecosyst.* 31 (7), 1611–1623. doi: 10.1002/aqc.3555

Schiel, D. R., and Foster, M. S. (2006). The population biology of large brown seaweeds: Ecological consequences of multiphase life histories in dynamic coastal environments. *Annu. Rev. Ecol. Evol. Syst.* 37 (1), 343–372. doi: 10.1146/annurev.ecolsys.37.091305.110251

Schneider, C. A., Rasband, W. S., and Eliceiri, K. W. (2012). NIH Image to ImageJ: 25 years of image analysis. *Nat. Methods* 9 (7), 671–675. doi: 10.1038/nmeth.2089

Silva, P. C., Pedroche, F. F., Chacana, M. E., Aguilar-Rosas, R., Aguilar-Rosas, L. E., and Raum, J. (2004). Geographic correlation of morphological and molecular variation in *Silvetia compressa* (Fucaceae, fucales, phaeophyceae). *Phycologia* 43 (2), 204–214. doi: 10.2216/i0031-8884-43-2-204.1

Steen, H., and Scrosati, R. (2004). Intraspecific competition in *Fucus serratus* and *F. evanescens* (Phaeophyceae: Fucales) germlings: Effects of settlement density, nutrient concentration, and temperature. *Mar. Biol.* 144 (1), 61–70. doi: 10.1007/s00227-003-1175-8

Stravisi, F. (1983). The vertical structure annual cycle of the mass field parameters in the gulf of Trieste. *Bollet. Ocean. Teor. Appl.* 1, 239–250. Available at: https://hdl.handle.net/11368/1701345.

Susini, M. L., Mangialajo., L., Thibaut., T., and Meinesz., A. (2007). Development of a transplantation technique of *Cystoseira amentacea* var. *stricta* and *Cystoseira compressa*. *Hydrobiologia* 580 (1), 241–244. doi: 10.1007/s10750-006-0449-9

Thibaut, T., Blanfuné, A., Boudouresque, C. F., and Verlaque, M. (2015). Decline and local extinction of fucales in French Riviera: the harbinger of future extinctions? *Medit. Mar. Sci.* 16 (1), 206–224. doi: 10.12681/mms.1032

Thibaut, T., Pinedo, S., Torras, X., and Ballesteros, E. (2005). Long-term decline of the populations of fucales (*Cystoseira* spp. and *Sargassum* spp.) in the albères coast (France, north-western Mediterranean). *Mar. pollut. Bull.* 50 (12), 1472–1489. doi: 10.1016/j.marpolbul.2005.06.014

Vadas, R. L., S.R., Johnson, S., and Norton, T. A. (1992). Recruitment and mortality of early post-settlement stages of benthic algae. *Br. phycol. Bull.* 27 (3), 331–351. doi: 10.1080/00071619200650291

Verdura, J., Sales, M., Ballesteros, E., Cefalì, M. E., and Cebrian, E. (2018). Restoration of a canopy-forming alga based on recruitment enhancement: methods and long-term success assessment. *Front. Plant Sci.* 9. doi: 10.3389/fpls.2018.01832

Vergés, A., Tomas, F., Cebrian, E., Ballesteros, E., Kizilkaya, Z., Verg, A., et al. (2014). Tropical rabbit fish and the deforestation of a warming temperate sea. *J. Ecol.* 102, 1518–1527. doi: 10.1111/1365-2745.12324

Vizetto-Duarte, C., Custódio, L., Acosta, G., Lago, J. H. G., Morais, T. R., Bruno de Sousa., C., et al. (2016). Can macroalgae provide promising anti-tumoral compounds? a closer look at *Cystoseira tamariscifolia* as a source for antioxidant and anti-hepatocarcinoma compounds. *PeerJ* 4, e1704. doi: 10.7717/peerj.1704

Waltham, N. J., Elliott, M., Lee, S. Y., Lovelock, C., Duarte, C. M., Buelow, C., et al. (2020). UN Decade on ecosystem restoration 2021–2030—What chance for success in restoring coastal ecosystems? *Front. Mar. Sci.* 7. doi: 10.3389/fmars.2020.00071

frontiers | Frontiers in Marine Science

TYPE Original Research
PUBLISHED 01 December 2022
DOI 10.3389/fmars.2022.1049765

Effects of habitat loss on migratory shorebird community structure at stopover sites: A case study in the Yellow River Delta, China

Houlang Duan[1,2]*, Xiubo Yu[1,2], Kai Shan[3], Chenghui Zhang[3] and Haifang Liu[3]

[1]Key Laboratory of Ecosystem Network Observation and Modelling, Institute of Geographic Sciences and Natural Resources Research, Chinese Academy of Sciences, Beijing, China, [2]College of Resources and Environment, University of Chinese Academy of Sciences, Beijing, China, [3]The Yellow River Delta National Nature Reserve Bureau Shandong, Dongying, Shandong, China

Coastal wetlands in China provide important stopover sites for migratory shorebird species. The loss of natural wetlands caused by land reclamation over the past few decades poses a major threat to shorebird populations. Although habitat loss at key stopover sites has been shown to lead to reductions in shorebird populations, the effects of habitat loss at specific stopover sites on shorebird populations remain unclear. Here, we used shorebird diversity indices and landscape metrics to elucidate the long-term (19952020) effects of habitat change on shorebird community structure in the Yellow River Delta, which is an important stopover site for shorebirds along the Yellow Sea coast. The results showed that the habitat area, largest patch index, mean patch area, and the aggregation index decreased over 25 years. By contrast, the number of patches and patch density increased over the same period. The richness, Shannon-Wiener index, Pielou index, and Simpson index of the shorebird community increased from 1995 to 2020, while abundance of shorebird declined by 90.14%. Declines in the abundance of species were more pronounced in larger-bodied ones than in smaller-bodied species (T=1.156, df=42, p=0.02). On the other hand, there were no significant differences in the decline in the abundance of threatened species and non-threatened species (T=-0.483, df=42, p=0.632) and coastal specialist species and generalist/inland specialist species (T=-1.197, df=42, p=0.239). The decrease in mean patch area significantly contributed to the reduction in abundance of shorebirds (N=6, p=0.01), and its effects were more pronounced on larger-bodied ones than on smaller-bodied species (T=-2.113, df=42, p=0.04). These results suggest that habitat loss in the Yellow River Delta has contributed to declines in shorebird populations and that larger-bodied ones are more sensitive to habitat change than smaller-bodied species. Existing wetlands are in urgent need of conservation, and further land reclamation in this region should be avoided. In addition, the development of conservation plans for coastal wetlands

OPEN ACCESS

EDITED BY
Caterina Bergami,
National Research Council (CNR), Italy

REVIEWED BY
Hong Mingsheng,
China West Normal University, China
Gaia Bazzi,
Istituto Superiore per la Protezione e la Ricerca Ambientale (ISPRA), Italy

*CORRESPONDENCE
Houlang Duan
duanhl@igsnrr.ac.cn

SPECIALTY SECTION
This article was submitted to Marine Conservation and Sustainability,
A section of the journal Frontiers in Marine Science

RECEIVED 21 September 2022
ACCEPTED 18 November 2022
PUBLISHED 01 December 2022

CITATION
Duan H, Yu X, Shan K, Zhang C and Liu H (2022) Effects of habitat loss on migratory shorebird community structure at stopover sites: A case study in the Yellow River Delta, China. *Front. Mar. Sci.* 9:1049765.
doi: 10.3389/fmars.2022.1049765

requires consideration of variation in the responses of different functional groups to habitat change.

KEYWORDS

habitat change, shorebird diversity, functional groups, land degradation, conservation and management

1 Introduction

China has over 18,000 km of coastline spanning 11 provinces, municipalities, and autonomous regions, and this coastline supports 40% of the Chinese population; it is also an economically important region that accounts for 58.6% of China's Gross Domestic Product (Yu and Zhang, 2020). Aside from their importance as natural resources, coastal wetlands are key components of the landscape and perform important ecological functions (Zhou et al., 2020). Coastal wetlands in China provide key habitats for migratory waterbirds and biodiverse groups of neritic organisms (Bai et al., 2015).

China's coasts are considered key habitats for biodiversity conservation. These habitats are continually being lost because of land reclamation and the invasion of alien species driven by economic development (Paulson Institute, 2016; Duan et al., 2022a). According to the second national survey of wetland resources in China in 2014 (SFA, 2014), the surface of coastal wetlands in China has decreased by 21.91% since the first national survey of wetland resources in 2003.

Waterbirds are important indicators of wetland ecosystem health, and their populations are highly sensitive to changes in coastal wetlands (Duan et al., 2020; Wang et al., 2022). Shorebird populations in particular are more sensitive to disturbance compared with other groups of waterbirds (Duan et al., 2022b). Previous surveys have shown that many shorebird populations are declining rapidly because of reductions in tidal flats along the Yellow Sea coast (Studds et al., 2017; Chan et al., 2019). However, these surveys have generally been conducted in wintering regions. A recently published study conducted at a broad geographical scale has shown that the relationship between coastal wetland loss and shorebird population change is weak according to stopover site data collected in the Yellow and Bohai Seas; although large changes in the abundances of shorebirds were observed, bird communities were generally similar between periods at the same sites (Wang et al., 2022). This suggests that the area of the stopover sites on which shorebird populations depend is small; thus, clarifying the relationship between coastal wetland loss and changes in shorebird populations requires studies conducted over small spatial scales.

In addition, quantifying the responses of waterbird populations to habitat changes caused by coastal wetland loss is important for determining which conservation actions need to be taken to mitigate declines in waterbird biodiversity. A previous study has shown that the efficiency of the conservation of waterbird populations and their habitat is enhanced when variation in the response of waterbird functional groups to habitat change is considered (Li et al., 2022). An increasing number of studies have shown that threatened shorebird species, larger-bodied species, and coastal specialist species are less likely to stopover or feed in artificial wetlands (Jackson et al., 2020). Whether the effects of changes in coastal habitats vary among functional groups remains unclear, yet this information is critically important for the development of habitat management plans.

The Yellow River Delta (YRD) is the largest estuarine wetland along the coasts of the Yellow and Bohai Seas. Shorebird populations of more than 20 species in the YRD meet the Ramsar 1% criterion (exceeding 1% of the total population in the flyway) (Xia et al., 2016). There is an inevitable conflict between land development and habitat conservation (Hou et al., 2021). We used shorebird survey data and land-use data to characterize the effects of long-term habitat change (1995–2020) on shorebird populations in the YRD. We hypothesized that habitat changes pose a more serious threat to threatened species, larger-bodied species, and coastal specialist species than to non-threatened species, smaller-bodied species, and generalist/inland specialist species. The findings of this study provide new insights that could aid the conservation and management of key shorebird habitats.

2 Materials and methods

2.1 Study area

This study was conducted in the YRD along the Dongying coast (37°35′N–38°12′N, 118°33′E–119°20′E), which is an important stopover site for migratory shorebirds along the East Asian–Australasian Flyway (EAAF) migratory route (Figure 1). The total area of YRD is 4785.5 km^2, and represents only 4.5% of Yellow and Bohai Seas. It is a Ramsar site and includes the YRD National Nature Reserve, which was established in 1992. This region includes multiple habitat

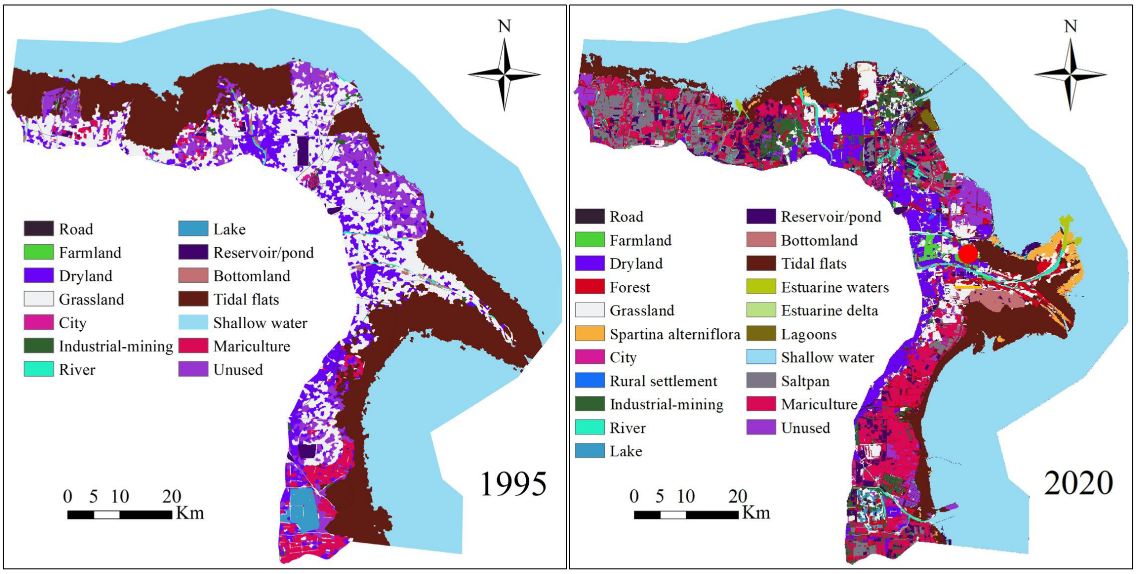

FIGURE 1
Study area of Yellow River Delta and its land use types in 1995 and 2020.

environment, i.e. tidal flats, estuarine delta, saltpan and mariculture. It hosts globally threatened species, such as the Eastern Curlew (Numenius madagascariensis) and Great Knot (Calidris tenuirostris), and the number of total shorebirds migrating northward through this region annually is greater than 130,000 (Li et al., 2018). Most coastal wetlands have been converted to artificial wetlands for mariculture, saltpans, and construction land because of land reclamation (Ma et al., 2019). This has had a significant effect on the surface and quality of shorebird habitat and thus the stability of shorebird populations (Hou et al., 2021).

2.2 Land cover data

Land cover maps of the YRD for 1995, 2000, 2005, 2010, 2015, and 2020 were interpreted using the object-oriented classification method on the basis of Landsat TM/ETM and Landsat 8 OLI data at a scale of 1:100000, and the spatial resolution of these data was 30 m × 30 m. Images with total cloud cover less than 5% were selected from the Geospatial Data Cloud (www.gscloud.cn/sources/) and the USGS Global Visualization Viewer (GloVis) (http://glovis.usgs.gov). The classification system for the land cover map was the same as that used in Di et al. (2014). Given that alien plant *Spartina alterniflora* is a major threat to shorebird species (Jackson et al., 2021), the distribution of *S. alterniflora* in 2010, 2015, and 2020 for the YRD (*S. alterniflora* has been spreading since 2010 [Yu et al., 2022]) at a spatial resolution of 30 m × 30 m was interpreted using object-based image analysis, support vector machine methods, and field investigations on the basis of Landsat OLI. *S. alterniflora* distribution data were obtained from the Northeast Institute of Geography and Agroecology, Chinese Academy Sciences (Mao et al., 2019). We used the “Mosaic To New Raster” tool in ArcGIS 10.5 to merge the *S. alterniflora* distribution layer with the land cover maps for 2010, 2015, and 2020. The land cover data in YRD for 1995 and 2020 see (Figure 1).

2.3 Identification of shorebird habitat

2.3.1 InVEST habitat quality model

The Natural Capital Project has developed a decision-making support software known as the InVEST model (Integrated Valuation of Environmental Services and Tradeoffs; version 3.7.0), and this was used to assess the value of ecosystem services and biodiversity (Hong et al., 2021). The habitat module of the InVEST model was used to assess habitat quality through consideration of habitat type and threat factors (Sharp et al., 2016). The specific equation is below:

$$Q_{xj} = H_j \left(1 - \left(\frac{D_{xj}^z}{D_{xj}^z + k^z} \right) \right) \tag{1}$$

where Q_{xj} is the habitat quality in grid cell x with land type j, H_j represents the habitat suitability in land type j, D_{xj} represents the effects of threat factors on grid cell x with land type j, and z and k are the scaling constant and half-saturation constant, which were 2.5 and 0.5 respectively considered as frequently used value in habitat module of InVEST model (Sharp et al., 2016).

2.3.2 Input data

The InVEST habitat model was affected by habitat type, habitat suitability, threat sources, the sensitivity of habitat to threat factors, threat characteristics, and habitat accessibility. (1) Habitat type for YRD in 1995, 2000, 2005, 2010, 2015, and 2020 was determined at the level of the grid cell at a resolution of 30 m × 30 m, and information on habitat type was extracted from land cover data between 1995 and 2020. Habitat types included farmland, reservoirs/ponds, bottomlands, tidal flats, estuarine waters, estuarine deltas, saltpans, mariculture, and unused land. (2) Habitat suitability was between 0 (lowest suitability) and 1 (highest suitability) and was determined following the method of Li et al. (2018). The habitat suitability of farmland, saltpan, and mariculture was adjusted on the basis of the field investigation. Habitat suitability can be found in Supplementary Table 1, and input Files was in.csv format.

(3) Potential threats to habitat include construction land, roads, invasion of alien species, and the human population. Thus, cities, rural settlements, industrial mining, mariculture, roads, unused land, and the presence of Spartina alterniflora are all considered threat sources. These were extracted from land cover data between 1995 and 2020 at a spatial resolution of 30 m × 30 m. (4) The sensitivity of habitat to threat factors indicates the relative sensitivity of habitat to each threat source. (5) Threat characteristics include the relative intensity, maximum disturbance distance, and type of distance-based decay. Specific parameter values for the sensitivity of habitat to threat factors and threat characteristics were collected from Li et al. (2018) and are provided in Supplementary Table 1; both input files were in.csv format.

(6) Habitat accessibility indicates the relative accessibility of the boundary of protected areas to each threat source. YRD National Nature Reserve was established in 1992 with the aim of reducing the intensity of human activity and conserving biodiversity. YRD National Nature Reserve was divided into three parts on the basis of permissible levels of human activity: the core area, experimental area, and buffer zone. Habitat accessibility data were obtained from the shapefile boundaries of the core area, experimental area, and buffer zone in ArcGIS 10.5. We set the attribute values for the shapefiles of the core area, experimental area, and buffer zone to 0.1, 0.5, and 1.0, respectively, with higher values indicating greater habitat accessibility. The shapefile boundaries of the core area, experimental area, and buffer zone were acquired from the Institute of Geographic Sciences and Natural Resources Research, Chinese Academy of Sciences (http://english.igsnrr.cas.cn/).

2.3.3 Habitat quality assessment

We ran the habitat module of the InVEST model (v3.7.0) using the above input data to estimate the distribution of shorebird habitat in 1995, 2000, 2005, 2010, 2015, and 2020. Habitat quality ranged from 0 to 1, with values closer to 1 indicating high habitat quality. We reclassified the habitat quality values into a binary format in which areas with habitat quality above and below 0.7 were considered suitable and unsuitable shorebird habitat, respectively (Sharp et al., 2016).

2.4 Measurements of landscape metrics

Landscapes can be defined by the spatial relationships among all components including landscape composition and landscape configuration. Landscape composition is mainly related to the presence and area of patches, and landscape configuration refers to the spatial distribution and spatial character of patches within the landscape. They are usually calculated using a spatial pattern analysis program in FRAGSTATS (Kevin and Marks, 1995).

The vector and raster versions of the FRAGSTATS program are used to process shapefiles and raster files, respectively. This study used the raster version to calculate landscape metrics. Raster images of shorebird habitat in.tif format in 1995, 2000, 2005, 2010, 2015, and 2020 were exported using ArcGIS 10.5 and used as the input data in the FRAGSTATS program.

Landscape composition metrics and landscape configuration metrics of shorebird habitat in 1995, 2000, 2005, 2010, 2015, and 2020 for the YRD were calculated using FRAGSTATS (v4.2.1). Landscape composition metrics included total area (TA), largest patch index (LPI), and mean patch area (AREA_MN). Landscape configuration metrics included number of patches (NP), patch density (PD), and the aggregation index (AI). Definitions and methods used to calculate these metrics are provided in Yohannes et al. (2020). TA is the total area of the landscape in hectares. LPI is the proportion of the largest patch to the total area of the landscape. NP represents the number of patches in the landscape. AREA_MN is the average area of patches in the landscape in hectares.

PD represents the sparseness of the patch distribution in the landscape, and it can be calculated by equation (2):

$$PD = \frac{NP}{TA} \tag{2}$$

AI represents the connectivity between patches in the landscape, and larger AI values indicate greater aggregation. It was calculated using equation (3):

$$AI = \left(\frac{g_{ii}}{Max \rightarrow g_{ii}} \right) \times 100 \tag{3}$$

where gii is the number of similar adjacent patches in the landscape.

We inputted the raster files (.tif format) of shorebird habitat between 1995 and 2020 into FRAGSTATS software (v4.2.1) and calculated the landscape metrics TA, LPI, AREA_MN, NP, PD, and AI at the landscape level. All results were output as.csv files.

2.4.1 Variation in landscape metrics

For each landscape metric, we calculated the percentage rate of change to quantify variation between 1995 and 2020. It was calculated using equation (4):

$$LM_{\text{change}} = \frac{LM_{2020} - LM_{1995}}{LM_{1995}} \times 100 \tag{4}$$

where $\mathrm{LM}_{\text{change}}$ is the percentage rate of change in each landscape metric from 1995 to 2020; LM_{2020} and LM_{1995} represent the landscape metric values in 2020 and 1995, respectively.

2.5 Shorebird data collection and processing

2.5.1 Shorebird data

Shorebird surveys in 2005, 2010, 2015, and 2020 for the YRD were conducted once a month by experienced observers from the YRD National Nature Reserve Management Bureau and Dongying City Bird Watching Association. In addition, shorebird population data for the peak of northward migration in March to May 1995 and 2000 were collected from Barter (2002). Generally, field surveys in the two different survey periods were conducted in the same regions during the daytime on sunny days. The number of shorebird species observed in the YRD is highest during the northward migration period according to previous studies (Bai et al., 2015) therefore, only survey data collected between March and May were compared. For each shorebird species, the highest number of observed individuals between March and May was used as the abundance for that species in each year. Eventually, we acquired the abundance of each shorebird species in 1995, 2000, 2005, 2010, 2015, and 2020.

2.6 Calculation of the diversity index

2.6.1 Diversity index measurement

We calculated several shorebird diversity indices, i.e. richness, abundance, Shannon Wiener index (SHDI), Pielou index (E), and Simpson's Index (D) in 1995, 2000, 2005, 2010, 2015, and 2020. The formulas for SHDI, E, and D are shown below:

$$SHDI = -\sum (p_i) Ln(p_i) \tag{5}$$

$$E = SHDI / Ln(S) \tag{6}$$

$$D = 1 - \sum p_i^2 \tag{7}$$

where p_i is the proportion of the abundance of ith shorebird species of the total abundance in the YRD, and S is the richness.

2.6.2 Change in diversity indices

We calculated differences from 1995 to 2020 in richness, abundance, SHDI, E, and D as follows:

$$DI_{\text{change}} = \frac{DI_{2020} - DI_{1995}}{DI_{1995}} \times 100 \tag{8}$$

where $\mathrm{DI}_{\text{change}}$ represents the difference in each diversity index between 1995 and 2000. DI_{2020} and DI_{1995} are the diversity indices in 2020 and 1995, respectively.

2.7 Relationships between landscape metrics and diversity indices

2.7.1 Test at the community level

To determine how changes in habitat affected shorebird diversity, we conducted partial Mantel tests. A partial Mantel test measures the correlation between two matrices containing measures of distance (Cox and Hinkley, 1974). It has been widely used to characterize the effects of environmental change on communities. Partial Mantel tests are more effective than other types of correlation analyses when sample sizes are low.

In this study, distance matrices were made using six predictor variables, TA, LPI, AREA_MN, NP, PD, and AI, in 1995, 2000, 2005, 2010, and 2020; distance matrices were also made using five response variables, i.e. richness, abundance, SHDI, E, and D, in 1995, 2000, 2005, 2010, and 2020. Partial Mantel tests were run using the linKET package in R version 4.0.4 (Huang, 2021). Detailed code is available at Figshare (http://doi.org/10.6084/m9.figshare.21406911).

2.7.2 Test at the functional group level

The abundance of threatened species, larger-bodied species, and coastal specialist species is lower than the abundance of non-threatened species, smaller-bodied species, and generalist/inland specialist species in artificial wetlands according to a previous study (Jackson et al., 2020). We thus hypothesized that threatened species, larger-bodied species, and coastal specialist species are more vulnerable to the effects of habitat change.

We divided all shorebird species into three sets of two functional groups: threatened species and non-threatened species, larger-bodied species and smaller-bodied species, and coastal specialist species and generalist/inland specialist species. We defined threatened species as globally threatened species, including critically endangered species, endangered species, vulnerable species, and near-threatened species, and non-threatened species as least concern species. The threatened status of shorebird species was determined using the IUCN Red List (https://www.iucnredlist.org/; IUCN, 2022). Jackson et al. (2020)

reported that shorebird species with body mass less than 250 g were more likely to feed in artificial wetlands; we divided shorebird species into two groups, larger-bodied species (i.e., species with body mass greater than 250 g) and smaller-bodied species (i.e., species with body mass less than 250 g). Coastal specialist species and generalist/inland specialist species were classified according to Jackson et al. (2020). Detailed species lists for these six functional groups can be found in Supplementary Table 2.

We calculated changes in the abundance of each species between 1995 and 2020, and using independent two-sample tests in SPSS 22.0 to compare differences in the magnitude of change between functional groups. We also conducted Pearson correlation analysis in SPSS 22.0 to determine the correlation coefficients between AREA_MN and the abundance between 1995 and 2020 for each species at the functional group level. We used independent two-sample tests in SPSS 22.0 to compare differences in correlation coefficients between functional groups. The magnitude of the change and correlation coefficients in the abundance of threatened species, larger-bodied species, and coastal specialist species was greater than that in the abundance of non-threatened species, smaller-bodied species, and generalist/inland specialist species, respectively. We thus suspect that habitat change has pronounced effects on threatened species, larger-bodied species, and coastal specialist species.

3 Results

3.1 Landscape metrics

Shorebird habitats in the Yellow River Delta (YRD) between 1995 and 2020 were mainly distributed along the coastal region according to the InVEST model (Figure 2). Habitat TA and LPI increased initially from 1995 to 2000 and then declined gradually between 2000 and 2020 (Table 1). Habitat total area (TA), largest patch index (LPI) declined by 34.99% and 58.87%, respectively, from 1995 to 2020 (Table 1). Mean patch area (AREA_MN) and aggregation index (AI) declined from 1995 to 2005, increased between 2005 and 2010, and then declined gradually from 2010 to 2020. Generally, AREA_MN decreased by 88.10%, and AI decreased by 2.65% between 1995 and 2020 (Table 1).

Number of patches (NP) and patch density (PD) increased by 441.73% and 725.00%, respectively, between 1995 and 2020. NP and PD increased initially from 1995 to 2005, declined from 2005 to 2010, and then increased gradually between 2010 and 2020 (Table 1).

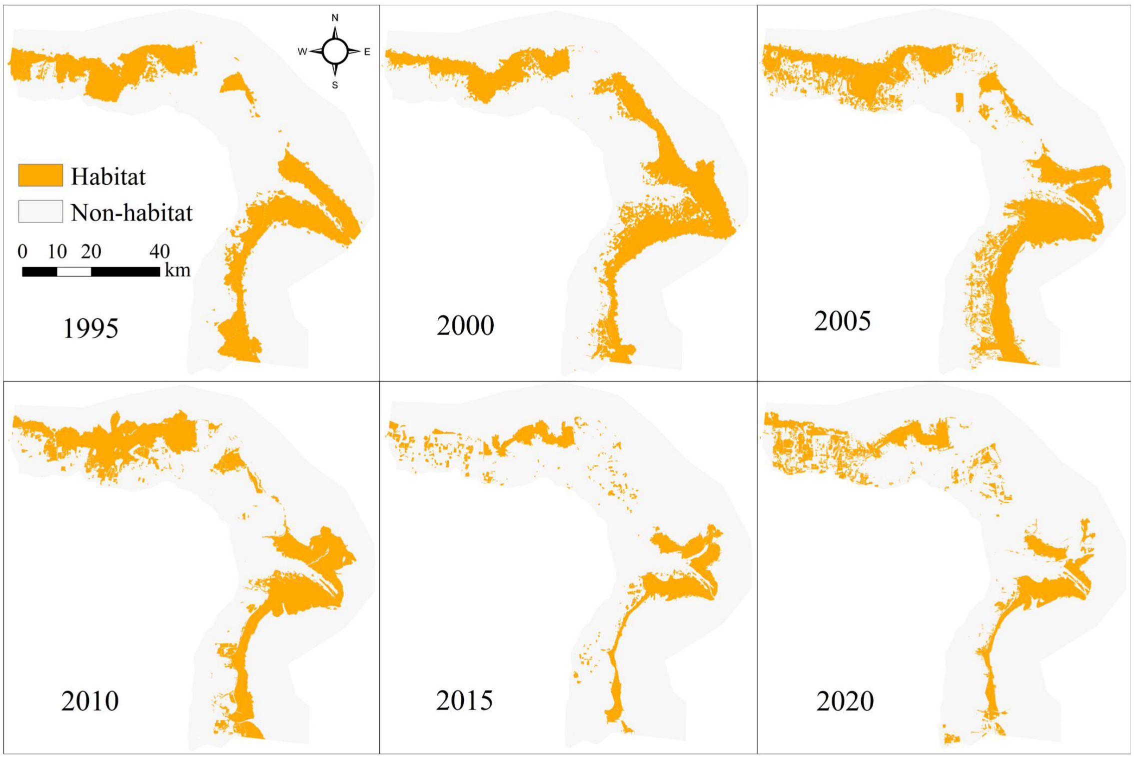

FIGURE 2
The distribution of shorebird habitat in the Yellow River Delta between 1995 and 2020 according to the InVEST model.

TABLE 1 Variation in the landscape metrics of shorebird habitat in the Yellow River Delta between 1995 and 2020.

Landscape metrics of habitat	Year						1995-2020
	1995	2000	2005	2010	2015	2020	Change ratio (%)
Total area (TA) (ha×10^3)	106.49	114.16	132.97	112.21	53.70	69.23	-34.99
Largest patch index (LPI)	53.08	67.79	50.91	50.73	32.58	21.83	-58.87
Mean patch area (AREA_MN)	0.84	0.68	0.28	0.39	0.15	0.10	-88.10
Number of patches (NP)	127	169	480	290	368	688	441.73
Patch density (PD)	0.12	0.15	0.36	0.26	0.69	0.99	725.00
Aggregation index (AI)	99.10	98.77	97.85	98.59	97.63	96.47	-2.65

3.2 Shorebird community structure

3.2.1 Observed shorebirds

A total of 45 shorebird species from 4 orders and 6 families were observed between 1995 and 2020, including 13 globally threatened species and 32 non-threatened species. A total of eight nationally protected species (NPS) were observed, including 1 NPS-Class I species, Nordmann's Greenshank (*Tringa guttifer*), and 7 NPS-Class II species, Eurasian Curlew (*Numenius arquata*), Asian Dowitcher (*Limnodromus semipalmatus*), Eastern Curlew, Great Knot, Ruddy Turnstone (*Arenaria interpres*), Broad-billed Sandpiper (*Limicola falcinellus*), and Little Curlew (*Numenius minutus*). A total of 17 shorebird species between 1995 and 2020 (37.8%) met the Ramsar 1% criterion (exceeding 1% of the total population in the flyway) (Table 2).

3.3 Variation in diversity indices

From 1995 to 2020, the richness, Shannon-Wiener index (SHDI), Pielou index (E), and Simpson index (D) increased by 2.63%, 17.60%, 16.77%, and 2.96%, respectively, and no significant changes were observed in any of these variables. By contrast, the abundance of shorebird species declined sharply from 1995 to 2020, and the overall decline in the abundance over this period was 90.14% (Table 3). The abundance of 19 shorebird species declined, including the Grey Plover (*Pluvialis squatarola*, 98.66% reduction), Dunlin (*Calidris alpina*, 98.59% reduction), Eastern Curlew (98.05% reduction), Lesser Sand Plover (*Charadrius mongolus*, 98.01% reduction), Kentish Plover (*Charadrius alexandrinus*, 97.74% reduction), Bar-tailed Godwit (*Limosa lapponica*, 96.72% reduction), Whimbrel (*Numenius phaeopus*, 96.26% reduction), Little Curlew (95.99% reduction), Common Greenshank (*Tringa nebularia*, 95.73% reduction), Great Knot (94.48% reduction), Spotted Redshank (*Tringa erythropus*, 88.89% reduction), Marsh Sandpiper (*Tringa stagnatilis*, 88.19% reduction), Eurasian Oystercatcher (*Haematopus ostralegus*, 81.58% reduction), Red-necked Stint (*Calidris ruficollis*, 81.54% reduction), Black-tailed Godwit (*Limosa limosa*, 69.43% reduction), Eurasian Curlew (67.67% reduction), Common Sandpiper (*Actitis hypoleucos*, 66.67% reduction), Wood Sandpiper (*Tringa glareola*, 52.63% reduction), and Ruff (*Philomachus pugnax*, 52.63% reduction) (Figure 3).

3.4 Responses of shorebird community structure to habitat change

At the community level, there was a significant positive relationship between the AREA_MN of shorebird habitat and the abundance of shorebird species (N=6, p=0.01) (Figure 4). This result indicated that decreases in the AREA_MN of shorebird habitat from 1995 to 2020 contributed to reductions in the abundance of species. In addition, the AREA_MN of shorebird habitat was not significantly related to other diversity indices including richness, SHDI, E, and D. There were no significant relationships of the landscape metrics TA, LPI, NP, PD, and AI with richness, abundance, SHDI, E, and D.

At the functional group level, the decline in the abundance of larger-bodied species was greater than that of smaller-bodied species (T=1.156, df=42, p=0.02) (Figure 5). There were no significant differences in the decline in the abundance of threatened species and non-threatened species (T=-0.483, df=42, p=0.632) and coastal specialist species and generalist/inland specialist species (T=-1.197, df=42, p=0.239). The correlation coefficient between AREA_MN and the abundance of larger-bodied species was significantly greater than that between AREA_MN and the abundance of smaller-bodied species (T=-2.113, df=42, p=0.04) (Figure 6). This indicates that decreases in AREA_MN had a stronger effect on the abundance of larger-bodied species than on the abundance of smaller-bodied species. The correlation coefficient between AREA_MN and the abundance in threatened species and coastal specialist groups was not significantly higher than that between AREA_MN and non-threatened species (T=1.502, df=42, p=0.141) and between AREA_MN and generalist/inland specialist species (T=1.713, df=42, p=0.09). These findings indicate that the effects of declines in the AREA_MN

TABLE 2 Maximum abundance of shorebirds and their IUCN Red List and conservation status throughout the 25-year survey period.

Taxonomic order	Scientific name	English name	Abundance	1 %criterion	IUCN Red List	Conservation status
Haematopodidae	*Haematopus ostralegus*	Eurasian Oystercatcher	76	Yes	NT	–
Recurvirostridae	*Himantopus himantopus*	Black-winged Stilt	1450	Yes	LC	–
	Recurvirostra avosetta	Pied Avocet	2750	Yes	LC	–
Charadriidae	*Charadrius veredus*	Oriental Dotterel	1	No	LC	–
	Vanellus vanellus	Northern Lapwing	550	No	NT	–
	Charadrius alexandrinus	Kentish Plover	24313	Yes	LC	–
	Pluvialis squatarola	Grey Plover	14899	Yes	LC	–
	Vanellus cinereus	Grey-headed Lapwing	6	No	LC	–
	Charadrius hiaticula	Common Ringed Plover	4	No	LC	–
	Pluvialis fulva	Pacific Golden Plover	62	No	LC	–
	Charadrius dubius	Little Ringed Plover	115	No	LC	–
	Charadrius mongolus	Lesser Sand Plover	201	Yes	LC	–
	Charadrius leschenaultii	Greater Sand Plover	80	No	LC	–
	Charadrius placidus	Long-billed Plover	2	No	LC	–
Rostratulidae	*Rostratula benghalensis*	Greater Painted-snipe	4	No	LC	–
Scolopacidae	*Numenius arquata*	Eurasian Curlew	9766	Yes	NT	II
	Tringa ochropus	Green Sandpiper	7	No	LC	–
	Limosa lapponica	Bar-tailed Godwit	10678	Yes	NT	–
	Limnodromus semipalmatus	Asian Dowitcher	8	No	NT	II
	Numenius madagascariensis	Eastern Curlew	1125	Yes	EN	II
	Calidris tenuirostris	Great Knot	11957	Yes	EN	II
	Arenaria interpres	Ruddy Turnstone	15	No	LC	II
	Tringa erythropus	Spotted Redshank	594	Yes	LC	–
	Calidris alpina	Dunlin	24106	Yes	LC	–
	Limosa limosa	Black-tailed Godwit	7197	Yes	NT	–
	Calidris canutus	Red Knot	450	No	NT	–
	Tringa totanus	Common Redshank	640	No	LC	–
	Calidris ruficollis	Red-necked Stint	2036	No	NT	–
	Actitis hypoleucos	Common Sandpiper	12	No	LC	–
	Calidris acuminata	Sharp-tailed Sandpiper	650	No	VU	–
	Limicola falcinellus	Broad-billed Sandpiper	6	No	LC	II
	Tringa glareola	Wood Sandpiper	321	No	LC	–
	Philomachus pugnax	Ruff	8	No	LC	–
	Xenus cinereus	Terek Sandpiper	220	No	LC	–
	Calidris temminckii	Temminck's Stint	20	No	LC	–
	Tringa nebularia	Common Greenshank	1368	Yes	LC	–
	Calidris alba	Sanderling	15	No	LC	–
	Gallinago gallinago	Common Snipe	25	No	LC	–
	Calidris ferruginea	Curlew Sandpiper	10	No	NT	–
	Numenius minutus	Little curlew	4300	Yes	LC	II
	Tringa guttifer	Nordmann's Greenshank	68	Yes	EN	I
	Tringa stagnatilis	Marsh Sandpiper	1135	No	LC	–
	Calidris subminuta	Long-toed Stint	13	No	LC	–
	Numenius phaeopus	Whimbrel	1444	Yes	LC	–
Glareolidae	*Glareola maldivarum*	Oriental Pratincole	1200	No	LC	–

Critically endangered; CR, endangered; EN, vulnerable; VU, near threatened; NT, Least concern; LC. Species in National Protected Species class I or II were assigned as protected; "-" was not protected. Species meet the Ramsar 1% criterion (exceeding 1% of the total population in the flyway) was marked by 'YES', if not was represented by 'No'.

TABLE 3 Changes in richness, abundance, Shannon-Wiener index, Pielou index, and Simpson index between 1995 and 2020 in the Yellow River Delta.

Indices	Year						1995-2020
	1995	2000	2005	2010	2015	2019	Change ratio (%)
Richness	38	21	21	35	39	39	2.63
Abundance	104564	59503	18083	11295	16750	10313	-90.14
Shonnon-Wiener index	3.15	2.39	3.18	4.16	3.44	3.70	17.60
Pielou index	0.87	0.79	1.04	1.17	0.94	1.01	16.77
Simpson index	0.86	0.75	0.86	0.93	0.82	0.88	2.96

of habitat on the abundance of threatened species and coastal specialist species are similar to the effects of the declines in the AREA_MN of habitat on non-threatened species and generalist/inland specialist species.

4 Discussion

Waterbird diversity is sensitive to environmental change, especially habitat change caused by land reclamation (Lei et al., 2017). In this study, we examined the response of shorebird community structure to habitat changes in the Yellow River Delta, an important stopover site for migratory shorebirds. The total area of habitat, largest patch index, mean patch area, and aggregation index decreased from 1995 to 2020, and the number of patches and patch density increased over this period. The abundance of shorebird species declined over this period, and the richness, Shannon-Wiener index, Pielou index, and Simpson index increased. The decline in the mean patch area of shorebird habitat significantly contributed to the reduction in the abundance of shorebirds, and the decline in the mean patch area had a stronger effect on the abundance of larger-bodied species than on the abundance of smaller-bodied species.

4.1 Changes in the landscape metrics of shorebird habitat

Natural wetlands have degraded and disappeared because of land reclamation and the invasion of *Spartina alterniflora* over the past few decades in the Yellow River Delta (Jackson et al., 2021). These changes have had major effects on the composition and configuration of shorebird habitat. The results of this study indicate that the largest patch index and mean patch area have decreased by more than 50% from 1995 to 2020, and the number of patches and patch density increased by more than 400% and 700%, respectively. This suggests that the continuous decline of coastal wetland habitat has resulted in habitat fragmentation

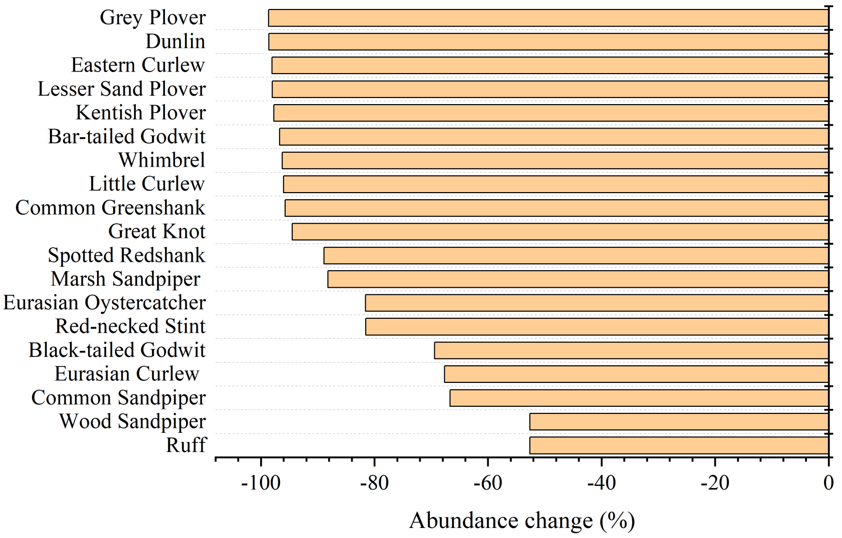

FIGURE 3
Changes in the abundance of shorebird species in the Yellow River Delta from 1995 to 2020.

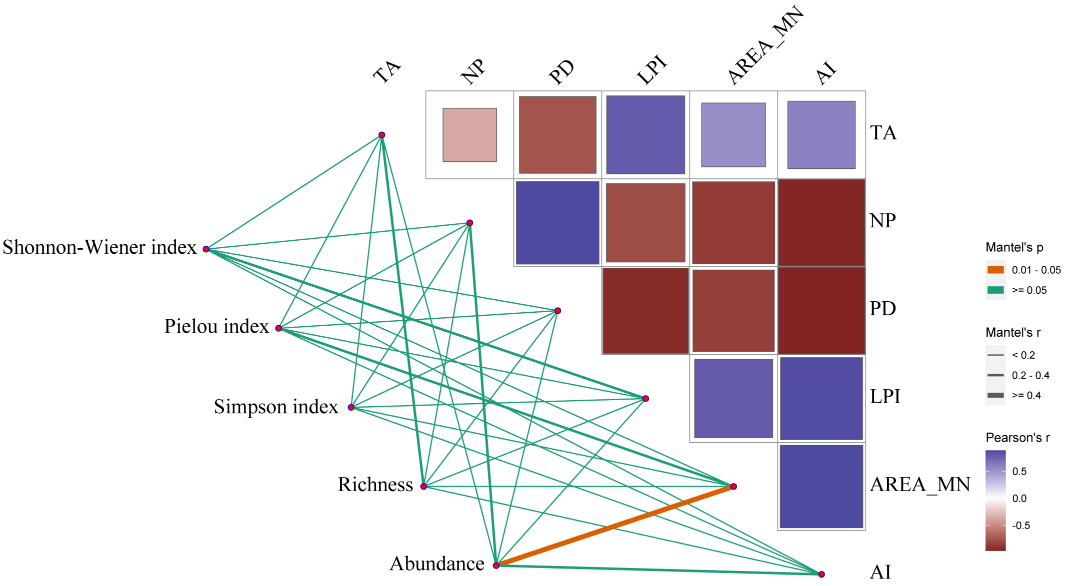

FIGURE 4
Relationships between the landscape metrics of shorebird habitat and shorebird diversity indices in the Yellow River Delta. Pairwise comparisons between shorebird diversity indices and landscape metrics of habitat are indicated by a color gradient denoting Pearson's correlation coefficients. The non-orange lines indicate non-significant relationships, and the orange line indicates a significant relationship ($p< 0.05$). The thickness of the line is positively correlated with the strength of the relationship. TA, total area; LPI, largest patch index; AREA_MN, mean patch area; NP, number of patches; PD, patch density; AI, aggregation index.

because most large patches have been converted to various small patches (Li et al., 2021). Previous studies have indicated that shorebird species prefer large habitat patches (Murray and Fuller, 2015; Zhang et al., 2017); thus, increases in the number of small habitat patches and decreases in habitat TA might pose major threats to the stability of migratory shorebird populations.

4.2 Changes in diversity indices

A total of 45 shorebird species, including 13 globally threatened species, were observed in the Yellow River Delta between 1995 and 2020 during the spring. The abundance of more than 30% of species met the Ramsar 1% criterion (exceeding 1% of the total population in the flyway). This indicates that the Yellow River Delta is a critically important site for the conservation of migratory shorebirds. Its importance has also been demonstrated in a previous study showing that the abundance of 17 shorebird species meets the Ramsar 1% criterion in the Yellow River Delta according to surveys conducted between 2005 and 2013 (Xia et al., 2016).

The total abundance of 45 shorebird species declined from 1995 to 2020, and the overall decline was greater than 90%. Decreases in the abundance of 19 shorebird species were greater than 50%, and these included globally threatened species, such as the Eurasian Oystercatcher, Eurasian Curlew, Bar-tailed Godwit, Eastern Curlew, Great Knot, Black-tailed Godwit, and Red-necked Stint. These findings are consistent with the results of Li et al. (2018) showing that the total abundance of shorebird species has declined by 60.27% and that the abundance of 11 shorebird species has decreased significantly over the last few decades in the Yellow River Delta. These patterns indicate that migratory shorebird species are in need of urgent conservation attention. In addition, the richness, Shannon-Wiener index, Pielou index, and Simpson index of the shorebird community slightly increased between 1995 and 2020. A previous study has shown that artificial wetlands can attract various shorebirds to feed or stopover (Jackson et al., 2019); the conversion of natural wetlands to saltpans and mariculture areas can provide diverse habitats that increase shorebird diversity in the Yellow River Delta.

4.3 Relationship between the shorebird community and habitat changes

At the community level, the sharp reduction in the mean patch area of shorebird habitat contributed to the continuous decline in the total abundance of shorebird species between 1995 and 2020 in the Yellow River Delta. Previous studies have shown that the loss of coastal wetlands in the Yellow Sea region has

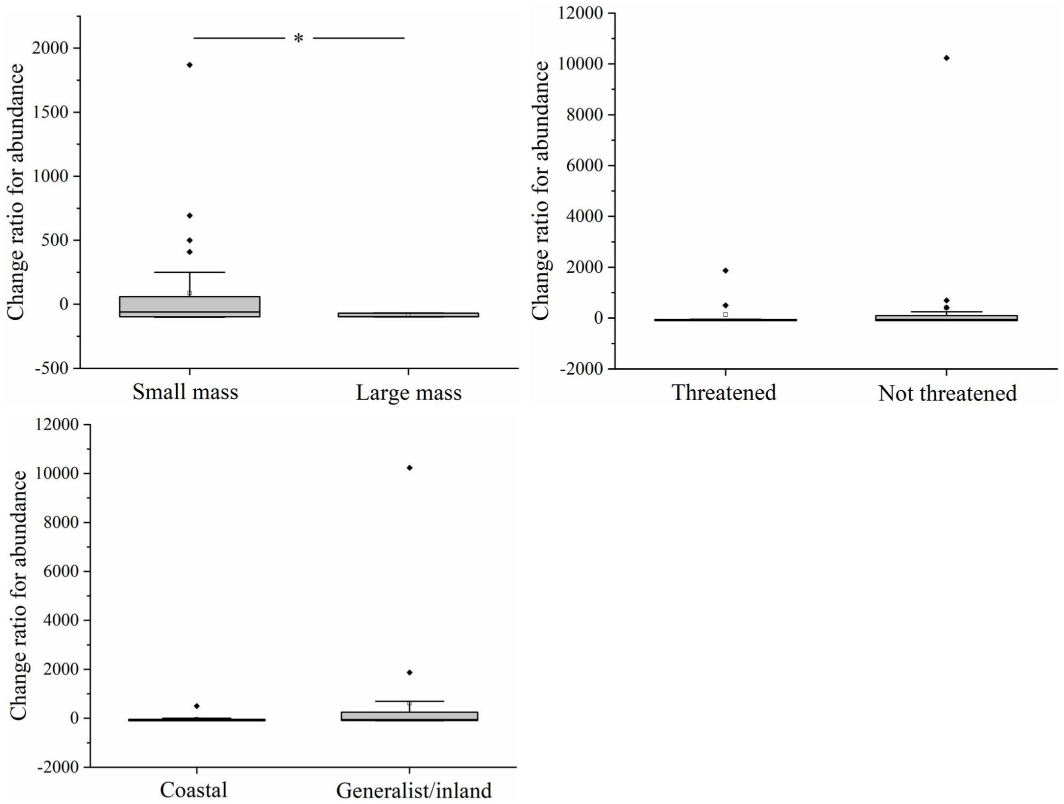

FIGURE 5
Differences in changes in the abundance of each species between functional groups in the Yellow River Delta. White squares represent mean values, horizontal bars within boxes represent median values, the upper and lower limits of boxes represent the maxima and minima, respectively, and whiskers represent 1% and 99%. Black squares represent abnormal value. *means significant at the 0.05 level.

caused declines in the populations of seven shorebird species at an annual rate of 8% (Studds et al., 2017). The Yellow River Delta is an important component of the Yellow Sea region, and this result indicates that habitat loss might pose a serious threat to migratory shorebird species.

At the functional group level, declines in the abundance of larger-bodied species over the past few decades have been more pronounced than those in smaller-bodied species. Larger-bodied shorebird species were more sensitive to declines in mean patch area than smaller-bodied species. A previous study has shown that larger-bodied species are less likely to feed in artificial wetlands (Jackson et al., 2020). This indicates that populations of these species are less capable of adapting to habitat change. Furthermore, there were no significant differences in the effects of declines in the mean patch area on the abundance of threatened species and non-threatened species and the abundance of coastal specialist species and generalist/inland specialist species. This might stem from the small sample sizes because survey data were collected over six periods between 1995 and 2020 in the Yellow River Delta. In addition, the comparison is between 1995 and 2020 only.

4.4 Conservation implications

This study indicate that the habitat loss posed a serious threat to shorebird species, especially larger-bodied species. A previous study has indicated that habitat loss at one stopover site is unlikely to be offset by the conservation of other habitats (Wang et al., 2022); thus, the conservation of existing natural wetlands in the Yellow River Delta is important for maintaining the stability of shorebird populations. The establishment of Yellow River Delta National Nature Reserve have been so far important for reducing human activity and conserving biodiversity. We recommend that the boundary of the reserve be enlarged to include the surrounding habitat that was included in the InVEST model. In addition, the results of this study highlight the urgency with which the conservation of larger-bodied species needs to be prioritized. We recommend that some larger-bodied, globally threatened shorebirds, such as the Eurasian Oystercatcher, Bar-tailed Godwit, and Black-tailed Godwit, be listed as nationally protected species to promote their conservation.

Long-term systematic survey data along with remote sensing data can provide insights into population trends and the factors

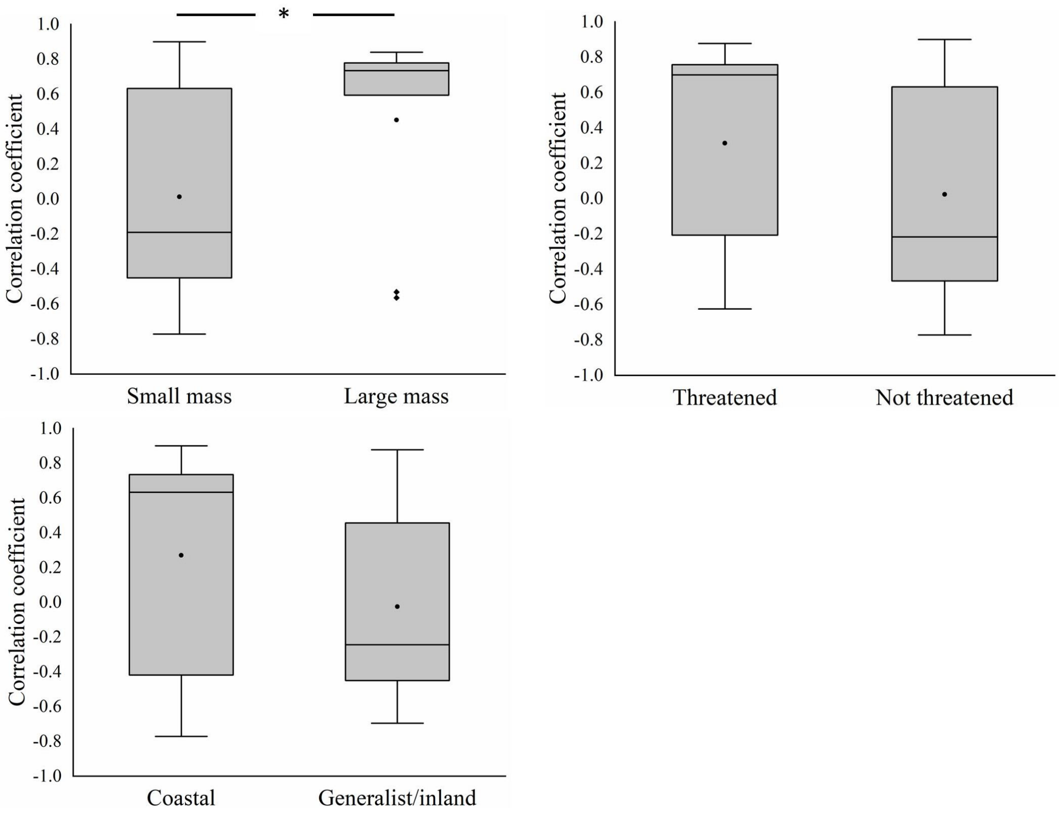

FIGURE 6
Differences in the correlation coefficients between mean patch area and the abundance of different groups of shorebird species in the Yellow River Delta. Black circles represent mean values, horizontal bars within boxes represent median values, the upper and lower limits of boxes represent the maxima and minima, respectively, and whiskers represent 1% and 99%. Black squares represent abnormal value. *means significant at the 0.05 level.

driving them; these data can also aid conservation and management. There is thus a need to clarify the responses of shorebird populations to changes in habitat at the scale of migratory networks, including breeding areas, stopover sites, and non-breeding areas. Shorebird surveys have been conducted in China, South Korea (Moores et al., 2016), Japan (Amano et al., 2010), New Zealand (Riegen and Sagar, 2020), and Australia (Clemens et al., 2016), but not in North Korea and Southeast Asia. The implementation of integrated and standardized monitoring systems is needed to acquire long-term shorebird survey data along the EAAF. Understanding the responses of shorebird populations to environmental changes along their migratory routes should be a central goal of future research.

Data availability statement

The raw data supporting the conclusions of this article will be made available by the authors, without undue reservation.

Ethics statement

Ethical review and approval was not required for the animal study because this study used the shorebird survey data and remote sensing data to reveal the relationship between landscape change on waterbird diversity. It did not include any actions to harm any animal.

Author contributions

XY and HD planned and designed the research; HD, KS, CZ, and HL collected data; HD analyzed data and wrote the manuscript; HD and XY. collaboratively revised the manuscript.

Funding

This research was jointly supported by the National Natural Science Foundation of China (42101105) and the Key

Laboratory of Coastal Environmental Processes and Ecological Remediation, YICCAS (Grant No. 2020KFJJ02).

Acknowledgments

We appreciate Lin Zhang for assistance with mapping. We thank Dehua Mao for providing *Spartina alterniflora* distribution data.

Conflict of interest

The authors declare that the research was conducted in the absence of any commercial or financial relationships that could be construed as a potential conflict of interest.

Publisher's note

Supplementary material

The Supplementary Material for this article can be found online at: https://www.frontiersin.org/articles/10.3389/fmars.2022.1049765/full#supplementary-material

References

Amano, T., Sz´ekely, T., Koyama, K., Amano, H., and Sutherland, W. J. (2010). A framework for monitoring the status of populations: an example from wader populations in the east asian-australasian flyway. *Biol. Conserv.* 143, 2238–2247. doi: 10.1016/j.biocon.2011.06.006

Bai, Q. Q., Chen, J. Z., Chen, Z. H., Dong, G. T., Dong, W. X., Fu Kan, V. W., et al. (2015). Identification of coastal wetlands of international importance for waterbirds: A review of China coastal waterbird surveys 2005–2013. *Avian Res.* 6, 1–16. doi: 10.1186/s40657-015-0021-2

Barter, M. (2002). Shorebirds of the yellow Sea: Importance, threats and conservation status. *Wetland Int. Oceania* 104, 1–299. doi: 10.1071/muv104n3_br1

Chan, Y. C., Tibbitts, T. L., Lok, T., Hasse, C. J., Peng, H. B., Ma, Z., et al. (2019). Filling knowledge gaps in a threatened shorebird flyway through satellite tracking. *J. Appl. Ecol.* 56, 2305–2315. doi: 10.1111/1365-2664.13474

Clemens, R., Rogers, D. I., Hansen, B. D., Gosbell, K., Minton, C. D. T., Straw, P., et al. (2016). Continental-scale decreases in shorebird populations in Australia. *Emu.* 116, 119–135. doi: 10.1071/MU15056

Cox, D. R., and Hinkley, D. V. (1974). *Theoretical statistics* (New York: Chapman and Hall).

Di, X. H., Hou, X. Y., and Wu, L. (2014). Land use classification system for China's coastal zone based on remote sensing. *Res Sci.* 36, 0463–0472.

Duan, H. L., Xia, S. X., Jackson, M. V., Zhao, N., Liu, Y., Teng, J. K., et al. (2020). Identifying new sites of significance to waterbirds conservation and their habitat modification in the yellow and bohai seas in China. *Glob. Ecol. Conserv.* 22, e01031. doi: 10.1016/j.gecco.2020.e01031

Duan, H. L., Yu, X. B., Xia, S. X., and Liu, Y. (2022b). Combining bootstrapping procedure and citizen science data to elucidate waterbirds' dependence on coastal wetland. *Front. Mar. Sci.* 9. doi: 10.3389/fmars.2022.888535

Duan, H. L., Yu, X. B., Zhang, L., Xia, S. X., Liu, Y., Mao, D. H., et al. (2022a). An evaluating system for wetland ecological risk: Case study in coastal mainland China. *Sci. Total Environ.* 828, 154535. doi: 10.1016/j.scitotenv.2022.154535

Hong, H. J., Kim, C. K., Lee, H. W., and Lee, W. K. (2021). Conservation, restoration, and sustainable use of biodiversity based on habitat quality monitoring: A case study on jeju island, south korea, (1989–2019). *Land* 10, 774. doi: 10.3390/land10080774

Hou, X. Y., Nin, J. C., Xing, Q. G., and Yu, X. B. (2021). *Remote sensing on wetland habitat evolution in the yellow river delta* (Beijng: Science Press).

Huang, H. (2021). *linkET: What the package does. r package version 0.0.1 (20200625).*

IUCN (2022) *The IUCN red list of threatened species.* Available at: https://www.iucnredlist.org (Accessed 20 July 2022).

Jackson, M. V., Carrasco, L. R., Choi, C. Y., Li, J., Ma, Z. J., Melville, D. S., et al. (2019). Multiple habitat use by declining migratory birds necessitates joined-up conservation. *Ecol. Evol.* 9, 2505–2515. doi: 10.1002/ece3.4895

Jackson, M. V., Choi, C. Y., Amano, T., Estrella, S. M., Lei, W. P., Moores, N., et al. (2020). Navigating coasts of concrete: Pervasive use of artificial habitats by shorebirds in the Asia-pacific. *Biol. Conserv.* 247, 1–11. doi: 10.1016/j.biocon.2020.108591

Jackson, M. V., Fuller, R. A., Gan, X. J., Li, J., Mao, D. H., Melville, D. S., et al. (2021). Dual threat of tidal flat loss and invasive spartina alterniflora endanger important shorebird habitat in coastal mainland China. *J. Environ. Manage.* 278, 111549. doi: 10.1016/j.jenvman.2020.111549

Kevin, M., and Marks, B. J. (1995). *FRAGSTATS: spatial pattern analysis program for quantifying landscape structure. gen. tech. rep. PNW-GTR-351. Portland, OR* (Pacific Northwest Research Station: U.S. Department of Agriculture, Forest Service), 122.

Lei, G. C., Zhang, Z. W., Yu, X. B., and Zhang, M. X. (2017). *Blueprint of coastal wetland conservation and management in China* (Beijing: Science Press).

Li, X. W., Hou, X. Y., Song, Y., Shan, K., Zhu, S., Yu, X. B., et al. (2018). Assessing changes of habitat quality for shorebirds in stopover sites: a case study in yellow river delta, China. *Wetlands* 39, 67–77. doi: 10.1007/s13157-018-1075-9

Li, Y. F., Mao, D. H., Wang, Z. M., Wang, X., Tan, X. Y., Jia, M. M., et al. (2021). Identifying variable changes in wetlands and their anthropogenic threats bordering the yellow Sea for water bird conservation. *Glob. Ecol. Conserv.* 27, e01613. doi: 10.1016/j.gecco.2021.e01613

Li, N., Tang, N., Wang, Z., and Zhang, L. (2022). Response of different waterbird guilds to landscape changes along the yellow sea coast: A case study. *Ecol. Indic.* 142, 109298. doi: 10.1016/j.ecolind.2022.109298

Ma, T. T., Li, X. W., Bai, J. H., and Cui, B. S. (2019). Habitat modification in relation to coastal reclamation and its impacts on waterbirds along china' s coast. *Glob. Ecol. Conserv.* 17, e00585. doi: 10.1016/j.gecco.2019.e00585

Mao, D. H., Liu, M. Y., Wang, Z. M., Li, L., Man, W. D., Jia, M. M., et al. (2019). Rapid invasion of spartina alterniflora in the coastal zone of mainland China: Spatiotemporal patterns and human prevention. *Sensors* 19, 2308. doi: 10.3390/s19102308

Moores, N., Rogers, D. I., Rogers, K., and Hansbro, P. M. (2016). Reclamation of tidal flats and shorebird declines in saemangeum and elsewhere in the republic of Korea. *Emu.* 116, 136–146. doi: 10.1071/MU16006

Murray, N. J., and Fuller, R. A. (2015). Protecting stopover habitat for migratory shorebirds in East Asia. *J. Ornithol.* 156, 217–225. doi: 10.1007/s10336-015-1225-2

Paulson Institute (2016). *Blueprint of coastal wetland conservation and management in China* (Beijing: Higher Education press. Institute of Geographic Sciences and Natural Resources Research, CAS).

Riegen, A. C., and Sagar, P. M. (2020). Distribution and numbers of waders in New Zealand, 1983-1994 *Notornis.* 67, 591634.

SFA (2014). Results of the second national wetland resources survey in China. *Land Greening* 2), 6–7.

Sharp, R., Tallis, H. T., Ricketts, T., Guerry, A. D., Wood, S. A., Chaplin-Kramer, R., et al. (2016). "InVEST +VERSION+ user's guide. 2018 International Conference on Computing Sciences and Engineering, ICCSE 2018 - Proceedings," (2018). 16 (3), 1–6.

Studds, C. E., Kendall, B. E., Murray, N. J., Wilson, H. B., Rogers, D. I., Clemens, R. S., et al. (2017). Rapid population decline in migratory shorebirds relying on yellow Sea tidal mudflats as stopover sites. *Nat. Commun.* 8, 1–7. doi: 10.1038/ncomms14895

Wang, X. D., Chen, Y., Melville, D. S., Choi, C. Y., Tan, K., Liu, J. J., et al. (2022). Impacts of habitat loss on migratory shorebird populations and communities at stopover sites in the yellow Sea. *Biol. Conserv.* 269, 109547. doi: 10.1016/j.biocon.2022.109547

Xia, S. X., Yu, X. B., Millington, S., Liu, Y., Jia, Y. F., Wang, L. Z., et al. (2016). Identifying priority sites and gaps for the conservation of migratory waterbirds in china's coastal wetlands. *Biol. Conserv.* 210, 72–82. doi: 10.1016/j.biocon.2016.07.025

Yohannes, H., Soromessa, T., Argaw, M., and Dewan, A. (2020). Changes in landscape composition and configuration in the beressa watershed, blue Nile basin of Ethiopian highlands: historical and future exploration. *Heliyon* 6, e04859. doi: 10.1016/j.heliyon.2020.e04859

Yu, X. B., and Zhang, L. (2020). *Green paper of china's coastal wetland conservation* (Beijing: Science Press).

Yu, X. B., Zhang, L., and Yang, B. (2022). *Green paper of china's coastal wetland conservation* (Beijing: Science Press).

Zhang, Q., Ma, K. M., Li, J. Y., and Zhang, Y. X. (2017). The effect of stopover wetlands on migratory waterbirds at different scales: a review. *Acta Ecol. Sin.* 37, 2520–2529. doi: 10.5846/stxb201510262158

Zhou, Y. M., Dou, Y. H., Yu, X. B., Huang, C., Wang, Y. Y., Li, X. W., et al. (2020). Examining health of wetlands with multiple ecosystem services as targets in china's coastal regions. *Chin. Geogr. Sci.* 30, 600–613. doi: 10.1007/s11769-020-1137-9

frontiers | Frontiers in Environmental Science

TYPE Original Research
PUBLISHED 13 December 2022
DOI 10.3389/fenvs.2022.1000087

Long-term monitoring of fish in a freshwater reservoir: Different ways of weighting complex spatial samples

Gashaw C. Tesfaye[1,2], Allan T. Souza[1], Daniel Bartoň[1], Petr Blabolil[1,3], Martin Čech[1], Vladislav Draštík[1], Jaroslava Frouzová[1], Michaela Holubová[1], Luboš Kočvara[1], Tomáš Kolařík[1], Carlos Martinez[1], Karlos R. Moraes[1], Milan Muška[1], Marie Prchalová[1], Milan Říha[1], Zuzana Sajdlová[1], Kateřina Soukalová[1], Marek Šmejkal[1], Michal Tušer[1], Mojmír Vašek[1], Lukáš Vejřík[1], Ivana Vejříková[1], Jiří Peterka[1], Tomáš Jůza[1] and Jan Kubečka[1]*

[1]Institute of Hydrobiology, Biology Centre of CAS, Ceske Budejovice, Czechia, [2]Ethiopian Institute of Agricultural Research, National Fishery and Other Aquatic Life Research Center, Sebeta, Ethiopia, [3]Faculty of Science, University of South Bohemia, Ceske Budejovice, Czechia

OPEN ACCESS

EDITED BY
Robert Ptacnik,
Wasser Cluster Lunz, Austria

REVIEWED BY
Maxime Logez,
Institut National de recherche pour l'agriculture, l'alimentation et l'environnement (INRAE), France
Carla Ferreira Rezende,
Federal University of Ceara, Brazil

*CORRESPONDENCE
Jan Kubečka,
kubecka@hbu.cas.cz

SPECIALTY SECTION
This article was submitted to Freshwater Science, a section of the journal Frontiers in Environmental Science

RECEIVED 21 July 2022
ACCEPTED 01 December 2022
PUBLISHED 13 December 2022

CITATION
Tesfaye GC, Souza AT, Bartoň D, Blabolil P, Čech M, Draštík V, Frouzová J, Holubová M, Kočvara L, Kolařík T, Martinez C, Moraes KR, Muška M, Prchalová M, Říha M, Sajdlová Z, Soukalová K, Šmejkal M, Tušer M, Vašek M, Vejřík L, Vejříková I, Peterka J, Jůza T and Kubečka J (2022), Long-term monitoring of fish in a freshwater reservoir: Different ways of weighting complex spatial samples.
Front. Environ. Sci. 10:1000087.
doi: 10.3389/fenvs.2022.1000087

Anthropogenic activities continue to pose the greatest challenges to freshwater ecosystems. Therefore, long-term monitoring is essential for the management and conservation of these resources. Monitoring programs for freshwater bodies often use a range of indicators, including biological elements such as fish. Existing European standard provides a depth-stratified gillnet sampling approach mainly in benthic habitats and at the deepest part of lakes to account for the uneven distribution of fish. However, the commonly used CEN (European Committee for Standardization) protocol does not weight sufficiently habitat volumes and underrepresent pelagic habitats to calculate whole-lake catch and biomass per unit effort (CPUE and BPUE, respectively). Extended European standard gillnet (4 larger mesh-sizes added in the geometric series) catch data collected over 18 years (2004–2021) in Římov Reservoir (Czech Republic) were used for a method comparison on indices for relative abundance and biomass of fish: CEN protocol without volume-weighting and two volume-weighted approaches. We also evaluated changes in species composition and trends in these fish population over time. Results indicated interannual changes in species composition, relative abundance, and biomass of fish community. The CEN protocol tended to put greater emphasis on benthic habitats which generally have larger CPUE and BPUE. Consequently, the two volume-weighting approaches produced lower estimates of the two parameters, with the exception of the most dominant pelagic bleak *Alburnus alburnus* (L.). All approaches consistently showed an increasing trend in whole-reservoir fish abundance and a decreasing trend in biomass over the study period. Following our assessment, we put forward the volume-weighting approach that considers the Volume of the depth Stratum

(VOST) for weighting as the most realistic approximation of fish populations and therefore recommend its use.

KEYWORDS

abundance, biomass, BPUE, CEN, CPUE, sampling design, species composition, volumeweighting

Introduction

Freshwater ecosystems are one of the most productive ecosystems and support high biodiversity (Dudgeon et al., 2006; Radinger et al., 2019). They provide a wide range of important socioeconomic services, and are vital in regulating and maintaining ecosystem services. In contrast, they are under severe threat due to anthropogenic impacts (Sala et al., 2000; Dudgeon et al., 2006). Anthropogenic influences such as climate change, habitat degradation, alteration of flow patterns, pollution (nutrients and toxic chemicals), over-exploitation, and biological invasions are among the greatest threats to freshwater biodiversity (Dudgeon et al., 2006; Ritterbusch et al., 2022). Freshwater systems are recipients of pollutants and all other anomalies in the watershed and are therefore often highly vulnerable. Unfortunately, they also have limited capacity to dilute significant amounts of wastes and other pressures (Dudgeon et al., 2006). Therefore, regular monitoring and taking timely corrective actions are imperative to address these challenges and sustain their societal benefits and ecological services.

Monitoring programs for freshwater often use a range of indicators, including biological elements, such as plants, invertebrates, fish, and microbes (Davis, 1995). Fish are considered an important bioindicator of the ecological quality of freshwater systems. The importance of fish as bioindicators stems from their biological and ecological attributes. For example, as long-lived organisms, fish can map integrated environmental influences and provide consolidated insight into the state of their environment over extended periods (Harris, 1995; Alexander et al., 2015a; Plessl et al., 2017). In addition, fish play a significant role in structuring ecosystems through trophic interactions and often have a strong influence on community composition, ecological condition, and water quality (Jeppesen et al., 2000; Jakobsen et al., 2004; Alexander et al., 2015a). Furthermore, in a healthy lake and reservoir ecosystem, fish generally occupy all major habitats (i.e., littoral, benthic, and pelagic) and a wide spectrum of trophic niches (Alexander et al., 2015a). However, different fish species prefer and tolerate different physicochemical regimes, so changes in fish community composition can reflect shifting ecological state (Mehner et al., 2005; Alexander et al., 2015a).

Fish community attributes specified in the EU Water Framework Directive (WFD) to be monitored by member states and used in the assessment of freshwater systems include species composition, abundance, and age structure of fish assemblages (European Commission, 2000). In the WFD and fisheries literature, whole-lake estimates of fish catch per unit effort (CPUE) and biomass per unit effort (BPUE) are used as measures of relative fish abundance and biomass, respectively. Information on long-term trends in these fish metrics is critical for most stock assessments, and fishery scientists often use commercial catch rate data (CPUE computed from commercial catch and effort records) to estimate such trends (Hilborn and Walters, 1992; Walters, 2003). However, this widely used approach has been criticized for not fully representing the whole lake system. Walters (2003) pointed out two common mistakes made when analyzing catch rate data. He indicated that the mistakes are related to the use of CPUE at an inappropriate spatial scale: data obtained only from limited fishing grounds are extrapolated to represent the large area (the entire system), and to the fact that unfished strata are usually ignored in the construction of abundance indices—he referred to these as "folly" and "fantasy", respectively. Some techniques have been proposed to address these issues (e.g., Walters, 2003; Campbell, 2004). It has been suggested that depth stratified random sampling, and the use of appropriate statistical techniques might overcome these limitations.

Accordingly, the European Committee for Standardization (CEN) requires member states to apply depth stratified sampling method mainly in benthic habitats, but also at the deepest part (locality) of the lake in pelagic habitats (for lakes with a maximum depth of >10 m) using European standard gillnets (ESG) to account for the uneven distribution of fish (CEN, 2005, 2015). However, whole-lake estimates of CPUE and BPUE derived from gillnet habitats without weighting by habitat volume (commonly referred to as the CEN protocol) may not provide a real picture of the system's fish population because the share of different depth strata is not uniform, and sampling of pelagic habitats is not fully covered. The distribution of fish in elongated reservoirs is also heterogeneous along the longitudinal axis (Vašek et al., 2004; Prchalová et al., 2009a; Vašek et al., 2016). Therefore, simply averaging the abundance and biomass indices of the different species caught by the total number of gillnet habitats (depth strata where gillnets were set) would mean that such habitat and distribution heterogeneity would be unrealistically equally weighted.

Researchers recommended volume-weighting of CPUE and BPUE by considering the volume of habitats and depth layers (strata) addresses this problem (Mehner et al., 2005; Lauridsen et al., 2008; Kubečka et al., 2013; Alexander et al., 2015a; Blabolil et al., 2016). However, previous volume weighting studies have

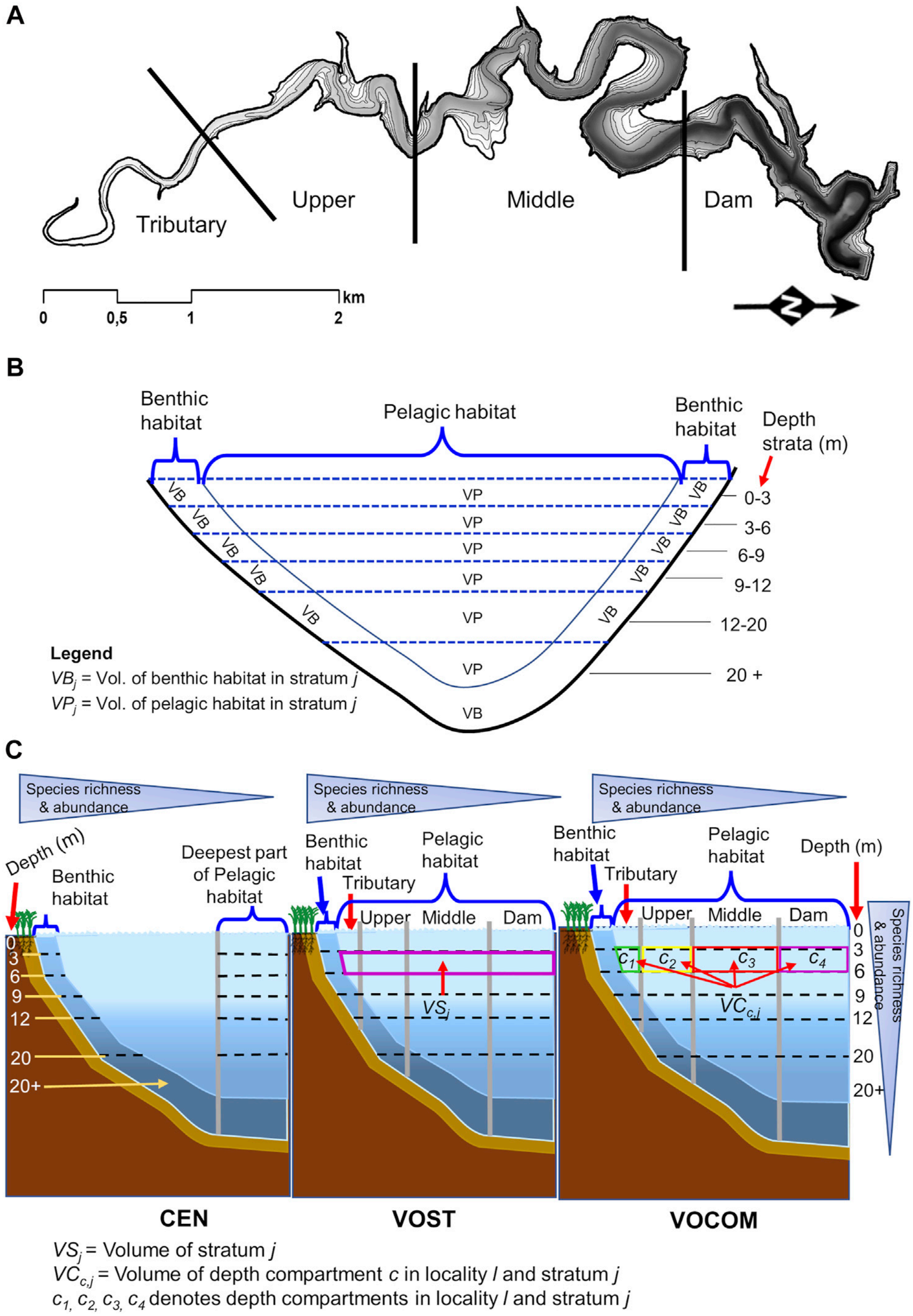

FIGURE 1
Map of Římov Reservoir with depth contours and four reservoir localities **(A)**, schematic representation of habitat definitions on the reservoir transversal cross-section with depth strata for middle and dam localities as an example **(B)**, and schematic representation of habitats on the reservoir cross-section with depth strata and gillnet settings of the three methods (CEN, VOST and VOCOM) **(C)**. The color depth of the gray shading in panel A indicates the depth of the reservoir, and the contour lines refer to the investigated depth strata starting from 0 to 3 m. The number of depth strata decreases from the dam (the deepest point) to the tributary. CEN refers to the European Committee for Standardization protocol, VOST is a method that weights catch rates using the volume of the depth stratum relative to the volume of the reservoir, while VOCOM is a method that weights catch rates using the volume of the depth compartment in each locality and stratum relative to the volume of the reservoir.

TABLE 1 List of fish species and their hybrids known to occur and caught during the sampling period (2004–2021) in Římov Reservoir (Czech Republic). Species caught, and not caught with the modified ESG or unreported before indicated with “yes” and “no”, respectively.

Family*	Scientific name	Common name	References	Present study	Remark[e]
Acipenseridae	*Acipenser* spp.	Sturgeon	a; d	yes	Non-native
Anguillidae	*Anguilla anguilla* (L.)	European eel	a; b	yes	
Nemacheilidae	*Barbatula Barbatula* (L.)	Stone loach	a; b	no	
Centrarchidae	*Lepomis gibbosus* (L.)	Pumpkin seed	a; d	yes	Non-native
Cottidae	*Cottus gobio* (L.)	Bullhead	a; b	no	
Leuciscidae	*Abramis brama* (L.)	Freshwater bream	a; b; c	yes	
Leuciscidae	*Alburnus alburnus* (L.)	Bleak	a; b; c	yes	
Xenocyprididae	*Hypophthalmichthys nobilis* (R.)	Bighead carp	a; d	no	Non-native
Leuciscidae	*Leuciscus aspius* (L.)	Asp	b; c; d	yes	
Cyprinidae	*Barbus barbus* (L.)	Barbel	b; c	yes	
Leuciscidae	*Blicca bjoerkna* (L.)	White bream	a; b; c	yes	
Cyprinidae	*Carassius gibelio* (B.)	Prussian carp	a; c	yes	Non-native
Xenocyprididae	*Ctenopharyngodon idella* (V.)	Grass carp	a; d	no	Non-native
Cyprinidae	*Cyprinus carpio* (L.)	Common carp	a; b; c	yes	Non-native
Gobionidae	*Gobio gobio* (L.)	Gudgeon	a; b; c	yes	
Xenocyprididae	*Hypophthalmichthys molitrix* (V.)	Silver carp	a	no	Non-native
Leuciscidae	*Leuciscus idus* (L.)	Ide	a; d	yes	
Leuciscidae	*Leuciscus leuciscus* (L.)	Dace	b; c	yes	
Leuciscidae	*Phoxinus phoxinus* (L.)	Minnow	a	no	
Gobionidae	*Pseudorasbora parva* (T. and S.)	Topmouth gudgeon	a; d	no	Non-native
Leuciscidae	*Rutilus rutilus* (L.)	Roach	a; b; c	yes	
Leuciscidae	*Scardinius erythrophthalmus* (L.)	Rudd	b; c	yes	
Leuciscidae	*Squalius cephalus* (L.)	Chub	a; b; c	yes	
Tincidae	*Tinca tinca* (L.)	Tench	a; c	yes	
Leuciscidae	*Vimba vimba* (L.)	Vimba bream	no	yes	
Leuciscidae	*A. brama X R. rutilus*	Hybrid bream x roach	b; c; d	yes	
Leuciscidae	*A. brama x S. erythrophthalmus*	Hybrid bream x rudd	no	yes	
Leuciscidae	*A. brama x B. bjoerkna*	Hybrid bream x white bream	d	yes	
Leuciscidae	*R. rutilus X B. bjoerkna*	Hybrid roach x white bream	d	yes	
Esocidae	*Esox lucius* (L.)	Pike	a; b; c	yes	
Percidae	*Gymnocephalus cernua* (L.)	Ruffe	a; b; c	yes	
Percidae	*Perca fluviatilis* (L.)	European perch	b; c	yes	
Percidae	*Sander lucioperca* (L.)	Pikeperch	b; c	yes	
Petromyzontidae	*Lamperta* spp.	Lamprey	a; b	no	
Salmonidae	*Coregonus* spp.	Whitefish	a; c	yes	Non-native
Salmonidae	*Oncorhynchus mykiss* (W.)	Rainbow trout	a; b; c	yes	Non-native

(Continued on following page)

TABLE 1 (*Continued*) List of fish species and their hybrids known to occur and caught during the sampling period (2004–2021) in Římov Reservoir (Czech Republic). Species caught, and not caught with the modified ESG or unreported before indicated with “yes” and “no”, respectively.

Family*	Scientific name	Common name	References	Present study	Remark^e
Salmonidae	*Salmo trutta* (L.)	Brown trout	a; b; c	no	
Salmonidae	*Salvelinus* spp.	Char	a	no	Non-native
Salmonidae	*Thymallus thymallus* (L.)	Grayling	a	no	
Siluridae	*Silurus glanis* (L.)	Wels catfish	a; b; c	yes	

*Family names are updated based on Fricke et al. (2022).

Source: a, Blabolil et al. (2021); b, Hladík et al. (2008); c, Prchalová et al. (2009b), d, Šmejkal et al. (2015); e, Musil et al. (2010).

used stratum volume as a proportion of total reservoir volume to weight catch rates according to the CEN sampling design (protocol). This means that pelagic fish are still underrepresented because sampling was only conducted in the deepest part of the lake or reservoir - which would ultimately result in lower volume-weighted relative abundance and biomass of fish populations and communities in pelagic habitats, so whole-lake estimates do not show a realistic picture of the lake or reservoir system. This is particularly important for large lakes and reservoirs, where nutrient enrichment by inflows and subsequent gradient formation along the longitudinal axis is inevitable (Prchalová et al., 2009a).

Therefore, this study aims to (a) estimate and compare reservoir-wide relative abundance and biomass indices of fish populations and communities, derived from the established CEN protocol and two volume-weighting approaches that consider both depth strata and horizontal gradients (new approach) and depth strata only, (b) assess whether species composition in Římov Reservoir has changed over time, and (c) examine trends in these fish population and community indices over time. To this end, we used gillnet catch data collected over 18 years (2004–2021) in Římov Reservoir (Czech Republic).

Materials and methods

The study area

The study was conducted in the canyon-shaped Římov Reservoir located (48°51′0.257″ N, 14°29′27.409″E) in the České Budějovice district of the Czech Republic (Figure 1A). The reservoir primarily serves as a drinking water supply for South Bohemia, helping to maintain a minimum downstream flow and flood control, and is not open to the public (neither recreational activities nor fishing are allowed). Although the water level fluctuates annually depending on annual precipitation and subsequent inflow from the Malše River (its main tributary), the reservoir has an average surface area of about 206 ha and maximum and average depths of 42 m and 16 m, respectively. The total volume of the reservoir used for the volume-weighting assessment (29.2 million m^3) refers to the volume of the reservoir at a usual water level of 469 m above sea level. It is a eutrophic and mono to dimictic reservoir with summer thermal stratification developing from April to October (Prchalová et al., 2009a).

The reservoir harbors more than 40 freshwater fish species belonging to 15 families (Table 1), including Acipenseridae, Anguillidae, Centrarchidae, Cottidae, Cyprindae, Esocidae, Gobionidae, Leuciscidae, Nemacheilidae, Percidae, Petromyzontidae, Salmonidae, Siluridae, Tincidae, and Xenocyprididae (Hladík et al., 2008; Prchalová et al., 2009b; Šmejkal et al., 2015; Blabolil et al., 2021). As shown in Table 1, about a quarter of the species are non-native species (Musil et al., 2010). Stock enhancement of predatory fish such as asp *Leuciscus aspius* L., pikeperch *Sander lucioperca* L., pike *Esox lucius* L., and wels catfish *Silurus glanis* L., as well as removal of planktivorous leuciscids such as freshwater bream *Abramis brama* L., roach *Rutilus rutilus* L., and bleak *Alburnus alburnus* L., are regular biomanipulation measures to control phytoplankton biomass and thus improve water quality (Jůza et al., 2022). The authors reported that the removal of planktivorous fish has been about 1–2 kg/ha of fish per year, and the rate has increased since 2020 with a new biomanipulation project. According to Vašek et al. (2013), the annual stocking rate of predatory fish in Římov Reservoir from 2004 to 2008 was 0.2 kg ha^{-1} one-summer old fish and about 86 ind. ha^{-1} advanced fry.

Gillnet setting and data collection

The reservoir was divided along its longitudinal axis into four main localities (tributary, upper, middle and dam) to cover the fish distribution following the longitudinal gradients (Figure 1A). These localities were further divided into benthic and pelagic habitats. In each habitat, multiple depth strata (layers) were considered to cover fish distribution along the vertical gradient (water column), and hence, depth-stratified random sampling was conducted in these compartments. Depth ranges generally included 0–3, 3–6, 6–9, 9–12, 12–20 and >20 m for both benthic and pelagic habitats (Figures 1B, C). Deeper layers >6 m of stratified eutrophic reservoir contain little or no fish in summer (Vašek et al., 2004, 2016; Prchalová et al., 2009a).

TABLE 2 Volume of depth strata and compartments (A), and the number of gillnets set (B) in different habitats and localities of the Římov Reservoir at 469 m above sea level–the common surface water level.

(A)	Stratum (m)	Volume of compartments by localities (m^3)				Volume of stratum (m^3)
Habitat		Dam	Middle	Upper	Tributary	
Benthic	0–3	61,602	136,064	70,312	82,377	350,355
Benthic	3–6	65,334	146,330	94,898	61,681	368,243
Benthic	6–9	64,129	144,188	103,022	11,218	322,558
Benthic	9–12	58,050	117,531	87,853	–	263,433
Benthic	12–20	444,980	1,009,980	–	–	1,454,960
Benthic	20 +	264,124	599,488	–	–	863,613
Pelagic	0–3	1,719,433	2,385,955	714,292	145,813	4,965,493
Pelagic	3–6	1,588,814	2,093,205	530,372	22,413	4,234,804
Pelagic	6–9	1,460,088	1,805,320	324,281	–	3,589,688
Pelagic	9–12	1,344,404	1,569,843	148,575	–	3,062,822
Pelagic	12–20	2,695,118	2,166,288	396,200	–	5,257,605
Pelagic	20 +	2,500,627	2,009,959	–	–	4,510,586
Total		12,266,703	14,184,150	2,469,804	323,502	29,244,159

(B)	Stratum (m)	Number of gillnets set in each locality and strata				
Habitat		Dam	Middle	Upper	Tributary	Total
Benthic	0–3	3	3	3	3	12
Benthic	3–6	3	3	3	3	12
Benthic	6–9 (m)	3	3	3	–	9
Benthic	9–12	3	3	–	–	6
Benthic	12–20	3	3	–	–	6
Benthic	20–40	3	3	–	–	6
Pelagic	0–3	3	3	3	3	12
Pelagic	3–6	3	3	–	–	6
Pelagic	6–9	3	3	–	–	6
Pelagic	9–12	-	–	–	–	-
Pelagic	12–20	3	3	–	–	6
Pelagic	20–40	3	3	–	–	6
Total		33	33	12	9	87

Following the recommendations of Blabolil et al. (2017), we reduced the netting effort and strata resolution in deeper layers by using greater depth intervals (12-20, 20 + m) to reduce the sampling effort. It was also found that samplings in deeper layers of many natural and artificial lakes were not informative in terms of relative abundance, and therefore a reduction of sampling effort in deeper layers was proposed (Deceliere-Vergès et al., 2009).

Fish were sampled annually in each stratum and locality during the summer (end of July–August) for 18 years (2004–2021) using modified ESG, which included 12 ESG meshes and an additional four large mesh size gillnets, because standard CEN gillnets capture fish well only up to a standard length of 300 mm (Šmejkal et al., 2015). As many fish in the Římov Reservoir are larger than this threshold, we included data from large mesh nets to ensure that the results cover the entire fish community. The mesh sizes of the ESG follow a geometric series with a ratio of approximately 1.25 (5, 6.25, 8, 10, 12.5, 15.5, 19.5, 24, 29, 35, 43, and 55 mm); each panel is 1.5 m height × 2.5 m length for benthic nets and 3 m × 2.5 m for pelagic nets, and a total panel length of 30 m (both types). The four large mesh nets roughly follow the mean geometric series of the ESG and include mesh sizes of 70, 90, 110, and 135 mm: each panel is 1.5 m height × 10 m length for benthic nets and 3 m × 10 m for pelagic nets, and a total length of 40 m. The large mesh nets (≥70 mm) had four times higher effort (net area) than the CEN standard nets (<70 mm) to catch sufficient numbers of larger fish. Therefore, the catches and net areas of the large mesh gillnets were divided by four to standardize the length of each panel to 2.5 m for all meshes. When all 16 meshes were the same length (2.5 m), catch data was standardized to 1,000 m^2 of net area.

Three gillnets were set parallel to the shore at each locality, depth stratum and habitat (Table 2). All gillnets were deployed 2 hours before dusk and hauled in 2 hours after dawn. All fish caught were then sorted by species, counted, a representative sample of common species and the entire catch weighed to the nearest 0.1 g. Only fish older than young-of-the-year (0+) were considered for this study (scale and otolith reading). Catch data were expressed as catch per unit effort (CPUE), measured as the number of fish caught per 1,000 m^2 of gillnet area, and biomass per unit effort (BPUE) when catch was expressed in kilograms of fish per 1,000 m^2 of gillnet area. The same approach was used to estimate whole-lake CPUE and BPUE. Therefore, for simplicity and to avoid unnecessary repetition, we have used a collective term "value per unit effort" (VPUE) for both CPUE and BPUE in the following formulas and discussion.

Volume estimation

The volume of the depth stratified compartment (denoted VC, in m^3) was calculated from the surface area (m^2) calculated in ArcMAP v10.6.1 (ESRI Inc., CA, United States) based on the depth contours of the bathymetric map (Figure 1A) generated before the reservoir was flooded, and the depth of the stratum (in m). The same depth strata (0–3, 3–6, 6–9, 9–12, 12–20 and >20 m) and localities (tributary, upper, middle and dam) were used during installation of gillnets. The depth of the stratum is the difference between the depth boundaries of two successive strata. Benthic volume was consistent with the results of Moraes et al. (2021) and was defined as the layer 1.5 m above the bottom within each stratum. All remaining volume in each depth stratum was considered pelagic. Then the volume of a stratum (VS., in m^3) was calculated by summing up compartment volumes for the benthic and pelagic habitats separately (Table 2). For example, the volume of a given depth stratum j in the pelagic habitat, VP_j (Figure 1C) was calculated as:

$$VP_j = VC_{jDam} + VC_{jMid} + VC_{jUpp} + VC_{jTrib} \tag{1}$$

Where, VC_{jDam} is the volume of the pelagic habitat of the dam locality of stratum j, $VC_{j\ Mid}$ is the same for the middle locality of stratum j, $VC_{j\ Upp}$ analogically for the upper locality of stratum j, and $VC_{j\ \mathrm{Trib}}$ for tributary locality of stratum j. The same approach applied to calculate the volume of benthic habitat strata, VB_j. The sum of the volumes of all strata in both pelagic and benthic habitat gives the total volume of the reservoir (Table 2).

Data analysis

Species composition

Temporal variation on fish species composition in the reservoir was examined by assessing the changes on percentage composition of dominant species over the sampling period. A literature review was also conducted to explore whether all known species in the system (Table 1) were sufficiently sampled with gillnets or not, and to find out if species were absent or introduced during the last 2 decades.

CEN and volume-weighted whole reservoir relative abundance and biomass

We compared the VPUEs derived from CEN protocol and two volume weighting approaches that considered the reservoir water volume of strata and compartments. Before beginning to determine VPUEs for the entire lake (reservoir) using all approaches, the mean VPUEs of the three nets deployed at each locality and depth stratum were calculated for each habitat. These VPUEs were then used as a baseline for all subsequent analyses.

a) CEN protocol

The whole-lake or reservoir CEN_VPUE$_i$ for species i was calculated as follows:

$$CEN\_VPUE_i = \frac{1}{G_{total}} \left(\sum_{l,j} VPUE_{i,l,j,b} + \sum_{j} VPUE_{i,dam,j,p} \right) \tag{2}$$

where, the first summation refers to the sum of the unweighted VPUEs for species i in locality l and stratum j, but only for benthic habitat b, while the second summation refers to the sum of the unweighted VPUEs for species *i* in stratum *j*, but only for pelagic habitat *p* of the dam (Figures 1B, C); the denominator "G_{total}" denote the total number of benthic gillnet sampling points plus the number of pelagic gillnets in the deepest locality (dam) of the reservoir.

The whole-reservoir unweighted VPUEs for the total fish community (CEN_VPUE) were then calculated as:

$$CEN\_VPUE = \sum_{i=1}^{n} CEN\_VPUE_i \tag{3}$$

b) VOST approach

This method used the **Vo**lume of the depth **St**ratum (hereinafter VOST) as a proportion of the volume of the reservoir for weighting (Figure 1C). This volume-weighting approach accounts for the heterogeneous fish distribution in the different water column layers (Lauridsen et al., 2008; CEN, 2015). Using the VOST approach, the whole-reservoir VPUE for species *i* (VOST_VPUE$_i$) was calculated following the next steps:

The first step is to calculate the mean VPUE of each species *i* in depth stratum *j* and habitat *h* using the following equation:

$$\overline{VPUE}_{i,\,j,\,h} = \frac{1}{n_j} \sum_{j} VPUE_{i,l,j,h} \tag{4}$$

Where, $\overline{VPUE}_{i,\,j,\,h}$ is the mean VPUE of species *i* (ranging from one to *n*) in strata *j* of each habitat *h* (benthic and pelagic) of all localities *l;* $n_{j,h}$ is the number of sampled localities in stratum *j* and habitat *h*, and the summation of VPUE for species *i* was done over all the localities *l* in stratum *j* and habitat *h*. Note that the mean VPUEs obtained using Eq. 4 were calculated separately for each habitat (benthic and pelagic), but to avoid unnecessary duplication, we used the expression *h* here for both habitats.

The mean VPUEs obtained using Eq. 4 were then multiplied by the volume of depth stratum *j* in each habitat *h* as:

$$\overline{VPUE}_{i,\,j,\,h} * VS_{j,h} \tag{5}$$

Where, $\overline{VPUE}_{i,\,j,\,h}$ as defined above, and $VS_{j,h}$ is the volume of the stratum *j* in habitat *h*.

The whole-reservoir VPUE for species *i* (VOST_VPUE$_i$) was then calculated by summing the results obtained in Eq. 5 for each species in all strata and habitats, and dividing by the total volume of the reservoir (V_{total}) as follows:

$$VOST\_VPUE_i = \frac{1}{V_{total}} \sum_{j} \overline{VPUE}_{i,j,h} * VS_{j,h} \tag{6}$$

Then, the annual whole-reservoir VPUEs for the total fish stock (VOST_VPUE) were calculated as:

$$VOST\_VPUE = \sum_{i=1}^{n} VOST\_VPUE_i \tag{7}$$

c) VOCOM approach

On the other hand, VOCOM - the new volume-weighting approach, accounts for the uneven fish distribution along the longitudinal gradient (reservoir localities), as well as the vertical (water column) gradients (Figure 1C; Table 2). Therefore, this weighting approach used the **Vo**lume of the depth Compartment (hereinafter VOCOM) in each locality and stratum as a proportion of the volume of the reservoir for weighting. Thus, the whole-reservoir VPUE for species *i* was calculated following the next steps:

First, the VPUE of species *i* in each locality *l* at the depth compartment *c* of the stratum *j* was multiplied by the volume of the depth compartment in each habitat *h* (Figure 1C; Table 2) as:

$$VPUE_{i,c,l,j,h} * VC_{c,l,j,h} \tag{8}$$

Where, $VPUE_{i,c,l,j,h}$ is VPUE of species *i* (ranging from one to *n*) in the depth compartment *c* of locality *l* and stratum *j* of each habitat *h* (benthic and pelagic), and $VC_{c,l,j,h}$ is volume of depth compartment *c* in locality *l* and stratum *j* of each habitat *h.*

The whole-reservoir VPUE for species *i* (VOCOM_VPUE$_i$) was then calculated by summing the results obtained in Eq. 8 for each species in all depth compartments of strata and habitats and dividing by the total volume of the reservoir (V_{total}) as:

$$VOCOM\_VPUE_i = \frac{1}{V_{total}} \sum_{l,j} \left(VPUE_{i,c,l,j,h} * VC_{c,l,j,h} \right) \tag{9}$$

Then, the whole-reservoir VPUEs for the total fish community (VOCOM_VPUE) were calculated as:

$$VOCOM\_VPUE = \sum_{i=1}^{n} VOCOM\_VPUE_i \tag{10}$$

Statistical analysis

The relative fish abundance and biomass for the whole community and the dominant species were compared using Analysis of covariance (ANCOVA). The ANCOVA was performed separately for each species and for CPUE and BPUE. The estimated weighted and unweighted CPUE and BPUE for each species and the whole community were used as dependent variables, method (CEN, VOST and VOCOM) as grouping or categorical variable (factor) and year as numeric variable (covariate). ANCOVA is a linear model similar to Analysis of variance (ANOVA), but unlike ANOVA, it includes at least one continuous variable, i.e., a covariate. Covariates represent sources of variation that are assumed to affect the dependent variable (response variable) but for which no control was conducted during the study procedures. Thus, including the covariate in the ANCOVA helps to control for the effects of the covariate on the response variable by making linear adjustments to the estimated group means. However, if this variable is not included in the analysis, it would be difficult to assess the true relationship between the factor and the response variable. In our case, we are interested in evaluating the differences between the outputs of the three methods (CEN, VOST and VOCOM) and thus year was included as a covariate so that its influence on the response variable could be accounted for in the model.

The interaction between the categorical and numeric variables was tested to cope with the ANCOVA assumptions of no interaction between these variables. Because their interaction was not significant for almost all groups, the final models were fitted without the interaction between the method (CEN, VOST, VOCOM) and the year. Models were fitted using the *stats* package (R Core Team, 2022). Model premises (e.g., linearity, heteroscedasticity and normality of residuals) and fits were evaluated using the *performance* package (Lüdecke et al., 2021). The means and slopes of the models were extracted using the *modelbased* package (Makowski et al., 2020). All VPUEs except for bleak were transformed (square root or log-transformed) to cope with the model premises as needed. For bleak, raw data were consistent with model premises and therefore were not transformed. Tukey *post hoc* test was then conducted to determine which method resulted in different estimates. Since the interaction between method and year was significant for roach CPUE, its marginal means were computed using the function *estimate_means* from the *modelbased* package. R software, v. 4.2.2 (R Core Team, 2022) was used to process the data and perform the statistical analysis. The figures were created using the *ggplot2* package (Wickham, 2016).

Results

Fish species composition

During the 18-year sampling period, 34,714 specimens of 29 fish species and their hybrids from 11 families were captured, including Acipenseridae, Anguillidae, Centrarchidae, Cyprindae, Esocidae, Gobionidae, Leuciscidae, Percidae, Salmonidae, Siluridae, and Tincidae. Leuciscids were by far the most diverse in terms of species richness (10 species and four hybrids, 48.3% of the total number of species caught), followed by cyprinids (three species, 10.3%) and percids (three species, 10.3%). The other families were represented by only one or two species (Table 1). Of the 29 species and their hybrids, 27 had been reported in previous studies (Table 1). However, about 11 species known to occur in the Římov Reservoir catchment have not been caught once with gillnets (ESG and large-mesh nets) since 2004. The species that were not caught belong to the families Nemacheilidae (stone loach *Barbatula barbatula* L.), Cottidae (bullhead *Cottus gobio* L.), Xenocyprididae (bighead carp *Hypophthalmichthys nobilis* R., sliver carp *Hypophthalmichthys molitrix* V., and grass carp *Ctenopharyngodon Idella* V.), Leuciscidae (minnow *Phoxinus phoxinus* L.), Gobionidae (Topmouth gudgeon), and Salmonidae (brown trout *Salmo trutta* L., char *Salvelinus spp.* and grayling *Thymallus thymallus* L.) (Table 1). However, we caught two leuciscids that have not been previously reported, including the vimba bream *Vimba vimba* L. (caught only in 2021) and hybrid bream *A. brama* x rudd *Scardinius erythrophthalmus* L. (caught in 2009 and 2017).

Of the species caught, about half were not regularly caught during the annual sampling campaign. Overall, only 12 to 17 species and hybrids (15 species on average) were caught annually, with the lowest and highest numbers of species and hybrids caught in 2007 and 2019, respectively (Supplementary Table S1), indicating interannual variation in species composition and abundance. Species such as European eel *Anguilla anguilla* L., Siberian sturgeon *Acipenser baerii B.*, pumpkinseed, rainbow trout *Oncorhynchus mykiss* W., whitefish *Coregonus* spp., barbel *Barbus barbus* L., Prussian carp, gudgeon *Gobio gobio* L., ide *Leucisus idus* L., dace *Leucisus leuciscus* L., chub *Squalius cephalus* L., tench *Tinca tinca* L., vimba bream and three leuciscid hybrids (bream *x* rudd, bream *x* white bream *Blicca bjoerkna* L., and roach *x* white bream) were not only caught less frequently, but their catch rates were also very low, so they were excluded from further analysis of relative abundance and biomass of dominant species (however they are still included in the total community results). In addition, although pike and rudd were frequently caught during the sampling period, they were not included in the subsequent analysis of relative abundance and biomass because they were less represented in the gillnet catches. Therefore, our analysis focused primarily on the remaining 10 important species and one hybrid, which accounted for 99.4% of the total fish sampled. These included bleak with a total catch of 14,774 (42.6%), roach 7,766 (22.4%), ruffe *Gymnocephalus cernua* L. 4,469 (12.9%), bream 3,750 (10.8%), perch *Perca fluviatilis* L.1,746 (5.0%), white bream 586 (1.7%), asp 578 (1.7%), pikeperch 362 (1.0%), hybrid bream x roach 307 (0.9%), common carp *Cyprinus carpio* L.110 (0.3%), and wels catfish 39 (0.1%).

Relative abundance and biomass

The different methods used to estimate CPUEs (Figure 2) and BPUEs (Figure 3) for the whole-reservoir yielded different VPUEs (Supplementary Table S2). In general, except for a few years, the CPUEs and BPUEs derived from CEN was bigger than VOST, which was bigger than VOCOM. However, CPUEs in 2009, 2012, 2013 and 2020, as well as BPUEs in 2009, were higher for VOCOM than for VOST, while CEN always generated higher VPUEs than either volume-weighting approach except for BPUEs in 2004 (Figure 3 Total). Comparing the estimated

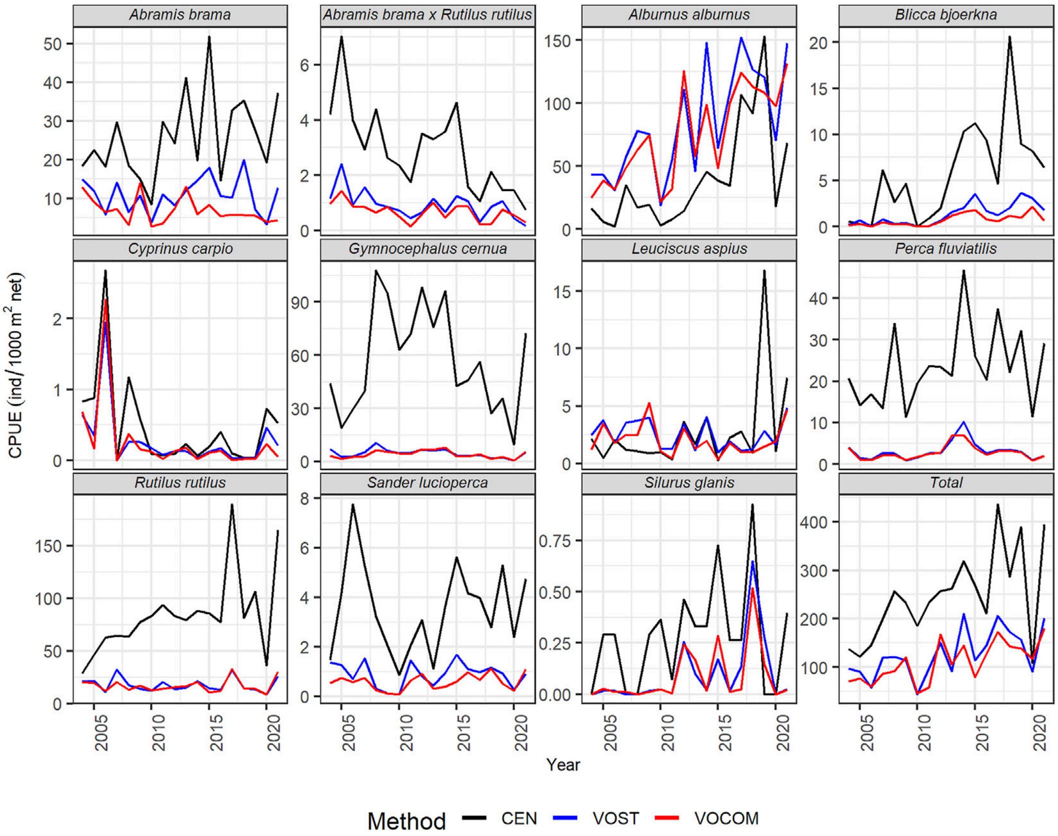

FIGURE 2
Estimated time-series whole-reservoir CPUE of the dominant fish species and the whole fish community (total) in the Římov Reservoir derived from CEN, VOST, and VOCOM approaches.

VPUEs of CEN with VOST VPUEs, the former provided on average of 47% (16%–76%) higher CPUEs and 46% (34%–63%) higher BPUEs. Similarly, the difference between estimates of CEN and VOCOM VPUEs increased by an average of 52% (35%–75%) for CPUEs and by 54% (34%–78%) for BPUEs. In contrast, the difference between the estimates of the two volume-weighting methods was an average of only 11% (−16%–41%) for the CPUEs and only 16% (−11%–44%) for the BPUEs. The negative values here indicate that VOCOM estimates were higher than VOST VPUEs, as noted above for some years.

Looking at the estimates by species, five most abundant species such as roach, ruffe, bleak, bream, and perch contributed an average of 93% (87%–97%) of the CEN CPUEs (Figure 4; Table 3), and 77% (68%–90%) of the BPUEs of the whole reservoir (Figure 4; Table 3). Of these species, roach and ruffe alone contributed a third and a quarter of the total CEN CPUE, respectively, while roach and bream accounted for the same proportion of the total CEN BPUEs. However, the contribution of bleak was only limited to about 14% and 5% for the total CEN CPUEs, and BPUEs, respectively. Moreover, predatory fish (asp, perch, pike, pikeperch, and wels catfish) accounted for 13% (6%–18%), and 21% (10%–36%) of the CEN relative abundance and biomass, respectively (Table 3). The CEN approach showed that perch was the most important predator species in the reservoir, accounting for about 10% of the total relative fish abundance and biomass, and more than three-quarters of the abundance and half of the biomass of the predatory fish (Tables 3).

The contribution of roach, ruffe, bleak, bream, and perch taken together reached to an average of 95% (89%–98%) of the VOST CPUEs, and 75% (47%–89%) of BPUEs of the whole reservoir (Figure 4; Table 3), suggesting that other species also made valuable contributions to VOST BPUEs. For example, common carp and asp contributed to 8% (ranging from <1% to 48%) and 5% (ranging from 1% to 17% of the total VOST BPUEs), respectively, although their contribution to total VOST CPUEs was not substantial. Unlike the CEN approach, bleak alone contributed to an average of 63% (43%–78%) of the total VOST CPUEs, followed by roach at 16% (9%–27%), while bleak, bream, and roach accounted for 21% (7–35%), 24% (12–39%), and 25% (12–40%) of the total VOST BPUEs, respectively (Table 3). Furthermore, in contrast to the CEN approach, the

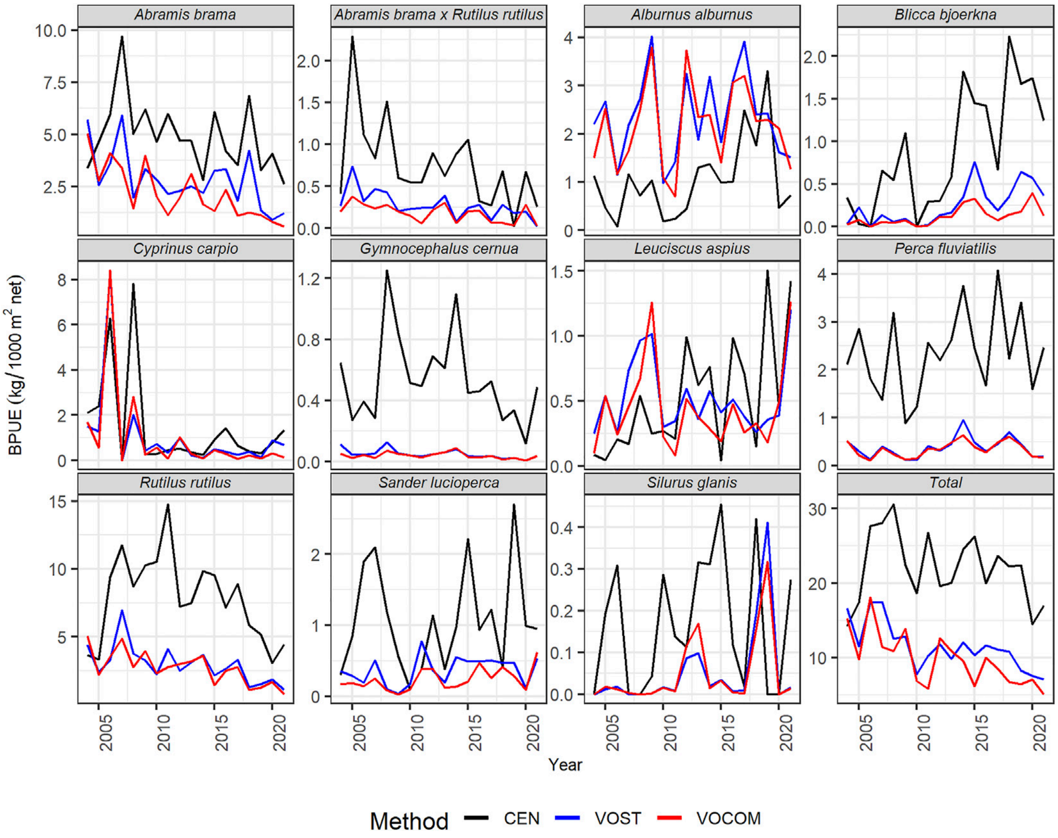

FIGURE 3
Estimated time-series whole-reservoir BPUEs of the dominant fish species and the whole fish community (total) in the Římov Reservoir derived from CEN, VOST, and VOCOM approaches.

five predatory fishes accounted for only 6% (3%–8%), and 13% (4%–30%) of VOST relative abundance and biomass, respectively (Table 3). In contrast to the CEN approach, perch contributed only about 45% of the predator abundance and a quarter of the estimated biomass of VOST.

Similarly, the contribution of roach, ruffe, bleak, bream, and perch reached to an average of 95% (91%–98%) of the VOCOM CPUEs, and 77% (49%–90%) of BPUEs of the whole reservoir (Figure 4; Table 3). In addition, common carp and asp contributed an average of 8% and 5%, respectively, to total VOST BPUEs, although their contribution to total VOCOM CPUEs was still low. Like VOST approach, bleak alone contributed to an average of 64% (36%–83%) of the total VOCOM CPUEs, followed by roach at 17% (8%–29%), while bleak, bream, and roach accounted for 24% (6%–38%), 21% (12%–33%), and 28% (15%–47%) of the total VOCOM BPUEs, respectively (Figure 4; Table 3). Moreover, the five predatory fishes accounted for only 6% (3%–8%), and 14% (3%–42%) of VOCOM relative abundance and biomass, respectively (Table 3). Perch alone contributed about 50% of the predator abundance and nearly a third of the estimated biomass (31%) of VOCOM. Worth noting is the contribution of ruffe (the smallest fish in the system), which accounted for an average of 24% of the total CEN CPUE reduced to only 5% of the total VOST CPUE and to 4% of the total VOCOM CPUE (Table 3).

Statistical evaluation of estimates from the three methods

Looking at the temporal trends in VPUEs, it is generally apparent that abundance of the total fish community showed an increasing trend through time (Figures 2, 5, total), while biomass showed a decreasing trend regardless of the methods used (Figures 3, 6, total). Interannual changes in VPUE varied by species and slightly by methods (Figures 2, 3).

However, the ANCOVA model with the interaction term (method: year) were found to be non-significant ($p > 0.05$) for the whole community and all species except roach CPUE, which showed marginal significance ($p = 0.046$; Tables 4, 5).

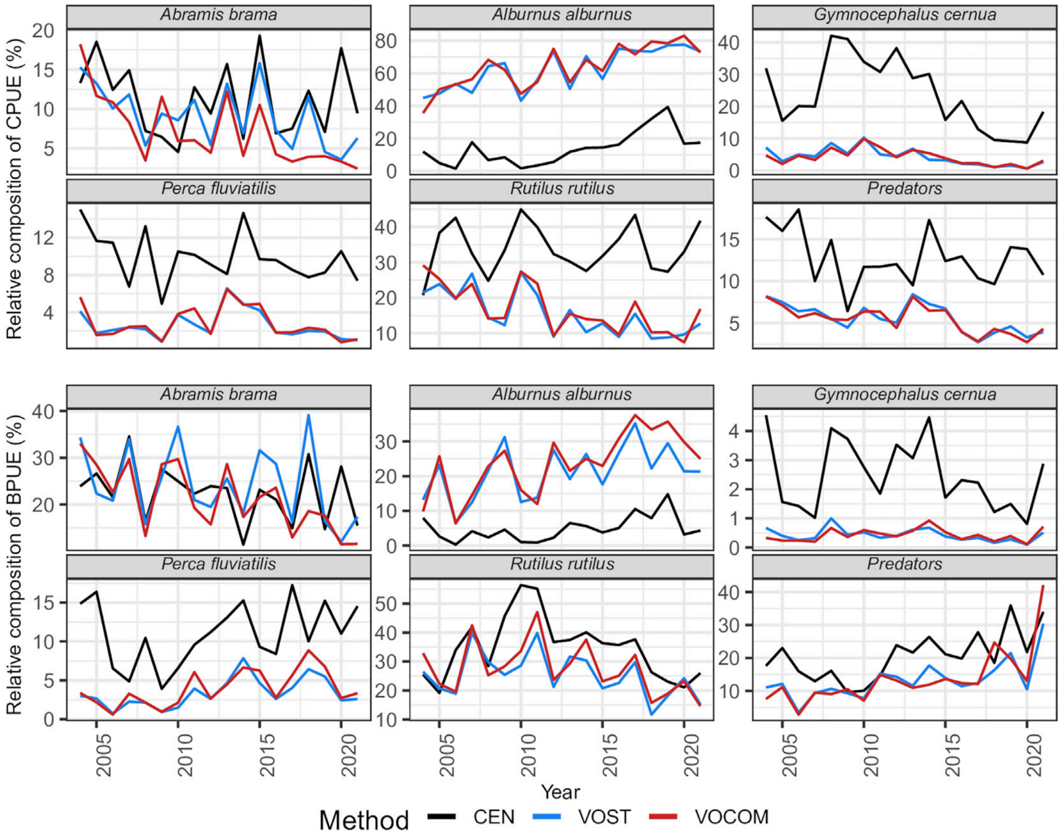

FIGURE 4
Relative composition of five predominant fish species and predators to the estimated total VPUEs of the time series obtained by three approaches (CEN, VOST and VOCOM) in Římov Reservoir.

The significant interaction between method and year for roach CPUE indicates that there were different responses between methods and that trends over time (i.e., slopes) were statistically different for the different methods (Figure 5). On the other hand, the lack of a significant interaction between method and year implies that although VPUEs from CEN were higher than VOST and VOCOM VPUEs for all species except bleak and asp (Figures 5, 6), VPUEs from all three methods decreased or increased at more or less similar extent during the study period. Therefore, the interaction term was not included in our further analysis.

Species that exhibited significant changes ($p < 0.05$) in CPUE over time with our final ANCOVA model (without interaction term) include: bleak, hybrid bream x roach, white bream, common carp and wels catfish, while about half of the species studied, such as bream, ruffe, asp, perch and pikeperch did not show significant changes ($p > 0.05$) over time (Table 6). In contrast, all dominant species except bleak, perch, and wels catfish showed significant changes in BPUE ($p < 0.05$) during the study period (Table 6). The analysis also showed that estimated VPUEs changed over time for the whole community.

Furthermore, comparison of VPUEs derived from CEN, VOST, and VOCOM indicated that community-wide VPUEs for total relative abundance and biomass were significantly different (Table 6). However, the Tukey *post hoc* test showed that VPUEs derived from VOST and VOCOM were similar for the pooled community data, but differed from CEN (Table 6). When examined by individual species, CPUEs and BPUEs derived from CEN, VOST, and VOCOM were also significantly different for all dominant species except common carp and asp ($p < 0.05$). However, the Tukey *post hoc* test for the species with significant test showed that VPUEs derived from VOST and VOCOM were similar for all dominant species but different from CEN (Table 6). Besides, the estimated marginal means, standard errors, and 95% confidence intervals of the three methods for roach CPUE (ind./1000 m^2 net) were 7.50, 0.52, and

TABLE 3 Average whole-reservoir CPUEs (ind./1,000 m^2 net) and BPUE (kg/1,000 m^2 net) from the gillnet catch and percentage contribution of five most dominant species and predators in Římov Reservoir (Czech Republic) obtained using the three different weighting methods.

Species	CEN				VOST				VOCOM			
	CPUE (range)	Mean (%) (range)	BPUE (range)	Mean (%) (range)	CPUE (range)	Mean (%) (range)	BPUE (range)	Mean (%) (range)	CPUE (range)	Mean (%) (range)	BPUE (range)	Mean (%) (range)
A. alburnus	39	14	1.0	5	83	63	2.4	21	75	64	2.2	24
	(2–153)	(2–39)	(0.1–3.3)	(0.3–15)	(19–152)	(43–78)	(1–4)	(7–35)	(22–132)	(36–83)	(0.7–3.8)	(6–38)
A. brama	26	11	4.9	23	11	9	2.8	24	7	7	2.2	21
	(8–52)	(5–19)	(2.6–9.7)	(11–35)	(3–20)	(4–16)	(1–6)	(12–39)	(3–14)	(2–18)	(0.6–5)	(12–33)
P. fluviatilis	24	10	2.4	11	3	3	0.4	3	3	3	0.3	4
	(11–47)	(5–15)	(0.9–4.1)	(4–17)	(1–10)	(1–7)	(0.1–1)	(1–8)	(1–7)	(1–7)	(0.1–0.6)	(1–9)
R. rutilus	84	34	7.8	35	18	16	3	25	17	17	2.7	28
	(29–189)	(21–45)	(3.1–14.8)	(19–56)	(9–32)	(9–27)	(1–7)	(12–40)	(9–33)	(8–29)	(0.7–5)	(15–47)
G. cernua	57	24	0.5	3	5	4	0.05	0.4	4	4	0.04	0.4
	(10–108)	(9–42)	(0.1–1.3)	(1–5)	(1–10)	(1–10)	(0.01–0.1)	(0.1–1)	(1–8)	(1–10)	(0.01–0.1)	(0.1–1)
Sum of five spp.	230	93	16.7	76	120	94	8.6	75	105	95	7.4	77
	(95–422)	(87–97)	(9.3–24.3)	(62–92)	(41–201)	(89–98)	(14–15.5)	(47–89)	(43–174)	(90–98)	(2.8–12.1)	(50–90)
Predators[a]	31	13	4.4	21	7	6	1.4	13	6	6	1.2	14
	(15–55)	(6–18)	(1.9–8.0)	(10–36)	(3–15)	(3–8)	(0.6–2.2)	(4–30)	(3–9)	(3–8)	(0.5–2.1)	(3–42)
Whole community	247		22		127		11.5		110		9.7	
	(109–436)		(14.2–30.6)		(44–210)		(7.1–17.7)		(46–181)		(5.1–18.1)	

Numbers in parentheses represent the minimum and maximum VPUEs, of the whole fish community, percentage contributions of five most dominant species and predators during 2004–2021.

[a] Predator fish in Římov include asp, wels catfish, perch, pike, and pikeperch.

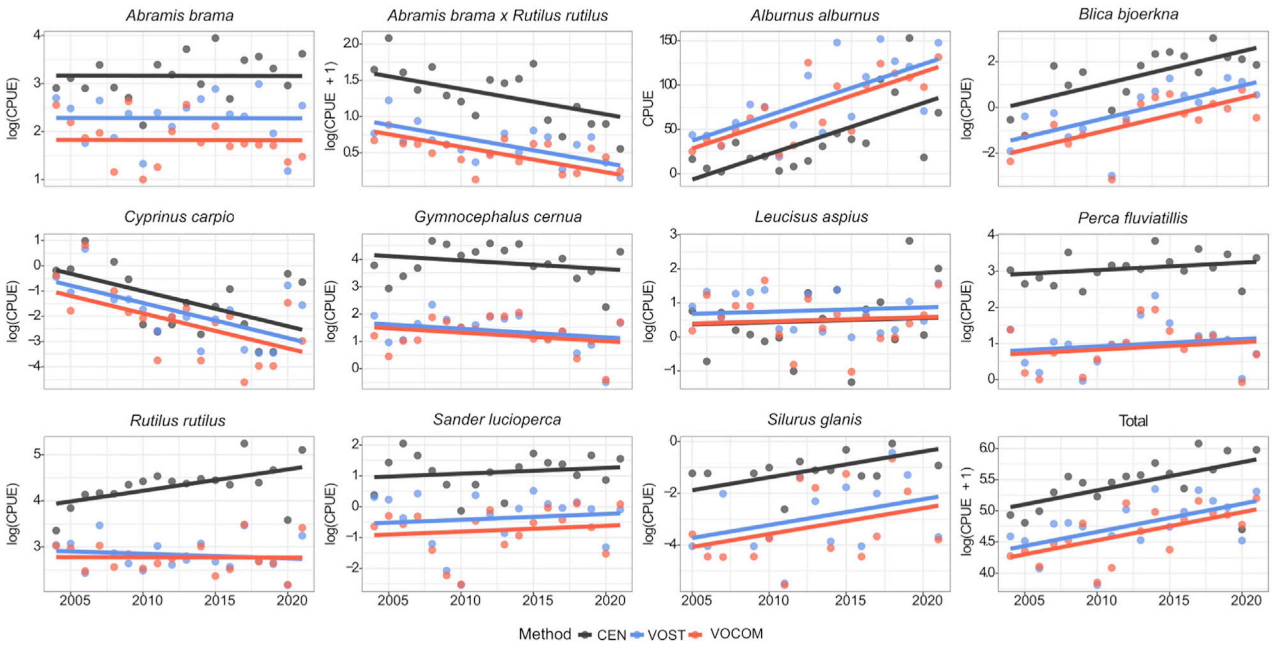

FIGURE 5
Temporal trends of CPUEs based on the ANCOVA model fits of transformed data determined by the three methods (CEN, VOST and VOCOM) for the dominant fish species and the whole fish community in the Římov Reservoir (Czech Republic).

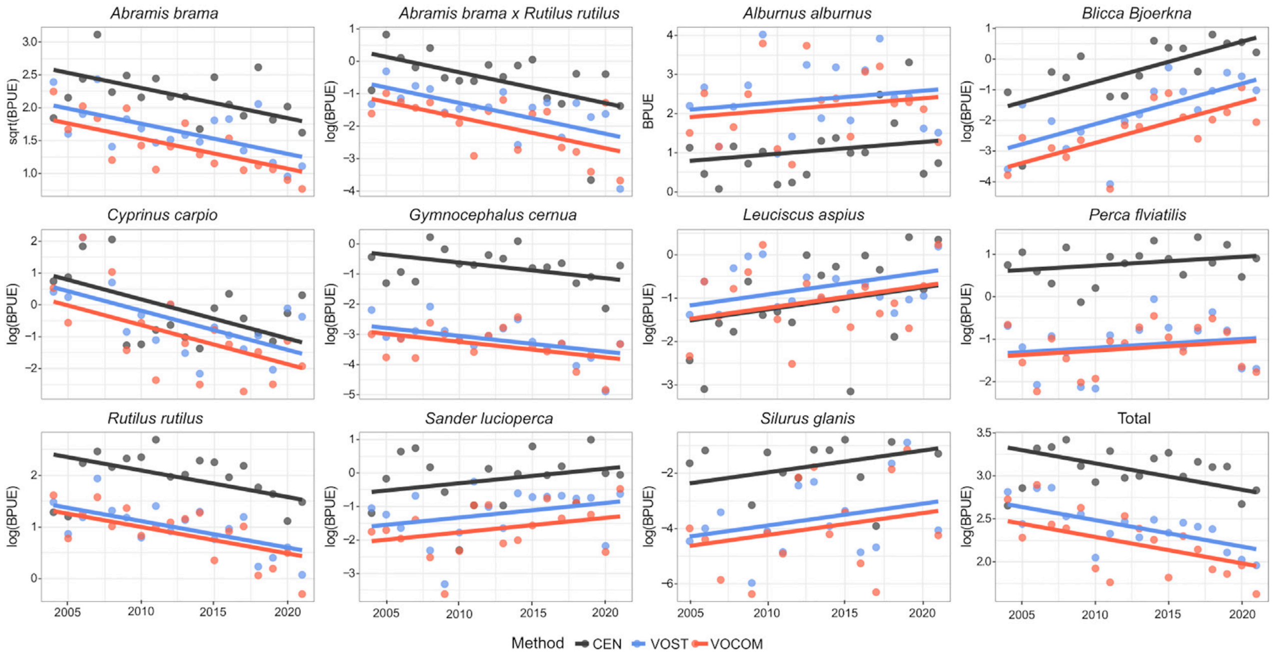

FIGURE 6
Temporal trends of BPUEs based on ANCOVA model fits of transformed data determined by the three methods (CEN, VOST and VOCOM) for the dominant fish species and the whole fish community in the Římov Reservoir (Czech Republic).

TABLE 4 ANCOVA results of the interaction test for CPUEs of the dominant species and the whole community sampled from 2004 to 2021 in Římov Reservoir, Czech Republic.

Species	Variable*	df	SS	MS	F	p**
A. alburnus	Method	2	19,332.647	9666.324	11.135	0.000
	Year	1	42,500.039	42500.039	48.958	0.000
	Method:Year	2	106.068	53.034	0.061	0.941
	Residuals	48	41,668.194	868.087		
A. brama	Method	2	56.153	28.076	43.636	0.000
	Year	1	0.206	0.206	0.320	0.574
	Method:Year	2	3.729	1.864	2.898	0.065
	Residuals	48	30.884	0.643		
A. brama x *R. rutilus*	Method	2	21.767	10.884	45.420	0.000
	Year	1	6.985	6.985	29.148	0.000
	Method:Year	2	0.191	0.095	0.398	0.674
	Residuals	48	11.502	0.240		
B. bjoerkna	Method	2	36.081	18.040	24.781	0.000
	Year	1	28.999	28.999	39.835	0.000
	Method:Year	2	0.200	0.100	0.137	0.872
	Residuals	42	30.575	0.728		
C. carpio	Method	2	0.347	0.174	1.958	0.153
	Year	1	1.753	1.753	19.766	0.000
	Method:Year	2	0.019	0.010	0.108	0.898
	Residuals	45	3.991	0.089		
G. cernua	Method	2	79.647	39.824	99.802	0.000
	Year	1	1.453	1.453	3.642	0.062
	Method:Year	2	0.451	0.225	0.565	0.572
	Residuals	48	19.153	0.399		
L. aspius	Method	2	1.084	0.542	0.903	0.412
	Year	1	0.198	0.198	0.330	0.568
	Method:Year	2	2.873	1.437	2.394	0.102
	Residuals	48	28.804	0.600		
P. fluviatilis	Method	2	56.031	28.016	94.461	0.000
	Year	1	0.622	0.622	2.096	0.154
	Method:Year	2	0.023	0.011	0.039	0.962
	Residuals	48	14.236	0.297		
R. rutilus	Method	2	28.270	14.135	104.358	0.000
	Year	1	0.207	0.207	1.526	0.223
	Method:Year	2	0.890	0.445	3.284	0.046
	Residuals	48	6.501	0.135		

(Continued on following page)

TABLE 4 (*Continued*) ANCOVA results of the interaction test for CPUEs of the dominant species and the whole community sampled from 2004 to 2021 in Římov Reservoir, Czech Republic.

Species	Variable*	*df*	*SS*	*MS*	*F*	*p***
S. lucioperca	Method	2	12.439	6.220	46.269	0.000
	Year	1	0.067	0.067	0.502	0.482
	Method:Year	2	0.033	0.016	0.123	0.885
	Residuals	48	6.452	0.134		
S. glanis	Method	2	37.732	18.866	13.228	0.000
	Year	1	9.244	9.244	6.481	0.015
	Method:Year	2	1.164	0.582	0.408	0.668
	Residuals	37	52.770	1.426		
Whole community	Method	2	276.128	138.064	34.608	0.000
	Year	1	111.927	111.927	28.056	0.000
	Method:Year	2	2.140	1.070	0.268	0.766
	Residuals	48	191.492	3.989		

*All CPUEs, derived from different methods, except those for *A. alburnus*, *A. brama x R. rutilus*, and the whole community, were log-transformed to cope with model premises. For the latter two, the CPUEs, were log (CPUE+1) transformed, and for *A. alburnus*, the raw data were consistent with the model premises and therefore were not transformed. ***$p \leq 0.05$ refers to a statistically significant difference, while $p > 0.05$ means that the difference is not significant. *SS*, the sum of squares; *MS*, the mean of squares; *F* = the *F*-statistic (i.e., variance ratio); *p* = the *p*-value.

6.48–8.59 for CEN; 2.82, 0.32, and 2.21–3.51 for VOST; and 2.55, 0.31, and 1.97–3.20 for VOCOM, respectively. Therefore, similar to the Tukey *post hoc* test for VPUEs of other dominant species and roach BPUE, only the estimated marginal mean of CEN differed from VOST and VOCOM, but the marginal means of VOST and VOCOM were similar.

Discussion

Methods for computing whole-reservoir relative fish abundance and biomass

The Římov Reservoir serves as a long-term ecological research site for monitoring all important components of aquatic biota (Znachor et al., 2017). Long-term, fishery-independent surveys conducted annually with standardized gear and a well-designed sampling approach can provide time series of fish population abundance - CPUE and biomass–BPUE indices (Martell and Froese, 2013; Froese et al., 2018; Froese et al., 2020) and ecosystem health indicators, as in the EU WFD (CEN, 2005; CEN, 2015). However, scientists long ago began to question the way we obtain input catch data and how these indices are determined (e.g., Walters, 2003; Campbell, 2004). Accordingly, depth-stratified sampling (*a priori*) (Walters, 2003; CEN, 2005) and volume-weighting of these indices (*a posteriori*) have been proposed (Mehner et al., 2005; Lauridsen et al., 2008; Kubečka et al., 2013; Alexander et al., 2015a). Here we discuss the results of three methods: the established CEN protocol and two volume-weighting approaches -VOST and VOCOM.

As expected, the three methods used to calculate the reservoir-wide relative abundance and biomass of the dominant species and the total fish community produced different VPUEs (Figures 2, 3). The CEN protocol places the greatest emphasis on benthic habitats, which generally harbor higher fish abundance, biomass, and species richness than pelagic habitats (Prchalová et al., 2008; Prchalová et al., 2009b; Moraes et al., 2021). Consequently, it provided higher reservoir-wide CPUEs and BPUEs by a factor of two when estimates are compared to the two volume-weighting approaches (Table 3). Similar differences were found by Lauridsen et al. (2008) for Danish lakes and by Alexander et al. (2015a) for many lakes in eastern France, Switzerland, and northern Italy. We see spatial scale problems in the CEN protocol that may have led to these differences. Walters (2003) pointed out that fisheries scientists typically use commercial catch rate data for stock assessments that come from only a few fishing areas to extrapolate to the entire system. Similarly, the CEN protocol uses ESG monitoring data primarily from benthic habitats and only at the deepest point of pelagic habitats to represent the entire lentic system. However, several authors have noted that the CEN protocol underrepresents pelagic species in whole-lake fish community assessments (Diekmann et al., 2005; Deceliere-Vergès and Guillard, 2008; Deceliere-Vergès et al., 2009; Specziár et al.,

TABLE 5 ANCOVA results of the interaction test for BPUEs of the dominant species and the whole community sampled from 2004 to 2021 in Římov Reservoir, Czech Republic.

Species	Variable*	*df*	*SS*	*MS*	*F*	*p***
A. alburnus	Method	2	17.999	9.000	11.897	0.000
	Year	1	1.332	1.332	1.760	0.191
	Method:Year	2	1.082	0.541	0.715	0.494
	Residuals	48	36.309	0.756		
A. brama	Method	2	5.631	2.816	28.556	0.000
	Year	1	3.069	3.069	31.120	0.000
	Method:Year	2	0.325	0.162	1.647	0.203
	Residuals	48	4.733	0.099		
A. brama x *R. rutilus*	Method	2	18.191	9.096	17.545	0.000
	Year	1	13.189	13.189	25.441	0.000
	Method:Year	2	0.001	0.000	0.001	0.999
	Residuals	48	24.884	0.518		
B. bjoerkna	Method	2	33.119	16.560	27.507	0.000
	Year	1	22.387	22.385	37.183	0.000
	Method:Year	2	0.219	0.110	0.182	0.834
	Residuals	42	25.285	0.602		
C. carpio	Method	2	2.815	1.408	0.412	0.665
	Year	1	47.375	47.375	13.861	0.001
	Method:Year	2	0.235	0.117	0.034	0.966
	Residuals	45	153.805	3.418		
G. cernua	Method	2	77.062	38.531	136.909	0.000
	Year	1	3.953	3.953	14.045	0.000
	Method:Year	2	0.691	0.346	1.228	0.302
	Residuals	48	13.509	0.281		
L. aspius	Method	2	1.300	0.650	1.157	0.323
	Year	1	3.320	3.320	5.911	0.019
	Method:Year	2	3.495	1.747	3.111	0.054
	Residuals	48	26.960	0.562		
P. fluviatilis	Method	2	46.544	23.272	83.766	0.000
	Year	1	0.620	0.620	2.230	0.142
	Method:Year	2	0.002	0.001	0.003	0.997
	Residuals	48	13.335	0.278		
R. rutilus	Method	2	13.029	6.514	43.077	0.000
	Year	1	3.834	3.834	25.351	0.000
	Method:Year	2	0.847	0.423	2.800	0.071
	Residuals	48	7.259	0.151		

(Continued on following page)

TABLE 5 (*Continued*) **ANCOVA results of the interaction test for BPUEs of the dominant species and the whole community sampled from 2004 to 2021 in Římov Reservoir, Czech Republic.**

Species	Variable*	*df*	*SS*	*MS*	*F*	*p***
S. lucioperca	Method	2	20.331	10.165	16.692	0.000
	Year	1	2.761	2.761	4.534	0.038
	Method:Year	2	0.194	0.097	0.159	0.853
	Residuals	48	29.231	0.609		
S. glanis	Method	2	40.409	20.205	11.285	0.000
	Year	1	5.825	5.825	3.253	0.079
	Method:Year	2	2.103	1.051	0.587	0.561
	Residuals	37	66.243	1.790		
Whole community	Method	2	25.927	12.963	73.328	0.000
	Year	1	3.902	3.902	22.070	0.000
	Method:Year	2	0.867	0.434	2.453	0.097
	Residuals	48	8.486	0.177		

*All BPUEs, derived from different methods, except for *A. alburnus* and *A. brama*, were log-transformed to cope with model premises. For *A. brama*, BPUEs, were square root transformed, and for *A. alburnus*, raw data were consistent with model assumptions and therefore were not transformed. **$p \leq 0.05$ refers to a statistically significant difference, while $p > 0.05$ means that the difference is not significant. *SS*, the sum of squares; *MS*, the mean of squares; *F*, the *F*-statistic (i.e., variance ratio), *P*, the *p*-value.

2009; Achleitner et al., 2012; Alexander et al., 2015b). In addition, sampling only the deepest spot of the lake/reservoir likely overlooks horizontal variation in fish communities in pelagic habitats (Lauridsen et al., 2008; Specziár et al., 2009; Alexander et al., 2015b). These issues are particularly important in large and deep lakes where pelagic habitats make up the majority of lake volume (Alexander et al., 2015b). Even in medium-sized reservoirs such as Římov Reservoir, the volume of pelagic habitats is much larger than that of benthic habitats (Table 2). In this respect, it seems correct to weight VPUEs by habitat volume.

CEN protocol is widely applied and suitable for assessing ecological quality and spatial and temporal comparisons of different water bodies (e.g., Diekmann et al., 2005; Mehner et al., 2005; Deceliere-Vergès and Guillard, 2008; Lauridsen et al., 2008; Prchalová et al., 2008; Achleitner et al., 2012; Alexander et al., 2015a; Šmejkal et al., 2015; Ritterbusch et al., 2022). However, high whole lake abundance and biomass indices of some species from CEN protocol could lead to expansion of resource use (e.g., by increasing fishing effort) or increased angling in recreational fisheries, which would have unforeseen ecological consequences for the freshwater system and ultimately affect long-term socioeconomic benefits. The volume weighting results presented here using nearly 2 decades of monitoring data and other previous studies (e.g., Lauridsen et al., 2008; Kubečka et al., 2013; Alexander et al., 2015a) clearly demonstrate the need to consider both vertical and horizontal weighted fish distribution to estimate realistic (less biased) fish metrics for the system when whole lake data are needed and for dealing with overall role of fish in the food web of the ecosystem.

The VOST approach used here is procedurally similar to previous volume weighting studies (e.g., Lauridsen et al., 2008; Kubečka et al., 2013; Alexander et al., 2015a). However, unlike the previous studies, VPUEs in VOST were calculated from the average catches of the four locations where pelagic nets were deployed to account for uneven horizontal fish distribution, whereas all previous volume-weighted studies used catches only from the deepest locality of the pelagic habitat and therefore have some of the limitations mentioned above. We therefore believe that the VOST-derived VPUEs better reflect the relative abundance and biomass of fish for the system.

Surprisingly, there are not many differences between the VPUEs derived from the VOST and VOCOM approaches for the Římov Reservoir. In the VOCOM calculation, the catch at each locality is weighted by the volume of its depth compartments. Lacustrine compartments in downstream localities (dam and middle) therefore have a greater weight in terms of volume than depth compartments in upper and tributary localities (Figure 1A), where the width of the reservoir and thus their volume is much smaller (Table 2). On the other hand, tributary and upper localities of the reservoir usually harbor more fish (Vašek et al., 2004, 2016; Prchalová et al., 2009a). When all localities are weighted equally using stratum volume (VOST), the increasing effect of tributary is not reduced by weighting their smaller strata volumes, and the numerical values of the estimates (VPUEs) are slightly larger than VOCOM. However, the

TABLE 6 Summary of comparisons (ANCOVA and Tukey *post hoc* test) for estimated VPUEs of fish community sampled in different years (2004–2021) in Římov Reservoir (Czech Republic) derived from CEN, VOST and VOCOM.

	Method			Year			Tukey *post hoc* test[c]		
Species	VPUE[a]	*F*	*p*	*df*[b]	*F*	*p*	CEN	VOST	VOCOM
A. alburnus	CPUE	11.57	0.000	2,50	50.87	0.000	a	b	b
	BPUE	12.03	0.000	2,50	1.78	0.188	a	b	b
A. brama	CPUE	36.79	0.000	2,50	0.002	0.965	a	b	b
	BPUE	27.84	0.000	2,50	30.34	0.000	a	b	b
A. brama x *R. rutilus*	CPUE	61.11	0.000	2,50	32.91	0.000	a	b	b
	BPUE	18.28	0.000	2,50	26.50	0.000	a	b	b
B. bjoerkna	CPUE	25.80	0.000	2,44	41.48	0.000	a	b	b
	BPUE	28.57	0.000	2,44	38.62	0.000	a	b	b
C. carpio	CPUE	2.78	0.072	2,47	22.17	0.000	a	a	a
	BPUE	2.97	0.061	2,47	21.82	0.000	a	a	a
G. cernua	CPUE	101.57	0.000	2,50	3.71	0.060	a	b	b
	BPUE	135.67	0.000	2,50	13.92	0.000	a	b	b
L. aspius	CPUE	0.86	0.431	2,50	0.31	0.579	a	a	a
	BPUE	1.07	0.352	2,50	5.45	0.024	a	a	a
P. fluviatilis	CPUE	98.24	0.000	2,50	2.18	0.146	a	b	b
	BPUE	87.25	0.000	2,50	2.32	0.134	a	b	b
R. rutilus	BPUE	40.18	0.000	2,50	23.65	0.000	a	b	b
S. lucioperca	CPUE	31.64	0.000	2,50	0.92	0.342	a	b	b
	BPUE	17.27	0.000	2,50	4.69	0.035	a	b	b
S. glanis	CPUE	13.64	0.000	2,39	6.68	0.014	a	b	b
	BPUE	11.53	0.000	2,39	3.32	0.076	a	b	b
Whole community	CPUE	30.55	0.000	2,50	27.21	0.000	a	b	b
	BPUE	62.29	0.000	2,50	23.52	0.000	a	b	b

[a] VPUEs, for *B. bjoerkna*, *C. carpio*, *G. cernua*, *L. aspius*, *P. fluviatilis*, *R. rutilus*, *S. lucioperca* and *S. glanis* were log transformed to cope with model premises. CPUEs, and BPUEs, for *A. brama* were log-transformed and square-root transformed, respectively. CPUEs, and BPUEs, for *A. brama x R. rutilus* and the whole community were log (VPUE+1) and log-transformed, respectively, and for *A. alburnus*, raw data were consistent with model assumptions and therefore were not transformed.

[b] The values of the degrees of freedom for the method (e.g., *df* = 2, 50) refer to the value for between groups and within groups (residuals), respectively; the latter vary slightly between species depending on the number of VPUEs, in 18 years. The degree of freedom for the covariate (year) is one for all dominant species and the whole community.

[c] A Tukey *post hoc* test with the same letters indicates no difference between the VPUEs, obtained with the three methods, whereas different letters indicate a difference between the methods. For roach CPUE, similar to the *post hoc* test for VPUEs, of other dominant species and roach BPUE, only the estimated marginal mean of CEN, differed from VOST, and VOCOM, but the marginal means of VOST, and VOCOM, were similar.

difference between the CPUEs (Figure 5) and BPUEs (Figure 6) of VOST and VOCOM was not statistically significant for both the total fish community and the dominant fish species, except for asp and common carp, where there was no difference between the three methods (Table 6). The similarity of results between VOST and VOCOM could be due to the limited morphological differences of the canyon-shaped Římov Reservoir along its longitudinal axis. In the case of extreme morphological differences along this axis, which could be the case for large lakes and reservoirs, the relative abundance and biomass indices could differ because there would be differences in the volume contribution of the different compartments. Mehner et al. (2005) and Lauridsen et al. (2008) also indicated that estimates would depend on lake morphology.

Fish assemblages of pelagic habitats in reservoirs are generally less diverse than those of benthic habitats. There are no truly pelagic fish species in Římov Reservoir, and the pelagic habitat is dominated by eurytopic species such as bleak, bream, roach, asp, and pikeperch (Moraes et al., 2021). Bleak is a highly successful species that dominates the pelagic habitat and thus the VOST and VOCOM species composition (Figure 4). The proportion of bleak in CEN protocol is most likely underestimated. The opposite phenomenon can be noticed for more benthic species such as perch and ruffe. More species are present in benthic habitats, so the species composition of CEN is more diverse, however the volume-weighted results are more realistic due to real ratios of habitat volumes. Many researchers have reached similar conclusions, noting that the CEN protocol not only underrepresents pelagic habitats, but whole-lake estimates of CPUE, BPUE, and community composition are also biased toward benthic communities, which are disproportionately influenced by the ecological conditions of benthic habitats (Diekmann et al., 2005; Mehner et al., 2005; Lauridsen et al., 2008; Achleitner et al., 2012; Alexander et al., 2015a). Since we found no significant differences between VOST and VOCOM, we put forward the VOST approach especially for small and medium lakes and reservoirs with less diverse bathymetric morphologies. In cases where bathymetric morphological differences are very large at different sites, which is often the case for large lakes and reservoirs, VOCOM would provide more realistic estimates of these population and community indices.

Monitoring fish species composition

The European Standard Gillnet (ESG) is becoming increasingly popular and is widely used for sampling in European waters. Our results show that despite the use of the modified-ESG series and a sampling scheme representing all habitats along the horizontal and vertical gradients, only a limited number of species (<50% of the fish species present in the reservoir) were caught annually (Table 1; Supplementary Table S1). Apparently, dominant, and subdominant species were caught regularly, while rare species were caught only occasionally. The newly emerged vimba bream probably originated from the inflow river since it was caught only in 2021 in the tributary locality of the reservoir. The hybrid bream x rudd, on the other hand, is probably the result of hybridization of the two species present in the reservoir. Hybridization of the two species in the wild has been reported in other systems (Donnelly et al., 1998; Wyatt et al., 2006). The observed interannual variation in species composition (Figure 4; Table 3) also suggests temporal variation in fish community composition and species accessibility to gillnets. Although the extended-ESG series solved the widely reported problem of size selectivity (Lauridsen et al., 2008; Šmejkal et al., 2015) and allowed capture of large specimens of common species, the problem of species selectivity–another inherent problem of gillnets that also applies to ESG, has not yet been resolved. Other studies also reported the problem of species selectivity in terms of low catchability in gillnets for eel and pike (Prchalová et al., 2013; CEN, 2015), burbot *Lota lota* and (Argillier et al., 2013) and wels catfish, which has a large, depressed head that is not suitable for gillnets. However, the comparisons with studies of the reservoir by other active methods (Říha et al., 2009; Říha et al., 2015) show that extended ESG cover the main players of the community.

Trends in fish abundance and biomass

Our study revealed trends in the abundance of some common species. Most striking is the increase in the abundance of the bleak in the volume-weighted VPUEs (Figures 2, 5). The population of this species has been gradually developing in the reservoir (Říha et al., 2009) and is clearly becoming more successful, while the total biomass of other fishes is decreasing, although bleak increase is seen only in numbers, not biomass. Another expanding species is white bream, which entered the reservoir relatively late and whose density is still relatively low. Perch abundance is increasing in the benthic habitat, which is inhabited primarily by small individuals. Predators (asp, pikeperch, and wels catfish) were found to have a slight population increase. They are regularly stocked into the reservoir, but their increase is limited by illegal fishing (Vašek et al., 2013). Common carp seldom breeds in central European reservoirs (Souza et al., 2022), and their population is supported by flood events that bring common carp from aquaculture ponds in the watershed (Boukal et al., 2012). The common carp population peaked in 2006, when significant flooding occurred (Znachor et al., 2017), and declined since then until 2020, when further flooding brought new inflow of common carps (Figure 2).

Roach abundance is also increasing in the benthic habitat, which is inhabited primarily by small individuals. In fact, the total biomass of roach is decreasing (Figures 3, 6), so the population consists of smaller individuals. These observed changes in roach size structure and shift in habitat from pelagic to littoral (benthic) may have greatly influenced the results of CEN for roach. This could also be why the CPUE interaction test for roach was significant over time for the different methods (Table 4), as the small (juvenile) roach prefer littoral habitats where plankton are abundant and the water is warmer, resulting in an increasing trend in their CPUE for CEN, but not for VOST and VOCOM (Figures 2, 6).

As a result, regardless of the methods used, a general downward trend in the relative biomass of the entire fish community was observed (Figures 3, 6), while abundance showed the opposite trend (Figures 2, 5). Also, the increasing trend in abundance clearly reflects the increase in abundance of small fish species (e.g., bleak) and small individuals of bream, roach, and white bream (Figure 2). Several factors may be responsible for this contrasting situation. Regular biomanipulation of fish (removal of planktivorous fish such as bleak, bream, and roach and enhancement of predators) could be a possible reason for this declining trend in size and thus total community biomass. Although biomass of predators has slowly increased over time (Figures 3, 6), they have generally remained at low levels (Figure 4). The most abundant predators, such as pikeperch, asp, and perch, consume small prey (Kubečka et al., 1998; Vašek et al., 2018) and are therefore unlikely to eliminate the largest individuals and reduce the average size of populations. Emerging wels catfish may play a role here. In addition, a fishery-induced evolution toward smaller size (Law, 2000; de Roos et al., 2006) is very unlikely, as the usual catches of planktivorous fish are only 1–2 kg/ha, except in the years from 2020 onwards, when more biomanipulation occurred (Jůza et al., 2022). Therefore, we can say that the direct impact on fish population size is unlikely. The most likely impact of fish removal could be more indirect through their food web. A study of bream growth performance in the Římov Reservoir using several decades of age structure and climate data showed a decreasing trend in the von Bertalanffy growth parameter K - a growth curvature parameter that indicates the growth rate of fish toward the asymptotic length ($L\infty$) or weight ($W\infty$) (Souza AT et al., unpublished data). This situation signals that predation pressure on zooplankton by abundant small planktivorous fish was high and these fish may have suffered from strong competition for food, resulting in a downward trend in their biomass.

Conclusion

This paper provides the most comprehensive description of long-term fish community dynamics, as it summarizes fish samples from all habitats (i.e., all fish older than 0+) collected with both European standard and large mesh gillnets. Using long-term fish catch data from Římov Reservoir, we present whole-reservoir species composition, abundance, and biomass indices for the dominant fish species and the entire community derived from volume-weighted and unweighted catch rates.

The CEN appeared to provided higher estimates of population and total community abundance and biomass by a factor of two when compared to the two volume weighting approaches. Therefore, using such a high VPUE could have serious implications for resource management plans and strategies, and food web models for ecosystem level assessments. We believe that the volume-weighted results are more realistic because habitat volumes are used for weighting and sampling accounts for heterogeneity in the vertical and horizontal distribution of fish. Since we found no significant differences between VOST and VOCOM, we put forward the VOST approach especially for small and medium lakes and reservoirs with less diverse bathymetric morphologies. In cases where bathymetric morphological differences are very large at different sites, which is often the case for large lakes and reservoirs, VOCOM would provide more realistic estimates of these population and community indices. To avoid overestimating the importance of benthic species at the expense of pelagic species (e.g., ruffe, perch, and roach vs bleak in Římov), we recommend pelagic sampling at more locations than just over the deepest part of the water body to cover heterogeneity of fish distribution in this habitat (usually the largest volume of the water body) as well, and weighting catches by the volume of a given depth stratum in a given water body to properly reflect actual volume proportions and provide the most representative picture of the whole community, as required by the WFD for ecosystem status assessment.

All approaches consistently showed an increasing trend in whole fish community abundance and a decreasing trend in biomass during the study period, which is supported by the observed increase in abundance of small fish. Overall, long-term fish monitoring data have proven critical for examining the status and understanding of fish community composition, relative abundance, and biomass trends, and for deciphering a realistic picture of fish populations and communities in the freshwater system by using habitat volume for weighting.

Data availability statement

The raw data supporting the conclusion of this article will be made available by the authors, without undue reservation.

Ethics statement

The animal study was reviewed and approved by Animal ethics committee of the Biology Centre CAS.

Author contributions

GT: Conceptualization, methodology, data processing, formal analysis, visualization, writing-original draft, review and editing; AS: Conceptualization, data processing, formal analysis, investigation, methodology, validation, visualization, and review and editing; DB: Investigation, writing—review and editing; PB: Investigation, writing—review and editing; MČ: Investigation, writing—review and editing; VD: Investigation, writing—review and editing; JF: Investigation, writing—review and editing; MH: Investigation, writing—review and editing; LK: Investigation, data curation, Writing—review and editing; TK: Investigation, data curation, Writing—review and editing; CM: Investigation, data curation, writing—review and editing; KM: Investigation, writing—review and editing; MM: Investigation, formal analysis, writing—review and editing; MP: Investigation, writing—review and editing; MŘ: Investigation, writing—review and editing; ZS: Investigation, writing—review and editing; KS: Investigation, writing—review and editing; MŠ: Investigation, writing—review and editing; MT: Investigation, writing—review and editing; MV: Investigation, writing—review and editing; LV: Investigation, writing—review and editing; IV: Investigation, writing—review and editing; JP: investigation, resources, writing—review and editing, funding acquisition and project administration; TJ: Investigation, writing—review and editing; JK: Conceptualization, investigation, methodology, review and editing, resources, validation, funding acquisition and project administration. All authors have agreed to be responsible for the content of the paper and approved it for publication.

Funding

European Union within ESIF in frame of Operational Program Research, Development and Education (Project No. CZ.02.1.01/0.0/0.0/16_025/0007417 administrated by the Ministry of Education, Youth and Sports of the Czech Republic)" and AV 21 strategy support program "Water for Life".

Acknowledgments

We acknowledge the help of many volunteers, colleagues and students helping occasionally with sampling in Římov reservoir, and Professor Gejza Dohnal (Czech Technical University) and Professor Tomaš Mrkvička (University of South Bohemia) for checking our statistical analyses. The suggestions of two reviewers and the associate editor, Prof. Robert Ptacnik greatly improved the manuscript.

Conflict of interest

The authors declare that the research was conducted in the absence of any commercial or financial relationships that could be construed as a potential conflict of interest.

Publisher's note

Supplementary material

The Supplementary Material for this article can be found online at: https://www.frontiersin.org/articles/10.3389/fenvs.2022.1000087/full#supplementary-material

References

Achleitner, D., Gassner, H., and Luger, M. (2012). Comparison of three standardised fish sampling methods in 14 alpine lakes in Austria. *Fish. Manag. Ecol.* 19, 352–361. doi:10.1111/j.1365-2400.2012.00851.x

Alexander, T. J., Vonlanthen, P., Periat, G., Degiorgi, F., Raymond, J. C., and Seehausen, O. (2015a). Estimating whole-lake fish catch per unit effort. *Fish. Res.* 172, 287–302. doi:10.1016/j.fishres.2015.07.024

Alexander, T. J., Vonlanthen, P., Periat, G., Degiorgi, F., Raymond, J. C., and Seehausen, O. (2015b). Evaluating gillnetting protocols to characterize lacustrine fish communities. *Fish. Res.* 161, 320–329. doi:10.1016/j.fishres.2014.08.009

Argillier, C., Caussé, S., Gevrey, M., Pédron, S., de Bortoli, J., Brucet, S., et al. (2013). Development of a fish-based index to assess the eutrophication status of European lakes. *Hydrobiologia* 704, 193–211. doi:10.1007/s10750-012-1282-y

Blabolil, P., Ricard, D., Peterka, J., Říha, M., Jůza, T., Vašek, M., et al. (2016). Predicting asp and pikeperch recruitment in a riverine reservoir. *Fish. Res.* 173, 45–52. doi:10.1016/j.fishres.2015.08.003

Blabolil, P., Boukal, D. S., Ricard, D., Kubečka, J., Říha, M., Vašek, M., et al. (2017). Optimal gillnet sampling design for the estimation of fish community indicators in heterogeneous freshwater ecosystems. *Ecol. Indic.* 77, 368–376. doi:10.1016/j.ecolind.2017.02.036

Blabolil, P., Harper, L. R., Říčanová, Š., Sellers, G., di Muri, C., Jůza, T., et al. (2021). Environmental DNA metabarcoding uncovers environmental correlates of fish communities in spatially heterogeneous freshwater habitats. *Ecol. Indic.* 126, 107698. doi:10.1016/j.ecolind.2021.107698

Boukal, D. S., Jankovský, M., Kubečka, J., and Heino, M. (2012). Stock–catch analysis of carp recreational fisheries in Czech reservoirs: Insights into fish survival, water body productivity and impact of extreme events. *Fish. Res.* 119-120, 23–32. doi:10.1016/j.fishres.2011.12.003

Campbell, R. A. (2004). CPUE standardisation and the construction of indices of stock abundance in a spatially varying fishery using general linear models. *Fish. Res.* 70, 209–227. doi:10.1016/j.fishres.2004.08.026

CEN (2005). *Water quality – sampling fish with multi-mesh gillnets*. Brussels: European Committee for Standardization. European Standard EN 14757:2005.

CEN (2015). *Water quality – sampling of fish with multi-mesh gillnets*. Brussels: European Committee for Standardization. European Standard EN 14757:2015.

Davis, W. S. (1995). "Bioassessment and criteria: Building on the past," in *Biological assessment and criteria: Tools for water resource planning and decision making*. Editors W. S. Davis and T. P. Simon (Boca Raton, FL: CRC Press), 15–29.

de Roos, A. M., Boukal, D. S., and Persson, L. (2006). Evolutionary regime shifts in age and size at maturation of exploited fish stocks. *Proc. R. Soc. B* 273, 1873–1880. doi:10.1098/rspb.2006.3518

Deceliere-Vergès, C., and Guillard, J. (2008). Assessment of the pelagic fish populations using CEN multi-mesh gillnets: consequences for the characterization of the fish communities. *Knowl. Manag. Aquat. Ecosyst.* 389, 04. doi:10.1051/kmae:2008005

Deceliere-Vergès, C., Argillier, C., Lanoiselée, C., de Bortoli, J., and Guillard, J. (2009). Stability and precision of the fish metrics obtained using CEN multi-mesh gillnets in natural and artificial lakes in France. *Fish. Res.* 99, 17–25. doi:10.1016/j.fishres.2009.04.012

Diekmann, M., Braemick, U., Lemcke, R., and Mehner, T. (2005). Habitat-specific fishing revealed distinct indicator species in German lowland lake fish communities. *J. Appl. Ecol.* 42, 901–909. doi:10.1111/j.1365-2664.2005.01068.x

Donnelly, R. E., Caffrey, J. M., and Tierney, D. M. (1998). Movements of a bream (*Abramis brama* (L.)), rudd x bream hybrid, tench (*Tinca tinca* (L.)) and pike (*Esox lucius* (L.)) in an Irish canal habitat. *Hydrobiologia* 371/372, 305–308. doi:10.1023/a:1017083423786

Dudgeon, D., Arthington, A. H., Gessner, M. O., Kawabata, Z. I., Knowler, D. J., Lévêque, C., et al. (2006). Freshwater biodiversity: Importance, threats, status, and conservation challenges. *Biol. Rev.* 81, 163. doi:10.1017/S1464793105006950

European Commission (2000). Directive 2000/60/EC of the European Parliament and of the Council of 23 October 2000 establishing a framework for Community action in the field of water policy action in the field of water policy. *Off. J. Eur. Communities* L327, 1–73.

Fricke, R. van der Laan, R., and Eschmeyer, W. (2022). Eschmeyer's catalog of fishes: Genera, species, references. Available at: https://researcharchive.calacademy.org/research/ichthyology/catalog/fishcatmain.asp (Accessed September 28, 2022).

Froese, R., Winker, H., Coro, G., Demirel, N., Tsikliras, A. C., Dimarchopoulou, D., et al. (2018). A new approach for estimating stock status from length frequency data. *ICES J. Mar. Sci.* 75, 2004–2015. doi:10.1093/icesjms/fsy078

Froese, R., Winker, H., Coro, G., Demirel, N., Tsikliras, A. C., Dimarchopoulou, D., et al. (2020). Estimating stock status from relative abundance and resilience. *ICES J. Mar. Sci.* 77, 527–538. doi:10.1093/icesjms/fsz230

Harris, J. H. (1995). The use of fish in ecological assessments. *Austral Ecol.* 20, 65–80. doi:10.1111/j.1442-9993.1995.tb00523.x

Hilborn, R., and Walters, C. (1992). *Quantitative fisheries stock assessment: Choice, dynamics, and uncertainty*. New York: Chapman & Hall.

Hladík, M., Kubečka, J., Mrkvička, T., Čech, M., Draštík, V., Frouzová, J., et al. (2008). Effects of the construction of a reservoir on the fish assemblage in an inflow river. *Czech J. Anim. Sci.* 53, 537–547. doi:10.17221/370-cjas

Jakobsen, T. S., Hansen, P. B., Jeppesen, E., and Søndergaard, M. (2004). Cascading effect of three-spined stickleback *Gasterosteus aculeatus* on community composition, size, biomass and diversity of phytoplankton in shallow, eutrophic brackish lagoons. *Mar. Ecol. Prog. Ser.* 279, 305–309. doi:10.3354/meps279305

Jeppesen, E., Lauridsen, T. L., Mitchell, S. F., Christoffersen, K., and Burns, C. W. (2000). Trophic structure in the pelagial of 25 shallow New Zealand lakes: Changes along nutrient and fish gradients. *J. Plankton Res.* 22, 951–968. doi:10.1093/plankt/22.5.951

Jůza, T., Blabolil, P., Čech, M., Draštík, V., Frouzová, J., Sajdlová, Z., et al. (2022). Fish stock mass reduction is indicated in standard abundance and biomass estimates from gillnets and hydroacoustics. *Fish. Res.* 253, 106389. doi:10.1016/j.fishres.2022.106389

Kubečka, J., Seda, J., and Matena, J. (1998). Fish-zooplankton interactions during spring in a deep reservoir. *Int. Rev. Hydrobiol.* 83, 431–441.

Kubečka, J., Prchalová, M., Čech, M., Draštík, V., Frouzová, J., Hladík, M., et al. (2013). Fish (osteichthyes) in biesbosch storage reservoirs (the Netherlands): a method for assessing complex stocks of fish. *Acta Soc. Zool. Bohem.* 77, 37–54.

Lauridsen, T. L., Landkildehus, F., Jeppesen, E., Jørgensen, T. B., and Søndergaard, M. (2008). A comparison of methods for calculating Catch Per Unit Effort (CPUE) of gill net catches in lakes. *Fish. Res.* 93, 204–211. doi:10.1016/j.fishres.2008.04.007

Law, R. (2000). Fishing, selection, and phenotypic evolution. *ICES J. Mar. Sci.* 57, 659–668. doi:10.1006/jmsc.2000.0731

Lüdecke, D. Ben-Shachar, M., Patil, I., Waggoner, P., and Makowski, D. (2021). performance: An R package for assessment, comparison and testing of statistical models. *J. Open Source Softw.* 6, 3139. doi:10.21105/joss.03139

Makowski, D., Ben-Shachar, M. S., Patil, I., and Lüdecke, D. (2020). Estimation of model-based predictions, contrasts and means. CRAN. Available at: https://easystats.github.io/modelbased/authors.html (Accessed August 8, 2022).

Martell, S., and Froese, R. (2013). A simple method for estimating MSY from catch and resilience. *Fish. Fish.* 14, 504–514. doi:10.1111/j.1467-2979.2012.00485.x

Mehner, T., Diekmann, M., Brämick, U., and Lemcke, R. (2005). Composition of fish communities in German lakes as related to lake morphology, trophic state, shore structure and human-use intensity. *Freshw. Biol.* 50, 70–85. doi:10.1111/j.1365-2427.2004.01294.x

Moraes, K., Souza, A. T., Vašek, M., Bartoň, D., Blabolil, P., Čech, M., et al. (2021). Openness of fish habitat matters: Lake pelagic fish community starts very close to the shore. *Water (Basel)* 13, 3291. doi:10.3390/w13223291

Musil, J., Jurajda, P., Adámek, Z., Horký, P., and Slavík, O. (2010). Non-native fish introductions in the Czech Republic - species inventory, facts and future perspectives. *J. Appl. Ichthyol.* 26, 38–45. doi:10.1111/j.1439-0426.2010.01500.x

Plessl, C., Otachi, E. O., Körner, W., Avenant-Oldewage, A., and Jirsa, F. (2017). Fish as bioindicators for trace element pollution from two contrasting lakes in the eastern rift valley, Kenya: spatial and temporal aspects. *Environ. Sci. Pollut. Res.* 24, 19767–19776. doi:10.1007/s11356-017-9518-z

Prchalová, M., Kubečka, J., Říha, M., Litvín, R., Čech, M., Frouzová, J., et al. (2008). Overestimation of percid fishes (Percidae) in gillnet sampling. *Fish. Res.* 91, 79–87. doi:10.1016/j.fishres.2007.11.009

Prchalová, M., Kubečka, J., Čech, M., Frouzová, J., Draštík, V., Hohausová, E., et al. (2009a). The effect of depth, distance from dam and habitat on spatial distribution of fish in an artificial reservoir. *Ecol. Freshw. Fish.* 18, 247–260. doi:10.1111/j.1600-0633.2008.00342.x

Prchalová, M., Kubečka, J., Říha, M., Mrkvička, T., Vašek, M., Jůza, T., et al. (2009b). Size selectivity of standardized multimesh gillnets in sampling coarse European species. *Fish. Res.* 96, 51–57. doi:10.1016/j.fishres.2008.09.017

Prchalová, M., Kubečka, J., Říha, M., Čech, M., Jůza, T., Ketelaars, H. A. M., et al. (2013). Eel attacks-A new tool for assessing European eel (*Anguilla anguilla*) abundance and distribution patterns with gillnet sampling. *Limnologica* 43, 194–202. doi:10.1016/j.limno.2012.09.003

R Core Team (2022). R: A language and environment for statistical computing. Available at: https://www.R-project.org/ (Accessed November 04, 2022).

Radinger, J., Britton, J. R., Carlson, S. M., Magurran, A. E., Alcaraz-Hernández, J. D., Almodóvar, A., et al. (2019). Effective monitoring of freshwater fish. *Fish. Fish.* 20, faf.12373. doi:10.1111/faf.12373

Říha, M., Kubečka, J., Vašek, M., Seďa, J., Mrkvička, T., Prchalová, M., et al. (2009). Long-term development of fish populations in the Římov Reservoir. *Fish. Manag. Ecol.* 16, 121–129. doi:10.1111/j.1365-2400.2008.00650.x

Říha, M., Ricard, D., Vašek, M., Prchalová, M., Mrkvička, T., Jůza, T., et al. (2015). Patterns in diel habitat use of fish covering the littoral and pelagic zones in a reservoir. *Hydrobiologia* 747, 111–131. doi:10.1007/s10750-014-2124-x

Ritterbusch, D., Blabolil, P., Breine, J., Erős, T., Mehner, T., Olin, M., et al. (2022). European fish-based assessment reveals high diversity of systems for determining ecological status of lakes. *Sci. Total Environ.* 802, 149620. doi:10.1016/j.scitotenv.2021.149620

Sala, O. E., Stuart, F., Iii, C., Armesto, J. J., Berlow, E., Bloomfield, J., et al. (2000). Global biodiversity scenarios for the year 2100. *Science* 287, 1770–1774. doi:10.1126/science.287.5459.1770

Šmejkal, M., Ricard, D., Prchalová, M., Říha, M., Muška, M., Blabolil, P., et al. (2015). Biomass and abundance biases in European standard gillnet sampling. *PLoS One* 10, e0122437. doi:10.1371/journal.pone.0122437

Souza, A. T., Argillier, C., Blabolil, P., Děd, V., Jarić, I., Monteoliva, A. P., et al. (2022). Empirical evidence on the effects of climate on the viability of common carp (*Cyprinus carpio*) populations in European lakes. *Biol. Invasions* 24, 1213–1227. doi:10.1007/s10530-021-02710-5

Specziár, A., Erős, T., György, Á. I., Tátrai, I., and Bíró, P. (2009). A comparison between the benthic Nordic gillnet and whole water column gillnet for characterizing fish assemblages in the shallow Lake Balaton. *Ann. Limnol. - Int. J. Lim.* 45, 171–180. doi:10.1051/limn/2009016

Vašek, M., Kubečka, J., Peterka, J., Čech, M., Draštík, V., Hladík, M., et al. (2004). Longitudinal and vertical spatial gradients in the distribution of fish within a canyon-shaped reservoir. *Int. Rev. Hydrobiol.* 89, 352–362. doi:10.1002/iroh.200410734

Vašek, M., Prchalová, M., Peterka, J., Ketelaars, H. A. M., Wagenvoort, A. J., Čech, M., et al. (2013). The utility of predatory fish in biomanipulation of deep reservoirs. *Ecol. Eng.* 52, 104–111. doi:10.1016/j.ecoleng.2012.12.100

Vašek, M., Prchalová, M., Říha, M., Blabolil, P., Čech, M., Draštík, V., et al. (2016). Fish community response to the longitudinal environmental gradient in Czech deep-valley reservoirs: Implications for ecological monitoring and management. *Ecol. Indic.* 63, 219–230. doi:10.1016/j.ecolind.2015.11.061

Vašek, M., Eloranta, A. P., Vejříková, I., Blabolil, P., Říha, M., Jůza, T., et al. (2018). Stable isotopes and gut contents indicate differential resource use by coexisting asp (*Leuciscus aspius*) and pikeperch (*Sander lucioperca*). *Ecol. Freshw. Fish.* 27, 1054–1065. doi:10.1111/eff.12414

Walters, C. (2003). Folly and fantasy in the analysis of spatial catch rate data. *Can. J. Fish. Aquat. Sci.* 60, 1433–1436. doi:10.1139/f03-152

Wickham, H. (2016). ggplot2: Elegant graphics for data analysis. Available at: https://ggplot2.tidyverse.org (Accessed September 29, 2022).

Wyatt, P. M. W., Pitts, C. S., and Butlin, R. K. (2006). A molecular approach to detect hybridization between bream *Abramis brama*, roach *Rutlius rutilus* and rudd *Scardinius erythrophthalmus*. *J. Fish. Biol.* 69, 52–71. doi:10.1111/j.1095-8649.2006.01104.x

Znachor, P., Hejzlar, J., Vrba, J., Nedoma, J., Seďa, J., Šimek, K., et al. (2017). in *Brief history of long-term ecological research into aquatic ecosystems and their catchments in the Czech Republic. Part I: Manmade reservoirs*. Editor P. Znachor (České Budějovice: Biology Centre CASInstitute of Hydrobiology), v.v.i.

frontiers | Frontiers in Marine Science

TYPE Original Research
PUBLISHED 16 December 2022
DOI 10.3389/fmars.2022.1070373

OPEN ACCESS

EDITED BY
Salvatore Siciliano,
Fundação Oswaldo Cruz (Fiocruz),
Brazil

REVIEWED BY
Valentina Asnaghi,
University of Genoa, Italy
Tomas Vega Fernandez,
Stazione Zoologica Anton Dohrn
Napoli, Italy

*CORRESPONDENCE
Fabrizio Gianni
fgianni@ogs.it

SPECIALTY SECTION
This article was submitted to
Marine Conservation and
Sustainability,
a section of the journal
Frontiers in Marine Science

RECEIVED 14 October 2022
ACCEPTED 21 November 2022
PUBLISHED 16 December 2022

CITATION
Gianni F, Manea E, Cataletto B,
Pugnetti A, Bergami C, Bongiorni L,
Pleslić G, Vilibić I and Bandelj V (2022)
Are we overlooking Natura 2000 sites?
Lessons learned from a transnational
project in the Adriatic Sea.
Front. Mar. Sci. 9:1070373.
doi: 10.3389/fmars.2022.1070373

Are we overlooking Natura 2000 sites? Lessons learned from a transnational project in the Adriatic Sea

Fabrizio Gianni[1]*, Elisabetta Manea[2], Bruno Cataletto[1,3], Alessandra Pugnetti[2], Caterina Bergami[4], Lucia Bongiorni[2], Grgur Pleslić[5], Ivica Vilibić[6] and Vinko Bandelj[1,3]

[1]National Institute of Oceanography and Applied Geophysics - OGS, Trieste, Italy, [2]National Research Council, Institute of Marine Sciences, CNR-ISMAR, Venice, Italy, [3]National Biodiversity Future Center - NBFC, Palermo, Italy, [4]National Research Council, Institute of Marine Sciences, CNR-ISMAR, Milan, Italy, [5]Blue World Institute of Marine Research and Conservation, Veli Lošinj, Croatia, [6]Ruđer Bošković Institute, Division for Marine and Environmental Research, Zagreb, Croatia

Since the adoption of the Habitats and Birds Directives by EU governments, marine Natura 2000 (N2K) sites have been established in the European Mediterranean Sea, creating one of the largest international networks of protected areas. Nevertheless, to date, marine N2K sites are generally scarcely implemented, studied and monitored, and thus their management effectiveness is weak, and their environmental status is often unknown. The Interreg Italy-Croatia ECOSS project aimed at establishing the ECOlogical observing system of the Adriatic Sea (ECOAdS), to integrate the existing research and monitoring activities in the area, and to promote data sharing at international level, for enhancing monitoring and conservation in Adriatic N2K network. In the framework of ECOSS, a conceptual model was developed and applied to selected N2K sites, to review the existing knowledge, assess site effectiveness, and suggest possible improvements in their monitoring and management based on the contribution that ECOAdS can provide to their implementation. Information on social, ecological, and oceanographic elements related to the conservation and management of these case studies was gathered by consulting the project partners involved in the management and monitoring of the sites and through a literature review. The results of this study revealed a discouraging condition with no management plan in most of the sites, while regulatory measures are generally in place but without surveillance. Monitoring activities are performed occasionally, and information on presence and status of protected species is often lacking or outdated. Although the N2K network provides a unique opportunity to advance marine conservation and achieve the 30% conservation target by 2030, the biggest challenge ahead is the proper management and monitoring of N2K sites. The proposed conceptual model may be taken as a framework to properly set up ecological observing systems in the N2K network and help overcome current limitations, integrating scientific research within the N2K conservation strategies.

KEYWORDS

marine conservation, monitoring, Natura 2000 sites, European directives, Adriatic

1 Introduction

Healthy ecosystems are critical for providing goods and services to human well-being. However, multiple stressors are leading to widespread changes in marine habitat structure and ecosystem functioning at all latitudes (Claudet and Fraschetti, 2010; Halpern et al., 2015; Zunino et al., 2017; Breitburg et al., 2018; Bucci et al., 2020).

Since the '70s, the European Union has demanded common policies to halt further biodiversity decline and protect the environment. In line with the provisions of the Convention on Biological Diversity (CBD) at the 1992 Rio Earth Summit, the Habitats Directive (HD; EC, 1992) and the Birds Directive (BD; EC, 2009) were among the first directives set off to ensure the conservation of a wide range of rare, threatened, or endemic flora and fauna. The HD and BD established, also thanks to the help of the funds provided by the LIFE Programme, a system of protected areas across Europe known as Natura 2000 (N2K), forming a transnational network (Evans, 2012). Currently, the N2K network includes more than 3000 marine sites and covers almost 9% of European seas (EEA, 2021). Their number is steadily growing (EC, 2017a), also to meet the requests of the latest environmental conservation policies and initiatives which include Agenda 30 (UN, 2015), the EU Biodiversity Strategy for 2030 (EC, 2020), and the 30 by 30 target (CBD, 2021). Such a vast network adds to other types of protected areas under national legislation and in the framework of different international legal instruments (e.g., Barcelona, Bern, Helsinki, OSPAR conventions).

As demonstrated by some decades of studies, when marine protected areas are well managed and adequately enforced, biodiversity and ecosystem functions can be preserved, in particular from fishing pressure (García-Rubies and Zabala, 1990; Marbà et al., 2002; Sala et al., 2012; Edgar et al., 2014; Zupan et al., 2018; Fraschetti et al., 2022). Fish are not the only organisms that can benefit from protection; other species, such as marine mammals, birds, and macrophytes can be safeguarded if their habitats are preserved (Ronconi et al., 2012; Filby et al., 2017; Tursi et al., 2022). The effects of protection measures in the ecosystems may then lead to the preservation of numerous ecosystem services needed to support both small and large-scale economies (e.g., increase in catches, income from other resources), and determine an improvement of human well-being and the social relevance of protected areas (Mascia et al., 2010; Ban et al., 2019).

To guarantee successful, well-managed protected areas and a possible return in benefits for local communities, all related socio-economic, governance, and ecological elements and their relationships need to be identified and taken into consideration (Cicin-Sain and Belfiore, 2005; Charles and Wilson, 2009). These elements are critical factors because they determine people's willingness to set and pursue conservation objectives, thus dramatically affecting the outcome of protected areas' implementation (Charles and Wilson, 2009; Di Franco et al., 2016; Giakoumi et al., 2018; Ban et al., 2019). Similarly, information on the status of species and habitats targeted for protection and the oceanographic processes affecting them is important to facilitate predictions of how marine environments will respond to anthropogenic alterations and assess if conservation objectives are achieved in the long term. In this context, integrated oceanographic and ecological observing systems, defined as networks of monitoring facilities and infrastructures collecting physicochemical and ecological data, may be the key to identify changes in ecosystems at multiple spatial and temporal scales (see Carr et al., 2011; Benedetti-Cecchi et al., 2018; Crise et al., 2018; Manea et al., 2020; Manea et al., 2021; Manea et al., 2022). Protected areas may, then, benefit from incorporating integrated observing systems into monitoring, as already demonstrated by several examples worldwide (e.g., Carr et al., 2011; Miranda et al., 2020; Perera-Valderrama et al., 2020). Indeed, through collection of ecological and oceanographic data and assessment of indicators by monitoring programs, the achievement of management goals and objectives can be tested and, if needed, additional regulatory actions implemented (Pomeroy et al., 2004; Cicin-Sain and Belfiore, 2005; Pomeroy et al., 2005). This approach is particularly useful for N2K sites, which represents an extraordinary tool for achieving international conservation targets. Nevertheless, marine N2K sites have been often overlooked with respect to terrestrial and freshwater N2K sites (e.g., Kati et al., 2015; Meinesz and Blanfuné, 2015; Orlikowska et al., 2016; Guidetti et al., 2019; Schéré et al., 2020), probably because the formers have been implemented more recently than the latter ones (Evans, 2012; Sundseth, 2013; EEA, 2021). Therefore, the greatest challenge that still lies ahead is the appropriate management and monitoring of marine N2K sites.

The Interreg Italy-Croatia project ECOSS[1] aimed to contribute filling these gaps through the establishment of the ECOlogical observing system in the Adriatic Sea (ECOAdS)[2] (Manea et al., 2021; Pugnetti et al., 2022). The scope behind this project was to connect tightly different actors through the science-society-policy interface at an international level, through a permanent and stable partnership between Italy and Croatia. ECOAdS is constituted by the facilities, infrastructures, and long-term ecological monitoring programs that already exist in the Adriatic Sea and that are managed by different research institutes, universities, and organizations. Data on ecological and oceanographic processes and variables collected in ECOAdS at local, national, and regional scales, can be used to get information on the status of target species and habitats, and assess the conservation effectiveness of N2K sites in the project area (Manea et al., 2022). The integration of marine ecological

---

[1] www.italy-croatia.eu/web/ecoss

observing systems would also provide a valuable tool for the implementation of EU Environmental Directives, for instance for defining Good Environmental Status (GES) under the Marine Strategy Framework Directive (MSFD; EC, 2008), and for achieving the objectives of the EUSAIR Action Plan (Manea et al., 2020; Solly and Berisha, 2021; Pugnetti et al., 2022).

In the framework of this project, a conceptual model was developed and applied to some selected N2K sites with the aim to review the existing information, assess the management and monitoring effectiveness, suggest possible improvements and highlight the contribution of ECOAdS in this context. In particular, for each case study, we identified social, ecological, and oceanographic elements, displayed and discussed the relationships among them, and highlighted possible pressures and gaps that management authorities should address to enhance the conservation of N2K sites. ECOAdS was connected to the management goals and target species of each N2K case study. Ecological and oceanographic variables and indicators that ECOAdS should monitor to assess the status of the conservation targets were also outlined.

The results of this study will inform the management of N2K sites and provide a baseline of knowledge to support the implementation of the ecological observing system in the Adriatic Sea. In addition, the conceptual model proposed here could be applied in other protected areas. Finally, since data on N2K sites is often difficult to gather, scattered, or not available, the information provided in this work can be useful to future studies aiming to investigate N2K management.

2 Materials and methods

2.1 Setting up of the conceptual model

The conceptual model was created using Cmaps v.6.04 free software[3], which allows constructing, sharing, and modifying online knowledge models represented as concept maps (Cañas et al., 2005). Specifically, the conceptual model consists of a schematic box-arrow model and was formulated following a stepwise process, as described in Grant et al. (1997). Firstly, the model required a deep understanding of all the key elements related to the management of protected areas. Social, ecological, and oceanographic elements of the N2K management were identified based on literature review on the subject (e.g., Pomeroy et al., 2004; Carr et al., 2011) and our own experience, represented graphically by boxes, and linked to one another according to their relationships. Efforts were done to keep the model as simple as possible, by avoiding an overcrowded scheme. Thus, only the most important elements and relationships were shown (Figure 1). The color of the box defines the typology of the element related to the N2K management, while the size is not relevant. Social elements (yellow boxes) are characterized by all those elements concerning the governance of N2K sites: EU Directives targeted by ECOSS (i.e., HD, BD, Water Framework Directive (WFD; EC, 2000), MSFD), the management authority, the management goal and objectives, the conservation measures, the stakeholders and the human activities. The identified ecological elements (green boxes) include the target species for which N2K sites were designated, the ecosystem services, the ecological monitoring programs, and the ecological variables measured. Oceanographic elements (blue boxes) include global changes, ocean processes, the oceanographic observing system, and the monitored oceanographic variables. Performance indicators used to assess environmental conditions or changes and to set environmental goals, constitute a cross-cutting element (orange box) since they can be obtained from a single ecological or oceanographic variable, or from multiple combinations of them. The monitoring programs, the variables, and the performance indicators were all included in the ECOAdS (red) box. A complete definition of the elements used in the conceptual model is provided in the Table S1.

The spatial arrangement of the boxes in the model follows a hierarchical organization: boxes at the top and bottom of the model refer to global aspects such as EU Directives, wide-scale monitoring programs, and ecosystem services, while in the center of the model, the elements are related to local aspects of the N2K sites, such as the goal, objectives, and target species. The ECOAdS box occupies a preeminent position in the conceptual model to make clear how ECOAdS can be integrated into the management workflow of the N2K sites. All the elements are strictly connected and the change of one determines changes in others. Arrows indicate the relationships among the elements. They can go in one direction from one box to another or can be bi-directional in case elements are expected to influence each other. Dotted lines indicate data flow, while continuous lines indicate a causal relationship between two boxes based on the direction of the arrow (Figure 1).

Starting from the top of the model, we outlined that the EU Environmental Directives ask management bodies to define the conservation measures and management goal of N2K sites. At the same time, the EU Directives also demand the effectiveness of these measures be assessed and this can be done by adopting performance indicators. The goal can be then split into more management objectives that in turn influence the choice of conservation measures. Management bodies generally engage stakeholders to discuss the limitation of the activities in the N2K sites and agree on the conservation measures. In fact, human activities in the N2K sites can directly affect species targeted for conservation, as well as functions and services provided by

---

[2] https://ecoads.eu/

[3] cmap.ihmc.us

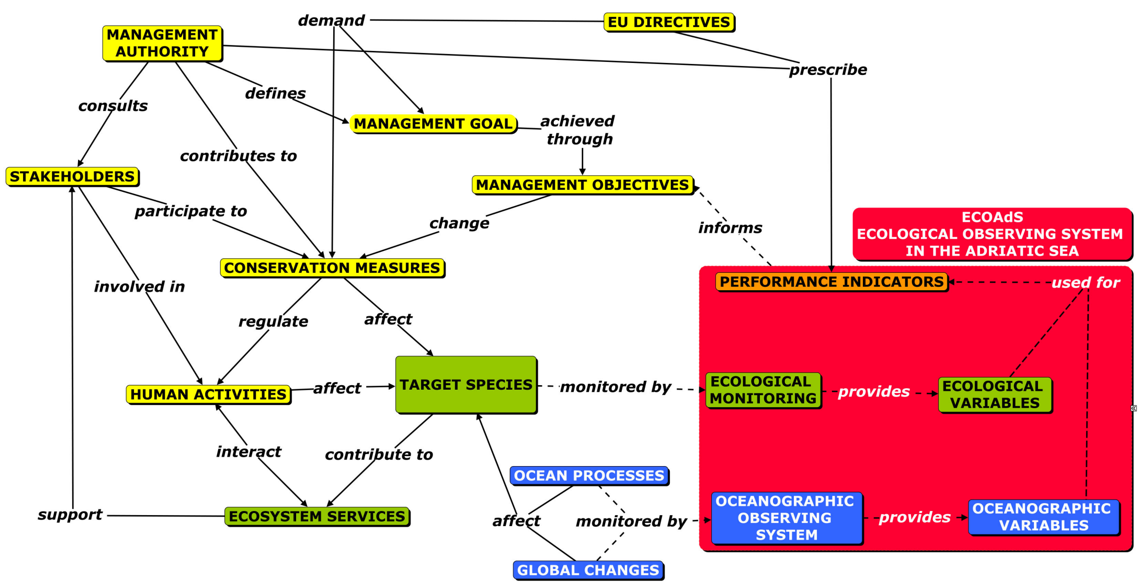

FIGURE 1
Generic conceptual model linking ECOAdS with N2K management and EU Directives. Dotted lines: data flow; continuous lines: causal relationship.

ecosystems. Natural processes and events can also affect target species. For instance, global changes, in particular those related to anthropogenically-driven climate alterations, and ocean processes are two of the main drivers of change for species and communities. Through ecological and oceanographic monitoring programs, ECOAdS collects data on environmental variables related to target species and both ecological and ocean processes. The variables, which depict the status of the system, are then used to obtain performance indicators that, in the end, track the progress towards objectives and evaluate the effects of management actions.

While the conceptual model was built around the need to manage N2K sites, i.e., with the 'Management Goal' box as an entry point, different users may start from different entry points according to their needs. For instance, an agency involved in monitoring activities may enter at the 'Ecological monitoring' box, while a public authority at the 'Management authority' box. In case, management objectives or conservation measures should be revised, the entry point could be based on these boxes.

2.2 Application of the model

The conceptual model was applied to seven Adriatic N2K sites (Figure 2) identified within the ECOSS project. These sites can be considered representative of the N2K network of the area since they include different typologies of habitats and environmental features. In addition, they are managed by the project partners, who therefore could provide information on the status of the target species and management activities. However, since some of these sites share similar ecological and geographical features, they were treated together and thus a total of four case studies were analyzed:

Case study 1: N2K sites Cres-Lošinj (HR3000161) and Viški akvatorij (HR3000469).
Case study 2: N2K site Malostonski zaljev (HR4000015).
Case study 3: N2K sites Trezze San Pietro e Bardelli (IT3330009) and Tegnùe di Chioggia (IT3250047).
Case study 4: N2K sites Delta del Po: tratto terminale e delta veneto (IT3270017) and Delta del Po (IT3270023).

Information to feed the application models was derived from questionnaires provided to the partners aimed to report the ecological monitoring programs they carry out (Vilibić and ECOSS Partnership, 2019), from technical tables at the project meetings, from the Standard Data Form (SDF) of the N2K sites[4], and from the project deliverables (Cataletto et al., 2019; Ciriaco et al., 2019; Markov and ECOSS Partnership, 2019; Golec and ECOSS Partnership, 2020; Miočić-Stošić et al., 2020; Pranovi et al., 2020). The management plan of the Delta del Po N2K site was also consulted to derive elements for this case study, even if it has not yet been approved (Ente Regionale Parco Delta del Po Veneto, 2010). When information was not available, elements were derived from literature review and knowledge available through our own experience. This was especially necessary for

---

[4] natura2000.eea.europa.eu

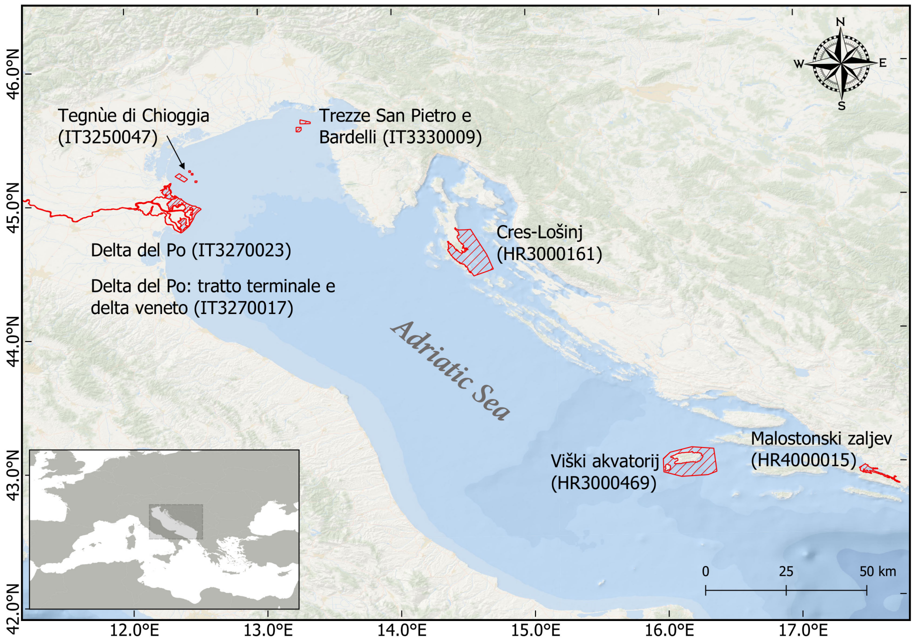

FIGURE 2
Map of the N2K sites considered as case studies in the ECOSS project. The two sites of Delta del Po are partially overlapping.

the management goals, objectives, conservation measures, monitoring variables and performance indicators that were missing in most cases. Criteria and requirements of the HD, BD, WFD (Annex V), and MSFD (Zampoukas et al., 2012; EC, 2017b) were also considered to identify such elements.

In particular, once target species, stakeholders, and human activities were identified, the management goals were outlined for N2K case studies reflecting the general objective of the HD and BD that aim at conserving the species and habitats of protection in a favorable status. To achieve these goals, specific management objectives and conservation measures were defined on the base of the target species of the case studies, and the human activities that may affect them. In the case pressures in N2K sites are expected to affect only one species, the management objectives were specifically focused on that species, otherwise, they were stated in a more general form, considering communities or ecosystems.

Ecological and oceanographic variables and performance indicators suitable to describe the status of the conservation targets and N2K effectiveness were also outlined based on the specific features of the target species and human activities, the identified management objectives, and the characteristics of the N2K case studies (Markov and ECOSS Partnership, 2019; Miočić-Stošić et al., 2020). Both state and pressure monitoring variables were considered, since they may also allow the detection of possible impacts acting on conservation targets and triggering changes in their original status. To keep the number of variables as low as possible and optimize efforts and costs for management authorities, they were also defined based on the general criteria of non-redundancy, sensitivity to change, feasibility, relevance for the N2K site, and cost-effectiveness (Pomeroy et al., 2004; Bundy et al., 2019). Even if none of the HD, BD, WFD, and MSFD specifically refer to performance indicators, the indicators here proposed are particularly in agreement with the eleven qualitative descriptors of the MSFD aimed to determine the GES. For instance, Descriptor 1, focused on biodiversity, can be investigated by different performance indicators such as change in species population demography, genetic diversity, and change in species home range and behavior. HD and BD also find correspondence in this descriptor since they do aim at conserving the species and habitats of protection in a favorable status. Descriptor 2, focused on non-indigenous species, can be monitored by analyzing trends in cover and density of invasive species. Descriptors 5 (eutrophication) and 8 (contaminants), also related to the requirements of the WFD, can be monitored by water quality indices.

To be in line with the aim of the ECOSS project, only management goals, objectives, conservation measures, variables, and indicators related to the biophysical-conservation aspects were considered (e.g., habitat quality, biological diversity, human activity regulation), while those related to socio-economic aspects (e.g., non-monetary benefits, food security, resource use conflicts) were not included.

3 Results

3.1 Case study 1: Viški akvatorij and Cres – Lošinj

3.1.1 Management aspects and target species

The N2K sites of Viški akvatorij and Cres – Lošinj in Croatia are managed by the Public Institution 'Sea and Karst' and Public Institution 'Priroda', respectively (Figure 3 and Tables S2, S3). These are two of the most important feeding and breeding areas for the common bottlenose dolphin (*Tursiops truncatus*, Montagu, 1821) in the Eastern Adriatic Sea (the only species listed in their respective SDF), so their main management goal is the preservation of the natural habitat of this species in a favorable status (Figure 3 and Tables S2, S3). However, to date, there is still no management plan, nor management objectives and other conservation measures in charge to effectively protect the target species (Markov and ECOSS Partnership, 2019). Management objectives necessary to achieve the N2K sites' goal should consider, for instance, the preservation and increase of *T. truncatus* population and its genetic connectivity with other populations, the preservation of dolphin prey species populations, the decrease of human-derived pressures, the preservation of a good seawater quality, and the mitigation of climate change and diseases impacts (Figure 3 and Tables S2, S3).

Different stakeholders act in this area including fishers, fish farmers, and, most of all, tourism companies due to the high touristic value of the area (Figure 3 and Tables S2, S3). Thus, fishing, aquaculture, tourism, and nautical sports including boating, are the main human activities in the N2K sites potentially causing dolphin bycatch (López, 2012), collision with boats, noise and water pollution (Rako-Gospić et al., 2013), change in dolphin habitat use (Pleslić et al., 2015), and marine debris pollution (Stagličić et al., 2021). Conservation measures that could effectively reduce such threats should be primarily focused on regulating all human activities, raising awareness of the local community, and increasing surveillance (Figure 3 and Tables S2, S3). In addition, the expansion of the size of the N2K site and protected area network beyond Cres-Lošinj and Viški akvatorij would guarantee the preservation of a larger portion of the home range of this highly mobile species (Pleslić et al., 2015; Fortuna et al., 2018), enhance genetic exchange between populations (Gaspari et al., 2015), and allow a better management of the source of threats that may be located outside the current borders of the N2K sites (Fortuna et al., 2018). The implementation of these measures would favor the resilience of the species to the effects of climate change (Wild et al., 2019; van Weelden et al., 2021).

3.1.2 ECOAdS and monitoring aspects

The Blue World Institute (BWI) conducts monitoring activities to assess the status of the bottlenose dolphin in the two studied sites. In addition, a considerable body of literature on the target species biology and ecology is available, especially for Cres-Lošinj (e.g., Bearzi et al., 2009; Genov et al., 2009; Rako-Gospić et al., 2013; Pleslić et al., 2015; Rako-Gospić et al., 2017; Pleslić et al., 2019). Based on the monitoring results, the dolphin populations in the two sites can be considered stable (Golec and ECOSS Partnership, 2020). Nevertheless, the main deficiency in the existing monitoring programs is that they are not conducted on a regular basis, because of the lack of resources (experts of marine mammals and funds) (Golec and ECOSS Partnership, 2020).

The effectiveness of the proposed conservation measures and the achievement of the management objectives can be assessed by some performance indicators, such as changes in dolphin population demography and behavior, genetic diversity, water quality indices, and trend in the amount of marine litter (Galgani et al., 2013; Jaiteh et al., 2013; Gaspari et al., 2015; Pavlidou et al., 2015; Pleslić et al., 2015; Fandel et al., 2020) (Figure 3 and Tables S2, S3). As an example of application of the conceptual model, the success of the regulatory actions aimed to reduce the impact of the marine traffic in the protected sites could be assessed by estimating the trend in the number of vessels inside the N2K sites and changes in dolphin home ranges or vocalizations. These performance indicators can be then calculated by collecting number, type and distribution of vessels, sound levels in water, the occurrence rate of dolphins in different areas and the characteristics of their vocalizations (Rako-Gospić et al., 2013; Pleslić et al., 2015; Fouda et al., 2018) (Figure 3 and Tables S2, S3).

Other useful monitoring variables could be, for instance, those related to the interaction of the species with fishing activities, as suggested by the project partners: signs of injuries in dolphins, number of interactions of dolphins with fishing gears or fish farms and, if possible, an estimate of the number of deaths due to bycatch (Jaiteh et al., 2013; Revuelta et al., 2018; Leone et al., 2019). These variables can be used to derive performance indicators such as the proportion of injured individuals, the interaction rate with fishing activities, and change in population demography (Figure 3 and Tables S2, S3). In addition, BWI recommended biopsy sampling for genetic and contamination analyses to better understand processes affecting the well-being of the local dolphin population (Gaspari et al., 2015; Zanuttini et al., 2019).

In relation to climate change, variables that may indicate an impact of extreme events on the species or alteration of oceanographic conditions may include the survival of dolphin offspring, dolphin prey population structure, spatial distributions of dolphins and their prey, time spent foraging by the target species per encounter, and frequency, duration, intensity of the heatwaves (Figure 3 and Tables S2, S3). In fact, different studies demonstrated that a catastrophic alteration of

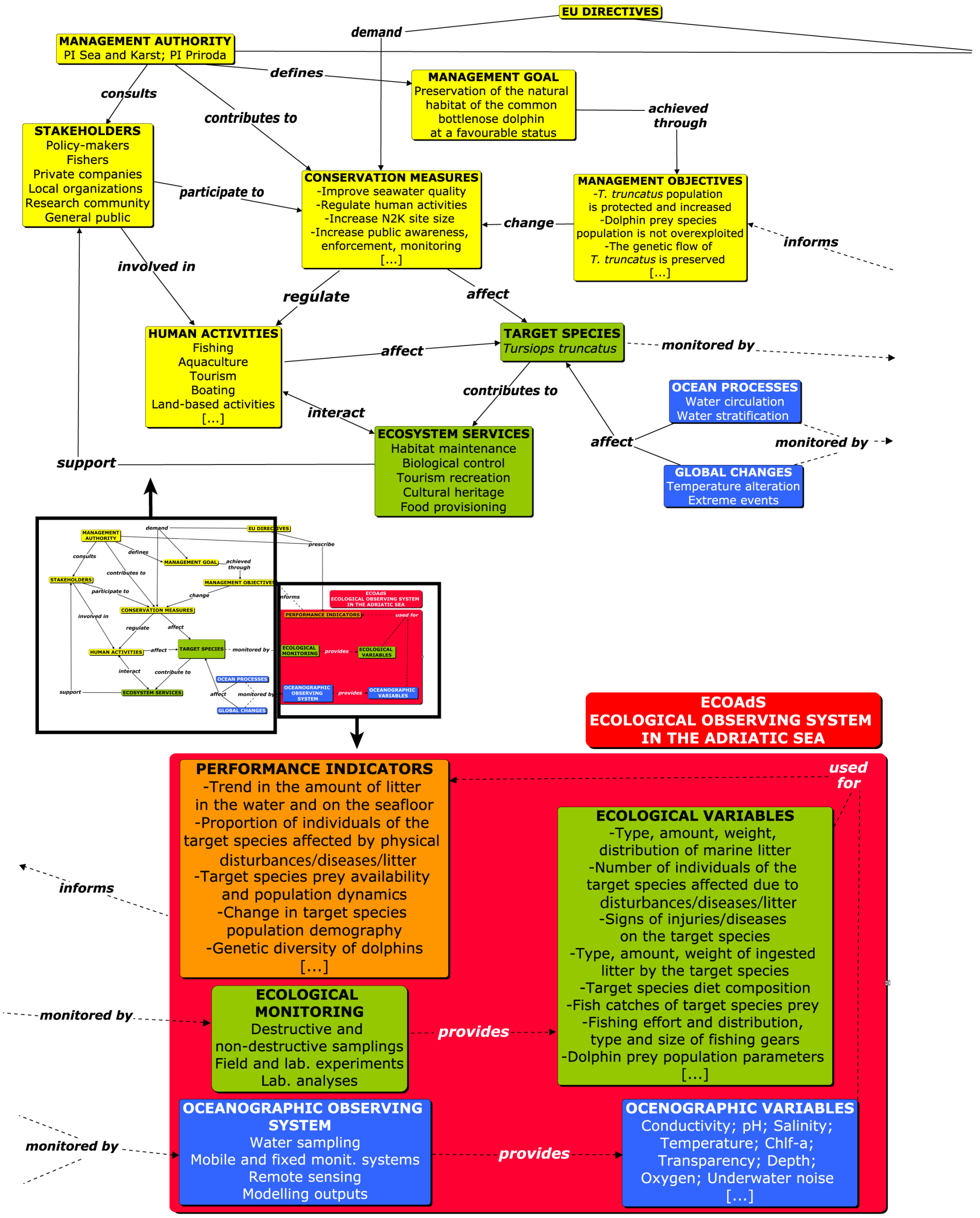

FIGURE 3
Application model of Cres-Lošinj and Viški akvatorij N2K sites for the target species *Tursiops truncatus*. For additional information see Tables S2, S3.

habitats, following marine heatwaves, caused a decline in reproductive success and survival of offspring (Wild et al., 2019); while alteration of distribution and behavior of dolphin prey species due to intense storm events, also induces a change in dolphin distribution and foraging behavior (Fandel et al., 2020).

Some of the variables proposed here are already collected in the two sites, and these include dolphin population demography, habitat use, spatial-temporal distribution, and underwater noise. The Croatian Institute of Oceanography and Fisheries (IZOR) also collects a wide range of data on physicochemical parameters, biological quality elements of the WFD, hydromorphological alterations, specific pollutants, benthic invertebrate fauna, macro-algae, and phytoplankton community (Ciriaco et al., 2019; Vilibić and ECOSS Partnership, 2019; Golec and ECOSS Partnership, 2020).

3.2 Case study 2: Malostonski zaljev

3.2.1 Management aspects and target species

The management body of Malostonski zaljev N2K site in Croatia is the Public Institution for the Management of Protected Natural Areas of Dubrovnik-Neretva County (PIDNIC), but a management plan has not been implemented yet, neither management objectives nor regulatory measures are officially defined (Markov and ECOSS Partnership, 2019). The N2K site protects two target habitats listed in the Annex I of the HD: 'Reefs' (1170) and 'Large shallow inlets and bays' (1160). This area is also under the significant influence of freshwater and characterized by the cultivation of the European flat oyster, a traditional, protected activity. Since there are no target species listed in the SDF, with the help of the project deliverables and partners, some relevant species deserving protection on the site were identified: seagrasses, the large brown algae *Fucus virsoides* J. Agardh, the noble pen shell *Pinna nobilis* (Linnaeus, 1758), the twaite shad *Alosa fallax* (Lacépède, 1803), and species forming coralligenous assemblages on the rocky substratum due to the presence of the 'Reefs' Habitat. Thus, the main management goal for this protected area could be the preservation of the target habitats ('Reefs' and 'Large shallow inlets and bays'), and the identified target species in a favorable status (Figure S1 and Tables S4, S5).

Management objectives necessary to achieve such goal should consider, for instance, the preservation of the target habitats and species in a good status, the preservation of the reef community diversity and gene pool, the decrease of human-derived pressures, the preservation of a good seawater quality and the mitigation of climate change, diseases, and the spread of invasive species impacts (Figure S1 and Tables S4, S5). As a primary conservation measure, PIDNIC suggested preserving the traditional shellfish cultivation together with natural habitats. To make this possible, it is necessary to actively support sustainable bivalve shellfish farming as part of cultural heritage and traditional value, and, at the same time, do an inventory of the biodiversity components, and monitor periodically the status of the marine environment (Golec and ECOSS Partnership, 2020). Indeed, aquaculture may impact the benthic habitats by increasing biodeposition to the seafloor (by mussel feces and pseudofeces) and induce variation in nutrient loading and fluxes, anaerobic metabolism in sediments and change in benthic community structure and functioning (Lacoste et al., 2020). In addition, the ecosystem in Malostonski zaljev N2K site is under the influence of the mainland, thus the surrounding land-based activities must be regulated to reduce water pollution and physical destruction of habitats due to urbanization. Other conservation measures that should be implemented are those aimed to limit several direct human pressures that may cause possible impact on target species, such as trampling on *F. virsoides*, anchoring and trawling on the seagrass *Cymodocea nodosa* (Ucria) (Asch. 1870) and *P. nobilis* (Francour et al., 1999; Vázquez-Luis et al., 2015), and poaching of the date mussel *Lithophaga lithophaga* (Linnaeus 1758) (Colletti et al., 2020). Installation of mooring buoys, a better surveillance, as well as the setting up of new regulations on the number of visitors, could be potential solutions to halt such threats. Regular monitoring activities in the area are required also to constantly assess the status of the target species and habitats (Figure S1 and Tables S4, S5).

3.2.2 ECOAdS and monitoring aspects

Currently, monitoring activities in the area are performed by IZOR and the University of Dubrovnik for the assessment of water quality and the status of MSFD descriptors. The activity includes the collection of physicochemical and biological parameters (e.g., chlorophyll-a, temperature, nutrients, pollutants, phytoplankton composition and abundance, sedimentation) (Vilibić and ECOSS Partnership, 2019; Golec and ECOSS Partnership, 2020). The variables collected by these monitoring activities may be particularly useful in the N2K site to assess the potential impact of the aquaculture (Ninčević-Gladan et al., 2015). The surface area devoted to aquaculture and abundance and biomass of benthic organisms, may also give us an indication of the impact of this activity in the bay (see for instance Borja et al., 2009; Valenti et al., 2018). At present, for most of the identified target species there is no adequate information (Markov and ECOSS Partnership, 2019), therefore, it is strictly urgent to create a knowledge base of their overall ecological status that would make a foundation for a management plan of the area. However, according to Miočić-Stošić et al. (2020), *C. nodosa* meadows seem to be stable, while *P. nobilis* is critically endangered due to a disease at regional scale (Carella et al., 2019; Šarić et al., 2020).

Other ecological and oceanographic variables that could be collected in the area to assess the efficacy of protection together with the corresponding performance indicators are listed in the Tables S4, S5 and in Figure S1. In particular, regarding *F. virsoides*, some monitoring variables that can give an indication of possible changes occurring to this species include, for example, spatial distribution, genetic information, individual size, biomass, adult and recruit density, mortality, and fertility rates. These variables should be then associated with data on temperature, nutrient concentration, and frequency, duration, and severity of sea storms and heatwaves. Indeed, *F. virsoides*, endemic to the Adriatic Sea, has faced an extensive regression in the last years (Battelli, 2016), probably due to the changes in the trophic status of this basin (Grilli et al., 2020) and climate change effects that seem to induce a shift in reproductive timing of this species (authors' personal observation), but further research is needed to clarify this aspect. Special attention should be also paid to other potential threats to this species, such as chemical pollutants (Falace et al., 2018) and intense herbivory (Battelli, 2016). Monitoring of contaminant concentration in *F. virsoides* tissues, as well as an assessment of the herbivore density is, hence, strictly recommended to implement adequate conservation actions (Figure S1 and Tables S4, S5).

Another destructive activity that has been reported in Mali Ston Bay is the date mussel poaching (Miočić-Stošić et al., 2020). This illegal practice often causes extensive and lasting reduction of the benthic habitat diversity with a shift from highly complex to structurally simplified habitats (i.e., biological deserts dominated by sea urchins) (Colletti et al., 2020). Efficacy of protection measures can be assessed by measuring percent cover of benthic habitat destructed by poaching and spatial and temporal extent of the disturbance (Figure S1 and Tables S4, S5). Useful information for managers may also infer from data on the number of reported offences in a year or kilograms of confiscated date mussels.

3.3 Case study 3: Trezze San Pietro e Bardelli and Tegnùe di Chioggia

3.3.1 Management aspects and target species

The Veneto Region is the main management authority of the Tegnùe di Chioggia N2K site, while the management authority of Trezze San Pietro e Bardelli N2K site is the Friuli Venezia Giulia Region, Italy (Figure S2 and Tables S6, S7). Both sites have been established to protect the mesophotic biogenic reefs of the Northern Adriatic Sea. They also share the same ecological and oceanographic processes and are subject to the same pressures. The loggerhead sea turtle *Caretta caretta* (Linnaeus, 1758) and *T. truncatus* are listed as target species in the SDFs of both sites, while *A. fallax*, and seabirds (the Mediterraneean gull *Ichthyaetus melanocephalus* (Temminck, 1820), the common shag *Phalacrocorax aristotelis desmarestii* (Payraudeau, 1826), and the yelkouan shearwater *Puffinus yelkouan* (Acerbi, 1827)) only for Trezze San Pietro e Bardelli N2K site. Many benthic species, such as the cushion coral *Cladocora caespitosa* (Linnaeus, 1758) and the stony cup coral *Astroides calycularis* (Pallas, 1766), are additionally listed in the SDFs and were here considered as relevant target species grouped under the name 'Coralligenous community', since most of them contribute to form coralligenous-like habitats with high biodiversity (Ponti et al., 2011; Falace et al., 2015). *P. nobilis* was also identified as a target species of these sites for its protected status under the HD and the recent threats it is facing (Carella et al., 2019) (Figure S2 and Tables S6, S7).

The management goal of these sites is the protection of the habitats and species identified in the N2K SDFs, and thus the conservation of all reef communities at a favorable status should be considered as the main management goal (Figure S2 and Tables S6, S7). Management plans have not been implemented for these sites. Management objectives should aim to maintain or restore a good status of the target species and their genetic diversity, minimize the effects of water pollution, the impact of invasive species, of the human activities and the effects of extreme events also linked to the climate change (Figure S2 and Tables S6, S7). Some conservation measures were issued by the management authorities including the prohibition of anchoring, professional and recreational fishing, organism collection, and the regulation of diving activities (Tables S6, S7). However, to date, the observance of the conservation measures is not guaranteed since surveillance and effective management of the sites is still lacking (S. Ciriaco personal observation). As additional conservation measures, it is advisable to remove marine litter that generally accumulates on these sites (e.g., Moschino et al., 2019) and install buoys signaling the N2K site boundaries for improving compliance with the current regulations. One of the main conservation strategies that should be put in place is increasing the protected area size and the creation of a network of mutually connected and protected sites in the Northern Adriatic Sea. Indeed, different studies have highlighted the high heterogeneity of these reefs and the importance to preserve more sites that are not currently protected, to guarantee connectivity through dispersal of the associated populations (Ponti et al., 2011; Falace et al., 2015; Fortuna et al., 2018; Bandelj et al., 2020). Joint management strategies, including offshore and terrestrial areas, with the adoption of ecosystem-based solutions are then necessary to avoid that high nutrient and sediment loads from rivers and the coast can affect the biogenic reef communities of these protected sites (Curiel et al., 2012; Falace et al., 2015) (Figure S2 and Tables S6, S7).

3.3.2 ECOAdS and monitoring aspects

Monitoring is performed only occasionally. There is no long, regular, and consistent data on species and oceanographic conditions, which is one of the main shortcomings in the management process, as highlighted by the project partners. Physicochemical or biological data can be partially derived from monitoring facilities in the proximity (e.g., buoys), or from remote sensing (e.g., chlorophyll-a from satellite), or modeling outputs (sea-current field components). This is not true for ecological data (e.g., community structure and composition) that were collected only during some projects (e.g., Interreg ITA-SLO TRECORALA, Italian PRIN ReefReseArcH) by different research institutions and companies investigating the diversity and connectivity of the mesophotic biogenic reefs (Vilibić and ECOSS Partnership, 2019; Golec and ECOSS Partnership, 2020).

Even less information is available on the spatial and temporal density and distribution of *T. truncatus, C. caretta*, *A. fallax* and seabirds in the N2K sites, and further monitoring programs should be carried out on these species (see La Mesa et al., 2015; Fortuna et al., 2018; Bearzi et al., 2021).

Taking as an example the application of the model for the 'coralligenous community', the effectiveness of the conservation measures aimed to reduce direct physical damages to the benthic organisms due to anchoring, scuba divers, or fishing can be assessed by different performance indicators, such as the proportion of injured organisms and changes in population demography. These indicators can be estimated by collecting data on population cover or density, signs of injuries on the target species, and number or cover of dead and injured organisms (e.g., Ferrigno et al., 2018) (Figure S2 and Tables S6, S7).

Particularly important for the benthic community is the early assessment of the presence, distribution, cover or density of invasive species to assess the potential risk posed by them (Figure S2 and Tables S6, S7). Similarly, the assessment of the amount, type, and weight of litter on the seafloor, as well as the number or cover of individuals adversely affected by litter is necessary to quantify the impact of such threat over time (Galgani et al., 2013) (Figure S2 and Tables S6, S7). The setting up of regular monitoring programs is, in these cases, an important strategy to report the spread of allochthonous species at their first stage or the presence of marine debris and to organize eradication and cleaning campaigns.

Alterations in pH and seawater temperature are the main consequences of climate change that interfere with the growth, body size, stress, reproductive success, and survival of many benthic species (Garrabou et al., 2009; Asnaghi et al., 2013; Zunino et al., 2017 and references therein). In addition, both processes have synergistic effects on species (Pörtner et al., 2014). To monitor such threats, it is advisable collecting data on the time of reproduction to assess potential phenological shifts, cover or density of organisms, presence of necrotic tissues, and growth, as well as data on oceanographic variables: temperature, number of extreme events (i.e., heatwaves), pH, and dissolved oxygen (Figure S2 and Tables S6, S7).

3.4 Case study 4: Delta del Po and Delta del Po: Tratto terminale e delta veneto

3.4.1 Management aspects and target species

The two Delta del Po N2K sites geographically overlap and compose a single delta system with shared habitats and species. The management body of both N2K sites is the Po Delta Veneto Regional Park Authority (Figure S3 and Tables S8, S9). A management plan was drafted for the Delta del Po N2K site (IT3270023), but to date, it has not been formally approved, even if it is used as a management tool for both sites (Ente Regionale Parco Delta del Po Veneto, 2010; Markov and ECOSS Partnership, 2019). Most of the species are exclusively related to freshwater and terrestrial habitats. For the aim of the ECOSS project, only those species strongly dependent on the marine environment were selected from the list of species under protection in these sites. These include different migratory and sedentary seabirds (the little tern *Sternula albifrons* (Pallas, 1764), the common tern *Sterna hirundo* (Linnaeus, 1758), the sandwich tern *Thalasseus sandvicensis* (Latham, 1787), the gull-billed tern *Gelochelidon nilotica* (Gmelin, 1789), the Caspian tern *Hydroprogne caspia* (Pallas 1770), the black-headed gull *Chroicocephalus ridibundus* (Linneus, 1766), the slender-billed gull *Chroicocephalus genei* (Breme, 1839), *I. melanocephalus*, and *P. aristotelis desmarestii*), all listed in the Annexes I and II of the BD. Some anadromous fish are also present (*A. fallax*, the Adriatic sturgeon *Acipenser naccarii* (Bonaparte, 1836), and the great sea lamprey *Petromyzon marinus* (Linnaeus, 1758)) that migrate from the sea to the upper part of the rivers for reproduction and listed in Annex II of the HD. Seagrasses used to thrive in the past in the Po Delta but they have not been recorded in recent years. However, since restoration activities are planned, and monitoring will be necessary for the next future, seagrasses were also considered as target species (Figure S3 and Tables S8, S9). The main management goal of these sites should include, therefore, the conservation of all these target species and their habitats (Figure S3 and Tables S8, S9).

Since both N2K sites extend on a vast terrestrial area characterized by numerous villages, human uses and pressures on target species are many and diffuse. Rivers, canals, and banks are modified by maintenance works, dike and barrier construction, soil erosion, rising of the salt wedge, and water level changes; all inducing alteration of sedimentation rate and water circulation. Recreational and commercial fishing, aquaculture and agriculture are also widely practiced in the area and are particularly important for the local economy; however, they contribute to cause changes in target species population and water quality, together with habitat fragmentation (Ente Regionale Parco Delta del Po Veneto, 2010). Finally, the river system is frequently visited by tourists as it is an attractive area for many outdoor activities (birdwatching, swimming, boating, trekking, etc.), but regulation measures should be improved since this sector represents another source of disturbance for the target species (Ente Regionale Parco Delta del Po Veneto, 2010; Verza and Cattozzo, 2015) (Figure S3 and Tables S8, S9).

Many management objectives and regulatory measures are reported in the management plan of the N2K to address the reported issues. They are mainly aimed to increase water circulation and passages for migratory fish, restore the Adriatic sturgeon population and the suitable habitats for seabirds, regulate human activities and predators' abundance to avoid impacts on target species and in particular on nesting seabirds, monitor target species status, assess pollution and improve water quality (Ente Regionale Parco Delta del Po Veneto, 2010; Markov and ECOSS Partnership, 2019) (Figure S3 and Tables S8, S9). In addition, one of the main objectives that should be considered is the implementation of integrated management strategies with other protected areas and in particular with a recent established N2K site offshore the Po River estuary (IT3270025 'Adriatico Settentrionale Veneto – Delta del Po') to enhance protection of target species whose home range includes also the marine realm. Major benefits for a more successful conservation, may also derive from involving stakeholders in the decision process and developing educational programs that could foster long-term interest and personal engagement in the management of ecosystems and natural resources (Giakoumi et al., 2018; Golec and ECOSS Partnership, 2020) (Figure S3 and Tables S8, S9).

3.4.2 ECOAdS and monitoring aspects

The Regional Agency for Environmental Protection and Prevention of the Veneto and the Institute of Marine Sciences – National Research Council perform monitoring activities in these N2K sites, assessing different physicochemical variables (e.g., temperature, salinity, current direction and velocity, organic matter, nutrients, and contaminants) and ecological variables (e.g., species composition, diversity, and abundance of phytoplankton, benthic macroinvertebrates, and macrophytes) (Vilibić and ECOSS Partnership, 2019; Golec and ECOSS Partnership, 2020). Occasionally, the management authority also monitors the spatial distribution of species, density, coverage, species richness, and community structure (Markov and ECOSS Partnership, 2019). Data on the status and distribution of *P. marinus*, *A. fallax*, and seagrasses are deficient, while much more information is available for the identified target seabirds (Ente Regionale Parco Delta del Po Veneto, 2010; Verza et al., 2011; Bon et al., 2013; Scarton et al., 2013; Verza, 2015; Scarton et al., 2018; Valle and Scarton, 2018; Miočić-Stošić et al., 2020; Scarton and Valle, 2020; Valle and Verza, 2020; Scarton, 2022). However, regular monitoring, necessary to detect population trends of these species and guide the adoption of adequate measure, is still lacking (Markov and ECOSS Partnership, 2019; Golec and ECOSS Partnership, 2020). Regarding, *A. naccarii*, this is an emblematic species of the Po River, endemic in the Adriatic Sea (Caramori et al., 2007; Arlati and Poliakova, 2009), and a priority species for conservation since its natural population has drastically decreased (Bronzi et al., 2011; Meadows and Coll, 2013). For this reason, the Adriatic sturgeon has been object of different reintroduction projects in the last decade (e.g., Life03nat/it/000113; Life04NAT/IT/000126; Life15 NAT/IT/0000989).

Conservation measures that can enhance restoration of the Adriatic sturgeon should include the improvement of river connectivity and water quality, control of illegal fishing, removal of invasive species, conservation and restoration of the spawning and foraging areas for *A. naccarii*, increase species abundance, and increase public awareness on the endangered status of this species (Caramori et al., 2007) (Figure S3 and Tables S8, S9). The effectiveness of such measures can be assessed by different performance indicators. For instance, the improvement of water circulation can be assessed by measuring some indicators of hydrological alteration (e.g., monthly magnitude of stream flow; magnitude, timing and duration of annual extreme stream flow; frequency and duration of flood and drought events) and their change over time (Richter et al., 1996; Lee et al., 2014) (Figure S3, Tables S8 and S9). To assess if the actions put in place to improve water quality are working, change in turbidity, water quality indices, the proportion of sick organisms and related contaminant level could be measured. These indicators are fed by several variables, some of which are already collected by local monitoring agencies, for instance, physicochemical water parameters, chlorophyll-a, nutrients and contaminants, and number of sick or dead organisms (Figure S3 and Tables S8, S9).

Special attention should be also given to monitoring the increase of the salinity in the delta system. Indeed, due to climate change, water extraction and alteration of river flow, salt-wedge intrusions into coastal zones are becoming more frequent and progressing upstream to the river, affecting numerous freshwater ecological processes, the migration of some target species, and the possibility to use water for drinking and soil irrigation (Simeoni and Corbau, 2009; Bellafiore et al., 2021). It is strictly urgent to adopt measures that regulate water extraction for different uses at the basin scale, creating phytodepuration basins, promoting the cultivation of plants that are more resistant to higher levels of salinity, and reducing those works that alter hydrological conditions (Zuazo and Pleguezuelo, 2009). Among the possible variables that can be monitored to detect environmental alterations are temperature, salinity, seawater level, water flow rate, amount of extracted water, number and frequency of heatwaves, amount of precipitation, population size of target species, number of dead or sick individuals, and species fertility (Figure S3 and Tables S8, S9).

4 Discussion

The application of the generic conceptual model to the four case studies selected in the ECOSS project, allowed to identify and analyze the main socio-ecological elements related to the management of these N2K sites, with the aim to understand the status of knowledge concerning such elements and the potential effectiveness of the existing management.

Overall, the management authorities were easily identified in our analysis since they have been already named locally or are represented by a regional or national institution, even if an effective management is still not in place. Also, the goal of the N2K sites can be considered well-defined since it follows the main objective of the HD and BD, which is maintaining and restoring the habitat types and species of community interest at a favorable conservation status. Human activities, and the relative stakeholders, were in part already available from the SDFs of the sites and from the questionnaires provided to the project partners (Vilibić and ECOSS Partnership, 2019). On the contrary, a general gap of information emerged regarding the management objectives and conservation measures, as well as a paucity of monitoring activities. This leads to a general lack of knowledge on the conservation status of target species in most of the considered N2K sites. In the two N2K sites protecting the mesophotic biogenic reefs of the Northern Adriatic Sea ('Trezze S. Pietro e Bardelli' and 'Tegnùe di Chioggia'), highly mobile species are listed in the SDFs as priorities for conservation, but very little information is available on their status (La Mesa et al., 2015; Fortuna et al., 2018; Bearzi et al., 2021), and they were observed only sporadically in the area. Hence they might be considered only occasional visitors. Much more information is available on the coralligenous communities present in these sites (e.g., Ponti et al., 2011; Falace et al., 2015; Nesto et al., 2020), but they are not monitored regularly. In the Malostonski zaljev N2K site, target species were not even identified and only two priority habitats were listed in the SDFs. The N2K sites where more efforts are invested in monitoring target species are Cres – Lošinj, Viški akvatorij, and Po Delta.

The lack of management plans and a concrete management process in these sites is the main reason for such data-deficiency. Even if management plans are not mandatory for N2K sites, as specified in the Article six of the HD, they may represent important tools for enhancing environmental conservation in N2K sites respect to the establishment of few regulatory measures. Indeed, in the absence of specific requirements from a management plan, objectives and conservation measures are often not defined, and monitoring activities are not performed or are often restricted to the time frame of specific research projects focusing on few processes or habitats (Golec and ECOSS Partnership, 2020). This also hampers the possibility to follow ecological trends and detect changes in population dynamics (White, 2019). The multiple human activities and pressures and the absence of surveillance are further constraints that limit the effectiveness of these protected areas.

In the light of these results, we tried to propose management objectives and conservation measures taking into consideration the target species, the human activities and their relationship, in order to address the potential sources of impact. The definition of clearly stated objectives is the primary step to specify the most appropriate performance indicators and variables to assess the achievement of the desired short-term management outcomes in the protected areas (Thomas and Middleton, 2003; Pomeroy et al., 2004). The variables and performance indicators linked to the expected objectives, target species and human pressures were identified here starting from the parameters that are already collected in the monitoring activities inside the N2K sites or in their proximity (Ciriaco et al., 2019). However, many other variables and indicators were suggested to be collected through ECOAdS, as the current monitoring is not sufficient to assess the status of the different target species and the impact of the many threats documented in the N2K sites. At this point, it is important to precise that the list of management objectives, performance indicators, and variables outlined for each N2K site are not intended to be used prescriptively but represent a starting point for effective management and appropriate monitoring programs in the N2K sites. In absence of specific and detailed information on the occurring species and their actual status, the definition of the elements to monitor is a difficult task. Future management authorities should adapt monitoring programs accordingly to the characteristics of the site, the available knowledge, the objectives, and the available human, technical and financial resources (Pomeroy et al., 2005). In the present study, only ecological indicators were considered within the ECOSS project. Other specific indicators for the assessment of stakeholder engagement, the role of leadership, the capacity of enforcement and compliance with protected areas' objectives need to be considered. Indeed, public support, and in particular strong commitment, education and participation of local stakeholders, has been found to be crucial for the long-term success of N2K management (Morris et al., 2014; Kati et al., 2015).

Our results particularly agree with those obtained by other authors that have investigated the N2K system in the last decade. Although this has an enormous potential to create a consistent network of interconnected protected areas, such a network does not still exist, and its implementation progress is considered slow in most Member States (MS). Mazaris et al. (2017) reported that the N2K system presently fails to meet several CBD targets (CBD, 2021): the relative percentage of protected marine surface area is variable among MS, offshore marine ecosystems are not well-represented, and ecological connectivity is not guaranteed. Moreover, less than 40% of the marine N2K sites have management plans, indicating limited or absent management activities in most cases (Mazaris et al., 2017). The effectiveness of the N2K network is even difficult to measure because the paucity of data due to sparse monitoring (Morris et al., 2014; Mazaris and Katsanevakis, 2018) and the absence of information on spatial distribution of threats, as in our cases (Mazaris and Katsanevakis, 2018; Mazaris et al., 2019). Our results also agree with a recent study that assessed the representativeness of the Adriatic N2K sites for the bottlenose dolphin and the loggerhead turtle (Fortuna et al., 2018). Authors found that, at present, site-based conservation tools are unlikely to be sufficient to protect a significant proportion (i.e., 60%) of both species, unless very large protected areas are designated and wide-scale mitigation measures of the threats are implemented (Fortuna et al., 2018).

Management bodies, governments and funding agencies are increasingly demanding information on management effectiveness of protected areas to assess whether results are in line with policy and management goals, and commensurate with efforts and resources (Roberts et al., 2018; Dunham et al., 2020). The conceptual model developed in this study can provide useful insights in protected areas' management and the proposed approach could be also extended to other N2K sites. Indeed, by summarizing the different components of N2K management, the model can help identify them and assess their relationship, highlight potential knowledge gaps, and provide a base for developing management plans. In addition, through the ecological observing system box, the model may help to develop adequate monitoring programs that collect data on ecological-oceanographic variables and performance indicators. Performance indicators then help to evaluate the effectiveness of conservation actions in each N2K site and revise related objectives, plans, and results. For example, if a performance indicator shows that a management objective is not being met, it may be necessary to modify or strengthen conservation measures; these will then regulate human activities and enable the conservation of target species. Vice versa, the model also allows detecting new human pressures that can act on the protected site or a new species that deserves protection, thus conservation measures or the variables necessary to monitor may require revision. Such a cyclic process follows an adaptive management approach, where the expectations of the set actions are systematically verified, and the results of such testing allow further revision and improvement of management practices (McCook et al., 2010; Nickols et al., 2019). Other types of stakeholders may also apply the model. For instance, environmental monitoring agencies may propose or change sampling techniques, variables, and performance indicators according to the target species and processes they are monitoring, and in relation to the management outcomes they are asked to verify. Thus, the observing system is not only important in the decision-making process but also in merging different fields: research, monitoring and nature management. For the aim of the ECOSS project, our conceptual model relies on ECOAdS[2], the ecological observing system in the Adriatic Sea established under the IT-HR project ECOSS[1]. However, any other observing systems or monitoring programs can be integrated in the model, according to the N2K site and local framework to which the model is applied.

To this regard, with the present study we also wanted to highlight the need to integrate existing monitoring initiatives and adopt a data sharing approach at transnational level in line with the principles of the Open Science (EC, 2018). This approach would facilitate the collection of data on ecological variables, which is generally expensive and difficult to achieve in the long-term. Ecological monitoring can be then further optimized by linking it to oceanographic monitoring, which can help predict the best timing of survey based on the ocean conditions that control the ecological process under study. For example, the optimal period for carrying out the surveys of anadromous fish populations could be derived by examining the physicochemical variables that trigger their migration (Thorstad et al., 2008). The creation of an observing system is also essential to enlarge the spatial and temporal scales of the monitoring activities and extend them outside the N2K sites, for taking into consideration different processes and species life stages (Garcìa-Charton et al., 2000; Edwards, 2004; Carr et al., 2011; Allen and Singh, 2016; Kaplan et al., 2019; Zipkin et al., 2021). While monitoring activities inside each N2K site can still be conducted by the management authority, local research institutes or private companies, large-scale data can derive only from a connected network of observing systems (Manea et al., 2022). This strategy links the potential of the protected areas to detect processes at local scales with that of the oceanographic monitoring systems at a larger scale. Thus, the response of habitats and species to both climate change and local human impacts can be revealed at multiple scales through the combination of N2K sites and observing system monitoring. Examples of extended and successful ocean monitoring systems that help to assess the effectiveness of protected area networks already exist worldwide, such as the Central and Northern California Ocean Observing System[5], and the Australia's Integrated Marine Observing System[6]. The extension and integration of the monitoring programs at different scales can also strengthen and elevate the role of the N2K sites in the Adriatic Sea: from a current condition of single isolated units to an efficient network of co-monitored and effective protected areas, as required by the CBD. This is particularly true for the N2K case studies here investigated because many of the species targeted for protection, such as seabirds, some fish, dolphins, and sea turtles, are expected to move significantly in the region (Fortuna et al., 2018). In addition, the complexity of some territories and the high number of human interests, such as in the Po Delta Park, require a broader and holistic management approach.

The results obtained in our study do not detract at all the role of N2K sites relative to the objectives for which they have been established. However, to achieve ecosystem-wide benefits, it is crucial to rethink and enlarge the aim of N2K sites. EU Member States should invest a great effort in the social and policy fields to greatly enhance N2K ability to meet its conservation targets. N2K site managers should follow an ecosystem-based approach and take into consideration the development of shared management processes between multiple N2K sites, as it is conceived in the HD (Bastmeijer, 2018). A stronger cooperation among different stakeholders is also needed to allow data and knowledge exchange (Bertzky and Stoll-Kleemann, 2009; Cvitanovic et al., 2014). In addition, to achieve broader coverage of the monitored area and focus on specific ecological factors, it may be useful to increase the

---

[5] www.cencoos.org

[6] imos.org.au

number of sampling stations within N2K sites and standardize the variables sampled (Manea et al., 2022). In the present study, an ecological observing system (ECOAdS) for the Adriatic Sea has been described, but, also, more generally, we suggest that existing or future ecological observing systems in other areas may be a suitable tool to improve monitoring programs, to share data between different producers and users, and ultimately to support the protection of marine habitats and species (Manea et al., 2022; Pugnetti et al., 2022).

Data availability statement

The original contributions presented in the study are included in the article/Supplementary Material. Further inquiries can be directed to the corresponding author.

Author contributions

FG: conceptualization, data collection and review, visualization, writing of the original draft. EM, CB, LB: inputs on the methodology. BC: work package leader, supervision. AP: project leader, supervision, inputs on the methodology. GP and IV: data provisioning. VB: conceptualization, visualization, supervision. All authors contributed to the article and approved the submitted version.

Funding

This research was supported by the EU funded project "ECOlogical observing system in the Adriatic Sea: oceanographic observations for biodiversity" (ECOSS; Interreg V-A Italy-Croatia CBC program 2014–2020, ID Number 10042301, from 01.01.2019 to 30.06.2021).

Acknowledgments

The authors want to thank all the ECOSS project partners for their suggestions and help at distinct stages of the study. Many thanks also to the two reviewers that helped to improve the manuscript.

Conflict of interest

The authors declare that the research was conducted in the absence of any commercial or financial relationships that could be construed as a potential conflict of interest.

Publisher's note

Supplementary material

The Supplementary Material for this article can be found online at: https://www.frontiersin.org/articles/10.3389/fmars.2022.1070373/full#supplementary-material

References

Allen, A. M., and Singh, N. J. (2016). Linking movement ecology with wildlife management and conservation. *Front. Ecol. Evol.* 3. doi: 10.3389/fevo.2015.00155

Arlati, G., and Poliakova, L. (2009). "Restoration of Adriatic sturgeon (*Acipenser naccarii*) in Italy: situation and perspectives," in *Biology, Conservation and Sustainable Development of Sturgeons*. Eds. R. Carmona, A. Domezain, M. García-Gallego, J. Hernando, F. Rodríguez and M. Ruiz-Rejón (Netherlands: Springer), 237–245. doi: 10.1007/978-1-4020-8437-9_14

Asnaghi, V., Chiantore, M., Mangialajo, L., Gazeau, F., Francour, P., Alliouane, S., et al. (2013). Cascading effects of ocean acidification in a rocky subtidal community. *PloS One* 8 (4), e61978. doi: 10.1371/journal.pone.0061978

Australia's Integrated Marine Observing System (IMOS). Available at: https://imos.org.au (Accessed September 30, 2022).

Bandelj, V., Solidoro, C., Laurent, C., Querin, S., Kaleb, S., Gianni, F., et al. (2020). Cross-scale connectivity of macrobenthic communities in a patchy network of habitats: the mesophotic biogenic habitats of the northern Adriatic Sea. *Estuar. Coast. Shelf Sci.* 245, 106978. doi: 10.1016/j.ecss.2020.106978

Ban, N. C., Gurney, G. G., Marshall, N. A., Whitney, C. K., Mills, M., Gelcich, S., et al. (2019). Well-being outcomes of marine protected areas. *Nat. Sustain.* 2 (6), 524–532. doi: 10.1038/s41893-019-0306-2

Bastmeijer, K. (2018). "The ecosystem approach for the marine environment and the position of humans: lessons from the EU Natura 2000 regime," in *The ecosystem approach in ocean planning and governance*. Eds. D. Langlet and R. Rayfuse (Leiden and Boston: Brill Nijhoff), 195–220. doi: 10.1163/9789004389984_008

Battelli, C. (2016). Disappearance of *Fucus virsoides* J. Agardh from the Slovenian coast (Gulf of Trieste, northern Adriatic). *Ser. Hist. Naturalis* 26 (1), 1–10. doi: 10.19233/ASHN.2016.1

Bearzi, G., Bonizzoni, S., Riley, M. A., and Santostasi, N. L. (2021). Bottlenose dolphins in the north-western Adriatic Sea: abundance and management implications. *Aquat. Conserv.: Mar. Freshw. Ecosyst.* 31 (3), 651–664. doi: 10.1002/aqc.3450

Bearzi, G., Fortuna, C., and Reeves, R. (2009). Ecology and conservation of common bottlenose dolphins *Tursiops truncatus* in the Mediterranean Sea. *Mammal Rev.* 39 (2), 92. doi: 10.1111/j.1365-2907.2008.00133.x

Bellafiore, D., Ferrarin, C., Maicu, F., Manfè, G., Lorenzetti, G., Umgiesser, G., et al. (2021). Saltwater intrusion in a Mediterranean delta under a changing climate. *J. Geophys. Res. Oceans* 126 (2), e2020JC016437. doi: 10.1029/2020JC016437

Benedetti-Cecchi, L., Crowe, T., Boehme, L., Boero, F., Christensen, A., Grémare, A., et al. (2018) *Strengthening Europe's capability in biological ocean observations.*

Eds. A. Piniella Muñiz, P. Kellett, K. Larkin and J. Heymans (Future Science Brief 3 of the European Marine Board, Ostend, Belgium), pp 76. Available at: https://marineboard.eu/sites/marineboard.eu/files/public/publication/EMB_FSB3_Biological_Ocean_Observation.pdf.

Bertzky, M., and Stoll-Kleemann, S. (2009). Multi-level discrepancies with sharing data on protected areas: What we have and what we need for the global village. *J. Environ. Manage.* 90 (1), 8–24. doi: 10.1016/j.jenvman.2007.11.001

Bon, M., Mezzavilla, F., and Scarton, F. (2013). *Carta delle vocazioni faunistiche del Veneto*. Associazione Faunisti Veneti. Regione del Veneto. pp 586. Available at: https://repository.regione.veneto.it/public/ad386f0479458f396c0feafb2cd47cae.php?lang=it&dl=true.

Borja, Á., Rodríguez, J. G., Black, K., Bodoy, A., Emblow, C., Fernandes, T. F., et al. (2009). Assessing the suitability of a range of benthic indices in the evaluation of environmental impact of fin and shellfish aquaculture located in sites across Europe. *Aquaculture* 293 (3-4), 231–240. doi: 10.1016/j.aquaculture.2009.04.037

Breitburg, D., Levin, L. A., Oschlies, A., Grégoire, M., Chavez, F. P., Conley, D. J., et al. (2018). Declining oxygen in the global ocean and coastal waters. *Science* 359 (6371), eaam7240. doi: 10.1126/science.aam7240

Bronzi, P., Castaldelli, G., Cataudella, S., and Rossi, R. (2011). "The historical and contemporary status of the European sturgeon, Acipenser sturio L., in Italy," in *Biology and Conservation of the European sturgeon*. Acipenser sturio L. 1758. Eds. P. Williot, E. Rochard, N. Desse-Besset, J. Gessner and F. Kirschbaum (Berlin, Heidelberg: Springer), 227–241. doi: 10.1007/978-3-642-20611-5_16

Bucci, K., Tulio, M., and Rochman, C. M. (2020). What is known and unknown about the effects of plastic pollution: a meta-analysis and systematic review. *Ecol. Appl.* 30 (2), e02044. doi: 10.1002/eap.2044

Bundy, A., Gomez, C., and Cook, A. M. (2019). Scrupulous proxies: defining and applying a rigorous framework for the selection and evaluation of a suite of ecological indicators. *Ecol. Indic.* 104, 737–754. doi: 10.1016/j.ecolind.2019.01.031

Cañas, A. J., Carff, R., Hill, G., Carvalho, M., Arguedas, M., Eskridge, T. C., et al. (2005). "Concept maps: integrating knowledge and information visualization," in *Knowledge and information visualization: searching for synergies*. Eds. S.-O. Tergan and T. Keller (Berlin, Heidelberg: Springer), 205–219. doi: 10.1007/11510154_11

Caramori, G. G., Barbieri, C., Galli, A., Lombardi, C., Marconato, E., Arlati, G., et al. (2007). *Il recupero dello storione cobice in Italia – Action Plan progetto Life 04NAT/IT/000126*. Ente Parco Regionale Veneto del Delta del Po. Regione Veneto, Regione Lombardia, Regione Emilia-Romagna - Italia. pp 162. doi: 10.13140/2.1.1085.7286

Carella, F., Aceto, S., Pollaro, F., Miccio, A., Iaria, C., Carrasco, N., et al. (2019). A mycobacterial disease is associated with the silent mass mortality of the pen shell *Pinna nobilis* along the Tyrrhenian coastline of Italy. *Sci. Rep.* 9 (1), 1–12. doi: 10.1038/s41598-018-37217-y

Carr, M. H., Woodson, C. B., Cheriton, O. M., Malone, D., McManus, M. A., and Raimondi, P. T. (2011). Knowledge through partnerships: integrating marine protected area monitoring and ocean observing systems. *Front. Ecol. Environ.* 9 (6), 342–350. doi: 10.1890/090096

Cataletto, B., Bandelj, V., Gianni, F., and ECOSS Partnership (2019). *D4.1.2. Report on the relationships between ecosystem-level management goals with ecological variables and oceanographic processes and the performance indicators. Deliverable of the Interreg Italy-Croatia ECOSS project Zenodo*. pp 30. doi: 10.5281/zenodo.6845444

Central and Northern California Coastal Ocean Observing System (CENCOOS). Available at: www.cencoos.org (Accessed September 30, 2022).

Charles, A., and Wilson, L. (2009). Human dimensions of marine protected areas. *ICES J. Mar. Sci.* 66 (1), 6–15. doi: 10.1093/icesjms/fsn182

Cicin-Sain, B., and Belfiore, S. (2005). Linking marine protected areas to integrated coastal and ocean management: a review of theory and practice. *Ocean Cost. Manage.* 48 (11-12), 847–868. doi: 10.1016/j.ocecoaman.2006.01.001

Ciriaco, S., Menon, S., Franzosini, C.ECOSS Partnership (2019). *D4.3.1. Review of the knowledge of the ecological processes in the selected Natura 2000 sites.* Deliverable of the Interreg Italy-Croatia ECOSS project. *Zenodo* pp. 30. doi: 10.5281/zenodo.6200186

Claudet, J., and Fraschetti, S. (2010). Human-driven impacts on marine habitats: a regional meta-analysis in the Mediterranean Sea. *Biol. Conserv.* 143 (9), 2195–2206. doi: 10.1016/j.biocon.2010.06.004

Cmap *CmapTools* (IHMC). Available at: https://cmap.ihmc.us (Accessed September 30, 2022).

Colletti, A., Savinelli, B., Di Muzio, G., Rizzo, L., Tamburello, L., Fraschetti, S., et al. (2020). The date mussel *Lithophaga lithophaga*: biology, ecology and the multiple impacts of its illegal fishery. *Sci. Total Environ.* 744, 140866. doi: 10.1016/j.scitotenv.2020.140866

Convention on Biological Diversity (CBD). (2021). *First draft of the post-2020 Global Biodiversity Framework, CBD/WG2020/3/3* (Montreal: CBD) pp. 12. Available at: https://www.cbd.int/doc/c/abb5/591f/2e46096d3f0330b08ce87a45/wg2020-03-03-en.pdf.

Crise, A., Ribera d'Alcalà, M., Mariani, P., Petihakis, G., Robidart, J., Iudicone, D., et al. (2018). A conceptual framework for developing the next generation of Marine OBservatories (MOBs) for science and society. *Front. Mar. Sci.* 5. doi: 10.3389/fmars.2018.00318

Curiel, D., Falace, A., Bandelj, V., Kaleb, S., Solidoro, C., and Ballesteros, E. (2012). Species composition and spatial variability of macroalgal assemblages on biogenic reefs in the northern Adriatic Sea. *Bot. Mar.* 55, 625–638. doi: 10.1515/bot-2012-0166

Cvitanovic, C., Fulton, C. J., Wilson, S. K., van Kerkhoff, L., Cripps, I. L., and Muthiga, N. (2014). Utility of primary scientific literature to environmental managers: an international case study on coral-dominated marine protected areas. *Ocean Coast. Manage.* 102, 72–78. doi: 10.1016/j.ocecoaman.2014.09.003

Di Franco, A., Thiriet, P., Di Carlo, G., Dimitriadis, C., Francour, P., Gutiérrez, N. L., et al. (2016). Five key attributes can increase marine protected areas performance for small-scale fisheries management. *Sci. Rep.* 6 (1), 1–9. doi: 10.1038/srep38135

Dunham, A., Dunham, J. S., Rubidge, E., Iacarella, J. C., and Metaxas, A. (2020). Contextualizing ecological performance: rethinking monitoring in marine protected areas. *Aquat. Conserv.: Mar. Freshw. Ecosyst.* 30 (10), 2004–2011. doi: 10.1002/aqc.3381

Edgar, G. J., Stuart-Smith, R. D., Willis, T. J., Kininmonth, S., Baker, S. C., Banks, S., et al. (2014). Global conservation outcomes depend on marine protected areas with five key features. *Nature* 506 (7487), 216–220. doi: 10.1038/nature13022

Edwards, M. S. (2004). Estimating scale-dependency in disturbance impacts: El niños and giant kelp forests in the northeast Pacific. *Oecologia* 138, 436–447. doi: 10.1007/s00442-003-1452-8

Ente Regionale Parco Delta del Po Veneto (2010). *Piano di gestione ZPS IT3270023–Delta del Po*. Regione del Veneto. Available at: http://www.istitutodelta.it/wp-content/uploads/2020/05/PdG_DeltaPoRev11.pdf.

European Commission (1992). Council directive 92/43/EEC of May 21, 1992 on the conservation of natural habitats and of wild fauna and flora. *Off. J. Eur. Union* 206, 7-50. Available at: https://eur-lex.europa.eu/legal-content/EN/TXT/?uri=celex%3A31992L0043.

European Commission (2000). Directive 2000/60/EC of the European Parliament and of the Council of 23 October 2000 establishing a framework for community action in the field of water policy (Water Framework Directive). *Off. J. Eur. Union* 327, 1–73. Available at: https://eur-lex.europa.eu/legal-content/EN/TXT/?uri=celex%3A32000L0060.

European Commission (2008). Directive 2008/56/EC of the European Parliament of the Council of 17 June 2008 establishing a framework for community action in the field of marine environmental policy (Marine Strategy Framework Directive). *Off. J. Eur. Union* 164, 19–40.

European Commission (2009). Directive 2009/147/EC of the European Parliament and of the Council of 30 November 2009 on the conservation of wild birds. *Off. J. Eur. Union* 20, 7–15. Available at: https://eur-lex.europa.eu/legal-content/EN/TXT/?uri=CELEX%3A32009L0147.

European Commission (2017a). *Communication from the Commission to the European Parliament, the Council, the European economic and social committee and the committee of the regions. An Action Plan for nature, people and the economy. Brussels, COM/2017/0198 final.* Available at: https://eur-lex.europa.eu/legal-content/EN/TXT/?uri=COM%3A2017%3A198%3AFIN.

European Commission (2017b). *Commission decision (EU) 2017/848 of 17 May 2017 laying down criteria and methodological standards on good environmental status of marine waters and specifications and standardized methods for monitoring and assessment, and repealing decision. Brussels, 2010/477/EU.* Available at: http://data.europa.eu/eli/dec/2017/848/oj.

European Commission (2018). *Directorate-general for research and innovation* (OSPP-REC: Open Science Policy Platform Recommendations, Publications Office, Brussels), pp. 18. doi: 10.2777/958647

European Commission (2020). *Communication from the Commission to the European Parliament, the Council, the European economic and social committee and the committee of the regions. EU Biodiversity strategy for 2030. Bringing nature back into our lives. Brussels, COM/2020/380 final.* Available at: https://eur-lex.europa.eu/legal-content/EN/TXT/?uri=celex%3A52020DC0380.

European Environment Agency (2021). *Natura 2000 coverage in Europe's seas, European Environment Agency.* Available at: https://www.eea.europa.eu/themes/biodiversity/natura-2000 (Accessed July 02, 2022).

Evans, D. (2012). Building the European Union's Natura 2000 network. *Nat. Conserv.* 1, 11–26. doi: 10.3897/natureconservation.1.1808

Falace, A., Kaleb, S., Curiel, D., Miotti, C., Galli, G., Querin, S., et al. (2015). Calcareous bio-concretions in the northern Adriatic Sea: habitat types, environmental factors that influence habitat distributions, and predictive modeling. *PloS One* 10 (11), e0140931. doi: 10.1371/journal.pone.0140931

Falace, A., Tamburello, L., Guarnieri, G., Kaleb, S., Papa, L., and Fraschetti, S. (2018). Effects of a glyphosate-based herbicide on *Fucus virsoides* (Fucales, Ochrophyta) photosynthetic efficiency. *Environ. Pollut.* 243, 912–918. doi: 10.1016/j.envpol.2018.08.053

Fandel, A. D., Garrod, A., Hoover, A. L., Wingfield, J. E., Lyubchich, V., Secor, D. H., et al. (2020). Effects of intense storm events on dolphin occurrence and foraging behavior. *Sci. Rep.* 10, 1–9. doi: 10.1038/s41598-020-76077-3

Ferrigno, F., Appolloni, L., Russo, G. F., and Sandulli, R. (2018). Impact of fishing activities on different coralligenous assemblages of gulf of Naples (Italy). *J. Mar. Biolog. Assoc.* 98, 41–50. doi: 10.1017/S0025315417001096

Filby, N. E., Christiansen, F., Scarpaci, C., and Stockin, K. A. (2017). Effects of swim-with-dolphin tourism on the behaviour of a threatened species, the burrunan dolphin *Tursiops australis*. *Endanger. Species Res.* 32, 479–490. doi: 10.3354/esr00826

Fortuna, C. M., Cañadas, A., Holcer, D., Brecciaroli, B., Donovan, G. P., Lazar, B., et al. (2018). The coherence of the European Union marine Natura 2000 network for wide-ranging charismatic species: a Mediterranean case study. *Front. Mar. Sci.* 5. doi: 10.3389/fmars.2018.00356

Fouda, L., Wingfield, J. E., Fandel, A. D., Garrod, A., Hodge, K. B., Rice, A. N., et al. (2018). Dolphins simplify their vocal calls in response to increased ambient noise. *Biol. Lett.* 14 (10), 20180484. doi: 10.1098/rsbl.2018.0484

Francour, P., Ganteaume, A., and Poulain, M. (1999). Effects of boat anchoring in *Posidonia oceanica* seagrass buds in the Port-Cros National Park (north-western Mediterranean Sea). *Aquat. Conserv.: Mar. Freshw. Ecosyst.* 9, 391–400.

Fraschetti, S., Fabbrizzi, E., Tamburello, L., Uyarra, M. C., Micheli, F., Sala, E., et al. (2022). An integrated assessment of the Good Environmental Status of Mediterranean marine protected areas. *J. Environ. Manage.* 305, 114370. doi: 10.1016/j.jenvman.2021.114370

Galgani, F., Hanke, G., Werner, S. D. V. L., and De Vrees, L. (2013). Marine litter within the European Marine Strategy Framework Directive. *ICES J. Mar. Sci.* 70 (6), 1055–1064. doi: 10.1093/icesjms/fst122

Garcìa-Charton, J. A., Williams, I. D., Pérez-Ruzafa, A., Milazzo, M., Chemello, R., Marcos, C., et al. (2000). Evaluating the ecological effects of Mediterranean marine protected areas: habitat, scale and the natural variability of ecosystems. *Environ. Conserv.* 27, 159–178. doi: 10.1017/S0376892900000199

García-Rubies, A., and Zabala, M. (1990). Effects of total fishing prohibition on the rocky fish assemblages of Medes islands marine reserve (NW Mediterranean). *Sci. Mar.* 54 (4), 317–328. Available at: http://hdl.handle.net/2445/32434.

Garrabou, J., Coma, R., Bensoussan, N., Bally, M., Chevaldonné, P., Cigliano, M., et al. (2009). Mass mortality in northwestern Mediterranean rocky benthic communities: effects of the 2003 heat wave. *Glob. Change Biol.* 15 (5), 1090–1103. doi: 10.1111/j.1365-2486.2008.01823.x

Gaspari, S., Holcer, D., Mackelworth, P., Fortuna, C., Frantzis, A., Genov, T., et al. (2015). Population genetic structure of common bottlenose dolphins (*Tursiops truncatus*) in the Adriatic Sea and contiguous regions: implications for international conservation. *Aquat. Conserv.: Mar. Freshw. Ecosyst.* 25 (2), 212–222. doi: 10.1002/aqc.2415

Genov, T., Wiemann, A., and Fortuna, C. M. (2009). Towards identification of the bottlenose dolphin (*Tursiops truncatus*) population structure in the north-eastern Adriatic Sea: preliminary results. *Varstvo Narave* 22, 73–80. Available at: https://zrsvn-varstvonarave.si/wp-content/uploads/2019/09/Genov_1574.pdf.

Giakoumi, S., McGowan, J., Mills, M., Beger, M., Bustamante, R. H., Charles, A., et al. (2018). Revisiting "success" and "failure" of marine protected areas: a conservation scientist perspective. *Front. Mar. Sci.* 5. doi: 10.3389/fmars.2018.00223

Golec, I., and ECOSS Partnership (2020). *D3.2.1. Report on the ecological monitoring, conservation strategies and management questions of Natura 2000 Marine sites. Deliverable of the Interreg Italy-Croatia ECOSS project. Zenodo* pp. 71. doi: 10.5281/zenodo.6135905

Grant, W., Pederson, E., and Marin, S. (1997). *Ecology and natural resource management: systems analysis and simulation* (New York: John Wiley and Sons, Inc), pp 400.

Grilli, F., Accoroni, S., Acri, F., Bernardi Aubry, F., Bergami, C., Cabrini, M., et al. (2020). Seasonal and interannual trends of oceanographic parameters over 40 years in the northern Adriatic Sea in relation to nutrient loadings using the EMODnet chemistry data portal. *Water* 12 (8), 2280. doi: 10.3390/w12082280

Guidetti, P., Addis, P., Atzori, F., Bussotti, S., Calò, A., Cau, A., et al. (2019). Assessing the potential of marine Natura 2000 sites to produce ecosystem-wide effects in rocky reefs: a case study from Sardinia island (Italy). *Aquat. Conserv.: Mar. Freshw. Ecosyst.* 29 (4), 537–545. doi: 10.1002/aqc.3026

Halpern, B. S., Frazier, M., Potapenko, J., Casey, K. S., Koenig, K., Longo, C., et al. (2015). Spatial and temporal changes in cumulative human impacts on the world's ocean. *Nat. Commun.* 6 (1), 1–7. doi: 10.1038/ncomms8615

Jaiteh, V. F., Allen, S. J., Meeuwig, J. J., and Loneragan, N. R. (2013). Subsurface behavior of bottlenose dolphins (*Tursiops truncatus*) interacting with fish trawl nets in northwestern Australia: implications for bycatch mitigation. *Mar. Mammal Sci.* 29 (3), E266–E281. doi: 10.1111/j.1748-7692.2012.00620.x

Kaplan, K. A., Yamane, L., Botsford, L. W., Baskett, M. L., Hastings, A., Worden, S., et al. (2019). Setting expected timelines of fished population recovery for the adaptive management of a marine protected area network. *Ecol. Appl.* 29 (6), e01949. doi: 10.1002/eap.1949

Kati, V., Hovardas, T., Dieterich, M., Ibisch, P. L., Mihok, B., and Selva, N. (2015). The challenge of implementing the European network of protected areas Natura 2000. *Conserv. Biol.* 29 (1), 260–270. doi: 10.1111/cobi.12366

Lacoste, É., McKindsey, C. W., and Archambault, P. (2020). Biodiversity–Ecosystem Functioning (BEF) approach to further understanding aquaculture–environment interactions with application to bivalve culture and benthic ecosystems. *Rev. Aquac.* 12, 2027–2041. doi: 10.1111/raq.12420

La Mesa, G., Annunziatellis, A., Filidei, E.Jr., and Fortuna, C. M. (2015). Modeling environmental, temporal and spatial effects on twaite shad (*Alosa fallax*) by-catches in the central Mediterranean Sea. *Fish. Oceanogr.* 24 (2), 107–117. doi: 10.1111/fog.12093

Lee, A., Cho, S., Kang, D. K., and Kim, S. (2014). Analysis of the effect of climate change on the nakdong river stream flow using indicators of hydrological alteration. *J. Hydro. Environ. Res.* 8, 234–247. doi: 10.1016/j.jher.2013.09.003

Leone, A. B., Bonanno Ferraro, G., Boitani, L., and Blasi, M. F. (2019). Skin marks in bottlenose dolphins (*Tursiops truncatus*) interacting with artisanal fishery in the central Mediterranean Sea. *PloS One* 14 (2), e0211767. doi: 10.1371/journal.pone.0211767

López, B. D. (2012). Bottlenose dolphins and aquaculture: interaction and site fidelity on the north-eastern coast of Sardinia (Italy). *Mar. Biol.* 159 (10), 2161–2172. doi: 10.1007/s00227-012-2002-x

Manea, E., Bergami, C., Bongiorni, L., Capotondi, L., De Maio, E., Oggioni, A., et al. (2021). A transnational marine ecological observatory in the Adriatic Sea to harmonize a fragmented approach to monitoring and conservation. *Adv. Oceanogr. Limnol.* 12 (1), pp 13. doi: 10.4081/aiol.2021.9811

Manea, E., Bergami, C., Pugnetti, A., Gianni, F., Oggioni, A., Bandelj, V., et al. (2022). An ecosystem-based system of variables to enhance marine species and habitat monitoring and conservation: the Adriatic Natura 2000 case study. *Front. Mar. Sci.* 9. doi: 10.3389/fmars.2022.920366

Manea, E., Bongiorni, L., Bergami, C., and Pugnetti, A. (2020). "Challenges for marine ecological observatories to promote effective GMS of Natura 2000 network. The case study of ECOAdS in the Adriatic Sea," in *Governing future challenges in protected areas*. Eds. L. Alfaré and E. Ruoss (Roma, Italy: CNR Edizioni), 23–39.

Marbà, N., Duarte, C. M., Holmer, M., Martínez, R., Basterretxea, G., Orfila, A., et al. (2002). Effectiveness of protection of seagrass (*Posidonia oceanica*) populations in Cabrera National Park (Spain). *Environ. Conserv.* 29 (4), 509–518. doi: 10.1017/S037689290200036X

Markov, M., and ECOSS Partnership (2019). *D4.1.1. Report on the characterization of the selected Natura 2000 sites. Deliverable of the Interreg Italy-Croatia ECOSS project*, Zenodo pp 86. doi: 10.5281/zenodo.6136088

Mascia, M. B., Claus, C. A., and Naidoo, R. (2010). Impacts of marine protected areas on fishing communities. *Conserv. Biol.* 24 (5), 1424–1429. doi: 10.1111/j.1523-1739.2010.01523.x

Mazaris, A. D., Almpanidou, V., Giakoumi, S., and Katsanevakis, S. (2017). Gaps and challenges of the European network of protected sites in the marine realm. *ICES J. Mar. Sci.* 75, 190–198. doi: 10.1093/icesjms/fsx125

Mazaris, A. D., Kallimanis, A., Gissi, E., Pipitone, C., Danovaro, R., Claudet, J., et al. (2019). Threats to marine biodiversity in European protected areas. *Sci. Total Environ.* 677, 418–426. doi: 10.1016/j.scitotenv.2019.04.333

Mazaris, A. D., and Katsanevakis, S. (2018). The threat of biological invasions is under-represented in the marine protected areas of the European Natura 2000 network. *Biol. Conserv.* 225, 208–212. doi: 10.1016/j.biocon.2018.07.007

McCook, L. J., Ayling, T., Cappo, M., Choat, J. H., Evans, R. D., De Freitas, D. M., et al. (2010). Adaptive management of the Great Barrier Reef: a globally significant demonstration of the benefits of networks of marine reserves. *Proc. Natl. Acad. Sci. U.S.A.* 107 (43), 18278–18285. doi: 10.1073/pnas.0909335107

Meadows, D., and Coll, H. (2013). *Status review report of five foreign sturgeon. Report to the National Marine Fisheries Service, Office of Protected Resources*, pp 78. Available at: https://web.archive.org/web/20141219084715/http://www.nmfs.noaa.gov/pr/pdfs/statusreviews/sturgeon_5foreign.pdf.

Meinesz, A., and Blanfuné, A. (2015). 1983–2013: development of marine protected areas along the French Mediterranean coasts and perspectives for achievement of the Aichi target. *Mar. Policy* 54, 10–16. doi: 10.1016/j.marpol.2014.10.025

Miočić-Stošić, J., Pleslić, G., and ECOSS Partnership (2020). *D4.2.1. Review of the knowledge of the target species at the selected Natura 2000 sites. Deliverable of the Interreg Italy-Croatia ECOSS project*. Zenodo pp 98 doi: 10.5281/zenodo.6199909

Miranda, R. J., Malhado, A. C. M., Fabré, N., Batista, V., Santos, R., Campos-Silva, J., et al. (2020). Integrating Long Term Ecological Research (LTER) and marine protected area management: challenges and solutions. *Oecol. Aust.* 24 (2), 279–300. doi: 10.4257/oeco.2020.2402.05

Morris, R. K., Bennett, T., Blyth-Skyrme, R., Barham, P. J., and Ball, A. (2014). Managing Natura 2000 in the marine environment–An evaluation of the effectiveness of 'management schemes' in England. *Ocean Coast. Manage.* 87, 40–51. doi: 10.1016/j.ocecoaman.2013.10.017

Moschino, V., Riccato, F., Fiorin, R., Nesto, N., Picone, M., Boldrin, A., et al. (2019). Is derelict fishing gear impacting the biodiversity of the northern Adriatic Sea? An answer from unique biogenic reefs. *Sci. Total Environ.* 663, 387–399. doi: 10.1016/j.scitotenv.2019.01.363

Nesto, N., Simonini, R., Riccato, F., Fiorin, R., Picone, M., Da Ros, L., et al. (2020). Macro-zoobenthic biodiversity of northern Adriatic hard substrates: ecological insights from a bibliographic survey. *J. Sea Res.* 160, 101903. doi: 10.1016/j.seares.2020.101903

Nickols, K. J., White, J. W., Malone, D., Carr, M. H., Starr, R. M., Baskett, M. L., et al. (2019). Setting ecological expectations for adaptive management of marine protected areas. *J. Appl. Ecol.* 56 (10), 2376–2385. doi: 10.1111/1365-2664.13463

Ninčević-Gladan, Ž., Bužančić, M., Kušpilić, G., Grbec, B., Matijević, S., Skejić, S., et al. (2015). The response of phytoplankton community to anthropogenic pressure gradient in the coastal waters of the eastern Adriatic Sea. *Ecol. Indic.* 56, 106–115. doi: 10.1016/j.ecolind.2015.03.018

Orlikowska, E. H., Roberge, J. M., Blicharska, M., and Mikusiński, G. (2016). Gaps in ecological research on the world's largest internationally coordinated network of protected areas: a review of Natura 2000. *Biol. Conserv.* 200, 216–227. doi: 10.1016/j.biocon.2016.06.015

Pavlidou, A., Simboura, N., Rousselaki, E., Tsapakis, M., Pagou, K., Drakopoulou, P., et al. (2015). Methods of eutrophication assessment in the context of the Water Framework Directive: examples from the Eastern Mediterranean coastal areas. *Cont. Shelf Res.* 108, 156–168. doi: 10.1016/j.csr.2015.05.013

Perera-Valderrama, S., Cerdeira-Estrada, S., Martell-Dubois, R., Rosique-de la Cruz, L., Caballero-Aragón, H., Valdez-Chavarin, J., et al. (2020). A new long-term marine biodiversity monitoring program for the knowledge and management in marine protected areas of the Mexican Caribbean. *Sustainability* 12 (18), 7814. doi: 10.3390/su12187814

Pleslić, G., Rako-Gospić, N., Mackelworth, P., Wiemann, A., Holcer, D., and Fortuna, C. (2015). The abundance of common bottlenose dolphins (*Tursiops truncatus*) in the former special marine reserve of the Cres-Lošinj archipelago, Croatia. *Aquat. Conserv.: Mar. Freshw. Ecosyst.* 25 (1), 125–137. doi: 10.1002/aqc.2416

Pleslić, G., Rako-Gospić, N., Miočić-Stošić, J., Blazinić Vučur, T., Radulović, M., Mackelworth, P., et al. (2019). Social structure and spatial distribution of bottlenose dolphins (*Tursiops truncatus*) along the Croatian Adriatic coast. *Aquat. Conserv.: Mar. Freshw. Ecosyst.* 29 (12), 2116–2132. doi: 10.1002/aqc.3213

Pomeroy, R. S., Parks, J. E., and Watson, L. M. (2004). *How is your MPA doing? A guidebook of natural and social indicators for evaluating marine protected area management effectiveness* (Gland, Switzerland and Cambridge, UK: IUCN). doi: 10.2305/IUCN.CH.2004.PAPS.1.en

Pomeroy, R. S., Watson, L. M., Parks, J. E., and Cid, G. A. (2005). How is your MPA doing? A methodology for evaluating the management effectiveness of marine protected areas. *Ocean Coast. Manage.* 48 (7-8), 485–502. doi: 10.1016/j.ocecoaman.2005.05.004

Ponti, M., Fava, F., and Abbiati, M. (2011). Spatial–temporal variability of epibenthic assemblages on subtidal biogenic reefs in the northern Adriatic Sea. *Mar. Biol.* 158, 1447–1459. doi: 10.1007/s00227-011-1661-3

Pörtner, H. O., Karl, D. M., Boyd, P. W., Cheung, W., Lluch-Cota, S. E., Nojiri, Y., et al. (2014). "Ocean systems," in *Climate change 2014: impacts, adaptation, and vulnerability. Part A: global and sectoral aspects. Contribution of working group II to the fifth assessment report of the intergovernmental panel on climate change*. Eds. C. B. Field, et al. (Cambridge, United Kingdom and New York, NY, USA: Cambridge University Press), 411–484. Available at: https://www.ipcc.ch/site/assets/uploads/2018/02/WGIIAR5-Chap6_FINAL.pdf.

Pranovi, F., Buffa, G., Rova, S., and ECOSS Partnership. (2020). *D3.4.1 Report on the ecosystem services to be used for monitoring ecological processes within the Natura 2000 sites. Deliverable of the Interreg Italy-Croatia ECOSS project*. Zenodo pp 71. doi: 10.5281/zenodo.6845234

Pugnetti, A., Manea, E., Vilibić, I., Sarretta, A., Capotondi, L., Cataletto, B., et al. (2022). The ecological observing system of the Adriatic Sea (ECOAdS): structure and perspectives within the main European biodiversity and environmental strategies. *Res. Ideas Outcomes* 8, e82597. doi: 10.3897/rio.8.e82597

Rako-Gospić, N., Fortuna, C. M., Holcer, D., Mackelworth, P., Nimak-Wood, M., Pleslić, G., et al. (2013). Leisure boating noise as a trigger for the displacement of the bottlenose dolphins of the Cres–Lošinj archipelago (northern Adriatic Sea, Croatia). *Mar. Pollut. Bull.* 68, 77–84. doi: 10.1016/j.marpolbul.2012.12.019

Rako-Gospić, N., Radulović, M., Vučur, T., Pleslić, G., Holcer, D., and Mackelworth, P. (2017). Factor associated variations in the home range of a resident Adriatic common bottlenose dolphin population. *Mar. Pollut. Bull.* 124 (1), 234–244. doi: 10.1016/j.marpolbul.2017.07.040

Revuelta, O., Domènech, F., Fraija-Fernández, N., Gozalbes, P., Novillo, O., Penadés-Suay, J., et al. (2018). Interaction between bottlenose dolphins (*Tursiops truncatus*) and artisanal fisheries in the Valencia region (Spanish Mediterranean Sea). *Ocean Coast. Manage.* 165, 117–125. doi: 10.1016/j.ocecoaman.2018.08.001

Richter, B. D., Baumgartner, J. V., Powell, J., and Braun, D. P. (1996). A method for assessing hydrologic alteration within ecosystems. *Conserv. Biol.* 10 (4), 1163–1174. doi: 10.1046/j.1523-1739.1996.10041163.x

Roberts, K. E., Valkan, R. S., and Cook, C. N. (2018). Measuring progress in marine protection: a new set of metrics to evaluate the strength of marine protected area networks. *Biol. Conserv.* 219, 20–27. doi: 10.1016/j.biocon.2018.01.004

Ronconi, R. A., Lascelles, B. G., Langham, G. M., Reid, J. B., and Oro, D. (2012). The role of seabirds in marine protected area identification, delineation, and monitoring: introduction and synthesis. *Biol. Conserv.* 156, 1–4. doi: 10.1016/j.biocon.2012.02.016

Sala, E., Ballesteros, E., Dendrinos, P., Di Franco, A., Ferretti, F., Foley, D., et al. (2012). The structure of Mediterranean rocky reef ecosystems across environmental and human gradients, and conservation implications. *PloS One* 7 (2), e32742. doi: 10.1371/journal.pone.0032742

Šarić, T., Župan, I., Aceto, S., Villari, G., Palić, D., De Vico, G., et al. (2020). Epidemiology of noble pen shell (*Pinna nobilis* L. 1758) mass mortality events in Adriatic Sea is characterized with rapid spreading and acute disease progression. *Pathogens* 9 (10), 776. doi: 10.3390/pathogens9100776

Scarton, F. (2022). Recent settlement of two new breeding species in the northern Po Delta (Veneto-Italy): the slender-billed gull (*Larus genei* Brème 1839) and the sandwich tern (*Thalasseus sandvicensis* Latham 1787). *Lavori - Società Veneziana di Scienze Naturali* 47, 121–123.

Scarton, F., Bon, M., Perco, F., and Verza, E. (2013). Gli uccelli acquatici svernanti nelle zone umide costiere del Friuli-Venezia Giulia e del Veneto: consistenza, dinamiche ed aspetti gestionali nel decennio 1997-2006. *Riv. ital. Orn. Milano* 82 (1-2), 94–99. Available at: https://caiscuola.cai.it/wp-content/uploads/2021/06/scarton.pdf.

Scarton, F., and Valle, R. (2020). Drone assessment of habitat selection and breeding success of gull-billed tern *Gelochelidon nilotica* nesting on low-accessibility sites: a case study. *Riv. Ital. Orn.* 90 (2), 69–76. doi: 10.4081/rio.2020.475

Scarton, F., Verza, E., Guzzon, C., Utmar, P., Sgorlon, G., and Valle, R. G. (2018). Laro-limicoli (Charadriiformes) nidificanti nel litorale nord Adriatico (Veneto e Ffriuli-Venezia Giulia) nel periodo 2008-2014: consistenza, trend e problematiche di conservazione. *RIO Res. Ornithol.* 88 (2), 33–41. doi: 10.4081/rio.2018.418

Schéré, C. M., Dawson, T. P., and Schreckenberg, K. (2020). Multiple conservation designations: what impact on the effectiveness of marine protected areas in the Irish Sea? *Int. J. Sustain. Dev. World Ecol.* 27 (7), 596–610. doi: 10.1080/13504509.2019.1706058

Simeoni, U., and Corbau, C. (2009). A review of the Delta Po evolution (Italy) related to climatic changes and human impacts. *Geomorphology* 107, 64–71. doi: 10.1016/j.geomorph.2008.11.004

Solly, A., and Berisha, E. (2021). "Towards the territorialisation of EU cohesion policy? The case of EUSAIR," in *Governing territorial development in the Western balkans*. Eds. E. Berisha, G. Cotella and A. Solly (Cham: Springer), 333–355. doi: 10.1007/978-3-030-72124-4_16

Stagličić, N., Varezić, D. B., Mrčelić, J. K., Pavičić, M., and Tutman, P. (2021). Marine litter on the shallow seafloor at Natura 2000 sites of the central Eastern Adriatic Sea. *Mar. Pollut. Bull.* 168, 112432. doi: 10.1016/j.marpolbul.2021.112432

Sundseth, K. (2013). *Natura 2000: managing sites in the Natura 2000 network. Nature and biodiversity newsletter*. Eds. S. Wegefelt (DG Environment European Commission). Available at: https://ec.europa.eu/environment/nature/info/pubs/docs/nat2000newsl/nat33_en.pdf.

Thomas, L., and Middleton, J. (2003). *Guidelines for management planning of protected areas*. IUCN Gland, Switzerland and Cambridge, UK. ix + pp 79. Available at: https://portals.iucn.org/library/efiles/documents/pag-010.pdf.

Thorstad, E. B., Økland, F., Aarestrup, K., and Heggberget, T. G. (2008). Factors affecting the within-river spawning migration of Atlantic salmon, with emphasis on human impacts. *Rev. Fish Biol. Fish* 18 (4), 345–371. doi: 10.1007/s11160-007-9076-4

Tursi, A., Mastrototaro, F., Montesanto, F., De Giosa, F., Lisco, A., Bottalico, A., et al. (2022). The Status of *Posidonia oceanica* at Tremiti Islands Marine Protected Area (Adriatic Sea). *Biology*, 11 (6), 923. doi: 10.3390/biology11060923

United Nations (2015). *Transforming our world: the 2030 Agenda for Sustainable Development, United Nations, A/RES/70/1*, pp 41. Available at: https://sustainabledevelopment.un.org/content/documents/21252030%20Agenda%20for%20Sustainable%20Development%20web.pdf.

Valenti, W. C., Kimpara, J. M., Preto, B. D. L., and Moraes-Valenti, P. (2018). Indicators of sustainability to assess aquaculture systems. *Ecol. Indic.* 88, 402–413. doi: 10.1016/j.ecolind.2017.12.068

Valle, R., and Scarton, F. (2018). Uso dei droni nel censimento degli uccelli acquatici nidificanti nel nord Adriatico. *Boll. Mus. Storia Naturale Venezia* 69, 69–75.

Valle, R. G., and Verza, E. (2020). I laro-limicoli (Charadriiformes) nidificanti nel Delta del Po Veneto (RO) nel periodo 2015–2018. *Boll. Mus. Storia Naturale Venezia* 71, 123–126.

van Weelden, C., Towers, J. R., and Bosker, T. (2021). Impacts of climate change on cetacean distribution, habitat and migration. *Clim. Change Ecol.* 1, 100009. doi: 10.1016/j.ecochg.2021.100009

Vázquez-Luis, M., Borg, J. A., Morell, C., Banach-Esteve, G., and Deudero, S. (2015). Influence of boat anchoring on *Pinna nobilis*: a field experiment using mimic units. *Mar. Freshw. Res.* 66, 786–794. doi: 10.1071/MF14285

Verza, E. (2015). "Popolazione e scelta dell'habitat riproduttivo di pernice di mare *Glareola pratincola* e sterna zampenere *Gelochelidon nilotica* nella parte veneta del Delta del Po (Rovigo); analisi del periodo 2001-2012," in *XVII Convegno Italiano di Ornitologia: Atti del Convegno di Trento* (MUSE-Museo delle Scienze Trento), 11-15 September 2013, 75-77. Available at: http://ciso-coi.it/wp-content/uploads/2015/12/CIO_2013_low.pdf#page=83.

Verza, E., and Cattozzo, L. (2015). *Atlante lagunare costiero del Delta del Po. Consorzio di bonifica Delta del Po, Regione del Veneto. Associazione Culturale Naturalistica Sagittaria, Adria (Ro)*, pp 341. Available at: https://www.bonificadeltadelpo.it/wp-content/uploads/2016/10/atlante-lagune_ott.pdf.

Verza, E., Scarton, F., Bon, M., and Trombin, D. (2011). "Confronto dei popolamenti di specie acquatiche di interesse conservazionistico nidificanti nel complesso laguna di Venezia–Delta del Po (Veneto)," in *XVI Convegno Italiano di Ornitologia: Atti del convegno di Cervia (RA)* (Scritti, Studi e Ricerche di Storia Naturale della Repubblica di San Marino), Cervia 21-25 September 2011, 237–239.

Vilibić, I., and ECOSS Partnership. (2019). *D3.1.1. Report on the assessment of existing ecological monitoring programs and observing systems*. Deliverable of the Interreg Italy-Croatia ECOSS project. *Zenodo* pp 84. doi: 10.5281/zenodo.6845435

White, E. R. (2019). Minimum time required to detect population trends: the need for long-term monitoring programs. *BioScience* 69 (1), 40–46. doi: 10.1093/biosci/biy144

Wild, S., Krützen, M., Rankin, R. W., Hoppitt, W. J., Gerber, L., and Allen, S. J. (2019). Long-term decline in survival and reproduction of dolphins following a marine heatwave. *Curr. Biol.* 29 (7), R239–R240. doi: 10.1016/j.cub.2019.02.047

Zampoukas, N., Piha, H., Bigagli, E., Hoepffner, N., Hanke, G., Cardoso, A. C., et al. (2012). *Monitoring for the Marine Strategy Framework Directive: requirements and options* (Luxembourg: Publications Office of the European Union), pp 42. doi: 10.2788/77640

Zanuttini, C., Gally, F., Scholl, G., Thomé, J. P., Eppe, G., and Das, K. (2019). High pollutant exposure level of the largest European community of bottlenose dolphins in the English channel. *Sci. Rep.* 9 (1), 1–10. doi: 10.1038/s41598-019-48485-7

Zipkin, E. F., Zylstra, E. R., Wright, A. D., Saunders, S. P., Finley, A. O., Dietze, M. C., et al. (2021). Addressing data integration challenges to link ecological processes across scales. *Front. Ecol. Environ.* 19 (1), 30–38. doi: 10.1002/fee.2290

Zuazo, V. H. D., and Pleguezuelo, C. R. R. (2009). Soil-erosion and runoff prevention by plant covers: a review. *Agron. Sustain. Dev.* 28, 65–86. doi: 10.1051/agro:2007062

Zunino, S., Canu, D. M., Bandelj, V., and Solidoro, C. (2017). Effects of ocean acidification on benthic organisms in the Mediterranean Sea under realistic climatic scenarios: a meta-analysis. *Reg. Stud. Mar. Sci.* 10, 86–96. doi: 10.1016/j.rsma.2016.12.011

Zupan, M., Fragkopoulou, E., Claudet, J., Erzini, K., Horta e Costa, B., and Gonçalves, E. J. (2018). Marine partially protected areas: drivers of ecological effectiveness. *Front. Ecol. Environ.* 16 (7), 381–387. doi: 10.1002/fee.1934

frontiers | Frontiers in Environmental Science

TYPE Original Research
PUBLISHED 04 January 2023
DOI 10.3389/fenvs.2022.989671

Consistency of six *in situ*, *in vitro* and satellite-based methods to derive chlorophyll *a* in two optically different lakes

Krista Alikas[1]*, Kersti Kangro[1,2], Kerttu-Liis Kõks[3], Marju Tamm[2], Rene Freiberg[2] and Alo Laas[2]

[1]Tartu Observatory, University of Tartu, Tartu, Estonia, [2]Chair of Hydrobiology and Fishery, Institute of Agricultural and Environmental Sciences, Estonian University of Life Sciences, Tartu, Estonia, [3]Civitta Estonia, Tartu, Estonia

OPEN ACCESS

EDITED BY
Elisabetta Manea,
UMR8222 Laboratoire d'Ecogéochimie des Environnements Benthiques (LECOB), France

REVIEWED BY
Zhigang Cao,
Nanjing Institute of Geography and Limnology, (CAS), China
Changchun Huang,
Nanjing Normal University, China
Monica Pinardi,
Institute for Electromagnetic Sensing of the Environment, Italy
Chiara Lapucci,
National Research Council (CNR), Italy

*CORRESPONDENCE
Krista Alikas,
✉ krista.alikas@ut.ee

SPECIALTY SECTION
This article was submitted to Freshwater Science, a section of the journal Frontiers in Environmental Science

RECEIVED 08 July 2022
ACCEPTED 12 December 2022
PUBLISHED 04 January 2023

CITATION
Alikas K, Kangro K, Kõks K-L, Tamm M, Freiberg R and Laas A (2023), Consistency of six *in situ*, *in vitro* and satellite-based methods to derive chlorophyll *a* in two optically different lakes.
Front. Environ. Sci. 10:989671.
doi: 10.3389/fenvs.2022.989671

Phytoplankton and its most common pigment chlorophyll a (Chl-a) are important parameters in characterizing lake ecosystems. We compared six methods to measure the concentration of Chl a ($C_{\text{Chl-a}}$) in two optically different lakes: stratified clear-water Lake Saadjärv and non-stratified turbid Lake Võrtsjärv. $C_{\text{Chl-a}}$ was estimated from: *in vitro* (spectrophotometric, high-performance liquid chromatography); fluorescence (*in situ* automated high-frequency measurement (AHFM) buoys) and spectral (*in situ* high-frequency hyperspectral above-water radiometer (WISPStation), satellites Sentinel-3 OLCI and Sentinel-2 MSI) measurements. The agreement between methods ranged from weak (R^2 = 0.26) to strong (R^2 = 0.93). The consistency was better in turbid lake compared to the clear-water lake where the vertical and short-term temporal variability of the $C_{\text{Chl-a}}$ was larger. The agreement between the methods depends on multiple factors, e.g., the environmental and in-water conditions, placement of sensors, sensitivity of algorithms. Also in case of some methods, seasonal bias can be detected in both lakes due to signal strength and background turbidity. The inherent differences of the methods should be studied before the synergistic use of data which will clearly increase the spatial (*via* satellites), temporal (AHFM buoy, WISPStation and satellites) and vertical (profiling AHFM buoy) coverage of data necessary to advance the research on phytoplankton dynamics in lakes.

KEYWORDS
chlorophyll-a, WISPstation, HPLC, fluorescence, high-frequency measurements, lakes, Sentinel-3 OLCI, Sentinel-2 MSI

1 Introduction

Phytoplankton forms the basis of the aquatic food web (Fenchel, 1988), reacts fast to the changes in the environment (Reynolds, 2006; Hama et al., 2015), and reflects the alterations in climate (Winder and Sommer, 2012; Guinder and Molinero, 2013). The main photosynthetic pigment in phytoplankton is chlorophyll a (Chl a), which has hence been used for a long time as a metric for describing phytoplankton properties, either as a proxy for biomass (Vörös and Padisak, 1991; Boyer et al., 2009; Bernát et al., 2020), a measure of eutrophication (Ferreira et al., 2011; Matthews, 2014; Guan et al., 2020), an indicator for blooms (Reinart and Kutser, 2006; Gittings et al., 2017), or basis for primary production calculations (Longhurst et al., 1995; Tilstone et al., 2014). It is also one of the important parameters in assigning the ecological status class of water bodies by various legislative acts, e.g. Water Framework Directive (European Commission, 2000) and Marine Strategy Framework Directive (European Commission, 2008) both in pan-European scale and regional conventions, such as OSPAR (Convention for the Protection of the Marine Environment of the North-East Atlantic) or HELCOM (Baltic Marine Environment Protection Commission) (HELCOM, 2006; OSPAR Commission, 2009).

The variety of ways to determine the concentration of Chl a ($C_{\mathrm{Chl\text{-}a}}$) is constantly increasing. In laboratory conditions, spectrophotometric method for $C_{\mathrm{Chl\text{-}a}}$ detection is widely used, although details in methodology (used solvent, calculation scheme, etc.) may differ among recommended standards and research groups (Gitelson et al., 2007; Zhang et al., 2009; Matthews et al., 2012; Pahlevan et al., 2020). High-performance liquid chromatography (HPLC) is by design more precise and has become a standard for analyzing phytoplankton pigments in marine and freshwaters (Simmons et al., 2016). Regardless of being relatively fast, objective and sensitive (Tamm, 2019), it is often unaffordable for smaller research teams or when high number of samples needs to be analyzed.

Automated high-frequency measurements (AHFM) of chlorophyll fluorescence with buoys equipped with various sensors, allow insight into processes within a lake in sub-hourly timescales (Laas et al., 2016). This enables the study of the diurnal and seasonal variations of $C_{\mathrm{Chl\text{-}a}}$ and lake metabolism in close details (Meinson et al., 2016) and provides a deeper insight into ecosystem dynamics, suits for assessing matter fluxes, and establishing precise chemical budgets (Rinke et al., 2013). AHFM systems are particularly useful to capture short-term events (e.g., cyanobacterial blooms) and fast water quality shifts in highly dynamic systems, together with enhancements in overall predictive capacity (Marcé et al., 2016). Profiling sensors in lakes give an overview of the vertical water column, while sensors deployed at fixed depths give information about one specific depth and location. Earlier, AHFM buoys were mainly equipped with underwater sensors to measure water temperature, electrical conductivity, pH, and dissolved oxygen properties, while information about biota, e.g., $C_{\mathrm{Chl\text{-}a}}$, was much scarcer (Meinson et al., 2016; Meinson, 2017). Over the last decade, most of the new AHFM systems have at least some sensors to detect algal pigment changes, and therefore many studies have also explained $C_{\mathrm{Chl\text{-}a}}$ variability in lakes (Brentrup et al., 2016; Rusak et al., 2018). Continuous AHFM monitoring allows comprehensive studies of fast-evolving processes in lakes in short-term scales (Snortheim et al., 2017; Woolway et al., 2017). The presence of sensors in many lakes around the globe (e.g., *via* GLEON network) gives means to draw broader conclusions about the effects of changing climate and resulting factors. This is important from both scientific and management point of view.

Spectral radiometric measurements allow the quantification of $C_{\mathrm{Chl\text{-}a}}$ *via* the absorption and scattering features in the recorded signal. *In situ* hyperspectral optical sensors (e.g., WISPStation) provide high spectral and temporal resolution, which enables the validation of visible and near-infrared bands of present and future satellite missions providing water reflectance data within minutes (Vansteenwegen, et al., 2019). WISPStation is an optical measurement system deriving above-water reflectance (spectral range 350–900 nm, spectral resolution 4.6 nm) and in-water substances (Peters et al., 2018) e.g., $C_{\mathrm{Chl\text{-}a}}$. High-frequency hyperspectral optical data can complement relatively scarce *in situ* measurements. This allows improving the knowledge about short-term processes in lakes and could be linked with Earth Observation (EO) measurements to increase knowledge in spatial scale (Siegel et al., 2013; Binding et al., 2018; Hu et al., 2019). EO data provides a frequent, large-scale synoptic overview of lakes and has been increasingly integrated operationally into inland water algal bloom monitoring (Binding et al., 2021). European Union's EO Programme Copernicus currently provides data access up to four Sentinel series satellites to derive optical water quality parameters in lakes. Sentinel-3 (S3) Ocean and Land Colour Instrument (OLCI) offers an opportunity to monitor inland and coastal waters with high spectral (21 bands) and temporal (global coverage every 2 days) resolution. Still, it is more suitable for monitoring large water bodies because of its spatial resolution (pixel size 300 m on the ground). Another European Space Agency satellite Sentinel-2 (S2) Multispectral Instrument (MSI) allows monitoring smaller water bodies, with spatial resolution of 10–60 m on the ground, but has lower spectral, radiometric and temporal resolution compared to Sentinel-3 OLCI. Although Sentinel-2 was initially created for land applications, water quality parameters can be still successfully mapped (Toming et al., 2016; Pahlevan et al., 2017; Ansper & Alikas, 2018; Bonansea et al., 2019; Page et al., 2019; Al-Kharusi et al., 2020).

Various methods to derive $C_{\mathrm{Chl\text{-}a}}$ are widely used depending on the traditional monitoring methods, availability of the resources, instruments, specialists and laboratory facilities. Data gathered with different methods are then used to conclude the phytoplankton properties from regional to global scales (Sayers et al., 2015; Pahlevan et al., 2020), despite methodological differences within a dataset. The monitoring requirements of $C_{\mathrm{Chl\text{-}a}}$ by different methods can vary and depend on multiple factors. The expected accuracy is variable: for example for the fluorescence measurements by sonde, the manufacturer gives ±5% as the accuracy estimation. The photometric accuracy of spectrophotometer is dependent on absorbance range (±0.002 absorbance at 0 to 0.5 absorbance range; ±0.003 absorbance at 0.5 to one absorbance range).

TABLE 1 Main morphological and bio-optical parameters in Võrtsjärv and Saadjärv. Mean values are given in parentheses. TSM refers to total suspended matter (mg/L) and $a_{CDOM}(442)$ to the absorption of coloured dissolved organic matter at 440 nm.

Parameter	Võrtsjärv	Saadjärv
Area (km^2)	270	7.24
Mean depth (m)	2.8	8
Max depth (m)	6	25
Volume (km^3)	0.75	0.056
Catchment Area (km^2)	3,104	28.4
Length (km)	34.8	6
C_{Chl-a} (μg/L)	5.1–83.18 (36.26)	3.23–9.15 (4.77)[a]
TSM (mg/L)	4–58.8 (19.88)	0.6–2.4 (1.52)[a]
$a_{CDOM}(440)$ (m^{-1})	1.2–13.8 (3.0)	0.8–1.2 (1.0)[a]
Secchi depth (m)	0.3–2.15 (0.7)	3–6.5 (4.25)
Surface elevation (m)	34.6	52.5

[a]indicates samples collected from the surface layer (down to 0.5 m).

Sentinel-3 Copernicus requirements have set 10% accuracy goal for C_{Chl-a} for both Case 1 and Case 2 waters, while thresholds are 30% and 70% respectively, depending on the optical complexity of the waters (Drinkwater and Rebhan, 2007). Here we have used a comprehensive dataset where C_{Chl-a} has been measured simultaneously by several methods, commonly used in limnology and satellite-based estimations. Despite high temporal frequency of some methods (e.g., AHFM of fluorescence for 24 h, radiometric measurements up to 10 h (depending on Sun elevation)), the focus is set on midday measurements to allow the minimum time gap between all methods constrained by satellite overpasses and *in vitro* sample analyses in the laboratory. In this study, we compared six different methods to derive CChl-a values, and analyzed the linkage and merging between different methods to estimate the consistency of the methods to derive CChl-a in two optically different lakes.

2 Materials and methods

2.1 Study lakes

Lake Võrtsjärv is a shallow eutrophic lake located in the southern part of Estonia (Table 1; Figure 1). The water in the lake is generally well mixed, and there is no significant stratification. The dominant algal groups are diatoms and cyanobacteria (*Limnothrix planctonica* and *L. redekei* tend to dominate during the entire year), the rest (green algae, cryptophytes and dinoflagellates) belong to a minority group (Järvet and Nõges, 1998).

Lake Saadjärv is a relatively deep (maximum 25 m) mesotrophic lake in South Estonia. It is dimictic, and is stratified for most of the year (Cremona et al., 2016), with significant temperature differences between the surface and bottom layer, especially in summer. The dominant algal groups by biomass are diatoms, cryptophytes, and cyanobacteria.

Both lakes differ greatly in terms of the amount of optically active substances (Table 1), the resulting underwater light field and seasonal dynamics in phytoplankton. Võrtsjärv has typically increasing phytoplankton biomass towards autumn, while in Saadjärv phytoplankton is more abundant in spring. Võrtsjärv has almost an order of magnitude higher C_{Chl-a} mean value compared to Saadjärv (36.3 μg/L and 4.8 μg/L respectively, Table 1). Absorption of colored dissolved organic matter (a_{CDOM}) is higher in spring in both lakes and decreases towards autumn. Total suspended matter (TSM) increases towards autumn in Võrtsjärv (from ~10 mg/L to 30 mg/L in 2018 and up to 40 mg/L in 2019) compared to low concentrations (~1.5 mg/L) during the entire year in Saadjärv.

2.2 Data

2.2.1 Laboratory measurements

Water samples for C_{Chl-a} analyses were gathered from surface water (e.g., 0.5 m depth) in Saadjärv and from various depth integrated water (surface, then after every 0.5 m) in Võrtsjärv. Water samples were kept in the dark and cooled container and filtered during the same day of the fieldwork.

Duplicate samples for C_{Chl-a} were filtered onto 25 mm ø GF/F filters (0.7 μm pore size). Filters were stored at −20°C until being extracted with 5 ml 96% ethanol for 24 h, centrifuged for 10 min (4,000 rpm), measured spectrophotometrically (Hitachi, 2020) and C_{Chl-a} was calculated for mixed phytoplankton assemblage according to Jeffrey and Humphrey (1975).

For HPLC analysis, 100–700 ml of sampled lake water was vacuum filtered through 47-mm Whatman GF/F, triplicate filters were stored in 5 ml plastic vials, frozen immediately and kept at −70°C before analysis. Phytoplankton pigments were extracted in 100% acetone (2 ml) containing internal standard and sonicated (Branson 1210) for 5 min. Samples were stored at −20°C for 24 h. After that, the extracts were filtered through 0.45 μm syringe filters (Millex LCR, Millipore) and stored in dark refrigerator until HPLC analysis (for details, see Tamm et al., 2015). C_{Chl-a} and Chlorophyllide a values were summed up for total C_{Chl-a}.

2.2.2 Fluorescence measurements

Data from two AHFM buoy stations measuring fluorescence were used (Figure 1). Võrtsjärv AHFM buoy (58.211798 N, 26.103163 E) was equipped with a Yellow Springs Instruments (YSI) model 6600 V2-4 multiparameter sonde in 1-m depth. The sonde has been fitted with a chlorophyll fluorescence probe

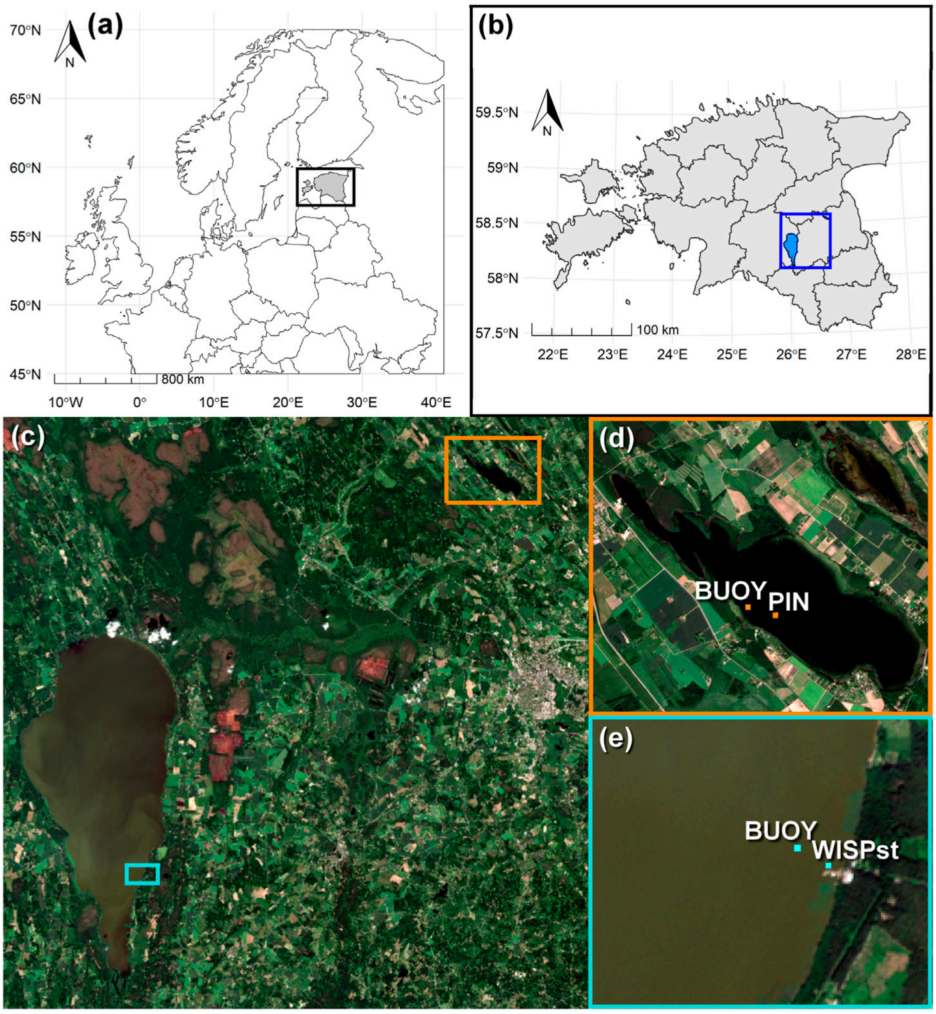

FIGURE 1
Location of the studied lakes on European scale **(A)** and within Estonia **(B)**. The location of AHFM buoy and pin location for the satellite data in Saadjärv are in the image with orange frame **(C,D)**. The location of WISPStation and AHFM buoy in Võrtsjärv are in light blue frame **(C,E)**. Estonian contour was obtained from the Estonian Land Board (2021).

(model 6025) and was recording after every 10 min frequency. Saadjärv AHFM buoy station (58.536963 N, 26.647558 E) was equipped with a YSI EXO-2 multiparameter sonde and worked as a vertical profiler within 2–20 m water column. This sonde was fitted with an EXO Total Algae-Phycocyanin sensor. The buoy was set to make profiles after every 30 min in 2018 and 1-h frequency in 2019, from surface to bottom and the data was recorded every 4–5 cm. The automated sensor-based measurements of chlorophyll fluorescence (ChlF) was converted into $C_{Chl\text{-}a}$ using standard manufactory coefficient and local conversion factors, derived *via* linear interpolation from monthly *in vitro* spectrophotometrically measured $C_{Chl\text{-}a}$. All underwater sensors in both AHFM systems were calibrated at least once per month according to the manufacturer instructions.

Both AHFM systems were also equipped with the multiparameter weather stations (Vaisala Weather Transmitter WXT520 in Võrtsjärv; Airmar 200WX Weather Station Instrument in Saadjärv) and solar irradiance sensors for above-water measurements. Photosynthetically active radiation (PAR) for Saadjärv was recorded with a Li-Cor quantum sensor (model LI-190SZ), while in Võrtsjärv, the buoy was equipped with a Li-Cor pyranometer (model LI-200SA), where PAR was calculated as 0.436 x Q (Q—incident global radiation) (Reinart and Pedusaar, 2008).

The non-photochemical quenching (NPQ) correction was performed according to Moiseeva et al. (2020):

$$PAR_z = PAR_0 \times e^{-(K_d \times z)} \tag{1}$$

$$d_{op} = e^{(-0.0019 \times PAR_z)} \tag{2}$$

TABLE 2 Selected algorithms for Sentinel-2 MSI and Sentinel-3 OLCI data over study lakes.

	S2	S3
Saadjärv	$Chl\ a = 1.7119^{*}\ \mathrm{chl\_conc} + 7.115$	$Chl\ a = 6.42 \times \left(\frac{\rho_{709}}{\rho_{665}}\right)^{1.2}$
Võrtsjärv	$Chl\ a = 2211.3 \times MCI + 22.77$	$Chl\ a = 8.8 \times MCI + 16.7$

$$F_{real} = F_t \times \left(2 - d_{op}\right) \tag{3}$$

where PAR_z is photosynthetically active radiation, which penetrates to depth z, PAR_0 is PAR falling to the lake surface, K_d is a diffuse attenuation coefficient, d_{op} is a portion of the open reaction centres (photosystem 2), F_t is a quasi-stationary level of fluorescence in an object adapted to light and F_{real} is a corrected chlorophyll fluorescence. In Võrtsjärv, K_d was obtained from the WISPStation radiometric data (Alikas et al., 2015). In Saadjärv, *in situ* measured Secchi depth was used to derive the euphotic depth (Z_{eu}) as a ratio between coefficient 2.69 and Secchi depth (Luhtala and Tolvanen, 2013), which was then converted to K_d (Koenings and Edmundson, 1991). The corresponding Z_{90} depth (depth at which 90% of the surface downwelling irradiance is attenuated) and Z_{eu} (reflects the depth where PAR is 1% of its surface value) were derived.

2.2.3 Spectral measurements

Fixed WISPStation was located in the pier of Võrtsjärv (Figure 1E, 58.211186 N, 26.107979 E). The station contains three radiometers that measure radiance and irradiance under fixed angles (Peters et al., 2018) with 15-min frequency. For a detailed description of the measurement setup, data processing and calibration of WISPStation, see Peters et al. (2018). Processed WISPStation data was downloaded from the WISPweb (https://wispweb.waterinsight.nl), where $C_{Chl\text{-}a}$ has been calculated from derived reflectance according to Gons (1999). Data was filtered based on the solar zenith angle (>70°), and exceptionally high values of $C_{Chl\text{-}a}$ (>200 μg/L), not consistent with the known natural background, were removed.

Satellite images from S2 MSI and S3 OLCI were used. Data was downloaded from Estonian National Satellite Data Centre ESTHub (ESTHub, 2022) with a pixel size of 60 m for S2 MSI and 300 m for S3 OLCI. First, S2 and S3 L1 data were processed with IDEPIX in SeNtinel Application Platform (SNAP) and pixels marked with cloud, cloud ambiguous, cloud sure, cloud buffer, cloud shadow, snow_ice and Sun glint risk flags were removed. Next, lake specific $C_{Chl\text{-}a}$ algorithms were applied (Table 2).

Previous studies (Mograne et al., 2019; Pereira-Sandoval et al., 2019; Warren et al., 2019; Alikas et al., 2020) have shown that C2RCC and POLYMER (Steinmetz et al., 2011) tend to work relatively well compared to other available atmospheric correction methods on MSI and OLCI data over optically different waters. The atmospherically corrected data, standard $C_{Chl\text{-}a}$ products from these processors together with previously developed approaches, based on L1 data (Alikas et al., 2015; Ansper and Alikas, 2018; Alikas et al., 2020), were tested over both lakes in terms of their accuracy and data availability.

In eutrophic Võrtsjärv (mean $C_{Chl\text{-}a}$ 36.3 μg/L, TSM 19.9 mg/L, $a_{CDOM}(440)$ 3.0 m^{-1}), L1 data based $C_{Chl\text{-}a}$ retrieval showed to be more robust and resulted in more retrievals than atmospherically corrected L2 or any standard product for deriving $C_{Chl\text{-}a}$. Therefore, the Maximum Chlorophyll Index (MCI) (Gower et al., 2008) was applied to L1 data and $C_{Chl\text{-}a}$ was derived by using empirical algorithms from S2 and S3 data in Võrtsjärv (Table 2).

In mesotrophic Saadjärv (mean $C_{Chl\text{-}a}$ 4.8 μg/L, TSM 1.5 mg/L, $a_{CDOM}(440)$ 1.0 m^{-1}), for S2 data POLYMER products resulted only in two quality controlled points in 2018 and four points in 2019, therefore C2RCC was chosen. C2RCC processor's standard $C_{Chl\text{-}a}$ product (chl_conc) with regional conversion factors was applied to S2 data. Also various empirical approaches were tested but due to high uncertainties in the shape and in the magnitude of the water-leaving reflectance from C2RCC, it did not result in more accurate $C_{Chl\text{-}a}$ retrievals. For S3 data, POLYMER atmospheric correction was applied to derive remote sensing reflectance (ρ) and a ratio of 709 and 665 after Gilerson et al. (2010) was applied with lake-specific coefficients (Table 2).

For S2 and S3 images, 3 × 3 pixel area centered at the coordinates (ROI—region of interest) of the *in situ* stations were extracted for further analyses (Figure 1). The mean (μ) and standard deviation (σ) were calculated within the ROI. Each ROI was checked for outliers following the OLCI validation guidelines (EUMETSAT, 2019). Single pixel outliers were removed if $C_{Chl\text{-}a} < (\mu—1.5\sigma)$ or $C_{Chl\text{-}a} > (\mu + 1.5\sigma)$. Entire ROI was excluded when the ratio between standard deviation and mean e.g., coefficient of variation (CV), was greater than 0.2 (e.g. 20%).

2.3 Temporal frequency of data

Depending on the setup of the different AHFM systems (WISPStation, fixed/profiler buoy) they provided from 50 to 900 measurements daily, covering more than 100 days of data during the vegetation period (Table 3). Availability of satellite data was mainly regulated by cloud cover and combination of signal strength versus lake size, which resulted on average in 40 images over Võrtsjärv compared to 15 over Saadjärv (Table 3).

2.4 Statistical analyses

Open-source software tool R was used for statistical analyses and graphics. Bias and error between different methods were estimated according to Seegers et al. (2018):

TABLE 3 Number of days with data used in this study. Slash (/) separates observations from years 2018 and 2019.

Method	Võrtsjärv[a]	Saadjärv[b]	Measurement depth	Nr of measurements in a day
Spectrophotometric	8/9	3/3	Integral[a], surface[b]	1
HPLC	8/–	3/2	Integral[a], surface[b]	1
Fluorescence	103/160	169/163	Subsurface[a], vertical profiler[b]	120–144[a] 900/400[b]
WISPStation	152/101	–	Z_{90} depth	30–51
Sentinel-2 MSI	38/36	14/16	Z_{90} depth	1
Sentinel-3 OLCI	44/74	15/25	Z_{90} depth	1–2

[a] Võrtsjärv.
[b] Saadjärv.

$$bias = 10^\wedge\left(\frac{\sum_{i=1}^{n} log_{10}\left(M_i\right) - log_{10}\left(Ref_i\right)}{n}\right) \tag{4}$$

$$MAE = 10^\wedge\left(\frac{\sum_{i=1}^{n} \left|log_{10}\left(M_i\right) - log_{10}\left(Ref_i\right)\right|}{n}\right) \tag{5}$$

where M_i is a model value, Ref_i is a reference value, and n is a number of paired observations. Bias represents log-transformed residuals, whereas MAE stands for the mean absolute error computed in log-space. These metrics are dimensionless, where the value of 1.5 indicates the model predicted value is 50% higher on average than the reference in case of bias and relative measurement error is 50% in case of MAE.

Mean Absolute Percentage Difference (MAPD) was used to study the short-term variability in respect of the midday reading

$$MAPD = \frac{\sum_{i=1}^{n} 100\left|\frac{x_{midday,i} - x_{day,i}}{x_{midday,i}}\right|}{n} \tag{6}$$

where $x_{\mathrm{midday,i}}$ is a $C_{\mathrm{Chl\text{-}a}}$ reference value on a midday (12.30 GMT+3), $x_{\mathrm{day,i}}$ $C_{\mathrm{Chl\text{-}a}}$ value before or after midday, n is a number of observations.

The non-parametric two-sample Mann-Whitney *U* test was used to detect statistically significant differences between paired measurements.

3 Results

We first show the results from the inter-comparison of all methods in both lakes and in a second step analyze the consistency between the methods in lakes separately in terms of the changing environmental and in-water background conditions. Third, based on the spectral and fluorescence high frequency measurements, the causes for seasonal bias and outliers between two methods are demonstrated.

3.1 Method based comparison to derive $C_{\mathrm{Chl\text{-}a}}$ in two optically different lakes

The combination of seasonal dynamics (Figure 2) and pairwise comparison (Figure 3) showed smaller differences between the methods in eutrophic Võrtsjärv compared to Saadjärv (Table 4). The bias between different methods was smaller in Võrtsjärv (average 3%, up to 31%) compared to Saadjärv (average 27%, up to 55%). Similarly, the average MAE was smaller in Võrtsjärv (average 28%, with a range from 7% to 51%) compared to Saadjärv (average 97%, with a range from 51%–159%) (Table 4). While the sparse *in vitro* measurements showed generally good agreement with all available methods, the results were more scattered between spectral and fluorescence measurements.

3.1.1 Laboratory measurements

Comparison of *in vitro* methods showed generally higher $C_{\mathrm{Chl\text{-}a}}$ by spectrophotometric approach compared to HPLC (Figure 3D). HPLC readings were, on average, 31% lower than spectrophotometrically measured $C_{\mathrm{Chl\text{-}a}}$ in Võrtsjärv (Table 4). In Saadjärv, the discrepancy was even more considerable.

The difference between the *in vitro* methods reflected also in the comparison with other methods. Comparison with WISPstation data showed underestimation of spectrophotometric $C_{\mathrm{Chl\text{-}a}}$ (24% bias, 29% MAE) and overestimation of HPLC $C_{\mathrm{Chl\text{-}a}}$ (11% bias, 13% MAE).

Compared to all methods, the smallest bias and MAE were derived between spectrophotometric and S3 (e.g., 2% bias in Võrtsjärv) and fluorescence (e.g., 6% bias in Võrtsjärv) based estimates in both lakes (Table 4).

3.1.2 Fluorescence measurements

In both lakes, the AHFM on ChlF delivered more than 100 days of data per year to study the seasonal dynamics of phytoplankton. As seen on Figure 2, the changes can be with high magnitude and rapid (e.g., daily changes in $C_{\mathrm{Chl\text{-}a}}$ ~10 μg/L

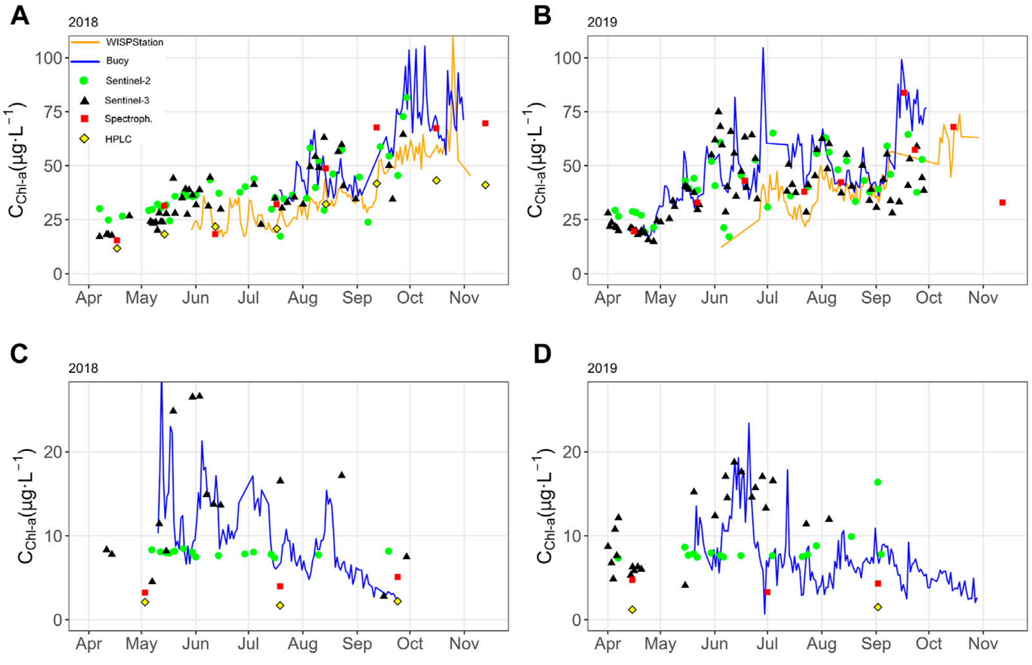

FIGURE 2
Midday $C_{Chl\text{-}a}$ time-series during vegetation period of 2018 and 2019, derived from various sensors in Võrtsjärv **(A,B)**: AHFM buoy, WISPStation, HPLC, spectrophotometric, S3, S2; and in Saadjärv **(C,D)**: AHFM buoy at Z_{90} depth, HPLC, spectrophotometric, S3, S2. Note the different y-scale in figures.

in Saadjärv and ~30 μg/L in Võrtsjärv). This seasonal dynamics is well captured by all methods with varying measurement frequency in Võrtsjärv (Figure 2A, B) with a bias from 6%–13% and MAE from 7%–38% in respective to fluorescence measurements (Table 4). In Saadjärv, there is a clear difference between the S2 and S3 derived seasonal dynamics (Figures 2C, D), with S3 tends to follow more similar pattern with fluorescence measurements than S2. It resulted in statistically significant different retrievals with 55% bias and 70% MAE.

In terms of the fluorescence measurements, in both lakes, the difference between the midday and night-time ChlF increased with increasing phytoplankton amount. Night-time ChlF tends to be higher during more abundant phytoplankton e.g. during the spring bloom in Saadjärv (up to 5.9 RFU) and late summer bloom in Võrtsjärv (up to 1.7 RFU). With this in mind, statistics between all methods in respective to ChlF night measurements were derived, which showed that the daytime ChlF measurements resulted in better consistency in eutrophic Võrtsjärv with all methods. In Saadjärv, the differences in the derived statistics were small and more data would be needed to study the impact of choosing between night or daytime ChlF as a reference data.

The comparison of in-water fluorescence measurements showed that the short-term temporal variability was 60% higher on average in the clear water Saadjärv (MAPD 11%) than in turbid Võrtsjärv (MAPD 4.5%) within the ±30 min time interval (Supplementary Figure S1). While in Saadjärv the short-term variability in recorded ChlF measurements was higher during spring bloom (in both day and night measurements), no seasonal dependence respective to the phytoplankton quantity was observed in Võrtsjärv. In comparison, spectral data (i.e., WISPStation) showed higher standard deviation around the midday measurements towards autumn—during low light conditions. The comparison of in-water fluorescence and above-water radiometric methods in Võrtsjärv showed the in-water measurements tend to be more stable while the above-water measurements are more prone to outliers (Supplementary Figure S1).

3.1.3 Spectral measurements

Despite the methodological similarities in deriving $C_{Chl\text{-}a}$ from WISPStation, S2 and S3 data, the comparison showed statistically significant differences, high scatter (Figures 3A1,2) and error up to 45% (Table 4) between WISPStation and EO data. Consistency was better between EO approaches in Võrtsjärv (Figure 3C; Table 4). In Saadjärv, although S2 and fluorescence measurements resulted in smallest bias (5%) and error (51%) from all methods in Saadjärv (Table 4), the C2RCC derived $C_{Chl\text{-}a}$ estimates from S2 data resulted in fairly stable

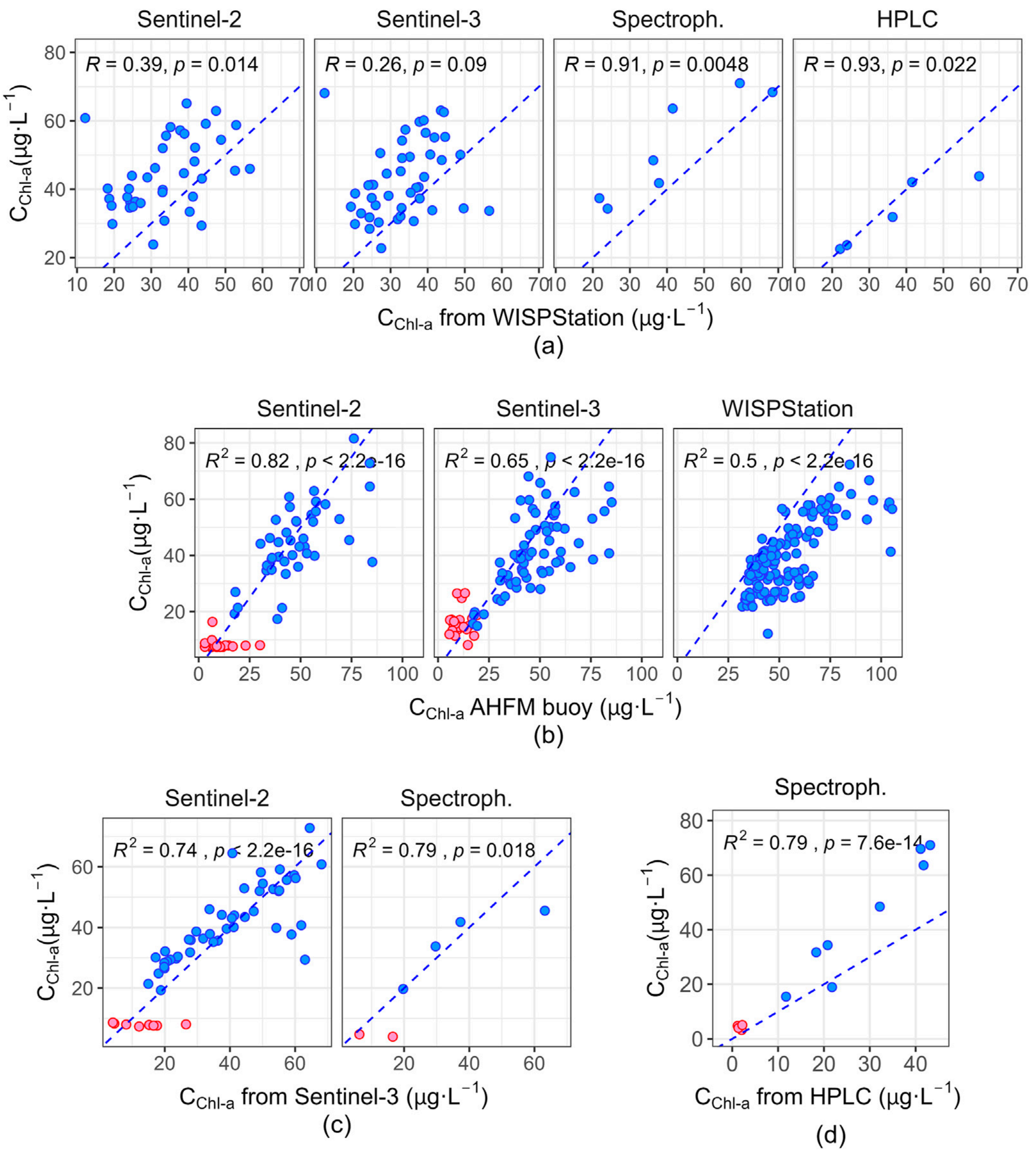

FIGURE 3
Comparison of C_{Chl-a} (µg·L^{-1}) acquired by various methods in Võrtsjärv (blue dots) and Saadjärv (red dots): **(A)** C_{Chl-a} from WISPStation in comparison with S2 (1), S3 (2), spectrophotometry (3) and HPLC (4), **(B)** C_{Chl-a} from fluorescence in comparison with S3 (1), S2 (2) and WISPStation (3), **(C)** C_{Chl-a} from S3 in comparison with S2 (1) and spectrophotometry (2) and **(D)** C_{Chl-a} from HPLC in comparison with spectrophotometry. R2 denotes the coefficient of determination about the entire dataset.

phytoplankton seasonal dynamics (Figures 2C, D) which was not supported by S3 and fluorescence based data.

In terms of spatial variability within the ROI, it was higher in Saadjärv during periods with more abundant phytoplankton (i.e. spring), but there were no systematic seasonal differences in S2 and S3 data over Võrtsjärv despite of the distinctive periods with higher C_{Chl-a} (Figures 2A, B).

The data from two AHFM systems (WISPstation and fluorescence buoy) in Võrtsjärv, resulted in 140 simultaneous measurements over 2 year period. Despite their moderate agreement (R^2 = 0.5), C_{Chl-a} from WISPStation was statistically significantly lower (on average 26%) than from fluorescence measurements (Table 4), larger values (>80 µg/L) were especially underestimated (Figure 3). Based on the statistics (Table 4), the fluorescence derived C_{Chl-a} tends to have better consistency with other methods than radiometric WISPStation measurements.

TABLE 4 Evaluated bias and mean absolute error (MAE) between studied methods according to Eqs 4, 5.

Model	Reference	Bias		MAE		N	
		Saadjärv	Võrtsjärv	Saadjärv	Võrtsjärv	Saadjärv	Võrtsjärv
HPLC	Spectrop	0.39	0.69	2.59	1.51	5	8
Spectrop	S3	0.43[a]	0.98	2.33[a]	1.15	2	4
S3	S2	1.39	0.91	1.95	1.22	8	46
S2	Fluoresc	1.05	0.94	1.51	1.23	26	42
S3	Fluoresc	1.55	0.88	1.7	1.25	23	69
Spectrop	Fluoresc	0.58[a]	0.94	1.72[a]	1.07	3	6
WISPstation	Fluoresc		0.87		1.38		140
HPLC	WISPstation		0.89		1.13		5
S2	WISPstation		1.32		1.45		40
S3	WISPstation		1.3		1.39		44
Spectrop	WISPstation		1.24		1.29		8

[a] Z_{90} vs. surface.

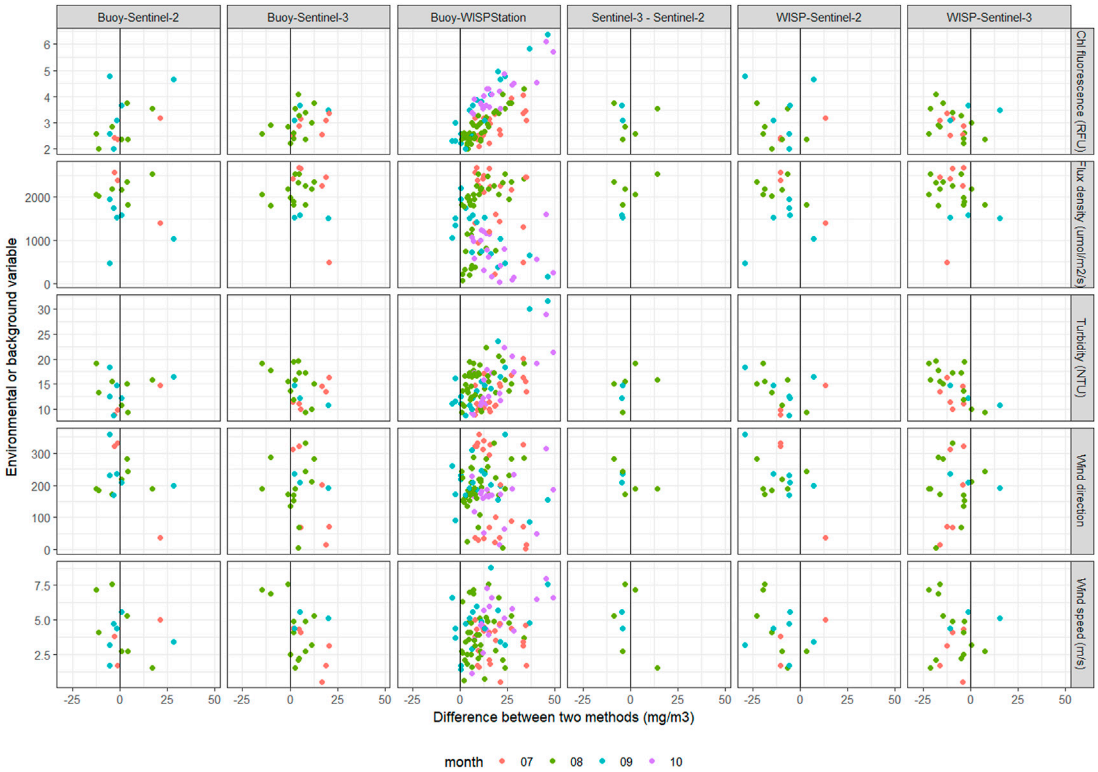

FIGURE 4
Impact of environmental and background conditions to method-based differences in estimating C_{Chl-a} in Lake Võrtsjärv.

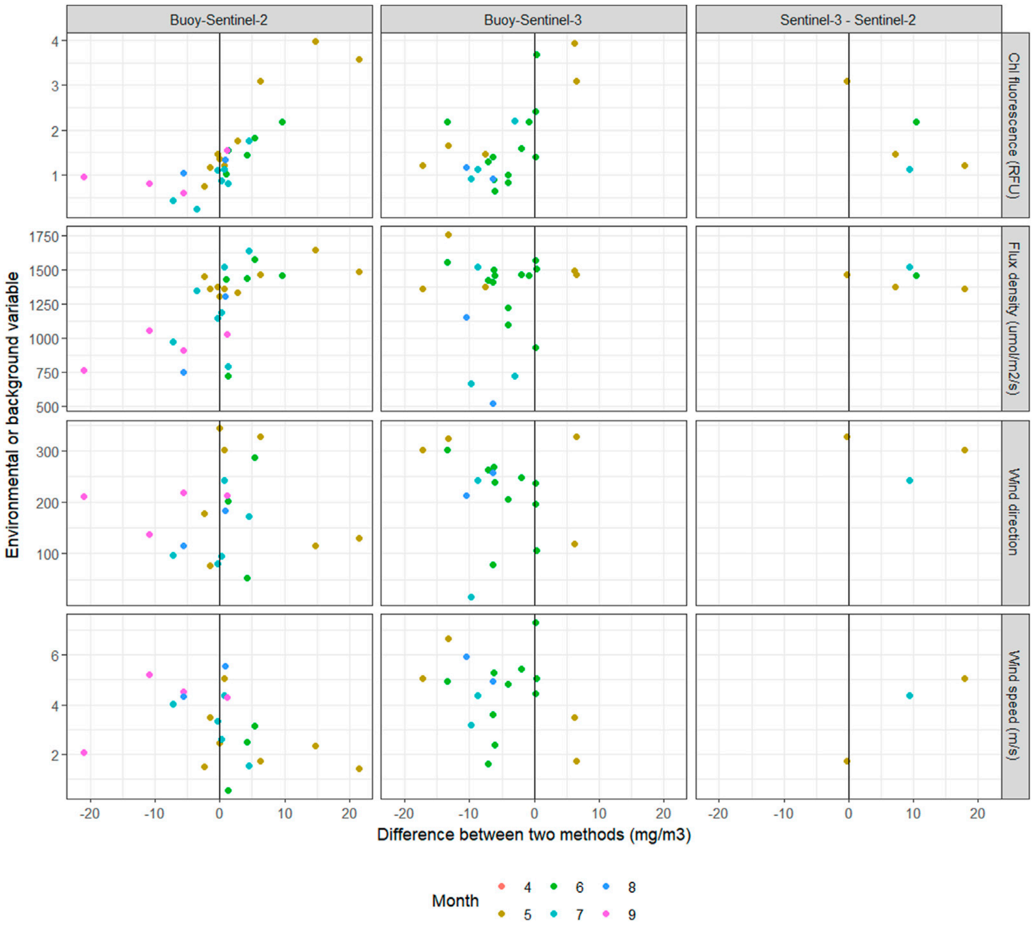

FIGURE 5
Impact of environmental and background conditions to method based differences in estimating $C_{Chl\text{-}a}$ in Lake Saadjärv.

3.2 Environmental and in-water background conditions

In vitro measurements have been mainly performed in good measurement conditions (low wind speed, low wave height) which can partly explain their good agreement with other available methods.

Pairwise comparison of $C_{Chl\text{-}a}$ estimates from radiometric (WISPStation, S2, S3) and fluorescence (buoy) measurements were coupled with buoy time series of observations of in-water and environmental conditions to determine their impact on the consistency of $C_{Chl\text{-}a}$ retrievals. Here again, the impact of the environmental and background conditions during the measurements had different effect in eutrophic shallow Võrtsjärv and in stratified mesotrophic lake Saadjärv.

The increase in turbidity (due to $C_{Chl\text{-}a}$ and TSM) tends to increase the differences between the methods in Võrtsjärv (Figure 4). This is evident especially in case of WISPStation data, whose $C_{Chl\text{-}a}$ tend to be smaller compared to S2, S3 and fluorescence retrievals during elevated turbidity. This results in an increasing systematic bias between fluorescence and WISPStation data. Similarly, the increase in wind speed, causing surface distortions (foam, waves, glint) and resuspension from the bottom, has an impact on WISPStation data but it also explains the switch from under- to overestimation of values in case of fluorescence and S3 data. Due to the location of the WISPStation (Figure 1E), poorer consistency with other methods is observed in case of northerly winds, when subsurface scum and foam are transported along the pier. High flux densities in July and August, and low flux densities in September and October explain some of the outliers. In Võrtsjärv, the consistency between S2 and S3 tend to have lowest impact from the environmental and background conditions.

In stratified clear water Saadjärv, the consistency between S2, S3, fluorescence measurements tend to depend largely on the signal strength e.g. ChlF and wind speed (Figure 5). The agreement between S2 and S3 decreases with decreasing ChlF, indicating the need for better algorithms for lower level of $C_{Chl\text{-}a}$.

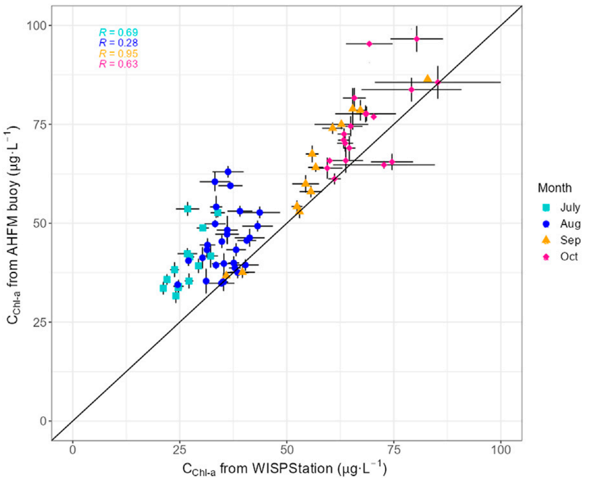

FIGURE 6
Hourly averaged and respective standard deviation for $C_{Chl\text{-}a}$ derived from fluorescence (*y*-axis) and $C_{Chl\text{-}a}$ derived from the spectral WISPStation data (*x*-axis) in Võrtsjärv during July-October 2018. Different months are coded with different colours. Time GMT+3 is used.

The dependence on signal strength is reflected also in the comparison of EO data with fluorescence measurements indicating larger biases during lower $C_{Chl\text{-}a}$. The low background turbidity (lower a_{CDOM} and TSM compared to Võrtsjärv, Table 1) results in higher amount of light available for phytoplankton in the subsurface layer and leads up to 81% change in ChlF due to the NPQ correction in Saadjärv. This could explain higher differences between fluorescence and spectral data during high flux density conditions, when the correction has the highest impact (Supplementary Figure S2). Despite the need for improved algorithms, the results also indicate improved consistency between fluorescence and EO based retrievals in case of increased wind speed, e.g. due to increased vertical mixing.

3.3 Method based differences to explain the seasonal bias and outliers

The inherent differences in the methods affect the consistency of $C_{Chl\text{-}a}$ retrievals and might therefore result in seasonal bias. For example, monthly-based difference in the consistency between fluorescence and WISPStation $C_{Chl\text{-}a}$ retrievals (Figure 6) could be explained by combined effect of various factors. First, timing of the *in situ* measurements to calibrate ChlF readings in high seasonal dynamics condition (Figure 2A). Second, increase of turbidity impacts both ChlF readings and sensitivity of the $C_{Chl\text{-}a}$ algorithm applied on WISPStation radiometric data. Third, outliers in September and October can be explained with low light and high wind speed conditions, while outliers in July and August more by wind direction (Figure 4). Fourth, higher short-term variability in WISPStation data in autumn measurements with more noise in the radiometric data during low light conditions increases the uncertainty of the measurements.

4 Discussion

The advancement of phytoplankton monitoring possibilities by various sensors requires the inter-comparison exercises to analyse the consistency of methods and outline the biases. The evaluation of $C_{Chl\text{-}a}$ derived by six methods over 2-year time period in optically different lakes indicated the importance to consider both environmental and method-based factors while interpreting the results.

4.1 Method-based factors affecting $C_{Chl\text{-}a}$ retrievals

4.1.1 Fluorescence measurements

There are various methods available to estimate the $C_{Chl\text{-}a}$ from the ChlF measurements (Ferreira et al., 2012; Zeng et al., 2017). The fluorescence yield per chlorophyll unit is very variable and depends on phytoplankton community composition, cell size, packaging effect and NPQ (Carberry et al., 2019 and references therein) and is difficult to account for regular basis. This is especially a challenge in the waters where phytoplankton community consists of many different species and various life cycle phases are present.

High-frequency measurements allow obtaining information from ChlF in sufficient temporal scale relevant to natural dynamics of the phytoplankton community. Photoprotection against high light induced by the xanthophyll cycle will lead to a non-photochemical quenching. The effect of NPQ correction clearly increased with increased PAR (Kromkamp et al., 2008; Ruban, 2016) and also depended on the level of OAS (optically active substances), leading up to 15% change in ChlF readings in Võrtsjärv compared to 81% in Saadjärv (Supplementary Figure S2). The amount of PAR of the total solar radiation depends on the wavelength, solar zenith angle, the aerosol amount in the atmosphere and clouds (Ross & Sulev, 2000). In Estonian geographic location the monthly total PAR is highest in June and decreases towards spring and autumn (Russak & Kallis, 2003). Here we showed the consistency between $C_{Chl\text{-}a}$ derived from above water radiometry (S2, S3, WISPStation) and fluorometers tended to decrease during high flux intensities in summer, especially pronounced in clear water Saadjärv (Figure 5). On the contrary, during autumn, when the illumination conditions were poorer, the consistency between the same methods was better during high flux intensities and decreased during low flux intensities (Figure 4). While in Võrtsjärv day-time ChlF was better reference based on the derived statistics (results not shown here), there was no clear pattern in Saadjärv. As the night-time ChlF tends to be higher during the bloom period and the difference was substantially higher in Saadjärv (up to 230%) compared to Võrtsjärv (up to 40%), it should be studied further in conjunction with inter-comparison of different methods to account for the NPQ.

It has been shown that CDOM and non-algal particles impede the accurate estimation of Sun-induced ChlF from the total reflectance spectra (McKee et al., 2007; Gilerson et al., 2008). Despite, the results from eutrophic Võrtsjärv show a strong correlation between $C_{Chl\text{-}a}$ derived from below water fluorometry and above-water radiometry (Figure 6), it was also shown that both methods depend on the background turbidity (Figure 4). Proctor & Roesler (2010) and Kuha et al. (2020) outlined that organic matter may lead to an underestimation of $C_{Chl\text{-}a}$ by absorbing excitation or emission wavelengths or, on the other hand, cause seemingly intensified Chl emission by contributing to the signal detected by Chl fluorometers. For example, a significant overestimation of $C_{Chl\text{-}a}$ with increased organic matter concentrations in an estuary was shown by Goldman et al. (2013). Results by Cremella et al. (2018) showed a linear response between ChlF and $a_{CDOM}(440)$ up to $20\,m^{-1}$ and a non-linear response between ChlF and CDOM at $a_{CDOM}(440) > 20\,m^{-1}$, also noting the negligible effect in CDOM ranges ($a_{CDOM}(440) < 2\,m^{-1}$) and pointing out the lack of interaction between turbidity and CDOM effects. In Saadjärv, the effect of CDOM and non-algal particles can be considered negligible. In Võrtsjärv, both the mean value and seasonal variation of $a_{CDOM}(440)$ and TSM were higher (Table 1), which requires the adaption of algorithms to different levels of OAS and more frequent measurements to calibrate ChlF readings.

4.1.2 Laboratory measurements

The fact that spectrophotometric measurements give higher values in comparison with HPLC, is not a new finding (Meyns et al., 1994; Sørensen et al., 2007). A strong positive correlation has been demonstrated between HPLC and spectrophotometrically measured $C_{Chl\text{-}a}$, with $C_{Chl\text{-}a}$ being 15%–20% higher *via* spectrophotometry than *via* HPLC (Sørensen et al., 2007; Tamm et al., 2015). Meyns et al. (1994) associated the differences in the measurements by HPLC and spectrophotometric methods with the degradation products of $C_{Chl\text{-}a}$ in the samples. Spectrophotometric measurements resulted in higher $C_{Chl\text{-}a}$ values, especially due to Chlorophyllide *a*. In this study Chlorophyllide *a* was included in HPLC measurements. This discrepancy could be attributed to the presence of other $C_{Chl\text{-}a}$ derivatives (allomers and epimers) and accessory pigments with overlapping spectra (Picazo et al., 2013; Tamm et al., 2015).

4.1.3 Spectral measurements

In case of above-water radiometry (S2, S3, WISPStation), $C_{Chl\text{-}a}$ is evaluated *via* indirect methods by the absorption and scattering features. In Lake Võrtsjärv, same type of approach was applied on both S2 and S3 data, which resulted in good agreement (9% bias and 22% MAE) even in the changing environmental and background conditions. The discrepancies were larger between WISPStation and EO-based approaches (bias ≥30%, MAE ≥39%) (Table 4). This can be due to sensor (i.e. different spectral response function, spatial resolution, sensitivity of the sensor) and also algorithm specific differences. This was especially evident during periods with elevated turbidity, indicating the need for optical water type specific algorithms. Similarly in Saadjärv, different approaches, the empirical (S3) and neural network (S2) derived $C_{Chl\text{-}a}$ showed clearly poorer agreement and stronger water type dependence. The study on optically different lakes indicates, despite the magnitude of seasonal dynamics of phytoplankton i.e. $C_{Chl\text{-}a}$ and other optically active substances, the change in the optical water type requires the adaption of algorithms to have confidence in the derived $C_{Chl\text{-}a}$ product throughout the season and over spatial scale.

Lake-specific approaches and previously developed regional conversion factors tuned with spectrophotometric $C_{Chl\text{-}a}$ (Alikas et al., 2010; Ansper and Alikas, 2018) were used. The tuning of the algorithm is sensitive to the calibration dataset, e.g., good agreement between spectrophotometric, S2, S3 derived $C_{Chl\text{-}a}$ in case of Võrtsjärv. The systematic underestimation of WISPStation $C_{Chl\text{-}a}$ (~20%) in Võrtsjärv compared to other methods (except HPLC) could be potentially corrected by further tuning or development of lake specific algorithm in order to minimize the differences between the methods. As shown also in previous studies, the agreement even between spectrophotometrically measured $C_{Chl\text{-}a}$ depends largely on the solvent but also on the calculation method. For example, the calculation method according to Lorenzen (1967) yielded on average 16% smaller $C_{Chl\text{-}a}$ values compared to Jeffrey and Humphrey (1975). Therefore, the inherent differences in the calibration dataset have to be considered and uncertainties evaluated, which will be then reflected in the higher order products (e.g., conversion factors, training dataset for neural network, satellite-based products, spatio-temporal analyses).

It was also observed, in case of both lakes and both S2 and S3 data, that the amount of quality-controlled data decreased towards autumn, which can be partly explained by clouds. However, this issue was stronger for narrower and smaller Saadjärv (width 1.8 km, length 6 km), where $C_{Chl\text{-}a}$ and TSM gradually decreased towards autumn, therefore the level of signal from the lake decreased, but the constant strong signal from the surrounding area continued. The land adjacency effect correction is known issue in the use of EO data over water surfaces (Kiselev et al., 2014; Bulgarelli & Zibordi, 2018) and might limit the use of data obtained over smaller water bodies or from coastal sites. In eutrophic Võrtsjärv, the propagated errors due to adjacency effect and atmospheric correction in the final $C_{Chl\text{-}a}$ measurement resulted in the use of L1 as the basis of the

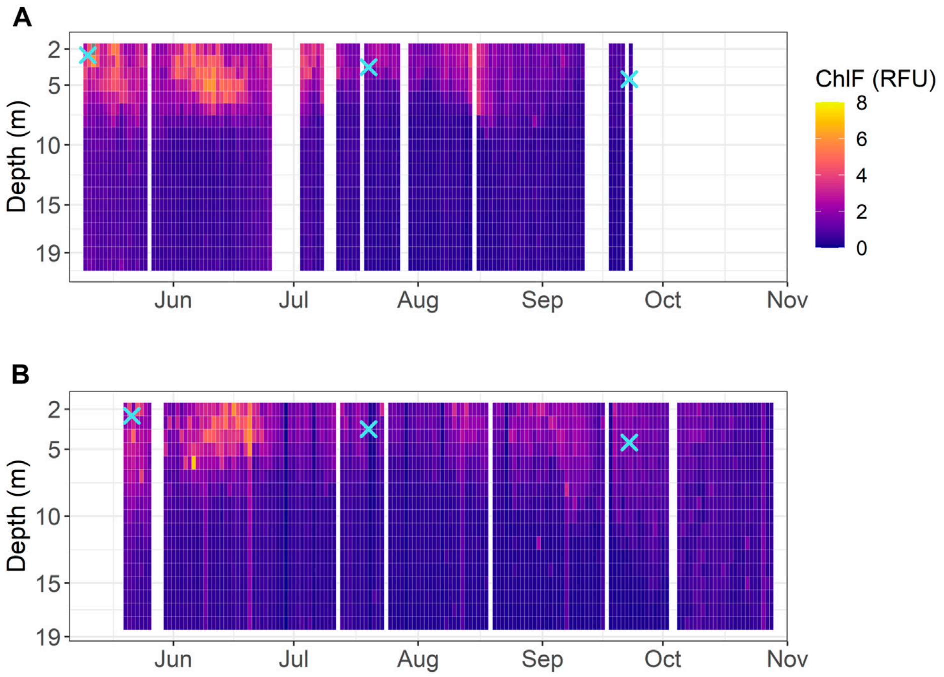

FIGURE 7
NPQ corrected ChlF midday profile in Saadjärv in 2018 **(A)** and in 2019 **(B)**. Crosses denote Z_{90} (derived from *in situ* Secchi depth).

processing which showed more reliable results. In clear Saadjärv, in case of S2 data, only few POLYMER processed pixels passed the quality control during 1 year, therefore C2RCC neural network C_{Chl-a} product was used. Despite providing continuous seasonal time series, it had low sensitivity to C_{Chl-a} patterns detected by fluorescence and S3 data. Due to the inaccuracies in the shape and the magnitude of the C2RCC derived Rrs, the application of various empirical algorithms did not improve the result.

The environmental effects had lower impact on S2 and S3 data compared to WISPStation measurements. High wind speed, increase in wave height and poor illumination conditions resulted in high uncertainties in the measured radiometric data (Alikas et al., 2020), which propagated errors to C_{Chl-a} retrievals (Figure 4) and could explain occasional outliers and seasonal patterns (e.g., increased variations in the recorded signal).

4.2 Consistency between the approaches

The synergistic use of various methods allows to create a linkage between them, crucial to develop and advance the study of phytoplankton C_{Chl-a} over different water types. As shown in this study, similar methods resulted in more consistent results (e.g., S2 and S3 over Võrtsjärv), while adding methods or moving towards clearer lake, the consistency decreased. Therefore, it is important to perform inter-comparison exercises to cover the vegetation period to see method-based differences but also outline potential cause for biases due to constantly varying environmental and background conditions present in the outdoors.

While all methods had better consistency in large, shallow, well-mixed, eutrophic Võrtsjärv, the discrepancies were larger in stratified clear-water mesotrophic Saadjärv. Inhomogeneous phytoplankton vertical distribution resulted in high variability on a profiler data (~10% on average) within the Z_{90} layer (Figure 7). Therefore, in these conditions, it is crucial that all methods (used for calibration, validation) would obtain signal exactly from the same water column. In traditional limnological water quality monitoring in stratified lakes, three water samples are taken (from surface, metalimnion and near-bottom layer). From vertical fluorescence distribution (Figure 7), it is evident that those sampling depths do not represent the actual biomass maximum, which in Saadjärv is generally between surface and the layer of temperature change, from where metalimnetic sample is gathered. Therefore the use of surface samples (as in this study), integral samples from discrete depths (waters samples, buoy) or from fixed layer e.g., Z_{90} (depends on wavelength) might cause seasonal biases depending on vertical distribution of phytoplankton.

With the advancement of sensors and new methods, ways to study phytoplankton are increasing. Here, we inter-compared three types of methods e.g., laboratory, fluorescence and spectral. While each method has its own advantages, the disadvantages should be or can be filled by alternative method included in the comparison. In parallel, research done on estimating full uncertainty budget for different methods would allow the user to estimate the suitability of each method for their application. Growing constellation of EO satellites allow already now global spatiotemporal analyses on lake phytoplankton, which can be complemented by present and future hyperspectral missions, however, the derived data, either used for calibration, validation or decision making, must be analyzed carefully to avoid artefacts due to selected method.

5 Conclusion

$C_{\text{Chl-a}}$ estimation obtained from six different methods complement each other but are not transferable due to method and season-based differences. Our study on optically different lakes showed:

- The consistency was better in large, well-mixed, eutrophic lake (average bias 0.97, MAE 1.28) compared to the clear-water mesotrophic lake (average bias 0.73, MAE 1.97) where the vertical and short-term temporal variability of the $C_{\text{Chl-a}}$ was larger.
- Similar methods resulted in more consistent results (e.g., S2 and S3 over Võrtsjärv), while adding methods or moving towards clearer lake, the consistency decreased.
- In eutrophic Võrtsjärv, both fluorescence and spectral WISPStation data had high impact on the $C_{\text{Chl-a}}$ retrievals during elevated turbidity indicating the need for more frequent calibration (fluorescence) and adaption of $C_{\text{Chl-a}}$ algorithm for different optical conditions.
- The consistency between $C_{\text{Chl-a}}$ derived from above water radiometry (S2, S3, WISPStation) and fluorescence tended to decrease during high flux intensities in summer (especially in clear water lake) and during low flux intensities in autumn.
- The inherent differences in the methods affect the consistency of $C_{\text{Chl-a}}$ retrievals and might therefore result in seasonal or spatial bias.

Perspectives for future studies include analysis of AHFM fluorescence data, focusing on extrapolation method of integral measurements, effect of frequent calibration and different corrections (e.g., removal of the influence of CDOM and non-algal particles to ChlF) to further investigate the intra-day variability and utilize possibilities by various new hyperspectral sensors (e.g., absorption and scattering features, shift of peaks).

Data availability statement

The raw data supporting the conclusions of this article will be made available by the authors, without undue reservation.

Author contributions

KA, KK, K-LK, and AL contributed to conception and design of the study, KA and K-LK performed data analyses and image processing, KK, AL, MT, and RF contributed with *in situ* and *in vitro* data acquisition, KA wrote the main draft of the manuscript, KK and K-LK wrote sections of the manuscript. All authors contributed to manuscript revision, read, and approved the submitted version.

Funding

This research was funded by EU's Horizon 2020 research and innovation programme (grant agreement no. 730066, EOMORES; grant agreement no. 101004186, Water-ForCE), Estonian Research Council grants PSG10, PSG32, PRG709 and PUTJD913.

Acknowledgments

Authors thank Water Insight for the WISPStation, Centre for Limnology for providing *in situ* $C_{\text{Chl-a}}$ data for Võrtsjärv. We thank ESA/Copernicus for S2 and S3 images and Estonian Land Board for the possibility to use ESTHub for image processing. We would like to acknowledge four reviewers for valuable comments and suggestions that helped improve this study.

Conflict of interest

The authors declare that the research was conducted in the absence of any commercial or financial relationships that could be construed as a potential conflict of interest.

Publisher's note

Supplementary material

The Supplementary Material for this article can be found online at: https://www.frontiersin.org/articles/10.3389/fenvs.2022.989671/full#supplementary-material

References

Al-Kharusi, E., Tenenbaum, D., Abdi, A., Kutser, T., Karlsson, J., Bergström, A.-K., et al. (2020). Large-scale retrieval of coloured dissolved organic matter in northern lakes using sentinel-2 data. *Remote Sens.* 12, 157. doi:10.3390/rs12010157

Alikas, K., Ansko, I., Vabson, V., Ansper, A., Kangro, K., Uudeberg, K., et al. (2020). Consistency of radiometric satellite data over lakes and coastal waters with local field measurements. *Remote Sens.* 12, 616. doi:10.3390/rs12040616

Alikas, K., Kangro, K., Randoja, R., Philipson, P., Asuküll, E., Pisek, J., et al. (2015). Satellite-based products for monitoring optically complex inland waters in support of EU water Framework directive. *Int. J. Remote Sens.* 36, 4446–4468. doi:10.1080/01431161.2015.1083630

Alikas, K., Kangro, K., and Reinart, A. (2010). Detecting cyanobacterial blooms in large North European lakes using the maximum chlorophyll Index. *Oceanologia* 52, 237–257. doi:10.5697/OC.52-2.237

Alikas, K., Kratzer, S., Noorma, A., Soomets, T., and Paavel, B. (2015). Robust remote sensing algorithms to derive the diffuse attenuation coefficient for lakes and coastal waters: Algorithm for diffuse attenuation coefficient. *Limnol. Oceanogr. Methods* 13, 402–415. doi:10.1002/lom3.10033

Ansper, A., and Alikas, K. (2018). Retrieval of chlorophyll a from sentinel-2 MSI data for the European union water Framework directive reporting purposes. *Remote Sens.* 11, 64. doi:10.3390/rs11010064

Bernát, G., Boross, N., Somogyi, B., Vörös, L., G.-Tóth, L., and Boros, G. (2020). Oligotrophication of lake balaton over a 20-year period and its implications for the relationship between phytoplankton and zooplankton biomass. *Hydrobiologia* 847, 3999–4013. doi:10.1007/s10750-020-04384-x

Binding, C. E., Pizzolato, L., and Zeng, C. (2021). EOLakeWatch, delivering a comprehensive suite of remote sensing algal bloom indices for enhanced monitoring of Canadian eutrophic lakes. *Ecol. Indic.* 121, 106999. doi:10.1016/j.ecolind.2020.106999

Binding, C., Zastepa, A., and Zeng, C. (2018). The impact of phytoplankton community composition on optical properties and satellite observations of the 2017 western lake erie algal bloom. *J. Gt. Lakes. Res.* 45, 573–586. doi:10.1016/j.jglr.2018.11.015

Bonansea, M., Ledesma, M., Bazán, R., Ferral, A., German, A., O'Mill, P., et al. (2019). Evaluating the feasibility of using sentinel-2 imagery for water clarity assessment in a reservoir. *J. S. Am. Earth Sci.* 95, 102265. doi:10.1016/j.jsames.2019.102265

Boyer, J., Kelble, C., Ortner, P., and Rudnick, D. (2009)., 9., S56–S67. doi:10.1016/j.ecolind.2008.11.013Phytoplankton bloom status: Chlorophyll a biomass as an indicator of water quality condition in the southern estuaries of Florida, USA, *Ecol. Indic.*

Brentrup, J., Williamson, C., Colom-Montero, W., Eckert, W., Eyto, E., Grossart, H.-P., et al. (2016). The potential of high-frequency profiling to assess vertical and seasonal patterns of phytoplankton dynamics in lakes: An extension of the plankton ecology group (PEG) model. *Inland Waters* 6, 565–580. doi:10.5268/IW-6.4.890

Bulgarelli, B., and Zibordi, G. (2018). On the detectability of adjacency effects in ocean color remote sensing of mid-latitude coastal environments by SeaWiFS, MODIS-A, MERIS, OLCI, OLI and MSI. *Remote Sens.Environ* 209, 423–438. doi:10.1016/j.rse.2017.12.021

Carberry, L., Roesler, C., and Drapeau, S. (2019). Correcting *in situ* chlorophyll fluorescence time series observations for non-photochemical quenching and tidal variability reveals non-conservative phytoplankton variability in coastal waters. *Limnol. Oceanogr. Methods* 17, 462–473. doi:10.1002/lom3.10325

Cremella, B., Huot, Y., and Bonilla, S. (2018). Interpretation of total phytoplankton and cyanobacteria fluorescence from cross-calibrated fluorometers, including sensitivity to turbidity and colored dissolved organic matter. *Limnol. Oceanogr. Methods* 16, 881–894. doi:10.1002/lom3.10290

Cremona, F., Laas, A., Nõges, P., and Noges, T. (2016). An estimation of diel metabolic rates of eight limnological archetypes from Estonia using high-frequency measurements. *Inland Waters* 6, 352–363. doi:10.1080/iw-6.3.971

Drinkwater, M., and Rebhan, H. (2007). Sentinel-3: Mission requirements document (MRD). ESA, EOP-SMO/1151/MD-md https://earth.esa.int/eogateway/documents/20142/1564943/Sentinel-3-Mission-Requirements-Document-MRD.pdf (Accessed September 7, 2022). 2, 19-22.

ESTHub (2022). ESTHub satellite data portal. Available at: https://ehdatahub.maaamet.ee/dhus/#/home (Accessed March 15, 2021).

EUMETSAT (2019). Recommendations for sentinel-3 OLCI ocean Colour product validations in comparison with *in situ* measurements – matchup protocols. https://www-cdn.eumetsat.int/files/2021-05/Recommendations%20for%20Sentinel-3%20OLCI%20Ocean%20Colour%20product%20validations%20in%20comparison%20with%20in%20situ%20measurements%20%E2%80%93%20Matchup%20Protocols_v7.pdf (Accessed April 12, 2021).

European Commission (2000). Directive 2000/60/EC of the European parliament and of the Council of 23 october 2000 establishing a Framework for community action in the field of water policy 2000. http://eur-lex.europa.eu/LexUriServ/LexUriServ.do?uri=CELEX:32000L0060:en:NOT (Accessed December 22, 2000).

European Commission (2008). Directive 2008/56/EC of the European parliament and of the Council of 17 June 2008 establishing a Framework for community action in the field of marine environmental policy 2008. http://eur-lex.europa.eu/LexUriServ/LexUriServ.do?uri=CELEX:32008L0056:en:NOT (Accessed June 25, 2008).

Fenchel, T. (1988). Marine plankton food chains. *Annu. Rev. Ecol. Syst.* 19, 19–38. doi:10.1146/annurev.es.19.110188.000315

Ferreira, J. G., Andersen, J. H., Borja, A., Bricker, S. B., Camp, J., Cardoso da Silva, M., et al. (2011). Overview of eutrophication indicators to assess environmental status within the European marine Strategy Framework directive. *Estuar. Coast. Shelf Sci.* 93, 117–131. doi:10.1016/j.ecss.2011.03.014(

Ferreira, R. D., Barbosa, C. C. F., and Novo, E. M. L. de M. (2012). Assessment of *in vivo* fluorescence method for chlorophyll-a estimation in optically complex waters (curuai floodplain, pará - Brazil). *Acta Limnol. Bras.* 24, 373–386. doi:10.1590/S2179-975X2013005000011

Gilerson, A. A., Gitelson, A. A., Zhou, J., Gurlin, D., Moses, W., Ioannou, I., et al. (2010). Algorithms for remote estimation of chlorophyll-a in coastal and inland waters using red and near infrared bands. *Opt. Express* 18, 24109. doi:10.1364/OE.18.024109

Gilerson, A., Zhou, J., Hlaing, S., Ioannou, I., Gross, B., Moshary, F., et al. (2008). Fluorescence component in the reflectance spectra from coastal waters. II. Performance of retrieval algorithms. *Opt. Express* 16, 2446. doi:10.1364/OE.16.002446

Gitelson, A. A., Schalles, J. F., and Hladik, C. M. (2007). Remote chlorophyll-a retrieval in turbid, productive estuaries: Chesapeake bay case study. *Remote Sens.Environ.* 109, 464–472. doi:10.1016/j.rse.2007.01.016

Gittings, J. A., Raitsos, D. E., Racault, M.-F., Brewin, R. J. W., Pradhan, Y., Sathyendranath, S., et al. (2017). Seasonal phytoplankton blooms in the gulf of aden revealed by remote sensing. *Remote Sens.Environ.* 189, 56–66. doi:10.1016/j.rse.2016.10.043

Goldman, E., Smith, E., and Richardson, T. (2013). Estimation of chromophoric dissolved organic matter (CDOM) and photosynthetic activity of estuarine phytoplankton using a multiple-fixed-wavelength spectral fluorometer. *Water Res.* 47, 1616–1630. doi:10.1016/j.watres.2012.12.023

Gons, H. (1999). Optical teledetection of chlorophyll a in turbid inland waters. *Environ. Sci. Technol.* 33, 1127–1132. doi:10.1021/ES9809657

Gower, J., King, S., and Goncalves, P. (2008). Global monitoring of plankton blooms using MERIS MCI. *Int. J. Remote Sens.* 29, 6209–6216. doi:10.1080/01431160802178110

Guan, Q., Feng, L., Hou, X., Schurgers, G., Zheng, Y., and Tang, J. (2020). Eutrophication changes in fifty large lakes on the yangtze plain of China derived from MERIS and OLCI observations. *Remote Sens. Environ.* 246, 111890. doi:10.1016/j.rse.2020.111890

Guinder, V., and Molinero, J. C. (2013). "Climate change effects on marine phytoplankton," in *Marine ecology in a changing world* (Boca Raton, FL, USA: CRC Press). ISBN 978-1-4665-9007-6.

Hama, T., Inoue, T., Suzuki, R., Kashiwazaki, H., Wada, S., Sasano, D., et al. (2015). Response of a phytoplankton community to nutrient addition under different CO2 and PH conditions. *J. Oceanogr.* 72, 207–223. doi:10.1007/s10872-015-0322-4

HELCOM (2006). "Manual for marine monitoring in the COMBINE programme of HELCOM. Part C," in *Programme for monitoring of eutrophication and its effects* (Helsinki, Finland, Europe: HELCOM).

HITACHI (2020). *Hitachi instruction manual for model U-3900/3933H spectrophotometer (maintenance manual).* Tokyo, Japan: Hitachi High-Tech Science Corporation. 2J2-9011-014 Ver15.

Hu, C., Feng, L., Lee, Z., Franz, B., Bailey, S., Werdell, J., et al. (2019). Improving satellite global chlorophyll a data products through algorithm refinement and data recovery. *J. Geophys. Res. Oceans* 124, 1524–1543. doi:10.1029/2019JC014941

Järvet, A., and Nõges, P. (1998). Research area and period of L.Võrtsjärv. In Present state and future fate of Lake Võrtsjärv. *Tampere* 13–22.

Jeffrey, S. W., and Humphrey, G. F. (1975). New spectrophotometric equations for determining chlorophylls a, b, C1 and C2 in higher plants, algae and natural phytoplankton. *Biochem. Physiol. Pflanz.* 167, 191–194. doi:10.1016/S0015-3796(17)30778-3

Kiselev, V., Bulgarelli, B., and Heege, T. (2014). Sensor independent adjacency correction algorithm for coastal and inland water systems. *Remote Sens.Environ* 157, 85–95. doi:10.1016/j.rse.2014.07.025

Koenings, J. P., and Edmundson, J. A. (1991). Secchi disk and photometer estimates of light regimes in alaskan lakes: Effects of Yellow color and turbidity. *Limnol. Oceanogr.* 36, 91–105. doi:10.4319/lo.1991.36.1.0091

Kromkamp, J., Dijkman, N., Peene, J., Simis, S., and Gons, H. (2008). Estimating phytoplankton primary production in Lake IJsselmeer (The Netherlands) using variable fluorescence (PAM-FRRF) and C-uptake techniques. *Eur. J. Phycol.* 43, 327–344. doi:10.1080/09670260802080895

Kuha, J., Järvinen, M., Salmi, P., and Karjalainen, J. (2020). Calibration of *in situ* chlorophyll fluorometers for organic matter. *Hydrobiologia* 847, 4377–4387. doi:10.1007/s10750-019-04086-z

Laas, A., Eyto, E., Pierson, D., and Jennings, E. (2016). "NETLAKE guidelines for automatic monitoring station development,". Technical Report (NETLAKE).

Longhurst, A., Sathyendranath, S., Platt, T., and Caverhill, C. (1995). An estimate of global primary production in the ocean from satellite radiometer data. *J. Plankton Res.* 17, 1245–1271. doi:10.1093/plankt/17.6.1245

Lorenzen, C. J. (1967). Determination of chlorophyll and pheo-pigments: Spectrophotometric equations. *Limnol. Oceanogr.* 12, 343–346. doi:10.4319/lo.1967.12.2.0343

Luhtala, H., and Tolvanen, H. (2013). Optimizing the use of Secchi depth as a proxy for euphotic depth in coastal waters: An empirical study from the baltic sea. *ISPRS Int. J. Geoinf.* 2, 1153–1168. doi:10.3390/ijgi2041153

Marcé, R., George, G., Buscarinu, P., Deidda, M., Dunalska, J., Eyto, E., et al. (2016). Automatic high frequency monitoring for improved lake and reservoir management. *Environ. Sci. Technol.* 50, 10780–10794. doi:10.1021/acs.est.6b01604

Matthews, M., Bernard, S., and Robertson Lain, L. (2012). An algorithm for detecting trophic status (Chlorophyll-a), cyanobacterial-dominance, surface scums and floating vegetation in inland and coastal waters. *Remote Sens. Environ.* 124, 637–652. doi:10.1016/j.rse.2012.05.032

Matthews, M. W. (2014). Eutrophication and cyanobacterial blooms in South African inland waters: 10years of MERIS observations. *Remote Sens. Environ.* 155, 161–177. doi:10.1016/j.rse.2014.08.010

McKee, D., Cunningham, A., Wright, D., and Hay, L. (2007). Potential impacts of nonalgal materials on water-leaving sun induced chlorophyll fluorescence signals in coastal waters. *Appl. Opt.* 46, 7720–7729. doi:10.1364/AO.46.007720

Meinson, P. (2017). PhD thesis. Tartu, Estonia: Estonian University of Life Sciences.High-frequency measurements – A new approach in limnology

Meinson, P., Idrizaj, A., Nõges, P., Noges, T., and Laas, A. (2016). Continuous and high-frequency measurements in limnology: History, applications and future challenges. *Environ. Rev.* 24, 52–62. doi:10.1139/er-2015-0030

Meyns, S., Illi, R., and Ribi, B. (1994). Comparison of chlorophyll-a analysis by HPLC and spectrophotometry: Where do the differences come from? *Arch. für Hydrobiol.* 132, 129–139. doi:10.1127/archiv-hydrobiol/132/1994/129

Mograne, M. A., Jamet, C., Loisel, H., Vantrepotte, V., Mériaux, X., and Cauvin, A. (2019). Evaluation of five atmospheric correction algorithms over French optically-complex waters for the sentinel-3a olci ocean color sensor. *Remote Sens.* 11 (6), 668. doi:10.3390/rs11060668

Moiseeva, N., Churilova, T., Efimova, T., and Matorin, D. (2020). Correction of the chlorophyll a fluorescence quenching in the sea upper mixed layer: Development of the algorithm. *Phys. Oceanogr.* 27, 60–68. doi:10.22449/1573-160X-2020-1-60-68

OSPAR Commission (2009). *Evaluation of the OSPAR system of ecological quality objectives for the North sea*, 102.

Page, B. P., Olmanson, L. G., and Mishra, D. R. (2019). A harmonized image processing workflow using sentinel-2/MSI and landsat-8/OLI for mapping water clarity in optically variable lake systems. *Remote Sens. Environ.* 231, 111284. doi:10.1016/j.rse.2019.111284

Pahlevan, N., Sarkar, S., Franz, B., V Balasubramanian, S., and He, J. (2017). Sentinel-2 MultiSpectral instrument (MSI) data processing for aquatic science applications: Demonstrations and validations. *Remote Sens. Environ.* 201, 47–56. doi:10.1016/j.rse.2017.08.033

Pahlevan, N., Smith, B., Schalles, J., Binding, C., Cao, Z., Ma, R., et al. (2020). Seamless retrievals of chlorophyll-a from sentinel-2 (MSI) and sentinel-3 (OLCI) in inland and coastal waters: A machine-learning approach. *Remote Sens. Environ.* 240, 111604. doi:10.1016/j.rse.2019.111604

Pereira-Sandoval, M., Ruescas, A., Urrego, P., Ruiz-Verdú, A., Delegido, J., Tenjo, C., et al. (2019). Evaluation of atmospheric correction algorithms over Spanish inland waters for sentinel-2 multi spectral imagery data. *Remote Sens.* 11 (12), 1469. doi:10.3390/rs11121469

Peters, S., Laanen, M., Groetsch, P., Ghezehegn, S., Poser, K., Hommersom, A., et al. (2018). *Wispstation: A new autonomous abowe water radiometer system, conference*. Dubrovnik: Ocean Optics.

Picazo, A., Rochera Cordellat, C., Vicente, E., Miracle, M., and Camacho, A. (2013). Spectrophotometric methods for the determination of photosynthetic pigments in stratified lakes: A critical analysis based on comparisons with HPLC determinations in a model lake. *Limnetica* 32, 139–158. doi:10.23818/limn.32.13

Proctor, C., and Roesler, C. (2010). New insights on obtaining phytoplankton concentration and composition from *in situ* multispectral chlorophyll fluorescence. *Limnol. Oceanogr. Methods* 8, 695–708. doi:10.4319/lom.2010.8.695

Reinart, A., and Kutser, T. (2006). Comparison of different satellite sensors in detecting cyanobacterial bloom events in the baltic sea. *Remote Sens. Environ.* 102, 74–85. doi:10.1016/j.rse.2006.02.013

Reinart, A., and Pedusaar, T. (2008). Reconstruction of the time series of the underwater light climate in a shallow Turbid Lake. *Aquat. Ecol.* 42, 5–15. doi:10.1007/s10452-006-9056-0

Reynolds, C. S. (2006). *The ecology of phytoplankton, ecology, biodiversity and conservation*. Cambridge, UK: Cambridge University Press.

Rinke, K., Kuehn, B., Bocaniov, S., Wendt-Potthoff, K., Büttner, O., Tittel, J., et al. (2013). Reservoirs as sentinels of catchments: The rappbode reservoir observatory (harz mountains, Germany). *Environ. Earth Sci.* 69, 523–536. doi:10.1007/s12665-013-2464-2

Ross, J., and Sulev, M. (2000). Sources of errors in measurements of PAR. *Agric. For. Meteorol.* 100, 103–125. doi:10.1016/S0168-1923(99)00144-6

Ruban, A. V. (2016). Nonphotochemical chlorophyll fluorescence quenching: Mechanism and effectiveness in protecting plants from photodamage. *Plant Physiol.* 170, 1903–1916. doi:10.1104/pp.15.01935

Rusak, J., Tanentzap, A., Klug, J., Rose, K., Hendricks, S., Jennings, E., et al. (2018). Wind and trophic status explain within and among-lake variability of algal biomass: Variability of phytoplankton biomass. *Limnol. Oceanogr. Lett.* 3, 409–418. doi:10.1002/lol2.10093

Russak, V., and Kallis, A. (2003). *Eesti kiirguskliima teatmik oü stilett trükikoda.* Tallinn, Estonia, Europe: Eesti meteoroloogia ja Hüdroloogia Instituut.

Sayers, M. J., Grimm, A. G., Shuchman, R. A., Deines, A. M., Bunnell, D. B., Raymer, Z. B., et al. (2015). A new method to generate a high-resolution global distribution map of lake chlorophyll. *Int. J. Remote Sens.* 36, 1942–1964. doi:10.1080/01431161.2015.1029099

Seegers, B. N., Stumpf, R. P., Schaeffer, B. A., Loftin, K. A., and Werdell, P. J. (2018). Performance metrics for the assessment of satellite data products: An ocean color case study. *Opt. Express* 26, 7404–7422. doi:10.1364/OE.26.007404

Siegel, D. A., Behrenfeld, M. J., Maritorena, S., McClain, C. R., Antoine, D., Bailey, S. W., et al. (2013). Regional to global assessments of phytoplankton dynamics from the SeaWiFS mission. *Remote Sens. Environ.* 135, 77–91. doi:10.1016/j.rse.2013.03.025

Simmons, L. J., Sandgren, C. D., and Berges, J. A. (2016). Problems and pitfalls in using HPLC pigment analysis to distinguish lake Michigan phytoplankton taxa. *J. Gt. Lakes. Res.* 42, 397–404. doi:10.1016/j.jglr.2015.12.006

Snortheim, C. A., Hanson, P. C., McMahon, K. D., Read, J. S., Carey, C. C., and Dugan, H. A. (2017). Meteorological drivers of hypolimnetic anoxia in a eutrophic, North temperate lake. *Ecol. Modell.* 343, 39–53. doi:10.1016/j.ecolmodel.2016.10.014

Sørensen, K., Grung, M., and Röttgers, R. (2007). An intercomparison of *in vitro* chlorophyll a determinations for MERIS level 2 data validation. *Int. J. Remote Sens.* 28, 537–554. doi:10.1080/01431160600815533

Steinmetz, F., Deschamps, P.-Y., and Ramon, D. (2011). Atmospheric correction in presence of sun glint: Application to MERIS. *Opt. Express* 19, 9783–9800. doi:10.1364/OE.19.009783

Tamm, M., Freiberg, R., Tõnno, I., Nõges, P., and Nõges, T. (2015). Pigment-based chemotaxonomy - a quick alternative to determine algal assemblages in large shallow eutrophic lake? *PLOS ONE* 10, e0122526. doi:10.1371/journal.pone.0122526

Tamm, M. (2019). PhD thesis. Tartu, Estonia: Estonian University of Life Sciences.Pigment-based chemotaxonomy – efficient tool to quantify phytoplankton groups in lakes and coastal sea areas

Tilstone, G., Miller, P., Brewin, B., and Priede, I. (2014). Enhancement of primary production in the North atlantic outside of the spring bloom, identified by remote sensing of ocean Colour and temperature. *Remote Sens. Environ.* 146, 77–86. doi:10.1016/j.rse.2013.04.021

Toming, K., Kutser, T., Laas, A., Sepp, M., Paavel, B., and Noges, T. (2016). First experiences in mapping LakeWater quality parameters with sentinel-2 MSI imagery. *Remote Sens.* 8, 640. doi:10.3390/rs8080640

Vansteenwegen, D., Ruddick, K., Cattrijsse, A., Vanhellemont, Q., and Beck, M. (2019). The pan-and-tilt hyperspectral radiometer system (PANTHYR) for autonomous satellite validation measurements-prototype design and testing. *Remote Sens.* 11, 1360. doi:10.3390/rs11111360

Vörös, L., and Padisak, J. (1991). Phytoplankton biomass and chlorophyll-a in some shallow lakes in central europe. *Hydrobiologia* 215, 111–119. doi:10.1007/BF00014715

Warren, M. A., Simis, S. G. H., Martinez-Vicente, V., Poser, K., Bresciani, M., Alikas, K., et al. (2019). Assessment of atmospheric correction algorithms for the Sentinel-2A MultiSpectral Imager over coastal and inland waters. *Remote Sens. Environ.* 225, 267–289. doi:10.1016/j.rse.2019.03.018

Winder, M., and Sommer, U. (2012). Phytoplankton response to a changing climate. *Hydrobiologia* 698, 5–16. doi:10.1007/s10750-012-1149-2

Woolway, R. I., Meinson, P., Nõges, P., Jones, I. D., and Laas, A. (2017). Atmospheric stilling leads to prolonged thermal stratification in a large shallow polymictic lake. *Clim. Change* 141, 759–773. doi:10.1007/s10584-017-1909-0

Zeng, C., Zeng, T., Fischer, A. M., and Xu, H. (2017). Fluorescence-based approach to estimate the chlorophyll-A concentration of a phytoplankton bloom in ardley cove (Antarctica). *Remote Sens.* 9, 210. doi:10.3390/rs9030210

Zhang, Y., Liu, M., Qin, B.-Q., Woerd, H., Li, J., and Li, Y. (2009). Modeling remote-sensing reflectance and retrieving chlorphyll-a concentration in extremely turbid case-2 waters (lake taihu, China). *IEEE Trans. Geosci. Remote Sens.* 47, 1937–1948. doi:10.1109/TGRS.2008.2011892

frontiers | Frontiers in Environmental Science

TYPE Methods
PUBLISHED 04 January 2023
DOI 10.3389/fenvs.2022.1038635

Check for updates

OPEN ACCESS

EDITED BY
Caterina Bergami,
National Research Council (CNR), Italy

REVIEWED BY
Taina Goncalves Loureiro,
Cape Peninsula University of Technology, South Africa
Fabio Ercoli,
Estonian University of Life Sciences, Estonia

*CORRESPONDENCE
Cristina Di Muri,
✉ cristina.dimuri@iret.cnr.it
Giorgio Mancinelli,
✉ giorgio.mancinelli@unisalento.it

SPECIALTY SECTION
This article was submitted to Conservation and Restoration Ecology, a section of the journal Frontiers in Environmental Science

RECEIVED 07 September 2022
ACCEPTED 07 December 2022
PUBLISHED 04 January 2023

CITATION
Di Muri C, Arvanitidis C, Basset A, De Giorgi R, Rosati I, Vaira L and Mancinelli G (2023), The validation case on invasive crustaceans of the LifeWatch ERIC Internal Joint Initiative: State of the art and next steps forward. *Front. Environ. Sci.* 10:1038635. doi: 10.3389/fenvs.2022.1038635

The validation case on invasive crustaceans of the LifeWatch ERIC Internal Joint Initiative: State of the art and next steps forward

Cristina Di Muri[1,2]*, Christos Arvanitidis[3], Alberto Basset[1,2,4], Raffaele De Giorgi[2], Ilaria Rosati[1,5], Lucia Vaira[2] and Giorgio Mancinelli[4,6,7]*

[1]Italian National Research Council, Institute of Research on Terrestrial Ecosystems–CNR-IRET, University of Salento, SP Lecce-Monteroni, Lecce, Italy, [2]LifeWatch ERIC, Service Centre, Ecotekne, SP Lecce-Monteroni, Lecce, Italy, [3]LifeWatch ERIC, Plaza España SN, SECTOR II-III, Seville, Spain, [4]Department of Biological and Environmental Sciences and Technologies–DiSTeBA, University of Salento, SP Lecce-Monteroni, Lecce, Italy, [5]LifeWatch Italy, University of Salento, SP Lecce-Monteroni, Lecce, Italy, [6]National Inter-University Consortium for Marine Sciences–CoNISMa, Piazzale Flaminio 9, Roma, Italy, [7]National Research Council, Institute of Marine Biological Resources and Biotechnologies–CNR-IRBIM, Lesina, Italy

LifeWatch ERIC, the e-Science European infrastructure for biodiversity and ecosystem research, launched an Internal Joint Initiative on Non-indigenous Species and Invasive Alien Species (NIS-IAS) as they are considered one of the major drivers of biodiversity and ecosystem change. Here, the case study focused on the trophic biogeography of invasive crustaceans is presented, describing the procedures, resources, and analytical web services implemented to investigate the trophic habits of these taxa by using carbon and nitrogen stable isotope data. The case study offers a number of analytical tools to determine the variability of the trophic position of invasive crustaceans in a spatially-explicit context and to model it as a function of relevant environmental predictors. Literature-based stable isotope data of the Atlantic blue crab *Callinectes sapidus* and of the Louisiana crayfish *Procambarus clarkii* have been used to evaluate the functionalities and outcomes of the workflow. The Tesseract Virtual Research Environment integrates all the analytical services offered by LifeWatch ERIC, including the ones developed for this case study, by means of a user-friendly interface. The analytical functions implemented for the crustacean workflow provide a proof of concept for future open e-science platforms focusing on NIS-IAS. The workflow conceptual structure can be adapted to a wide range of species, and can be further improved to support researchers in monitoring and predicting trophic-related impacts of NIS-IAS. In addition, it can support policymakers and stakeholders in the implementation of effective management and control measures to limit the negative effects of bioinvaders in recipient environments.

KEYWORDS

virtual research environment, invasive species, carbon 13, nitrogen 15, *Callinectes sapidus*, *Procambarus clarkii*, trophic position, ecological impact

1 Introduction

The modern era of globalization is characterized by an intensification of human activities, such as the transport of people and goods and the creation of artificial corridors, facilitating the introduction of species outside their native geographic ranges (Banks et al., 2015). The European Union has recognized that Non-Indigenous Species (NIS hereafter) require immediate consideration and adequate management and control actions, and has addressed this issue in Regulation 1143/2014 (European Commission, 2014) and in the Biodiversity Strategy to 2030 (European Commission, 2020). The former requires member states to provide lists of NIS that could determine significant negative impacts on biodiversity and on related ecosystem services. However, the availability of comprehensive and measurable impact estimates is still limited (see e.g., Katsanevakis et al., 2014; Tsirintanis et al., 2022 for the Mediterranean Sea), partly due to the scarce information on NIS ecology in nature and on the type and strength of the interactions they establish with the native biota (Cardeccia et al., 2018; Katsanevakis and Moustakas, 2018). The need for a thorough assessment of NIS impacts is particularly imperative when they cause adverse ecological and economic effects and reach the "invasive" status (after UNEP, 1992; Invasive Alien Species–IAS: Russell and Blackburn, 2017).

To date, the impacts of IAS have been mostly evaluated by using qualitative evidence-based knowledge of experts rather than quantitative evidence (Corrales et al., 2020; Essl et al., 2020). In addition, it is difficult to infer common patterns from the observed impacts, as this evidence is generally context-dependent and limited in space and time (Courchamp et al., 2017; Torchin et al., 2021; Watkins et al., 2021). A number of recent regional and global scale investigations, focusing on the impact of bioinvaders, have demonstrated that meta-analytical approaches can overcome the paucity and diversity of available information, and can identify and test the primary factors affecting the context-dependency of IAS impacts. Moreover, they have indicated relatively straightforward ecological rules to locally predict the threat of biological invasions on native communities (Thomsen et al., 2014; Gallardo et al., 2016; Mollot et al., 2017; Anton et al., 2019; Bradley et al., 2019). These studies have shown that the impact of invaders on the biodiversity and functioning of recipient ecosystems depend critically on their trophic habits. For example, Thomsen et al. (2014), Mollot et al. (2017), and Anton et al. (2019) indicated that the trophic position of aquatic invaders controls their adverse effects on biodiversity, a result confirmed by a global meta-analysis on community responses to invasion performed by Bradley et al. (2019). Additionally, Gallardo et al. (2016) indicated that introduced predators and omnivores are the trophic groups that exert the most negative effects on the lowest levels of benthic food webs in aquatic ecosystems as also acknowledged by other studies (Vazquez, 2006; Romanuk et al., 2009; Havel et al., 2015; Mancinelli et al., 2017b; Médoc et al., 2018).

Building on this evidence, a validation case focused on the trophic habits of crustacean IAS and their impact on invaded benthic food webs was conceived. The case study has been developed by LifeWatch ERIC (https://www.lifewatch.eu/), the e-Science European infrastructure offering e-science tools and facilities to the scientific community committed to biodiversity and ecosystems research. Nowadays, a large variety of projects/initiatives provides datasets, databases, and data analysis tools to tackle different emerging challenges in the field of biodiversity and ecosystem conservation (Escribano et al., 2018; Stephenson and Stengel, 2020). However, the fragmentation of available data often hinders the capacity to reveal key ecological patterns and hampers analytical efforts aiming at integrating such a heterogeneous body of information (Bingham et al., 2017). To overcome the existing limitations in data accessibility, discoverability, and interoperability, LifeWatch ERIC has devoted its efforts to collate and harmonize biodiversity and ecosystems-related data according to the FAIR principles (Findable, Accessible, Interoperable, Reusable: Wilkinson et al., 2016). Most importantly, LifeWatch ERIC provides a diverse range of data and analytical web services, arranged in purpose-built pipelines of work or workflows, and properly structured in Virtual Research Environments (VREs). The latter are web-based, community-oriented, comprehensive, flexible, and secure working environments, allowing users to perform and complete their analyses in biodiversity and ecosystems research (Basset and Los, 2012; see also Enke et al., 2012; Candela et al., 2013). Given the strict association between biological invasions on one hand and the conservation and management of biodiversity in natural ecosystems on the other, in 2019 the executive board of LifeWatch ERIC launched an Internal Joint Initiative (https://www.lifewatch.eu/internal-joint-initiative/). Through the identification of demonstrative case studies on NIS-IAS, the aim of the initiative was to implement validation cases providing data and e-tools to the scientific community to develop evidence-based knowledge on key ecological topics in different research areas of invasion ecology. They included the prediction of dispersion scenarios of keystone NIS in terrestrial ecosystems, the early-detection and monitoring of NIS spread in aquatic habitats through conventional ecological monitoring procedures and DNA metabarcoding, the EUNIS (European Nature Information System, https://eunis.eea.europa.eu/) habitat and ecosystem vulnerability to NIS invasion, and the evaluation of the spatial variability and predictability of trophic-related ecological impacts of invasive crustaceans.

Here the latter validation case is presented, describing the spatially-explicit trophic variations of two study species, i.e., the

FIGURE 1
Photographs of *Procambarus clarkii* (upper side) and *Callinectes sapidus* (lower side), the two model crustaceans used for the validation of the LifeWatch ERIC case study on trophic habits of omnivorous invasive species. Note that the two photos are not in scale.

Louisiana crayfish *Procambarus clarkii* and the Atlantic blue crab *Callinectes sapidus*, two omnivorous invasive species in European freshwaters and coastal waters. The possibility that climatic drivers acting at large spatial scales may influence the trophic behavior of omnivorous species, independently from their native or non-indigenous nature, remains to date unexplored. This occurs notwithstanding the increasing interest in the linkage between species' trophic-related traits and the ongoing global climate change, since global warming has the potential to determine trophic shifts and variations in the trophic niche of aquatic organisms, ultimately altering the structure and functions of both freshwater and marine food webs (Bartley et al., 2019; Wallingford et al., 2020; Henry and Sorte, 2022).

Specifically, here an effort was made to describe: 1) the procedures used to conceive, design, and define the structure and the tools needed to assess the trophic habits of invasive crustaceans using stable isotope data; 2) the methodological approaches adopted to implement the validation case and the workflow design, and 3) the structure of the datasets on which the analytical workflow relies.

Moreover, two preliminary examples focused on the analysis of stable isotope datasets collated for the validation case and resolved at both population- and individual-scale are provided, illustrating the potential outcomes expected from the advanced implementation of the analytical workflow at the core of the validation case.

2 Methods

2.1 Study species

The validation case focused on two widely distributed species of invasive omnivorous crustaceans, i.e., the Louisiana crayfish *P. clarkii* and the Atlantic blue crab *C. sapidus* (Figure 1).

Procambarus clarkii (Girard, 1852) is native to the southern United States and northern Mexico, but it has been introduced widely in all continents, with the exception of Australia and Antarctica (Loureiro et al., 2015), for economic purposes, i.e., aquaculture and fishing activities (Hobbs et al., 1989; Oficialdegui et al., 2019) and for the biological control of schistosomes and of other snail-transmitted parasites, as occurred in a number of African countries (Hofkin et al., 1991; Sulieman et al., 2013). *Procambarus clarkii* is included in the European list of IAS of greatest concern (European Commission, 2008). Due to its biological and ecological characteristics (Hänfling et al., 2011), this species causes serious harm to the biodiversity and functions of the invaded environments as well as to ecosystem services and human infrastructures (e.g. irrigation canals and rice crops: Twardochleb et al., 2013; Souty-Grosset et al., 2016).

The origin of the Atlantic blue crab *C. sapidus* (Rathbun, 1896) is the western Atlantic coast and its native range spans from New England to Uruguay (Millikin and Williams, 1984). This omnivorous crab was introduced in Europe in 1901 and first recorded in the Mediterranean basin in 1947, although it has been suggested that it had arrived a decade earlier (Nehring, 2011). In the last decade, *C. sapidus* has spread almost ubiquitously in the Black Sea and in the eastern and central Mediterranean Sea, with the western and southern sectors of the basin as fronts of the most recent range expansions (Mancinelli et al., 2021). Since 2006, *C. sapidus* has been recognized as an invasive species in the Mediterranean Sea (Streftaris and Zenetos, 2006), however, a review published in 2017 (Mancinelli et al., 2017a) and a risk assessment performed in 2021 for the EU (Rabitsch et al., 2022), highlighted the rather scant information on its actual impact on recipient communities. Clavero et al. (2022) provided the first quantitative assessment of the adverse effects exerted by the blue crab on the biodiversity of recipient communities.

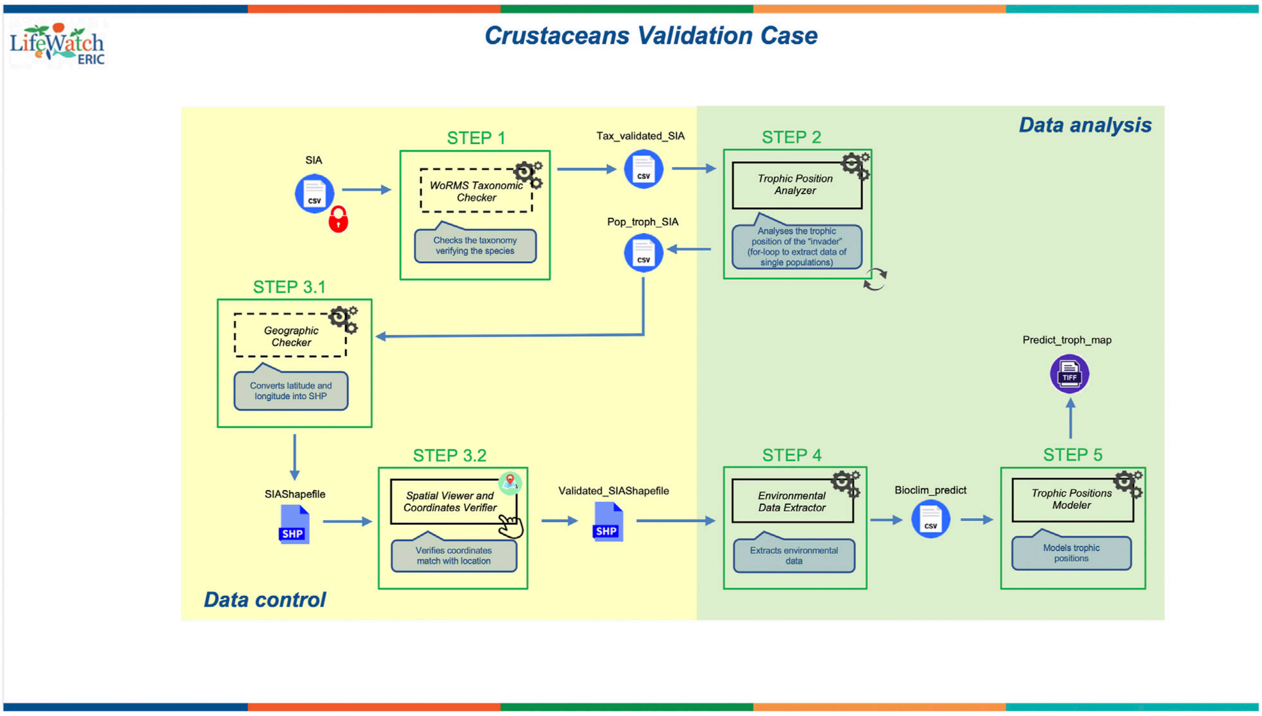

FIGURE 2
Crustacean Validation Case diagram. The diagram shows the analytical workflow and its components including services (steps in green boxes) and input/output datasets produced. A detailed guide to the symbols included in the diagram is provided in the Supplementary Material "Workflow Standard–Guidelines".

2.2 Data collection

Stable isotopic data were collated from the literature to provide extensive, standardized, and spatially-explicit information on the trophic habits of the study species at different spatial scales. Stable isotopes analysis has gained huge popularity for the study of aquatic food webs in the last decades, allowing for robust comparisons of species dietary habits at a local as well as regional and global scale (e.g., Mancinelli, 2012; Annabi et al., 2018; Pethybridge et al., 2018; Mancini et al., 2021; Mancini et al., 2022). This methodology is currently recognized as a key tool to deepen the understanding of ecosystem processes and functioning and to evaluate the response of aquatic ecosystems to anthropogenic impacts, including global climate change (Mancinelli and Vizzini, 2015; Gautam and Lee, 2016).

An extensive literature search was performed to collate geo-referenced stable isotope data resolved at individual- and population-scale. Extensive details on the adopted procedures are provided in Di Muri et al. (2022a); Di Muri et al. (2022b). In brief, the online databases ISI Web of Science and Scopus were searched by using a multiple search criterion and the term "*Procambarus clarkii*" or "*Callinectes sapidus*" in conjunction with "stable isotopes". The results were complemented with those obtained from queries on Google Scholar (https://scholar.google.com/) using identical keywords. The entries obtained from the literature search had their titles and abstracts screened in order to remove manipulative studies and reviews. The full text of the remaining studies was examined in detail to select those where the occurrence of the two species was reported explicitly, together with information on the country, latitude and longitude, the year of the record, and at least the $\delta^{15}N$ value of the sampled specimens. Publications where the sampling locations were reported in maps were also included in the selection and Google Earth was used to extract the geographic coordinates. In addition, the literature sources to be eligible had to include isotopic information on potential vegetal or animal prey. The publications meeting the aforementioned criteria were eventually selected and $\delta^{15}N$ and $\delta^{13}C$ values were extracted from tables and figures. Figures were digitized after a fivefold enlargement and converted to numerical form using the graph capture freeware WebPlotDigitizer (ver. 4.5; https://automeris.io/WebPlotDigitizer/). In the dataset resolved at individual scale, $\delta\ ^{15}N$ and $\delta\ ^{13}C$ values refer to single specimens, whereas in the population-scale dataset, mean values of carbon and nitrogen

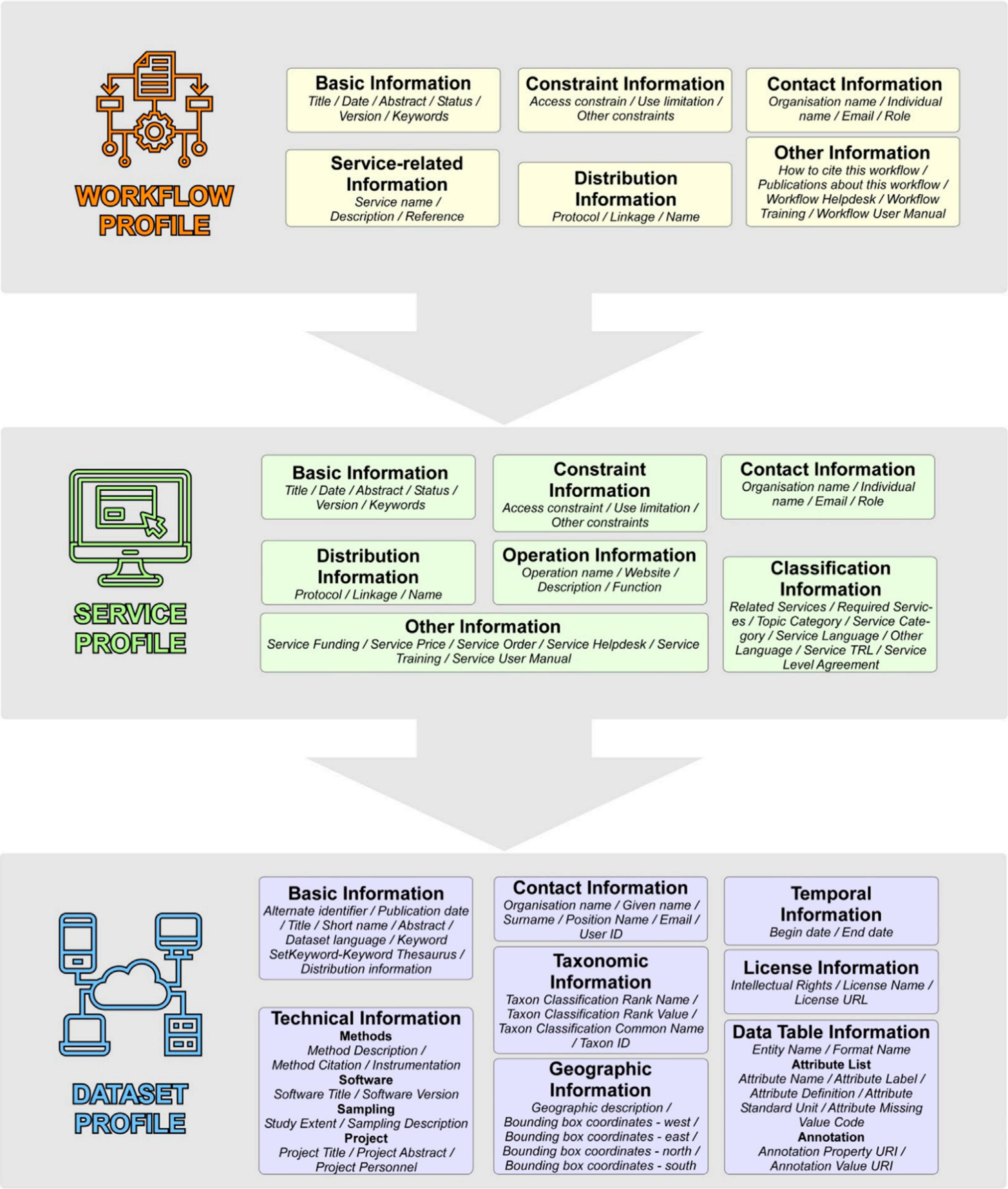

FIGURE 3
LifeWatch ERIC metadata profile for workflows (yellow), services (green), and datasets (blue). The asterisks (*) indicate the mandatory attributes. A complete description of the LifeWatch ERIC Application profiles is available in Vaira et al. (2022).

stable isotopes were extracted from the literature along with their standard deviations and sample sizes if available. Lastly, the authors of the selected publications were contacted directly to obtain additional unpublished information and raw data, hence, the collated datasets include published data from peer-reviewed articles and grey literature as well as data gathered from unpublished sources, ultimately offering visibility to previously unavailable information.

2.3 The workflow

The datasets are conceived and designed to be analyzed by means of a number of sequential analytical web services included in a workflow. The structure of the workflow is presented as a diagram in Figure 2 and was developed using the LifeWatch ERIC guidelines as a general reference and through a collaborative approach between scientists and ICT

TABLE 1 List of climatic variables and related databases and layer names used for the multiple correlation analysis.

Database	Variable name	Layer name
MARSPEC	Mean annual SST	biogeo13
MARSPEC	SST of the coldest ice-free month	biogeo14
MARSPEC	SST of the warmest ice-free month	biogeo15
MARSPEC	Annual Range in SST	biogeo16
MARSPEC	Annual Variance in SST	biogeo17
MERRAclim	Annual Mean Temperature	BIO1
MERRAclim	Mean Diurnal Range	BIO2
MERRAclim	Isothermality	BIO3
MERRAclim	Temperature Seasonality	BIO4
MERRAclim	Max Temperature of Warmest Month	BIO5
MERRAclim	Min Temperature of Coldest Month	BIO6
MERRAclim	Temperature Annual Range	BIO7
MERRAclim	Mean Temperature of Wettest Quarter	BIO8
MERRAclim	Mean Temperature of Driest Quarter	BIO9
MERRAclim	Mean Temperature of Warmest Quarter	BIO10
MERRAclim	Mean Temperature of Coldest Quarter	BIO11

*SST, sea surface temperature.

experts. The overall goal of the workflow is to analyze the trophic geography of the two crustacean species under analysis, assuming their trophic position as an indirect indicator of their ecological impact on recipient aquatic food webs. This is performed by first running a spatially-explicit quantitative assessment of the trophic position of the two species and then by finding potential correlations between the invaders' trophic position and climatic drivers that are expected to change in the future (e.g., water temperature or salinity for marine ecosystems and air temperature for terrestrial ecosystems).

Specifically, the workflow was designed to include three functional analytical services for calculating the impact of the invaders (data analysis, in green in Figure 2) and three additional services to check the quality of the data entered by the users (data control, in yellow in Figure 2) and allowing for automatic corrections and adjustments if required.

The key data analysis steps and services included therein consist of: 1) the calculation of the trophic position of the invasive species through a Bayesian approach (Trophic Position Analyzer); 2) the extraction of environmental predictors from cloud-based repositories (Environmental Data Extractor); this service fetches and downloads from available repositories oceanographic and bioclimatic raster layers for the geographic coordinates included in the input dataset; and 3) the modelling of the invaders' trophic position as a function of the environmental variables using a Generalized Additive Model (Trophic Positions Modeler). The data control steps allow the user to: 1) check the scientific names of the species included in the input dataset (WoRMS Taxonomic Checker); 2) create a shapefile using the geographic coordinates included in the input dataset (Geographic Checker); and 3) verify the accuracy of the geographic coordinates (Spatial Viewer and Coordinates Verifier) by matching the latitude and the longitude with the corresponding locations and countries included in the input dataset, and by using the shapefile created within the previous service (i.e., Geographic Checker).

The resources created for the workflow (i.e., workflow, services, and datasets) are described using the LifeWatch ERIC application profiles and are published on the LifeWatch ERIC Metadata Catalogue (https://metadatacatalogue.lifewatch.eu). The metadata records of the workflow and services are documented with the ISO19139 standard and include respectively 24 and 34 metadata attributes (Figure 3). Dataset metadata records are documented with EML2.2.0 standard and the metadata schema includes 77 attributes (Figure 3). A complete description of the LifeWatch ERIC Application profiles is available in Vaira et al. (2022).

Links to metadata resources within the LifeWatch ERIC Metadata Catalogue and used for this case study are provided in the Supplementary Material.

2.4 Data analysis

The analyses are implemented within the workflow through the R statistical environment (R Development Core Team, 2022). Specifically, the trophic position of the invasive species (Trophic Position Analyzer, Figure 2) is calculated using the *tRophicPosition* package (version 0.7.7; Quezada-Romegialli et al., 2018; Quezada-Romegialli et al., 2019). Trophic position estimations are conventionally performed using:

$$TP_{\delta^{15}N} = \left(\delta^{15}N_{Consumer} - \delta^{15}N_{Baseline}\right) / \Delta^{15}N + \lambda$$

This equation is a generalization of that presented in Vander Zanden et al. (1997), where $\delta^{15}N_{Consumer}$ is the nitrogen isotopic signature of the invasive species under investigation (i.e., *P. clarkii* or *C. sapidus*), $\Delta^{15}N$ is the trophic discrimination factor of $\delta^{15}N$ (TDF hereafter), and $\delta^{15}N_{Baseline}$ and λ are, respectively, the nitrogen isotopic signature and the trophic level of the baseline species.

In the *tRophicPosition* package, the trophic position is estimated using a Bayesian approach whereby nitrogen values of consumers and baselines as well as the TDF are modelled as random variables, each having a prior normal distribution on their means and a uniform prior distribution on their standard deviations, and the trophic position is treated as a random

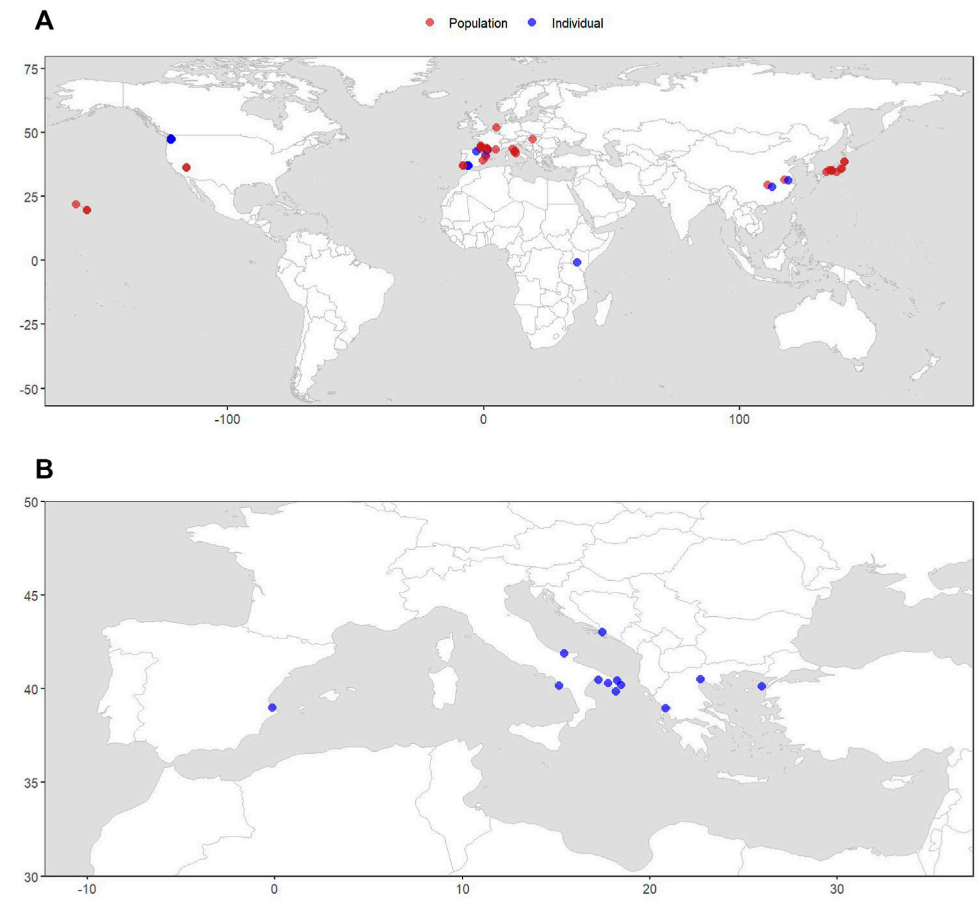

FIGURE 4
Maps of the locations included in the datasets of stable isotope data for *Procambarus clarkii* **(A)** and *Callinectes sapidus* **(B)**. The isotopic records shown in red are resolved at population-scale and the ones in blue are resolved at individual-scale.

parameter. The trophic position is also modelled as having a uniform prior distribution whereas λ is fixed. Given the omnivorous trophic habits of the species considered in this case study, the values of the trophic positions are estimated adopting a TDF of 0.27 ± 2.15 for carbon and a TDF of 2.58 ± 1.96 for nitrogen (mean ± 1SD, n = 49 and 91, respectively), calculated as the average of published enrichment factors for aquatic crustaceans (including *C. sapidus* and the crayfish *Orconectes viridis* and *Cherax destructor*) feeding on both vegetal and animal items (De Giorgi et al., 2022), and more consistent with other literature syntheses focused on crustaceans (Vanderklift and Ponsard, 2003; Carrozzo et al., 2014). The complete list of species selected as baselines and their assigned trophic levels can be found in Mancinelli and Di Muri. (2022a); Mancinelli and Di Muri. (2022b).

The Environmental Data Extractor service (Figure 2) performs the selection of a suite of oceanographic and climatic data from Bio-Oracle v2.0 (Tyberghein et al., 2012; Assis et al., 2018 for *C. sapidus*) and from WorldClim 2 (Fick and Hijmans, 2017 for *P. clarkii*). Bio-Oracle is a high-resolution GIS database of oceanic climate layers obtained from remotely sensed and *in situ* oceanographic observations with a common spatial resolution of five arcmin. The database additionally includes future projections produced for 2040–2050 and for 2090–2100 by averaging data from distinct Atmosphere/Ocean Global Climate Models (AOGCMs). WorldClim is a dataset with a global coverage including satellite-based climatic layers that have been built for the period 1970–2000 with a 30 arc-seconds spatial resolution and including downscaled future climate projections. The bioclimatic variables from these repositories are retrieved in R using the package *sdmpredictors* (v. 0.2.12; Bosch et al., 2022).

In the Trophic Position Modeler service (Figure 2), a generalized additive mixed model (GAMM; Wood, 2017) is used to examine relationships between the values of the trophic position and the suite of selected environmental predictors. GAMMs are built in R using the *gamm4*

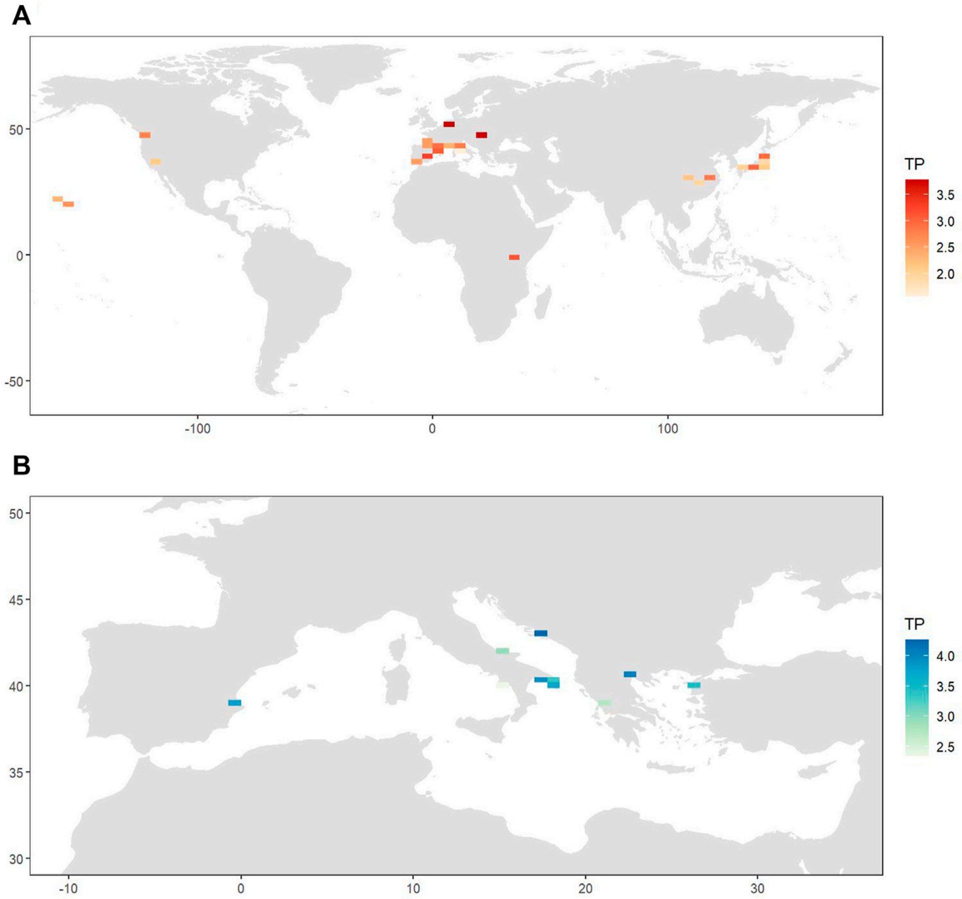

FIGURE 5
Heatmaps showing the values of the trophic position for *Procambarus clarkii* **(A)** and *Callinectes sapidus* **(B)** calculated respectively using the population-scale and the individual-scale dataset. Trophic position values were mediated for locations occurring within the same tile of the heatmap.

package (Wood and Scheipl, 2020) with a Gaussian error distribution and an identity link function; smoothing splines are used to examine non-linear fits for all marginal terms considered in the model. Exclusive economic zones and countries are incorporated as random effects to account for intra-group correlations and over-dispersion frequently arising in spatial analyses (Wood, 2017), whereas a scale-invariant tensor product is used to model the covariates for the geographical locations. Model selection is then performed manually using a backward elimination approach (starting with all candidate variables), and the best model fit is selected using the Akaike Information Criterion for small sample sizes (AICc).

Here, for illustrative purposes, the analyses presented focus on the population-scale dataset of *P. clarkii* (Mancinelli and Di Muri, 2022b) and on the individual-scale dataset of *C. sapidus* (Mancinelli and Di Muri, 2022a) using temperature-related continuous predictors for present conditions. The geo-referenced trophic position values were estimated according to Vander Zanden et al. (1997) and temperature-related oceanographic and climatic high-resolution layers were selected from MERRAclim (Carrete Vega et al., 2017 for *P. clarkii*) and MARSPEC (Sbrocco and Barber, 2013 for *C. sapidus*) (Table 1). Sea surface temperatures were used for *C. sapidus*, whereas air temperatures were used as a proxy of inland water temperatures for *P. clarkii* due to the unavailability of detailed raster layers for surface water temperatures in freshwater habitats (Piccolroaz et al., 2018; Table. 1). Subsequently, a simplified procedure based on a multiple correlation approach was performed with the aim of identifying the most adequate temperature-related variables to predict the variation in the trophic positions observed within the two datasets. Climatic variables and trophic position values were log-transformed and mean-centered for the analysis. The identification of the Minimum Adequate Model (MAM hereafter; Whittingham et al., 2006) was based on the heuristic generation of

TABLE 2 Bayesian Information Criterion (BIC) values and Bayes factors (B) estimated by the heuristic procedure implemented for Minimum Adequate Model (MAM) selection for *Procambarus clarkii*. Only the 10 models showing the lowest BIC values are reported. See Table 1 for layer acronyms.

Layers included in the model	BIC	B
BIO8	3.66	
BIO1	4.43	1.47
BIO10	5.12	2.08
BIO6	5.21	2.17
BIO9	5.53	2.55
BIO6-BIO8	6.43	3.99
BIO5-BIO8	6.73	4.64
BIO8-BIO10	6.74	4.66
BIO7-BIO8	6.93	5.13
BIO2-BIO8	7.28	6.11

alternative regression models. Model selection was performed by adopting an information theoretic criterion (Burnham and Anderson, 2002; Hegyi and Garamszegi, 2011) based on the estimation of the Bayesian Information Criterion (BIC; Schwarz, 1978) calculated for each combination of *n* explanatory variables. For model comparisons, approximate Bayes factors $B_{1,2}$ were calculated as:

$$B_{1,2} = exp\left\{\frac{-1}{2}\Delta_{1,2}\right\}$$

where $B_{1,2}$ = BIC(k_1)−BIC(k_2), and BIC(k_n) are the BIC values of models k_1 and k_2. If $B_{1,2} > 1$, then model k_1 is the model selected by the procedure (Neath and Cavanaugh, 2012) and identified as the best MAM. Model building and statistical analyses were performed following Fox and Weisberg. (2011).

Further analyses, not included in the current version of the workflow, were performed to provide an example of metrics that could be inferred by using stable isotope data, as well as to present the possible future implementations of the workflow. Using the individual-resolved data of *C. sapidus* six quantitative population metrics, originally described by Layman et al. (2007), were estimated for each location including the mean distance to centroid (CD) as a measure of population trophic diversity, nitrogen range (NR) and carbon range (CR) as indicators of the total nitrogen and carbon range exploited by each population, the standard deviation of nearest neighbor distance (SDNND) as an index of population trophic evenness, the total area (TA) as a measure of each population niche area estimated using a convex hull drawn around the most extreme data points on an isotope bi-plot. As TA is expected to increase with sample size (Jackson et al., 2011), additional estimations of niche areas were performed using the corrected standard ellipse area (SEAc) as a measure of each population niche area estimated using a standard ellipse calculated from the variance and covariance of $\delta^{13}C$ and $\delta^{15}N$ values and corrected for small sample sizes. All metrics were calculated using the package *SIBER* (Jackson and Parnell, 2021) in the R statistical computing environment (R Development Core Team, 2022).

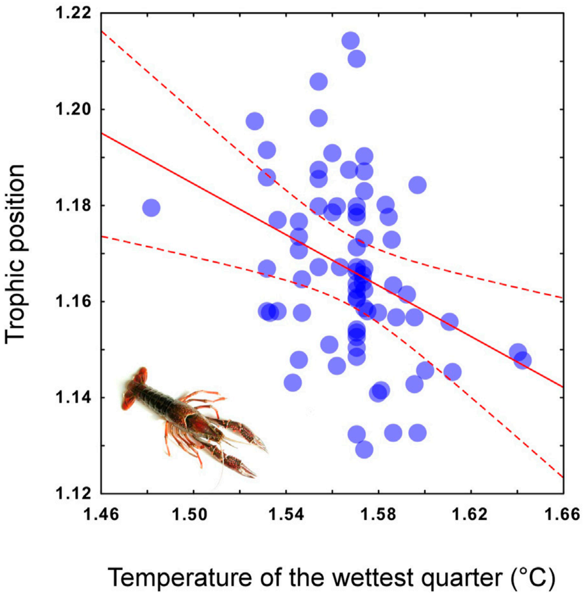

FIGURE 6
Trophic position of *Procambarus clarkii* calculated from the population-scale dataset as predicted by local mean temperature of the wettest quarter values. For the regression curve (solid line) 95% confidence intervals are included (dashed line). Log-transformed and mean-centered data are used in the scatterplot.

3 Results

Two datasets for *P. clarkii* and one dataset for *C. sapidus* were collated and included carbon and nitrogen isotopic values of the species and of their potential prey, and used as baselines for the analyses, within invaded habitats Mancinelli and Di Muri. (2022a); Mancinelli and Di Muri. (2022b). An additional dataset with stable isotope values of *C. sapidus* collected within the native area is currently under completion.

The literature search on *P. clarkii* identified 41 studies, performed between 2005 and 2021 within the global invaded range of the species, including geo-referenced stable isotope information. A population-scale dataset with mean and standard deviation values of 160 carbon and nitrogen isotopic records for *P. clarkii* and its potential prey was collated. In addition, a dataset resolved at the individual scale and

TABLE 3 Sample number (n), trophic position (TP), mean distance to centroid (CD), nitrogen range (NR), carbon range (CR), standard deviation of nearest neighbor distance (SDNND), total area (TA), and corrected standard ellipse area (SEAc) of the 12 *Callinectes sapidus* populations included in the individual-scale dataset.

Location	n	TP	CD	NR	CR	SDNND	TA	SEAc
Acquatina	20	3.35	2.06	3.24	8.63	0.4	15.96	6.52
Gandia	19	3.8	2.91	7.55	9.22	0.78	35.46	15.14
Lesina	24	2.96	0.85	2.65	3.31	0.25	4.83	1.4
Loudias	15	4.04	2.52	6.57	6.97	0.83	24.91	12.17
Pogonitsa	19	2.73	1.77	5.18	4.78	0.51	14.96	6.32
Parila	15	4.26	1.12	2.78	3.37	0.19	5	2.59
Alimini	7	3.34	1.29	3.29	3.14	1.1	5.23	4.46
Mar Piccolo	13	4.49	3.63	4.93	8.34	0.26	20.87	17.57
Torre Colimena	48	3.4	2.61	8.76	7.85	0.43	34.9	11.95
Spunderati	16	3.74	3.16	2.04	11.57	0.25	9.53	4.41
Alento River	10	2.34	0.88	2.51	2.19	0.28	2.44	1.5
Gokceada	30	3.46	0.74	3.2	2	0.24	2.9	0.82

consisting of 1,168 isotopic records was produced. The isotopic values included within the two datasets were gathered from 39 locations and 10 countries across Europe, Asia, Africa, and North America and, therefore, including all continents where *P. clarkii* has been found (Figure 4A).

The average trophic position of *P. clarkii* calculated from the population-scale isotopic dataset was 2.7 ± 0.07 (mean ± SE); estimations varied considerably among locations and ranged between values close to 2, indicating fully herbivorous trophic habits, and values >4, suggesting a carnivorous diet including other predatory species (Figure 5).

The multiple regression and the subsequent heuristic search for the MAM performed using the trophic positions of *P. clarkii* as the response variable and the 11 temperature-related MERRAclim variables as predictors, indicated that the best MAM was a single-variable model including the mean temperature of the wettest quarter as the only significant predictor (Table 2: BIC; Figure 6) and a significant negative relationship was observed (Pearson correlation: r = -0.35; p = 0.002; Figure 6). Noticeably, a significant inverse correlation was observed also with the mean annual temperature (Pearson correlation: r = -0.24, p = 0.03).

For *C. sapidus*, an individual-scale dataset was collated including 360 isotopic records gathered from 12 Mediterranean locations where *C. sapidus* has been introduced and is currently considered invasive.

The mean trophic position of *C. sapidus* was 3.5 ± 0.2 (mean ± SE), with values showing a two-fold variation between 2.3 and 4.5 (Table 3; Figure 5). The multiple regression and MAM identification procedure performed to find relations between the trophic positions of *C. sapidus* and five MARSPEC temperature-related variables indicated that the best predictive MAM was provided by the mean annual sea surface temperature (Table 4; Figure 7). Specifically, a significant negative relationship was observed (Figure 7; Pearson correlation: r = -0.59, p = 0.04), indicating that the highest trophic positions were related with the lowest sea surface temperatures. The isotopic niche metrics estimated for the 12 populations of *C. sapidus* included in the individual-scale dataset are reported in Table 3. None of them was correlated with sample size or trophic position estimations (Table 5); furthermore, total

TABLE 4 Bayesian Information Criterion (BIC) values and Bayes factors (B) estimated by the heuristic procedure implemented for Minimum Adequate Model (MAM) selection for *Callinectes sapidus*. Only the 10 models showing the lowest BIC values are reported. See Table 1 for layer acronyms.

Layers included in the model	BIC	B
biogeo13	−0.1	
biogeo15	3.31	5.5
biogeo14	4.42	9.58
biogeo16	4.94	12.43
biogeo17	4.97	12.62
biogeo13-biogeo15	0.78	1.55
biogeo13-biogeo14	1.84	2.64
biogeo13-biogeo17	2.35	3.4
biogeo13-biogeo16	2.35	3.4
biogeo15-biogeo16	5.56	16.95

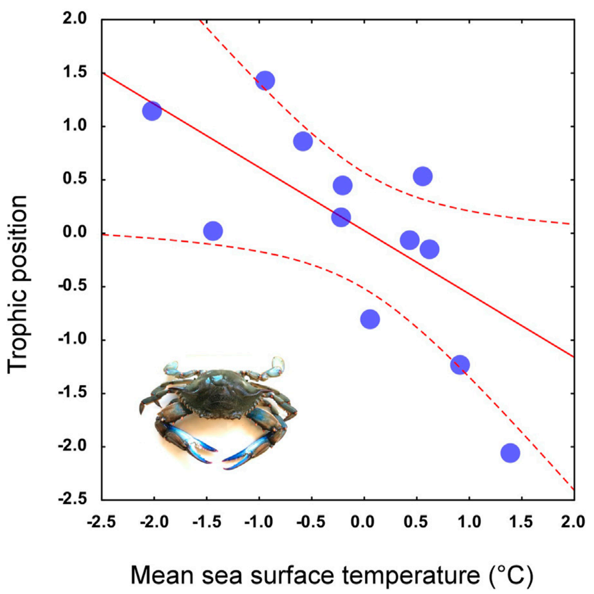

FIGURE 7
Trophic position of *Callinectes sapidus* calculated from the individual-scale dataset as predicted by local annual mean sea surface temperature. For the regression curve (solid line) 95% confidence intervals are included (dashed line). Log-transformed and mean-centered data are used in the scatterplot.

TABLE 5 Correlation matrix (Pearson r coefficient) among sample number (n), trophic position (TP), mean distance to centroid (CD), nitrogen range (NR), carbon range (CR), standard deviation of nearest neighbor distance (SDNND), total area (TA), and corrected standard ellipse area (SEAc) of the 12 *Callinectes sapidus* populations included in the individual-scale dataset. All metrics log-transformed and mean-centered before analysis. Significant correlations with $p < 0.05$ are highlighted in bold.

	TP	CD	NR	CR	SDNND	TA	SEAc
N	0.01	0.07	0.40	0.19	-0.34	0.33	0.04
TP		0.55	0.25	0.49	0.04	0.43	0.51
CD			0.53	**0.94**	0.21	**0.86**	**0.90**
NR				0.42	0.48	**0.84**	**0.78**
CR					0.14	**0.84**	**0.80**
SDNND						0.38	0.46
TA							**0.94**

area (TA), and corrected standard ellipse area (SEAc) estimations resulted highly correlated with each other and with mean distance to centroid (CD), nitrogen range (NR), and carbon range (CR) values. No significant bivariate relationships were observed between isotopic niche metrics and temperature-related MARSPEC predictors (Table 6), even though total area (TA) and corrected standard ellipse area (SEAc) values showed a positive relationship with the sea surface temperature of the warmest ice-free month ($p < 0.09$; Table 5).

4 Discussion

This paper described the procedures employed to collect data and design the workflow at the basis of the validation case focused on the two invasive crustaceans, i.e., *C. sapidus* and *P. clarkii*, and developed within the LifeWatch ERIC Internal Joint Initiative on non-indigenous and invasive species. The functionalities of the workflow have been illustrated by carrying out a preliminary analysis of the data performed both at population- and individual-scale. Independently from the resolution of the datasets, the results revealed the existence of significant relationships between temperature-related variables and the trophic positions of the two invasive crustaceans.

Ultimately, the outcomes showed the ability of the workflow to identify environmental-driven trophic patterns at different spatio-temporal scales by using stable isotope analysis.

The availability of stable isotope information is crucial to investigate drivers of changes in the trophic structure within different ecosystems; however, such studies are often hampered by the availability of stable isotope data. For example, within this case study, an extensive and labour-intensive literature search was performed to gather stable isotope information across a variety of sources. Isotopic data collected by researchers worldwide are currently spread over a variety of sources, including peer-reviewed articles, gray literature, datasets stored in different repositories, or other resources which are not accessible to users (Woo and Scheipl, 2020). The lack of a unique and standardized data repository for stable isotopes hinders the possibility of casting these data into wide, continental or global, spatial contexts and of using them beyond the scope for which they were originally generated (Pauli et al., 2017). Therefore, potential drivers of trophic variations acting at large geographical scales may remain undetected and the possibility of estimating the role of global environmental pressures, such as climate warming, in species trophic habits may be overlooked. It follows that this precious body of information deserves to be properly standardized, managed and disseminated, and made available in the long-term in a stable, reliable, and organized repository. Scientists have long acknowledged the need to build centralized databases for stable isotope data obtained from ecological studies in order to facilitate the integration and re-usability of such data across multiple scientific disciplines (Pauli et al., 2017; Eftimov et al., 2019; Woo et al., 2021). Such a centralized repository of stable isotope data would prevent the time-consuming efforts of data collection from different sources. In

TABLE 6 Correlation matrix (Pearson r coefficient) between MARSPEC temperature-related predictors (see Table 1 for acronyms) and sample number (n), mean distance to centroid (CD), nitrogen range (NR), carbon range (CR), standard deviation of nearest neighbor distance (SDNND), total area (TA), and corrected standard ellipse area (SEAc) of the 12 *Callinectes sapidus* populations included in the individual-scale dataset. All metrics log-transformed and mean-centered before analysis.

	biogeo13	biogeo14	biogeo15	biogeo16	biogeo17
n	−0.20	−0.24	−0.12	0.20	0.23
CD	0.20	0.24	0.46	0.03	0.03
NR	0.27	0.15	0.40	0.08	0.13
CR	0.14	0.13	0.42	0.13	0.13
SDNND	0.40	0.15	0.55	0.16	0.22
TA	0.24	0.13	0.49	0.16	0.20
SEAc	0.29	0.27	0.49	0.01	0.05

addition, it would facilitate data integration, standardization, harmonization, and ensure data interoperability by making each dataset accessible in a both human and machine-readable format through the use of controlled metadata and defined ontologies (Eftimov et al., 2019). In this context, the LifeWatch e-Infrastructure with its distributed nodes and facilities offers suitable features to guarantee the long-term storage of data, metadata, and semantic resources, such as those of the LifeWatch Italy Data Portal (https://dataportal.lifewatchitaly.eu), the LifeWatch ERIC Metadata Catalogue (https://metadatacatalogue.lifewatch.eu), and EcoPortal (http://ecoportal.lifewatch.eu/). The e-Infrastructure provides stable and reliable web-based solutions to share data and analytical tools and to make them findable, accessible, interoperable, and reusable according to the FAIR principles (Wilkinson et al., 2016), and it would, therefore, represent an ideal repository of stable isotope data for both ecological and environmental studies.

The validation of our analytical workflow on the population-scale dataset for *P. clarkii* and on the individual-scale dataset for *C. sapidus* indicated that the collection of geo-referenced stable isotope information on invasive species and on their potential prey can be used to explore ecologically-meaningful relationships between environmental variables and the trophic positions of the invaders and, ultimately, develop scenarios for future trends. The preliminary analytical outcomes presented here are supported by other studies where such associations were also observed. For example, the use of a global meta-analysis of stable isotope data demonstrated that changes in the trophic positions of three tuna species were associated with latitudinal and oxygen gradients (Pethybridge et al., 2018). Using a similar analytical approach, this study revealed that temperature-related variables may be associated with the variations in the trophic positions of *P. clarkii* and *C. sapidus* within invaded aquatic food webs (Figures 6,7). It follows that, independently from ecological constraints related to the structure of the recipient communities in terms of e.g., resource availability, species composition, or local environmental conditions, the trophic role played by an invader within a food web is related with large-scale environmental drivers ultimately influenced by climate change. Specifically, the results of this study indicated that at relatively high temperatures omnivorous invaders occupy higher trophic levels in food webs, whereas at lower temperatures they may shift to lower positions within the trophic network. To provide an in-depth analysis of the factors involved in the observed relationships goes beyond the scope of the present study; however, as it is acknowledged that the whole-body metabolic costs increase with higher external temperatures (Brown et al., 2004; Arim et al., 2007; Bonnaffé et al., 2021), the observed shifts in the trophic positions of *P. clarkii* and *C. sapidus* may be explained by changes in the metabolic responses of the species as a result of their trophic plasticity. How and to what extent the observed trophic shifts affect the ecological impact of omnivorous invasive species on recipient communities is an open question which requires additional investigation. Yet it is likely the variation from omnivorous to primarily carnivorous trophic habits may increase their overall impact as previously suggested (Thomsen et al., 2014; Gallardo et al., 2016; Mollot et al., 2017; Anton et al., 2019; Bradley et al., 2019). The observed relationships between external temperature and trophic position additionally indicate that future changes in the climatic conditions experienced by the two species may affect their trophic positions and, in turn, their impact in invaded food webs. To date, while a considerable effort has been made to evaluate the effects of climate warming on the frequency of introduction and invasiveness of NIS-IAS (Bellard et al., 2018; Ricciardi et al., 2021), less consideration has been given to the study of climatic variations and on their influence on the impact of established invaders. This study clearly shows that aquatic predators and their functional role in food webs may be particularly vulnerable to climate change and that global warming may play a major role in determining future functional characteristics of the species, and, in the case of bioinvaders, their trophic impact on recipient communities and ecosystems.

To provide higher flexibility to the end-users and to expand the current scope of the workflow it would be essential to widen its analytical features by, for instance, adding trophic niche metrics calculation and accounting for all possible combinations of climatic variables that could shape the trophic habits of invasive species. The future implementations will allow for the testing of bioclimatic predictors of trophic positions of different species, native and non-indigenous, in potentially all types of environments, including aquatic and terrestrial. The possibility of querying and extracting environmental variables of all kinds from different repositories, online platforms, and databases, beyond the ones used within the case study, will allow for greater customization by end-users and make the potentiality of this workflow unlimited.

In conclusion, the present work clearly demonstrated how collaboration between scientific and ICT communities for the development of cutting-edge e-tools could greatly facilitate scientists in finding evidence on rapid responses of biodiversity and ecosystems to the most critical issues for conservation and inform environmental managers to take prompt action. The LifeWatch ERIC Internal Joint Initiative on invasive species and the specific case study described herein focuses on evaluating and predicting the trophic geography and, indirectly, trophic-related impacts of large invasive omnivorous crustaceans in invaded food webs. Such types of workflows could be implemented and deployed to address a variety of key questions in ecology including biodiversity and ecosystem responses to climate change or to other anthropogenic pressures acting at global scales.

Data availability statement

The datasets generated and analyzed for this study can be found in the LifeWatch Italy Data Portal (https://dataportal.lifewatchitaly.eu/view/urn%3Auuid%3Ae869c2cc-2011-461d-99cc-8d6d642b1624; https://dataportal.lifewatchitaly.eu/view/urn%3Auuid%3A18a8256c-0e31-4800-af5b-958ea88faf34).

Author contributions

MG conceived and designed the case study and workflow. DMC and MG performed data collection, dataset creation and standardization, data analysis, and writing including the original draft of the manuscript, the final review, and editing. RI and VL contributed to the datasets formatting and quality check, to the workflow development, and to the manuscript final review and editing. AC and BA reviewed the manuscript. DGR contributed to the final editing and revision.

Funding

LifeWatch ERIC Internal Joint Initiative.

Acknowledgments

The Authors thank González-Aranda Juan Miguel, Huguet-Vives Antoni, Minadakis Nikos, and Sáenz-Albanés Antonio José from the LifeWatch ERIC ICT Core for the technical support in the development of the crustaceans workflow.

Conflict of interest

The authors declare that the research was conducted in the absence of any commercial or financial relationships that could be construed as a potential conflict of interest.

Publisher’s note

Supplementary material

The Supplementary Material for this article can be found online at: https://www.frontiersin.org/articles/10.3389/fenvs.2022.1038635/full#supplementary-material

References

Annabi, A., Bardelli, R., Vizzini, S., and Mancinelli, G. (2018). Baseline assessment of heavy metals content and trophic position of the invasive blue swimming crab *Portunus segnis* (Forskål, 1775) in the Gulf of Gabès (Tunisia). *Mar. Pollut. Bull.* 136, 454–463. doi:10.1016/j.marpolbul.2018.09.037

Anton, A., Geraldi, N. R., Lovelock, C. E., Apostolaki, E. T., Bennett, S., Cebrian, J., et al. (2019). Global ecological impacts of marine exotic species. *Nat. Ecol. Evol.* 3 (5), 787–800. doi:10.1038/s41559-019-0851-0

Arim, M., Bozinovic, F., and Marquet, P. A. (2007). On the relationship between trophic position, body mass and temperature: Reformulating the energy limitation hypothesis. *Oikos* 116 (9), 1524–1530. doi:10.1111/j.0030-1299.2007.15768.x

Assis, J., Tyberghein, L., Bosch, S., Verbruggen, H., Serrão, E. A., De Clerck, O., et al. (2018). Bio-ORACLE v2.0: Extending marine data layers for bioclimatic modelling. *Glob. Ecol. Biogeogr.* 27 (3), 277–284. doi:10.1111/geb.12693

Banks, N. C., Paini, D. R., Bayliss, K. L., and Hodda, M. (2015). The role of global trade and transport network topology in the human-mediated dispersal of alien species. *Ecol. Lett.* 18 (2), 188–199. doi:10.1111/ele.12397

Bartley, T. J., Mccann, K. S., Bieg, C., Cazelles, K., Granados, M., Guzzo, M. M., et al. (2019). Food web rewiring in a changing world. *Nat. Ecol. Evol.* 3 (3), 345–354. doi:10.1038/s41559-018-0772-3

Basset, A., and Los, W. (2012). Biodiversity e-science: LifeWatch, the European infrastructure on biodiversity and ecosystem research. *Plant Biosyst. Int. J. Deal. all Aspects Plant Biol.* 146 (4), 780–782. doi:10.1080/11263504.2012.740091

Bellard, C., Jeschke, J. M., Leroy, B., and Mace, G. M. (2018). Insights from modeling studies on how climate change affects invasive alien species geography. *Ecol. Evol.* 8 (11), 5688–5700. doi:10.1002/ece3.4098

Bingham, H. C., Doudin, M., Weatherdon, L. V., Despot-Belmonte, K., Wetzel, F. T., Groom, Q., et al. (2017). The biodiversity informatics landscape: Elements, connections and opportunities. *Res. Ideas Outcomes* 3, e14059. doi:10.3897/rio.3.e14059

Bonnaffé, W., Danet, A., Legendre, S., and Edeline, E. (2021). Comparison of size-structured and species-level trophic networks reveals antagonistic effects of temperature on vertical trophic diversity at the population and species level. *Oikos* 130 (8), 1297–1309. doi:10.1111/oik.08173

Bosch, S., Tyberghein, L., De Clerck, O., Fernandez, S., and Schepers, L. (2022). sdmpredictors: Species distribution modelling predictor datasets. Avaliable at: http://cran.r-project.org/web/packages/sdmpredictors.

Bradley, B. A., Laginhas, B. B., Whitlock, R., Allen, J. M., Bates, A. E., Bernatchez, G., et al. (2019). Disentangling the abundance–impact relationship for invasive species. *Proc. Natl. Acad. Sci. U. S. A.* 116 (20), 9919–9924. doi:10.1073/pnas.1818081116

Brown, J. H., Gillooly, J. F., Allen, A. P., Savage, V. M., and West, G. B. (2004). Toward a metabolic theory of ecology. *Ecology* 85 (7), 1771–1789. doi:10.1890/03-9000

Burnham, K. P., and Anderson, D. R. (2002). *Model selection and multi-model inference: A practical information-theoretic approach*. New York, NY: Springer.

Candela, L., Castelli, D., and Pagano, P. (2013). Virtual research environments: An overview and a research agenda. *Data Sci. J.* 12, GRDI75–GRDI81. doi:10.2481/dsj.grdi-013

Cardeccia, A., Marchini, A., Occhipinti-Ambrogi, A., Galil, B., Gollasch, S., Minchin, D., et al. (2018). Assessing biological invasions in European seas: Biological traits of the most widespread non-indigenous species. *Estuar. Coast. Shelf Sci.* 201, 17–28. doi:10.1016/j.ecss.2016.02.014

Carrete Vega, G., Pertierra, L. R., and Olalla-Tárraga, M. Á. (2017). MERRAclim, a high-resolution global dataset of remotely sensed bioclimatic variables for ecological modelling. *Sci. Data* 4 (1), 170078. doi:10.1038/sdata.2017.78

Carrozzo, L., Potenza, L., Carlino, P., Costantini, M. L., Rossi, L., and Mancinelli, G. (2014). Seasonal abundance and trophic position of the Atlantic blue crab *Callinectes sapidus* Rathbun 1896 in a Mediterranean coastal habitat. *Rend. Fis. Acc. Lincei* 25 (2), 201–208. doi:10.1007/s12210-014-0297-x

Clavero, M., Franch, N., Bernardo-Madrid, R., López, V., Abelló, P., Queral, J. M., et al. (2022). Severe, rapid and widespread impacts of an Atlantic blue crab invasion. *Mar. Pollut. Bull.* 176, 113479. doi:10.1016/j.marpolbul.2022.113479

Corrales, X., Katsanevakis, S., Coll, M., Heymans, J. J., Piroddi, C., Ofir, E., et al. (2020). Advances and challenges in modelling the impacts of invasive alien species on aquatic ecosystems. *Biol. Invasions* 22 (3), 907–934. doi:10.1007/s10530-019-02160-0

Courchamp, F., Fournier, A., Bellard, C., Bertelsmeier, C., Bonnaud, E., Jeschke, J. M., et al. (2017). Invasion biology: Specific problems and possible solutions. *Trends Ecol. Evol.* 32 (1), 13–22. doi:10.1016/j.tree.2016.11.001

De Giorgi, R., Cilenti, L., Falco, S., Katselis, G., Kevrekidis, K., Papadia, P., et al. (2022). Trace metals in five Mediterranean populations of the invasive Atlantic blue crab *Callinectes sapidus*: do variations in trophic position matter? Manuscript in preparation.

Di Muri, C., Alcorlo, P., Bardelli, R., Catalan, J., Gacia, E., Guerra, M. T., et al. (2022a). Individual and population-scale carbon and nitrogen isotopic signatures of *Procambarus clarkii* in invaded freshwater ecosystems. *Biodivers. Data J.* 10, e94411. doi:10.3897/bdj.10.e94411

Di Muri, C., Rosati, I., Bardelli, R., Cilenti, L., Veli, D. L., Falco, S., et al. (2022b). An individual-based dataset of carbon and nitrogen isotopic data of *Callinectes sapidus* in invaded Mediterranean waters. *Biodivers. Data J.* 10, e77516. doi:10.3897/bdj.10.e77516

Eftimov, T., Ispirova, G., Potočnik, G., Ogrinc, N., and Koroušić Seljak, B. (2019). ISO-FOOD ontology: A formal representation of the knowledge within the domain of isotopes for food science. *Food Chemistry* 277, 382–390.

Enke, N., Thessen, A., Bach, K., Bendix, J., Seeger, B., and Gemeinholzer, B. (2012). The user's view on biodiversity data sharing - investigating facts of acceptance and requirements to realize a sustainable use of research data -. *Ecol. Inf.* 11, 25–33. doi:10.1016/j.ecoinf.2012.03.004

Escribano, N., Galicia, D., and Ariño, A. H. (2018). The tragedy of the biodiversity data commons: A data impediment creeping nigher? *Database.* 2018, bay033. doi:10.1093/database/bay033

Essl, F., Lenzner, B., Bacher, S., Bailey, S., Capinha, C., Daehler, C., et al. (2020). Drivers of future alien species impacts: An expert-based assessment. *Glob. Chang. Biol.* 26 (9), 4880–4893. doi:10.1111/gcb.15199

European Commission (2014). Regulation (EU) No 1143/2014 of the European Parliament and of the Council of 22 October 2014 on the prevention and management of the introduction and spread of invasive alien species. *Official J. Eur. Union* 317, 35–55. Available at: https://eur-lex.europa.eu/legal-content/EN/TXT/PDF/?uri=CELEX:32014R1143andrid=5

European Commission (2020). "Communication from the commission to the European parliament, the Council, the economic and social committee and the committee of the regions," in *EU Biodiversity Strategy for 2030 - bringing nature back into our lives* (Brussels: Publication Office of the European Union). Avaliable at: http://eur-lex.europa.eu/LexUriServ/LexUriServ.do?uri=CELEX:52012DC0673:EN:NOT.

European Commission (2008). *Towards an EU strategy on invasive species*. Brussels: European Commission.

Fick, S. E., and Hijmans, R. J. (2017). WorldClim 2: New 1-km spatial resolution climate surfaces for global land areas. *Int. J. Climatol.* 37 (12), 4302–4315. doi:10.1002/joc.5086

Fox, J., and Weisberg, H. S. (2011). *An R companion to applied regression*. Second Edition. Thousand Oaks, CA: Sage Publications, Inc.

Gallardo, B., Clavero, M., Sánchez, M. I., and Vilà, M. (2016). Global ecological impacts of invasive species in aquatic ecosystems. *Glob. Chang. Biol.* 22 (1), 151–163. doi:10.1111/gcb.13004

Gautam, M. K., and Lee, K. S. (2016). Application of stable isotopes in ecosystem research. *Curr. Sci.* 110 (7), 1288–1306. Available at: https://www.jstor.org/stable/24908018

Hänfling, B., Edwards, F., and Gherardi, F. (2011). Invasive alien Crustacea: Dispersal, establishment, impact and control. *BioControl* 56 (4), 573–595. doi:10.1007/s10526-011-9380-8

Havel, J. E., Kovalenko, K. E., Thomaz, S. M., Amalfitano, S., and Kats, L. B. (2015). Aquatic invasive species: Challenges for the future. *Hydrobiologia* 750 (1), 147–170. doi:10.1007/s10750-014-2166-0

Hegyi, G., and Garamszegi, L. (2011). Using information theory as a substitute for stepwise regression in ecology and behavior. *Behav. Ecol. Sociobiol.* 65 (1), 69–76. doi:10.1007/s00265-010-1036-7

Henry, A. K., and Sorte, C. J. B. (2022). Impact assessment of coastal marine range shifts to support proactive management. *Front. Ecol. Environ.* 20 (3), 161–169. doi:10.1002/fee.2447

Hobbs, H., Jass, J. P., and Huner, J. V. (1989). A review of global crayfish introductions with particular emphasis on two North American species (Decapoda, Cambaridae). *Crustaceana* 56 (3), 299–316. doi:10.1163/156854089x00275

Hofkin, B. V., Koech, D. K., Oumaj, J., and Loker, E. S. (1991). The North American crayfish *Procambarus clarkii* and the biological control of schistosome-transmitting snails in Kenya: Laboratory and field investigations. *Biol. Control* 1 (3), 183–187. doi:10.1016/1049-9644(91)90065-8

Jackson, A. L., Inger, R., Parnell, A. C., and Bearhop, S. (2011). Comparing isotopic niche widths among and within communities: SIBER – stable isotope bayesian ellipses in R. *J. Animal Ecol.* 80 (3), 595–602. doi:10.1111/j.1365-2656.2011.01806.x

Jackson, A. L., and Parnell, A. C. (2021). Siber: Stable isotope bayesian ellipses in R. R package version 2.1.6. Avaliable at: http://cran.r-project.org/web/packages/SIBER.

Katsanevakis, S., and Moustakas, A. (2018). Uncertainty in marine invasion science. *Front. Mar. Sci.* 5, 38. doi:10.3389/fmars.2018.00038

Katsanevakis, S., Wallentinus, I., Zenetos, A., Leppäkoski, E., Çinar, M. E., Oztürk, B., et al. (2014). Impacts of invasive alien marine species on ecosystem services and biodiversity: A pan-European review. *Aquat. Invasions* 9 (4), 391–423. doi:10.3391/ai.2014.9.4.01

Layman, C. A., Arrington, D. A., Montaña, C. G., and Post, D. M. (2007). Can stable isotope ratios provide for community-wide measures of trophic structure? *Ecology* 88, 42–48. doi:10.1890/0012-9658(2007)88[42:csirpf]2.0.co;2

Loureiro, T. G., Anastácio, P. M. S. G., Araujo, P. B., Souty-Grosset, C., and Almerão, M. P. (2015). Red swamp crayfish: Biology, ecology and invasion - an overview. *Nauplius* 23, 1–19. doi:10.1590/s0104-64972014002214

Mancinelli, G., Bardelli, R., and Zenetos, A. (2021). A global occurrence database of the Atlantic blue crab *Callinectes sapidus*. *Sci. Data* 8 (111), 111–210. doi:10.1038/s41597-021-00888-w

Mancinelli, G., Chainho, P., Cilenti, L., Falco, S., Kapiris, K., Katselis, G., et al. (2017a). The atlantic blue crab *Callinectes sapidus* in southern European coastal waters: Distribution, impact and prospective invasion management strategies. *Mar. Pollut. Bull.* 119 (1), 5–11. doi:10.1016/j.marpolbul.2017.02.050

Mancinelli, G., and Di Muri, C. (2022a). An individual-based dataset of carbon and nitrogen isotopic data of *Callinectes sapidus* in invaded Mediterranean waters [Data set]. *LifeWatch ERIC.* doi:10.48372/9CD2907F-8F44-4DF6-9070-6B21E1991B94

Mancinelli, G., and Di Muri, C. (2022b). Individual and population-scale carbon and nitrogen isotopic signatures of *Procambarus clarkii* in invaded freshwater ecosystems. *LifeWatch ERIC.* doi:10.48372/D25219D3-FE11-4052-879A-EB2E15CA295C

Mancinelli, G., Guerra, M. T., Alujević, K., Raho, D., Zotti, M., and Vizzini, S. (2017b). Trophic flexibility of the atlantic blue crab *Callinectes sapidus* in invaded coastal systems of the apulia region (SE Italy): A stable isotope analysis. Estuarine. *Coast. Shelf Sci.* 198, 421–431. doi:10.1016/j.ecss.2017.03.013

Mancinelli, G. (2012). On the trophic ecology of gammaridea (Crustacea: Amphipoda) in coastal waters: A European-scale analysis of stable isotopes data. *Estuar. Coast. Shelf Sci.* 114, 130–139. doi:10.1016/j.ecss.2011.12.003

Mancinelli, G., and Vizzini, S. (2015). Assessing anthropogenic pressures on coastal marine ecosystems using stable CNS isotopes: State of the art, knowledge gaps, and community-scale perspectives. *Estuar. Coast. Shelf Sci.* 156, 195–204. doi:10.1016/j.ecss.2014.11.030

Mancini, F., De Giorgi, R., Ludovisi, A., Vizzini, S., and Mancinelli, G. (2021). Ontogenetic shift in the trophic role of the invasive killer shrimp *Dikerogammarus villosus*: A stable isotope study. *Biol. Invasions* 23, 1803–1817. doi:10.1007/s10530-021-02472-0

Mancini, F., Lillo, A. O., Bardelli, R., Vizzini, S., and Mancinelli, G. (2022). Variation in the stable isotope trophic position of the bluefish *Pomatomus saltatrix* (linnaeus, 1766) from two mediterranean sites: Insights from a global meta-analysis. *Mediterr. Mar. Sci.* 23, 850–863. doi:10.12681/mms.29325

Médoc, V., Thuillier, L., and Spataro, T. (2018). Opportunistic omnivory impairs our ability to predict invasive species impacts from functional response comparisons. *Biol. Invasions* 20 (5), 1307–1319. doi:10.1007/s10530-017-1628-5

Millikin, M. R., and Williams, A. B. (1984). Synopsis of biological data on blue crab, *Callinectes sapidus* Rathbun. *FAO Fish. Synop.* 38, 138.

Mollot, G., Pantel, J. H., and Romanuk, T. N. (2017). The effects of invasive species on the decline in species richness: A global meta-analysis. *Adv. Ecol. Res.* 56, 61–83.

Neath, A. A., and Cavanaugh, J. E. (2012). The bayesian information criterion: Background, derivation, and applications. *WIREs Comp. Stat.* 4 (2), 199–203. doi:10.1002/wics.199

Nehring, S. (2011). *In the wrong place - alien marine Crustaceans: Distribution, biology and impacts.* Netherlands: Springer, 607–624.

Oficialdegui, F. J., Clavero, M., Sánchez, M. I., Green, A. J., Boyero, L., Michot, T. C., et al. (2019). Unravelling the global invasion routes of a worldwide invader, the red swamp crayfish (*Procambarus clarkii*). *Freshw. Biol.* 64 (8), 1382–1400. doi:10.1111/fwb.13312

Pauli, J. N., Newsome, S. D., Cook, J. A., Harrod, C., Steffan, S. A., Baker, C. J. O., et al. (2017). Opinion: Why we need a centralized repository for isotopic data. Proceedings of the National Academy of Sciences 114 (12), 2997–3001.

Pethybridge, H., Choy, C. A., Logan, J. M., Allain, V., Lorrain, A., Bodin, N., et al. (2018). A global meta-analysis of marine predator nitrogen stable isotopes: Relationships between trophic structure and environmental conditions. *Glob. Ecol. Biogeogr.* 27 (9), 1043–1055. doi:10.1111/geb.12763

Piccolroaz, S., Healey, N. C., Lenters, J. D., Schladow, S. G., Hook, S. J., Sahoo, G. B., et al. (2018). On the predictability of lake surface temperature using air temperature in a changing climate: A case study for lake tahoe (USA). *Limnol. Oceanogr.* 63 (1), 243–261. doi:10.1002/lno.10626

Quezada-Romegialli, C., Jackson, A. L., and Harrod, C. (2019). tRophicPosition: Bayesian trophic position calculation with stable isotopes. Avaliable at: http://cran.r-project.org/web/packages/tRophicPosition.

Quezada-Romegialli, C., Jackson, A. L., Hayden, B., Kahilainen, K. K., Lopes, C., and Harrod, C. (2018). tRophicPosition, an r package for the Bayesian estimation of trophic position from consumer stable isotope ratios. *Methods Ecol. Evol.* 9, 1592–1599. doi:10.1111/2041-210x.13009

R Development Core Team (2022). *R: A language and environment for statistical computing.* Vienna, Austria: R Foundation for Statistical Computing. Avaliable at: http://www.R-project.org/.

Rabitsch, W., Kudrnovsky, H., Roy, H., Beckmann, B., Peyton, J., Purse, B., et al. (2022). Study on invasive alien species development of risk assessments to tackle priority species and enhance prevention : Final report (and annexes). [Technical Report] European Commission: European Commission.

Ricciardi, A., Iacarella, J. C., Aldridge, D. C., Blackburn, T. M., Carlton, J. T., Catford, J. A., et al. (2021). Four priority areas to advance invasion science in the face of rapid environmental change. *Environ. Rev.* 29 (2), 119–141. doi:10.1139/er-2020-0088

Romanuk, T. N., Zhou, Y., Brose, U., Berlow, E. L., Williams, R. J., and Martinez, N. D. (2009). Predicting invasion success in complex ecological networks. *Phil. Trans. R. Soc. B* 364 (1524), 1743–1754. doi:10.1098/rstb.2008.0286

Russell, J. C., and Blackburn, T. M. (2017). Invasive alien species: Denialism, disagreement, definitions, and dialogue. *Trends Ecol. Evol.* 32 (5), 312–314. doi:10.1016/j.tree.2017.02.005

Sbrocco, E. J., and Barber, P. H. (2013). Marspec: Ocean climate layers for marine spatial ecology. *Ecology* 94 (4), 979. doi:10.1890/12-1358.1

Schwarz, G. (1978). Estimating the dimension of a model. *Ann. Stat.* 6 (2), 461–464. doi:10.1214/aos/1176344136

Souty-Grosset, C., Anastácio, P. M., Aquiloni, L., Banha, F., Choquer, J., Chucholl, C., et al. (2016). The red swamp crayfish *Procambarus clarkii* in Europe: Impacts on aquatic ecosystems and human well-being. *Limnologica* 58, 78–93. doi:10.1016/j.limno.2016.03.003

Stephenson, P. J., and Stengel, C. (2020). An inventory of biodiversity data sources for conservation monitoring. *PLOS ONE* 15 (12), e0242923. doi:10.1371/journal.pone.0242923

Streftaris, N., and Zenetos, A. (2006). Alien marine species in the Mediterranean - the 100 'Worst Invasives' and their impact. *Mediterr. Mar. Sci.* 7 (1), 87–117. doi:10.12681/mms.180

Sulieman, Y., Pengsakul, T. T., Guo, Y., Huang, S. Q., and Peng, W. X. (2013). Laboratory and semi-field evaluation on the biological control of *Oncomelania hupensis* snail (Gastropoda: Pomatiopsidae), the intermediate host of *Schistosoma japonicum*, using *Procambarus clarkii* crayfish (Crustacea: Cambaridae). *Egypt. J. Biol. Pest Control* 23 (2), 215–220.

Thomsen, M. S., Byers, J. E., Schiel, D. R., Bruno, J. F., Olden, J. D., Wernberg, T., et al. (2014). Impacts of marine invaders on biodiversity depend on trophic position and functional similarity. *Mar. Ecol. Prog. Ser.* 495, 39–47. doi:10.3354/meps10566

Torchin, M. E., Freestone, A. L., Mccann, L., Larson, K., Schlöder, C., Steves, B. P., et al. (2021). Asymmetry of marine invasions across tropical oceans. *Ecology* 102 (8), e03434. doi:10.1002/ecy.3434

Tsirintanis, K., Azzurro, E., Crocetta, F., Dimiza, M., Froglia, C., Gerovasileiou, V., et al. (2022). Bioinvasion impacts on biodiversity, ecosystem services, and human health in the Mediterranean Sea. *Aquat. Invasions* 17, 308–352. doi:10.3391/ai.2022.17.3.01

Twardochleb, L. A., Olden, J. D., and Larson, E. R. (2013). A global meta-analysis of the ecological impacts of nonnative crayfish. *Freshw. Sci.* 32 (4), 1367–1382. doi:10.1899/12-203.1

Tyberghein, L., Verbruggen, H., Pauly, K., Troupin, C., Mineur, F., and De Clerck, O. (2012). Bio-ORACLE: A global environmental dataset for marine species distribution modelling. *Glob. Ecol. Biogeogr.* 21 (2), 272–281. doi:10.1111/j.1466-8238.2011.00656.x

UNEP (1992). Convention on biological diversity. Nairobi: Avaliable at: https://digitallibrary.un.org/record/223428?ln=en.

Vaira, L., Fiore, N., and Rosati, I. (2022). LifeWatch ERIC Application Profiles (Version 1). *LifeWatch ERIC.* doi:10.48372/8528-9Z45

Vander Zanden, M. J., Cabana, G., and Rasmussen, J. B. (1997). Comparing trophic position of freshwater fish calculated using stable nitrogen isotope ratios (15N) and literature dietary data. *Can. J. Fish. Aquat. Sci.* 54 (5), 1142–1158. doi:10.1139/f97-016

Vanderklift, M., and Ponsard, S. (2003). Sources of variation in consumer-diet δ^{15}N enrichment: A meta-analysis. *Oecologia* 136 (2), 169–182. doi:10.1007/s00442-003-1270-z

Vazquez, D. P. (2006). *Conceptual ecology and invasion biology: Reciprocal approaches to nature*. Dordrecht: Springer Netherlands, 307–322.

Wallingford, P. D., Morelli, T. L., Allen, J. M., Beaury, E. M., Blumenthal, D. M., Bradley, B. A., et al. (2020). Adjusting the lens of invasion biology to focus on the impacts of climate-driven range shifts. *Nat. Clim. Chang.* 10 (5), 398–405. doi:10.1038/s41558-020-0768-2

Watkins, H. V., Yan, H. F., Dunic, J. C., and Côté, I. M. (2021). Research biases create overrepresented "poster children" of marine invasion ecology. *Conserv. Lett.* 14 (3), e12802. doi:10.1111/conl.12802

Whittingham, M. J., Stephens, P. A., Bradbury, R. B., and Freckleton, R. P. (2006). Why do we still use stepwise modelling in ecology and behaviour? *J. Animal Ecol.* 75 (5), 1182–1189. doi:10.1111/j.1365-2656.2006.01141.x

Wilkinson, M. D., Dumontier, M., Aalbersberg, I. J., Appleton, G., Axton, M., Baak, A., et al. (2016). The FAIR Guiding Principles for scientific data management and stewardship. *Sci. Data* 3 (1), 160018. doi:10.1038/sdata.2016.18

Woo, J., Zhao, L., and Bowen, G. J. (2021). Streamlining geospatial data processing for isotopic landscape modeling. *Concurrency and Computation: Practice and Experience* 33 (19), e6324.

Wood, S. N. (2017). *Generalized additive models: An introduction with R*. Boca Raton, FL: Chapman and Hall/CRC Press.

Wood, S., and Scheipl, F. (2020). gamm4: Generalized Additive Mixed Models using 'mgcv' and 'lme4'. R package. Avaliable at: http://cran.r-project.org/web/packages/gamm4.

frontiers | Frontiers in Environmental Science

TYPE Original Research
PUBLISHED 04 January 2023
DOI 10.3389/fenvs.2022.1058515

High-frequency monitoring through *in-situ* fluorometric sensors: A supporting tool to long-term ecological research on lakes

Michela Rogora[1]*, Tommaso Cancellario[1], Rossana Caroni[1], Lyudmila Kamburska[1], Dario Manca[1], Simona Musazzi[1], Rocco Tiberti[2] and Andrea Lami[1]

[1]National Research Council, Water Research Institute (CNR IRSA), Verbania Pallanza, Italy, [2]Department of Earth and Environmental Sciences DSTA, University of Pavia, Pavia, Italy

Lake Maggiore is a site of the Long-Term Ecosystem Research (LTER) network, belonging to the deep subalpine Lake District in Northern Italy. Studies on the physical, chemical, and biological features of the lake have been performed continuously since the 1980s. The lake recovered from eutrophication reaching the present oligotrophic condition. In the last decade, climate change represents the main driving factor for the long-term evolution of the lake, affecting its hydrodynamics, nutrient status, and biological communities. In 2020 a high-frequency monitoring (HFM) system was deployed, with the aim to integrate long-term monitoring based on discrete sampling and analysis. The system consists of a buoy equipped with sensors for limnological variables and algal pigments. The high-frequency monitoring program is part of a cross-border project between Italy and Switzerland focusing on lake quality monitoring as a critical input for successful lake management. In this paper we focus on Chlorophyll-*a* data, with the aim to test whether *in-situ* fluorescence measurements may provide a reliable estimate of lake phytoplankton biovolume and its seasonal dynamic. Sensor's performance was regularly tested comparing chlorophyll-*a* data taken by the *in-situ* fluorescent sensors (Cyclops7, Turner Design), data from laboratory fluorescence analysis (FluoroProbe, BBE Moldaenke), values obtained from chlorophyll-*a* analysis by UV-VIS spectrophotometry and data from phytoplankton microscopy analysis. We found a general good agreement between the Chlorophyll-*a* data obtained with the different methods, confirming the use of *in-situ* sensors as a reliable approach to measure algal pigments, especially to assess their variability in the short-term, but also to describe the seasonal pattern of phytoplankton biovolume. However, phytoplankton community composition played a substantial role in the performance of the different methods and in the reliability of *in-situ* data as a tool to assess algal biovolume. This study demonstrates that high-frequency monitoring (HFM), used in conjunction with discrete chemical and biological monitoring, represents an important advance and support in the long-term monitoring of freshwaters and is a useful tool to detect ecological changes.

EDITED BY
Robert Ptacnik,
Wasser Cluster Lunz, Austria

REVIEWED BY
Arda Özen,
Cankiri Karatekin University, Turkey
Joaquim I. Goes,
Columbia University, United States

*CORRESPONDENCE
Michela Rogora,
michela.rogora@cnr.it

SPECIALTY SECTION
This article was submitted to Freshwater Science,
a section of the journal
Frontiers in Environmental Science

RECEIVED 30 September 2022
ACCEPTED 01 December 2022
PUBLISHED 04 January 2023

CITATION
Rogora M, Cancellario T, Caroni R, Kamburska L, Manca D, Musazzi S, Tiberti R and Lami A (2023), High-frequency monitoring through *in-situ* fluorometric sensors: A supporting tool to long-term ecological research on lakes.
Front. Environ. Sci. 10:1058515.
doi: 10.3389/fenvs.2022.1058515

Regular checking and validation of the sensor readings through laboratory analyses are important to get trustworthy data.

KEYWORDS

chlorophyll, fluorimetry, high frequency monitoring, LTER, phytoplankton

1 Introduction

Monitoring the surface water quality is compulsory for the current environmental policies under the EU Water Framework Directive (WFD, 2000/60/EC) (European Commission, 2000). This directive commits EU member countries to achieve good qualitative status for their water bodies and prevent further deterioration. The first step to reaching these ambitious goals is to assess the ecological status of aquatic environments through monitoring and assigning them to specific quality classes. This is central to the operation of the WFD, though the monitoring itself also has other objectives such as increasing system understanding and designing mitigation options (Skeffington et al., 2015).

Traditionally, freshwater monitoring involves fieldwork for sample collection and subsequent laboratory work. Samples are collected manually from selected waterbody stations and depth at scheduled intervals throughout the year. The amount of manual work required makes these methods costly and time-consuming. Moreover, because of the low sampling frequency, this approach often fails to capture the dynamics of biotic and abiotic processes within freshwater ecosystems. Despite the usefulness of traditional monitoring programs, the discrete nature of sampling means it is vital to fill the knowledge gaps related to short-lived, extremely episodic, or unpredictable events, and in general to any process with a characteristic temporal scale shorter than the sampling frequency (Jennings et al., 2012; Meinson et al., 2016).

The WFD requires the classification of the ecological status of surface waters in an integrative way, by using multiple taxonomic groups (biological quality elements, BQEs) together with supporting physico-chemical and hydro-morphological variables (Caroni et al., 2013). For lake monitoring, phytoplankton is one of the required BQEs to be assessed. Phytoplankton biomass is widely used as an indicator of the status assessment of surface waters (Salmaso et al., 2006; Boyer et al., 2009). Microscopy identification and enumeration of phytoplankton performed in the laboratory are essential to provide reliable data for assessing the ecological state of lakes. However, phytoplankton microscopy analysis is a time-consuming method, requiring specialized scientific personnel to determine taxonomy and to make biomass calculations of phytoplankton communities in lakes.

Chlorophyll-*a* (hereinafter Chl-*a*) concentration is often used as a proxy for phytoplankton biomass (Vörös, and Padisák, 1991; Kasprzak et al., 2008). It represents one of the key indicators of water quality for lakes, in particular concerning eutrophication-related problems (e.g., deterioration of water quality, development of algal blooms). Chl-*a* is traditionally quantified in the laboratory from water samples using ethanol or acetone extraction followed by spectrophotometric measurement (Lorenzen, 1967; ISO 10260, 1992). Although it is nowadays a well-established technique, Chl-*a* extraction protocols may have some shortcomings as they require the manual collection of large water sample volumes, sample transportation, and laboratory personnel to perform extraction and spectrophotometric analyses.

A global increase in the frequency, intensity, and duration of cyanobacterial blooms is raising concerns as many bloom-forming species produce harmful compounds that pose a risk to human and animal health (Taranu et al., 2015; Harke et al., 2016). To evaluate the threat posed by cyanobacteria bloom formations and to assist in the understanding of bloom dynamics, the biomass of cyanobacteria is required to be quantified. The identification of taxa and estimation of the abundance of cyanobacteria, as well as of pigment and cyanotoxin concentrations, are important tasks given the increase in the frequency, intensity, and duration of cyanobacterial blooms that are raising concerns worldwide. However, laboratory determination procedures for the quantification of cyanobacterial pigments, such as phycocyanin, are labour-intensive and time-consuming (Sarada et al., 1999; Randolph et al., 2008).

Laboratory analysis to assess phytoplankton biomass and algal pigments have been extensively used in long-term monitoring programs of lakes and the time series produced have contributed to extended datasets and synoptic studies across different ecosystems (e.g., Salmaso et al., 2003; Morabito et al., 2018a; Stockwell et al., 2020). However, both phytoplankton microscopy analysis and Chl-*a* determination in the laboratory do not allow the monitoring of lake productivity and phytoplankton variations in real time or at high frequency: these methods are indeed not able to detect accurately phytoplankton successions and bloom formation with a sufficient temporal resolution. In particular, the short-lived nature of cyanobacterial blooms makes traditional laboratory methods difficult to be used for their early detection and monitoring (Hunter et al., 2009; Stumpf et al., 2012; Bertone et al., 2018).

The limited spatial and temporal coverage of discrete monitoring methods prompted the development of alternative and complementary monitoring techniques. As regards algal pigment, during the last 2 decades, field fluorometers for *in-situ* measurement have become increasingly common worldwide (Marcé et al., 2016; Meinson et al., 2016). Fluorometric quantification of Chl-*a* and other common algal pigments such as phycocyanin and phycoerythrin is generally cost-effective and allows frequent observations during sudden phenomena such as mixing events or short-lived algal blooms (Jennings et al., 2012; Klug et al., 2012). These sensors have been incorporated into *in-situ* monitoring systems across the globe (McQuaid et al., 2011; Hamilton et al., 2014; Hodges et al., 2018), showing potential for assessment of phytoplankton biomass spatially and temporally.

Lake Maggiore is a deep oligomictic lake belonging to the "IT-08 Southern Alpine Lake" LTER site. The lake has been studied for its physical, chemical, and biological aspects since the 1980s. It recovered from eutrophication thanks to the reduction of catchment loads and reached a stable oligotrophic status by the end of the 1990s. Nowadays, dissolved oxygen and nutrient dynamics are mainly driven by in-lake processes, in particular, the stratification and mixing regime, which in turn are affected by climate change (Rogora et al., 2018, Rogora et al., 2021). Water temperature increased, at different rates according to depth and season, causing increased stability of the water column and a decreasing frequency of deep mixing events, the last full turnover having occurred in 2006 (Fenocchi et al., 2018). As an effect, oxygen is steadily decreasing and phosphorus, nitrate, and silica are accumulating in the deep layers, with limited replenishment of the trophogenic layers (Rogora et al., 2021). These changes are affecting phytoplankton composition and seasonal succession (Morabito et al., 2012; Tanentzap et al., 2020), with a slightly increasing trend of Chl-*a* concentrations and the evidence of short-lived phytoplankton blooms triggered by heavy precipitation events (Morabito et al., 2018b).

To integrate the discrete monitoring of the lake, in particular, to get information on short-term lake dynamics, an HFM of Lake Maggiore was started in 2020 within the cross-border cooperation project SIMILE (Italian acronym for "Integrated monitoring system for knowledge, protection, and valorization of the subalpine lakes and their ecosystems"). Its general objectives are the improvement/optimization of the monitoring of the deep subalpine lakes (Lugano, Maggiore, and Como) in the so-called "Insubric" region of Northern Italy and the strengthening of the coordinated management of water through an intensification of stakeholders' participation in the processes of knowledge gain and monitoring of the water resource. The first aim of SIMILE is the testing and developing of an innovative monitoring approach, integrating satellite data, *in-situ* high-frequency sensor data, and user-contributed georeferenced data (Brovelli et al., 2019).

Within the SIMILE project, an assessment of the high-frequency data quality was started, with a focus on algal pigment data. This paper presents a comparison of the *in-situ* high-frequency measurements of Chl-*a* provided by the sensors with those obtained from laboratory analysis on water samples collected in 2020–21. We also measured phytoplankton abundance and composition in each sample by microscopy analysis. Finally, we aimed to critically discuss HFM as a complementary approach to the discrete monitoring of lakes, highlighting both its strong points and major drawbacks, focusing on the contribution that HFM may provide in long-term ecological research.

2 Methods

2.1 Study site

Lake Maggiore is the second deepest (370 m) and largest (212.5 km^2) lake in Italy. It belongs to the subalpine lake district, and together with lakes Lugano, Como, Garda, and Iseo, it contributes to almost 80% of the total volume of freshwater in Italy. These lakes altogether are an invaluable water resource for several uses including hydroelectric power production, potabilization, irrigation, as well as they are key elements for the tourist economy of the Alpine region (Salmaso et al., 2020). Lake Maggiore is oligotrophic by nature; a eutrophication process started in the 1960s, when nutrient concentration, mainly phosphorus, started to rise, followed by an increase in phytoplankton abundance, biovolume, and primary production. After reaching a eutrophic state in the late 1970s-early 1980s, a recovery process started, thanks to the reduction of catchment loads and the lake gradually returned to an oligotrophic condition, with total phosphorus concentrations around 10 μg P L^{-1} (Ruggiu et al., 1998; Morabito et al., 2012). Since the late 1980s, changes in phytoplankton species diversity and composition appeared, with a decrease in average cell size, Chl-*a*, and total biovolume, as well as of annual primary production (Ruggiu et al., 1998).

Lake Maggiore watershed (about 6,600 km^2) is shared almost equally between Italy and Switzerland, so issues related to the lake water quality and its restoration and management have been afforded through cooperation between the two countries. In particular, lake monitoring has been performed monthly since the 1980s at the deepest point (Ghiffa station), within the limnological campaigns funded by the International Commission for the Protection of Italian-Swiss Waters (CIPAIS; www.cipais.org). The monitoring covered several physical, chemical, and biological variables, and these long-term data series allowed us to evaluate the lake trophic evolution i.e., oligotrophication, as well as its response to climate drivers (Tanentzap et al., 2020; Rogora et al., 2021). However, until recently, only discrete data, based on regular field campaigns, have been collected, except for meteo-hydrological data for which high-frequency monitoring stations have been established in the lake watershed (Ciampittiello et al., 2021).

As regards phytoplankton, integrated samples (0–20 m) have been regularly collected and analyzed by microscopy to identify

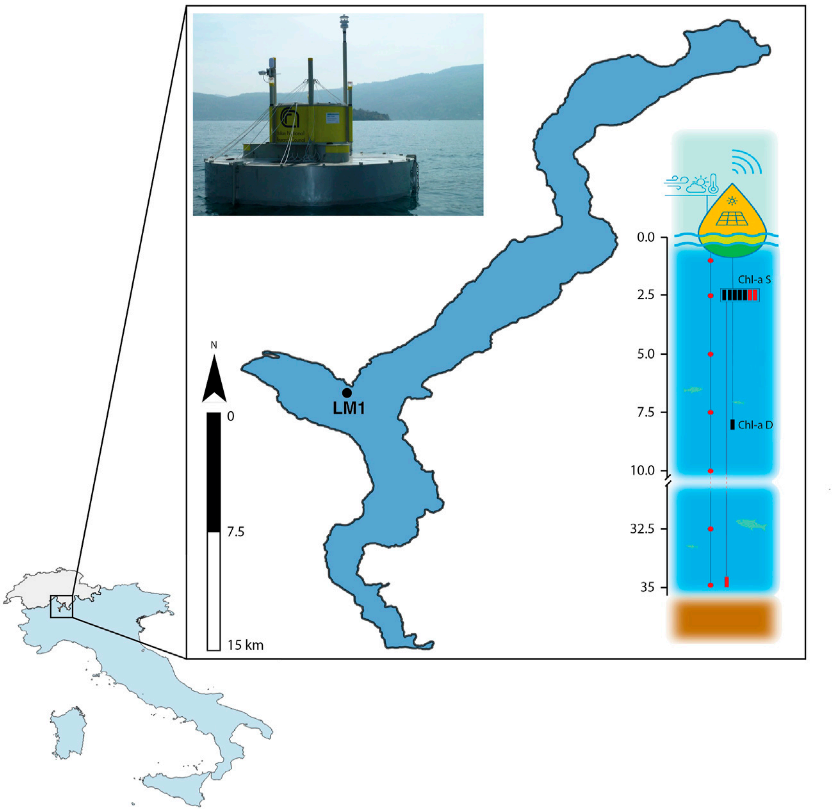

FIGURE 1
Location and main characteristics of the monitoring buoy LM1 in Lake Maggiore (see Tiberti et al., 2021 for the details). On the bottom-left map, Italy is coloured blue while Switzerland is grey.

taxa at the species level (Morabito et al., 2012) and assess biovolume of the main groups (Ruggiu et al., 1998). Chl-*a* concentration was also measured on integrated samples by spectrophotometric technique in the period 1984–2009 (APAT-IRSA-CNR, 2003), while from 2010 measurements were taken using a vertical profiling instrument (FluoroProbe, BBE Moldaenke) after a careful check of the comparability of the two methods.

2.2 LM1 buoy

The monitoring buoy LM1 was deployed in Lake Maggiore in the Pallanza basin (about 50 m from the shoreline, anchored at a depth of about 40 m; Figure 1). The buoy was developed in-house and conceived as a low-cost modular system (Tiberti et al., 2021). It is equipped with sensors for pH, conductivity, dissolved oxygen—surface (1.5 m depth) and deep (10 m depth)—and algal pigments (Chl-*a*, both at surface and deep, phycocyanin (PC) and phycoerythrin (PE) at surface), a thermistor chain, a weather station, and a live webcam (https://www.meteolivevco.it/boa-limnologica-sul-lago-maggiore/). Sensors used for pigment monitoring (Cyclops7, Turner Design) include two Chl-*a* sensors (surface and deep) which were deployed in 2020, and one PC and one PE sensors which were added in March 2021. Each sensor is wire connected to the electronic control unit, which has been specifically designed within the project for signal acquisition from the sensors, data storage, basic data elaboration, and wireless transfer. The open-source data management software istSOS (http://istsos.org/) was selected for managing and dispatching the observations from the monitoring sensors (Strigaro et al., 2022). Further details on the system hardware and software are provided by Tiberti et al. (2021).

For the present study, pigment raw data (in Volt) were stored in daily text files at 1 minute frequency. Successively, the data were processed by applying quality assurance/quality control (QA/QC) procedures and aggregated on an hourly basis. Sensor signal at the surface was clearly affected by quenching during daylight, as shown by the daily cycle in fluorescence data (Tiberti et al., 2021). As suggested by McBride and Rose (2018), night measurements should be considered the most indicative of Chl-*a* concentration. In particular, for the comparison with laboratory data, we selected fluorescence sensor data between 00:00 and 05:00 a.m. on the day of the sampling. The conversion

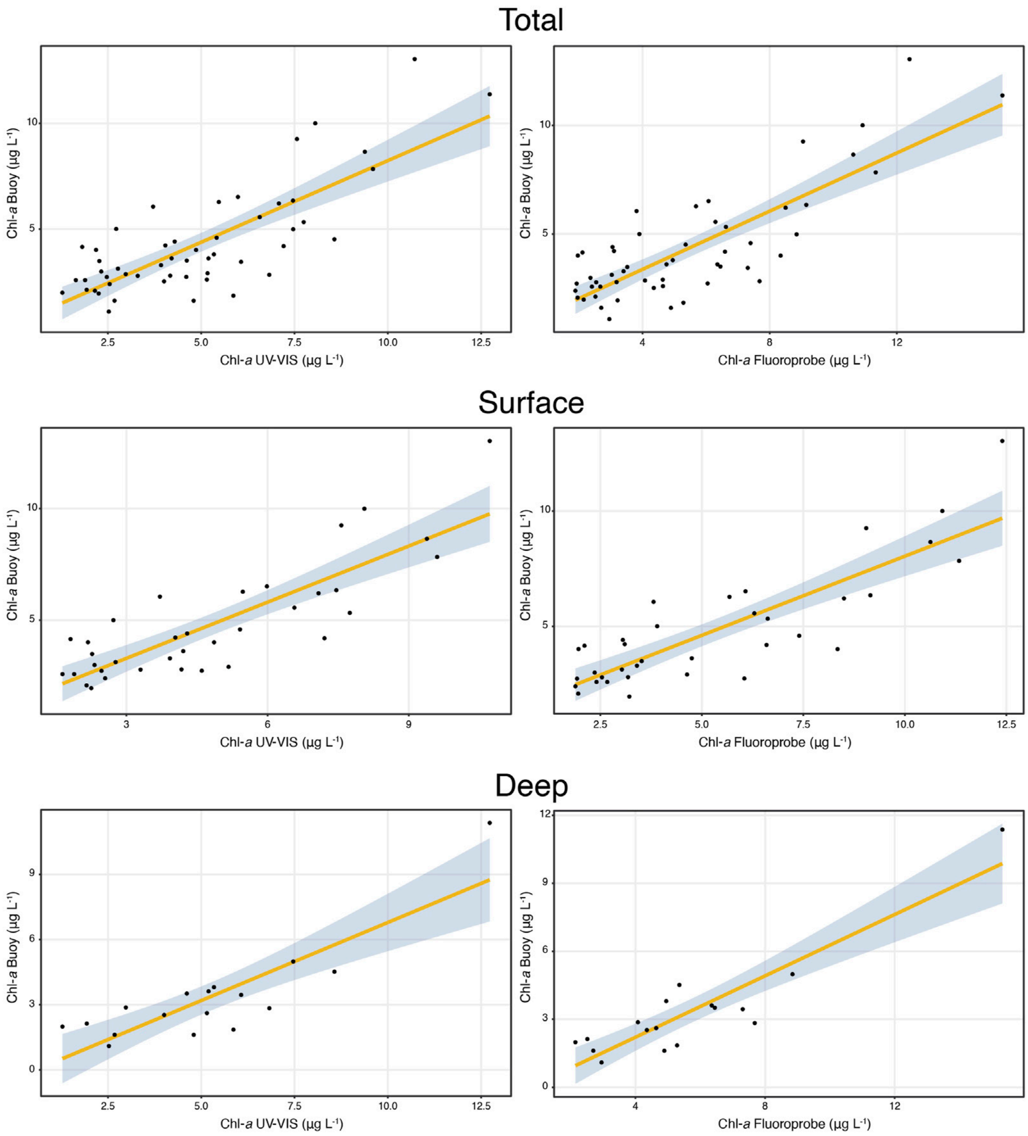

FIGURE 2
Comparison between Chl-*a* concentrations obtained from the *in-situ* sensors (buoy) and laboratory analysis UV-VIS (left panels) and FP (right panels). In the panels data are shown for all the samples, surface and deep samples. Statistics of the linear regressions are provided in Table 1.

from signal data (in Volt) to Chl-*a* concentrations (μg L^{-1}) was done by applying a measured factor obtained from laboratory calibration (Tiberti et al., 2021).

2.3 Chl-*a* analysis

During the first 2 years of the HFM (2020-2021) we collected 54 water samples within 37 sampling dates, approximatively fortnightly, during the periods of high biological activity, and monthly in the other months. Samples were collected close to the buoy using a Ruttner bottle. Part of the samples were taken at 1 m depth (n = 37), and part at 10 m depth (n = 17), where the surface and deep Chl-*a* sensors are placed, respectively. Data covered the periods January-September 2020 and March-December 2021. Unfortunately, no data were available between October 2020 and February 2021 because a violent storm seriously damaged the buoy and the sensors on 2 October 2020 and the repairing operation took several months before the monitoring could be restarted.

All the samples were analyzed as follows:

- acetone extraction followed by UV-VIS spectrophotometrical reading (APAT IRSA 9020) to quantify Chl *a*, *b*, *c*, according to APAT—IRSA/CNR, 2003.

- fluorometric determination of total Chl-*a* and of the contribution by the main algal classes through the multi-wavelength probe FluoroProbe (bbe Moldaenke GmbH), used as a Workstation benchtop unit. The instrument can detect four phytoplankton classes: green algae, xanthophyll-containing brown algae (dinoflagellates, diatoms, chrysophyceae), blue-green algae (PC-rich cyanobacteria), and red algae (PE-rich cyanobacteria, cryptophyceae) (Callieri et al., 2021).

On a subset of the surface samples (n = 23), microscopy analysis of phytoplankton based on the inverted microscopy techniques (Utermöhl, 1931; Lund et al., 1958) and the CEN guidance (CEN, 2004) was performed. Taxa were classified at species or genus level by an inverted microscope (Zeiss) at intermediate (200x) and high (×400) magnification. Community composition was estimated as taxa relative abundance. The total biovolume and biovolume of each group were estimated from density data and original measurements of cell volume (Morabito et al., 2012).

To evaluate how well *in-situ* sensor data reflect the results of laboratory techniques, we used a series of linear regressions, with the average *in-situ* night values (from 00:00 and 05:00 a.m.) of Chl-*a* as the dependent variable and the laboratory measures of Chl-*a* (by UV-VIS and FP) as independent variables, both considering all samples together (n = 54) and surface and deep samples separately (n = 37 and n = 17, respectively). In addition, we described the linear relationship between the *in-situ* Chl-*a* measures and the estimated algal biovolume (available only for 23 surface samples) with a further regression analysis. All analyses were performed in the R environment for statistical computing (R Core Team, 2022).

3 Results

3.1 Evaluation of Chl-*a* estimation by *in-situ* sensors

Chl-*a* concentrations measured in Lake Maggiore during the study period through HFM ranged between 2 and 13 μg L^{-1} at the surface and 1 and 12 μg L^{-1} at the deep sample points, with average values of 4.7 and 3.3 μg L^{-1}, respectively. These values are typical of mesotrophic lakes; however, they lie in the low range of Chl-*a* concentrations characterizing freshwater lakes worldwide (Filazzola et al., 2020). Some peaks (above 10 μg L^{-1}) were detected in spring and summer, usually in correspondence with diatom blooms, such as in May 2021.

Altogether the results of the linear regression indicate a good fit between the values recorded by the buoy and both UV-VIS and FP data (Table 1; Figure 2). The slopes of the regression lines are frequently significantly lower than 1 (1 is not included in the 95% Confidence Intervals), which indicates that laboratory calibration, based on dilutions of algal cultures, may be inaccurate under natural conditions, i.e., natural algal communities. Because of this, discrete laboratory measures from discrete samples could be used to recalibrate the sensors.

The high frequency (HF) data collected in 2020 and 2021 (hourly average) allowed us to describe the seasonal pattern of Chl-*a* concentrations in great detail (Figure 3): sensor readings were able to describe the annual Chl-*a* dynamics, its main peaks (e.g., March, late April and June 2020 and May 2021) and a number of short-lived peaks of Chl-*a* (Figure 3) that would have passed unnoticed or poorly described by discrete data. Some discrepancy was observed between HF and laboratory data in late summer 2020, when the *in-situ* data slightly underestimated the Chl-*a* values.

3.2 Algal groups and their role in Chl-*a* detection

To get additional data on phytoplankton biovolume and composition, a subset of surface samples were counted by microscope (Figure 4). As regards the phytoplankton community composition, our results confirmed those obtained from the long-term monitoring of Lake Maggiore (Morabito et al., 2012; Rogora et al., 2021). We found a limited presence of cyanobacteria, which were present in small amounts mostly in late summer (e.g., 290 $mm^3\ m^{-3}$ in August 2020). Bacillariophyceae were dominant in almost all the samples, representing between 50 and 80% of the total biovolume. The second most important group was that of cryptophyceae, which were dominant in a few spring samples (e.g., about 500 and 750 $mm^3\ m^{-3}$ in March and May 2021).

The Chl-*a* values, both from the buoy and UV-VIS analysis, closely followed the pattern of the Bacillariophyceae group (Figure 4). Diatoms are indeed the dominant taxon in Lake Maggiore, and their blooms in spring and summer are the main responsible for the Chl-*a* peaks observed in the lake, especially in recent years (Rogora et al., 2021).

When considering total biovolume, the highest values were measured in early March 2020 (2,800 $mm^3\ m^{-3}$), June 2020 (2,500 and 2,800 $mm^3\ m^{-3}$ respectively on the 16 and 30 of June), and May 2021 (4,200 $mm^3\ m^{-3}$). Despite the limited number of samples available in 2021, the seasonal pattern in both years was similar to the long-term monitoring of the lake, with the highest biovolume measured in spring (Rogora et al., 2021). The pattern of total biovolume followed well that of Chl-*a* concentrations resulting from the HFM (Figure 4). The linear regression parameters ($R^2 = 0.72$, $p < 0.001$; a = 1.82 (0.77–2.87 95% CI); b = 0.002 (0.001–0.003 95% CI)) indicate a good fit between *in-situ* Chl-*a* sensor and the biovolume estimates from the microscopic analysis, as shown in Figure 5.

TABLE 1 Results from linear regressions between chlorophyll-*a* concentrations measured by *in-situ* sensors (buoy) and by UV-VIS spectrophotometry or FluoroProbe (FP). The intercept (a), slope (b), coefficient of determination (R^2), and *p*-values are reported; lower and upper 95% confidence intervals of a and b are reported in brackets.

		Buoy vs. UV-VIS				Buoy vs. FP			
	n	a	b	p	R^2	a	b	p	R^2
All data	52	0.52 (−0.44, 1.47)	0.77 (0.60, 0.94)	<0.001	0.62	0.71 (−0.13, 1.55)	0.67 (0.53, 0.80)	<0.001	0.66
Surface	35	0.78 (−0.27 1.83)	0.84 (0.64, 1.03)	<0.001	0.70	1.18 (0.24, 2.11)	0.69 (0.53, 0.84)	<0.001	0.71
Deep	17	−0.41 (−1.80,0.99)	0.72 (0.48,0.96)	<0.001	0.73	−0.50 (−1.61, 0.61)	0.68 (0.50, 0.85)	<0.001	0.82

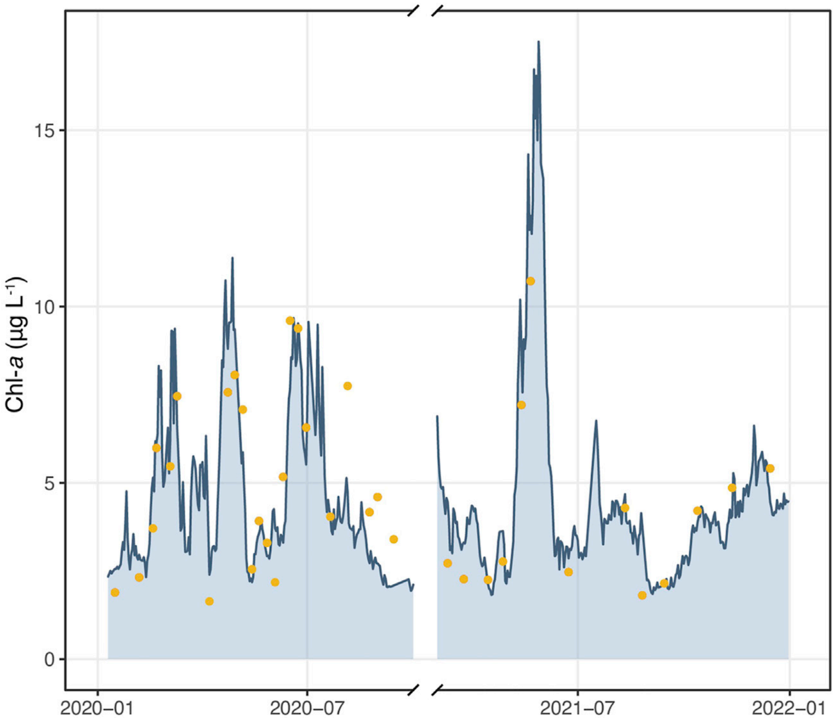

FIGURE 3
Hourly average data of Chl-*a* concentrations from *in-situ* sensors (bluish area) and Chl-*a* concentrations in the surface samples collected in 2020–21 and analysed by UV-VIS spectrophotometry (yellow dots).

4 Discussion

The comparison between field and laboratory methods to estimate Chl-*a* concentrations in Lake Maggiore showed an overall good agreement. In particular, *in-situ* fluorimetric sensors provided a reliable estimate of Chl-*a* values and captured peaks occurring during algal blooms in spring and summer. Linear regressions were statistically significant between the data from the buoy and those from laboratory analyses. As expected, we found a higher correlation coefficient with the buoy sensor and FP data since both estimate Chl-*a* concentrations through a fluorimetric measure. A better fit with laboratory data emerged for the deep sensor, with respect to the surface one, possibly due to the more limited variability of deep Chl-*a* concentrations. A fair agreement was also found between the *in-situ* fluorometric data and the total phytoplankton biovolume estimated by cell counting, suggesting *in-situ* HF data as a tool to assess phytoplankton biomass variability in the short term. However, the phytoplankton community composition should be considered in this evaluation.

In this study, during most of the year, the phytoplankton community of Lake Maggiore was dominated by diatoms, and their biovolume variation during the 2-year period had a fair agreement with the *in-situ* HF Chl-*a* sensor trend. However, during the summer, cyanobacteria started to be an important part of the phytoplankton community. In particular, in late

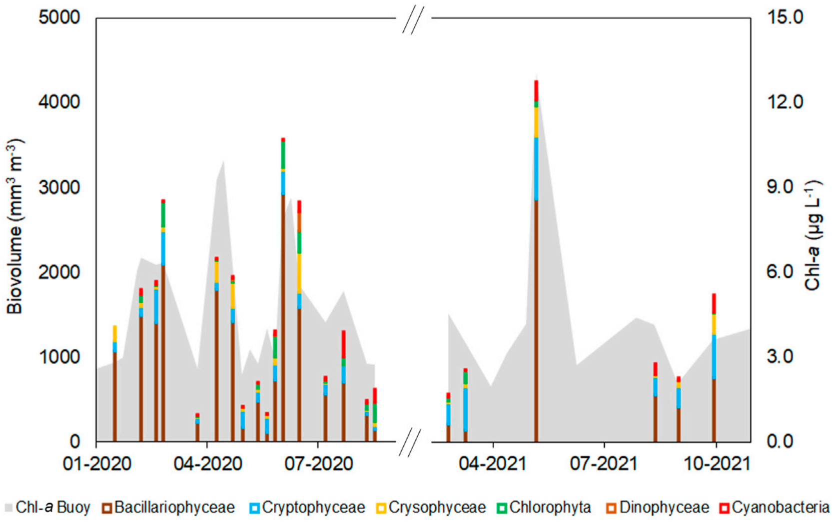

FIGURE 4
Biovolume of the main phytoplankton groups based on microscopy analysis of surface samples (n = 23) collected in 2020 and 2021. The grey area shows the pattern of HF Chl-*a* data from the *in-situ* sensor.

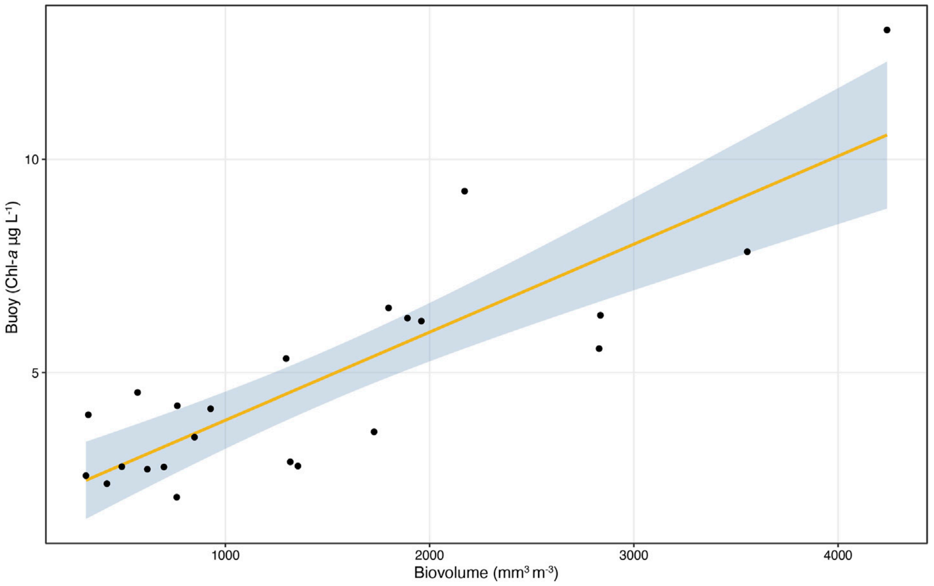

FIGURE 5
Linear regressions between Chl-*a* concentrations obtained from the *in-situ* sensors (buoy) and total phytoplankton biovolume by microscopy analysis (n = 23).

summer and early autumn small cell-sized (Chroococcales, cell sizes 2–4 µm) colonial cyanobacteria taxa such as *Aphanoteche* sp. and *Aphanocapsa* sp. reached considerable density values. During this period, Chl-*a* concentration by *in-situ* sensors recorded lower values with respect to laboratory methods and phytoplankton counting. A similar discrepancy was observed by other studies that highlighted how at low Chl-*a* concentrations (approx. below 10 µg L^{-1}), the percentage contribution of picocyanobacteria to total phytoplankton biomass can be high (Voros et al., 1998). PE-rich picocyanobacteria are commonly found in oligotrophic waters where green and blue-green light is available, as in the case of Lake Maggiore (Callieri et al., 2021).

Picocyanobacteria are characterized by a low Chl:biomass ratio with respect to other phytoplankton groups, so their presence could lead to an underestimate of total phytoplankton biomass based on *in-situ* Chl-*a* data.

Our results confirmed what was highlighted by other studies about the limitations of sensor use to estimate Chl-*a* variations, including interference from water turbidity and the different contribution by phytoplankton classes (Zamyadi et al., 2012; Kong et al., 2014; Kasinak et al., 2015). In fact, *in-situ* fluorescence estimation mainly depends on phytoplankton biomass, its community composition, and its physiological state (Richardson et al., 2010). However, other physical and chemical factors such as water temperature, water column stratification, underwater light, back light scattering, and light absorption by organic and inorganic particles can affect the final measure of chlorophyll and phycobiliprotein values (Proctor & Roesler 2010; Ostrowska 2012).

A limitation of our study consists in the narrow range of Chl-*a* values considered in the method comparison: Chl-*a* in Lake Maggiore is in the low range of concentrations for freshwater, with most of the data between 2 and 3 μg L^{-1} and only a few data above 10 μg L^{-1}, during spring algal density increases. Moreover, the phytoplankton community was dominated by diatoms, which also contributed to the highest Chl-*a* values recorded, followed by green algae. PC-containing cyanobacteria were rarely detected in the lake, and this prevented us from assessing the use of phycocyanin *in-situ* sensors as early warning systems for potentially toxic cyanobacteria blooms.

A further limitation of our assessment lies in the uneven distribution of samples (more frequent sampling in 2020 and a higher number of surfaces with respect to deep samples) and in the lack of replicates, which prevented the evaluation of random errors. However, we tested the agreement between methods on a total of 54 samples covering the seasonal pattern of Chl-*a* and the results clearly demonstrate an overall agreement between *in-situ* sensor data and extracted Chl-*a*.

A further problem we encountered was the presence of gaps in the HF data due to technical issues (e.g., sensor damages, fouling, lack of data transmission), the most relevant being a 5-month interruption between 2020 and 2021 due to the damages caused to the buoy by a severe storm. However, these issues are not rare in HFM applications and should be considered when designing the monitoring system and evaluating the costs and benefits of the system itself (Seifert-Dähnn et al., 2021). Despite these drawbacks, the HFM systems in Lake Maggiore performed well in depicting the seasonal pattern of Chl-*a* concentrations, which in turn proved to be a good proxy of phytoplankton biovolume. We still need to test the performance of the PC and PE sensors deployed in 2021. However, we think these sensors will be a useful integration to the HFM of Lake Maggiore, for a more comprehensive evaluation of the phytoplankton succession. Overall, our results confirmed that *in-situ* sensors may be useful in measuring diagnostic pigments and estimating algae abundance in near real-time, especially when sensors for different pigments are combined (Pace et al., 2017; Bertone et al., 2018; Chegoonian et al., 2022). These data may be relevant in planning field campaigns for institutional monitoring purposes, e.g., targeting the sampling and analysis effort on bringing information on critical or representative periods in terms of algal blooms.

It is worth mentioning that in some periods of 2020 (March-May and November-December) the field campaigns for the monitoring of Lake Maggiore had to be delayed due to the lockdowns caused by the outbreak of the COVID-19 pandemic. In those situations, the HF data provided by the buoy were the only data available and, even though limited to a few variables, provided useful information on the lake dynamics. Some relative maxima in Chl-*a* concentrations recorded by the buoy (e.g., 7.8–8.6 μg L^{-1} on 16 and 23 of June 2020) were not detected by the discrete monitoring program based on monthly surveys (3.1 μg L^{-1} for June 2020; CIPAIS, 2022) confirming that monthly or even lower-frequent sampling is likely to miss the short-term variability of some lake processes. HF data may not only detect short-term events but also improve the estimate of key parameters for water quality assessment, such as Chl-*a* concentrations (Bresciani et al., 2011). Further, the HF Chl-*a* data may be employed in assessing the performance of the monitoring systems based on satellite data, also under development within the SIMILE project (Luciani et al., 2021; Bratic et al., 2022).

Long-term monitoring has proved to disproportionately contribute to a better understanding of ecosystems as well as to support management and restoration policy (Hughes et al., 2017). However, a multi-scale approach is required in ecological study, combining monitoring at different temporal and spatial scales (Sparrow et al., 2020). In-depth information on lake productivity and phytoplankton biomass, such as those provided by microscopy and laboratory analysis of discrete samples, cannot be replaced by sensor data. Nevertheless, HFM, even when limited to a few basic variables, may supplement time series of highly detailed data, contributing to a deeper knowledge of ecosystem dynamics, especially as regards short-term and highly variable processes (Carpenter et al., 2020).

5 Conclusion

Our study confirmed that *in-situ* sensors measuring *in vivo* fluorescence are an interesting approach for monitoring algal blooms in lakes and are an effective tool to detect and track bloom formation, complementing the more classical laboratory analysis. HFM is not limited to Chl-*a*, but also includes other algal pigments (i.e., PC and PE) that may improve the evaluation of lake productivity and phytoplankton succession: used in conjunction with discrete chemical and biological monitoring, it represents an important advance in the monitoring of freshwaters and a useful tool to detect ecological changes.

However, regular check and validation of the sensor readings through laboratory analyses is needed to get reliable data.

Automated *in-situ* monitoring can warn water managers and local authorities when measures against blooms are required and data can be used for successive selection of sites to be sampled and analyzed in the laboratory. In summary, lake monitoring, programs based on discrete sample collection and analysis may be successfully integrated by HFM and other approaches, such as the use of satellite data and of observations provided by citizens: this can hold both for lakes subject to operational monitoring under the WFD, where early warning systems could be needed to assess critical issue such as algal blooms, but also for lakes under the surveillance monitoring, to supplement and validate long-term discrete data.

Data availability statement

The raw data supporting the conclusion of this article will be made available by the authors, without undue reservation.

Author contributions

MR conceptualised the study and prepared the original draft, with the support of AL and LK. AL, SM, RC, and LK performed the laboratory analyses. TC and DM were in charge for the buoy data management. TC and RT led the data analysis for the manuscript. All the authors contributed to writing, reviewing, and editing.

Funding

The development of the LM1 buoy and all the activities related to the evaluation of pigment data have been supported by SIMILE, an Interreg Italian-Swiss project funded by the European Regional Development Fund (ERDF) ID: 523544. Long-term limnological research on Lake Maggiore is partly funded by the International Commission for the Protection of Swiss-Italian Waters (CIPAIS).

Acknowledgments

Investigations on Lake Maggiore are also carried out in the framework of the LTER (Long Term Ecological Research) Italian network, site “IT-08 Southern Alpine lakes” (http://www.lteritalia.it/). We want to thank the other partners and collaborators of the SIMILE project: Lombardy Region, Ticino Canton, Fondazione Politecnico di Milano, IREA CNR, and the Regional Agency for Environmental Protection (ARPA) of the Lombardy Region, for the fruitful cooperation within the project. We also wish to thank the technicians, postdocs and students who have contributed to the fieldwork and laboratory analysis described in this study.

Conflict of interest

The authors declare that the research was conducted in the absence of any commercial or financial relationships that could be construed as a potential conflict of interest.

Publisher’s note

References

APAT – IRSA/CNR (2003). Metodi analitici per le acque. Manuali e Linee guida 29/2003.

Bertone, E., Burford, M. A., and Hamilton, D. P. (2018). Fluorescence probes for real-time remote cyanobacteria monitoring: A review of challenges and opportunities. *Water Res.* 141, 152–162. doi:10.1016/j.watres.2018.05.001

Boyer, J. N., Kelble, C. R., Ortner, P. B., and Rudnick, D. T. (2009). Phytoplankton bloom status: Chlorophyll a biomass as an indicator of water quality condition in the southern estuaries of Florida, USA. *Ecol. Indic.* 9, S56–S67. doi:10.1016/j.ecolind.2008.11.013

Bratic, G., Carrion, D., Cannata, M., Rogora, M., Strigaro, D., and Brovelli, M. A. (2022). lake water quality monitoring tools. Int. Arch. Photogramm. *Remote Sens. Spat. Inf. Sci.*, 599–606. doi:10.5194/isprs-archives-XLIII-B4-2022-599-2022

Bresciani, M., Stroppiana, D., Odermatt, D., Morabito, G., and Giardino, C. (2011). Assessing remotely sensed chlorophyll-a for the implementation of the Water Framework Directive in European perialpine lakes. *Sci. Total Environ.* 409, 3083–3091. doi:10.1016/j.scitotenv.2011.05.001

Brovelli, M. A., Cannata, M., and Rogora, M. (2019). SIMILE, a geospatial enabler of the monitoring of sustainable development goal 6 (ensure availability and sustainability of water for all). Int. Arch. Photogramm. *Int. Arch. Photogramm. Remote Sens. Spat. Inf. Sci.XLII-4/W20*, 3–10. doi:10.5194/isprs-archives-xlii-4-w20-3-2019

Callieri, C., Hernández-Avilés, J. S., Eckert, E. M., Rogora, M., Tartari, G., Sforzi, T., et al. (2021). Transparent exopolymer particles (TEP), phytoplankton and picocyanobacteria along a littoral-to-pelagic depth-gradient in a large subalpine lake. J. *Limnol* 80 (3). doi:10.4081/jlimnol.2021.2021

Caroni, R., Van de Bund, W., Clarke, R. T., and Johnson, R. K. (2013). Combination of multiple biological quality elements into waterbody assessment of surface waters. *Hydrobiologia* 704 (1), 437–451. doi:10.1007/s10750-012-1274-y

Carpenter, S. R., Arani, B. M., Hanson, P. C., Scheffer, M., Stanley, E. H., and Van Nes, E. (2020). Stochastic dynamics of Cyanobacteria in long-term high-frequency observations of a eutrophic lake. *Limnol. Oceanogr. Lett.* 5 (5), 331–336. doi:10.1002/lol2.10152

CEN (2004). Water quality – guidance standard for the routine analysis of phytoplankton abundance and composition using inverted microscopy (Utermöhl technique) CEN TC 230/WG 2/TG 3/N83, May 2004.

Chegoonian, A. M., Zolfaghari, K., Leavitt, P. R., Baulch, H. M., and Duguay, C. R. (2022). Improvement of field fluorometry estimates of chlorophyll *a* concentration in a cyanobacteria-rich eutrophic lake. *Limnol. Ocean. Methods* 20 (4), 193–209. doi:10.1002/lom3.10480

Ciampittiello, M., Manca, D., Dresti, C., Grisoni, S., Lami, A., and Saidi, H. (2021). Meteo-hydrological sensors within the lake Maggiore catchment: System establishment, functioning and data validation. *Sensors* 21 (24), 8300. doi:10.3390/s21248300

European Commission. Brussels: European Commission.Directive 2000/60/EC of the European parliament and of the council of 23 october 2000 establishing a framework for community action in the field of water policy*Off. J. L327/1*

Fenocchi, A., Rogora, M., Sibilla, S., Ciampittiello, M., and Dresti, C. (2018). Forecasting the evolution in the mixing regime of a deep subalpine lake under climate change scenarios through numerical modelling (Lake Maggiore, Northern Italy/Southern Switzerland). *Clim. Dyn.* 51 (9), 3521–3536. doi:10.1007/s00382-018-4094-6

Filazzola, A., Mahdiyan, O., Shuvo, A., Ewins, C., Moslenko, L., Sadid, T., et al. (2020). A database of chlorophyll and water chemistry in freshwater lakes. *Sci. Data* 7 (1), 310–10. doi:10.1038/s41597-020-00648-2

Hamilton, D. P., Carey, C. C., Arvola, L., Arzberger, P., Brewer, C., Cole, J. J., et al. (2014). A global lake ecological observatory network (GLEON) for synthesising high-frequency sensor data for validation of deterministic ecological models. *Inland Waters* 5, 49–56. doi:10.5268/iw-5.1.566

Harke, M. J., Steffen, M. M., Gobler, C. J., Otten, T. G., Wilhelm, S. W., Wood, S. A., et al. (2016). A review of the global ecology, genomics, and biogeography of the toxic cyanobacterium, Microcystis spp. *Harmful algae*. 54, 4–20. doi:10.1016/j.hal.2015.12.007

Hodges, C. M., Wood, S. A., Puddick, J., McBride, C. G., and Hamilton, D. P. (2018). Sensor manufacturer, temperature, and cyanobacteria morphology affect phycocyanin fluorescence measurements. *Environ. Sci. Pollut. Res.* 25 (2), 1079–1088. doi:10.1007/s11356-017-0473-5

Hughes, B. B., Beas-Luna, R., Barner, A. K., Brewitt, K., Brumbaugh, D. R., Cerny-Chipman, E. B., et al. (2017). Long-term studies contribute disproportionately to ecology and policy. *BioScience* 67 (3), 271–281. doi:10.1093/biosci/biw185

Hunter, P. D., Tyler, A. N., Gilvear, D. J., and Willby, N. J. (2009). Using remote sensing to aid the assessment of human health risks from blooms of potentially toxic cyanobacteria. *Environ. Sci. Technol.* 43 (7), 2627–2633. doi:10.1021/es802977u

ISO 10260, 1992. Water quality — measurement of biochemical parameters — spectrometric determination of the chlorophyll-a concentration

Jennings, E., Jones, S., Arvola, L., Staehr, P. A., Gaiser, E., Jones, I. D., et al. (2012). Effects of weather-related episodic events in lakes: An analysis based on high-frequency data. *Freshw. Biol.* 57 (3), 589–601. doi:10.1111/j.1365-2427.2011.02729.x

Kasinak, J. E., Holt, B. M., Chislock, M. F., and Wilson, A. E. (2015). Benchtop fluorometry of phycocyanin as a rapid approach for estimating cyanobacterial biovolume. *J. Plankton. Res.* 37, 248–257. doi:10.1093/plankt/fbu096

Kasprzak, P., Padisák, J., Koschel, R., Krienitz, L., and Gervais, F. (2008). Chlorophyll a concentration across a trophic gradient of lakes: An estimator of phytoplankton biomass? *Limnologica* 38, 327–338. doi:10.1016/j.limno.2008.07.002

Klug, J. L., Richardson, D. C., Ewing, H. A., Hargreaves, B. R., Samal, N. R., Vachon, D., et al. (2012). Ecosystem effects of a tropical cyclone on a network of lakes in northeastern North America. *Environ. Sci. Technol.* 46 (21), 11693–11701. doi:10.1021/es302063v

Kong, Y., Lou, I., Zhang, Y., Lou, C. U., and Mok, K. M. (2014). Using an online phycocyanin fluorescence probe for rapid monitoring of cyanobacteria in Macau freshwater reservoir. *Hydrobiologia* 741, 33–49. doi:10.1007/s10750-013-1759-3

Lorenzen, C. J. (1967). Determination of chlorophyll and pheo-pigments: Spectrophotometric equations. *Limnol. Oceanogr.* 12, 343–346. doi:10.4319/lo.1967.12.2.0343

Luciani, G., Bresciani, M., Biraghi, C. A., Ghirardi, N., Carrion, D., Rogora, M., et al. (2021). Satellite Monitoring system of Subalpine lakes with open source software: The case of SIMILE Project. Baltic J. *Mod. Comput.* 9, 135–144. doi:10.22364/bjmc.2021.9.1.08

Lund, J. W. G., Kipling, C., and Le Cren, E. D. (1958). The inverted microscope method of estimating algal numbers and the statistical basis of estimations by counting. *Hydrobiologia* 11, 143–170. doi:10.1007/bf00007865

Marcé, R., George, G., Buscarinu, P., Deidda, M., Dunalska, J., de Eyto, E., et al. (2016). Automatic high frequency monitoring for improved lake and reservoir management. *Environ. Sci. Technol.* 50 (20), 10780–10794. doi:10.1021/acs.est.6b01604

McBride, C. G., and Rose, K. C. (2018). "Automated high-frequency monitoring and research", K. Collier, J. Quinn, and C. Howard-Williams (Hamilton: Springer), 419–461. doi:10.1007/978-3-319-93043-5*Lake restoration handbook*

McQuaid, N., Zamyadi, A., Prévost, M., Bird, D. F., and Dorner, S. (2011). Use of *in vivo* phycocyanin fluorescence to monitor potential microcystin-producing cyanobacterial biovolume in a drinking water source. *J. Environ. Monit.* 13 (2), 455–463. doi:10.1039/c0em00163e

Meinson, P., Idrizaj, A., Nõges, P., Nõges, T., and Laas, A. (2016). Continuous and high-frequency measurements in limnology: History, applications, and future challenges. *Environ. Rev.* 24 (1), 52–62. doi:10.1139/er-2015-0030

Morabito, G., Mazzocchi, M. G., Salmaso, N., Zingone, A., Bergami, C., Flaim, G., et al. (2018a). Plankton dynamics across the freshwater, transitional and marine research sites of the LTER-Italy Network. Patterns, fluctuations, drivers. *Sci. Total Environ.* 627, 373–387. doi:10.1016/j.scitotenv.2018.01.153

Morabito, G., Oggioni, A., and Austoni, M. (2012). Resource ratio and human impact: How diatom assemblages in Lake Maggiore responded to oligotrophication and climatic variability. *Hydrobiologia* 698, 47–60. doi:10.1007/s10750-012-1094-0

Morabito, G., Rogora, M., Austoni, M., and Ciampittiello, M. (2018b). Could the extreme meteorological events in Lake Maggiore watershed determine a climate-driven eutrophication process? *Hydrobiologia* 824 (1), 163–175. doi:10.1007/s10750-018-3549-4

Ostrowska, M. (2012). Model of the dependence of the sun-induced chlorophyll a fluorescence quantum yield on the environmental factors in the sea. *Opt. Express* 20 (21), 23300–23317. doi:10.1364/oe.20.023300

Pace, M. L., Batt, R. D., Buelo, C. D., Carpenter, S. R., Cole, J. J., Kurtzweil, J. T., et al. (2017). Reversal of a cyanobacterial bloom in response to early warnings. *Proc. Natl. Acad. Sci. U. S. A.* 114 (2), 352–357. doi:10.1073/pnas.1612424114

Proctor, C. W., and Roesler, C. S. (2010). New insights on obtaining phytoplankton concentration and composition from *in situ* multispectral Chlorophyll fluorescence. *Limnol. Oceanogr. Methods* 8, 695–708. doi:10.4319/lom.2010.8.0695

R Core Team (2022). R: A language and environment for statistical computing, *Found. Stat. Comput*. Vienna: Austria. https://www.R-project.org/.

Randolph, K., Wilson, J., Tedesco, L., Li, L., Pascual, D. L., and Soyeux, E. (2008). Hyperspectral remote sensing of cyanobacteria in turbid productive water using optically active pigments, chlorophyll a and phycocyanin. *Remote Sens. Environ.* 112 (11), 4009–4019. doi:10.1016/j.rse.2008.06.002

Richardson, T. L., Lawrenz, E., Pinckney, J. L., Guajardo, R. C., Walker, E. A., Paerl, H. W., et al. (2010). Spectral fluorometric characterization of phytoplankton community composition using the Algae Online Analyser®. *Water Res.* 44, 2461–2472. doi:10.1016/j.watres.2010.01.012

Rogora, M., Austoni, M., Caroni, R., Giacomotti, P., Kamburska, L., Marchetto, A., et al. (2021). Temporal changes in nutrients in a deep oligomictic lake: The role of external loads versus climate change. *J. Limnol.*, 80(3). doi:10.4081/jlimnol.2021.2051

Rogora, M., Buzzi, F., Dresti, C., Leoni, B., Lepori, F., Mosello, R., et al. (2018). Climatic effects on vertical mixing and deep-water oxygen content in the subalpine lakes in Italy. *Hydrobiologia* 824 (1), 33–50. doi:10.1007/s10750-018-3623-y

Ruggiu, D., Morabito, G., Panzani, P., and Pugnetti, A. (1998). Trends and relations among basic phytoplankton characteristics in the course of the long-term oligotrophication of Lake Maggiore (Italy). *Hydrobiologia* 369, 243–257. doi:10.1023/a:1017058112298

Salmaso, N., Buzzi, F., Capelli, C., Cerasino, L., Leoni, B., Lepori, F., et al. (2020). Responses to local and global stressors in the large southern perialpine lakes: Present status and challenges for research and management. *J. Gt. Lakes. Res.* 46, 752–766. doi:10.1016/j.jglr.2020.01.017

Salmaso, N., Morabito, G., Buzzi, F., Garibaldi, L., Simona, M., and Mosello, R. (2006). Phytoplankton as an indicator of the water quality of the deep lakes south of the alps. *Hydrobiologia* 563, 167–187. doi:10.1007/s10750-005-0003-1

Salmaso, N., Morabito, G., Mosello, R., Garibaldi, L., Simona, M., Buzzi, F., et al. (2003). A synoptic study of phytoplankton in the deep lakes south of the Alps (lakes Garda, Iseo, Como, Lugano and Maggiore). *J. Limnol.* 62 (2), 207–227. doi:10.4081/jlimnol.2003.207

Sarada, R. M. G. P., Pillai, M. G., and Ravishankar, G. A. (1999). Phycocyanin from spirulina sp: Influence of processing of biomass on phycocyanin yield, analysis of efficacy of extraction methods and stability studies on phycocyanin. *Process Biochem.* 34 (8), 795–801. doi:10.1016/s0032-9592(98)00153-8

Seifert-Dähnn, I., Furuseth, I. S., Vondolia, G. K., Gal, G., De Eyto, E., Jennings, E., et al. (2021). Costs and benefits of automated high-frequency environmental monitoring–The case of lake water management. *J. Environ. Manage.* 285, 112108. doi:10.1016/j.jenvman.2021.112108

Skeffington, R. A., Halliday, S. J., Wade, A. J., Bowes, M. J., and Loewenthal, M. (2015). Using high-frequency water quality data to assess sampling strategies for the EU Water Framework Directive. *Hydrol. Earth Syst. Sci.* 19 (5), 2491–2504. doi:10.5194/hess-19-2491-2015

Sparrow, B. D., Edwards, W., Munroe, S. E., Wardle, G. M., Guerin, G. R., Bastin, J. F., et al. (2020). Effective ecosystem monitoring requires a multi-scaled approach. *Biol. Rev.* 95 (6), 1706–1719. doi:10.1111/brv.12636

Stockwell, J. D., Doubek, J. P., Adrian, R., Anneville, O., Carey, C. C., Carvalho, L., et al. (2020). Storm impacts on phytoplankton community dynamics in lakes. *Glob. Change Biol.* 26 (5), 2756–2784. doi:10.1111/gcb.15033

Strigaro, D., Cannata, M., Lepori, F., Capelli, C., Lami, A., Manca, D., et al. (2022). Open and cost-effective digital ecosystem for lake water quality monitoring. *Sensors* 2, 6684. doi:10.3390/s22176684

Stumpf, R. P., Wynne, T. T., Baker, D. B., and Fahnenstiel, G. L. (2012). Interannual variability of cyanobacterial blooms in Lake Erie. *PLoS ONE* 7 (8), e42444. doi:10.1371/journal.pone.0042444

Tanentzap, A. J., Morabito, G., Volta, P., Rogora, M., Yan, N. D., and Manca, M. (2020). Climate warming restructures an aquatic food web over 28 years. *Glob. Change Biol.* 26 (12), 6852–6866. doi:10.1111/gcb.15347

Taranu, Z. E., Gregory-Eaves, I., Leavitt, P. R., Bunting, L., Buchaca, T., Catalan, J., et al. (2015). Acceleration of cyanobacterial dominance in north temperate-subarctic lakes during the Anthropocene. *Ecol. Lett.* 18 (4), 375–384. doi:10.1111/ele.12420

Tiberti, R., Caroni, R., Cannata, M., Lami, A., Manca, D., Strigaro, D., et al. (2021). Automated high frequency monitoring of Lake Maggiore through *in situ* sensors: System design, field test and data quality control. *J. Limnol.* 80 (2). doi:10.4081/jlimnol.2021.2011

Utermöhl, von H. (1931). Neue Wege in der quantitativen Erfassung des Planktons. (Mit besondere Beriicksichtigung des Ultraplanktons). *SIL Proc. 1922-2010* 5, 567–596. doi:10.1080/03680770.1931.11898492

Vörös, L., Callieri, C., Balogh, K. V., and Bertoni, R. (1998). Freshwater picocyanobacteria along a trophic gradient and light quality range. *Hydrobiologia* 369, 117–125. doi:10.1023/a:1017026700003

Vörös, L., and Padisák, J. (1991). Phytoplankton biomass and chlorophyll-a in some shallow lakes in central Europe. *Hydrobiologia* 215, 111–119. doi:10.1007/bf00014715

Zamyadi, A., McQuaid, N., Prévost, M., and Dorner, S. (2012). Monitoring of potentially toxic cyanobacteria using an online multi-probe in drinking water sources. *J. Environ. Monit.* 14, 579–588. doi:10.1039/c1em10819k

frontiers | Frontiers in Environmental Science

TYPE Methods
PUBLISHED 22 May 2023
DOI 10.3389/fenvs.2023.1057742

Check for updates

OPEN ACCESS

EDITED BY
Caterina Bergami,
National Research Council (CNR), Italy

REVIEWED BY
Alessandro Oggioni,
National Research Council (CNR), Italy
Agnieszka Karolina Kolada,
Institute of Environmental Protection (IOS), Poland

*CORRESPONDENCE
S. Jannicke Moe,
✉ jmo@niva.no

RECEIVED 30 September 2022
ACCEPTED 06 April 2023
PUBLISHED 22 May 2023

CITATION
Moe SJ, Mentzel S, Welch SA and Lyche Solheim A (2023), From national monitoring to transnational indicators: reporting and processing of aquatic biology data under the European Environment Agency's State of the Environment data flow.
Front. Environ. Sci. 11:1057742.
doi: 10.3389/fenvs.2023.1057742

From national monitoring to transnational indicators: reporting and processing of aquatic biology data under the European Environment Agency's State of the Environment data flow

S. Jannicke Moe[1]*, Sophie Mentzel[1], Samuel A. Welch[1] and Anne Lyche Solheim[2]

[1]Norwegian Institute for Water Research (NIVA), Section for Ecotoxicology and Risk Assessment, Oslo, Norway, [2]Norwegian Institute for Water Research (NIVA), Section for Freshwater Ecology, Oslo, Norway

Biological monitoring data from aquatic ecosystems are collected from European countries on a yearly basis by the European Environment Agency (EEA) through the Water Information System for Europe (WISE). The WISE-SoE (State of Environment) data flows provide indicators of pressures, states and impacts of surface waters and groundwaters on a pan-European scale. The WISE-2 Biology was established to obtain a harmonised flow of biology data reported annually as Ecological Quality Ratios (EQRs) from European surface waters, as a supplement to the mandatory 6-yearly reporting of ecological status of water bodies for the Water Framework Directive. The purposes of this paper are 1) to describe the compilation of national aquatic biology monitoring data indicators and to inform about the public availability of these data, 2) to give an overview of the reported data and indicate the potential for assessments based on these data, and 3) to illustrate the potential for further use of the underlying species abundance data in biodiversity research and assessment. WISE-2 data are reported for the following biological quality elements: phytoplankton, phytobenthos, macrophytes, macroalgae, angiosperms, benthic invertebrates and fish in rivers, lakes, transitional and/or coastal waters. The EQR values represent the deviation from reference conditions. The final processed and quality-checked data are published in EEA's database Waterbase - Biology, which currently holds data from more than 13,000 waterbodies in 26 countries from the reporting years 2011–2021. Examples of time series aggregated by geographic regions give an indication of the type of trends that can be obtained from the reported data at the nEQR scale. However, the current results are representative only for certain geographic regions with high coverage of water bodies. Within the European research project EuropaBON (Europa Biodiversity Observation Network), the use of WISE-2 data can be leveraged to support biodiversity policy and conservation planning. EuropaBON's online database provides an overview of how biodiversity monitoring schemes across Europe flows through different integration nodes, to produce Essential Biodiversity Variables and other policy-relevant indicators. Here, we use the EuropaBON visualisation tool to illustrate the WISE-2 as a European integration node for 157 biology datasets via the national integration nodes.

KEYWORDS

Water Framework Directive (2000/60/EC), biological quality elements (BQE), surface water bodies, ecological quality ratio (EQR), Water Information System of Europe, essential biodiversity variables (EBV), temporal trend analysis

1 Introduction

The European Water Framework Directive (WFD) requires monitoring and assessment of the ecosystems of surface water bodies in rivers, lakes, transitional and coastal waters in all EU member states (European Commission, 2000). The ecological status assessment should be based primarily on metrics representing a selection of biological quality elements (BQEs) and supported abiotic quality elements (physical, chemical and hydromorphological variables) (Hering et al., 2015). Ecological status of water bodies is reported according to river basin management plans (RBMP) every 6 years through the Water Information System for Europe (WISE); the 3rd WFD reporting cycle was completed in 2022.

In addition to the mandatory reporting to WISE-WFD, biological data from monitoring of aquatic ecosystems are collected and integrated by the European Environment Agency (EEA) through the voluntary State of the Environment reporting (WISE-SoE). The data are collected on a yearly basis through the European Environment Information and Observation Network (EIONET), and used by EEA in State of the Environment reports which are published every 5 years (EEA, 2019). Since the reporting to WISE-SoE is voluntary, the selection of water bodies often constitutes a subset of those reported to the WFD. Still, the WISE-SoE data flows aim to provide a representative set of indicators of pressures, states and impacts of waters on a pan-European scale.

Within the WISE-SoE system, the WISE-2 Biology data flow (https://cdr.eionet.europa.eu/help/WISE_SoE/wise2) was established to obtain a harmonised flow of biology data reported as ecological quality ratios (EQRs) from all surface water categories; rivers, lakes, transitional and coastal waters.

The added value of the WISE-SoE biology data in comparison to other main relevant data sources is illustrated in a conceptual diagram (Figure 1). Other data sources such as national monitoring data can provide even longer time series and higher resolution of information, such as abundance per species. However, compilation of raw species data is beyond the scope of EEA. While the WISE-2 data flow has a lower spatial coverage than the WFD reporting, the former has several benefits in the context of biodiversity information:

(1) more frequent reporting: annual SoE data calls vs. WFD reporting every 6 years.
(2) higher resolution: EQR (Ecological quality ratio) values on continuous scale (0-1) vs. categorical (5 status classes) (see Section 2.1 below).
(3) the biological determinands of SoE can be related to physical or chemical pressures and impacts (e.g., eutrophication vs. general degradation).

WISE-2 Biology data is the most recent of the four current WISE-SoE data flows: chemical emission (WISE-1), water quantity (WISE-3) and water quality (WISE-6). In this context, the WISE-2 data can fill the gap in the DPSIR (Drivers—Pressures—States—Impacts—Responses) model used for water management in Europe (EEA, 2018), by representing the biotic states and impact part of the DPSIR cycle (Moe et al.,

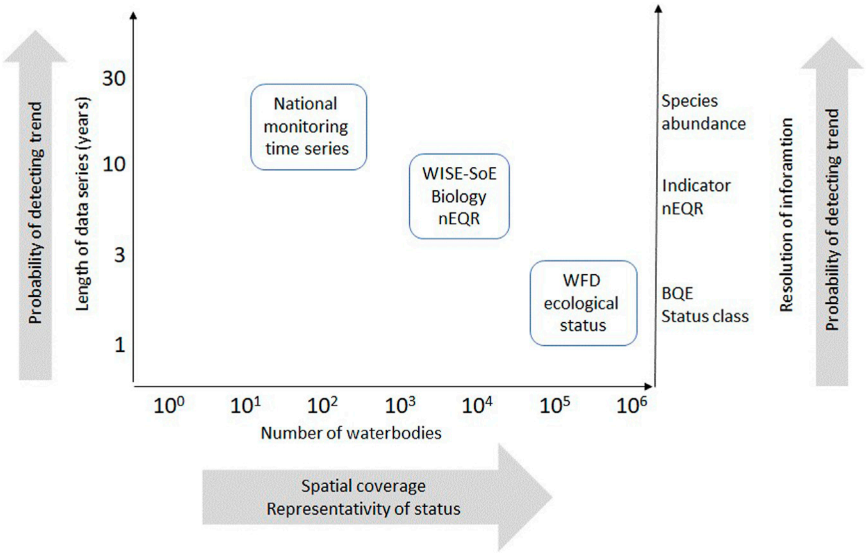

FIGURE 1
Schematic diagram of the spatial and temporal extent and resolution of WISE-SoE biology data, compared to alternative monitoring data sources (national data and WISE-WFD data). Note: the position and extent of the text boxes do not represent exact values.

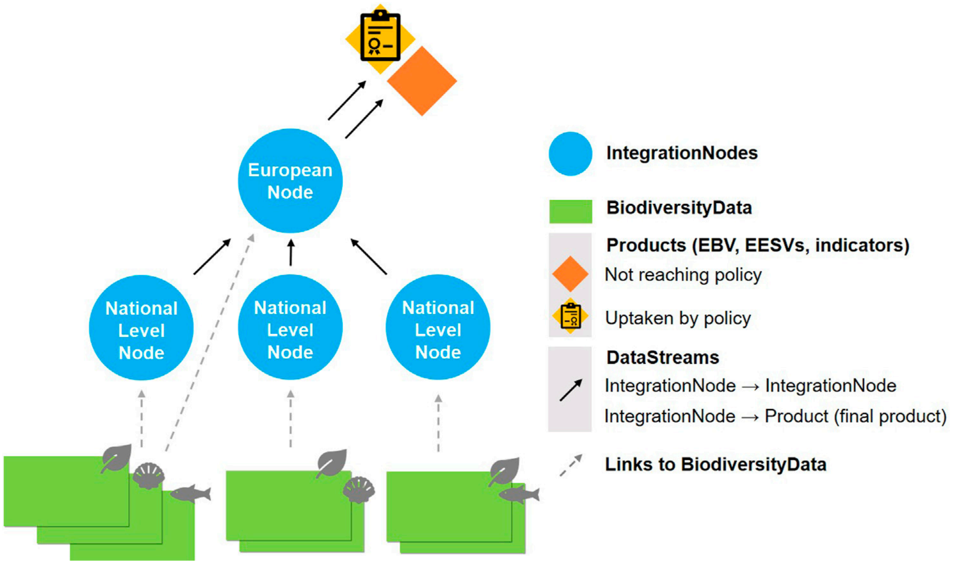

FIGURE 2
The EuropaBON biodiversity monitoring database: Schematic diagram of the dataflow across an integration initiative. The European node corresponds to WISE-2; the Sub-EU level nodes corresponds to national data compilation for reporting to WISE-2. Modified after Figure 1 in Morán-Ordóñez et al. (2023).

2016). These data can provide an important building block towards the development of a new aquatic biology indicator (sensu EEA) with relevance for the WFD as well as other EU directives and policies. EEA indicators are designed to answer key policy questions and to support all phases of environmental policy making from policy monitoring and evaluation to communicating to policymakers and the public, and to inform the reader about the trend or status of the phenomenon being investigated over a given period of time.

The assessment of SoE biology data is also relevant for the focus on Biodiversity in the new EU Commission. An assessment based on the biological data can be expected to give added value compared to the assessment of the overall ecological status for river and lake water bodies reported in the RBMPs in several ways:

- Good ecological status is an objective of the WFD for rivers and lakes and should be assessed primarily by using BQEs and secondarily by physico-chemical quality elements. While the assessment of ecological status of water bodies according to WFD should be based on several different BQEs (e.g., phytoplankton, macrophytes, macroinvertebrates and fish in lakes), only a subset of the BQEs are requested by reporting to EEA (e.g., phytoplankton, macrophytes and fish in lakes). The selected BQEs are typically those for which assessment methods are best developed by the countries implementing the WFD.
- Most of the biological indicators can provide direct information on the impacts of specific pressures, e.g., nutrient enrichment and organic pollution, hydromorphological pressures, acidification etc., and can therefore provide a link to the underlying causes for change in the ecological status of river and lake water bodies.
- The normalised EQR values (ecological quality ratio on a scale from 0 to 1) provide more accurate measurement of ecological status than the categorical status class given in the WFD-RBMP reporting and can be used to assess changes within a status class, as well as between status classes.

While the WISE-2 data are publicly available in tabular format, further evaluation and context is needed for these data to become useful to support biodiversity policy and conservation planning. This is an ongoing activity of the European Horizon 2020 project EuropaBON (Europa Biodiversity Observation Network: integrating data streams to support policy) (Pereira et al., 2022). The project's mission is to overcome existing data gaps and workflow bottlenecks by designing an EU-wide framework for monitoring biodiversity and ecosystem services (Santana et al., 2023). EuropaBON has set up a web-based platform to collect and record the current biodiversity monitoring data workflows across Europe in a database (Figure 2) (Morán-Ordóñez et al. 2023). This database is in essence a metadatabase, which will provide an overview of how biodiversity data collected in monitoring schemes across Europe flows through different institutions and programs and is processed to produce Essential Biodiversity Variables (EBVs) (Pereira et al., 2013), Essential Ecosystem Services Variables (EESVs) (Balvanera et al., 2022), and other EU policy-relevant indicators. This database will also provide more detailed information on the individual national biodiversity datasets, underlying monitoring programs, species lists, contact information and other metadata, which can be relevant information for scientists interested in accessing the original monitoring data. As such, the EuropaBON monitoring database will provide useful information on aquatic biological data

TABLE 1 Number of waterbodies reported per country and water category, by one or more BQEs (see Table 2) for one or more years. Countries are grouped into geographic regions for assessment of trends. Abbreviations: RW = river water bodies, LW = lake water bodies, TW = transitional water bodies, CW = coastal water bodies. "Status class" is the count of waterbodies with status class reported (mandatory). "nEQR" is the count number of waterbodies with normalised Ecological Quality Ratio values, either reported or calculated based on the reported national EQR values and classification systems. Note: For countries that have not implemented the WFD (e.g CH), the national classification is not necessarily WFD-compliant.

Country code	Geographic region	RW status class	RW nEQR	LW status class	LW nEQR	TW status class	TW nEQR	CW status class	CW nEQR
Austria (AT)	Southeast	242	242	156	26	—	—	—	—
Belgium (BE)	West	3,942	3,942	6	6	10	10	—	—
Bulgaria (BG)	Southeast	831	831	2	2	—	—	—	—
Switzerland (CH)	West	108	—	—	—	—	—	—	—
Cyprus (CY)	South	160	139	3	—	—	—	—	—
Germany (DE)	West	28	—	89	—	—	—	—	—
Denmark (DK)	West	144	—	—	—	—	—	—	—
Estonia (EE)	East	394	392	13	7	—	—	—	—
Spain (ES)	South	7,617	7,375	118	118	173	157	257	80
Finland (FI)	North	67	67	48	48	—	—	—	—
France (FR)	West	1,681	1,681	—	—	—	—	—	—
Croatia (HR)	Southeast	156	156	8	8	—	—	—	—
Ireland (IE)	West	498	458	325	186	—	—	—	—
Italy (IT)	South	5,130	5,034	382	317	601	499	914	887
Lithuania (LT)	East	2,422	2,420	946	946	24	24	6	6
Luxembourg (LU)	West	19	18	—	—	—	—	—	—
Latvia (LV)	East	89	89	35	35	11	11	21	21
Netherlands (NL)	West	158	127	349	343	—	—	—	—
Norway (NO)	North	442	270	137	35	—	—	210	128
Poland (PL)	East	4,293	3,781	2,124	1,845	4	4	—	—
Portugal (PT)	South	53	—	1	—	—	—	—	—
Romania (RO)	Southeast	1,060	885	10	10	—	—	—	—
Sweden (SE)	North	324	314	2,563	2,437	—	—	4	—
Slovenia (SI)	East	112	—	65	10	—	—	—	—
Slovakia (SK)	East	272	252	—	—	—	—	—	—
United Kingdom (UK)	West	7,570	6,373	326	235	—	—	—	—
Sum		37,812	34,846	7,706	6,614	823	705	1,412	1,122

at all levels from the national monitoring programs to European indicators of ecosystem state and services.

The objective of this paper is to provide information on the WISE-2 biology data, how they can be accessed and used, and to illustrates current or planned applications and indicator development for European-scale assessments. Moreover, we describe how information on these dataflows are used in the EU project EuropaBON, which can in turn provide more detailed information on the original monitoring data underlying the WISE-2 data flow.

2 Reporting and processing of WISE-2 biology data

2.1 Biological quality elements (BQEs)

Response to stress differs between organism groups, water types and stressors. A conceptual model from the EU project WISER (Hering et al., 2013) summarises how the individual organism groups respond to different types of degradation in rivers, lakes, transitional and coastal waters. A recent comprehensive study across

TABLE 2 Number of records per determinand reported to WISE-2 and published in Waterbase—Biology 2021. Each determinand represents a biological quality element (BQE), as well as a specific impact type (for rivers and lakes). Retired determinands are not included in the table. Abbreviations for water categories: RW = river water bodies, LW = lake water bodies, TW = transitional water bodies, CW = coastal water bodies: Abbreviations for water BQEs: PB = phytobenthos, MI = benthic macroinvertebrates, FI = fish, PP = phytoplankton, MP = macrophytes, MA = macroalgae, AN = angiosperms. Abbreviations for water impact types (suffixes to determinand labels): _E = eutrophication, _A = acidifiction, _G = general degradation, H = hydromorphological pressures.

Water category	Biological quality element	Determinand code	Determinand label	No. of status class values	No. of normalised EQR values
RW	PB	EEA_124-04-9	PhytobenthosEQR_E	15,670	9,925
RW	MI	EEA_13-03-6	InvertebrateEQR_A	470	469
RW	MI	EEA_13-01-4	InvertebrateEQR_G	20,548	13,106
RW	FI	EEA_14-01-7	FishEQR_G	554	479
RW	FI	EEA_14-02-8	FishEQR_H	570	400
LW	PP	EEA_11-04-1	PhytoplanktonEQR_E	5,788	5,030
LW	MP	EEA_123-04-6	MacrophyteEQR_E	1,571	1,416
LW	FI	EEA_14-01-7	FishEQR_G	281	275
LW	FI	EEA_14-02-8	FishEQR_H	66	0
TW	PP	EEA_11-08-5	PhytoplanktonEQR	253	51
TW	MA	EEA_121-01-7	MacroalgaeEQR	193	65
TW	AN	EEA_122-02-1	AngiospermsEQR	45	4
TW	MI	EEA_13-05-8	InvertebrateEQR	288	163
TW	FI	EEA_14-05-1	FishEQR	44	36
CW	PP	EEA_11-08-5	PhytoplanktonEQR	731	361
CW	MA	EEA_121-01-7	MacroalgaeEQR	186	107
CW	AN	EEA_122-02-1	AngiospermsEQR	94	29
CW	MI	EEA_13-05-8	InvertebrateEQR	401	138
Total				**47,753**	**32,054**

spatial scales and water categories reported that nutrient enrichment was the overriding stressor for lakes, while for rivers the effects of nutrient enrichment were dependent on the specific stressor combination and biological response variable {Birk, 2020 #24}.

The WISE-2 data include data from rivers, lakes, transitional and/or coastal water bodies in 26 countries (Table 1). The data are reported for the following biological quality elements (BQEs) (Table 2): phytobenthos and macroinvertebrates in rivers; phytoplankton and macrophytes in lakes; phytoplankton, macroalgae, angiosperms and invertebrates in coastal and transitional waters; as well as fish in rivers, lakes and transitional waters. Specific information on pressure-response relationships for the different BQEs and water categories can be found in the overview by (Birk et al., 2012) and the references within.

For rivers, phytobenthos is used as an indicator for the impact of nutrient enrichment, based on changes in taxonomic composition of diatoms or non-diatom algae. Macroinvertebrates in rivers respond to several pressures, e.g., organic enrichment, hydromorphological pressures, acidification, or general degradation, which is usually a mixture of point source pollution causing organic enrichment and hydromorphological pressures causing altered habitats. For lakes, phytoplankton is a sensitive indicator for the impact of nutrient enrichment caused by diffuse and point source pollution. Macrophytes are also responding to nutrient enrichment caused by diffuse and point source pollution. In addition, macrophytes respond to siltation and to hydromorphological pressures, but the metrics selected for reporting to WISE-2 are those responding to nutrient enrichment. Likewise, the determinands for coastal and transitional waters have been selected as those most suitable to indicate the ecological status of water bodies in these water categories.

The biology data include the status classes (high, good, moderate, poor, bad) for each determinand, as a mandatory element in the SoE data reporting. The ecological status assessment is based on the ecological quality ratio (EQR values) as required by the Water Framework Directive (WFD). Reporting of EQR values is not mandatory but strongly encouraged. The EQR is a measure of the deviation from reference conditions for each biological quality element (BQE). The national metrics used to measure the EQR are normally based on a general response to increasing pressure seen as a decrease of the sensitive taxa usually dominating under reference conditions and an increase of tolerant taxa, and a change in abundance for some of the metrics (e.g., increase in phytoplankton chlorophyll). The national EQR values reported by each country are normalised to a common scale, either by the reporters or by the EEA as part of the data processing (see section Calculation and processing of normalised EQR values).

Biological data can also be reported to WISE-SoE in absolute scale (original metric scale) for certain determinands for phytoplankton: Chlorophyll a, Cyanobacteria biomass, Cyanobacteria proportion and Total phytoplankton biomass. These determinands are also relevant for an aquatic biological indicator, but are subject to another data flow (WISE-6 water quality) for data-technical reasons. Therefore, these data will not be presented further in this paper.

2.2 Data sources

Waterbase is the generic name given to the EEA's databases on the status and quality of Europe's rivers, lakes, groundwater bodies and transitional, coastal and marine waters, on the quantity of Europe's water resources, and on the emissions to surface waters from point and diffuse sources of pollution. Waterbase data is collected and published to produce comparable indicators of pressures, state and impacts on European waters. Waterbase is intended for a European-wide scale of analysis. It is not intended for assessing compliance with any European Directive or any other legal instrument. Information on the national and sub-national scales should be sought from other sources.

Data reported to WISE-2 Biology are published in Waterbase Biology (https://www.eea.europa.eu/data-and-maps/data/waterbase-biology-1), which comprises four tables: EQR values by site, EQR values by water body, classification procedures, and spatial data (derived from WFD and from WISE-5). The WISE-2 Biology data presented in Section 2 were downloaded from the 2021 version of Waterbase Biology, published 16.05.2022 (see Data Availability Statement). This database contains all officially reported and quality-assured biological data from the first reporting cycle in 2011 until the 2021 reporting cycle, which ended in January 2022. Additional data may have been delivered but not passed the automatic quality checking in the Central Data Repository (https://cdr.eionet.europa.eu). The overviews reported here used data from the following tables:

1) Waterbase_v2021_1_T_WISE2_BiologyEQRData. Data reported by monitoring site. Mandatory values: determinand status class, i.e., status class at the determinand level (impact-specific BQE). Recommended values: national EQR values and/or normalised EQR values (nEQR).
2) Waterbase_v2021_1_T_WISE2_BiologyEQRDataByWaterbody. Data as above but aggregated to waterbody level before reporting.
3) Waterbase_v2021_1_T_WISE2_BiologyEQRClassificationProcedure. National class boundaries used for calculation of nEQR values from the reported national EQR values for each determinand. (Some countries have multiple impact-specific determinands for the same BQE, e.g., for invertebrates' responses to acidification and general degradation).
4) Waterbase_v2021_1_T_WISE4_MonitoringSite_DerivedData. This table provides a link from monitoringSiteIdentifier to waterBodyIdentifier and coordinates (longitude and latitude).

Spatial information for the water bodies of biology data includes information on water category, water body type, natural/artificial/highly modified water body, and coordinates. This information was extracted from the WISE-WFD database as far as possible (i.e., for all water bodies already reported to the WFD). For the remaining water bodies (e.g., for EEA member states not reporting to the WFD), the spatial information was extracted from EEA's WISE-5 Spatial data flow.

The overview of the four tables (https://www.eea.europa.eu/data-and-maps/data/waterbase-biology/#tab-european-data) contains a definition of each element (i.e., table column), including additional metadata information for individual records such as the status and the reliability of the record. Further information for all tables, elements and allowable values (codes) are available from the WISE-2 data dictionary (https://dd.eionet.europa.eu/datasets/latest/WISE-SoE_Biology). The published data furthermore contains fields with metadata information such as the version ID, status code, observation status, and statements from expert-based quality checking.

The metadata associated with this dataset (https://www.eea.europa.eu/data-and-maps/data/waterbase-biology-1/#tab-metadata) provides more information on the reporting obligation (WISE SoE Biology data), the rights to use, disclaimers, methodology and data sources. For more detailes, see the Data Availability Statement.

As a more user-friendly alternative to downloading tables from Waterbase with additional functionalities, the Discodata server (https://discodata.eea.europa.eu/) is a public tool and service where anybody can access data published by the European Environment Agency (EEA). It offers two functionalities: A human-readable web application to inspect and query databases using Structured Query Language (SQL), and a machine-readable application programming interface (API) to get data from databases, using SQL queries, as JavaScript Object Notation information.

Biological data in EQR scale were extracted from the tables BiologyEQRData and BiologyEQRDataByWaterbody. The number of status class values and normalised EQR values available for each determinand is shown in Table 2. Data reporters have also been encouraged to report more of their existing monitoring data to WISE-2 to fill the gaps both in space, time and taxonomy (biological quality elements).

2.3 Calculation and processing of normalised EQR values

All countries reporting to WFD have developed national classification systems for assessment of ecological status based on EQR values. However, the boundaries defined between status classes (e.g., Good/Moderate) in national EQR scale vary among countries, as well as among determinands and water body types (Birk et al., 2012). For example, the Good/Moderate boundary of a given BQE could be 0.62 in one country and 0.66 in another case; an EQR value of 0.64 would then mean Good status in the former case but Moderate status in the latter case. This means that national EQR values are not directly comparable between countries, without considering the distance to their respective class boundaries (Birk et al., 2013). Therefore, the national EQR values are being normalised to a scale of 0–1, in order to obtain a consistent scale across all countries (Figure 3). On the normalised scale, the status

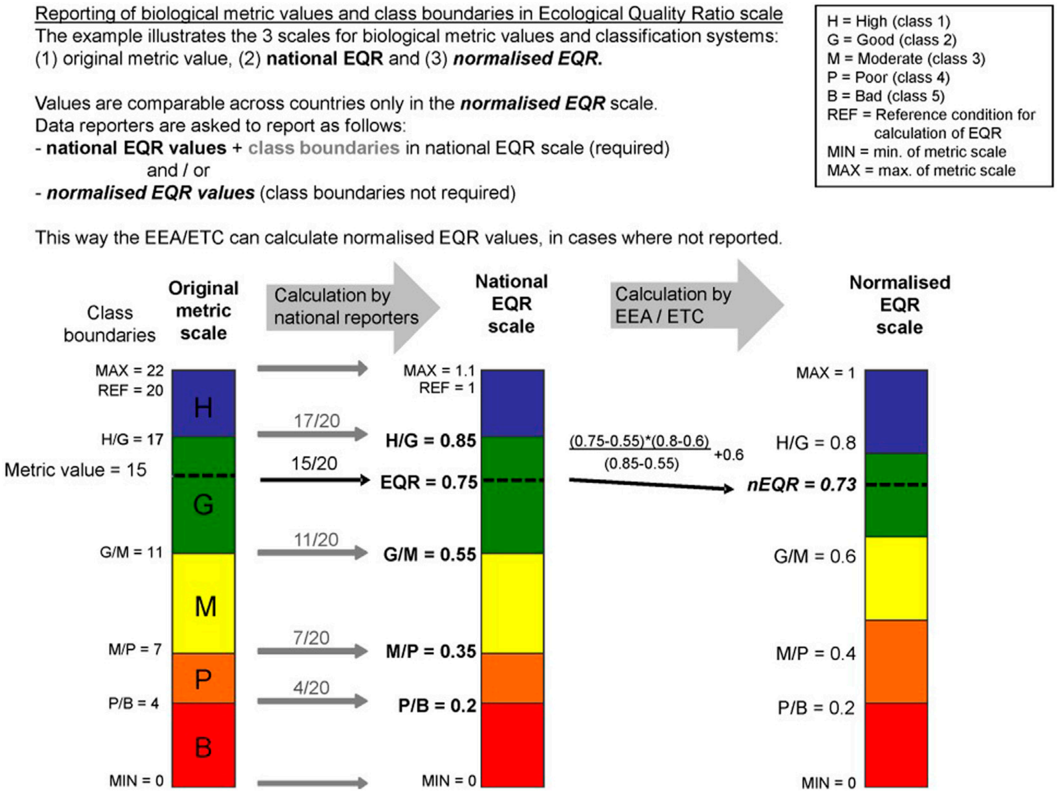

Reporting of biological metric values and class boundaries in Ecological Quality Ratio scale
The example illustrates the 3 scales for biological metric values and classification systems:
(1) original metric value, (2) **national EQR** and (3) ***normalised EQR.***

Values are comparable across countries only in the ***normalised EQR*** scale.
Data reporters are asked to report as follows:
- **national EQR values** + class boundaries in national EQR scale (required)
and / or
- ***normalised EQR values*** (class boundaries not required)

This way the EEA/ETC can calculate normalised EQR values, in cases where not reported.

H = High (class 1)
G = Good (class 2)
M = Moderate (class 3)
P = Poor (class 4)
B = Bad (class 5)
REF = Reference condition for calculation of EQR
MIN = min. of metric scale
MAX = max. of metric scale

FIGURE 3
Example of calculation of normalised ecological quality ratios (EQRs) from national EQRs. Colour codes represent ecological status classes: blue = H(igh), green = G(ood), yellow = M(oderate), orange = P(oor), red = B(ad). REF = reference condition, defined as the metric value of unimpacted water bodies. Note that the maximum value of the metric scale can exceed the reference condition, therefore the national EQR value can exceed 1. Source: https://dd.eionet.europa.eu/datasets/latest/WISE-SoE_Biology/tables/BiologyEQRData.

class boundaries are identical for all countries (high: 0.8–1.0, good: 0.6–0.8, moderate: 0.4–0.6, poor: 0.2–0.4, bad: 0.0–0.2). An EQR value identical to the boundary between two status classes belongs to the worse of the two status classes.

The conversion from national to normalised EQR requires the information on class boundaries (in EQR scale) which can be specific for the determinand and for the national water body type, as well as for natural vs. artificial and highly modified water bodies. The normalised EQR are calculated using the formula:

$$\begin{aligned}\text{normalisedEQR} = {} & (\text{EQR} - \text{LowerBoundaryEQR}) \\ & \times 0.2/(\text{UpperBoundaryEQR} - \text{LowerBoundaryEQR}) \\ & + \text{LowerBoundaryNormEQR}\end{aligned}$$

where LowerBoundaryEQR and UpperBoundaryEQR are the lower and upper status class boundaries in the national EQR scale, respectively, the factor 0.2 is the width of any status class at the normalised EQR scale, and LowerBoundaryNormEQR is the lower class boundary in the normalised EQR scale. The calculation can be performed by the WISE-2 reporters before reporting, or by EEA after reported if sufficient information is provided on the national classification system.

To maximise the number of so-called indicator values for aggregated time series plots and for trend analysis, missing yearly values were replaced with imputed values as far as possible. Gaps of up to 3 years within a data series have been interpolated as the average of the previous and following years. Likewise, gaps of up to 3 years at the beginning or end of a series were extrapolated to be identical as the first or last available value. This procedure follows the methodology used for the EEA indicator “Nutrients in Freshwater”, as described in its Supplementary Material section (https://www.eea.europa.eu/ims/nutrients-in-freshwater-in-europe).

3 Overview of data reported to WISE-2 biology

3.1 Quantity and quality of data reported to WISE-2

The official biology data reporting started in 2011 (with records from sampling year 2010), after 2 years of test reporting in 2009-2010. The published dataset Waterbase - Biology 2021, which is based on WISE-2 reporting from 2021, now contains more than 47,000 indicator values in the form of ecological status class, and more than 32,000 indicator values quantified as normalised EQR values. These data are reported from more than 11,000 river waterbodies, 1,800 lake water bodies, 260 transitional water

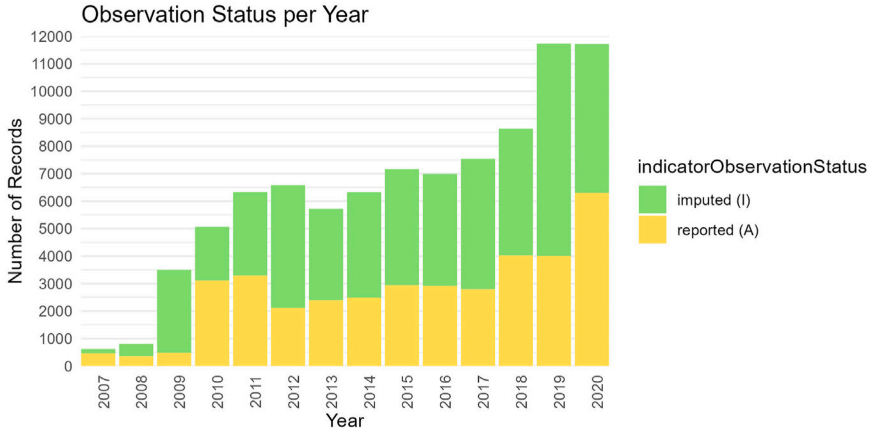

FIGURE 4
Number of indicator values reported and imputed for the years 1990–2020. Indicator values are unique combinations of water bodies (Table 1) and determinands (Table 2). Imputed indicator values result from interpolation and extrapolation of time series (described in Section 2.3). Data source: Waterbase Biology 2021.

bodies and 440 coastal water bodies, in 26 countries (Table 1). The dataset from rivers is dominated by Spain, Italy, Poland and Lithuania, while the dataset from lakes are dominated by Sweden and Poland. Italy is currently also the dominating country in reporting from transitional and coastal waters.

The biological data described in this report are available from approximately 13,500 waterbodies. The majority of waterbodies have values from 1–5 years (Figure 1), while a few water bodies have series lasting 15 years. The number of waterbodies in the WFD database is an order of magnitude higher, but so far only from three reporting years. For the WISE-SoE data, the longer series and the more detailed data type both contribute to higher probability of detecting temporal trends with statistical significance.

Normalised EQR values are now available for the majority of water bodies with status class reported (Table 1). A few countries have still reported only status class (e.g., Switzerland, Germany, Denmark and Portugal).

WISE-2 contains >3,000 indicator values (reported or imputed) for each of the sampling years from 2009 to 2020 (Figure 4). The latest year of reporting in 2021 (sampling year 2020) resulted in more than 6,000 reported indicator values, and almost 12,000 indicator values when imputed values are included.

3.2 Spatial patterns in reported ecological status class

The maps (Figure 5) display the latest BQE status (or potential) class of each waterbody (from Waterbase Biology 2019). The left panel shows the reported determinand status class for valid determinands and aggregated to the BQE level, while the right panel shows the BQE status class calculated based on available nEQR values. The lack of coloured points in the right panel is due to lack of reported EQR data or class boundaries in only a few cases (e.g., Switzerland, Germany, Denmark). The missing values are usually due to missing coordinates, inconsistencies in the spatial information or other technical issues. The map of invertebrates in rivers does not include the determinand InvertebrateEQR_A (response to acidification), due to the limited geographic representativity (United Kingdom, Germany, Norway, Sweden).

Earlier versions of WISE-SoE Biology maps have been published previously (2015, last modified 2019):

- https://www.eea.europa.eu/data-and-maps/explore-interactive-maps/phytobenthos-in-rivers
- https://www.eea.europa.eu/data-and-maps/explore-interactive-maps/macroinvertebrates-in-rivers
- https://www.eea.europa.eu/data-and-maps/explore-interactive-maps/phytoplankton-in-lakes
- https://www.eea.europa.eu/data-and-maps/explore-interactive-maps/macrophytes-in-lakes

3.3 Temporal patterns of normalised EQR aggregated to European level

This section shows one example of how the time series for individual water bodies can be aggregated to trans-national level in different ways - here by the geographic regions of Europe (defined in Table 1). Other types of aggregation that has been explored for these data are by initial ecological status class as well as to the pan-European level (not shown here). The selection of data series includes only waterbodies nEQR values for all 8 years 2011–2018 after the imputation of missing values (described in the section Calculation and processing of normalised EQR values).

When all indicator value series are aggregated to the European level, the time series so far display only weak tendencies (not shown here). Invertebrates in rivers show a decrease from the upper range to the lower range of good status, which is the WFD management target. This tendency would not have been possible to document from reporting of ecological status class only. For the three botanical BQEs, the aggregated time series do not display any clear or monotonous trend.

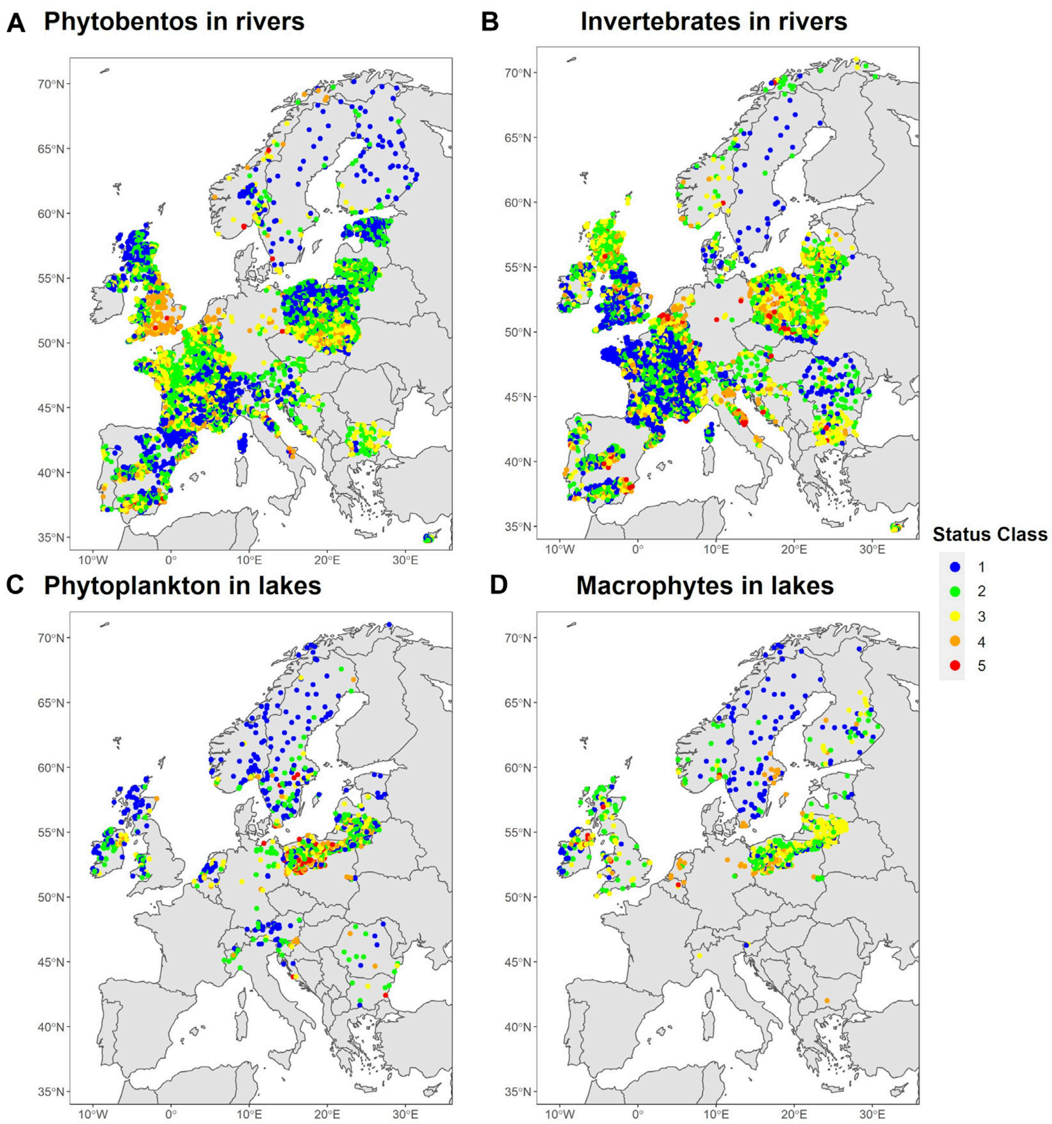

FIGURE 5
Spatial patterns in ecological status: Reported ecological status class for a selection of biological quality elements: **(A)** phytobenthos in rivers, **(B)** invertebrates in rivers, **(C)** phytoplankton in lakes, **(D)** macrophytes in lakes (see also Table 2). For each water body, the latest reported value is used. Colour code: blue = High, green = Good, yellow = Moderate, orange = Poor, red = Bad. Colour code for artificial and highly modified water bodies with incomplete class boundaries: green = good potential, orange = moderate/poor/bad. Data source: Waterbase Biology 2019.

The time series aggregated by geographic region (Figure 6) reveal more differences. For example, the invertebrate nEQR values reported from Eastern Europe show a decreasing trend from the mid-range to the lower range of Good status, approaching the Good/Moderate boundary. Moreover, invertebrates nEQR values reported from Southern Europe show a decreasing trend from High to the upper range of Good status, but this trend is based on 3 series only. (More series of invertebrates have been reported from Southern Europe recently, but most series have length up to 5 years, and are therefore not yet included in this figure). The average invertebrate nEQR values in Western Europe, which is the region with the highest number of series, has been fluctuating below the Good/Moderate boundary until 2015 and remained just above boundary since 2016.

As another example, phytoplankton values reported from Eastern Europe started in the upper range Moderate status, and barely reached Good status in the period 2013–2016. Since 2017, the nEQR values have returned to the upper range of Moderate status. In this example, reporting of WFD status classes only show Good status for the period 2013–2016, without revealing that the ecological status was still very close to the Good/Moderate boundary, implying a high risk of decline back to Moderate status.

The number of complete series per BQE is unevenly distributed among the regions of Europe. Western Europe has the highest number of both phytobenthos ($n = 230$) and invertebrates ($n = 221$) in rivers. A high number of series from rivers are also reported from East (phytobenthos: $n = 199$) and Southeast (invertebrates: $n = 70$). Northern Europe has the most series of lake phytoplankton ($n = 117$). However, the count of complete series depends on the criteria set; for example, setting the start year to 2012 will result in a higher number of series.

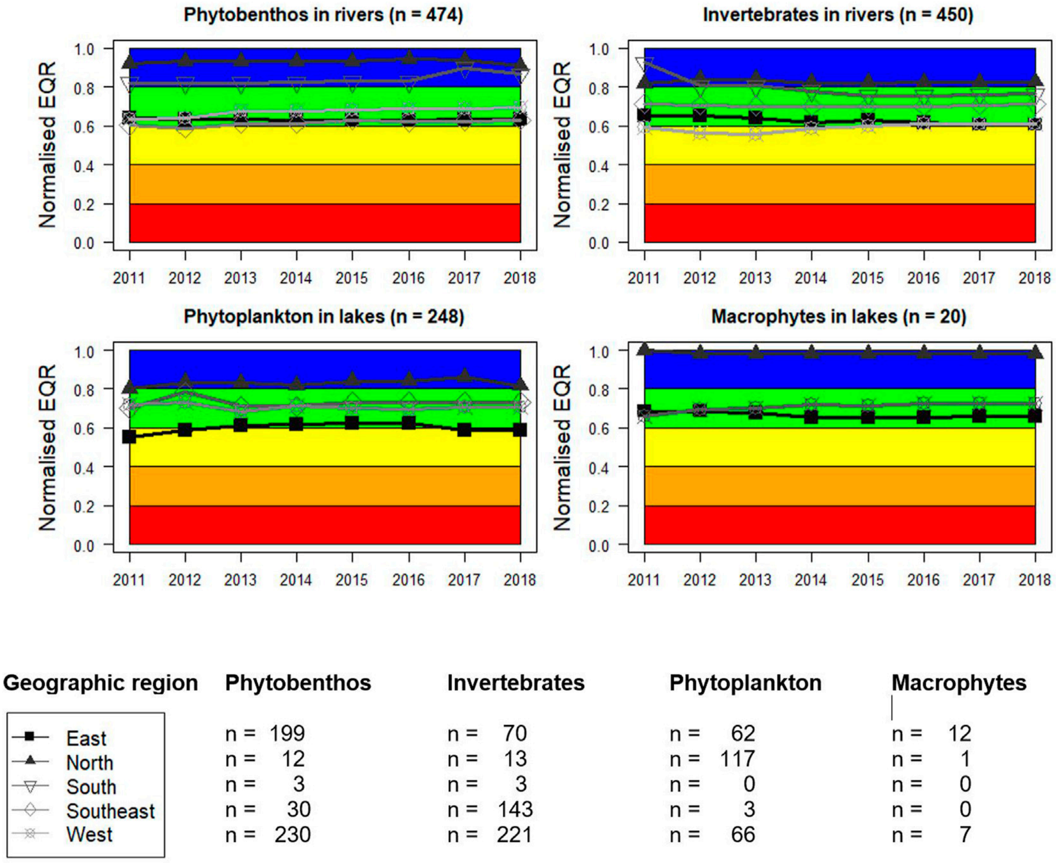

Geographic region	Phytobenthos	Invertebrates	Phytoplankton	Macrophytes
East	n = 199	n = 70	n = 62	n = 12
North	n = 12	n = 13	n = 117	n = 1
South	n = 3	n = 3	n = 0	n = 0
Southeast	n = 30	n = 143	n = 3	n = 0
West	n = 230	n = 221	n = 66	n = 7

FIGURE 6
Temporal patterns in ecological status: Time series of normalised EQR values for the years 2011–2018 aggregated by geographic regions of Europe (see Table 1). The numbers above the plots show the total number of water bodies for each BQE. The number of water bodies per geographic region for each BQE is given below the figure. Data source: Waterbase Biology 2019.

Obtaining a representative picture of pan-European trends across will require time series from a higher number of waterbodies than what has reported until now, and better representativity both across geographic regions and across the different status classes. For the version of Waterbase Biology presented here (published 2019), assessments can only be representative for certain geographic regions with high coverage of water bodies. Nevertheless, these figures give an indication of the type of results and trends that can be obtained from the reported SoE biology data at the nEQR scale.

4 Potential use of WISE-2 biology data

4.1 Development of an aquatic biological indicator for EEA

The biological data (normalised EQR values) accumulated in Waterbase since 2010 have the potential to be applied as an indicator of environmental status and trends in regions of Europe, in a similar way as nutrients data reported to WISE-6. Assessment of the nutrients data show that nutrient conditions in European surface waters have improved in recent decades, as the average nitrate and phosphate concentrations in rivers and total phosphorus concentration in lakes have decreased (https://www.eea.europa.eu/ims/nutrients-in-freshwater-in-europe). The data reported to WISE-2 Biology can be supplemented by the phytoplankton data reported in original metric scale stored in WISE-6 (Water quality), including data on chlorophyll and cyanobacteria in original metric scale, as these are clear indicators of eutrophication in lakes (Ho et al., 2019). Moreover, the biology data can be analysed as responses to the chemical data in WISE-6 representing specific pressures (Phillips et al., 2008). Preliminary analyses (not shown) suggest that the biological determinands show significant relationships with the selected general physico-chemical quality elements, such as total phosphorus representing eutrophication, and biological oxygen demand representing general degradation. However, these estimated relationships also contain large variation, which warrants more detailed analysis.

As the biology data provide longer time series with each reporting year, analysis of the series can be used to address questions such as:

- Can we see any progress in ecological status for biology in rivers and lakes, in response to the decrease in nutrients and BOD concentrations reported for freshwater indicators?
- Are further measures to reduce pressures needed to achieve progress in the biological conditions in rivers and lakes?

- Is there a time lag in the biological response to the decrease in nutrients and organic pollution?
- Will the European Green Deal make progress towards restoration of biodiversity in rivers and lakes?

A biological indicator can be developed with a similar structure as the existing indicator "Nutrients in freshwater" (https://www.eea.europa.eu/data-and-maps/ indicators/nutrients-in-freshwater/nutrients-in-freshwater-assessment-published-6), but could be specific to regions or and/or broad water types, which may have different levels of environmental pressures (Lyche Solheim et al., 2019). However, dynamic tableaus with an online user interface will be preferable to static pictures. Further work on an aquatic biological indicator based on the WISE-2 data is planned to take place within the European Topic Center on Biodiversity and Ecosystems (ETC BE, 2023–2026) (https://www.eionet.europa.eu/etcs/etc-be).

The indicator outlined here is related to specific policy targets of the Water Framework Directive (WFD) "good ecological status" of rivers and lakes and prevention of deterioration of ecological status, also including no deterioration from high to good or worse. The indicator can also be linked to other water related directives, e.g., the Nitrates Directive (91/676/EEC) dealing with pollution pressures from agriculture and the Urban Wastewater Directive (91/271/EEC), as well as to the Habitats Directive target of favourable conservation status for freshwater habitats and species and the EU Biodiversity strategy 2020. Diffuse pollution from agriculture is still one of the most important pressures on European rivers and lakes (EEA, 2018). Indicators showing the biological impacts of this pollution are essential to plan pollution reduction measures and assess their effectiveness in terms of improvements of ecological status. Most of the BQEs included in this dataflow are particularly sensitive to nutrients and/or organic pollution.

The biological data would provide a better aquatic SEBI (Streamlined European Biodiversity Indicator) (Feest, 2013) than the currently used abiotic indicators. The overall ecological status class is not a good option because it is less comparable across countries than the BQE status class, due to different combination rules for BQEs vs. supporting quality element, and since overall ecological status class is reported only once every 6 years. In addition, the uncertainty associated with the classification of each individual BQE is accumulated at the water body level (Moe et al., 2015).

4.2 Use of WISE-2 biology data through EuropaBON

The project EuropaBON (https://europabon.org/) work package 3.1 has developed a web-based platform to collect and record the current biodiversity data workflows across Europe, with the underlying database (https://monitoring.europabon.org/monitoring). The purpose of this database is to give an overview of existing biodiversity datasets and describe the major workflows used to generate and use these data in policy and research environments. The focus of WP3.1 is not to map all monitoring initiatives in Europe, but to ensure that those monitoring initiatives providing data for current biodiversity workflows are well represented in the underlying database. This database will help understand how biodiversity data collected in monitoring schemes across Europe flows through different institutions and programs and gets processed to produce Essential Biodiversity Variables (EBVs) and Ecosystem Services Indicators (ESS) other EU policy-relevant indicators. The term "integration initiatives" refers to each one of these full biodiversity data workflows. The priority is to collect integration initiatives at the European level, but integration initiatives at lower levels (e.g., National) are also be accommodated.

The compilation of national datasets and reporting to WISE-2 as a European integration node is illustrated in (Figure 7), using the EuropaBON database's visualisation tool. In total 157 national biology datasets from WISE-2 are reported in the EuropaBON database, where each biological quality element constitutes a separate dataset (Table 2). The European-level integration node (WISE-2; by EEA) and the national-level integration nodes (national WISE-2 deliveries; typically by national environmental agencies) have so far been completed with the information that is publicly available for all countries. The national integration node for Norway has been elaborated with more details on the underlying biodiversity data, monitoring methods and indicator calculation from three ecological monitoring programmes, as well as contact persons for the national data flow. These types of information can also be registered for other countries, if made available to the EuropaBON project Additional information on the national dataset that can be extracted from Waterbase Biology, such as the number of water bodies per dataset, as well as the first and last sampling year of sampling, has also been registered in the EuropaBON database. This additional information is displayed in the Supplementary Material.

The concept of Essential Biodiversity Variables (EBVs) was introduced to structure biodiversity monitoring globally, and to harmonize and standardize biodiversity data from disparate sources to capture a minimum set of critical variables required to study, report and manage biodiversity change. (Kissling et al., 2018). The list of EBVs has been used as an analytical framework to help bridge the gap between biodiversity data and policy reporting needs (Geijzendorffer et al., 2016). Within EuropaBON, EBVs have been defined for terrestrial, freshwater and marine ecosystems by the research partners in close dialogue with stakeholders (Moersberger et al., 2022), and is currently being further specified in another deliverable from the EuropaBON project (D4.1) (Junker et al., 2023). Three of the groups of EBVs are particularly relevant to WISE-2 Biology data:

1) Species distribution and abundance, incl. macrophytes, invertebrates, fish.
2) Community composition, including EQR values for all BQEs.
3) Ecosystem structure, including distribution of EUNIS inland water habitats, which are mostly comparable to broad surface water body types (Lyche Solheim et al., 2019).

A fourth group of EBVs is Ecosystem function, which includes harmful algal blooms (i.e., cyanobacteria biomass) is reported to WISE-6.

Regarding the need for data on community composition (group 2 above), the data flow through WISE-2 is already established and the normalised EQR values are comparable across countries. However, the spatial and temporal

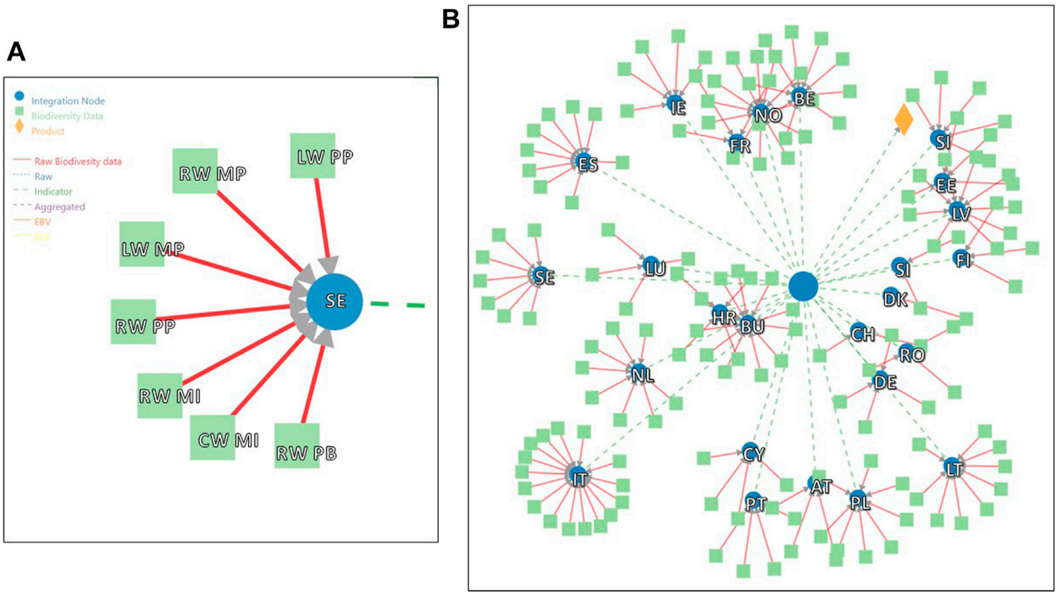

FIGURE 7
Integration of biodiversity data flows within WISE-2 as registered in and visualised by the EuropaBON database (simplified diagrams). **(A)** Example of a national integration node (Sweden) with each biodiversity dataset labelled (for abbreviations, see Table 1; Table 2); **(B)** overveiw of all national integration nodes (individual biodiversity datasets not labelled). The large blue circle represents the European integration node (WISE-2); the smaller blue circles represent national integration nodes (e.g., databases at national environmental agencies). Red lines represent original biological monitoring data compiled at the national integration nodes; dashed green lines represent indicator values (EQR values) compiled at the European integration node.

resolution is currently insufficient for assessing representative spatial status and trends in biodiversity. The EQR data are based on taxonomic analysis of samples from stations used for WFD surveillance and/or operational monitoring. If these underlying data could become accessible, they would support the EBV group 1 above as a basis for further species modeling at the European scale.

4.3 Conclusion and outlook

Biological data have been reported as EQR values from 26 countries, mostly from river and lakes, and to a lower degree from transitional and coastal waters. The growing number of records and water bodies, as well as the growing length of the time series, suggest that these indicator values can become useful in assessments of ecological status and trends in Europe. The use of normalised EQR values enables both analysis of geographical and temporal patterns, as well as statistical trend analysis, with higher resolution than the status class data reported to WFD. However, the WISE-2 Biology data still show large variations in number of sites and years among countries, which indicate challenges concerning geographical representativity in the context of a European-scale indicator. To obtain more representative data, reflecting the actual distribution of status classes, the countries should report more data from water bodies in less than good status, which are mainly included in the operational monitoring programmes.

While the normalised EQR values presented here can serve as essential biodiversity variables, as they show the deviation from natural aquatic biodiversity at the community composition level, the underlying georeferenced species data could provide an added value for biodiversity modeling and assessment, if those data were accessible. We hope that the information provided on the national WISE-2 data flows in the EuropaBON monitoring database, currently and in future updates, can help to provide a connection from these national data resources to support assessment and conservation/restoration of biodiversity in aquatic ecosystems.

Data availability statement

The original contributions presented in the study are included in the article/Supplementary Material, further inquiries can be directed to the corresponding author.

Author contributions

Conceptualization: ALS and SJM; methodology: SJM and ALS; software: SJM; validation: SJM and ALS; formal analysis: SJM; data curation: SJM and SM; writing—original draft: SJM and ALS; writing—review and editing: SJM, SAW, SM, and ALS; visualization: SJM, SAW, and SM; supervision: SJM and ALS; project administration: SJM and ALS; funding acquisition: ALS and SJM. All authors contributed to the article and approved the submitted version.

Funding

This paper has been written within the project EuropaBON (Grant agreement No. 101003553, EU Horizon 2020 Coordination and Support Action). The author's work with WISE-2 has been carried out within the European Topic Centre on Inland, Coastal and Marine waters (ETC/ICM), an international consortium working with the European Environment Agency (EEA) under a Framework Partnership Agreement for the periods 2014—2018 (No. EEA/NSV/13/002-ETC/ICM) and 2019—2022 (No. OCP/EEA/NSS/18/002-ETC/ICM). The WISE-2 data flow has been established and operated in collaboration with several persons at EEA, including Peter Kristensen, Monika Peterlin, Marek Staron, Fernanda Nery and Jørgen Olsen. Colleagues at NIVA are acknowledged for support with data processing: Kari Austnes, Jan-Erik Thrane, Eivind E. Andersen, Jonas Persson and Cathrine Gundersen.

Acknowledgments

The WISE-2 data flow has been established and operated in collaboration with several persons at EEA, including Peter Kristensen, Monika Peterlin, Marek Staron, Fernanda Nery and Jørgen Olsen. Colleagues at NIVA are acknowledged for support with data processing: Kari Austnes, Jan-Erik Thrane, Eivind E. Andersen, Jonas Persson and Cathrine Gundersen. We thank Alejandra Moran-Ordóñez, David Martí and other collaborators from EuropaBON for support with entering the WISE-2 information into the EuropaBON database.

Conflict of interest

The authors declare that the research was conducted in the absence of any commercial or financial relationships that could be construed as a potential conflict of interest.

Publisher's note

Supplementary material

The Supplementary Material for this article can be found online at: https://www.frontiersin.org/articles/10.3389/fenvs.2023.1057742/full#supplementary-material

References

Balvanera, P., Brauman, K. A., Cord, A. F., Drakou, E. G., Geijzendorffer, I. R., Karp, D. S., et al. (2022). Essential ecosystem service variables for monitoring progress towards sustainability. *Curr. Opin. Environ. Sustain.* 54, 101152. doi:10.1016/j.cosust.2022.101152

Birk, S., Bonne, W., Borja, A., Brucet, S., Courrat, A., Poikane, S., et al. (2012). Three hundred ways to assess Europe's surface waters: An almost complete overview of biological methods to implement the Water Framework Directive. *Ecol. Indic.* 18, 31–41. doi:10.1016/j.ecolind.2011.10.009

Birk, S., Willby, N. J., Kelly, M. G., Bonne, W., Borja, A., Poikane, S., et al. (2013). Intercalibrating classifications of ecological status: Europe's quest for common management objectives for aquatic ecosystems. *Sci. Total Environ.* 454-455, 490–499. doi:10.1016/j.scitotenv.2013.03.037

European Commission (2000). Directive 2000/60/EC of the European parliament and of the Council establishing a framework for the community action in the field of water policy. The water framework directive (WFD).

European Environment Agency (2018). European waters - assessment of status and pressures. EEA Report No 7/2018. ISSN 1977-8449.

European Environment Agency (2019). The European environment — State and outlook 2020. Knowledge for transition to a sustainable Europe.

Feest, A. (2013). The utility of the streamlining European biodiversity indicators 2010 (SEBI 2010). *Ecol. Indic.* 28, 16–21. doi:10.1016/j.ecolind.2012.10.015

Geijzendorffer, I. R., Regan, E. C., Pereira, H. M., Brotons, L., Brummitt, N., Gavish, Y., et al. (2016). Bridging the gap between biodiversity data and policy reporting needs: An Essential Biodiversity Variables perspective. *J. Appl. Ecol.* 53, 1341–1350. doi:10.1111/1365-2664.12417

Hering, D., Borja, Á., Carvalho, L., and Feld, C. K. (2013). Assessment and recovery of European water bodies: Key messages from the WISER project. *Hydrobiologia* 704, 1–9. doi:10.1007/s10750-012-1438-9

Hering, D., Carvalho, L., Argillier, C., Beklioglu, M., Borja, A., Cardoso, A. C., et al. (2015). Managing aquatic ecosystems and water resources under multiple stress — an introduction to the MARS project. *Sci. Total Environ.* 503-504, 10–21. doi:10.1016/j.scitotenv.2014.06.106

Ho, J. C., Michalak, A. M., and Pahlevan, N. (2019). Widespread global increase in intense lake phytoplankton blooms since the 1980s. *Nature* 574, 667–670. doi:10.1038/s41586-019-1648-7

Junker, J., Beja, P., Brotons, L., Fernandez, M., Fernández, N., Kissling, W. D., et al. (2023). D4.1. List and specifications of EBVs and EESVs for a European wide biodiversity observation network. ARPHA Preprints. doi:10.3897/arphapreprints.e102530

Kissling, W. D., Ahumada, J. A., Bowser, A., Fernandez, M., Fernández, N., García, E. A., et al. (2018). Building essential biodiversity variables (EBVs) of species distribution and abundance at a global scale. *Biol. Rev.* 93, 600–625. doi:10.1111/brv.12359

Lyche Solheim, A., Globevnik, L., Austnes, K., Kristensen, P., Moe, S. J., Persson, J., et al. (2019). A new broad typology for rivers and lakes in Europe: Development and application for large-scale environmental assessments. *Sci. Total Environ.* 697, 134043. doi:10.1016/j.scitotenv.2019.134043

Moe, S. J., Haande, S., and Couture, R.-M. (2016). Climate change, cyanobacteria blooms and ecological status of lakes: A bayesian network approach. *Ecol. Model.* 337, 330–347. doi:10.1016/j.ecolmodel.2016.07.004

Moe, S. J., Lyche Solheim, A., Soszka, H., Gołub, M., Hutorowicz, A., Kolada, A., et al. (2015). Integrated assessment of ecological status and misclassification of lakes: The role of uncertainty and index combination rules. *Ecol. Indic.* 48, 605–615. doi:10.1016/j.ecolind.2014.08.018

Moersberger, H., Martin, J. G. C., Junker, J., Georgieva, I., Bauer, S., Beja, P., et al. (2022). Europa biodiversity observation network: User and policy needs assessment. ARPHA Preprints 3.

Morán-Ordóñez, A., Beja, P., Fraixedas, S., Herrando, S., Junker, J., Kissling, W. D., et al. (2023). D3.3 Identification of current monitoring workflows and bottlenecks. ARPHA Preprints. doi:10.3897/arphapreprints.e103765

Pereira, H. M., Ferrier, S., Walters, M., Geller, G. N., Jongman, R. H. G., Scholes, R. J., et al. (2013). Essential biodiversity variables. *Science* 339, 277–278. doi:10.1126/science.1229931

Pereira, H. M., Junker, J., Fernández, N., Maes, J., Beja, P., Bonn, A., et al. (2022). Europa biodiversity observation network: Integrating data streams to support policy. ARPHA Preprints 3.

Phillips, G., Pietiläinen, O. P., Carvalho, L., Solimini, A., Lyche Solheim, A., and Cardoso, A. C. (2008). Chlorophyll–nutrient relationships of different lake types using a large European dataset. *Aquat. Ecol.* 42, 213–226. doi:10.1007/s10452-008-9180-0

Santana, J., Porto, M., Brotons, L., Junker, J., Kissling, W. D., Lumbierres, M., et al. (2023). D3.2 Report on gaps and important new areas for monitoring in Europe. ARPHA Preprints. doi:10.3897/arphapreprints.e103657

frontiers | Frontiers in Environmental Science

TYPE Original Research
PUBLISHED 06 July 2023
DOI 10.3389/fenvs.2023.1075458

OPEN ACCESS

EDITED BY
Caterina Bergami,
National Research Council (CNR), Italy

REVIEWED BY
Pilar Diaz-Tapia,
Spanish Institute of Oceanography (IEO),
Spain
Luigi Piazzi,
University of Sassari, Italy

*CORRESPONDENCE
Antonella Petrocelli,
✉ antonella.petrocelli@irsa.cnr.it

RECEIVED 20 October 2022
ACCEPTED 21 June 2023
PUBLISHED 06 July 2023

CITATION
Petrocelli A, Wolf MA, Sciuto K, Sfriso A, Rubino F, Ricci P and Cecere E (2023), Long-term data prove useful to keep track of non-indigenous seaweed fate. *Front. Environ. Sci.* 11:1075458. doi: 10.3389/fenvs.2023.1075458

Long-term data prove useful to keep track of non-indigenous seaweed fate

Antonella Petrocelli[1]*, Marion Adelheid Wolf[2], Katia Sciuto[3], Adriano Sfriso[2], Fernando Rubino[1], Pasquale Ricci[4] and Ester Cecere[1]

[1]Institute for Water Research (IRSA)-CNR, Taranto, Italy, [2]Department of Environmental Sciences, Informatics and Statistics, University of Venice Ca' Foscari, Venice, Italy, [3]Department of Chemical, Pharmaceutical and Agricultural Sciences, University of Ferrara, Ferrara, Italy, [4]Department of Biosciences, Biotechnologies, and Environment, University of Bari, Bari, Italy

The Mar Piccolo of Taranto (southern Italy, Mediterranean Sea), a site of the European LTER network, is a transitional water system, where a century-old intensive mussel farming activity has been carried out, together with an intense import-export business of bivalve mollusks. Previous studies showed that this basin is third for NIS seaweed introduction in the Mediterranean Sea, after the Thau Lagoon and the Venice Lagoon. The present paper deals with the results of 11-year monitoring activity on non-indigenous species (NIS) of seaweeds, which was performed in the Mar Piccolo. In the studied period (2011–2021), two different time frames (i.e., 2011–2015 and 2016–2021) were considered, since they were based on a different number of sampling sites. To investigate spatial and temporal differences in the seaweed assemblage, a multivariate analysis was performed considering the NIS and the most important native species in terms of temporal occurrence. Fourteen NIS were recorded in total in the Mar Piccolo of Taranto during this period, with variable abundances among sites and years: nine species in the first time period, and thirteen species in the second one. *Caulerpa cylindracea*, recorded with negligible biomass in the first period, was absent in the second-period samplings. Molecular analyses confirmed the taxonomy of three species (i.e., *Grateloupia minima*, *Neopyropia koreana*, and *Polysiphonia morrowii*), previously identified only through morphological features. The most abundant species was *Hypnea corona*, which almost doubled its biomass in the second time period compared to the first one. Three species (i.e., *Caulacanthus okamurae*, *G. minima*, and *P. morrowii*) increased their biomass by an order of magnitude in the second time period. No significant differences were found over years. Site 1 resulted in significant differences among the sites and different seasonal pattern occurred among the investigated sites. No significant long-term changes occurred in the seaweed assemblages, suggesting the absence of strong disturbances due to the settlement of NIS.

KEYWORDS

long term ecological research, Mar Piccolo, Mediterranean Sea, non-indigenous species, seaweeds, transitional water systems

1 Introduction

It is well known that long-term ecosystem observations and measurements are an invaluable means to understanding the causes and consequences of perturbations occurring (Turner et al., 2003). For this reason, Long Term Ecological Research (LTER) networks have been established over the years both at national and international levels, starting from the first United States network that began its activities in 1980 (Callahan, 1984). Nowadays, the LTER series have become a starting point to assess and interpret the effects of climate change and other anthropogenic pressures (Pugnetti et al., 2013; Zingone et al., 2019). In particular, the importance of LTER datasets for biodiversity studies has been underlined (Compagnoni et al., 2020), and the United Nations Convention on Biological Diversity considers them recommended indicators (Zilioli et al., 2019).

Since 2011 the Mar Piccolo of Taranto has been part of the Italian and European LTER network (https://deims.org/ac3f674d-2922-47f6-b1d8-2c91daa81ce1), mainly due to the presence of historical data sets on chemical-physical variables and benthic macrophyte biodiversity (Petrocelli et al., 2021). It is a transitional water system, where intensive mussels farming activity has been carried out for approximately 100 years, as well as a strong import site for bivalve mollusks. For this reason, it is highly exposed to the introduction of non-indigenous species (NIS) (Newton et al., 2014), in particular, seaweeds (Mineur et al., 2014; Wolf et al., 2018). According to Copp et al. (2007), the frequency and success rate of NIS introduction are closely related to propagule pressure too. In Australia, after a boom-population, the invasive *Codium fragile* heavily declined up to densities lower than 2 thalli/m^2, most likely due to the presence of very few propagules with limited viability (Trowbridge et al., 2016). Conversely, in a newly-built marina in Brittany (France) *Undaria pinnatifida* (Harvey) Suringar reached densities of up to 50 specimens/m^2 in 2 years, due to a continuous propagule supply from populations settled on adjacent rocky shores (Salamon et al., 2020). Climate conditions are another important factor that affects the establishment of NIS, becoming more limiting in transitional waters. The tropical *Grateloupia yinggehaiensis* H.W. Wang *et* R.X. Luan had a considerable spread in the industrial area of Porto Marghera (northern Adriatic, Mediterranean Sea), due to the thermal pollution caused by a thermoelectric power plant operating in the area (Wolf et al., 2014).

In the Mar Piccolo of Taranto, the regular and longtime LTER data collection has allowed a continuous update of the basin phytobenthic biodiversity, the prompt detection of newly introduced NIS, the assessment of NIS fate, and the detection of the most important factors for either their success or decline (Petrocelli et al., 2019). For example, two seaweed species have been observed only temporarily and disappeared without establishing in the basin. In June 2012, for the first time and no longer after that date, very few thalli of *Ascophyllum nodosum* (Linnaeus) Le Jolis were observed on sparse pebbles in the Mar Piccolo. This species was first reported in the Mediterranean in 2009, after the casual finding of very few floating specimens in the Mar Grande basin, near a mollusk import-export center (Petrocelli and Cecere, 2010). This led to the hypothesis that the introduction vector for *A. nodosum* in Taranto seas was oyster imports from France. *Ascophyllum nodosum* thalli were most likely used to cover and keep the mollusks fresh during transportation (Verlaque et al., 2007), and then dumped in the seawater. Since this species is native to the cold-temperate waters of the North Atlantic, with a temperature tolerance not higher than 25°C (Keser et al., 2005), and the temperature of Mar Piccolo seawater is often higher than 27°C (Petrocelli et al., 2020a), this conceivably prevented the establishment of *A. nodosum* (Petrocelli et al., 2013). *Undaria pinnatifida*, a cold-temperate species native to the Pacific Japanese seawaters, underwent a similar fate in the Mar Piccolo. After first detection in 1998, this species showed a short initial period of increasing settlement, followed by a quick decline and its final disappearance over 11 years (Cecere et al., 2016). Laboratory and field observations in the native area have suggested an optimum temperature of 19°C for *U. pinnatifida* reproduction and survival (Akiyama and Kurogi, 1982; Sanderson, 1990; Watanabe et al., 2014). The temperature extremes recorded in Mar Piccolo seawater, both in the coldest week and in the warmest one in the last year of *U. pinnatifida* flourishing growth, were far from the optimum. This most likely contributed to *U. pinnatifida* disappearing, even though the additional and combined influence of low salinity and heavy metal contamination could not be excluded (Cecere et al., 2016).

The presence of NIS seaweeds is often overlooked due to their possible morphological similarity with native species. In this case, molecular analyses through the DNA barcoding method have proved to be fundamental in discriminating cryptic introduced species (Zucarello et al., 2002; Saunders, 2009; Montes et al., 2016; 2017; Piñeiro-Corbeira et al., 2020). In the Mar Piccolo, DNA barcoding analyses confirmed the taxonomic identity of several species previously identified through classical morphological methods. *Agardhiella subulata* was initially identified through a morphological analysis (Perrone and Cecere, 1994). In 2011, after a new introduction event, its identification was confirmed by the *rbc*L gene analysis (Cecere et al., 2011a). In December 2000, specimens of *Hypnea cornuta* (Kützing) J. Agardh were collected in the Mar Piccolo for the first time. The species identification was based on anatomical features and the presence of stellate propagules (Cecere et al., 2004), as well as confirmed by molecular analysis (Yamagishi et al., 2003). Since the taxonomic identity of this taxon became less defined over time, recently a molecular study was focused on the *H. cornuta* complex, detecting three different clades inside this group (Jesus et al., 2019). The Taranto specimens, together with those from Western Australia, New Zealand, and Japan were ascribed to a generic Clade#3, which was then named *Hypnea corona* Huisman and Petrocelli (Huisman et al., 2021). Due to the presence of ambiguous morphological features, some specimens of a rhodophycean seaweed collected in the Mar Piccolo in 2010, were doubtfully identified as *Grateloupia* cf. *filicina* (J.V. Lamouroux) C. Agardh, a species exclusively distributed in the Mediterranean Sea (De Clerck et al., 2005; Wilkes et al., 2005). Molecular analyses, based on the *rbc*L gene, were therefore carried out on these specimens from Mar Piccolo and also on specimens from the French Thau Lagoon collected in 1998 and tagged as *Grateloupia* sp. This molecular survey identified all the samples as *G. minima* P. and H. Crouan, described in 1867 from the Atlantic

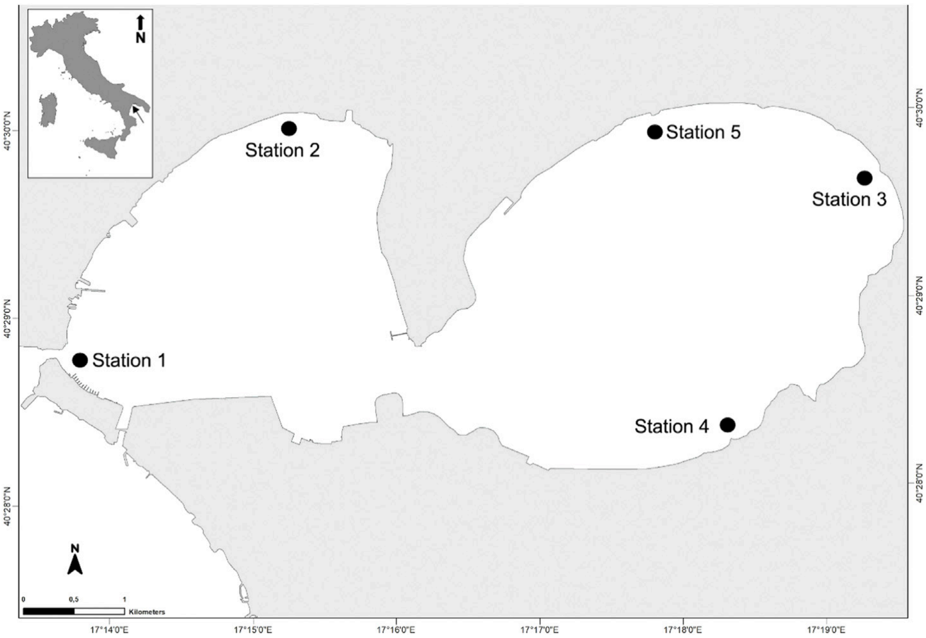

FIGURE 1
Map of the Mar Piccolo of Taranto and location of sampling sites. The arrow in the frame indicates the location of Taranto in Italy.

Ocean, allowing its first report as a NIS both in the Mar Piccolo and in the Mediterranean Sea (Cecere et al., 2011b). The taxonomic identity of *Grateloupia turuturu* specimens collected in the Mar Piccolo and the Venice Lagoon in 2007, was confirmed through DNA analysis in recent years (Cecere et al., 2011c). A turf-forming rhodophycean species, observed for the first time in the Mar Piccolo in 2012, was identified based on the morphological analysis as *Caulacanthus ustulatus* (Turner) Kützing (Rhodophyta, Gigartinales), a taxon commonly distributed in the Mediterranean Sea. Some specimens from the French Mediterranean coast were successively ascribed to the NIS taxon *Caulacanthus okamurae* (Verlaque et al., 2015). Therefore, *rbc*L gene molecular analyses were carried out on *C. ustulatus* specimens collected both in the Mar Piccolo and in the Venice Lagoon, confirming the presence of the non-indigenous taxon also in these two Mediterranean hot spots (Petrocelli et al., 2020b).

With this background and exploiting the long-term data potential, this paper aims to take stock of the NIS seaweed situation in the Mar Piccolo of Taranto, also through the help of molecular methods. Continuous introductions have been recorded over time, with the different species displaying many adaptive strategies. Therefore, several years after their first detection, they show different distribution pathways and fates. Based on their growth and reproduction requirements, if known, their further development has been hypothesized too. Climate change, and in particular heat waves, are becoming well-known phenomena; thus, the less adaptive species will most likely disappear from the basin. Finally, the DNA barcoding method has further proved to be a useful means for cryptic introduced species issues, otherwise doubtfully identified with classical approaches.

2 Materials and methods

This research was carried out in the Mar Piccolo of Taranto (40°28′46″ N, 17°13′41″ E) (southern Italy, Mediterranean Sea). It has a somewhat elliptical shape and is divided into two sub-basins, the First Inlet and the Second Inlet (Figure 1). The Mar Piccolo is a transitional water system, characterized by the input of brackish water, at a mean temperature of 18°C and a salinity range of 2.3–4.7, coming from 34 submarine springs, locally named “citri,” variously distributed in the two Inlets. In the basin, seawater temperature ranges between 7.5°C and 32.3°C, while salinity ranges between 33.0 and 37.8.

During the 11-year study, two time periods were considered due to a different number of investigated sites. From 2011 to 2015, the sampling sites were four, two in the First Inlet and two in the Second Inlet (Figure 1). In 2016, a fifth site, located in the Second Inlet, was added (Figure 1).

Seasonal manual harvests were carried out at a maximum depth of 50 cm. For each site, three 50 cm × 50 cm quadrats were collected by scraping the surface within the quadrats and picking all the seaweeds. Seaweeds were put in plastic bags identified by an encoded box for each replicate and brought to the laboratory, where they were stored in plastic nets and dipped in concrete tanks filled with seawater. Harvested samples were individually sorted to separate single species. After sorting, taxonomic identification of each taxon was performed through stereomicroscopes (LEICA MZ 12 Stereoscope, Leica Microsystems GmbH, Wetzlar, Germany) and light microscopes (LEICA DMR Trinocular Microscope, Leica Microsystems GmbH, Wetzlar, Germany). Successively, biomass (drained wet weight) was measured by means of a double-digit analytical balance (Sartorius L2200P, Sartorius Lab Instruments GmbH, Göttingen, Germany).

2.1 Molecular analyses

Since the identification was considered dubious for some specimens, a small part of the thallus was carefully cleaned from epiphytes and debris and dried in silica gel (J.T. Baker, Deventer, Holland) for molecular analyses.

Silica-dried fragments of thalli were ground in a mortar with quartz sand (Honeywell Fluka, Charlotte, NC, United States), and total genomic DNA was extracted with the Genomic DNA Purification Kit (Thermo Fisher Scientific, Waltham, Massachusetts, United States) following the manufacturer's recommendations. Since the dubious specimens belonged to the phylum Rhodophyta, the 5P portion of the *rbc*L gene (*rbc*L-5P) was selected to identify them following the DNA barcoding method.

The *rbc*L-5P fragment (about 700 bp) was amplified using the primer pairs F57-R753 (Freshwater and Rueness, 1994) and the PCR conditions reported by Wolf et al. (2011). The obtained amplicons were verified by agarose gel electrophoresis and purified with ExoSAP-IT (Thermo Fisher Scientific, Waltham, Massachusetts, United States) before sequencing. Sequencing was performed at the Eurofins Genomics Sequencing Service (Eurofins Genomics GmbH, Ebersberg, Germany) with the same primer pairs used for amplification. Final consensus sequences were assembled with the help of the GeneStudio program (http://genestudio.com/) and then compared with the sequences available in the INSDC (International Nucleotide Sequence Database Collaboration) archives using the BLAST tool (Altschul et al., 1990). The newly obtained sequences were also deposited in the INSDC archives through the GenBank platform BankIt.

2.2 Multivariate analysis

A multivariate analysis was carried out to explore spatial and temporal differences in the macroalgae assemblages. Three sites (1, 3, 4) were chosen, since they were sampled along the entire time series and represent different zones in the First and Second Inlet of the Mar Piccolo (Figure 1). In this way the sampling design resulted less unbalanced. The characteristic species of the assemblage were selected according to their frequency of occurrence (FO%, expressed in percentage) during the entire period, selecting the species with a FO% > 5% and maintaining all NIS in the analysis (Supplementary Table S1). A total of 37 species were selected and the biomass data (g m^{-2}) were four-root transformed to balance the contribution of rare and very abundant species. Multivariate analyses were conducted by means of a Bray-Curtis similarity calculated on a "stations × species" matrix (377 × 37).

The null hypothesis of no spatial variation or temporal differences in seaweed assemblage structure was investigated by adopting a multifactorial model tested by the Permutational Multivariate Analysis of Variance (Anderson et al., 2008). Data collected from each site were considered independent because they were carried out in random positions within each site, and thus, the exchangeability of the observations under the null hypothesis was assumed, fulfilling the requirements of hypothesis testing with permutation methods (Anderson, 2001). Year (fixed with 11 levels), Season (fixed with 4 levels), and Site (random with 3 levels) were tested as orthogonal factors in the PERMANOVA test, with *p-values* calculated through 9,999 permutations using the "Permutation of residuals under a reduced model" as permutation method. In the model, "Year × Site" and "Season × Site" interactions were tested. When the PERMANOVA test result was significant ($p < 0.05$), a *post hoc* PAIRWISE *t*-test was carried out to evaluate differences between the levels of each factor and their interactions, calculating Monte Carlo *p-values* (Anderson et al., 2008). Data were plotted using both unconstrained ordinations, the nonmetric multidimensional scaling (nMDS, Clarke and Warwick, 2001), and Principal Coordinate Analysis, PCoA, Gower, 1966). In both ordination methods, the sites were plotted together with the species mainly correlated to the first two axes in the PCoA using Spearman's correlation coefficient (rs). In addition, the distances among centroids were explored for significant complex interactions between factors using both ordination methods to visualize complex spatio-temporal patterns (Guerra-Castro et al., 2016).

The contribution of species to the differences among sites was explored through the Similarity Percentage analysis (SIMPER; Clarke, 1993; Clarke and Warwick, 2001). All multivariate analyses were carried out by means of PRIMER v.6+PERMANOVA (Primer-E Ltd., Plymouth, United Kingdom).

3 Results

3.1 NIS species

In the studied period (2011–2021), fourteen NIS were recorded in the Mar Piccolo of Taranto. In the 2011–2015 time frame, nine species were recorded in four sites. In the 2016–2021 time frame, thirteen species were found in five sites. Eight species were recorded throughout the study period, one species was present only from 2011 to 2015, and five species were present only from 2016 to 2021 (Table 1).

Figure 2 reports the biomass trend of NIS species in the studied period. Due to their very low biomass values, *A. subulata*, *Asparagopsis taxiformis*, *Caulerpa cylindracea*, and *Solieria filiformis* were not plotted. In both time frames, the highest total biomass values were reached by *H. corona* (Table 1). It was observed only in the Second Inlet, from spring to autumn with ups and downs throughout the study period. From 2011 to 2015, it was present at Site 3 and Site 4, while from 2016 to 2021 also at Site 5. For each year, summer was the season of maximum abundance. For each year and in all the seasons, Site 3 collected quantities were higher than those of Site 4, while starting from 2016, *H. corona* abundance at Site 5 sometimes exceeded that at Site 3. The highest yearly total biomass value was measured in 2018 and corresponded to 28.8 × 10^3 g_{wwt} m^{-2}.

In the summer of 2012, for the first time and with very few specimens, *C. okamurae* was recorded at Site 4; it was settled on basal parts of *Chondracanthus acicularis* (Mertens *ex* Turner) Kützing. Since then, it was observed every year and in every season, mainly at Site 4, but also occasionally with small

TABLE 1 List of NIS and their total abundances (g_{wwt} m^{-2}) recorded in the Mar Piccolo of Taranto in the study period 2011–2021.

Species	2011–2015	2016–2021	Total
Agardhiella subulata (C. Agardh) Kraft & M.J. Wynne	0	18	18
Asparagopsis cf. *taxiformis* (Delile) Trevisan	0	2	2
Caulacanthus okamurae Yamada	1,498	12,614	14,112
Caulerpa cylindracea Sonder	0.1	0	0.1
Codium fragile (Suringar) Hariot	222	0.4	222
Colpomenia peregrina Sauvageau	1,408	2,113	3,526
Cutleria multifida (Turner) Greville	0	1,188	1,188
Grateloupia minima P. Crouan & H. Crouan	1,621	11,641	13,261
Grateloupia turuturu Y. Yamada	85	39	124
Hypnea corona Huisman & Petrocelli	51,928	98,879	150,807
Neopyropia koreana (M.S. Hwang & I.K. Lee) L.-E. Yang & J. Brodie	89	1,161	1,250
Osmundea oederi (Gunnerus) G. Furnari	0	3,076	3,076
Polysiphonia morrowii Harvey	175	1,721	1,896
Solieria filiformis (Kützing) Gabrielson	0	0.3	0.3

quantities at the other sites (except for Site 2), reaching the peak in spring 2016 (i.e., 6.4 × 10^3 g_{wwt} m^{-2}). From 2017, a considerable decrease was observed, with ups and downs until autumn 2021.

Grateloupia minima was collected for the first time in 2011 at Site 4. Successively, it was recorded every year mainly at Site 4, and since 2016 also at Site 5, where it became one of the most luxuriant species in the last 3 years. The highest total yearly biomass value, corresponding to 2.7 × 10^3 g_{wwt} m^{-2}, was reached in 2019.

Colpomenia peregrina was observed for the first time in the winter of 2012 at Site 1. Since then, it was observed every year only at the same site, with the following seasonal occurrence: always in spring, several times in winter (except in 2014, 2015, and 2017), and fewer occurrences in autumn (i.e., 2014, 2015, and 2020). The yearly biomass peak was reached in 2014, with 9.0 × 10^2 g_{wwt} m^{-2}. Considering the whole study period, *C. peregrina* biomass showed ups and downs in the first time frame and reached a certain uniformity in the second time frame, with values considerably lower compared to the peak.

The presence of *Cutleria multifida* was detected for the first time in 2017, even though it was collected with measurable biomass only in the winters of 2018 and 2021 at Site 1. The highest yearly total biomass value was reached in 2021 and corresponded to 1.2 × 10^3 g_{wwt} m^{-2}. Concerning *Neopyropia koreana*, a very low biomass was recorded for the first time in winter 2012 at Site 4. Successively, this species was collected always in winter only at Site 1 and with highly variable biomass values. The highest total yearly value was recorded in 2017 and corresponded to 6.1 × 10^2 g_{wwt} m^{-2}. *Polysiphonia morrowii* was found for the first time in the winter of 2012 at Site 1; since then, starting from 2014, it was recorded every year at the same site, and from 2015 also at Site 4. The highest

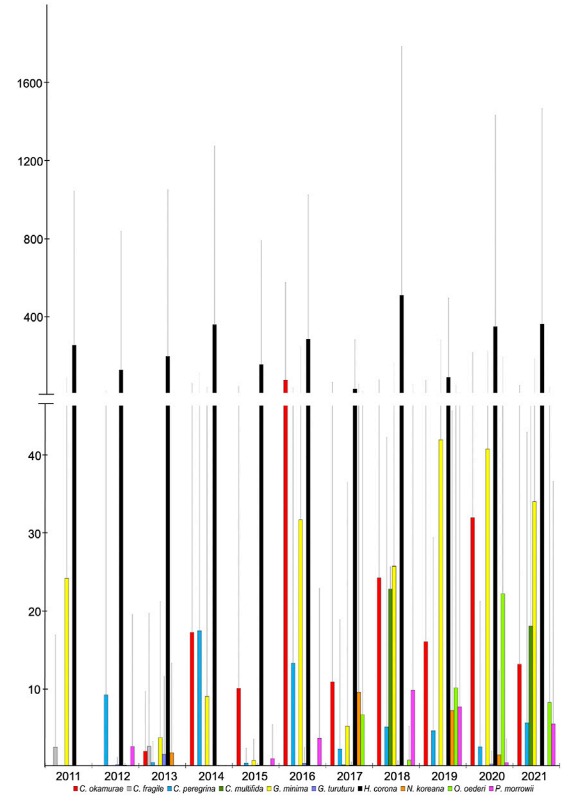

FIGURE 2
Abundances (mean total value + s.d.) of NIS collected in the Mar Piccolo for each year in the study period 2011–2021.

TABLE 2 List of NIS detected in the Mar Piccolo of Taranto with the DNA barcoding method. For each specimen, the recognized species and the highest BLAST percent identity are reported.

Morphological identification	Sampling date	Collection site	Recognized species	GenBank accession number	BLAST percent identity (%)
Grateloupia cf. *filicina*	16.04.2018	Site 4	*Grateloupia minima*	OP503631	100
Grateloupia cf. *filicina*	16.04.2018	Site 4	*Grateloupia minima*		
Grateloupia cf. *filicina*	03.06.2019	Site 5	*Grateloupia minima*		
Grateloupia cf. *filicina*	10.06.2019	Site 4	*Grateloupia minima*		
Polysiphonia cf. *morrowii*	26.02.2013	Site 1	*Polysiphonia morrowii*	OP503632	100
Polysiphonia cf. *morrowii*	11.04.2018	Site 4	*Polysiphonia morrowii*		
Porphyra cf. *leucosticta*	16.12.2014	Site 1	*Neopyropia koreana*	OP503633	100
Porphyra sp	25.03.2019	Site 1	*Neopyropia koreana*		
Porphyra sp	03.06.2019	Site 1	*Neopyropia koreana*		

TABLE 3 Summary of PERMANOVA test based on Bray-Curtis similarity for four-root transformed biomass data on the basis of a multifactorial model with 3 factors (Year, Ye, Season, Se, Site, Si). The probabilities of each Pseudo-F value were obtained with 9,999 permutations of residuals under a reduced model. In red significant *p-value*, with significance levels coded by asterisks ($^*p < 0.05$, $^{**}p < 0.01$, $^{***}p < 0.001$).

Source	df	SS	MS	Pseudo-F	P(perm)	perms
Ye	10	73,588	7,359	1.5779	0.0013**	9,832
Se	3	100,290	33,428	2.2176	0.0276*	9,942
Si	2	377,060	188,530	90.7370	0.0001***	9,921
Ye × Si	20	93,330	4,667	2.2460	0.0001***	9,720
Se × Si	6	90,513	15,085	7.2606	0.0001***	9,838
Res	335	696,040	2,078			
Total	376	1,443,000				

biomass values were found at Site 1. The highest total yearly biomass was measured in 2018 and reached 6.3×10^2 g_{wwt} m^{-2}.

Codium fragile was recorded in the summers of 2011 and 2013 at Site 1, with a biomass peak of 128 g_{wwt} m^{-2} in 2013. In the springs of 2016 and 2018, few thalli were observed with negligible biomass. *Grateloupia turuturu* was detected every year except in 2014. It was observed at Site 1, mainly in winter, but sometimes in spring and autumn, with few thalli attached to plastic nets. The highest total yearly biomass was measured in spring 2013 and reached 75.3 g_{wwt} m^{-2}.

Agardhiella subulata was recorded, with very few thalli, at Site 4 only in spring 2016 and in winter 2017, when the highest total yearly biomass was reached (i.e., 18.2 g_{wwt} m^{-2}). Very few tetrasporic thalli of *A. taxiformis* (i.e., *Falkenbergia rufolanosa*) were collected for the first time in the summer of 2016 at Site 1 and, then, in the autumn of 2021. It was then detected at Site 2 in the summers of 2018, 2020, and 2021, and in winter 2021. *Caulerpa cylindracea* was found, with undetectable biomass, only in summer 2013 at Site 4. *Solieria filiformis* was also observed only once, with undetectable biomass, at Site 4 in spring 2017.

3.2 Molecular analysis

Some of the analyzed specimens were attributed to non-indigenous species that are difficult to recognize based only on morphology. For two species, the molecular analyses confirmed their belonging to NIS already reported in the study area such as *G. minima* (four specimens sequenced), and *P. morrowii* (two specimens sequenced). A newly introduced NIS was detected (three specimens sequenced) (Table 2), that is *Neopyropia koreana*, reported for the first time in the Mar Piccolo of Taranto.

3.3 Multivariate analysis of the seaweed's assemblages

PERMANOVA analysis showed a significant difference in the seaweed assemblages for the Site factor and both interactions between "Year × Site" and "Season × Site" (Tables 3, 4). Site 1 was separated from the others, as detected by nMDS ordination and PCoA (Figures 3, 4), although the variance explained by the first two axes was low (PCo1 = 25.1% and PCo2 = 14.7%). The main species positively correlated to the first axis (rs > 0.35) were *Dictyota dichotoma* var. *intricata, Ellisolandia elongata*, *Amphiroa beauvoisii,* and *C. peregrina* (NIS), which were associated with Site 1 (Supplementary Table S2). Replications of sites 3 and 4 showed a gradient of separation along the PCo2 axis, confirmed by the *post hoc* test (Table 4). *Hypnea corona* (NIS), *Alsidium corallinum,* and *Spyridia filamentosa* were the main species correlated to Site 3, while *C. acicularis*, *Gelidium crinale*, and *C. okamurae* (NIS) were characteristic of Site 4.

Considering the "Season × Site" interaction, differences in the seasonal pattern within the sites were detected by *post hoc* test and the centroids' ordinations (Table 4; Figure 5; Supplementary Figure S1). In the PCoA, the sites were distributed along the first axis (55.2% of explained variance), with Site 1 characterized by different seasonal assemblages composed by *D. dichotoma* var. *intricata, D. dichotoma* var. *dichotoma, E. elongata, G. turuturu* (NIS), *Corallina officinalis, Padina pavonica, A. beauvoisii, P. morrowii* (NIS), *C. peregrina* (NIS) (correlation to PCo1, rs > 0.75; Supplementary

TABLE 4 **Summary of PAIRWISE *t*-test among levels of Site and Season × Site interaction, with the seasons levels within the sites (Spring Sp, Summer Su, Autumn Au, Winter Wi). Values *t*-test (t), number of permutations (perms), Monte Carlo *p-values* (PMC) and Average Similarity (Av. Sim. %) between seasons pairs are reported. In red significant *p-value*, with significance levels coded by asterisks (*$p < 0.05$, **$p < 0.01$, ***$p < 0.001$).**

PAIRWISE test: Site					
	Site pairs	t	perms	P(MC)	Av. Sim. (%)
	1, 3	13.726	9,944	0.0001***	2.2
	1, 4	10.928	9,936	0.0001***	3.8
	3, 4	6.0823	9,935	0.0001***	17.6
PAIRWISE test: Site × Season					
Site	Season pairs	t	perms	P(MC)	Av. Sim. (%)
1	Sp, Su	42.548	9,943	0.0001***	24.9
	Sp, Au	38.166	9,954	0.0001***	31.8
	Sp, Wi	20.179	9,946	0.0028**	35.9
	Su, Au	16.068	9,967	0.0818	36.3
	Su, Wi	32.721	9,959	0.0001***	26.5
	Au, Wi	25.472	9,949	0.0006***	33.5
3	Sp, Su	56.971	9,953	0.0001***	27.6
	Sp, Au	3.548	9,948	0.0001***	26.8
	Sp, Wi	25.835	9,933	0.0001***	20.7
	Su, Au	56.981	9,948	0.0001***	40.8
	Su, Wi	77.651	9,949	0.0001***	88.3
	Au, Wi	43.358	9,947	0.0001***	21.7
4	Sp, Su	28.642	9,941	0.0001***	19.5
	Sp, Au	31.065	9,927	0.0001***	17.6
	Sp, Wi	14.228	9,939	0.0645	23.9
	Su, Au	20.909	9,936	0.0003***	23.3
	Su, Wi	30.672	9,933	0.0001***	17.4
	Au, Wi	24.887	9,920	0.0001***	20.5

Table S2). Along the second axis (21.6% of explained variance), Site 3 assemblage showed the greatest differences between seasons, with *H. corona* (NIS) as the typical species in summer and autumn, while *A. corallinum* and *Chaetomorpha linum* were abundant in spring. In winter, Site 3 assemblage was characterized by *C. acicularis*. In Site 4, small but significant changes among the seasons were observed, except for the winter-spring season pair, with *Gracilaria gracilis*, *C. okamurae* (NIS), and *G. crinale* as characteristic of these seasons.

Considering the "Year × Site" interaction, the distance among centroids confirmed the separation of sites in the nMDS plot, resulting in line with *post hoc* test results (Supplementary Figure S2; Supplementary Table S3). Indeed, the seaweed assemblages of Site 1 were more similar in terms of year (centroids close among them), while a higher temporal variability in the assemblages was observed in Sites 3 and 4 (increase in the distance among centroids). Site 3 showed the highest variability in the assemblages over time, and *H. corona* was the most important NIS to contribute to seasonal changes. The remaining *post hoc* tests on seasons and year pairs are reported in Supplementary Table S3.

4 Discussion

Over the past 11 years, long-term observations have allowed for the detection of an increasing number of seaweed NIS in the Mar Piccolo of Taranto, confirming the susceptibility of this basin to biopollution. The Mar Piccolo is a very important place for mussel farming and shellfish imports, mainly consisting of Japanese oysters from Atlantic waters, which are supposed to be the main introduction vector for most seaweed NIS (Manghisi et al., 2010; Verlaque and Breton, 2019). In the Mar Piccolo, local mussel farmers' observations have confirmed the introduction of *U. pinnatifida* since the 1990s through imported oysters (Cecere et al., 2000).

With a total number of 16 non-indigenous seaweeds recorded in the last 35 years, the Mar Piccolo basin is confirmed as the third seaweed NIS hot spot among the Mediterranean transitional water systems, after the Thau Lagoon and the Venice Lagoon (Boudouresque et al., 2020). These seaweed species show different behaviors mainly linked to their area of origin and their eco-physiological requirements. Therefore, different fates can be foreseen for each of them in the next years.

The warm tolerant *H. corona* (Rhodophyta, Gigartinales), which is the most abundant NIS in the basin until now, has proved to be the only NIS that behaves as an invasive species since it was first detected in 2000 (identified as *H. cornuta*). It spread into two zones of the Mar Piccolo Second Inlet (Cecere et al., 2016), seasonally monitored within the framework of LTER activities, until 2011. In 2016, observations along the NE coast of the basin showed the presence of *H. corona* in considerable amounts also in another zone, and in response, a new sampling site was added to the routine monitoring. According to recent studies, this species is part of the *H. cornuta* complex and has a tropical and subtropical distribution (Jesus de et al., 2019; Huisman et al., 2021). This indicates its long-lasting establishment in the increasingly warm Mar Piccolo seawaters, and, at the same time, enables us to make previsions on its permanence and further spread in the basin. The present study has confirmed that *H. corona* is widespread in the Mar Piccolo, likely enhanced by the high production of stellate propagules, which are an important means of vegetative propagation (Cecere et al., 2004).

Eight NIS species, native from cold-temperate oceanic waters, either in the Pacific or Atlantic Ocean, can be considered established in Mar Piccolo, ups and downs of biomass. *Caulacanthus okamurae, C. peregrina, Neopyropia koreana,* and *P. morrowii* have optimum growth temperatures between 18°C and 23°C (Kudo and Masuda, 1981; Vandermeulen, 1986; Choi et al., 2001; Choi and Nam, 2001; Croce and Parodi, 2017; Kim et al., 2022). Starting from 2011, the temperature in the Mar Piccolo seawaters generally exceeded 27°C in the warmest week, and, in recent years, these values have persisted for several weeks (Petrocelli et al., 2020a). At the same time, ever more frequent heat waves have affected wide areas around the world (Mentaschi et al., 2017). Therefore, for these species limited growth and their eventual disappearance in the long run, are predictable in the Mar Piccolo basin. For *C. multifida, G. minima,* and *Osmundea*

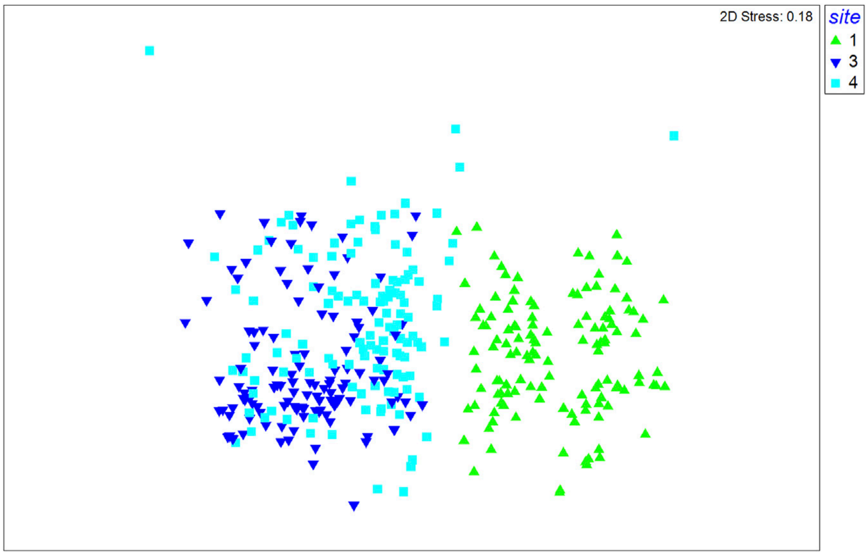

FIGURE 3
Nonmetric multidimensional scaling ordination (nMDS) based on the Bray−Curtis similarity matrix with the sites marked in the plot (1 = green; 3 = dark blue; 4 = light blue).

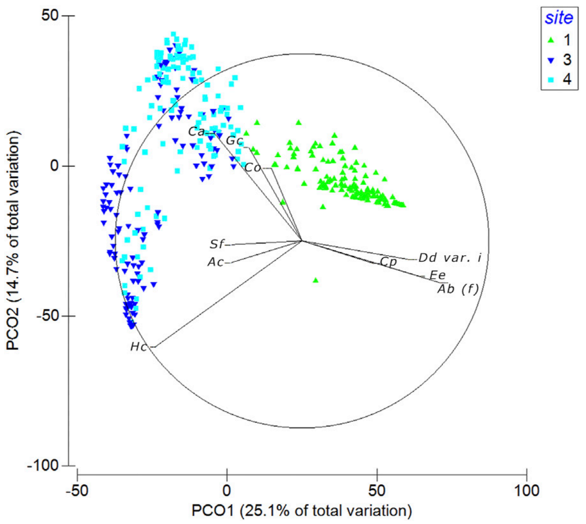

FIGURE 4
Principal Coordinate Analysis ordination (PCoA) based on the Bray−Curtis similarity measure of the stations labeled as sites (1 = green; 3 = dark blue; 4 = light blue). The percentages of explained variance (%) of both PCO1 and PCO2 axes are reported, and vectors indicate the main correlated species with the two axes (rs > 0.35). Species' names are coded as: *Ac, Alsidium corallinum; Ab (f), Amphiroa beauvoisii (f); Co, Caulacanthus okamurae; Cl, Chaetomorpha linum; Ca, Chondracanthus acicularis; Cp, Colpomenia peregrina; Co (f), Corallina officinalis (f); Dd* var. *d, Dictyota dichotoma* var. *dichotoma; Dd* var. *i, Dictyota dichotoma* var. *intricata; Ee, Ellisolandia elongata; Gc, Gelidium crinale; Gg (t), Gracilaria gracilis (t); Gt, Grateloupia turuturu; Hc, Hypnea corona; Pp, Padina pavonica; Pm, Polysiphonia morrowii; Sf, Spyridia filamentosa.*

oederi there is no information about the environmental requirements for their growth, so it is hard to gain an understanding of the reasons for fluctuations in their biomass as well as to foresee the fate of their populations in the basin. Concerning *C. multifida,* since the species has been present in the Mediterranean for a long time (Cormaci et al., 2012), we can also hypothesize that it has adapted to this environment and, therefore, it will become a constant element of the Mar Piccolo macrobenthic flora.

Grateloupia turuturu showed a first phase of population growth in the Mar Piccolo of Taranto, followed by a considerable fall, up to the current vestigial community (Petrocelli et al., 2020a). This species is considered among the most dangerous invasive seaweeds, due to its ability to replace both animal and plant native species on hard substrata in coastal ecosystems (Freitas et al., 2016), taking particular advantage in the absence of well-structured benthic communities (Mulas and Bertocci, 2016). Recent studies using an Ecological Niche Model based on ecophysiological responses forecast its future geographical distribution in temperate and warm-temperate seawaters (Koerich et al., 2020). Indeed, *G. turuturu* tolerates wider ranges of both temperature and salinity and nutrient concentrations up to eutrophication (Simon et al., 2001), which explains its permanence in the Mar Piccolo 15 years after its first record. No detrimental effect on the local communities has been observed to date, despite the presence of predisposing conditions.

Five NIS species were sporadically observed. Few thalli of *C. fragile* were not continuously observed. We suggest that these were most probably separate introductions, without a propagule pressure that can sustain its establishment. *Codium fragile* is considered a warm-temperate species with optimal growth temperatures between 21°C and 24°C (Fralick and Mathieson, 1973), and temperature is the most important environmental factor controlling its seasonal growth (Hanisak, 1979). Therefore, we suppose that *C. fragile* will never establish in the Mar Piccolo, due to the currently reported temperatures higher regimes than the optimal growth ones. *Agardhiella subulata* was particularly abundant in the Mar Piccolo from the end of the 1980s up to the second half of the 1990s (Cecere et al., 1992). Afterward, it underwent a complete disappearance, until sporadic new findings were recorded during this study, most probably due to different secondary re-introductions through shellfish import (Petrocelli et al., 2013), as already hypothesized in the Ganzirri Lake (Sicily, Ionian Sea) (Manghisi et al., 2010). Both male and female gametophytic thalli were collected in 2011, but to date, *A. subulata* has not been re-established in the Mar Piccolo. This species, preferentially distributed in shallow and sheltered environments, is native to the cold temperate Atlantic Ocean. P and N in seawater are limiting growth factors (Chopin et al., 1990). *Agardhiella subulata* is well established in the Venice lagoon, where temperatures can rise to 32.5°C (Sfriso et al., 2020), and was observed as a dominant species in the Po Delta lagoons, where high P and N concentrations were recorded (Sfriso et al., 2016). Therefore, temperature could seem less important than nutrients in fostering *A. subulata* settlement and establishment in the Mar Piccolo. Indeed, in the last 20 years a trend of temperature increase has been recorded (Cecere et al., 2016), but a considerable improvement in seawater quality was also observed in the basin, due to the closure of several urban sewage disposals (Kralj et al., 2016); this can be a disadvantage for *A. subulata* establishment in the basin.

In the studied period, negligible quantities of the tetrasporophyte (stage *Falkenbergia*) of *Asparagopsis* sp. were occasionally collected in the First Inlet. The genus *Asparagopsis* has still unsolved taxonomic questions and, thus, for the correct identification of species, the DNA barcoding method is imperative (Andreakis et al., 2007). Unfortunately, up to now, not enough quantities of *Asparagopsis* have been collected in the Mar Piccolo to perform molecular analysis. Therefore, in this study, we refer to *Asparagopsis* cf. *taxiformis*, since this species was reported for the first time in the basin in 2014 according to morphological identification (Bottalico et al., 2015). However, it is worth remembering that the congeneric NIS *Asparagopsis armata* Harvey is present in the nearby Mar Grande (Cecere et al., 1996). *Solieria filiformis* was the first NIS recorded in the Mar Piccolo. Indeed, its presence in the basin was already witnessed in a herbarium sheet dating back to 1922 (identified as *Gracilaria confervoides* Greville) (Perrone and Cecere, 1994). However, the first record of this species, which was also the first report for the Mediterranean, was based on a collection in 1987 (Cecere, 1990) when several unattached floating and sterile thalli of Solieriaceae (including *A. subulata* and *S. filiformis*) were sampled in both the basin inlets. Since then, recurring observations have shown that *S. filiformis* has spread considerably in the Mar Piccolo, becoming one of the dominant species in summer in the Second Inlet (Cecere et al., 1992). At the end of the 1990s, *S. filiformis* disappeared from the basin, because it was used in an experimental cultivation with mussels, starting in 1994, which led to the massive harvest of thalli (Cecere and Petrocelli, 2009). *Solieria filiformis* growth is strongly enhanced by a high content of N, mainly ammonium (Peñuela et al., 2018). During this study, in spring 2017, few sterile thalli were collected in the Mar Piccolo, most likely due to a new introduction event, not followed by the species re-establishment. The failure to find again this species in the following years could be due to a reduced propagule pressure, combined with the lower N content in seawater (Kralj et al., 2016). *Caulerpa cylindracea* was detected for the first time in the Mar Piccolo in 2001 (reported as *Caulerpa racemosa*), and continuously until 2004 by research projects focused solely on NIS (E. Cecere and A. Petrocelli unpublished data). It was widely distributed in the First Inlet, with some spots in the north-eastern part of the Second Inlet, at a depth between 0.5 and 3 m. Since then, a few filaments of *C. cylindracea* were collected again as part of this study in summer 2013. In the Tyrrhenian Sea, *in situ* studies showed that *C. cylindracea* is a nitrophilic species, but while N does not represent a limitative nutrient, P is limitative (Gennaro et al., 2015). Light is another limiting environmental factor for *C. cylindracea* growth. This species has elevated photosynthetic plasticity, but the energetic costs required for the acclimation often reduce its survival at low light conditions (Bernardeau-Esteller et al., 2015). These could have been the main factors leading to the disappearance of *C. cylindracea* in the Mar Piccolo, where urban effluents were mainly closed, but sedimentation remained very high (Bellucci et al., 2016). *Caulerpa cylindracea* is considered the first among the ten most invasive non-indigenous seaweed species in the Mediterranean Sea, with both negative and positive impacts on the invaded communities (Tsirintanis et al., 2022). However, for the moment, it can be considered another unsuccessful NIS in the Mar Piccolo of Taranto.

The DNA barcoding method has proved a very useful investigative tool for species identification, as it has enabled the identification of several other doubtful taxa present in the basin. Indeed, within the framework of the National Biodiversity Future Center (NBFC), funded by the Italian National Recovery and Resilience Plan (PNRR), a specific task is devoted to this issue in the future. Concerning *G. minima*, the molecular analyses helped the inclusion of morphologically different specimens under the same taxon. For *P. morrowii*, the first report for the Mar Piccolo was tentatively attributed to this taxon, because all the specimens collected in the Mediterranean Sea belonged to this species (Petrocelli et al., 2013). However, a misidentification with *Polysiphonia senticulosa* Harvey (Kudo and Masuda, 1981) could not be excluded. *Polysiphonia morrowii* was very probably present as an epiphyte on several other seaweeds: for some seaweed specimens the sequencing signal was disturbed, indicating the presence of more than one species (despite our efforts to clean the samples before the molecular analyses), and thus these results could not be included in this paper. However, it is worth underlining that, based on the BLAST search, the readable part of the sequence of each of these specimens had a 100% identity with *P. morrowii* sequences. Finally, it was possible to solve the misidentification of *Neopyropia koreana* with other congeneric species, commonly based only on morphological features until now (Kim et al., 2022).

The multivariate analysis results highlight the absence of long-term changes in the structure of seaweed assemblages, indicating no relevant disturbances due to NIS settlement in the Mar Piccolo. Indeed, most NIS species seem to follow a seasonal cycle in equilibrium with native species. This condition is particularly evident in Site 1, where the assemblage seems to maintain stability during the entire year, driven by high abundances of Corallinales, Dictyotales, and the regular occurrence of some NIS, as *C. peregrina* and *P. morrowii*. The main differences detected in the analyses could be affected by the spatial positions of investigated sites, with the assemblage in the First Inlet of Mar Piccolo (Site 1) being different from other sites in the Second Inlet (Sites 3 and 4). In the last two sites, the difference between the assemblages arises at a seasonal scale, with Site 3 showing the most relevant seasonal differences due to the high abundance of *H. corona* in the summer. This observation is in line with the studies on the seasonal cycle of this species in the Mar Piccolo (Cecere et al.,

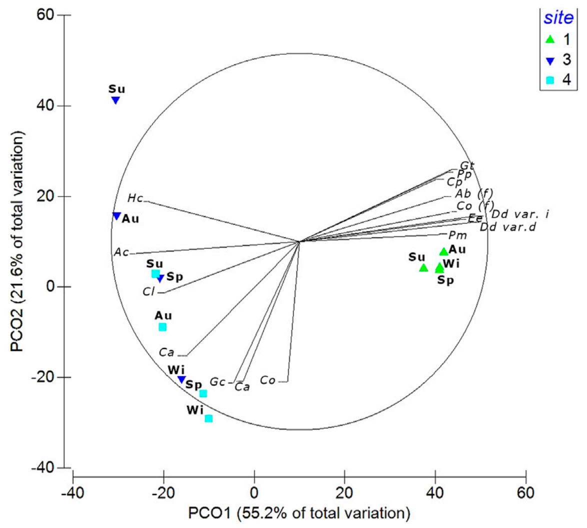

FIGURE 5
Principal Coordinate Analysis ordination (PCoA) based on the Bray−Curtis similarity measure of centroids calculated for the Season × Site interaction. The percentages of explained variance (%) of both PCo1 and PCo2 axes are reported, and vectors indicate the main correlated species with the two axes (rs > 0.75). Seasons are coded in the labels (Sp, Spring; Su, Summer; Au, Autumn; Wi, Winter). Species' names are coded as: *Ac, Alsidium corallinum; Ab (f), Amphiroa beauvoisii (f); Co, Caulacanthus okamurae; Cl, Chaetomorpha linum; Ca, Chondracanthus acicularis; Cp, Colpomenia peregrina; Co (f), Corallina officinalis (f); Dd* var. *d, Dictyota dichotoma* var. *dichotoma; Dd* var. *i, Dictyota dichotoma* var. *intricata; Ee, Ellisolandia elongata; Gc, Gelidium crinale; Gg (t), Gracilaria gracilis (t); Gt, Grateloupia turuturu; Hc, Hypnea corona; Pp, Padina pavonica; Pm, Polysiphonia morrowii; Sf, Spyridia filamentosa.*

2016; Petrocelli et al., 2019). On the other hand, Site 4 showed a pattern of small changes in the macroalgal assemblages, with the summer-autumn and winter-spring periods showing slightly different results, and the latter being characterized by *C. okamurae* as the most important NIS, as observed in previous analyses (Petrocelli et al., 2020b).

Since 2011, a substantial increase in imported bivalve mollusks has been registered at the Taranto market. This was mainly due to a strong decline in local production, caused by the detection of organic pollutants beyond the limits permitted by current legislation (Cecere et al., 2016). Once they arrive by track, adult organisms (for direct sale) and juveniles (for fattening) were both indiscriminately immersed in the Mar Piccolo, also in contravention of European law (Cecere et al., 2016). During an informal conversation, two local shellfish importers and sellers reported that 200,000 quintals of bivalve mollusks officially reached the Taranto market in 2021. Moreover, they outlined that this value is surely underestimated due to the massive amount of product that is unlawfully imported, which could be estimated at around 500,000 quintals. Most of the imported bivalve mollusks (mainly mussels and clams) came from the Northern Adriatic, Greece, and Spain. Only a small percentage (mainly oysters) was imported from France. Most likely, the imported organisms have contributed to the continuous NIS introduction in the Mar Piccolo assessed in this study, as has already been demonstrated in other world zones (Mineur et al., 2007; 2014; Wolf et al., 2018). In this respect, continuous dialogue among researchers, mollusk producers, and local authorities has recently led the mayor of Taranto to enact a specific issue that bans juveniles and adults of allochthonous bivalve mollusks from the Mar Piccolo, to preserve both the original animal genetic pool from hybridization and the environment from the introduction of new NIS.

Higher quantities of imported products can also explain the significant differences among sites, with the separation of Site 1 in the First Inlet. Indeed, there are numerous bivalve mollusk retailers, restaurants, and immersed packets near this site, containing adult bivalve mollusks (mainly oysters), which have often been observed, with heaps of shells discarded there. The situation is different in the other investigated sites located in the Second Inlet, which are instead characterized by the presence of farming plants where the imported juvenile products are improvidently immersed for fattening. This could explain similarities.

Based on the current study, the Mar Piccolo seems not particularly suitable for NIS settlement and development. Most NIS native to cold-temperate zones have either disappeared or did not succeed in forming luxurious populations. The only exception is *H. corona*, a warm-tolerant species well adapted to the increasing seawater temperatures of the basin. Further systematic seasonal LTER observations will allow for the continuous monitoring of the situation and the early detection of any new NIS. Recently, the relevance of these activities was sealed by the Italian PNRR, which funded the enhancement of the e-LTER infrastructure, to which the Mar Piccolo belongs, thereby ensuring the continuation of data collection over time.

Data availability statement

The sequences produced in this study can be found in the INSDC online repositories. To access the sequences use the accession numbers OP503631, OP503632, and OP503633 in the search box that can be found at: https://www.ncbi.nlm.nih.gov/genbank/.

Author contributions

AP: conceptualization, investigation, data curation, writing—original draft, writing—review and editing. MW: molecular analyses, writing—original draft, and writing–review. KS: molecular analyses, writing—original draft, and writing–review. AS: writing–review. FR: statistical analysis and writing–review. PR: statistical analysis and writing—review. EC: investigation, data curation, and writing–review. All authors contributed to the article and approved the submitted version.

Funding

The authors acknowledge the support of activities from the Apulian Region, through POR PUGLIA FESR-FSE 2014/2020—Axis VI, Action 6.5 "Interventions for protection and valorization of marine and terrestrial biodiversity" Sub Action 6.5.a., and funded by EU-NextGenerationEU within the National Biodiversity Future Center, Project CN00000033.

Acknowledgments

This research was carried out within the framework of the LTER network (www.lteritalia.it). Giuseppe Portacci continuously and actively contributed to the sampling and sorting activities. The suggestions of the two referees are warmly acknowledged.

Conflict of interest

Publisher's note

Supplementary material

The Supplementary Material for this article can be found online at: https://www.frontiersin.org/articles/10.3389/fenvs.2023.1075458/full#supplementary-material

References

Akiyama, K., and Kurogi, M. (1982). Cultivation of *Undaria pinnatifida* (Harvey) Suringar, the decrease in crops from natural plants following crop increase from cultivation. *Bull. Tohoku Reg. Fish. Res. Lab.* 44, 91–100.

Altschul, S. F., Gish, W., Miller, W., Myers, E. W., and Lipman, D. J. (1990). Basic local alignment search tool. *J. Mol. Biol.* 215, 403–410. doi:10.1016/S0022-2836(05)80360-2

Anderson, M. J. (2001). A new method for non-parametric multivariate analysis of variance. *Austral Ecol.* 26, 32–46. doi:10.1046/j.1442-9993.2001.01070.x

Anderson, M. J., Gorley, R. N., and Clarke, K. R. (2008). *PERMANOVA+ for PRIMER: Guide to software and statistical methods*. Plymouth: PRIMER-E Ltd.

Andreakis, N., Procaccini, G., Maggs, C., and Kooistra, W. H. (2007). Phylogeography of the invasive seaweed *Asparagopsis* (Bonnemaisoniales, Rhodophyta) reveals cryptic diversity. *Mol. Ecol.* 16, 2285–2299. doi:10.1111/j.1365-294X.2007.03306.x

Bellucci, L. G., Cassin, D., Giuliani, S., Botter, M., and Zonta, R. (2016). Sediment pollution and dynamic in the Mar Piccolo of Taranto (southern Italy): Insights from bottom sediment traps and surficial sediments. *Environ. Sci. Pollut. Res.* 23, 12554–12565. doi:10.1007/s11356-016-6738-6

Bernardeau-Esteller, J., Ruiz, J. M., Tomas, F., Sandoval-Gil, J. M., and Marín-Guirao, L. (2015). Photoacclimation of *Caulerpa cylindracea*: Light as a limiting factor in the invasion of native Mediterranean seagrass meadows. *J. Exp. Mar. Biol. Ecol.* 465, 130–141. doi:10.1016/j.jembe.2014.11.012

Bottalico, A., Russo, C., and Pati, R. (2015). Sulla presenza del genere *Asparagopsis* Montagne (Bonnemaisoniales, Rhodophyta) in Puglia (Italia meridionale). *Inf. Bot. Ital.* 47, 291–313.

Boudouresque, Ch.-F., Blanfuné, A., Pergent, G., Pergent-Martini, C., Perret-Boudouresque, M., and Thibaut, T. (2020). Impacts of marine and lagoon aquaculture on macrophytes in Mediterranean benthic ecosystems. *Front. Mar. Sci.* 7, 218. doi:10.3389/fmars.2020.00218

Callahan, J. T. (1984). Long-Term Ecological Research. *BioScience* 34, 363–367. doi:10.2307/1309727

Cecere, E., Alabiso, G., Carlucci, R., Petrocelli, A., and Verlaque, M. (2016). Fate of two invasive or potentially invasive alien seaweeds in a central Mediterranean transitional water system: Failure and success. *Bot. Mar.* 59, 451–462. doi:10.1515/bot-2016-0053

Cecere, E., Cormaci, M., Furnari, G., Petrocelli, A., Saracino, O., and Serio, D. (1996). Benthic algal flora of Cheradi Islands, (Gulf of Taranto, Mediterranean Sea). *Nova Hedwig.* 62, 191–214.

Cecere, E., Moro, I., Wolf, M. A., Petrocelli, A., Verlaque, M., and Sfriso, A. (2011c). The introduced seaweed *Grateloupia turuturu* (Rhodophyta, Halymeniales) in two Mediterranean transitional water systems. *Bot. Mar.* 54, 23–33. doi:10.1515/bot.2011.009

Cecere, E., Petrocelli, A., Portacci, G., Mineur, F., and Verlaque, M. (2011b). *Grateloupia minima* (Rhodophyta, Gigartinales) in the Thau lagoon and in the Mar Piccolo of Taranto: First report for the Mediterranean Sea. *Boll. Musei Ist. Biol. Univ. Genova* 73, 78.

Cecere, E., Petrocelli, A., and Saracino, O. D. (2000). *Undaria pinnatifida* (Fucophyceae, Laminariales) spread in the central Mediterranean: Its occurrence in the Mar Piccolo of Taranto (Ionian Sea, southern Italy). *Cryptogam. Algol.* 21, 305–309. doi:10.1016/S0181-1568(00)00113-6

Cecere, E., and Petrocelli, A. (2009). "The Mar Piccolo of Taranto," in *Flora and vegetation of the Italian transitional water systems*. Editors E. Cecere, A. Petrocelli, G. Izzo, and A. Sfriso (Spinea, Venice: CoRiLa, Stampa Multigraf), 195–227.

Cecere, E., Petrocelli, A., and Verlaque, M. (2004). Morphology and vegetative reproduction of the introduced species *Hypnea cornuta* (Rhodophyta, Gigartinales) in the Mar Piccolo of Taranto (Italy), Mediterranean Sea. *Bot. Mar.* 47, 381–388. doi:10.1515/BOT.2004.056

Cecere, E., Portacci, G., Petrocelli, A., Wolf, M. A., Sciuto, K., and Moro, I. (2011a). "Corsi e ricorsi storici: Il ritorno dell'alga alloctona *Agardhiella subulata* (Rhodophyta, Gigartinales) nel Mar Piccolo di Taranto," in *Proceedings of Gruppo di Algologia riunione scientifica annuale* (Ancona, Italy: CSI), 8.

Cecere, E., Saracino, O. D., Fanelli, M., and Petrocelli, A. (1992). Presence of a drifting algal bed in the Mar Piccolo basin, Taranto (Ionian Sea, southern Italy). *J. Appl. Phycol.* 4, 323–327. doi:10.1007/BF02185789

Cecere, E. (1990). Sulla presenza nel Golfo di Taranto di una specie nuova per il Mediterraneo: *Solieria filiformis* (Kützing) Gabrielson (Rhodophyta, Gigartinales). *Oebalia* 16, 629–631.

Choi, H. G., and Nam, K. W. (2001). Growth, tetrasporogenesis, and life history in culture of *Caulacanthus okamurae* (Gigartinales, Rhodophyta) from Korea. *Bot. Mar.* 44, 315–320. doi:10.1515/BOT.2001.040

Choi, H. G., Nam, K. W., and Norton, T. A. (2001). No whirlwind romance: Typhoons, temperature and the failure of reproduction in *Caulacanthus okamurae* (Gigartinales, Rhodophyta). *Eur. J. Phycol.* 36, 353–358. doi:10.1080/09670260110001735498

Chopin, T., Hanisak, M. D., Koehn, F. E., Mollion, J., and Moreau, S. (1990). Studies on carrageenans and effects of seawater phosphorus concentration on carrageenan content and growth of *Agardhiella subulata* (C. Agardh) Kraft and Wynne (Rhodophyceae, Solieriaceae). *J. Appl. Phycol.* 2, 3–16. doi:10.1007/BF02179764

Clarke, K. R. (1993). Nonparametric multivariate analyses of changes in community structure. *Aust. J. Ecol.* 18, 117–143. doi:10.1111/j.1442-9993.1993.tb00438.x

Clarke, K. R., and Warwick, R. M. (2001). *Change in marine communities: An approach to statistical analysis and interpretation*. Plymouth: PRIMER-E.

Compagnoni, A., Bibian, A. J., Ochocki, B. M., Levin, S., Zhu, K., and Miller, T. E. (2020). popler: An R package for extraction and synthesis of population time series from the long-term ecological research (LTER) network. *Methods Ecol. Evol.* 11, 258–264. doi:10.1111/2041-210X.13319

Copp, G. H., Templeton, M., and Gozlan, R. E. (2007). Propagule pressure and the invasion risks of non-native freshwater fishes: A case study in England. *J. Fish. Biol.* 71, 148–159. doi:10.1111/j.1095-8649.2007.01680.x

Cormaci, M., Furnari, G., Catra, M., Alongi, G., and Giaccone, G. (2012). Flora marina bentonica del Mediterraneo: Phaeophyceae. *Boll. Accad. Gioenia Sci. Nat. Catania* 45, 1–508.

Croce, M. E., and Parodi, E. R. (2017). The establishment of the non-native seaweed *Polysiphonia morrowii* in Northern Patagonia: Size of thallus and reproduction. *Aquat. Bot.* 136, 35–38. doi:10.1016/j.aquabot.2016.09.002

De Clerck, O., Gavio, B., Fredericq, S., Bárbara, I., and Coppejans, E. (2005). Systematics of *Grateloupia filicina* (Halymeniaceae, Rhodophyta), based on rbcL sequence analyses and morphological evidence, including the reinstatement of *G. minima* and the description of *G. capensis* sp. nov. *J. Phycol.* 41, 391–410. doi:10.1111/j.1529-8817.2005.04189.x

Fralick, R. A., and Mathieson, A. C. (1973). Ecological studies of *Codium fragile* in New England, USA. *Mar. Biol.* 19, 127–132. doi:10.1007/BF00353583

Freitas, C., Araújo, R., and Bertocci, I. (2016). Patterns of benthic assemblages invaded and non-invaded by *Grateloupia turuturu* across rocky intertidal habitats. *J. Sea Res.* 115, 26–32. doi:10.1016/j.seares.2016.07.002

Freshwater, D. W., and Rueness, J. (1994). Phylogenetic relationships of some European *Gelidium* (Gelidiales, Rhodophyta) species, based on *rbcL* nucleotide sequence analysis. *Phycologia* 33, 187–194. doi:10.2216/i0031-8884-33-3-187.1

Gennaro, P., Piazzi, L., Persia, E., and Porrello, S. (2015). Nutrient exploitation and competition strategies of the invasive seaweed *Caulerpa cylindracea*. *Eur. J. Phycol.* 50, 384–394. doi:10.1080/09670262.2015.1055591

Gower, J. C. (1966). Some distance properties of latent root and vector methods used in multivariate analysis. *Biometrik* 53, 325–338. doi:10.2307/2333639

Guerra-Castro, E. J., Conde, J. E., and Cruz-Motta, J. J. (2016). Scales of spatial variation in tropical benthic assemblages and their ecological relevance: Epibionts on caribbean mangrove roots as a model system. *Mar. Ecol. Prog. Ser.* 548, 97–110. doi:10.3354/meps11693

Hanisak, M. D. (1979). Growth patterns of *Codium fragile* ssp. *tomentosoides* in response to temperature, irradiance, salinity, and nitrogen source. *Mar. Biol.* 50, 319–332. doi:10.1007/BF00387009

Huisman, J. M., D'Archino, R., Nelson, W., Boo, S. M., and Petrocelli, A. (2021). Cryptic cryptogam revealed: *Hypnea corona* (Gigartinales: Cystocloniaceae), a new red algal species described from the *Hypnea cornuta* complex. *Pac. Sci.* 75, 263–268. doi:10.2984/75.2.8

Jesus de, P. B., Costa, A. L., Castro Nunes de, J. M., Manghisi, A., Genovese, G., Morabito, M., et al. (2019). Species delimitation methods reveal cryptic diversity in the *Hypnea cornuta* complex (Cystocloniaceae, Rhodophyta). *Eur. J. Phycol.* 54, 135–153. doi:10.1080/09670262.2018.1522454

Keser, M., Swenarton, J. T., and Foertch, J. F. (2005). Effects of thermal input and climate change on growth of *Ascophyllum nodosum* (Fucales, Phaeophyceae) in eastern Long Island Sound (USA). *J. Sea Res.* 54, 211–220. doi:10.1016/j.seares.2005.05.001

Kim, H.-S., Choi, H. G., Hwang, M. S., Jeon, Y. J., Yarish, C., and Kim, J. K. (2022). Concise review of the genus *Neopyropia* (Rhodophyta: Bangiales). *J. Appl. Phycol.* 34, 1805–1824. doi:10.1007/s10811-022-02776-1

Koerich, G., Assis, J., Burle Costa, G., Nasri Sissini, M., Serrão, E. A., Rubi Rörig, L., et al. (2020). How experimental physiology and ecological niche modelling can inform the management of marine bioinvasions? *Sci. Tot. Environ.* 700, 134692. doi:10.1016/j.scitotenv.2019.134692

Kralj, M., De Vittor, C., Comici, C., Relitti, F., Auriemma, R., Alabiso, G., et al. (2016). Recent evolution of the physical–chemical characteristics of a site of national interest—The Mar Piccolo of Taranto (Ionian Sea)—And changes over the last 20 years. *Env. Sci. Pollut. Res.* 23, 12675–12690. doi:10.1007/s11356-015-5198-8

Kudo, T., and Masuda, M. (1981). A taxonomic study of *Polysiphonia morrowii* Harvey (Rhodophyta, Ceramiales). *Jap. J. Phycol.* 29, 263–272.

Manghisi, A., Morabito, M., Bertuccio, C., Le Gall, L., Couloux, A., Cruaud, C., et al. (2010). Is routine DNA barcoding an efficient tool to reveal introductions of alien macroalgae? A case study of *Agardhiella subulata* (Solieriaceae, Rhodophyta) in Cape Peloro lagoon (Sicily, Italy). *Cryptogam. Algol.* 31, 423.

Mentaschi, L., Vousdoukas, M. I., Voukouvalas, E., Dosio, A., and Feyen, L. (2017). Global changes of extreme coastal wave energy fluxes triggered by intensified teleconnection patterns. *Geophys. Res. Lett.* 44, 2416–2426. doi:10.1002/2016GL072488

Mineur, F., Belsher, T., Johnson, M. P., Maggs, C. A., and Verlaque, M. (2007). Experimental assessment of oyster transfers as a vector for macroalgal introductions. *Biol. Conserv.* 137, 237–247. doi:10.1016/j.biocon.2007.02.001

Mineur, F., Le Roux, A., Maggs, A., and Verlaque, M. (2014). Positive feedback loop between introductions of non-native marine species and cultivation of oysters in Europe. *Conserv. Biol.* 28, 1667–1676. doi:10.1111/cobi.12363

Montes, M., Rico, J. M., García-Vázquez, E., and Borrell, Y. J. (2016). Morphological and molecular methods reveal the Asian alga *Grateloupia imbricata* (Halymeniaceae) occurs on Cantabrian Sea shores (Bay of Biscay). *Phycologia* 55, 365–370. doi:10.2216/15-112.1

Montes, M., Rico, J. M., García-Vazquez, E., and Pichs, Y. J. B. (2017). Molecular barcoding confirms the presence of exotic Asian seaweeds (*Pachymeniopsis gargiuli* and *Grateloupia turuturu*) in the Cantabrian Sea, Bay of Biscay. *PeerJ* 5, e3116. doi:10.7717/peerj.3116

Mulas, M., and Bertocci, I. (2016). Devil's tongue weed (*Grateloupia turuturu* Yamada) in northern Portugal: Passenger or driver of change in native biodiversity? *Mar. Environ. Res.* 118, 1–9. doi:10.1016/j.marenvres.2016.04.007

Newton, A., Icely, J., Cristina, S., Brito, A., Cardoso, A. C., Colijn, F., et al. (2014). An overview of ecological status, vulnerability and future perspectives of European large shallow, semi-enclosed coastal systems, lagoons and transitional waters. *Estuar. Coast. Shelf Sci.* 140, 95–122. doi:10.1016/j.ecss.2013.05.023

Peñuela, A., Robledo, D., Bourgougnon, N., Bedoux, G., Hernández-Núñez, E., and Freile-Pelegrín, Y. (2018). Environmentally friendly valorization of *Solieria filiformis* (Gigartinales, Rhodophyta) from IMTA using a biorefinery concept. *Mar. Drugs* 16, 487. doi:10.3390/md16120487

Perrone, C., and Cecere, E. (1994). Two solieriacean algae new to the Mediterranean: *Agardhiella subulata* and *Solieria filiformis* (Rhodophyta, Gigartinales). *J. Phycol.* 30, 98–108. doi:10.1111/j.0022-3646.1994.00098.x

Petrocelli, A., Acquaviva, M. I., Alabiso, G., Belmonte, M., Biandolino, F., Cardellicchio, N., et al. (2021). "IT22-M Mar Piccolo di Taranto," in *La Rete Italiana per la Ricerca Ecologica di Lungo Termine. Lo studio della biodiversità e dei cambiamenti*. Editors L. Capotondi, M. Ravaioli, A. Acosta, F. Chiarini, A. Lami, A. Stanisci, et al. (Roma, Italy: CNR Edizioni), 675–700. doi:10.5281/zenodo.5570272

Petrocelli, A., Alabiso, G., Cecere, E., Ricci, P., and Carlucci, R. (2020a). Invasive or not? The case of *Grateloupia turuturu* (Rhodophyta, Halymeniales) in the northern Ionian Sea (Mediterranean Sea). *Mar. Pollut. Bull.* 161, 111748. doi:10.1016/j.marpolbul.2020.111748

Petrocelli, A., and Cecere, E. (2010). Biodiversity and mollusc transfer: Need of observance of the laws to avoid alien seaweeds introduction. *Biol. Mar. Mediterr.* 17, 175–176.

Petrocelli, A., Cecere, E., and Rubino, F. (2019). Successions of phytobenthos species in a Mediterranean transitional water system: The importance of long term observations. *Nat. Conserv.* 34, 217–246. doi:10.3897/natureconservation.34.30055

Petrocelli, A., Cecere, E., and Verlaque, M. (2013). Alien marine macrophytes in transitional water systems: New entries and reappearances in a Mediterranean coastal basin. *BioInvasions Rec.* 2, 177–184. doi:10.3391/bir.2013.2.3.01

Petrocelli, A., Wolf, M. A., Cecere, E., Sciuto, K., and Sfriso, A. (2020b). Settlement and spreading of the introduced seaweed *Caulacanthus okamurae* (Rhodophyta) in the Mediterranean Sea. *Diversity* 12, 129. doi:10.3390/d12040129

Piñeiro-Corbeira, C., Verbruggen, H., and Díaz-Tapia, P. (2020). Molecular survey of the red algal family Rhodomelaceae (Ceramiales, Rhodophyta) in Australia reveals new introduced species. *J. Appl. Phycol.* 32, 2535–2547. doi:10.1007/s10811-019-01932-4

Pugnetti, A., Acri, F., Bernardi Aubry, F., Camatti, E., Cecere, E., Facca, C., et al. (2013). The Italian Long-Term Ecological Research (LTER-Italy) network: Results, opportunities, and challenges for coastal transitional ecosystems. *Transit. Waters Bull.* 7, 43–63. doi:10.1285/i1825229Xv7n1p43

Salamon, M., Lévêque, L., Ballenghien, M., and Viard, F. (2020). Spill-back events followed by self-sustainment explain the fast colonization of a newly built marina by a notorious invasive seaweed. *Biol. Invasions* 22, 1411–1429. doi:10.1007/s10530-019-02193-5

Sanderson, J. C. (1990). A preliminary survey of the distribution of the introduced macroalga *Undaria pinnatifida* (Harv) Suringar on the East Coast of Tasmania. *Bot. Mar.* 33, 153–158. doi:10.1515/botm.1990.33.2.153

Saunders, G. W. (2009). Routine DNA barcoding of Canadian Gracilariales (Rhodophyta) reveals the invasive species *Gracilaria vermiculophylla* in British Columbia. *Mol. Ecol. Resour.* 9, 140–150. doi:10.1111/j.1755-0998.2009.02639.x

Sfriso, A., Buosi, A., Wolf, M. A., and Sfriso, A. A. (2020). Invasion of alien macroalgae in the Venice Lagoon, a pest or a resource? *Aquat. Invasions* 15, 245–270. doi:10.3391/ai.2020.15.2.03

Sfriso, A., Facca, C., Bon, D., and Buosi, A. (2016). Macrophytes and ecological status assessment in the Po delta transitional systems, Adriatic Sea (Italy). Application of Macrophyte Quality Index (MaQI). *Acta Adriat.* 57, 209–225.

Simon, C., Ar Gall, E., and Deslandes, E. (2001). Expansion of the red alga *Grateloupia doryphora* along the coasts of Brittany. *Hydrobiologia* 443, 23–29. doi:10.1023/A:1017587918604

Trowbridge, C. D., Little, C., and Stirling, P. (2016). Post-proliferation population of introduced seaweed: Decline of a parthenogenetic green seaweed in Irish marine reserve. *Biol. Environ. Proc. R. Ir. Acad.* 116, 87–102. doi:10.3318/bioe.2016.10

Tsirintanis, K., Azzurro, E., Crocetta, F., Dimiza, M., Froglia, C., Gerovasileiou, V., et al. (2022). Bioinvasion impacts on biodiversity, ecosystem services, and human health in the Mediterranean Sea. *Aquat. Invasions* 17, 308–352. doi:10.3391/ai.2022.17.3.01

Turner, M. G., Collins, S. L., Lugo, A. L., Magnuson, J. J., Rupp, T. S., and Swanson, F. J. (2003). Disturbance dynamics and ecological response: The contribution of Long-Term Ecological Research. *BioScience* 53, 46–56. doi:10.1641/0006-3568(2003)053[0046:DDAERT]2.0.CO;2

Vandermeulen, H. (1986). Growth of *Colpomenia peregrina* (Phaeophyceae) in culture: Effects of salinity, temperature and daylength. *J. Phycol.* 22, 138–144. doi:10.1111/j.1529-8817.1986.tb04156.x

Verlaque, M., Boudouresque, Ch.-F., and Mineur, F. (2007). Oyster transfers as a vector for marine species introductions: A realistic approach based on the macrophytes. *CIESM Workshop Monogr.* 32, 39–48.

Verlaque, M., and Breton, G. (2019). Biological invasion: Long term monitoring of the macroalgal flora of a major European harbor complex. *Mar. Pollut. Bull.* 143, 228–241. doi:10.1016/j.marpolbul.2019.04.038

Verlaque, M., Ruitton, S., Mineur, F., and Boudouresque, Ch.-F. (2015). *CIESM atlas of exotic species in the mediterranean. 4: Macropytes*. Monaco: CIESM Publishers, 362.

Watanabe, Y., Nishihara, G. N., Tokunaga, S., and Terada, R. (2014). The effects of irradiance and temperature responses and the phenology of a native alga, *Undaria pinnatifida* (Laminariales), at the southern limit of its natural distribution in Japan. *J. Appl. Phycol.* 26, 2405–2415. doi:10.1007/s10811-014-0264-z

Wilkes, R. J., McIvor, L. M., and Guiry, M. D. (2005). Using rbcL sequence data to reassess the taxonomic position of some *Grateloupia* and *Dermocorynus* species (Halymeniaceae, Rhodophyta) from the north-easten Atlantic. *Eur. J. Phycol.* 40, 53–60. doi:10.1080/09670260400024634

Wolf, M. A., Buosi, A., Juhmani, A. S. F., and Sfriso, A. (2018). Shellfish import and hull fouling as vectors for new red algal introductions in the Venice Lagoon. *Estuar. Coast. Shelf Sci.* 215, 30–38. doi:10.1016/j.ecss.2018.09.028

Wolf, M. A., Sciuto, K., Maggs, C. A., Barros-Barreto, M. B., Andreoli, C., and Moro, I. (2011). *Ceramium* Roth (Ceramiales, Rhodophyta) from Venice lagoon (Adriatic Sea, Italy): Comparative studies of mediterranean and atlantic taxa. *Taxon* 60, 1584–1595. doi:10.1002/tax.606004

Wolf, M. A., Sfriso, A., and Moro, I. (2014). Thermal pollution and settlement of new tropical alien species: The case of *Grateloupia yinggehaiensis* (Rhodophyta) in the Venice Lagoon. *Estuar. Coast. Shelf Sci.* 147, 11–16. doi:10.1016/j.ecss.2014.05.020

Yamagishi, Y., Masuda, M., Abe, T., Uwai, S., Kogame, K., Kawaguchi, S., et al. (2003). Taxonomic notes on marine algae from Malaysia. XI. Four species of Rhodophyceae. *Bot. Mar.* 46, 534–547. doi:10.1515/BOT.2003.056

Zilioli, M., Oggioni, A., Tagliolato, P., Pugnetti, A., and Carrara, P. (2019). Feeding Essential Biodiversity Variables (EBVs): Actual and potential contributions from LTER-Italy. *Nat. Conserv.* 34, 477–503. doi:10.3897/natureconservation.34.30735

Zingone, A., D'Alelio, D., Mazzocchi, M. G., Montresor, M., and Sarno, D.LTER-MC team (2019). Time series and beyond: Multifaceted plankton research at a marine Mediterranean LTER site. *Nat. Conserv.* 34, 273–310. doi:10.3897/natureconservation.34.30789

Zuccarello, G. C., West, J., and Rueness, J. (2002). Phylogeography of the cosmopolitan red alga *Caulacanthus ustulatus* (Caulacanthaceae, Gigartinales). *Phycol. Res.* 50, 163–172. doi:10.1111/j.1440-1835.2002.tb00147.x

Frontiers in
Environmental Science

Explores the anthropogenic impact on our natural world

An innovative journal that advances knowledge of the natural world and its intersections with human society. It supports the formulation of policies that lead to a more inhabitable and sustainable world.

Discover the latest Research Topics

See more →

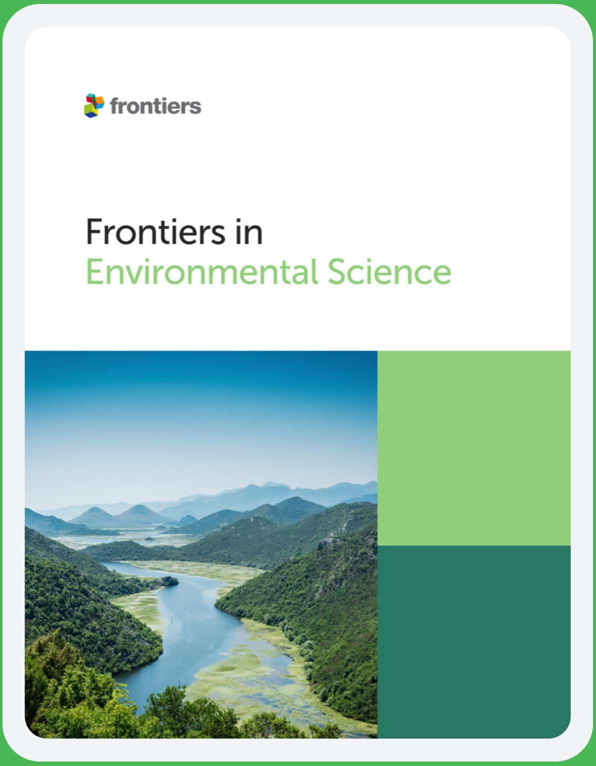

Frontiers

Avenue du Tribunal-Fédéral 34
1005 Lausanne, Switzerland
frontiersin.org

Contact us

+41 (0)21 510 17 00
frontiersin.org/about/contact